# *Advances in Printing and Media Technology*

## Vol. XXXVII

Edited by Nils Enlund and Mladen Lovreček

# Advances in Printing and Media Technology

Proceedings of the 37th International Research Conference of iarigai

Montreal, Canada, September 2010

Published by the International Association
of Research Organizations for the Information,
Media and Graphic Arts Industries

Darmstadt, Germany 2010

Co-edited by
Nils Enlund, Stockholm, Sweden
Mladen Lovreček, Zagreb, Croatia

Scientific Committee

Anne Blayo (Grenoble),
Tim Claypole (Swansea),
Edgar Dörsam (Darmstadt),
Nils Enlund (Stockholm),
Patrick Gane (Espoo),
Jon Yngve Hardeberg (Gjovik),
Ulrike Herzau-Gerhardt (Leipzig),
Gunter Hübner (Stuttgart),
Per-Åke Johansson (Stockholm),
John Kettle (Espoo),
Helmut Kipphan (Schwetzingen),
Björn Kruse (Norrköping),
Magnus Lestelius (Karlstad),
Ulf Lindqvist (Espoo),
Patrice Mangin (Trois Rivieres),
Pirkko Oittinen (Helsinki),
Jouko Peltonen (Turku),
Anastasios Politis (Athens),
Renke Wilken (Munich),
Scott Williams (Rochester)

# Contents

## 4. Innovative use of printing

*Introduction*

...

# Preface

*Nils Enlund*

Co-editor, Chairman of the Program Committee

KTH - Royal Institute of Technology
SE-10044 Stockholm, Sweden
E-mail: nilse@kth.se

## Trendspotting in print and media technology research

The volume that you now hold in your hands contains the scientific and technical research contributions presented at the 37th International Research Conference of iarigai, the International Association of Research Organizations for the Information, Media and Graphic Arts Industries, held in Montreal, Canada, on September 12-15, 2010. The contributions for this conference were selected by a scientific committee of international experts through a double-blind review process.

The yearly iarigai conference is the main international forum for scientific exchange in the print and media technology field. The proceedings provide an excellent overview of current industry trends and research foci among universities and research organizations in the field.

In 2009, the main emerging research trend was the challenges of creating and maintaining sustainability in production, distribution and consumption of media content and products. In 2010, this trend continues strongly. Scientific studies address the problems of assessing the carbon footprint of newspaper production, performing comparative life-cycle analyses of alternative media channels, and developing sustainable strategies for media companies.

Another trend that was already apparent in 2009 is now visibly gathering strength: investigations of the user experience when consuming media content and products. How does the feel of a paper quality between your fingertops affect your attitudes toward the printed product and its content? How does the use of special effects influence the credibility and attractivity of the media product? How should we design products in order to recognize and address consumer preferences? In an environment where the competition between media forms is growing stronger by the day, answering these and similar questions is becoming increasingly important.

A third strong trend within the research community is the development of innovative uses of printing technology. As printing of text and images is loosing ground due to the success of screen-based information, there is a surge of interest in alternative uses for the already existing and fine-tuned printing technology. There is an increasing body of research on functional printing: printing of electronic components, batteries and curcuits; the use of nanotechnologies; printing on non-conventional substrates; thermochromic prints. This development is paralleled by research on new types of paper and substrates for functional printed products. These areas hold tremendous opportunities. Print is definitely not dying.

In addition to the unfolding and expanding research topics above, this volume presents an abundance of new and exciting work on topics that may not have the same novelty value but form the solid basis of print technology research - questions of print and reproduction quality, color management, ink and paper characteristics, printing productivity, and standardisation.

So, whatever your research interest, you will certainly find valuable information in this book.

# Surface modification of a PCB substrate for improved adhesion of inkjet printed circuit structures[*]

*Ashok Sridhar*[1]*, D. J. van Dijk*[2]*, R. Akkerman*[2]

[1] Printed Functionalities, Fraunhofer ENAS
 Technologie-Campus 3, D-09126, Chemnitz, Germany
 E-mail: ashok.sridhar@enas.fraunhofer.de

[2] Production Technology Group, University of Twente
 Drienerlolaan 5, NL-7500AE, Enschede, the Netherlands

**Abstract**

The robustness and service life of inkjet printed electronic circuit structures are highly influenced by the state of the interface between these structures and the substrate. In the case of polymeric substrate materials, surface modification is, in many cases, necessary to realise a favourable interface, as these materials are generally not very receptive to chemical bond formation with the deposited ink. This paper deals with the surface modification of a high frequency laminate (substrate) using two different techniques to improve interfacial adhesion. The techniques deployed are $CF_4/O_2$ based plasma treatment and micro structuring using pulsed laser. The plasma treatment parameters were varied systematically using a statistical design of experiments. Substrates with varying surface characteristics, resulting from different plasma treatment parameter sets, were subjected to surface energy and surface roughness measurements. Similarly, the influence of laser treatment parameters on surface characteristics of the substrate was also studied. The outcomes of these two surface modification techniques are discussed in this paper.

**Keywords:** inkjet printing; adhesion, surface modification; plasma etching; laser ablation

## 1. Background

Inkjet printing of functional inks is widely researched as a technique for electronics fabrication. However, being able to print the required circuit structures is a job half done if the robustness, reliability and lifetime expectancy requirements are not met. The response of a printed structure to mechanical, thermal and environmental stresses is a key aspect to be considered before deeming it suitable for practical applications. One of the most important factors that determine the robustness and reliability of a circuit structure is its adhesion to the substrate material. In general, adhesion of a thin film to a substrate depends on the affinity between the two materials, the mode and rate of deposition, the film thickness, the process temperature, the process pressure etc [1]. This holds true for inkjet printing as well, as a single layer of inkjet-deposited structure is typically less than a micron in thickness, and hence can be classified as a thin film.
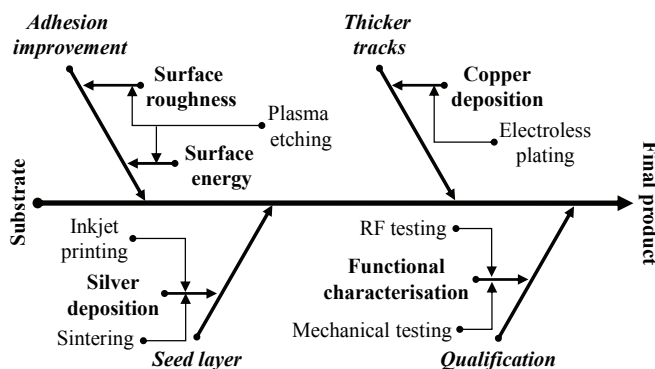


*Figure 1: An inkjet printing-based process chain for fabrication of conducting (metallic) circuit structures*

---

Within the framework of this research, inkjet printing is deployed as a technique to deposit silver seed layers for a subsequent electroless plating process, for the fabrication of conducting circuit structures, especially for high radio frequency (RF) applications. Figure 1 depicts the individual components of this research and where inkjet printing fits in.

*Table 1: Materials and equipments used for experiments relevant to this paper*

| Type | Description |
|---|---|
| Substrate | Rogers RO4003 high-frequency laminate |
| Ink | Harima Nanopaste (60% silver nanoparticles by weight) |
| Plating bath | Enthone Envision-2130 electroless copper system |
| Inkjet printer | Jetlab-4 drop-on-demand, piezo-actuated printer |
| Plasma etcher | TePla 3067-E barrel-type plasma etcher |
| Laser setup | Coherent Vitesse Duo with Coherent RegA regenerative amplifier |

Special RO4003 substrates for inkjet printing (without copper cladding) were procured from Rogers Corporation, USA. The adhesion of inkjet printed silver structures on this substrate was insufficient, as indicated by scotch tape tests. Poor adhesion was also evident from the electroless plating trials, during which the silver seed layers delaminated from the substrate. This delamination is shown in figure 2.
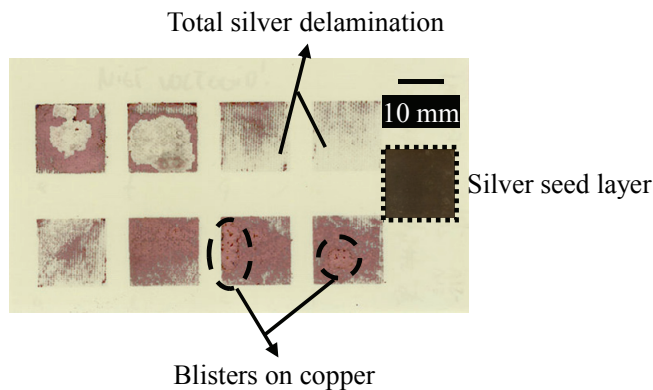


*Figure 2: Square-shaped silver seed layers inkjet printed on a RO4003 substrate and subjected to copper plating; the delamination of silver due to poor adhesion can be clearly seen. Inset: a silver seed layer prior to plating*

To improve adhesion of the silver structures to the substrate, two different surface modification techniques were used: plasma etching and laser ablation. Plasma etching was investigated in greater detail using a statistical design of experiments (DoE). Conclusions concerning the substrate surface characteristics suitable for inkjet printing-electroless plating and the importance of surface modification for good adhesion were expected to be the outcomes of this research at the outset.

## 2. Plasma etching

### 2.1 Introduction

$CF_4/O_2$ plasma was chosen for this study based on prior experience and the available literature that extensively discusses the application of this gas combination to etch thermoset as well as thermoplastic polymers [2,3]. The chemical reactions are promoted by radicals in $O_2$ and $CF_4$. Within certain limits, the addition of $CF_4$ to an oxygen plasma greatly enhances the etch rate. Even though oxygen is the etchant for polymers, atomic fluorine creates radicals at the surface of the polymer for further attack by oxygen [4]. The plasma treatment was intended to modify the wettability of the substrate surface and to impart sufficient surface roughness, so that mechanical interlocking is enhanced. However, very rough substrates or substrates with surface pores, as discussed in [5,6] were not intended, as they will have a detrimental effect on the accuracy of inkjet printing. In addition to that, roughened polymer surfaces have a deleterious effect on (RF-) electrical performance, especially in the case of high frequency circuits [7]. The DoE was used to identify the process parameter window that yields the most suitable substrate surface characteristics.

## 2.2 Design of experiments

The experimental design technique chosen for this study is the central composite rotatable design (CCRD). It gives sufficient information to describe majority of steady-state process responses and requires far fewer runs when compared to the full factorial design, and gives a clearer picture about interactions between the process variables than a fractional factorial design. The CCRD was chosen in such a way that it contains '$2^n$' factorial treatment designs, '2n' axial or star points and sufficient replications at the centre of the design. Here, 'n' represents the number of process variables under study. Initial plasma etching trials showed that four factors, namely power, time of exposure to plasma, flow rate of $O_2$ and flow rate of $CF_4$ are most relevant parameters that need to be studied. The operating pressure, which is generally considered important in plasma etching, could not be pre-set in the available equipment. As a result, the CCRD consisted of 16 factorial treatment designs, with 8 star points and 7 centre points, thus 31 experiments in total. Power was varied from 2500 W to 4100 W in steps of 400 W, time was varied from 10 min to 50 min in steps of 10 min, $O_2$ flow rate from 0 ml/min to 2000 ml/min in steps of 500 ml/min and $CF_4$ flow rate from 0 ml/min to 200 ml/min in steps of 50 ml/min. The magnitude of the process parameters are much higher than those found in the literature. The reason for this is that the plasma etching equipment used for the experiments is an industrial-scale equipment with a large chamber ($\approx 0.7$ m$^3$) that necessitated these parameter values for effective etching. A detailed explanation of the CCRD model is not presented in this paper; the model has been dealt with in detail in a separate paper [8].

## 2.3 Experiments and measurements

As per the experimental design, 31 substrates, each measuring 100 mm × 100 mm, were cut and subsequently plasma etched. In this etching process, the specimen i.e. substrate is immersed in plasma-containing gases that react with it. At a relatively high process pressure of more than 0.2 mbar, the mechanism for etching is predominantly chemical, the physical bombardment being minimal. The chosen gas flow rates were such that the process pressure was always above 0.2 mbar for all the experimental trials. The initial temperature of the plasma chamber was set as 80°C.

After etching, the contact angle of water on these substrates was measured with the purpose of calculating the surface energy of the latter, using the Neumann's equation of state [9]. The next step was the surface roughness measurement using a DEKTAK surface profiler, followed by analysis of the substrate surface topography using a scanning electron microscope (SEM). Subsequent to surface characterisation, rectangular test patterns of arbitrarily determined dimensions (30 mm × 10 mm) were inkjet printed on these substrates. The thickness of the pattern was highly dependant on surface roughness and surface energy of the individual substrates, and was difficult to characterise due to the pronounced roughness of certain substrates. Measurements on selected substrates after sintering of the test patterns indicated that the thicknesses were in the order of 1 μm. Scotch tape tests were done on these patterns to qualitatively rank the adhesive strength of the substrates under study. The spreading of the ink on the substrates was also studied to identify the optimal substrate surface characteristics.

## 3. Laser ablation

### 3.1. Introduction

Plasma treatment etches the substrate as a whole, unless a mask is used to make the process selective. However, making a mask containing micro-patterns that allow the plasma to attack the substrate on specific locations is a time-consuming and expensive process. Hence, it was decided to use a laser ablation setup that directly etches desired patterns on the substrate i.e. it enables selective patterning of the substrate. The advantage of selective patterning is that if different inks have to be used on the same substrate to inkjet print different functional components, the size and shape of the patterns can be locally varied depending on the flow properties of the ink. The setup used in this study is a femto-second laser with a wavelength of 800 nm and a pulse length of 250 fs. Due to the extremely short pulse duration and small beam size, the material is ablated locally, resulting in minimal substrate damage due to the reduced heat-affected zone [10].

### 3.2. Experiments and measurements

The output power was maintained at 1 W. The focal spot size was varied between 5 and 20 μm, the pulse repetition rate was varied between 10 and 250 kHz, and the scanning speed, from 20 to 200 mm.s$^{-1}$. Three different patterns were ablated: lines, hatches and holes. The patterned substrates resulting from the various parameter combinations were analysed using SEM and subsequently, silver structures were inkjet printed on selected substrates. Finally, scotch tape tests were done to qualitatively check for adhesion.

## 4. Results and discussion

The plasma treatment yielded substrates with varying surface roughnesses and surface energies, depending on the parameter set used. Based on surface roughness and surface energy measurements, as well as adhesion tests and droplet spreading observations, a substrate that was etched at 3300 W for 10 minutes, with $O_2$ and $CF_4$ flow rates maintained at 1000 ml/min and 100 ml/min respectively, was selected as the one with optimal surface characteristics. Figure 3 shows SEM images of the selected substrate before and after plasma treatment.
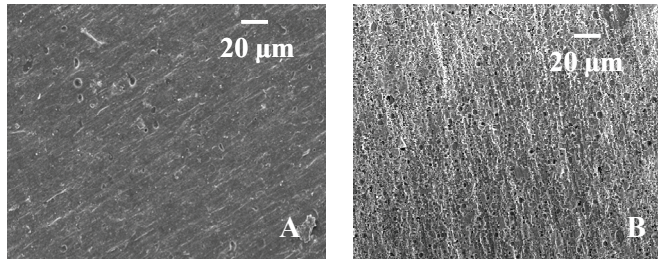


*Figure 3: A RO4003 substrate (A) before plasma etching and (B) after plasma etching with the optimal parameter set*

The selected substrate had a Ra value of 0.56 μm and a surface energy of 47.2 mN/m. The scotch tape test indicated an improvement in adhesion. Only minimal amount of silver was peeled off from the plasma etched substrate. That too, the failure was not adhesive but cohesive. This indicates that the adhesion between silver and the plasma treated substrate is higher than the cohesive strength of silver. The increase in adhesion can be attributed to the greater mechanical interlocking due to the increase in surface roughness of the substrate, and to the change in functional groups on the surface of the polymeric substrate. It was also possible to electroless plate copper on silver seed layers printed on this substrate, as shown in figure 4.
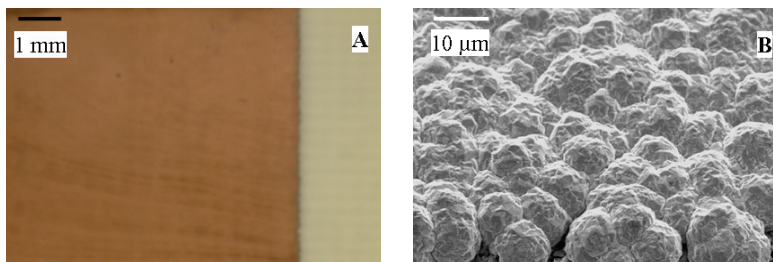


*Figure 4: Images of an inkjet printed-electroless plated structure on a plasma treated RO4003 substrate: (A) macroscopic and (B) microscopic*

Finding the correct laser ablation parameters proved to be difficult due to the composite nature of the substrate. The substrate is comprised of 3 materials: polymer matrix, glass fibre reinforcements and ceramic fillers. The laser beam penetrated the polymer top layer and encountered the other two materials. The parameters optimised to ablate the polymer did not hold good for the other materials. SEM analysis of ablated substrates showed that the laser-generated patterns were as much as 10 μm deep, much more than the intended depth of 1 to 3 μm. The problem with deeper patterns is they can lead to local agglomeration of functional ink particles during printing, resulting in huge variations in the cross-section of printed structures. This will affect both the electrical functionality and mechanical properties of these structures. The laser-generated patterns experimented with are shown in figure 5.
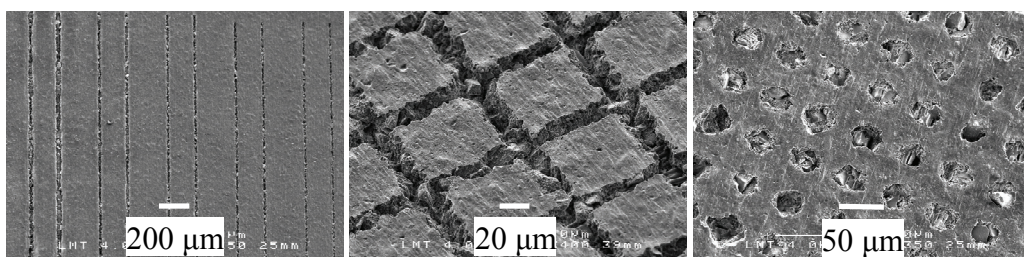


*Figure 5: Laser ablated structures on RO4003 substrate material*

Similar investigations carried out on FR4 substrate material proved to be successful, resulting in ablation of holes with a diameter of 10 μm and depth of 3.5 μm. Since FR4 does not contain large filler particles, it was far easier and accurate to ablate than RO4003.

## 5. Conclusions

- Inkjet printed structures on plasma treated substrates showed improved adhesion.
- Increase in surface energy and surface roughness is responsible for improved adhesion.
- Improved adhesion enabled electroless copper plating on silver seed layers without adhesive failure.
- Laser ablated patterns were too deep (~10 μm), leading to local agglomeration of the ink.
- Ink agglomeration leads to cross-sectional variation, which affects mechanical as well as (RF-) electrical properties of the printed structures.

## References

[1] K. L. Mittal: "Adhesion measurement of thin films", *Electrocomponent Science and Technology,* Vol. 3, p. 21, (1976).

[2] G. Turban and M. Rapeaux: "Dry etching of polyimide in $O_2$-$CF_4$ and O2-SF6 plasmas", *Journal of Electrochemical Society: Solid-state Science and Technology,* Vol. 130 (11), p. 2231, (1983).

[3] I. Garnev, K. Oshinov, V. Orlinov, K. Popova and B. Spangenberg: "Optimising plasma etching of base polymer materials for MLB using response surface methodology", *Bulgarian Journal of Physics,* Vol. 19 (3-4), p. 74, (1992).

[4] M. Ghosh and K.L. Mittal: "Polyimides: fundamentals and applications", *CRC Press,* p. 432-434, (1996).

[5] J. Ge, R. Tuominen and J.K. Kivilahti: "Adhesion of electrolessly-deposited copper to photosensitive epoxy", *Journal of Adhesion Science and Technology,* Vol. 15 (10), p. 1133, (2001).

[6] A. Sridhar, D.J. van Dijk and R. Akkerman: "Inkjet printing and adhesion characterisation of conductive tracks on a commercial printed circuit board material", *Thin Solid Films (2009),* doi: 10.1016/j.tsf.2009.03.133.

[7] J. Ge: "Interfacial adhesion in metal/polymer systems for electronics", *PhD Thesis - Helsinki University of Technology, Finland,* p. 9, (2003).

[8] A. Sridhar, M. A. Perik, J. Reiding, D. J. van Dijk and R. Akkerman: "Fabrication of RF circuit structures on a PCB material by inkjet printing-electroless plating and the substrate preparation therefor", *Proceedings of International Conference on Electronics Packaging 2009,* p. 322.

[9] OCA20 Web Help, OCA video-based contact meter, DataPhysics Instruments GmbH, Germany.

[10] S-H. Ko, H. Pan, C. P. Grigoropoulos, J. M. J. Frechet, C. K. Luscombe and D. Poulikakos: "Lithography-free high-resolution organic transistor arrays on polymer substrate by low energy selective laser ablation of inkjet-printed nanoparticle film", *Applied Physics A: Materials Science & Processing,* Vol. 92 (3), p. 579, (2008).

**1**

*Print media, the consumer
and the sustainable society*

# Accessibility and multi-channel publishing: Different aims, similar solutions?

*Ulrich Nikolaus*

Leipzig University of Applied Sciences (HTWK Leipzig)
Gutenbergplatz 2 - 4, D-04103 Leipzig, Germany
E-mail: nikolaus@fbm.htwk-leipzig.de

**Abstract**

Accessibility, the attempt to make publications available for as many people as possible (especially for people with disabilities), seems at first glance to have little in common with (single-source) multi-channel publishing, the concept of using one single data source for the publication on different publication channels. However, both the technical solutions and the document structures used to achieve these goals sometimes turn out to be surprisingly similar. The similarities and differences between both concepts will be discussed, using the XML-based e-book standard "ePUB" and the accessible document format "DAISY 3" as an example. Furthermore, remaining technical issues and limitations that inhibit the seamless integration of accessibility in multi-channel publishing will be covered in detail.

**Keywords:** accessibility; single-source multi-channel publishing; XML; ePUB; DAISY

## 1. Introduction

The integration of disabled individuals into society is an ancient social issue - and an important part of it is the attempt to make any information available to the general public accessible to handicapped persons as well. Unfortunately, our society is slow to fix chronic problems even after discovering solutions (Dick & Golshani 2008). Although equal treatment of people with disabilities is required by law in many countries[1], unrestricted information access still remains an unfulfilled dream. At present, only two, at most three percent of all literature published in Germany every year (and less than five percent in Canada) is available in accessible formats (Dittmer 2007, CNIB 2009). An important reason for this may be that the production of accessible documents is an often tedious task. Documents for visually impaired people[2], for instance, are mostly edited, formatted and produced independently and in parallel to conventional publications; in general by specialized institutions like, in Canada, the Canadian National Institute for the Blind (CNIB) or, in Germany, the German Central Library for the Blind (DZB). This duplicated production process is both time-consuming and expensive.

Electronic publishing, however, has simplified information access for handicapped users in various ways. For many blind and visually impaired persons, using computers, browsing the World Wide Web or shopping on the internet have become everyday tasks (cf. Figure 1). In order to do this, disabled persons need input and output devices that can adapt electronic publications to their specific needs. Depending on the type of disability, there are a great variety of assistive technologies available (Ribera 2008, 26). Computer mouses or trackballs, for instance, are not suitable for blind or visually impaired persons, because they require visual tracking of mouse pointer position (Scherrer 2010, 141). Therefore, users with print impairments have to rely on keyboard shortcuts and tab navigation instead. As for information output, screen readers and refreshable Braille displays are probably the most important tools (Ribera 2008, 26). Screen readers are software applications that convert textual information to computer-generated speech using a text-to-speech (TTS) engine. (Refreshable) Braille displays are tactile devices that use several groups of six to eight moveable pins to form Braille characters that can be read by many blind users. Obviously, an I/O interface like the one

---

[1] Examples are the Americans with Disabilities Act and Section 508 of the Rehabilitation Act (508 ACT) in the U.S. or the Disability Discrimination Act in Great Britain. In Germany, equal rights for handicapped persons are even guaranteed by the constitution (German Basic Law, Art. 3, par. 3).

[2] There are many forms of disabilities, requiring various devices for information access. This paper, however, will be focused on documents for persons with print disabilities, this being the author's main area of research. Nevertheless, the needs of deaf, hearing impaired or dyslexic users have to be taken into account as well - and in some cases, the approach may even be similar (cf. Eberius & Haffner 2010).

shown in Figure 1 is fundamentally different compared to the one customarily used by non-handicapped users. Nonetheless, electronic publications should be accessible for all users - regardless of their preferred way of information access.

This, however, entails changes in information structure: In order to make automatic content adaptation to assistive I/O technology possible, strict semantic structuring is indispensable (Dick & Golshani 2008, 22). As the production of supplemental accessible publications is too time consuming and expensive in the long run, publications for the general public have to become adaptable to assistive technology. This, however, can only be done if document content and structure can be accessed, analysed and, if necessary, altered automatically in order to adapt presentation and navigation according to the user's needs. Mark-up languages like XML have already proven that they are well suited to meet these demands. XML, designed in 1998 with the purpose to become the "future lingua franca for the exchange of structured data" (Bosak 1998, 120), has become a key technology for electronic publishing, mainly due to its major design principles including extensibility (to define new semantic structures as needed), structure (to model data to any level of complexity), validation (to automatically check data for structural correctness), media independence (to publish content in multiple formats), and vendor and platform independence (l.c.). Implementing the principle to separate content, structure and layout, XML applications use mark-ups to tag semantic document structures in such a way that they can be parsed, altered and processed automatically. Thus, information contained in one single source can, in principle, be published without manual intervention on different output channels in order to become a printed book, a website, an e-book - or an accessible document adapted to the special needs of handicapped users.



*Figure 1: User interaction with keyboard (right) and refreshable Braille display (left)*

At this point, it becomes evident that there is an obvious connection between accessibility and single-source multi-channel publishing: If one considers refreshable Braille displays or screen readers as being just additional output channels beside paper, computer screens or mobile devices, it becomes apparent that technical solutions and document structures used in multi-channel publishing might be advantageous for the production of accessible documents as well.

## 2. Methods

The objective of this paper is to determine, whether the above-mentioned similarities between accessibility and multi-channel publishing can be put to practical use. In order to do this, two XML-based standards, the International Digital Publishing Forum's "EPUB" (designed for cross-media publication of print documents as electronic books) and "DAISY" (the main standard for the publication of Digital Talking Books accessible for visually impaired people) are compared on a technical level. This includes an analysis of both the external and the internal document structure (i.e. packaging formats of both standards including comprised files, semantic structure of the corresponding XML element sets, navigation, linking and document layout, respectively).

In a second step, it shall be tested to which degree these structural correlations can be used to ease the conversion of e-books in EPUB format to DAISY 3 and vice versa, thus facilitating the integration of accessibility in an XML-based multi-channel publishing process.

## 3. Comparison of EPUB and DAISY - Results

The **Digital Accessible Information SYstem (DAISY)** was developed in 1996 by the Swedish Library of Talking Books and Braille (Talboks- och punktskriftsbiblioteket, TPB 2009), in order to increase the usage of electronic publications by people with print impairments. Originally a proprietary document format, DAISY 3 is now a free, international standard (ANSI/NISO Z39.86), developed, maintained and promoted by the DAISY Consortium (DAISY 2010a). The history of the development of the DAISY standard is described in (Leas, Persoon et. al. 2008, 29). DAISY publications - also known as "Digital Talking Books" or "DAISY DTBs" - are a collection of digital files that provide an accessible representation of printed books for individuals who are blind, visually impaired, or print-disabled. They may contain digital audio recordings of human or synthetic speech, marked up text, and a range of machine-readable files. In contrast to the linear presentation of analogue audio recordings, DAISY DTBs are navigable, searchable, support bookmarking and highlighting. Because all content can be synchronized to audio playback, DAISY DTBs offer a significantly enhanced reading experience not only to print-disabled users, but to learning-disabled readers as well (ANSI/NISO 2005).

There are three basic types of DAISY DTBs: audio-only DTBs (containing mostly audio files and navigation; though further information on document structure, linking information or narrated footnotes may be added), text-only DTBs (comprising the full text and structure of a book, but no audio data; intended for synthetic speech engines or refreshable Braille displays), and DTBs containing both audio and full text, providing the richest reading experience and the greatest level of access (DAISY 2010b).

The **EPUB standard** was developed by the International Digital Publishing Forum (IDPF) in 2007, superseding the older Open eBook Publication Structure (OEBPS; IDPF 2010a). IDPF promotes the development of electronic publishing applications and standards, and of digital publications that are interoperable between disparate EPUB-compliant reading devices and applications (IDPF 2010b). Its members include, amongst others, book, newspaper, journal and magazine publishers, booksellers, software and reading system developers (IDPF 2010c). A founding member of the IDPF is the DAISY Consortium, who is also a leading member in the maintenance of the IDPF Standards (IDPF 2010d). The EPUB content publication standard consists of three specifications, the Open Publication Structure (OPS, describing the representation of its content), the Open Packaging Format (OPF, defining structure and semantics to the electronic publication) and the OEBPS Container Format (OCF, the packaging format that describes the bundling of all EPUB data in one single ZIP archive, IDPF 2010a). Additionally, EPUB uses the Navigation Control File for XML Applications (NCX), which is a part of the DAISY specification, to describe e-book navigation and the table of contents. In exchange, the Open packaging format is reused in DAISY DTBs.

In this section, both standards will be examined in greater detail. The analysis is based on the official specification of both standards in (ANSI/NISO 2005) and (IDPF 2010e), respectively. A schematic representation of both document structures can be seen in Figure 2.

### 3.1 Basic components and main folder

A DAISY DTB is a collection of various XML based, text-only or image data files gathered in one simple, uncompressed document folder (cf. no. [1] in Figure 2). In order to facilitate the transfer of DAISY books via http, this folder may be compressed by ZIP, but it has to be unpacked again for playback purposes. There is no strict specification of file order and sub folder structure, and until now, there is no file extension (like, for instance, *.dtb) associated with DAISY books, although there has been a submission in the DAISY Requirements Gathering forum concerning this issue (DAISY 2008). An EPUB document is also a collection of XML based, text-only or image data files, compressed in one single ZIP archive, whose file extension has to be changed to *.epub. Here, file order and sub folder structure are regulated more strictly than in the DAISY specification, but the files contained therein are, for the most part, quite similar. The first file in the main ZIP container must be a file named 'mimetype', describing the EPUB MIME type ("application/epub+zip") in one simple ASCII string (IDPF 2010f, 18). Next, the container must include a directory named "META-INF" at root level, containing several files describing contents, meta data, signatures, encryption or digital rights. Amongst them, only an XML based file named "container.xml" is man-

datory (l.c., 12), which must identify the MIME type of, and path to, the root file of the publication (cf. no. [2] in Figure 2). The other, optional files that may be included in the "META-INF" sub folder shall not be discussed here. A more detailed description of them may be found in (IDPF 2010f, 12 et seq.).
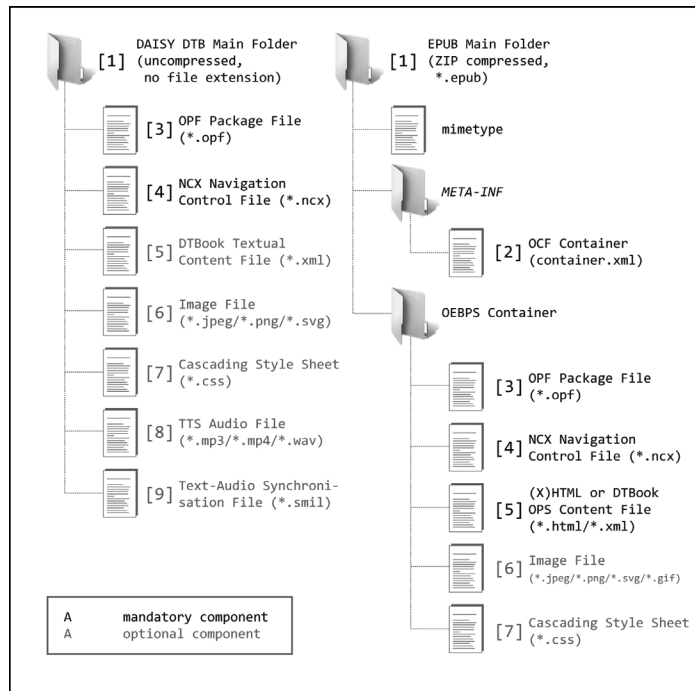


*Figure 2: Comparison of DAISY and EPUB document structure and data formats*

## 3.2 OPF package file

The *Open Packaging Format File (OPF)* is drawn from the IDPF OPF Specification 2.0 (IDPF 2007) and is used by DAISY DTBs and EPUB books alike. In DAISY books, it can be located in the main folder, whereas in EPUB, it has to be placed in an OEBPS sub folder (cf. no. [3] in Figure 2). In both cases, it contains a set of meta data describing the electronic publication, a list (the *manifest*) of the files that make up the electronic book, and a *spine* that defines the default reading order of the document (ANSI/NISO 2005, #OPF). In short, this XML based file contains mainly administrative information about the electronic publication, the files that comprise it, and how these files interrelate (l. c.), which is needed by DAISY and EPUB reading devices for technical reasons.

## 3.3 The navigation control file (NCX)

Whereas the OPF Packaging format is a part of the EPUB standard that was reused in DAISY DTBs, it's just the other way round with the *Navigation Control File for XML Applications* (NCX), which was developed for DAISY DTBs, but which is now used for the same purpose in EPUB books. Again, the location within the document folder is slightly different (cf. no. [4] in Figure 2), but both have the purpose to provide the reader efficient and flexible access to the major structural elements of the document (i.e. part, chapter, or section). Direct access to additional elements such as pages, footnotes, figures, tables, etc. may be included as well in separate, non-hierarchical lists (ANSI/NISO 2005, #NCX). Thus, the NCX file is necessary for the generation of the table of contents and other navigational purposes.

## 3.4 OPS Textual content files (DTBook or XHTML)

The textual content of DAISY DTBs and EPUB books is contained in one or more *textual content files*. While the document structures of both publication standards were so far quite similar, the correlation is more complex in this regard. The Open Publication Structure (OPS) specification (IDPF 2009) defines two "preferred vocabularies" for the description of EPUB document content: XHTML and the XML based *Digital Talking Book*[3] (DTBook) format (cf. no. [5] in Figure 2). DTBook is an XML based document format

---

[3] It might be confusing that both the DAISY textual content file and the complete DAISY book are sometimes referred to as "Digital Talking Book". In this paper, the complete DAISY book will be called a "DAISY DTB", whereas the textual content file and its specification will be referred to as "DTBook".

originally developed to describe the textual content of DAISY books. Thus, e-books in EPUB format might even share content files with DAISY DTBooks, which could certainly ease conversion. At present, EPUB books using DTBook as content format are quite rare, XHTML still being the prevailing format. This is quite unfortunate, as DTBook provides a semantically much richer environment that would be beneficial for e-book production as well.

In the current version 3 of the DAISY standard, DTBook is the only feasible document type for content definition. Earlier versions of the standard used HTML 4.01 strict or XHTML 1.1 (ANSI/NISO 2002, #Dtbookhtm), but this has been changed beginning with DAISY 2.01 (DAISY 1999). The DTBook specification shares 47 element types with (X)HTML, omits 30 others and adds 32 new ones (NLS 2002, #evolution). Some element types shared with (X)HTML may be used to mark up semantic structures important for assistive technology (which are, unfortunately, rarely used in (X)HTML), like abbreviations, acronyms, foreign language expressions (essential for screen readers) and alternative text versions for media content, respectively (l. c., #elementuses). Here, only minor additions were made (for instance producer's notes, providing supplemental information for print-disabled people that were not included in the original printed document; cf. Kerscher 2001).

A large number of new DTBook element types are intended to faithfully and unambiguously preserve the structure of the printed version of an electronic publication (l. c.), describing semantic elements such as front, body and rear matter, sidebars or page numbers (NLS 2002, #elementuses). These elements not only improve citability, but facilitate the production of DTBook documents in a variety of accessible formats (like automatic translation to Braille, large print or "on the fly" rendering by refreshable Braille displays or screen readers; cf. ANSI/NISO 2005, #Text). In (X)HTML, originally developed for the description of hypertext documents rather than for accurate representations of printed books, these mark-ups are dispensable – at least for the usage in a WWW context. For the description of e-books in EPUB format, however, these semantic elements might be advantageous as well.

Another important addition in DTBook are element types that are intended to enhance navigation by using not only hierarchical global navigation targets (e.g. headings, nested chapters, sections, sub-sections, etc.) to access information, but giving immediate access to page numbers, (narrated) footnotes or annotations, respectively (Kerscher 2001). Last but not least, DTBook may contain optional synchronisation information via the smilref attribute for sentence- or word-level synchronization between XML-encoded text and audio files (see below).

### 3.5 Additional files

In addition to the documents listed above, EPUB e-books and DAISY DTBs may contain some optional files as well, for instance image data or presentation styles in *Cascading Style Sheets (CSS)* format (cf. no. [6] and [7] in Figure 2).The META-INF container of EPUB e-books, may contain additional meta data, digital signatures or information on digital rights management (DRM) and encryption (IDPF 2010f, 11 et. seq.). DAISY DTBs may include MP3, MPEG-4 or WAV audio and *Synchronized Multimedia Integration Language (SMIL)* files destined to choreograph the playback of text and audio data (in user agents that support both; cf. no. [8] and [9] in Figure 2). For the purposes discussed here, however, the OPF package file, the NCX navigation control file and the OPS content files are the most important.

## 4. Comparison of EPUB and DAISY - Discussion

Summarizing the results of the previous section, it can be stated that there are some striking similarities between the DAISY and EPUB file formats. Both are open source, non-proprietary, XML based international standards. Though the sub folder structure varies in detail, there are three fundamental analogies: In both cases, the internal document structure is defined in OPF, the navigation is specified in NCX, and the document content *can* be described in both cases by using a DTBook file. Furthermore, presentation styles can be included using CSS, and the handling of image data is also quite similar.

All this being true, some important differences remain. One possible obstacle for a smooth conversion of one format into the other is the optional contents: EPUB books may be encrypted or protected by DRM, DAISY DTBs, in general, are not. In audio-only DAISY DTBs, the textual representation of document content may be omitted - whereas in EPUB e-books with (X)HTML based textual content files, several mark-ups important for accessibility purposes (and included in the DTBook specification) may be missing. In short, a

certain subset of DAISY DTBs and EPUB e-books achieves the highest level of conformity: unencrypted, DRM-free EPUB books and full-text DAISY DTBs, both using DTBook as textual content format. For books in this subset, a joint production of DAISY DTBs and EPUB e-books or an automated conversion of one format into the other might be done with reasonable overhead.

## 5. E-book reader test - Results

This, however, only applies if documents built according to these rules are supported by the respective user agents. Like all XML based mark-up languages, OPF, NCX and DTBook files have to be parsed and rendered for presentation purposes - and just like in (X)HTML, not all rendering engines offer full support for all element types defined in the standard. In general, problems of interpretation arise with uncommon or rarely used document structures. Fortunately, most of the preconditions mentioned above are quite common: unencrypted, DRM-free EPUB e-books can be found on various sites on the web, e. g. (Project Gutenberg 2010), and most sample DTBs published by the DAISY Consortium are either Full Text Full Audio or Text Only (DAISY 2009). Thus, the main issue remaining is the file format used for the textual content document. (X)HTML is a common and proven mark-up language, but several semantic structures important for accessibility purposes are missing. DTBook, on the other hand, supports these element types and is a preferred vocabulary according to the EPUB standard (IDPF 2009), but is still rather uncommon in e-books. Therefore, in this section, it shall be examined if an EPUB using DTBook as textual content file can be parsed and rendered correctly by selected EPUB reading devices.

To answer this question, a sample document was constructed. For this purpose, issue no. 14 of "Streifband", an educational journal for apprentices in publishing companies and the book selling trade, was used. This journal is published once a year by students of Book and Media Production at the Leipzig University of Applied Sciences. Since this journal is also used as an example of multi-channel publishing for educational purposes, the source data was already available in an XML based format (DocBook). This data was converted into DTBook (one file for each article). Subsequently, all other EPUB components (OPF, NCX etc.) were generated and validated automatically by using the so-called DAISY pipeline. This is a cross-platform, open source framework for DTB-related document transformations (DAISY 2010c), using DTBook as pivot format. Launched in 2005 and maintained by the DAISY Consortium, the DAISY pipeline is not only capable of producing, transforming and validating all types of DAISY books, but of generating (X)HTML, LaTeX or EPUB versions of DTBook documents as well.

The sample document generated by the "EPUB Creator" component of DAISY pipeline was then inspected and validated manually by the author to ensure conformance to the EPUB standard. In this step, some minor errors had to be corrected (e. g. a missing namespace attribute in the NCX file, inconsistent naming of Dublin Core user IDs or superfluous text-audio synchronization information that had to be removed). Some changes were made to the CSS style sheet for DTBook documents provided by the DAISY Consortium (DAISY 2010e), in order to permit the display of images (disabled in the default version) or to add some class definitions (for instance to change the font weight of abstracts from regular to bold).

Next, this EPUB sample document was tested on the following hardware e-book readers: Amazon Kindle, Apple iPad, iRex Digital Reader 1000 S, and Sony Reader PRS-505. Of those, only the latter offered native EPUB support. However, both on iPad and iRex, an installation of third-party software (Lexcycle Stanza and FBReader, respectively) was possible. Unfortunately, this was not possible for Amazon Kindle, whose content formats are restricted to Kindle (AZW), TXT, PDF, unprotected MOBI, and PRC, respectively (Amazon 2010).

For the purpose of comparison, some selected software e-book readers - namely Adobe Digital Editions, Lexcycle Stanza, the open source tool FBReader, and a Mozilla Firefox Add-On named EPUB reader - were tested as well. As it turned out, the test results of hardware and software e-readers using the same rendering engines were identical. Therefore, only the Firefox EPUB Reader is listed in Table 1, since its Gecko engine is the only one that is not used in one of the hardware user agents as well. Table 1 gives an overview of the test results. Here, the following markers were used: If all features were supported according to the EPUB specification by the tested user agent, the corresponding cell is marked as "+". If support was missing in a few cases, but existent in most, it is marked as "o", and as "-" if the order was reversed. If the lack of support was such that reading or navigation were impossible altogether, the corresponding cell is marked as "--". Below, the test results will be described in detail.

*Table 1: Results of e-book reader test*

|  | Amazon Kindle | Apple iPad | iRex DR 1000S | Sony Reader PRS-505 | Mozilla Firefox |
|---|---|---|---|---|---|
| **Rendering Engine** | none | Lexcycle Stanza | FBReader (Open Source) | native/Adobe Digital Editions | EPUB Reader (Add-on) |
| **Document and meta data access** | no EPUB support | + | + | + | + |
| **Content rendering** |  | -- | o | o | o |
| **Formatting** |  | not testable | – | o | o |
| **Navigation** |  | o | – | + | o |

## 5.1 Document and meta data access

In a first step, it was tested whether the sample document was accepted as a valid EPUB document and if it could be opened without provoking any error messages. Aside from Amazon Kindle, which has no EPUB support at all, all readers accepted the test document as a valid e-book. Furthermore, meta information on book title and book author could be accessed on any user agent (aside from Kindle).

## 5.2 Content rendering

In the second test stage, it was examined if all document content was displayed by the test candidates (layout and design notwithstanding). Here, unfortunately, another complete failure was to report, because Apple iPad (with Lexcycle Stanza) displayed nothing but blank pages. All other e-book readers visualized standard content elements like headlines, paragraphs etc. more or less correctly - on iRex (with FBReader), even automatic hyphenation was available. DTBook specific element types like producer's notes or bylines (containing information about the author(s) of each journal article) were also displayed correctly - the only exception being iRex, where bylines were omitted. The rendering of images and ordered lists was quite error-prone. iRex and Mozilla Firefox (EPUB Reader) displayed pictures correctly; iPad ignored them. On Sony Reader, image support was unstable: Some pictures were visible, others not, and even the addition of a single blank or tab character could make an image disappear. Furthermore, the presentation of ordered lists was incorrect. Both iRex and Sony Reader implicitly converted them to bulleted lists. Mozilla Firefox identified the list type correctly, but failed at automatic enumeration (all list items having the same number "0"). Thus, each content element (except for the ordered lists) was displayed correctly by at least one of the tested user agents, but unfortunately, none of them was able to render all content as desired.

## 5.3 Formatting

In test stage number three, the presentation style was examined. As was mentioned before, a custom style sheet in CSS format had been used - now it was tested if the sample document was rendered according to its specifications. Since Amazon Kindle and Apple iPad displayed no content at all, they were not included in this step. In iRex (FBReader), custom styles were mostly ignored: Abstracts had "normal" font weight instead of "bold", the black border surrounding producer's notes was missing, and even table data cells were displayed as ordinary paragraphs. Headlines were distinguishable from other block level elements in size and font width, but their styling did not match the specification in the custom style sheet. Thus, most content was presented in a readable way on iRex - but using a styling of its own, not the one specified by the author. In Sony Reader and Mozilla Firefox, the support for custom styles was better. In both cases, most of the content was rendered according to the CSS specification - except for the incorrect display of ordered lists and images that was already mentioned above.

## 5.4 Navigation

In a last step, document navigation was examined. Ironically, this worked quite well on Apple iPad (Lexcycle Stanza), even if there was no content to access: the table of contents was displayed correctly, its main items could be selected, and it was even possible to leaf through the empty pages. Quite the opposite was true for iRex (FBReader), where the presentation of content was acceptable, but only page-by-page navigation (forward and backward) and a return to the begin of the document was possible. The table of contents, however, could not be accessed, the appropriate icon missing in the iRex tool bar. The most flexible navigation was offered by Sony Reader (and Adobe Digital Editions), where all buttons (previous, next, begin of document) and the table of contents worked fine. Navigation support was quite extensive in Mozilla Firefox (EPUB reader) as well - except for one problem with internal links: If a navigation point in the NCX navigation control file aimed at the beginning of a document (i. e. a new article), the link could be followed.

If, however, the navigation point was aimed at a subsection, EPUB Reader jumped to the beginning of the document nonetheless. Thus, only navigation points on the highest level of hierarchy could be accessed.

## 6. E-book reader test - Discussion

In short, the results of the e-book reader test were quite unsatisfactory. Although the test document was built according to EPUB standards, none of the user agents examined was able to render it in an accurate way - though each feature (with the exception of ordered lists) was displayed correctly by at least one of the test candidates.

A possible explanation for the effects described above is a limited XML/CSS support. Following the principle to separate content and presentation, (X)HTML and XML files should describe document content and structure only, whereas all information on typography, colours, layout etc. should be defined using cascading style sheets. The respective user agents (web browsers, e-book readers etc.) then have to re-combine these descriptions for presentation. Originally developed for web design purposes, CSS is quite a reliable way to style (X)HTML documents. For XML based documents like DTBook, however, some limitations in native CSS support remain. One important difference between (X)HTML and XML in relation to CSS is that most user agents have a default rendering of (X)HTML documents implemented even if no custom style sheet is defined. This, however, is not always the case for XML documents - which might explain the completely empty document on Apple iPod (Lexcycle Stanza).

Limited support of custom CSS by Stanza is a known issue (Lexcycle 2009); in general, Stanza intentionally overrides them and uses styles of its own. If, however, such default styles were only defined for (X)HTML, documents using the XML based DTBook format can not be rendered at all. As for iRex (FBReader), missing support for custom style sheets is even conceded by the FBReader online documentation (FBReader n.d.). Contrary to Stanza, unknown semantic elements are not ignored by FBReader, but rendered as standard paragraphs. Thus, the appearance of DTBook specific element types is quite uniform - but at least it is possible to access them at all.

A limited XML/CSS support might also explain the image display problems on Sony Reader. To display graphics, the style sheet supplied by the DAISY consortium uses both the CSS "img:before" pseudo element and the "content:url()" property. The support of this pseudo element has been limited for quite some time - even the Microsoft Internet Explorer introduced it only in version 8 (Microsoft 2010). It is probable that the support of this feature is still an issue on the Sony Reader, because images were visible on some occasions, but on others not. For (X)HTML based content, however, native image support seems to be implemented, as images in (X)HTML based EPUB books are displayed reliably. Furthermore, the linking problems in Mozilla Firefox' EPUB Reader might be due to a limited XLink support. For the definition of links, XML uses the XML Linking Language (XLink), which is more powerful but also more complex than the linking model used in (X)HTML. Because of its complexity, only so-called "simple links" are yet fully implemented by Firefox' rendering engine (Mozilla 2009). Links to subsections of the document, however, are considered as "extended links". Again, the (X)HTML linking mechanism is different, so that internal links in (X)HTML based EPUB books work fine.

## 7. Conclusions

Accessibility and multi-channel publishing: the comparison of these concepts showed that structural and technical requirements for the production of accessible material and cross media publishing are indeed quite similar. In both cases, the usage of XML-based mark-up languages and open standards (XHTML, DTBook, NCX, CSS) and the separation of content, structure and presentation turned out to be important principles. Consequently, some obvious structural correlations of document structures could be found: DAISY and EPUB share many structural and semantic properties (container structure, main content document format, navigation control file, etc.) that might ease both the joint creation of both document formats and the conversion of one format into another. Unfortunately, the support of DTBook based EPUB books, which would be an ideal source format for the conversion in the accessible DAISY format, is still very limited: none of the e-book readers tested here was able to render the whole sample document according to specification. Whereas the document structures seem to be adequate for a merging of accessibility and multi-channel publishing, there is still room for improvement concerning the applications responsible for interpretation and presentation of those document formats.

Once again, a technical solution is discovered, but the problem is not yet fixed[4]. Nonetheless, the production of accessible documents was probably never easier and the additional effort necessary never lower than in a cross media publishing environment. Some institutions have already taken the opportunity to improve information access for handicapped users: The American Physical Society, for instance, is planning to publish all its scientific journals in accessible formats (Gardner & Kelly 2010), DAISY support can be added to Microsoft and Open Office (Microsoft 2008, Spiewak, Strobbe & Engelen 2010), and there is a prototypic DSpace extension that would make open access repositories accessible to disabled end users (Ribera 2010). It would be desirable that others soon follow these examples.

## Acknowledgements

## References

Amazon.com Inc. (2010). *Kindle Wireless Reading Device*. Retrieved 2010-07-06
from: http://www.amazon.com/Kindle-Wireless-Reading-Display-Generation/dp/B0015T963C

American National Standards Institute (2002). *Specifications for the Digital Talking Book, Release 2002*.
Retrieved 2010-07-02 from: http://www.niso.org/workrooms/daisy/Z39-86-2002.html#Dtbookhtm

American National Standards Institute (2005). *Specifications for the Digital Talking Book*.
Retrieved 2010-06-10 from: http://www.niso.org/workrooms/daisy/Z39-86-2005.html

Bosak, Jon (1998). *Media-Independent Publishing: Four Myths about XML*. In: Computer 10 (31), pages 120 -122

Canadian National Institute for the Blind (2009). *About the CNIB Library*.
Retrieved 2010-02-09 from: http://www.cnib.ca/en/services/library/about/Default.aspx

DAISY Consortium (1999). *DAISY 2.01 Specification*.
Retrieved 2010-07-02 from: http://www.daisy.org/daisy201.html

DAISY Consortium (2008). *DAISY Requirement Submission: ZIP archive as directly supported DTB package format*. Retrieved 2010-06-29 from: http://www.daisy.org/z3986-requirements-detail?i=56

DAISY Consortium (2009). *Sample Content*. Retrieved 2010-07-02 from: http://www.daisy.org/sample-content

DAISY Consortium (2010a). *About the DAISY Consortium*.
Retrieved 2010-06-22 from: http://www.daisy.org/about-us/

DAISY Consortium (2010b). *DAISY Technology. What is a DTB?*
Retrieved 2010-06-22 from: http://www.daisy.org/dtbooks/

DAISY Consortium (2010c). *DAISY Pipeline: DTB-related Document Transformations*.
Retrieved 2010-07-06 from: http://www.daisy.org/pipeline

DAISY Consortium (2010e). *DAISY/NISO Standard DTD and CSS files*.
Retrieved 2010-07-06 from: http://www.daisy.org/daisyniso-standard-dtd-and-css-files

Dick, Wayne / Golshani, Forouzan (2008). *An Accessible Lane on the Information Superhighway*.
In: IEEE Multimedia 4 (15), pages 22 - 26

Dittmer, Elke (2007). *11 Jahre DAISY Consortium - Gemeinsam die Zukunft gestalten*.
Retrieved 2010-02-09 from: http://www.dzb.de/aktuelles/veranstaltungen/daisyday_dittmer.html

Eberius, Wolfram & Haffner, Alexander (2010). *Multimodal enhancements and distribution of DAISY-books*.
In: Proceedings of the DAISY 2009 International Technical Conference, Leipzig, pages 36 - 41

FBReader Documentation (n.d.). *Electronic Book Formats (supported and unsupported)*.
Retrieved 2010-07-07 from: http://www.fbreader.org/docs/formats.php

Gardner, John A. / Kelly, Robert A. (2010). *Scientific journals go DAISY*.
In: Proceedings of the DAISY 2009 International Technical Conference, Leipzig, pages 62 - 66

German Basic Law (2002). *Grundgesetz für die Bundesrepublik Deutschland,
zuletzt geändert durch das Änderungsgesetz vom 26. Juli 2002*. München: DTV-Beck

---

[4] Significantly, analyses of the built-in accessibility functions of Adobe Acrobat and Macromedia (now Adobe) Flash and Director provided similar results (Nikolaus & Dobroschke 2010, Nikolaus 2005).

International Digital Publishing Forum (2007). *IDPF Open Packaging Format (OPF) 2.0 1.0. Recommended Specification*. Retrieved 2010-07-01 from: http://www.openebook.org/2007/opf/OPF_2.0_final_spec.html

International Digital Publishing Forum (2009). *IDPF Open Publication Structure (OPS) 2.0 Recommended Specification September 11, 2007*. Retrieved 2010-07-02 from: http://www.idpf.org/2007/ops/ops2.0/download/

International Digital Publishing Forum (2010a). *International Digital Publishing Forum (formerly Open eBook Forum)*. Retrieved 2010-06-22 from: http://www.idpf.org/

International Digital Publishing Forum (2010b). *International Digital Publishing Forum: About*. Retrieved 2010-06-29 from: http://www.idpf.org/about.htm

International Digital Publishing Forum (2010c). *IDPF Membership: Current Members*. Retrieved 2010-06-29 from: http://www.idpf.org/membership/currentmembers.asp

International Digital Publishing Forum (2010d). *IDPF Groups: EPUB Standards Maintenance Working Group*. Retrieved 2010-06-29 from: http://www.idpf.org/idpf_groups/epubmaint.htm

International Digital Publishing Forum (2010e). *IDPF Specifications*. Retrieved 2010-06-28 from: http://www.idpf.org/specs.htm

International Digital Publishing Forum (2010f). *IDPF Specifications: Open Container Format (OCF) v 2.01*. Retrieved 2010-07-01 from: http://www.idpf.org/doc_library/epub/OCF_2.0.1_draft.doc

Kerscher, George (2001). *Theory Behind the DTBook DTD*. Retrieved 2010-07-08 from: http://data.daisy.org/publications/docs/theory_dtbook/theory_dtbook.html?q=publications/docs/theory_dtbook/theory_dtbook.html

Leas, Dennis; Persoon, Emilia; Soiffer, Neil & Zacherle, Michael (2008). *DAISY 3: A Standard for Accessible Multimedia Books*. In: IEEE Multimedia 4 (15), pages 28 - 37

Lexcycle Forums (2009). *Is there a list of CSS/ePub features/tags that iPhone Stanza does/doesn't support?* Retrieved 2010-07-07 from: http://www.lexcycle.com/node/1625

Microsoft Corporation (2008). *Microsoft, DAISY Make Reading Easier for People With Print Disabilities*. Retrieved 2010-07-08 from: http://www.microsoft.com/presspass/press/2008/may08/05-07SaveAsDAISYPR.mspx

Microsoft Corporation (2010). *CSS Improvements in Internet Explorer 8*. Retrieved 2010-07-07 from: http://msdn.microsoft.com/en-us/library/cc304082%28VS.85%29.aspx

Mozilla Developer Center (2009). *XLink support*. Retrieved 2010-07-07 from: https://developer.mozilla.org/en/XLink

National Library Service for the Blind and Physically Handicapped (NLS) (2002). *Digital Talking Book Expanded Document Type Definition Documentation for Version V110*. Retrieved 2010-07-02 from: http://www.loc.gov/nls/z3986/v100/dtbook110doc.htm

Nikolaus, Ulrich (2005). *Barrierefreies Authoring. Entwicklung barrierefreier Anwendungen mit grafischen Entwicklungswerzeugen*. In: Information Management & Consulting 20 (3), pages 3 - 20

Nikolaus, Ulrich & Dobroschke, Julia (2010). *Automatic conversion of PDF-based, layout-oriented typesetting data to DAISY: potentials and limitations*. In: Proceedings of the DAISY 2009 International Technical Conference, Leipzig, pages 115 – 127. URN: http://nbn-resolving.de/urn:nbn:de:bsz:14-qucosa-38042

Project Gutenberg (2010). *Project Gutenberg, the first producer of free electronic books (ebooks). Main Page*. Retrieved 2010-07-07 from: http://www.gutenberg.org/wiki/Main_Page

Ribera Turró, Mireia (2008). *Are PDF Documents Accessible?* In: Information technology and libraries 3 (27), pages 25 - 43

Ribera Turró, Mireia (2010). *Open repositories made accessible through XML transformations*. In: Proceedings of the DAISY 2009 International Technical Conference, Leipzig, pages 135 - 140

Scherrer, Yvonne Seraphine (2010). *First professional workstation for the visual impaired at DRS1*. In: Proceedings of the DAISY 2009 International Technical Conference, Leipzig, pages 141 - 142

Spiewak, Vincent; Strobbe, Christophe & Engelen, Jan (2010). *ODT2DAISY: Authoring full DAISY books with OpenOffice.org*. In: Proceedings of the DAISY 2009 International Technical Conference, Leipzig, pages 149 - 154

Talboks- och punktskriftsbiblioteket (Swedish Library of Talking Books and Braille) (2009). *History of DAISY*. Retrieved 2010-06-22 from: http://www.tpb.se/english/talking_books/history_

# Using consumer preferences in setting the target for product development

*Maiju Aikala[1], Mari Ojanen[2], Kaisa Vehmas[1]*

[1] VTT Technical Research Centre of Finland, P.O.Box 1000, FIN-02044 VTT, Finland
  E-mails: maiju.aikala@vtt.fi, kaisa.vehmas@vtt.fi

[2] Kemira Oyj, P.O.Box 44, 02271 Espoo, Finland
  E-mail: mari.ojanen@kemira.com

**Abstract**

The objective of the study was to identify the required and attractive properties of silk coated papers in the end user point of view. The linking of end use evaluations with paper characteristics through sensory properties was also studied. The target was to find out how paper could be developed in order to differentiate positively from competitors within the silk coated paper grade.

The differences between the depths of the mental impressions could be estimated quite well using visual and tactile sensory panels in the laboratory scale. Thus, when the target of the impressions is defined, less time consuming panel evaluations can be used to verify, if the target is achieved.

**Keywords:** mental impression; perceived quality; tactile; visual

## 1. Introduction

The need for market-driven product development in the paper industry has been realized. Traditionally, the product development in paper industry has focused on the production process and improving the existing products at competitive prices. However, the reason behind most of the unsuccessful product development projects has been the gap between product properties and the needs and expectations of the market. (Jokinen and Heinonen, 1987) The efforts to change the development strategies from product-oriented to customer-oriented have only recently intensified in response to global competition, market consolidation, overcapacity, price weakness and new technologies. (Lail, 2003)

Printing paper marketing is a typical example of business-to-business marketing. Although the decisions on the paper selection are made by the publisher or the advertiser, the final user is consumer - the reader. Thus, the preferences of the consumers are of the utmost importance also in paper development.

The objective of the study was to identify the required and attractive properties of silk coated papers in the end user point of view. The relationships between end use evaluations and sensory properties were also studied. The target was to find out how paper could be developed in order to differentiate positively from competitors within the silk coated paper grade.

## 2. Methods

Seven silk coated papers were studied. Papers were printed and the visual and tactile profiles of the papers were conducted. The visual and tactile properties of the papers were evaluated by using sensory evaluation panels with 11 panellists. The visual panel was a panel of experts and the touch and feel panel was a trained evaluation panel. End user studies were carried out both with the professionals in print product's value chain and with the consumers.

The printing trials were carried out at KCL, Finland on sheet-fed offset press 4-unit Roland Favorit RVF. Two different layouts were used. KCL standard layout (Figure 1) was used for evaluation the visual and tactile properties. The layout for end use evaluations (Figure 2) included elements of the products where silk coated papers are typically used: customer magazine, advertising leaflet and other high quality images. During the printing trials the speed of the printing machine was 5000 sheets / hour. The colour order was KCMY. Target density for black was 1.90, for cyan 1.55, magenta 1.20 and yellow 1.20. Fountain solution included 2 % of Vegra VP 546 additive and 10 % of IPA (isopropyl alcohol). The printing hall temperature was 21 °C and humidity 45 %.
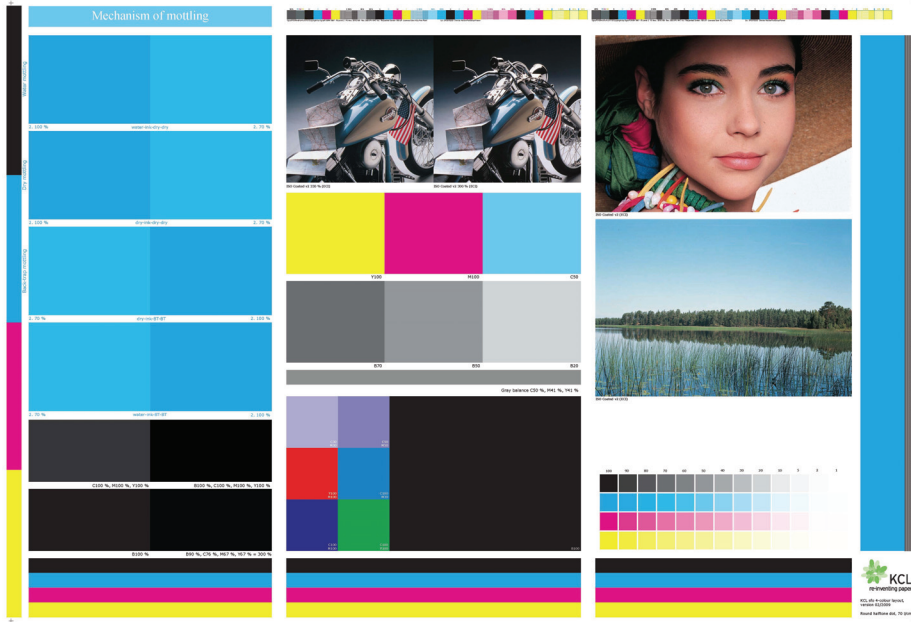
*Figure 1: KCL standard layout for sensory evaluations*



*Figure 2: Layout for end use evaluations*

VTT Touch and feel panel (11 panelists) evaluated the **feel of roughness**, **stickiness**, and **silky feeling** of unprinted and printed samples (KCL standard layout: B100 field). The definitions of the tested touch and feel attributes are presented in the Table 1.

*Table 1: Definitions of the touch and feel attributes*

| Attribute | Definition |
|---|---|
| ROUGHNESS | - amount of grainy particles on the surface |
| Smooth - Rough | - lack of smoothness |
| STICKINESS | - adhesive |
| Unsticky - Sticky | - waxy |
| SILKY FEELING | - soft |
| Unsilky - Silky | - unsticky |
|  | - fingers glide softly |

VTT Visual panel (11 panelists) evaluated the **visual unevenness**, **gloss difference** between unprinted and printed area, and **colorfulness** of the samples. The evaluated fields are presented in the Table 2. Open questions concerning the samples were presented and they are listed in the Table 2.

*Table 2: Visually evaluated attribute*

| Attribute | Field in KCL standard layout | Open questions |
|---|---|---|
| VISUAL UNEVENNESS<br>Even - Uneven | B90%, C76%, M67%, Y67% = 300% | - Which is dominating: gloss unevenness or mottling?<br>- Is the unevenness disturbing? |
| GLOSS DIFFERENCE<br>Small difference - Large difference | B90%, C76%, M67%, Y67% = 300% | - Has the sample low quality?<br>- How? |
| COLORFULNESS<br>Pale - Strong colors | | - Has the sample low quality?<br>- How? |

Both panels used numerical category scale, where the panelist placed the extremes on the beginning and on the end of the scale, and the rest of the samples between the extremes. The distance between the samples correlates with the degree of difference. For example, when the roughness perception was evaluated, the panelists placed the smoothest sample to 0 and the roughest to the other end of scale. Then they placed rest of the samples between the smoothest and roughest ones. The panelists were also encouraged to comment the samples in their own words.

The result of the touch and feel evaluation is the mean of the panelists' evaluations. The significance of difference between papers is estimated by calculating Least Significant Difference (LSD-value). LSD-value is calculated with following equation (Meilgaard, 1999):

$$LSD = t_{\alpha/2, df_E} \sqrt{2MS_E / b}$$

(1)

where:

$t_{\alpha/2, df_E}$ is the upper-$\alpha/2$ critical value of t-distribution with $df_E$ degrees of freedom,

$MS_E$ is the mean square of error from the ANOVA table and

$b$ is number of panelists.

If the mean evaluations between samples differ more than the LSD-value, then the difference between the samples is statistically significant. More information about the touch and feel analysis is available e.g. in (Aikala et al. 2003), (Forsell et al. 2004) and (Aikala and Seisto 2009).

The samples were also characterized with laboratory measurements. The measurements are listed in Appendix 1.

End use evaluations included interviews in print product's value network and consumer focus groups. In the value network the interviewees represented professionals in advertising agencies, customer magazine publishers and printing houses (altogether 12 interviewees). Two consumer focus group interviews were conducted. A semi-structured interviewing method was used. 'Semi-structured' means that the interviewing themes were set beforehand for all interviews, although the actual questions and their order had variations.

## 3. Results

### 3.1 Interviews

In the end-user interviews it could be noted that silk papers caused a wide variation of mental impressions. Silky feeling of the paper was described to be pleasant, warm, soft, smooth, slippery, non sticky, sophisticated. Paper is used to give an impression on the product's quality: high quality paper – high quality product. In the interviews the professionals in publishing and advertising business considered paper through its functionality. The visual impression was the most critical perceptual property of printed products. Paper should be pleasant to eyes; it should have good readability. Visual evenness is a prerequisite for good visual appearance. According to the professionals a certain threshold of acceptance of the visual quality needs to be exceeded before other senses can play any role.

For consumers high quality meant good color rendering, low tendency to wrinkles, slightly thicker paper, soft and glossy, high opacity and easy to leaf through. One of the drawbacks of silk papers was the finger prints. Finger prints were left on silk papers rather easily and they were also visible. The consumers paid more attention to the overall impressions instead of concentrating on one sense at the time. The visual properties naturally played an important role; however, the consumers let different senses compensate more each other than the professionals. For example, one sample *"felt so pleasant that the finger prints didn't disturb."*

## 3.2 Visual evaluations

The sensory evaluation method used forces the samples on the scale from 0 to 100 in spite of the strength of the perceived differences between the samples. The large error bars in the gloss difference and colorfulness as well as rather small difference between the maximum and minimum indicate that the visual differences between the samples were rather small, especially in visual gloss difference between printed and unprinted area and colorfulness (Figure 3). However, the samples could be differentiated based on their visual unevenness. Visual unevenness was highly affected by the gloss unevenness. The results also indicated that especially higher paper gloss increased the impression of the unevenness of the print quality.
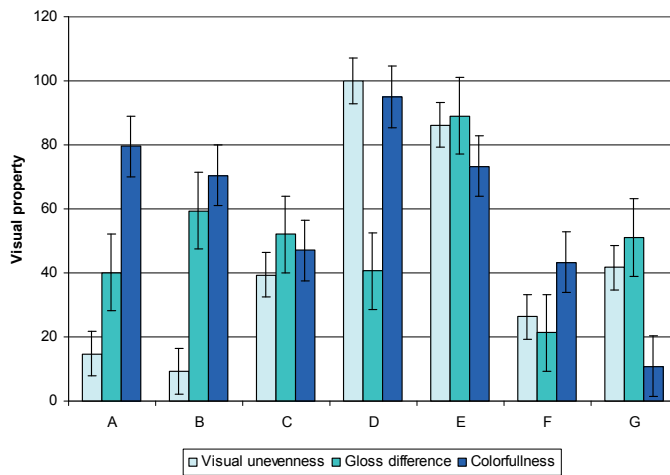


*Figure 1: Differences between the tested papers A-G based on their visual properties*

In the end user interviews the professionals in the print product's value network mentioned the surface evenness and pictures that stand out as the most relevant visual properties. Figure 4 shows how the evaluations of the visual panel (bars) correspond to the mental impression of evenness of surface (triangles). The samples have been ranged from left to right based on the panel evaluation of visual evenness. The results indicate that the visual evenness can be reliably evaluated with the visual panel in laboratory conditions. However, the standing out pictures does not correlate with any of the evaluated visual property. This could be due to the small differences between the samples, and thus the panel did not have a consensus in detecting them.
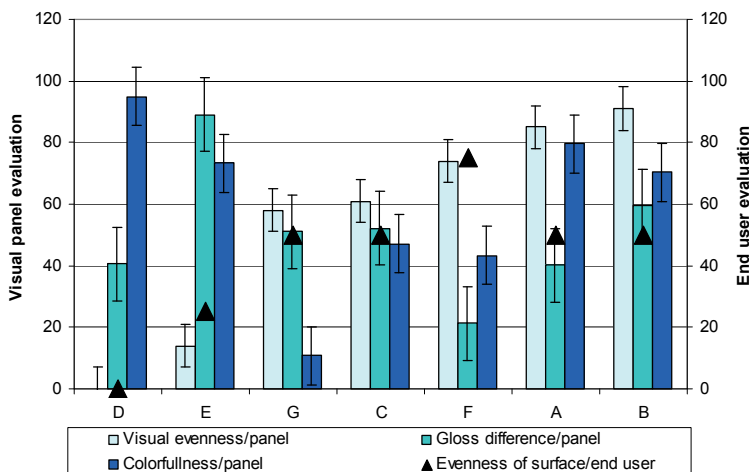


*Figure 2: Relationships between the mental impression of evenness of surface and subjective visual evaluations. The order of the samples is based on the visual evenness evaluated by the visual panel*

### 3.3 Touch and feel evaluations

The results of panel evaluation of the tactile properties are shown in Figure 5 and in Appendix 1. Correlation analysis indicated that the evaluation of silky feeling is dominated by the feel of smoothness. Also feel of stickiness has an impact in the silky feeling, as we can see from the tactile profile of sample G. It felt smooth but also sticky, and thus, less silky than e.g. samples A and F. The paper surface should be smooth enough to emphasize the silky feeling but not too strongly calendered to give glossy, plastic like appearance. It should be kept in mind that the differences between the samples were quite small, for example, it was mentioned that *"only the samples D and E were rough"*.
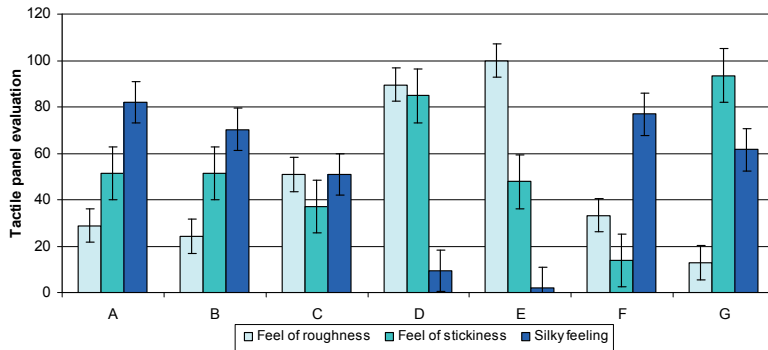


*Figure 5: The tactile properties of tested paper samples A-G*

Figure 6 shows the relationships between the soft and silky impressions mentioned in end user interviews (triangles and dots) with the tactile properties evaluated by the trained testing panel (bars). The order of the samples is based on the feel of smoothness evaluated by the tactile panel. In consumer interviews mental impressions *soft* and *silky* were mostly linked with the sample F. The feel of roughness and feel of stickiness of sample F were evaluated as low. Samples D and E couldn't be linked with neither silky nor soft impression according to the consumers. The feel of roughness and the feel of stickiness were evaluated rather high for both of these samples. The results indicate that the mental impressions of softness and silkiness can be estimated by using the trained testing panel. It also looks like the feel of roughness has the dominant effect on the silky and soft image. Feel of stickiness also plays a role, but the effect is not linear.
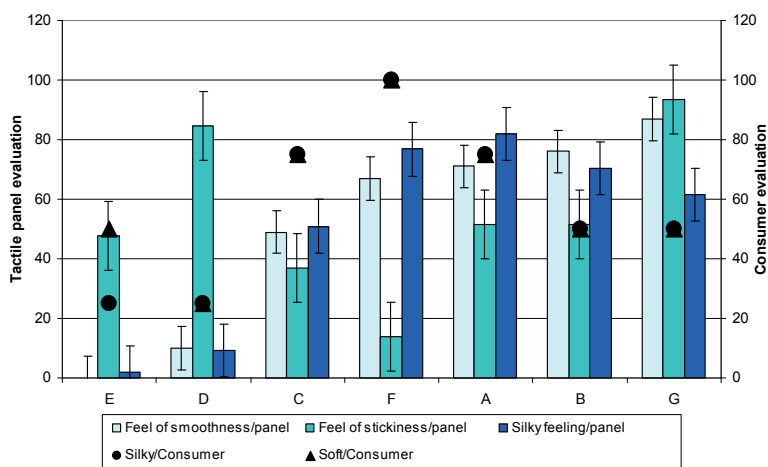


*Figure 6: Relationships between the mental impressions and subjective tactile evaluations. The order of the samples is based on the feel of smoothness evaluated by the trained tactile panel*

### 4. Discussion

Although the product development strategy in paper industry has started to move from product-oriented to customer-oriented, it is still a fact that paper properties are usually defined using certain technical parameters and their specifications. (Jernström, Haarla 2003) When paper is selected for a specific end product, technical parameters play a minor role. They are important for predicting the functioning of the paper in the processes,

but customer's satisfaction never rises above the neutral no matter how functional the paper becomes. Thus, it is quite evident that the concentration on improving the technical parameters is not enough. It is necessary to identify the relationships between the impressions related to the paper and measurable paper properties, and how to utilize them in brand building. (Haarla 2000, Aikala)

The results strengthen the assumption that the paper property and print quality measurements do not tell the whole truth about the samples. Based on the interview data, the tested samples can be divided into three groups: 1) 'Above average' including samples A, C and F, 2) 'Average' including samples B and G, and 3) 'Below average' with samples D and E. Roughly the same groups can be detected from the sensory data. On the other hand, the same groups cannot be detected from the laboratory measurements. The similar behaviour, i.e. the differences in tactile properties cannot be solely explained with laboratory measurements, has been earlier detected in several cases. (Aikala et al. 2003, Aikala et al. 2009b, Forsell et al., Vihavainen)

In this study, the sensory evaluations of trained testing panel correlated very well with the selected mental impressions mentioned in the end user interviews. However, it should be kept in mind that at this point the mental impressions were not measured but estimated from the interview data.

## 5. Conclusions

The objective of the study was to identify the required and attractive properties of silk coated papers in the end user point of view. The target was to find out how paper could be developed in order to differentiate positively from competitors within the silk coated paper grade.

The interviews in the print product's value network show that silk coated papers gives the message of high quality, sophisticated products. Following expressions were used to describe silky feeling: pleasant, warm, gentle, soft, smooth, slippery, non sticky. The professionals in the print products' value network pay more attention to the visual perception than to other senses. If the product is visually acceptable, also other senses can affect the overall perception. The consumers use different senses more equally, and thus, different senses can complement one another.

The differences between the magnitudes of the mental impressions could be estimated to some extent using visual and tactile sensory panels in the laboratory scale. Thus, when the target for the impressions is set, less time consuming panel evaluations can be used to verify, if the target is achieved. This is very important because the laboratory measurements do not solely explain the differences between the samples.

## References

Aikala, M., (2009), *Quality space of the magazine - A methodological approach to customer requirements as a driver for product development. Doctoral Thesis, Helsinki University of Technology, Department of Forest Products Technology. KCL Communications 14, 117 p.*

Aikala, M., Nieminen, S., Poropudas, L. & Seisto, A., (2003), *The end user aspects in print product development. 30th IARIGAI Conference, 7-10 September, 2003, Dubrovnik, Croatia, 11 p.*

Aikala, M. & Seisto, A., (2009), *Tactile quality. Print Media - Principles, Processes and Quality. P. Oittinen and H. Saarelma (ed.) Fapet Oy, pp. 355-371.*

Aikala, M., Seisto, A &. Vaittinen, H., (2009)*, Beyond traditional measurements - getting closer to the end user with a touch and feel method. PTS Coating Symposium, 22-24 September, 2009, Baden-Baden, Germany, pp. 31-1 - 31-2.*

Forsell, M., Aikala, M., Seisto A. & Nieminen, S., (2004), *End users' perception of printed products. PulPaper Conference, 1-3 June, 2004, Helsinki, Finland, 6 p.*

Haarla, A., (2000), Printing and writing papers. Paper and Board Grades. H. Paulapuro (ed.), Fapet Oy, pp. 14-53.

Haarla, A., (2003), *Product differentiation: Does it provide competitive advantage for a printing paper company? Doctoral Thesis, Helsinki University of Technology, Laboratory of Paper Technology, Reports, Series A17, 227 p.*

Jernström, E., (2000), *Assessing the technical competitiveness of printing paper. Doctoral Thesis, Acta Universitatis Lappeenrantaensis 95, Lappeenranta University of Technology, 156 p.*

Jokinen, A. & Heinonen, J., (1987) *Tutkimus ja tuotekehitys yritysjohdon työvälineenä paperiteollisuudessa. Tekes Teollisuussihteeriraportti 17/1987, 22 p.*

Lail, P. W., (2003), *Supply chain best practices for pulp and paper industry. TAPPI Press, Atlanta, 191 p.*

Meilgaard, M., Civille, G. V. & Carr, B. T., (1999), *Sensory Evaluation Techniques, 3rd ed., CRC Press, Boca Raton, p. 291.*

Vihavainen, S., (2004), *Measurement of perceived quality - Data analysis of quality assessments and measurable properties of paper. Master's Thesis, Tampere University of Technology, Department of Automation, 65 p.*

## Appendix 1

Summary of the results

| MEASUREMENT | Unit | Method | A | B | C | D | E | F | G |
|---|---|---|---|---|---|---|---|---|---|
| CIE Whiteness D65 | | ISO 11475 | 126,5 | 125,6 | 125,6 | 125,2 | 122,2 | 125,0 | 140,1 |
| Paper Gloss | % | ISO 8254-1 | 26,6 | 23,2 | 19,2 | 50,5 | 29,6 | 21,9 | 47,2 |
| PPS Roughness | $\mu$m | ISO 8791-4 | 1,22 | 1,25 | 1,50 | 2,01 | 2,31 | 1,24 | 1,16 |
| $\Delta$Gloss | % | | 46,6 | 49,2 | 50,0 | 26,1 | 41,8 | 37,5 | 35,2 |
| Relative contrast | | | 0,25 | 0,24 | 0,27 | 0,35 | 0,32 | 0,37 | 0,23 |
| Mottling value, BT C70 | | PapEye | 3,7 | 3,87 | 3,72 | 3,73 | 4,07 | 3,73 | 3,73 |
| SENSORY EVALUATIONS | | | | | | | | | |
| Feel of roughness (unprinted) | | | 18 | 32 | 63 | 80 | 94 | 28 | 1 |
| Feel of roughness (printed) | | | 29 | 24 | 51 | 90 | 100 | 33 | 13 |
| Feel of stickiness (unprinted) | | | 73 | 62 | 31 | 61 | 40 | 3 | 82 |
| Feel of stickiness (printed) | | | 51 | 51 | 37 | 85 | 48 | 14 | 94 |
| Silky feeling (unprinted) | | | 75 | 61 | 48 | 19 | 0 | 92 | 82 |
| Silky feeling (printed) | | | 82 | 70 | 51 | 9 | 2 | 77 | 62 |
| Visual unevenness | | | 15 | 9 | 39 | 100 | 86 | 26 | 42 |
| Visual gloss difference | | | 40 | 59 | 52 | 41 | 89 | 21 | 51 |
| Visual colourfullness | | | 80 | 70 | 47 | 95 | 73 | 43 | 11 |
| INTERVIEWS* | | | | | | | | | |
| Soft | | | + | 0 | + | - | 0 | ++ | 0 |
| Silky | | | + | 0 | + | - | - | ++ | 0 |
| Velvety | | | + | 0 | 0 | - | + | 0 | 0 |
| Evenness of surface | | | 0 | 0 | 0 | -- | - | + | 0 |
| Pictures stand out | | | + | 0 | 0 | ++ | + | ++ | 0 |

* 0 denotes average level, ++ clearly above average level and -- clearly below average level.

# Communication within the value chain of paper-print: visual perception and colour management on commercial publication paper grades

*Luc Lanat*

Stora Enso Publication Paper, Corbehem mill
Rue de Corbehem, F-62117 Brebrieres, France
E-mail: luc.lanat@storaenso.com

### Abstract

Paper and forest products are renewable, recyclable, sustainable, and bring emotions to end-user. Emotions and quality images are linked. This topic motivates active research.

In Communication within the value chain paper-printing, several misunderstandings appear:
* Misunderstandings due to differences between printing equipments and papermaking equipments.
* Misunderstandings due to differences in lighting conditions between papermakers and printers.
* Misunderstandings between colour management prepress specifications and visual perception of white paper colour by itself.
* Misunderstandings on printing relevant properties. Which paper properties are relevant for paper during printing?
* Misunderstandings motivated by different interests between stakeholders: printing machine suppliers, papermakers suppliers, materials and software suppliers.

To clarify these misunderstandings, main conclusions of this paper are:
* Perception of paper whiteness, evaluated visually through panels indoor, but close to Nordic daylight showed that Whiteness measurement is superior to Brightness.
* Printing at constant target density, colour gamut, calculated as per C* sum reported in literature earlier, gave deceiving results. It is suggested that PPS roughness, although primitive, is more distinctive than shade references to select the right colour management profile, mainly linked to a paper type.
Definitely, further work is here needed to come to any conclusion on Colour Gamut potential.
* Colour Gamut discussions should integrate data made available by papermakers, as described in ISO NWI 15397 proposed standard and also detailed in this paper. Papermakers of Paperdam working group agreed to make available paper white point and publicly available characterization data to be used with their grades to their best knowledge. This is not a guarantee for "conformance" or "standardized printing", but of course it is a preferred starting point and should bring printing consistency.
* To reach targeted colours, ISO specified paper colour targets do not cover all market conditions. There is a clear need for evaluation of paper white point as a colour for best colour management calculations and avoid colour shifts versus targets.

**Keywords**: quality; paper; printing; colour gamut; whiteness

## 1. Introduction

Nowadays, paper and thus papermaker's efforts must concentrate on what they do best: offering emotions and images of quality to the end-user. Emotions and quality images are linked. This topic motivates active research.

We showed in a previous paper (Kolseth, Lanat, Sävborg, 2009) the importance of paper optics and equipments in printing evaluations and also how optical dot gain, because intrinsic paper property, could introduce incorrect dot gain evaluations in Sheet Fed Offset.

In another unpublished internal study, we verified the influence of Stora Enso Press Selection paper grades on Colour Gamut in the a* and b* plane  on samples printed in rotogravure. Results were in line with usual paper classification. The ranking, namely from low to high colour gamut in the a* and b* plane was: Improved News 52 gsm, White Improved News 55 gsm, SC B 56, SC A 56 gsm, SC A+ 56 gsm, SC A ++ 54 gsm, LWC 54 gsm, LWC 57 gsm, LWC + 70 gsm. This ranking was close to L* coordinate ranking and encouraged us to study further the a* and b* plane, as an approach to colour gamut evaluation.

We present here internal studies on:
* Paper whiteness and perception evaluated through panels.
* Colour Gamut of commercial papers both in Heat Set Web Offset and Gravure printing through specific but reproducible and consistent printing trials.

Also, this paper is motivated by developments of Standardization within ISO TC 130 (Printing) and TC 6 (Paper). A list of print relevant paper properties was published recently by VDMA Germany and by virtually all printing market players. (Papierkennwerte/Characteristic paper values, 2009). As a follow up, ISO WD 15397 "Communication of optical and surface properties of printing substrates - Graphic papers for rotogravure, heat-set web offset, offset sheets, proofing" is in development.

The objective of this paper is three-fold:
* To contribute to use in the market and within mills optical paper measurements which match visual perception with human eye in usual home-office conditions.
* To contribute to develop methods to quantify paper performance when evaluating colour coordinates of the CMY-RGB hexagon.
* To give ground and encourage further standardization developments.


## 2. Methods

### 2.1 Visual panel for paper whiteness perception

We asked a group of 12 experienced people to rank a set of papers from the markets from Improved News up to WFC (Wood Free Coated) (Jordan, O'Neill 1991). The test was operated in Falun mid-Sweden indoor but behind a window under noon overcast Nordic daylight. We compared this ranking with several available optical laboratory properties (Brightness D65, C Brightness, Whiteness, Colour L*, a*, b*.

### 2.2 Equipments

We used an Elrepho spherical spectrophotometer (d/0°), available in paper industry and i-one X-Rite angular spectrophotomer (45°/0°) used in graphic industry for printing evaluations. Elrepho is classical equipment for papermakers, and allows to follow deviations due to UV content. Routines are available to measure Colour L*, a*, b* D50, with the UV calibration of C illuminant. See ISO 5631-3.

### 2.3 Colour Management and Colour Gamut calculation

Colour rendering is an important component of print quality, the other being detail rendering. The size of the colour gamut depends on both printing process and material including paper type. A larger colour gamut, or colour range, is commonly accepted as a potentially better print quality. It is however not generally established how much larger one specific colour gamut should be to be perceived as a significantly better print quality. One straightforward approach was made by Kurt Schläpfer (2000), who proposed a simple classification of colour gamut's of different printing processes. He suggested that the colour gamut of any printing process (for a given combination of ink strength and substrate) is primarily determined by the chroma (saturation) values of the primary colours - Cyan C, Magenta M, Yellow Y -and the secondary colours - Red (M+Y), Green (C+Y) and Blue (C+M).

Using this approach, he suggested that the colour gamut of a printing process can be described by one single number, the gamut area in the a* b*-plan. The gamut area is defined by Chroma (C*) and hue (h*) angle values, but Schläpfer showed that the area correlates very well with the sum of the Chroma values. Therefore the Chroma sum (C* Sum) is used in this paper as a characterization of the colour gamut. Chroma sum is given by Equation 1 where n is the six primary and secondary colours. Schläpfer suggested steps of 50 units in Chroma sum to identify different categories.

This calculation does not take L* coordinate in consideration, while ISO 12647 series does. This approach is a comparative tool and an approximation and cannot be used yet as a tool to evaluate paper as such. The use of this calculation should be linked to consistent and reproducible printing conditions. This is what we focused on. We used internal printing forms, with standard colour patches, FOGRA Media Wedge or ECI 2002.

$$C^* Sum = \sum_{n=1}^{6} \sqrt{\left(a_n^*\right)^2 + \left(b_n^*\right)^2} \tag{1}$$

## 2.4 Printing trials HSWO and Gravure

For each presented study, we performed our printing trials keeping most parameters constant, and concentrated on paper changes.

Target ink densities were kept constant, coated and uncoated papers being printed at different ink densities, as usual. Inks were industrial inks.

HSWO trials were printed at KCL pilot plant in Finland. Gravure trials were specifically prepared by industrial printer and operated in France.

## 3. Results

### Study 1. Whiteness panel ranking of European commercial papers, indoor but Nordic light

Figure 1 gives the results of the ranking panel. The x-axis gives panel visual perception of papers, lowest to the left to highest to the right. Measured whiteness, brightness and fluorescence are compared with the results from the ranking panel.



**Whiteness-Brightness scale on left, Fluorescence scale on right.**

Legend: □ Fluorescence, D65/10°   ■ D65-Brightness   ● CIE-Whiteness, C/2°
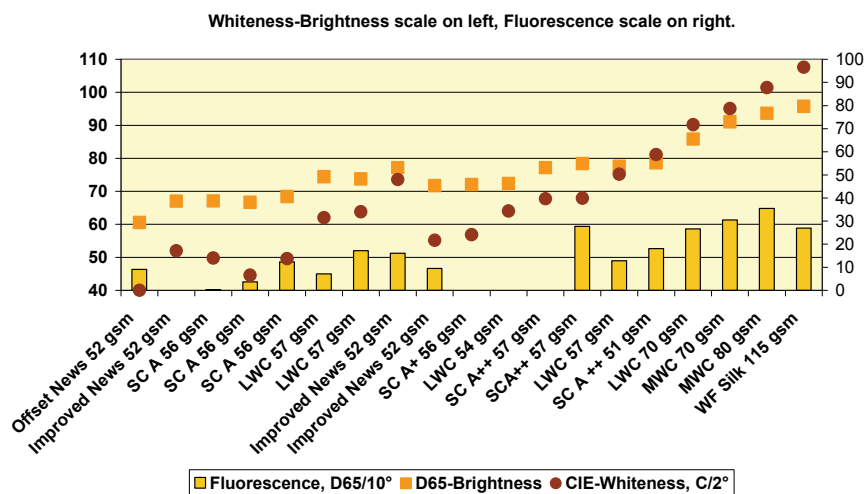
*Figure 1: Visual whiteness perception under indoor conditions but Nordic overcast daylight, papers in x-axis in order of visual ranking*

* Whiteness C values range from 40 to 110, while D65 Brightness values range from 60 to 95. Whiteness is thus more distinctive.
* For Whiteness values above 60, Whiteness C gives closer match than D65 Brightness to panel ranking.
* For Whiteness values below 60, the shade and fluorescence become more evident for the panel than Whiteness as such. This is logical, shade is more important for less white papers and visual evaluations may differ due to shade (b* values in particular on the yellow-blue axis) and fluorescence.

### Study 2. ISO12647-2 targets and evaluation of Colour Gamut at full tones in Heat Set Web Offset MWC papers from European market 2009

This study gathers HSWO MWC papers from 70 to 115 gsm from European market. Printing was operated at KCL printing pilot plant in April 2009 under consistent conditions and approaching daily practice at printing plants, namely at constant target densities. Tested samples were printed at following target densities: Black 1,70 / Cyan 1,50 (+/-0,05) / Magenta 1,30 / Yellow 1,20 and kept constant for all grades. The out coming web temperature was kept constant at 130 °C. Target densities were not optimised to reach CIELAB values for primary and secondary colours as specified in ISO 12647-2.

The measurements were made on prints over a white backing with a Gretag Spectrolino spectrophotometer without polarising filter. The calculations were made with the D50 illuminant and the 2° observer weight functions.

Our goal was to position the colour gamut variations versus **ISO-ECI-FOGRA targets** described in characterization data for the related grades and to evaluate colour gamut to rank papers with possible links to paper properties.

Figure 2abcd shows colour coordinates for white paper, black print and primary and secondary colours. Tolerances allowed by ISO 12647-2 are shown as circles. Full circle is centered on the shades target of ISO 12647-2 and dotted circle is centered on the average of all papers.
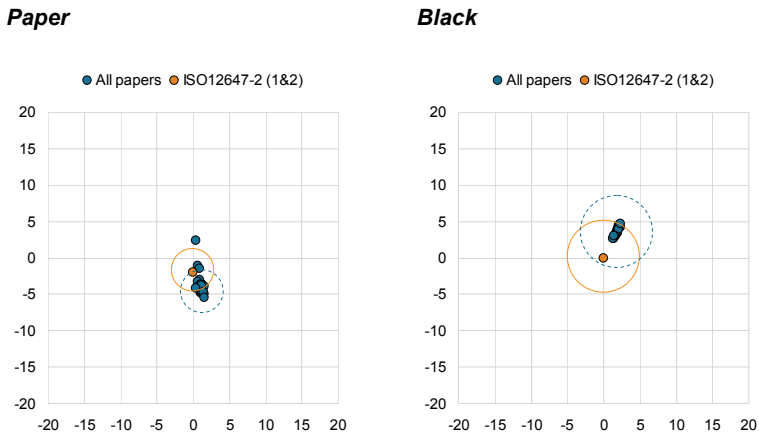
*Figure 2a: Colour coordinate b\* versus a\* for white paper and black print*
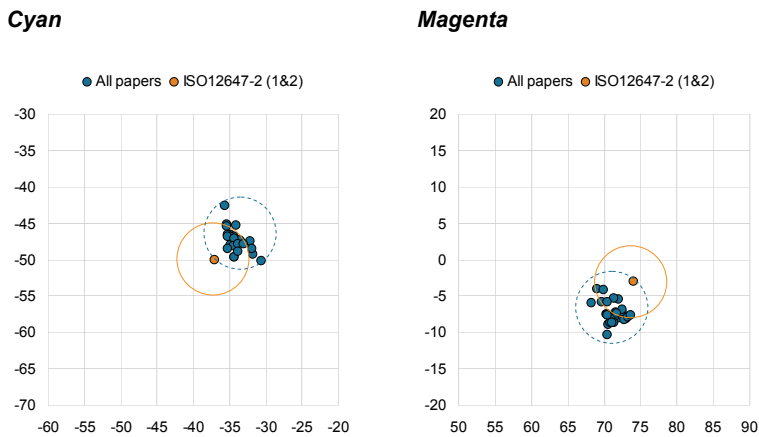
*Figure 2b: Colour coordinate b\* versus a\* for cyan and magenta*
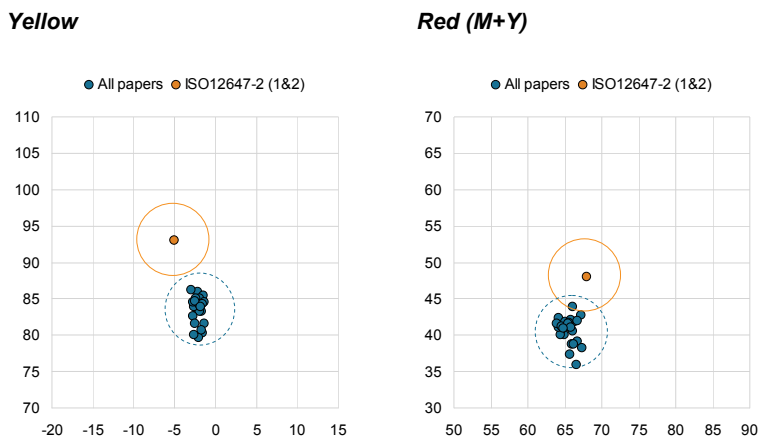
*Figure 2c: Colour coordinate b\* versus a\* for yellow and red (M+Y)*
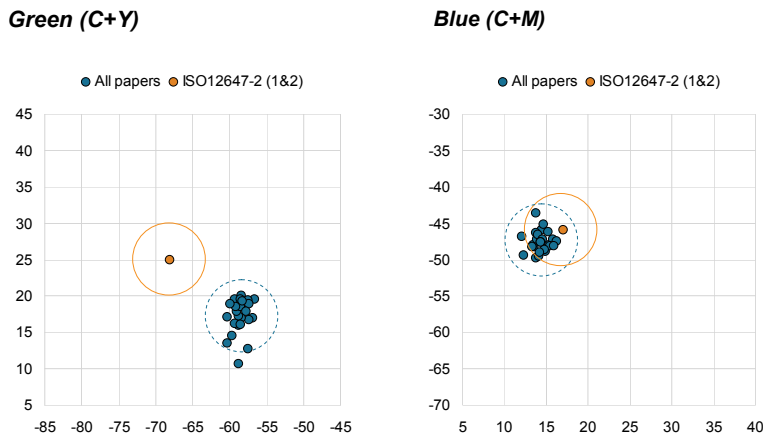
**Green (C+Y)**                    **Blue (C+M)**



*Figure 2d Colour coordinate b\* versus a\* for green (C+Y) and blue (C+M)*

Figure 3 presents the Colour Gamut of the printed result by one single number, the Chroma sum or C\* sum, as per Equation 1.
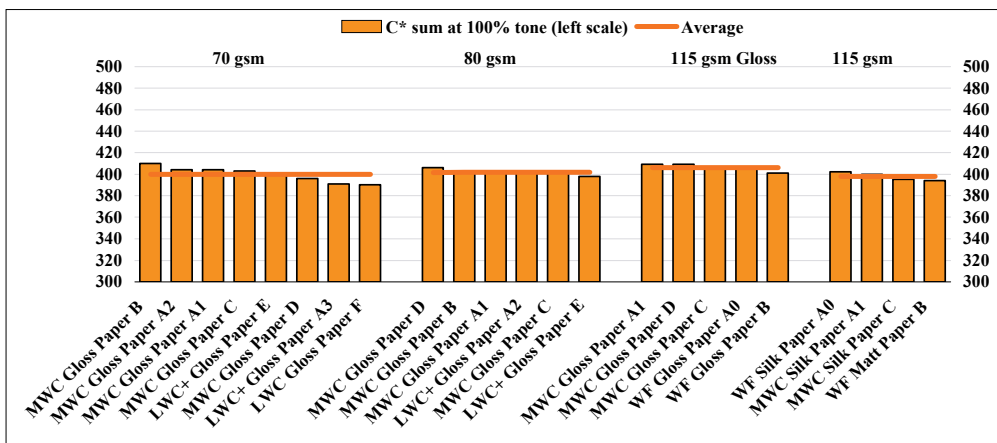


*Figure 3: Chroma sum C\* at 100% tone. HSWO European papers 70-115 gsm*

Figure 3 shows a tendency towards that higher grammage offers better Chroma sum. As expected, higher grammages and smoother papers give better results. As expected also, when comparing 115 gsm Gloss with 115 gsm Silk, Silk paper being less smooth shows indeed lower C\* sum. Chroma sum is intended to be useful as a comparison between and within paper type, but the difference within paper types is here negligible.

### Study 3. Gravure trial 2010 at industrial printer to compare LWC and LWC high brightness from same mill

We run another trial to compare 2 papers rather close for end-user, namely only different in brightness-shade and in touch and feel properties (silk touch). The ECI 2002 colour patches (more than 1600) were printed. Paper properties are described in Table 1 and results in Figure 4a and 4b. Table 1 gives the delta b\* measured with a papermaker equipment with D65 illuminant, namely 6,6. Figure 4 data use a printer equipment with D50 illuminant.

*Table 1 Paper properties Gravure trial LWC Silk high brightness versus LWC Gloss*

|  | gsm | Gloss | PPS roughness | Bulk | L\*/a\*/b\* D65 |
|---|---|---|---|---|---|
| LWC Silk high brightness | 60 | 55 | 0,97 | 0,8 | 91/0,1/-4 |
| LWC Gloss | 57 | 48 | 0,74 | 0,8 | 90/-0,8/2,6 |
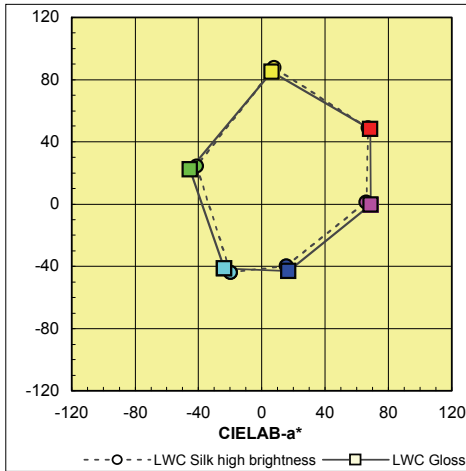
*Figure 4a Colour coordinates at 100% tone*    *Figure 4b Colour coordinates at 40% tone*
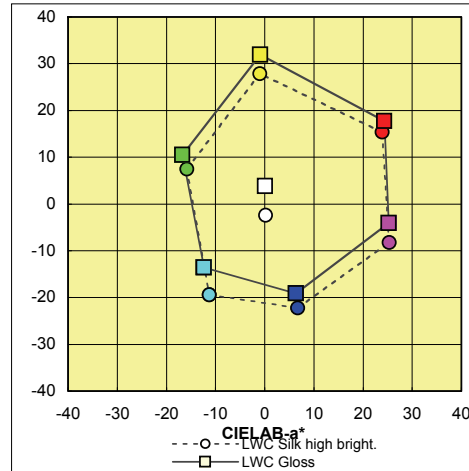
Figure 4 shows that at full tone, the Colour Gamut, calculated as C* sum, is close for both papers (382 versus 376). At 40 %, they are also exactly equivalent (146 versus 146), but shifted about 5 units in the b* axis.

## 4. Discussion

**Communication within the value chain of paper-print**

It is important to distinguish paper visual perception and paper optics needed to fine-tune colour parameters during printing. These concepts are different, targets, equipments, people in charge are different, but both informations are needed.

There are also several misunderstandings to clarify in communication within the value chain.

* Misunderstandings due to differences between printing equipments and papermaking equipments.

   Both papermaking and printing processes are industrial processes and do need different methods. They do not measure the same processes. As an example, printers optical equipments geometry is 45°/0° or 0°/4 5°, this satisfactory and widely used, while papermakers use d/0° more suitable, because more accurate for them.

* Misunderstandings due the differences in lighting conditions between papermakers and printers.

   Papermakers use D65 illuminant, needed to evaluate high brightness grades, and mostly Xenon light sources. Printers use D50 illuminant for historical reasons (Jordan, 2006).

   The new CIE illuminant, ID65 (indoor D65), Nordic daylight behind a window, (Jordan, 2002 and Gombos, 2008) is adding even more confusion. We believe, but this must still be proven, that it may be close to Whiteness calculated with illuminant C and thus would not bring any new information  for our industries.

* Misunderstandings between colour management prepress specifications and visual perception of white paper colour by itself. The white point of paper is needed as a zero point for colour management software and characterization data. But each paper grade should have a characterization data independently of its colour or white point. The visual aspect of white paper is a different concept than paper colour measurement needed for colour management settings.

* Misunderstandings on printing relevant properties. Which paper properties are relevant for paper during printing? Paper is defined through a very long list of physical and chemical parameters, and depending on the end-use, some properties are relevant and other not. Thousands of data are indeed available within the papermaking process and it is a must to identify those relevant.

* Misunderstandings motivated by different interests between stakeholders: printing machine suppliers, papermakers suppliers, materials and software suppliers. All want to promote quality and consistent printing and standardization is an excellent tribune for this. But they all have different interests and vocabulary. Papermaking process is heavy industry and consistency is needed for our operations and costs even more than for our paper users. Also, papermakers develop, beside the printers' needs, what their customers, publishers and advertisers are asking, and they all want to differentiate at best costs.

*Study 1*

Papers with same Brightness D65 / observer 10° differed in visual perception with Whiteness illuminant C / observer 2°. Whiteness C is here more in accordance with visual ranking and thus preferred. Whiteness calculation formula integrates already the shade. Other studies showed that b* shade and L* are most influent on whiteness.

*Study 2*

We conclude from Figure 2 that variation tolerances allowed in 12647-2 are reached. They are rather wide and even allow papers ranging from LWC 70 gsm up to WF 115 gsm, Silk and Gloss to be within the tolerances allowed by the standard.

We also conclude that ISO targets (see figure 2a tests on blank Paper) differ from average of papers tested. So, there is a clear need for evaluation of paper white point as a colour for best colour management calculations.

Schläpfer (2000), mentions a 50 points difference as being relevant to differentiate printing processes. It seems that the calculation may still give too much importance to shade. We tried to correlate the Figure 3 results with several paper properties. Most relevant were Gloss, PPS roughness, b* shade, but we could not draw a clear conclusion to link Colour Gamut as calculated above and a paper property.

Still PPS gave the best tendency and this suggests that PPS may be used, although primitive, to forecast the potential Colour Gamut, more than anything else. PPS being available easily this would allow to select the correct paper type and characterization data. In our example, ISO shade classification as per ISO 12647-2, distinguishes 2 paper types thru 2 shade classes : (a*=0/b*=-3) for WF Gloss, WF Matt, WF Silk, MWC Gloss, MWC Silk and (a*=-1/b*=3) for LWC + Gloss, LWC Gloss. PPS below 1 (115 gsm Gloss) or PPS above 1 (70 gsm Gloss) will be more distinctive.

Definitely, further work is here needed to come to any conclusion on Colour Gamut potential. Colour Gamut as such is quite difficult to evaluate. To define information capacity of printed matter is the important issue and depends of colour gamut, but also printing conditions, inks, dot gain, screen ruling, etc… All this factors need to be addressed. Recent standardization work introduces the concept of Achievable Colour Gamut, also known as "Process agnostic", and this is to be supported but worked out.

So, our message is that Colour Gamut discussions should integrate data made available by papermakers, as described in ISO NWI 15397 and also detailed later in this paper. Also, papermakers of Paperdam working group agreed to make available paper white point and publicly available characterization data to be used with their grades to their best knowledge. This is not a guarantee for "in conformance" or "standardized" printing, but of course it is a preferred starting point and should bring printing consistency.

*Study 3*

Study 3 shows again that the white point of paper will influence colour qualities. Colour gamut is not only a plane in colour space, it is a non-symmetric 3D volume space from black CMYK (overprinting) up to white end (paper whiteness). Our experience is that, visually, at higher L* values, paper shade a* and b* values affect more printed colour, reddish paper shade giving warm colour to white human skin and too bluish paper shade giving "sick" colour to the human face.

*Link with ISO Standardization*

Numeric data files introduction and need for consistent printing independent of printing equipments and locations is pushing standardization developments. (McDowell 2006).

Printing industry standards developed within ISO TC 130 do refer to several paper properties, paper being a widely used printing substrate.

ISO TC 6 Pulp, Paper and Board successfully developed standards to allow papermaking processes to stay reproducible and reliable within paper mills. They are of course used for paper specifications when needed.

As mentioned above, an important issue is the prepress white point settings. To determine the colour of unprinted paper, we recommend using ISO 5631-3 or to approach the results obtained with ISO 5631-3.

Calibration routines are widely available and in operation worldwide. This can be done with either paper-maker's equipments or printer's equipments. Printing equipments differ from equipments used within paper mills, meant for paper process control. Results of correctly calibrated equipments are often close, but not always.

*Proposal for paper specifications and paper requirements*
The use of a paper-based standard is recommended. This includes and starts with paper proofing substrates.

Paperdam working group is promoting a Standard proposal NWI 15397 on "Communication of optical and surface properties of printing substrates - Graphic paper for proofing, rotogravure, heat-set web offset, sheet-fed offset". This tentative standard gives an extended list of ISO standardized paper properties as per below:

Print relevant properties for Proofing, Roto, HSWO, SFO:
- Paper mill and brand name.
- Grammage.
- Bulk or specific volume.
- Roughness PPS (Parker-print Surf) for coated grade, Roughness Bendtsen for Mat, Silk or Uncoated grade. Only PPS for Gravure.
- Gloss. (or classification Gloss, Silk, Matt for Proof substrates).
- Opacity.
- Brightness or Whiteness. For visual evaluation on unprinted paper.
- Colour as per L*, a*, b* D50 (printing conditions). For evaluation of paper white point under D50 illuminant.
- Colour as per L*, a*, b* D65 (outdoor conditions). For evaluation of unprinted substrate under D65 illuminant.
- Prepress Colour Management deviations to be expected due to UV content of light.

Print relevant properties for Roto, HSWO, SFO:
- Prepress information. Publicly available characterization data recommendations.

Print relevant properties for Roto:
- Tensile strength.

Print relevant properties for SFO:
- Resistance to bending (rigidity).


## 5. Conclusions

**Paper whiteness** evaluation needs to be addressed, depending of lighting conditions. We recommend to use Whiteness C illuminant 2° observer as hint to evaluate paper whiteness. Since D65 Brightness 10° is also commercially widely available, linked to commercial decisions, and anyhow useful for papermaking process monitoring, it is also mentioned in most Technical Data Sheets.

Introducing Indoor and Outdoor Whiteness with reviewed calculations may further do improvements or simplification:

* Above 420 nm, calculate Indoor and Outdoor Whiteness as per Whiteness D65 to day.
* Below 420 nm, calculate as per illuminant C for Indoor Whiteness and as per illuminant D65 for Outdoor Whiteness.

This concept is under development for next ISO TC 6 meeting in Paris, together with modified CIE Whiteness calculation for values above 140 (Coppel, 2007).

It is clear that the **12647 paper colour targets** have an interest for printing consistency and standardization. But targets given in these standards are misleading. Market may change and determination of white point of paper is a must. Colour L*, a*, b* D50 paper data are made available by papermakers for printers when needed. Besides this, papermakers will give hints on how to best use their products by recommending best publicly available paper profiles and characterization data (see Paperdam working group statement).

Achievable Colour Gamut depends of printing process, printing conditions. It does not depend of paper shade only, but is linked to surface mainly, in less extent to L* values and even less extend to shade (or fluorescence thus).

Further work is needed to agree on standardized and reproducible methodologies, because this issue is complex but full of potential. A suggested method could be as follows: print with same conditions (ink, blankets-cylinder engraving) at several densities. To determine Colour Gamut at a given density, evaluate Colour Gamut at several densities and extrapolate at the given density.

Quality: "I know it when I see it". (Guaspari, 1985)

We want paper users to get the full benefit of the daily quality improvements made in our mills.

## Acknowledgements

## References

Coppel L, Lindberg S, Rydefalk, S. Whiteness assessment of paper samples in the vicinity of upper CIE whiteness limit, 26th session of the CIE, Beijing, China, pp D1-10. And other Innventia studies.

Gombos, Katalin, Pointer Michael, Sik-Lànyi Cecilia, Schanda Jànos, Tarczali Tünde, 2008, Proposal for an Indoor Daylight Illuminant. Color Research and application pp 08-25.

Guaspari, John, 1994. Quality, I know it when I see it. Book, AMACOM, American management Association.

Jordan, Byron, O'Neill, M.A. 1991.The whiteness of paper colorimetry and visual ranking. TAPPI 74 (5): 93-101.

Jordan, Byron, 2002. Accurate Colorimetry of fluorescent papers. ISO TC6 WG 3: N 528.

Jordan, Byron, 2003. More thoughts on Illuminants. ISO TC6 WG 3: N 537.

Mc Dowell, David Q., 2006, The Synergistic Relationship between Standards for Data Exchange, Metrology, Process Control, and Color Management, TAGA Proceedings pp 151-156.

Kolseth Peter, Lanat Luc, Sävborg Örjan. 2009. Printing by numbers on commercial paper grades. Presented at iarigai conference Stockholm.

Puebla, Claudio, 2003. Whiteness assessment, a primer. Concepts, Determination and Control of Perceived Whiteness. Axiphos Gmbh, Germany. See www.axiphos.com.

Schläpfer, Kurt, 2000. Classification of Colour Gamut's of Printing Processes. TAGA Proceedings, pp112-129.

## Other references and standards cited

Kolseth Petter, Nicander Anna, 2006 Colour Gamut in Rotogravure, Stora Enso Research Falun Internal report.

Paperdam presentations to ISO TC 6 and TC 130. See www.paperdam.com.

Papierkennwerte in German/Characteristic paper value, Recommended characteristic paper values for communication within the value chain of paper-print. Initiative of VDAM and Zellcheming 2009-2010. See www.zellcheming.de or www.vdma.org or  www.paperdam.org.

## ISO Standards of TC 6 and TC 130 cited

ISO 2470-2. Paper, board and pulps - Measurement of diffuse blue reflectance factor - Part 2: Outdoor daylight conditions (D65 brightness).

ISO 11476. Paper and board - Determination of CIE whiteness, C/2° (indoor illumination conditions).

ISO 11475. Paper and board - Determination of CIE whiteness, D65/10° (outdoor daylight).

ISO 5631-2. Paper and board - Determination of colour by diffuse reflectance - Part 2: Outdoor daylight conditions (D65/10°).

ISO 5631-3. Paper and board - Determination of colour by diffuse reflectance - Part 3: Indoor illumination conditions (D50/2°).

ISO 12647-1 to -8. Graphic technology - Process control for the production of half-tone colour separations, proofs and production prints.

ISO TS 10128. Methods of adjustment of the colour reproduction of a printing system to match a set of characterisation data.

ISO WD 15397 Graphic Technology - Communication of optical and surface properties of printing substrates. - Graphic papers for rotogravure, heat-set web offset, offset sheets, proofing.

# Multisensory evaluation of the paper products

*Aino Mensonen*, *Maiju Aikala, Janne Laine*

VTT Technical Research Centre of Finland
P. O. Box 1000, FIN-02044 VTT, Finland

E-mails: aino.mensonen@vtt.fi, maiju.aikala@vtt.fi, janne.laine@vtt.fi

**Abstract**

The tradition in evaluating the paper products has been making the assessment sense by sense. The subjective evaluations of the products have been focused on visual assessments as they support the quality control during the printing process. Recently the focus in print product development has been shifting towards brand building and mental impressions, and thus, methodology for the subjective evaluation of tactile properties has been developed. The next development trend is obviously towards evaluation of multisensory perception. Multisensory evaluation of paper products is essential in order to understand the overall experience the product evokes in the end-use.

The purposes of this work were to study visual and haptic perception and their possible interaction with paper roughness discrimination tasks. The study was conducted further to the multisensory evaluation of paper products where all senses are involved. Furthermore the impressions that the product evokes in the end-user were connected to sensory results. In paper roughness discrimination tasks no interaction between vision and touch was found. Discrimination performance where both vision and touch were used and the roughness evaluation based on touch was found superior to other conditions. The information from unattended modality was applied if attended sensory system could not provide enough details to make a judgment. In the end-use situation all modalities are involved, thus multisensory evaluation is needed. A novel way of presenting the results, where the results of multisensory evaluation of printed products are combined with the images evoked from the product, has been developed.

**Keywords:** multisensory; touch; sight; paper products

## 1. Introduction

The product development in paper industry has traditionally concentrated on efficiency and cost savings. Based on the efficiency, the paper producers have fine-tuned the raw materials and production processes. It has been discovered quite recently that the products need new features which differentiate them from competitor's similar products. Also, the producers need marketing arguments. Measurable sensory properties give an answer to this. Traditionally these measurements have focused only on visual evaluations, and recently also on tactile evaluations (Aikala et al. 2003, Aikala et al. 2010, Forsell et al. 2004). In the end-use situation all senses are involved, thus multisensory evaluation, where all senses are allowed to take an action to judgment, is needed. Also the impressions evoked from the product should be linked to the sensory results.

When exploring the printed paper products, vision is likely to dominate touch because of the faster information processing speed. Could the slower tactile perception have modifying effect to the visual perception of the product? And could the visual perception have an effect on tactile perception?
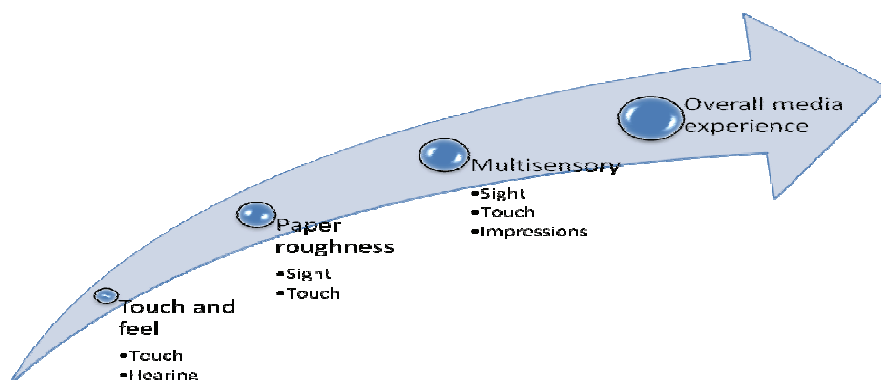


*Figure 1: Progress of the research*

Our aim is to study multisensory evaluation of different kind of media products. In this study we have concentrated on paper roughness by assessing what impact the touch has on vision and vice versa in paper roughness discrimination task. After that we have developed a method for evaluation of multisensory perception and a novel way for presenting the results of the multisensory evaluation of paper products combined with the images evoked from the product. Figure 1 presents the progress of the research; step 1 has been carried out earlier (Aikala et. al 2003, Forsell et. al 2004), this study concentrates on steps 2 and 3, and step 4 is our final goal.

## 2. Methods

In the first part of the study, five paper samples were assessed in two different tasks regarding the paper roughness. The first task was to examine the differences in the discrimination accuracies between different evaluation conditions (visual, haptic, both visual and haptic, but decision based on either one). The second task was to examine what kind of influence touch has on visual perception of the paper roughness and vice versa. Samples used in the experiment were of wood containing medium weight coated (MWC) gloss papers. Three samples were of the same custom made paper, which was calendared to different roughness levels. Two samples were commercial papers.

Two-alternative forced-choice (2-AFC) method was used. 2-AFC method is a psychophysical method in which the test person is forced to choose one of the alternatives. Results were tested with two-way within-subjects ANOVA (analysis of variance) to find the dependencies and differences between modalities, i.e. vision and touch, and comparison pairs and further analyzed with pair wise t-tests.

The testing device was custom made. The apparatus was composed of two 50 cm-diameter discs having common axis around which they could be freely turned. The system was covered with wooden box. It had openings both for the top disc (viewing) and for the bottom disc (touching) so that the test persons couldn't see the sample which they were touching. The illumination was arranged so that the test person couldn't make the decision based on gloss differences. Although the smell and hearing were not studied, they were taken into account: all participants wore hearing protectors and the smell of the wooden box masked the paper's odor. Test persons sat on adjusted chair and used chin rest in order to get the distance and viewing angle constant independent of the test person (Figure 2). The apparatus is described in Turtola (2008) in detail.



*Figure 2: The test arrangement (Turtola 2008)*

Test persons were shown two stimuli, one at the time, and their task was to tell, which one they considered to be the rougher one. Discrimination performance was tested in four possible conditions. Two of them were unimodal: 1) visual, where the samples were viewed but not touched and 2) tactile, where the samples were touched but not seen. Two of the conditions were bimodal, both of them the samples were seen and touched, but in 3) the evaluation was based on vision and in 4) the evaluation was based on touch.

In the second part of the study, nine heat-set offset printed samples were evaluated in two different tasks. The test page used in evaluations is presented in Figure 3 and the procedure is presented in Figure 4. In the first

task the samples were evaluated in multimodal conditions: by letting touch and sight impact simultaneously on the perception. The criteria used in the assessments were: roughness, sharpness, lightness, colorfulness, slipperiness, stiffness and gloss. The mental impressions were collected from interviews made among consumers, advertising agents and publishers, made in an earlier project (Aikala et. al 2010). In the second task the test persons assessed the magnitudes of chosen impressions: trustworthy, high-quality, silky, peaceful, sophisticated, warm, cheap, environmentally friendly, relaxed and pleasant. In both tasks the attributes were assessed by a scaling method



*Figure 3: The test page in the second part of the study*



*Figure 4: The tasks in the second part of the study*

Principal component analysis (PCA) was used in the interpretation and visualization of the results. The original data consisted of a total of 17 observations (assessments of the 7 sensory attributes and 10 mental impressions listed above) of each sample by each observer. The locations of the samples were mapped from the 17-dimensional space of the original scales to the plane of the first two principal component axes. This reduced the redundancy in the original data (arising from the correlations between the original scales) and allowed the most significant perceived differences between the samples to be visualized in a 2-dimensional graph. The principal components are calculated as linear combinations of the original variables so that the maximum amount of variance in the data is explained by the minimum number of principal components. By mapping the samples and also the original sensory and mental impression scales to the principal component axes, the sensory perceptions and mental impressions evoked by the samples, and the relationships between different sensory attributes can be better visualized and interpreted, as shown in the next section. Jackson (2003) describes principal component analysis in detail.

## 3. Results and discussion

In the first part of the study, where the paper samples were assessed based on their roughness perception, the bimodal (vision and touch together) discrimination performance where the evaluation was based on touch, was superior to the other conditions. Pure touch was found to function better than pure vision. In conditions requiring tactile evaluation the participants were both more consistent with each other and more capable to differentiate the samples. The results indicate that if the information provided by one modality is not enough to discriminate the stimuli, participants use also the information provided by the other modality, which at the time might be more suitable for the task.

It was found that the best way of carrying out paper roughness discrimination tests is to make the evaluation using touch and letting the vision to help the assessment. It was also found that the trained evaluators made the test based on the sense which he was told to use in the task, until the evaluation task was too hard for evaluator, and hence the other sense was used. Conflicting information provided by unattended sense had no effect on the discrimination accuracy. Hence, in roughness evaluation there was no interaction between vision and touch.

In the end-use situation naturally all senses influence on how the product is perceived. In the second part of the study all senses were allowed to influence on the evaluation, although the assessment based on visual and touch evaluations. The results of multisensory evaluation were combined with the magnitudes of impressions evoked by the samples. Principal component analysis was applied to this combined set of psychometric data as described above. The result of mapping the samples, sensory attributes, and mental impressions to the plane spanned by the first two principal components is presented in Figure 5. This diagram can be called the experience map of this set of samples. In this figure the length and direction of each attribute vector indicates the contribution of the attribute to the first two principal component axes. The attributes with the longest vectors had the largest contribution to the first two principal axes. As the first two principal components represent the majority of the observed total variance between the samples, approximately 65 percent, the attributes with the longest vectors can be considered as having the most significant role in describing the perceived differences between the samples.

The locations of the samples can be compared to the direction of the attribute vectors for an overall view of which attributes describe the samples and what kind of mental impressions are associated with the samples. The directions of the vectors further indicate positive and negative correlations (vectors pointing in the same or opposite directions, respectively) between the attributes, or the lack of significant correlation (vectors approximately perpendicular to one another) between the attributes for this set of samples.

It should be noted that some attributes that have relatively small contribution to the first two principal components may still differentiate significantly between some samples, which can be illustrated by plotting the samples in the plane of the 3rd and 4th principal component.

In the Figure 5 it can be seen that samples A and B are found more stiff, trustworthy, high-quality and glossy than the other samples. Samples C and I are on the opposite side of A and B and they can be described as warm, sharp and colorful samples. Environmentally friendly goes together with relaxed and cheap impressions and results indicate that the samples C and E can be characterized as such samples. Those three impressions are far from trustworthy and high-quality. It can also be seen that none of the attributes describe sample F very well, although it appears that F is on the opposite side of slippery feel. It can also be seen, that the sample-set did not include samples which could be characterized as silky, peaceful and high lightness. Figure shows that there were attributes which differentiate the samples well regardless of other attributes. For example, roughness distinguishes this sample set well regardless of samples' trustworthy or cheap impressions.

Paper samples can be divided into four groups:

A and B, which are glossy, high-quality, trustworthy and stiff samples.

G and H, which are pleasant, sophisticated and slippery samples.

C and I, which are warm, sharp and colorful samples. They are close to environmentally friendly, relaxed and cheap impressions. This group is opposite to group 1 and its characteristics.

D and F, which are rougher compared to other samples and opposite of group 2.
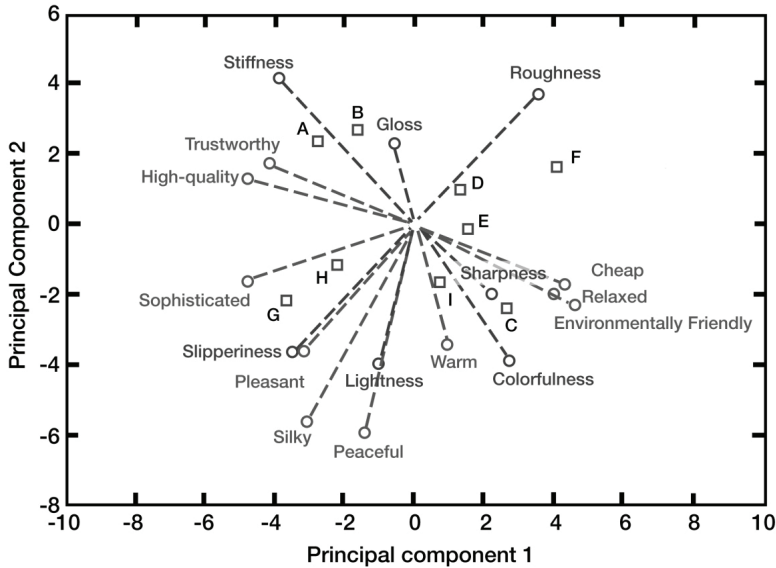
*Figure 5: The experience map*

## 4. Conclusions

In roughness perception the role of visual roughness is not as clear as felt roughness. Roughness is a feature that is more connected to touch than vision. However, the participants that performed poorly in haptic-only condition gained relatively much help from the availability of the other modality. In roughness evaluation the vision and touch seem to be working as independent sources of the information. The information from unattended modality was applied only if attended sensory system could not provide enough details to make a judgment.

The experience map visualizes how the mental impressions that describe the papers, their sensory properties and other characteristics are linked together. It can be utilized in product development as well as in marketing purposes. The experience map gives the paper and printing industry a novel way to differentiate their products. It gives also tools to communicate product's properties to the customer. The method of assessment can be expanded to evaluation of other products as well, for example touch screens or packaging.

## Acknowledgements

## References

Aikala, M., Nieminen, S., Poropudas, L. & Seisto, A., (2003) *The end user aspects in print product development. 30th IARIGAI Conference, 7-10 September, 2003, Dubrovnik, Croatia, 11p.*

Aikala., M., Ojanen, M. & Vehmas, K., (2010) *Using consumer preferences in setting the target for product development. Will be published in 37th IARIGAI Conference, 12-15 September, 2010, Montreal, Canada, 7p.*

Forsell, M., Aikala, M., Seisto, A. & Nieminen, S., (2004) *End users' perception of printed products. PulPaper Conference, 1-3 June, 2004, Helsinki, Finland, 6p.*

Jackson, J. E., (2003) *A User's guide to principal components. John Wiley & Sons, USA 2003, 569p.*

Turtola, P., (2008) *Visual, Haptic, and Visual-Haptic Perception of Paper Roughness. Master's Thesis, Faculty of Information and Natural Sciences, Helsinki University of Technology, November 2008, 61p.*

# The influence of special effects on the perception of printed products

*Janne Laine, Tapio Leppänen, Olli Nurmi*

VTT Technical Research Centre of Finland
P. O. Box 1000, FIN-02044 VTT
Espoo, Finland
E-mail: janne.laine@vtt.fi

**Abstract**

The influence of special effects on the perception and mental impressions associated with printed products was investigated in a psychometric study. The procedures used in this work were based on the results of the earlier study, but the subjective experiments were streamlined, concentrating on measuring only a few key perceptual dimensions. The basic approach was to build certain numerical psychometric scales to describe the mental impressions evoked by the set of print samples subjectively assessed in the experiments. This paper concentrated mainly on the average observer, and in these averaged results the above mentioned trends were consistent. However, the results indicate significant positive overall trends in the examined perceptual dimensions resulting from the use printed special effects.

**Keywords:** special effects; printing; perception; user experience; psychometry

## 1. Introduction

The work described in this paper is a continuation of a study that concentrated on measuring the influence of the printed special effects on the subjective experience and mental impressions evoked by printed products. The psychometric scaling procedures used in this work were based on the results of the earlier study [Laine et al., 2008]. Compared to the earlier study, the subjective experiments were streamlined, concentrating on measuring only a few key perceptual dimensions that were identified as being central in describing the perceptual and experiential shifts resulting from the use of printed special effects. The use of this focused experimental setup allowed a considerably larger amount of print samples to be assessed by a considerably larger group of observers. Indeed, this was the main motivation for this study: to collect a larger set of subjective assessment data for a larger set of special effects print samples, in order to verify and possibly expand the findings of the earlier study, which had been carried out with a more limited set of print samples and observers.

The basic approach was to build certain numerical psychometric scales to describe the mental impressions evoked by the set of print samples subjectively assessed in the experiments. By comparing the positions of special effect print samples on the psychometric scales to those of reference samples printed without special effects, significant trends could be observed in how the special effects shifted the mental impressions associated with the print samples.

## 2. Experiments

A total of 60 different print samples were collected for the subjective assessments. 26 of these samples were standard CMYK print samples without special effects. They had the same content as the corresponding special effect print samples, and served as references for analyzing the perceptual shifts caused by the special effects. Metallic effects were used in 15 of the print samples. The class of metallic effects included metal-laminated paper, metallic inks, and metallic foil elements. Varnishing was used in 15 of the prints samples. Typically spot gloss or pearlescent varnishing was used to highlight certain objects in the printed image. In 10 samples a design paper with visible surface structure or special optical properties was used. The print sample set also had a single print sample in which a 3D effect had been created by printing on a lenticular sheet. Some of the samples had more than one special effect; both metallic and varnishing effects could be used in the same print sample, for example. In contrast to the previous project in which several different special effect versions of the same content were made specifically for the psychometric experiments, most of the samples used here were taken from earlier production or demonstration samples that already were enhanced with special effects. The reference versions were produced by printing the same content without the

special effect, in some cases mimicking the effect, as well as possible, with modified CMYK separations. Thus there were typically two versions with the same content, a special effect print sample and a standard CMYK print sample for reference.

The set of print samples were assessed by a total of 177 observers. Although the majority of the observers (145) were Finnish, a total of 10 nationalities were represented. The second largest group, 21 observers, were from Germany. The other countries among the ten were represented by 1 to 3 observers each.

All the samples were attached to gray cardboard backing that extended beyond the borders of the print sample. Each observer assessed a subset of 28 randomly selected print samples in random order, one sample at a time. The observers were allowed to hold the samples in their hands, but were instructed to touch only the cardboard backing, not the sample itself.

Before assessing the samples the observers completed a background questionnaire. In addition to basic demographic data, the questionnaire included a short section concentrating on media use.

The observers were asked to indicate their level of agreement with seven statements concerning the perceived properties of each sample by making a mark on a visual ruler such as the one shown in Figure 1.

**This sample is interesting.**

| Completely disagree | Slightly disagree | Undecided | Slightly agree | Completely agree |
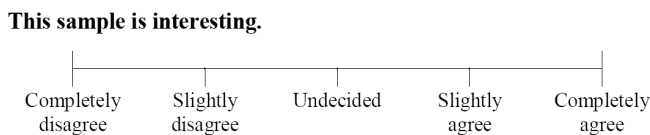
*Figure 1: The visual ruler used in assessing the print samples*

The seven statements were:
1. This sample is stylish.
2. This sample is interesting.
3. This sample is beautiful.
4. This sample catches one's attention.
5. This sample is pleasant to look at.
6. This sample is memorable.
7. The visual appearance of this sample supports the content.

The agreement levels were converted to integer numbers from 0 (corresponding to the left end of the ruler, "Completely disagree") to 100 (corresponding to the right end of the ruler, "Completely agree"). This data was analyzed to form numerical scales representing the perceptual differences between the print samples, as described in the following section. The first six statements were used to form ratings for "Noteworthiness" and "Aesthetic Value", as described below.

## 3. Results and discussion

The results of the earlier work suggested that the influence of the printed special effects on the perception of printed products was mainly reflected on two perceptual dimensions. These dimensions were termed Noteworthiness and Aesthetic value. Statements 2 (This sample is interesting), 4 (This sample catches one's attention), and 6 (This sample is memorable) in the previous chapter were intended to measure the Noteworthiness of the print samples. Likewise, statements 1 (This sample is stylish), 3 (This sample is beautiful), and 5 (This sample is pleasant to look at) were intended to measure the Aesthetic Value of the samples.

Multivariate data analysis method known as principal component analysis (PCA), described in detail by Jackson (2003), was used to verify that the six attributes indeed measured these two approximately independent underlying dimensions, as was assumed based on the results of the earlier study. Examination of Figure 2 confirms that this was the case. Vectors corresponding to the attributes "Interesting", "Memorable", and "Catches attention" all point in the same general direction, indicating high correlation between these

variables. This is also the case for attributes "Pleasant to look at", "Beautiful", and "Stylish". Furthermore, the fact that the angle between the vectors of these two groups of attributes is approximately 90 degrees indicates low correlation between the groups and suggests that the two underlying attributes indeed correspond to two separate aspects in perceiving the special effects in printed products, as expected.
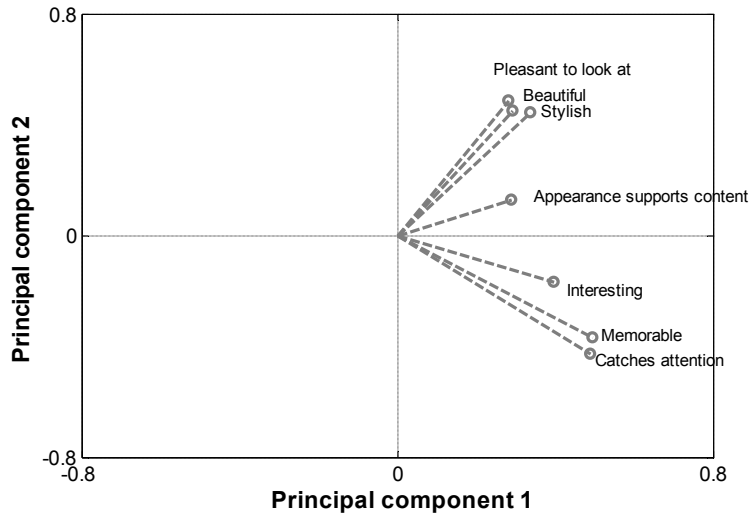


*Figure 2: The seven original attributes in the space of principal components 1 and 2*

Rotating the vectors counter-clockwise by roughly 40 degrees would put the vectors in positions that closely correspond to their locations in the earlier study. This would align the horizontal axis with the dimension of Noteworthiness, and the vertical axis with Aesthetic Value.

The seventh variable, corresponding to the statement "Appearance supports content" was included in the assessments in order to identify possible cases where the use of special effects was perceived to be in disharmony with the message of the content. This variable is seen to have some positive correlation with both Noteworthiness and Aesthetic Value.

Instead of actually rotating the axes in the principal component space of the above diagram (which would not have affected the interpretation of the results), Noteworthiness was calculated in a more straightforward manner as the average of the ratings on the "Interesting", "Memorable", and "Catches attention" rulers. Aesthetic Value was similarly calculated as the average of "Pleasant to look at", "Beautiful", and "Stylish".

Figure 3 summarizes the overall results of the study, showing the locations of all 60 print samples in the Noteworthiness-Aesthetic Value diagram (values averaged over all 177 observers).
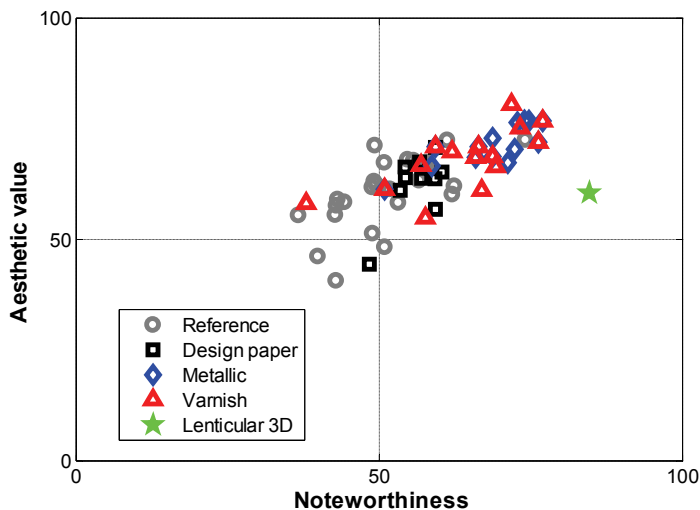


*Figure 3: Noteworthiness and Aesthetic Value of all print samples, averaged over all observers*

The gray circles in Figure 3 correspond to the reference print samples that had the same content as some of the special effect samples but without any special effects above conventional CMYK printing. These reference samples form a cluster roughly in the middle of the diagram. The distribution of these points results from the perceived differences in the Noteworthiness and Aesthetic Value of the content of the samples. Without yet looking specifically at the reference and special effect samples of identical content, it can be seen that generally the special effect sample clusters occupy areas to the top right of the reference samples, indicating increased Noteworthiness and Aesthetic Value in the special effect samples.

While no general conclusions can be drawn from the position of a single sample, it is interesting to note that the only sample with a 3D effect created by lenticular printing, is considerably separated from the cluster of the other samples by its significantly higher Noteworthiness.

Looking more closely at the perceptual shifts produced by a certain type of special effect, Figure 4 shows locations of the print samples with metallic effects (whether produced by laminated paper, metallic inks, or foil) and the corresponding reference print samples with the same content but no special effects. Although the results are generally not discussed at the level of individual print samples in this paper the samples are still assigned numeric labels in the graphs in order to facilitate references to certain cases. The arrows point from the reference sample to the corresponding metallic-effect sample, indicating the perceived shift in Noteworthiness and Aesthetic Value in that case. A trend is evident in the perceived shifts: the arrows point toward the top right corner, indicating increases in both Noteworthiness and Aesthetic Value. In all cases an increase in both of these dimensions was achieved with metallic effects. The shifts can generally be said to be statistically significant. The confidence intervals for the mean values of both Noteworthiness and Aesthetic Value (not shown in the figures), averaged over all observers, are in the range from 2.1 to 4.7 scale units, for all samples.



*Figure 4: Noteworthiness and Aesthetic Value of samples with a metallic special effect and the corresponding reference samples, averaged over all observers*

The results for the varnish samples, plotted in Figure 5, are very similar to those of the samples with metallic effects. Again increases in both Noteworthiness and Aesthetic Value were generally achieved compared to the reference samples, apart from a few cases in which only the Noteworthiness was significantly increased, Aesthetic Value having remained practically at the same level as that of the reference sample. The increases in Noteworthiness tended to be larger, but only slightly, than increases in Aesthetic Value for the other samples also, as was the case with the samples with metallic effects.

The design paper print samples were more experimental in nature than the other samples. A set of contents from previous productions, originally printed on conventional paper, were printed on a set of design papers with special surface properties for the purposes of these experiments.

The varying suitability of the given design paper to each content appears to be evident in the results for the design papers, plotted in Figure 6. The graph indicates that increases in Noteworthiness were achieved for most samples, compared to samples of the same content printed on normal paper. However, there were both

increases and decreases in the Aesthetic Value. Indeed, for the same content, Aesthetic Value was in some cases increased when a certain design paper was used, but decreased with another kind of design paper (arrows pointing towards both top right and bottom right from the reference sample; see samples 8, 9, and 10, for instance).
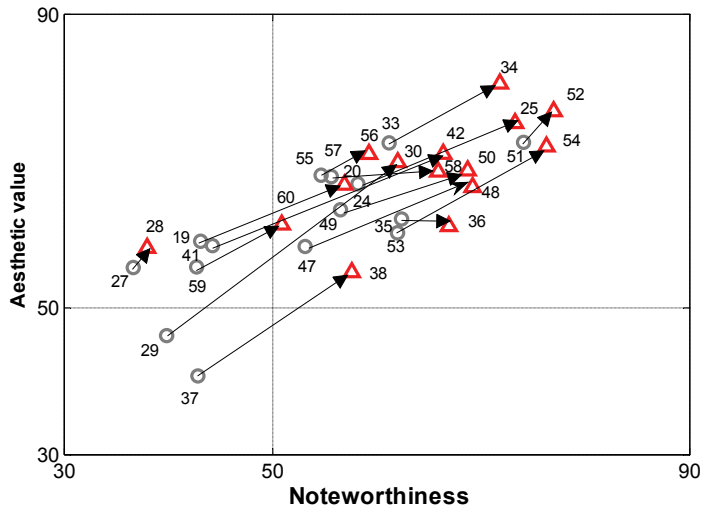


*Figure 5: Noteworthiness and Aesthetic Value of samples with a varnish special effect and the corresponding reference samples, averaged over all observers*
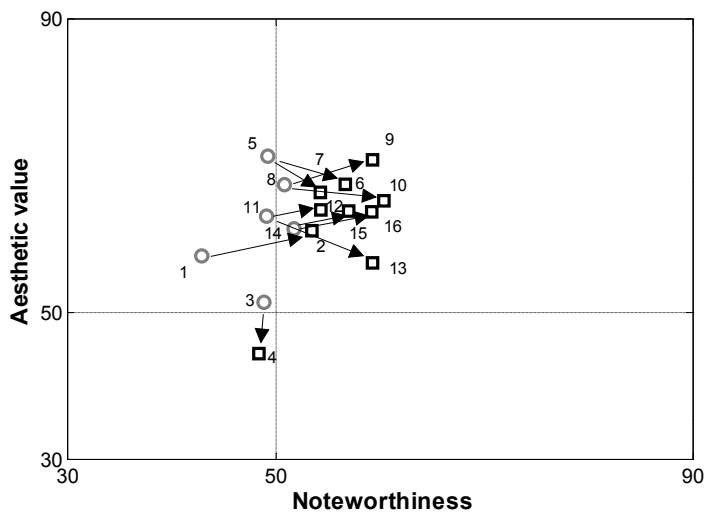


*Figure 6: Noteworthiness and Aesthetic Value of design paper samples and the corresponding reference samples, averaged over all observers*

The results for the design papers resemble the results of the previous study, in which the special effect print samples were also for the most part made by adding different types of special effects to existing content [Laine et al., 2009]. In those results the trend of increases in Noteworthiness was evident, with both increases and decreases in Aesthetic Value. This was interpreted as having resulted from the success (or lack of it) with which a special effect had been designed and implemented, and the suitability (or lack of it) of a given special effect to certain content. It was further speculated that with more carefully designed special effects increases in Aesthetic Value as well as Noteworthiness could be usually achieved.

The results of this study support the above assumptions: a strong trend of increases in both Noteworthiness and Aesthetic Value was evident with the carefully designed metallic and varnish special effect samples (Figures 5 and 6).

For the purposes of comparison to the results of the previous study, note that samples 37 and 38 (the cover of annual report without special effects and the same cover with spot gloss varnishing, respectively) of this study were also included in the previous study (identified by sample labels Report and ReportGloss in Laine et al. (2009)).

While the results presented above in this paper generally showed a strong trend of increased Noteworthiness and Aesthetic Value when the values were averaged over all observers, observer groups could be found that deviated from these averages. An interesting approach would be to cluster observers sharing similar attitudes towards printed special effects by statistical analysis of the assessment data. The identified observer clusters could then be profiled based on the background data. This kind of analysis was beyond the scope of this work, however.

The results for some basic demographic groups were examined, however. When examining these results, it should be noted that because the number of observers in each group is considerably lower than the total number of observers, there is more uncertainty in the sample mean locations for the observer groups. Note also that the observers were not completely randomly selected, and cannot be assumed to fully represent the general population. While there were some significant differences for individual samples in the assessments made by women and men, the results of the both sexes share the similar trend of increasing Noteworthiness and Aesthetic Value for the metallic and varnish samples.
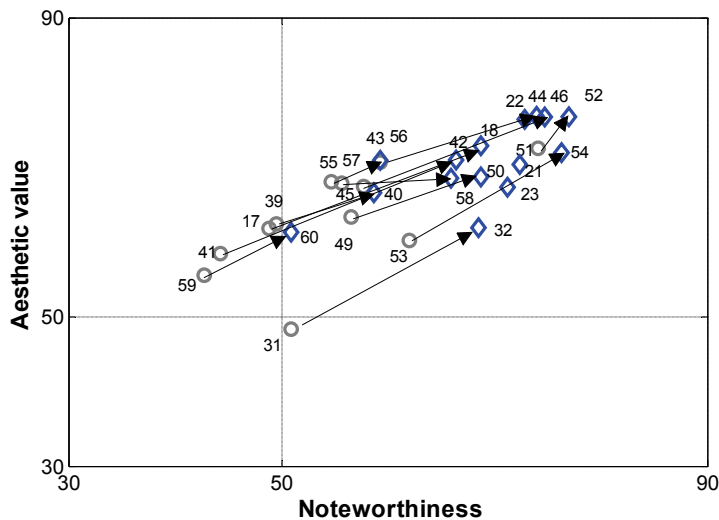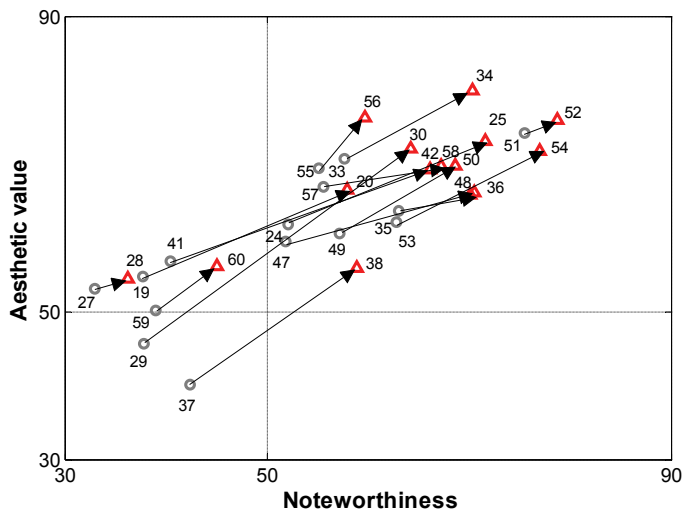


*Figure 7: Noteworthiness and Aesthetic Value of samples with a varnish special effect and the corresponding reference samples, averaged over observers aged 20 to 39*
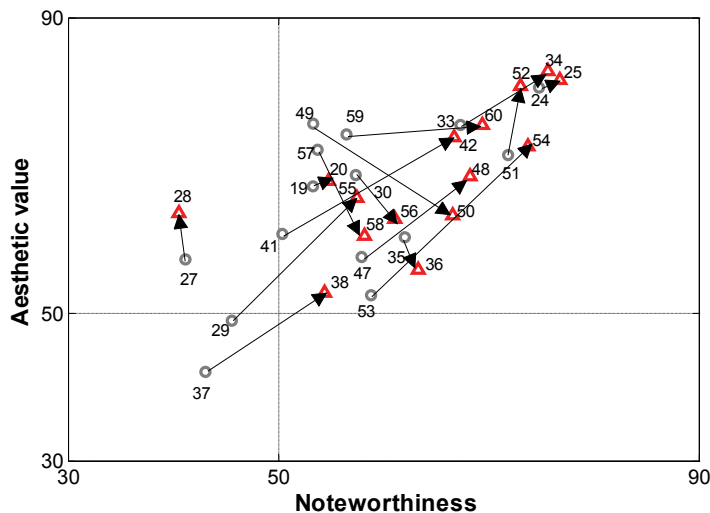


*Figure 8. Noteworthiness and Aesthetic Value of samples with a varnish special effect and the corresponding reference samples, averaged over observers aged 40 to 63*

The differences were more pronounced when observers aged 20 to 39 (120 observers) were compared to observers aged 40 to 63 (53 observers), as seen in Figures 7 and 8 for the samples with varnish effects. The older observer group ranked some special effect samples considerably lower in Aesthetic Value than the younger observer group. However, there were still a considerable number of special effect samples that were highly ranked by the older observers also.

## 4. Conclusions

The influence of special effects on the perception and mental impressions associated with printed products was investigated in a psychometric study. A set of 60 print samples containing different types of printed special effects, such as varnishing and metallic effects, was subjectively assessed by 177 observers. The number of print samples and observers was increased from an earlier study, allowing more general conclusions to be drawn from the results.

The shifts produced by the use special effects along perceptual dimensions termed Noteworthiness and Aesthetic Value were examined. These dimensions were found in the previous study to efficiently capture a considerable part of the influence of printed special effects on the subjective experience of printed products. The positions of the special effect print samples were compared on the psychometric scales of Note-worthiness and Aesthetic Value to the positions of the reference samples that had the same content but no special effects beyond conventional CMYK printing. A strong trend of increased Noteworthiness and Aesthetic Value in the special effect print samples, compared to the reference samples, was found.

This paper concentrated mainly on the average observer, and in these averaged results the abovementioned trends were consistent. Further examples showed how groups of observers could be found that significantly differed from the average observer in their assessments of some of the samples.

It should be stressed that due to the complexity of perceptual interactions involving factors such as the content of the printed product, colour reproduction, the visual design and technical implementation of the special effects, and the varying preferences and expectations among the users of printed products, the results cannot be taken as a categorical indication of how the use of a given type of special effect will influence the user perception of the printed product in a specific case. However, the study reported in this paper did indicate significant positive overall trends in the examined perceptual dimensions resulting from the use printed special effects.

### References

Laine, J. S., Leppänen, T., Nurmi, O. (2009) *Perception of printed special effects*, iarigai 36th International Research Conference, 13-16 September 2009, Stockholm.

Jackson, J. E. (2003). *A User's guide to principal components*, John Wiley & Sons, U.S.A. 569 p.11-16.

# Computer-displayed images in the subjective assessment of visual packaging designs

*Janne Laine, Elina Rusko, Anne Arvola, Janne Pajukanta, Olli Nurmi*

VTT Technical Research Centre of Finland
P.O. Box 1000, FIN-02044 VTT Espoo, Finland
E-mails: firstname.lastname@vtt.fi

**Abstract**

The basic approach of this research was to test a limited number of packages presented on computer screen and compare the results with assessing the real packages. The eye tracking device was used to record the eye movements of the observers and scan path and relative dwell time were used to describe the result.

In this limited study we used data from only 10 observers but it indicates that it is possible to compare different packaging designs using images presented on the screen. The digital images of the packages can be used to evaluate new layouts quickly and objectively, thereby significantly reducing the time to establish a new package design, and at the same time ensuring that the design works well with the target group.

The results showed that similar patterns for eye movements could be observed for both cases which indicate that it is possible to evaluate the packaging design by using the digital images.

**Keywords:** packaging design; perception; user experience; eye tracking

## 1. Introduction

The work described in this paper deals with the visual design of packages. Specifically, eye-tracking was used to investigate the feasibility of using images of packages viewed on computer displays, instead of real packages, when studying the subjective response to visual packaging design. The research question was whether or not similar gaze patterns were obtained if the observers assessed digital images of the packages presented on a computer screen instead of real packages.

Typically similar types of consumer goods are placed next to each other in stores, on the shelves of the grocery shops for instance. This grouping is especially strong along the horizontal axis. The consumers use only few seconds to make the final purchasing decision between the different brands. The packaging has to communicate brand, product and price information efficiently and thus the visual design of the packages is very important. Real packages or physical mock-ups are used in many consumer tests. This is somewhat time-consuming and not always possible. The motivation for the study was to test whether it is possible to speed up the testing by using computer generated images instead of physical packages in consumer tests. The research question was whether or not similar gaze patterns were obtained if the observers assessed digital images of the packages presented on a computer screen instead of real packages. This was studied by comparing the eye-tracking results obtained in these two conditions.

Conclusive results were not expected due to the limited scope of the experiments, compared to the complexity of the perceptual and cognitive processes involved in the perception of packages. Instead, the motivation for the study was to test the measuring of gaze pattern data in two types of simplified experimental setups, and to find clues of possible significant differences, if any, in the way that computer-displayed images of packages and real packages are viewed. These findings could then be taken into account in future research of visual package design and positioning, and could be used as a basis for more in-depth studies of the observed perceptual phenomena.

The experimental setup involved a package evaluation task during which the eye-tracking data was recorded and a subsequent interview of the observers. The evaluation task was designed to give the observers a realistic motivation for viewing the packages, and the interview was done in order to obtain further information for interpreting the eye-tracking data. The experimental setup is described in the following sections. The results of the experimented are then presented. Finally, the results are discussed, and conclusions are made.

## 2. Experiment

A set of three different juice cartons, shown in Figure 1, was prepared for the experiments. Each carton was approximately 7 cm wide and 23 cm high.

10 people (2 females, 8 males, aged from 16 to 51) participated in the subjective evaluation. 5 of the observers evaluated the samples while sitting on a chair so that their eyes were approximately 60 cm from the cartons. The cartons were placed side by on a neutral grey cardboard in front of the observer. The cardboard extended behind the samples and to the sides, providing a uniform background for the evaluation. The movement of the observers' heads was not restricted but they were instructed to avoid moving their heads during the experiment.

The other half of the observers sat on a chair in front of an Eizo ColorEdge CG220 computer display in a similar viewing configuration. These observers performed the same evaluation task by viewing a picture of the juice cartons on the computer monitor. A satisfactory appearance match between the displayed image and the real cartons was obtained by using a colour-managed workflow from photography to display. The original RAW image from the Canon 20D digital SLR camera, shot in controlled lighting conditions, was processed in Adobe Photoshop Lightroom and Adobe Photoshop, using an image of the GretagMacbeth ColorChecker as a reference for colour reproduction. The display was calibrated and its ICC profile was used in producing the final display image. The size of the packages in the displayed image matched the size of their real-world counterparts.



*Figure 1: The set of three juice cartons used as samples in the experiments*

The luminance levels were similar between the computer display and the real cartons. Both the computer display and the real cartons were evaluated in VTT's research environment for visual communications under controlled illumination. The room is not exposed to outside light and has adjustable illumination and mid-grey walls. Indirect illumination from fluorescent daylight tubes, reflected from the ceiling and approximating the D50 standard daylight illuminant was used during the experiments. The illuminance at table level, on which the samples were placed, was approximately 500 lx. The lighting conditions corresponded to the conditions P2 defined in the standard ISO 3664:2000 for practical appraisal of printed products. The white point of the computer display was set to the luminance of 120 cd/m$^2$ and the chromaticity coordinates of the D65 standard illuminant.

The eye movements of the observers and the corresponding gaze patterns were recorded with the Sensomotoric Instruments (SMI) iView X HED eye tracking system. The system consists of two head-mounted cameras (an eye camera for tracking the movement of the pupil and a scene camera for recording the scene viewed by the observer) and a workstation with the necessary software for calibrating and controlling the cameras and capturing the eye movements. The system uses infrared illumination and real-time computer-based image processing to detect the centre of pupil and track its movements. System calibration makes it possible to map pupil location to a point in the subject's view. The subject's view is captured by the scene camera. The system output includes pupil and gaze position, and video data of the scene being viewed, as well as other data such as pupil size. This initial data can be further analyzed by pro-

ducing various kinds of visualizations and indices describing the gaze path, as exemplified by the results presented in the following section.

The observers were given the task of assessing the healthiness of the three products shown to them. They were told that they would be given 30 seconds to view the products, after which they would be asked to indicate which one of the products was the healthiest. The juice cartons, or their image on the computer display, were hidden behind a mid-grey cardboard before and after this 30-second assessment interval.

After making the choice, the observer's were briefly interviewed. They were asked to give reasons for their choice, describing what aspects of the packages they paid attention to when assessing the healthiness of the products. They were also asked to describe the other aspects of the juice cartons that they noticed and remembered, and their overall impression of each product.

## 3. Results

The initial eye and gaze tracking data was analyzed in the SMI BeGaze™ software. The data was also exported from the SMI BeGaze software to Matlab for further statistical analysis. Figure 2 shows an example of the scan path for an observer viewing the packages of the physical products. This can be compared to the example scan path from an observer viewing the computer display in Figure 3.



*Figure 2: Scan path for an observer viewing the real packages. Frame capture from a video showing the gaze location overlaid on the scene video. The point and crosshair cursor indicates the current gaze location. The trailing line depicts the gaze path during the last 10 seconds*
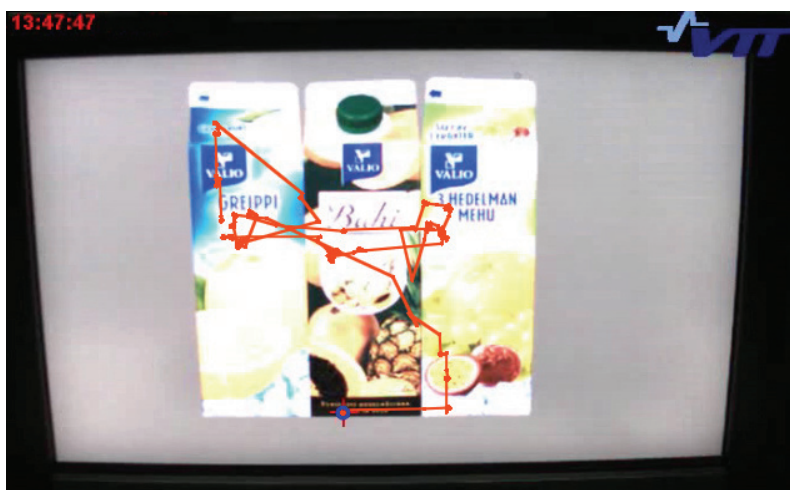


*Figure 3: Scan path for an observer viewing the picture of the packages on a computer display*

The scan paths in Figures 2 and 3 show a typical pattern of fixations around points of interest (text, signs, and salient features in the images) in the packages and pictures, and the saccades during which the gaze moves from one point of interest to another.

Overall inspection of the gaze paths using the scan path videos and still images, and other visualization methods such as heat maps (using a scale of colours superimposed over the scene image to depict the areas receiving most attention from the observer) showed that while there were expected differences between individual observers in the way they viewed the scene there did not appear to be consistent differences between the two cases. Typically the eye movements could be roughly divided into three sequences: the scanning phase to get an overview, detailed comparison of the products and the final decision stage.

Several numerical indices were used to describe and compare the gaze paths. A total of 31 indices such as fixation and saccade frequencies, average, minimum, and maximum values for variables such fixation duration, saccade amplitude and velocity were calculated for each observer's gaze path. Eye blinks were also detected and included in the indices. Student's t-test suggested no significant differences in any of the variables between the two groups of observers (those who viewed the real packages and those who viewed the images on computer display).

Specification of areas of interest in the scene facilitates further analysis of the gaze path relative to the objects in the scene. In this case each juice carton was specified as an area of interest for data analysis purposes, as indicated in Figure 4. Note that an area of interest is specified after the experiment by the researcher purely for data analysis purposes. The observer is not aware of such areas during the experiment and the areas do not necessarily have any connection to the observer's perception of the scene.



*Figure 4: Three areas of interest (AOI) specified for the analysis of the gaze path data*

A number of graphs and indices can be derived by relating the gaze path to the specified areas of interest. Figures 5 and 6 show the relative dwell time of the observer' gaze on the three areas of interest (the three juice cartons) as a function of time during the 30 second viewing period for an observer viewing the real packages and another observer viewing the picture on screen, respectively. The time intervals in the graph during which the relative dwell time percentages do not sum up to 100% (the columns do not reach the top of the graph) indicate that for a part of that time interval the observer's gaze was not on any of the areas of interest.
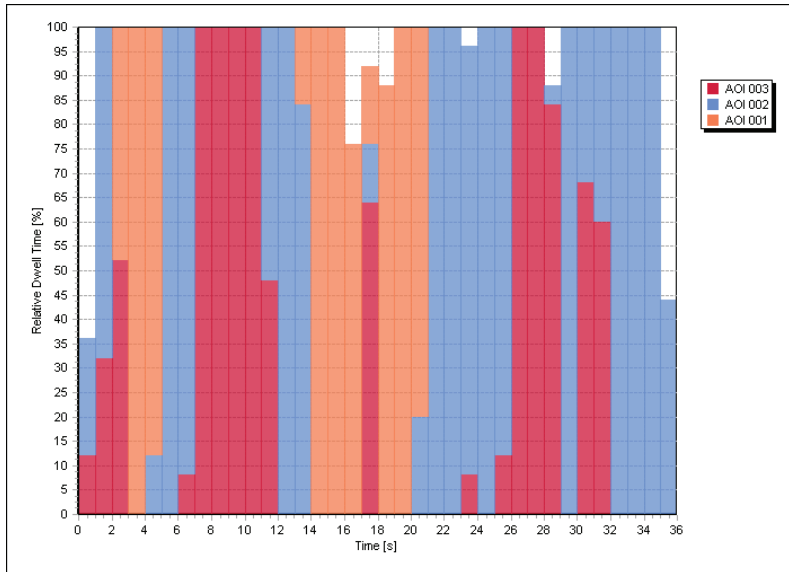
*Figure 5: Relative dwell time of an observer's gaze on the three juice cartons in 0.5 second intervals.
This observer viewed the real packages.*
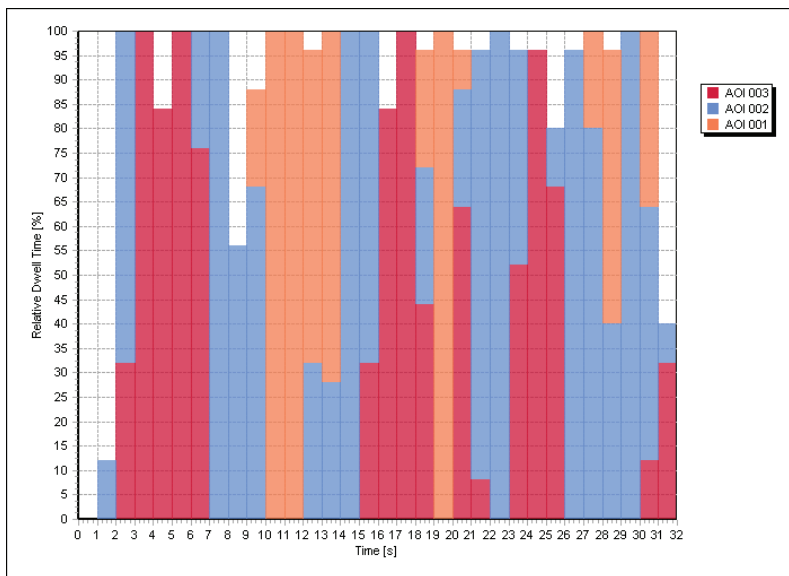


*Figure 6: Relative dwell time of an observer's gaze on the three juice cartons in 0.5 second intervals.
This observer viewed the picture of the packages on a computer display*

As with the gaze path graphs above, the graphs related to the areas of interest give no indication of any significant bias in the observer's gaze pattern when viewing the picture on the computer display instead of the real packages.

A number of further numerical indices related to the areas of interest were calculated for each observer and each area of interest. In addition to dwell time data presented above indices such as glances count (the number of saccades that entered the area from outside) and fixation count (the number of fixations inside the area) were analyzed. As with the other indices above, the t-test revealed no significant differences between the two experimental conditions in any of the indices related to the areas of interest.

Incidentally, the distribution of choices among the three juices was also identical between the two cases. In both groups 3 observers chose juice 2 as the healthiest one, and juices 1 and 3 were each chosen by a single observer in both groups. The interview results were consistent with the gaze patterns, and did not suggest any considerable differences between the two experimental conditions either.

## 4. Discussion

Summing up the results presented in the previous section, no evidence was found of consistent differences in gaze patterns when viewing pictures of packages on a computer screen instead of the real packages. It should be stressed, however, that the low number of subjects used in the experiments means that differences in the gaze paths would have needed to be quite obvious to show up as statistically significant. A considerably larger number of observations would be needed to reliably identify less remarkable, but still possibly practically significant differences in the gaze patterns when viewing computer-displayed images of packages. Furthermore, a simplified experimental setup was used that forced the observers to view the real packages from a fixed angle. This essentially reduced the subjective assessment task to a visual inspection of 2-dimensional surfaces in both cases. The results would likely have been different, and certainly much more difficult to compare between the two cases, if the subjects had been allowed to touch the packages or even to view them from different angles.

Indeed, in this case care was taken to make the viewing conditions as similar as possible in the two cases. This kind of side-by-side viewing of packages without touching can be seen to be reasonably similar to the real-life scenario of initial viewing of products tightly arrayed on the shelves of a store. The fact that no striking differences was found between viewing the computer-displayed pictures and the real packages in this experimental setup suggests that computer-displayed images could be used at least in the first stages of testing the subjective response to different package designs, simulating the visual experience of viewing packages on the shelves of a store. Even then care needs to be taken not to bias the results by introducing error from factors such as inaccurate colour reproduction or geometric distortions of the packages in the computer-displayed images. In practice, instead of using computer-displayed photographic pictures of packages (as was done here) computer-generated images based on package design files would likely be used. A natural progression would then be to render 3D models of package designs on computer screens. This kind of evaluation setup could include interaction, allowing the subject to control the angle from which he package is being viewed. This would facilitate more realistic visualization of the 3-dimensional nature of the package, as well as visualization of special effects such as metallic elements or spot varnish that depend on the specific illumination and viewing geometry to catch the eye of the viewer.

Although benefits are seen in using soft-proofing in studying the subjective response to visual packaging designs, the above discussion does not intend to suggest that physical packages are not needed in the research of consumer response to different kinds of variations in the attributes of packages. On the contrary, in practice multiple types of research methods are often used and the results from multiple experiments integrated in the analysis to gain a more complete understanding of how the various attributes together form the overall subjective experience of the product. The multimodal nature of perceiving packages alone makes it necessary to use physical samples in subjective experiments: the role of the touch and feel attributes in the consumer experience cannot be evaluated using computer-simulated packages. In this framework gaze tracking is a tool that, when used in conjunction with other methods such as interviews or psychometric scaling, can provide useful additional information that helps in interpreting the results.

## 5. Conclusion

The difference of subjectively assessing visual package designs using either the real physical packages or their pictures on a computer screen was studied in experiments using an eye tracking device. Analysis of the gaze path during the viewing of the packages or pictures of the packages showed similar patterns between the two cases. The variation between the observers appeared larger than the variation between the two cases. Due to the limited scale of the experiments, the results cannot be taken as conclusive evidence that there are no significant differences in the gaze patterns between viewing real packages and their images on computer screens. On the other hand, neither did the data point to any obvious differences, suggesting that simulating package designs on computer screens could be a feasible option to producing actual packages or physical mock-ups to test the consumer response to visual package design, at least in some instances in which the 3-dimensional form and the touch and feel attributes of the packages are of lesser interest.

## References

Duchowski, A. Eye Tracking Methodology, Springer London, 2007, 328 p

# A market survey of Variable Data Print (VDP) on fibre-based packaging in North America and Europe

*Marcus Rehberger*[1, 2] *and Valériane Vigne*[3]

[1] Innventia AB, Drottning Kristinas Väg 61, 114 86 Stockholm, Sweden
[2] Royal Institute of Technology Stockholm, School of Computer Science and Communication, Sweden
[3] ICGQ - The Quebec Institute of Graphic Communications, Montréal, Canada

E-mails: marcus.rehberger@innventia.com and vvigne@icgq.qc.ca

**Abstract**

Variable data will play a decisive role in the future of packaging and product promotion. Inkjet printing is the most suitable technology to apply variable data on packaging and to offer customized and even personalized prints for the industry and the end-consumer. To obtain a picture of the industries' view on variable data print on fibre-based packaging, a market survey was initiated and was addressed to people in the development, marketing and decision-making sectors of the packaging and printing industry, including manufacturers of machinery, producers of packaging and prints and print buyers. The goal was to draw an overview map covering the people's view on their market, trends in their fields and how they envision the future of VDP on fibre-based packaging.

**Keywords:** market survey; inkjet; variable data print; packaging

## 1. Introduction

The packaging industry is one of the largest industries world-wide. Its turnover in 2008 with packaging container sales was USD 500 billion (Anon, 2008), a USD 203 billion packaging printing market (Davis, 2010) and estimated packaging machinery sales of USD 25 billion. Packaging is used in almost every industry sector and besides protecting goods for safe transport from A to B, it needs to be labelled with variable or static information, e.g. logistics data or information/description for the customer. For variable data, a common method is to use sticky labels, but static data on fibre-based packaging is generally printed by flexography or lithographic offset. Nowadays, package printing is very diverse and can be high quality for advertising reasons or fulfil minimum requirements for marking, such as logotypes or basic information.

The type of package, e.g. primary, secondary or tertiary packaging, is a further crucial factor with regard to print quality. A primary packaging (pP) is defined as being the packaging in direct contact with the product, and depending on the product, it is printed or unprinted. This means that a plastic bag for cereals is not printed, but the milk carton is. When the primary packaging is not printed, the secondary packaging (sP) fulfils this task. The tertiary packaging (tP) is mainly used for distribution of the product within its primary and secondary packaging. Print quality, therefore, has to fulfil minimum requirements. For the tP, it is most important that bar codes, 2D codes and other taggings / markings are readable with automatic devices or by a person. For pP's and sP's, high print quality is a crucial factor, especially for products sold to the end-consumer. Industrial customers are less demanding and their choice of which product to buy is not dependent on the print quality.

In the case of the end-consumers, the product has to be outstanding on the shelf and she needs to be attracted by the print (Calver, 2004; Meyers, et al., 1998; Paine, 1992) because most buying decisions are in-store decisions (Ambrose, et al., 2003; Shimp, 2008). The behaviour of the consumers and the industry confirms the trend that the packaging is playing an increasingly important role in the marketing (Löfgren, 2006; Olsmats, 2002).

Very precise machinery is necessary to achieve high print quality. In packaging printing, the flexographic method has developed as the most applicable technique because its soft printing forme adapts to the substrate surface and is thus capable of printing uneven and rough surfaces such as corrugated board and cardboard. Packaging printing has developed into a very sophisticated process, and the very high print quality achieved is used by marketing divisions for the smart advertising of products. However, to sell a product in-store and to have an outstanding packaging compared with other competing products on the shelf, new commercial gimmicks need to be found and adapted to catch the customer's attention.

Variable data is commonly used in a magazine's mailing process, when the recipient's address is printed with inkjet technology (Mejtoft, 2006a), and in packaging printing for tagging / marking the package (Dante, et al., 2000; Stack, 2003). However, in none of these applications is the variable data printed in high quality into the printed static image. It shall not be possible for a consumer to distinguish between variable and static printed elements, and the variable elements can consist of regional or seasonal content, local languages, bar codes or anything else that can be customized on primary and/or secondary packaging.

In the case of fibre-based packaging, variable data printing (VDP), e.g. inkjet, is used in combination with a conventional printing method, e.g. flexography or offset. This combination of two different printing methods is called hybrid printing and the elements involved combine to offer completely new possibilities (Viström, et al., 2006).

The trend within the industry towards inkjet printing on packaging is visible in various ways. Numerous printing and packaging conferences and trade fairs have inkjet printing as a major topic, and Davis (2010) predicts in his forecast an increase from 8,5 % (2008) to 19,3 % (2014) regarding the machinery on the US market. Nevertheless, little research is evident within this area, especially regarding technical issues, but Mejtoft (2006b) and Viström (2008) have published papers regarding the economic and theoretical issues, and Rehberger et.al (2010; two publications) studied the technical issues of inkjet printing on fibre-based packaging.

To show the possibilities of hybrid print in combination with printed VDP features on fibre-based packaging, this survey was initiated. A questionnaire was sent to people in the development, marketing and decision-making sectors of the packaging industry (manufacturer, producer and print buyer). The goal was to draw an overview map covering people's view on their market, trends in their fields and how they envision the future of VDP on fibre-based packaging.

## 2. Method

The questionnaire was designed and deployed by Innventia AB, Stockholm, Sweden, and The Quebec Institute of Graphic Communications (QIGC), Montréal, Canada. It was a collaborative project to cover the North American and European markets.

### 2.1 Questionnaire structure
The questionnaire incorporated 20 questions and Figure 1 shows the general structure of the questionnaire starting with a welcome note (part 1) followed by general questions regarding business-related details of the participant (part 2) and his company (part 3). Part 3 included questions designed to assign each participant a place in the later analysis and a more detailed statistical examination.



*Part includes a question which is mandatory to continue

**In part 4 is questioned the knowledge regarding the converting process of fibre-based packaging. Participants without this knowledge skipped part 5 and were directly forwarded to part 6
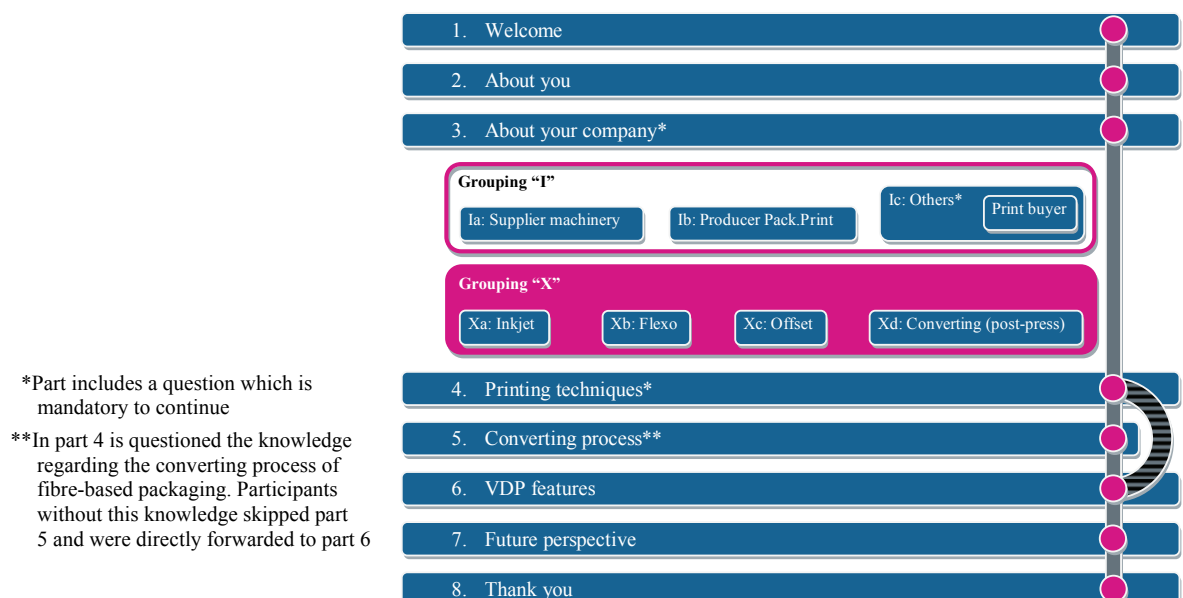
*Figure 1: General structure of the questionnaire*

The first grouping of participants "I" was related to the business area, whether the participant was a) supplier machinery (Ia), b) producer packaging print (Ib), c) print buyer or d) other (Ic). Since there were very few participants in group C, this group was assigned to group D (Ic). In the grouping "X", the relevant data was based on how large a percentage of the company's business was assigned to substrate, inkjet, flexography, offset, screen and converting (post-press) and the following percentage steps were selected: less than 10%, 10 - 25%, 25 - 50%, 50 - 75%, 75 - 90%, 100% or not applicable (n/a). In group Ia, the choice substrate was excluded (see Figure 4), because the questionnaire was not addressed to manufacturers of paper machines. For the later analysis of grouping "X" only the following groups were included: inkjet (Xa), flexo (Xb), offset (Xc) and converting (post-press) (Xd).

Part 4 sought to assess how familiar the participant was with printing techniques and his impression of inkjet within the conventional printing industry. If the participant was familiar with printing and converting processes of the fibre-based packaging industry, he continued with part 5, otherwise he continued to part 6. Part 5 "Converting process" included technical questions regarding the implementation of inkjet, whereas part 6 discussed concrete VDP features. The final part discussed the future perspective of inkjet, VDP and conventional print before the participant was thanked and asked to fill in his name and email address for preliminary results, final results and publications.

## 2.2 Questions

The detailed structure of the technical questions of parts 4 to 8 is shown in Table 1. Part 4 sought to establish how familiar the participant was with the printing and converting processes of fibre based packaging and how they see inkjet printing, if it is a complement to the conventional printing world or not.

*Table 1: Detailed structure of questionnaire beginning with part 4, incl. the questions with answers or instructions*

**4. Printing techniques**

    4.1. How familiar are you with printing and converting techniques and its technical and/or economic state-of-the-art possibilities?

        *a) Not so familiar, b) Quite familiar, c) Very familiar*

    4.2. Conventional printing techniques are very well developed within packaging print on fiber-based packaging. What is your opinion: will the new emerging inkjet technology be a competitor to conventional printing systems or will it complement them in the future?

        a) It will complement, b) A competitor, c) Both, it will complement but is a competitor, d) Neither of the above

**5. Converting process**

    5.1. Several locations are possible to implement an inkjet unit "in-line" in the converting process. Could you mark the most applicable location(s), which is/are in your opinion easy upgradeable with an inkjet unit and would NOT impact the production process.**

        *a) Conventional printing machine*         *d) Packer (stacking and packing of finished packages)*

        *b) Die-cutter*         *e) Other unit (Please specify "Other unit")*

        *c) Folding-gluing machine*         *f) It is NOT possible to implement*

    5.2. Implementation of an inkjet unit in the converting process of corrugated board or cardboard could raise technical and/or financial issues. Such issues could stop your company to invest in VDP. Please rate the following issues:*

        *a) Lack of speed*         *d) Costs for upgrading existing machinery*

        *b) Insufficient space for integration*         *e) Costs for new machines equipped with inkjet units*

        *c) Environmental issues (e.g. dust)*         *f) Other Issue (Please specify "Other issue")*

**6. VDP features**

    6.1. Could you rate the importance of the following VDP features printed on fiber-based packaging?*

        *a) Catch of attention of a consumer at the Point of-Sale (e.g. promotion campaign)*

        *b) Enhanced security features (e.g. pharmaceutical products)*

        *c) Simplified communication of information between product and consumers (e.g. customized info on packaging)*

        *d) Variable data for logistics and distribution*

        *e) Customized data to target consumers directly (e.g. consumers name on packaging)*

    6.2. Do you have 1 or 2 concrete packaging example(s) in your mind, where VDP features could be printed with a hybrid process? (hybrid process = combination of a conventional printing process with inkjet)

        *Examples and/or descriptions of applications can be written in two textboxes (A and B).*

**7. Future perspective**

    7.1. Please rate the following statements regarding the near future of inkjet and its applications in the packaging print of fiber-based packaging:*

        *a) The usage of VDP features on "primary" packaging will increase quite a lot with increasing opportunities*

        *b) The usage of VDP features on "secondary" packaging will increase quite a lot with increasing opportunities*

        *c) The keyword is to print VDP features "inline" in the converting process rather than off-line*

        *d) Your companies strategy will change with more advanced VDP features*

        *e) Conventional printing and converting machines will be sold with implemented inkjet units to print VDP features,*

        *f) De-inking of inkjet printed materials is still an issue and it will affect your decision to invest in inkjet technology*

\* Question is built-up as a matrix where the matrix row is mentioned above and the rating is done as follows:
  Not significant, Less significant, Neutral, Quite significant, Extremely significant, N/A

\*\* Multiple choices possible

The implementation of inkjet "inline" in the converting process is a key factor for variable data printing on fibre-based packaging. The technical part (5) therefore asked the participants to rate a number of possible implementation locations. The second question in this part asked about economic issues that might stop companies from investing in VDP. Inkjet print combined with conventional print offers many new VDP features and in part 6 the participant was asked to rate the significance of 6 mentioned examples. He was also asked to indicate possible practical examples of VDP features printed with a hybrid technology. In the final part, future perspectives of VDP were indicated with 6 examples and the participant again had to rate their significance.

## 2.3 Data collection

The questionnaire was announced in several groups on a business-oriented social networking site named LinkedIn (www.linkedin.com). These groups were exclusively for people from industry and an approval from the group leader is necessary to become a member. These groups covered inkjet business, general printing business and packaging business. In addition to this networking site, e-mails were sent to known companies and contacts. A blog webpage was also created for the public to reach the questionnaire, to distribute first information and to inform the participants of the preliminary and final results (http://mcrehberger.blogspot.com). The actual data collection was achieved with the internet tool Survey Monkey (http://www.surveymonkey.com). It allows a survey to be created online and all participants can access the survey through a link. All answers were collected automatically and the final result was downloaded for analysis.

## 2.4 Data analysis

After the data has been transferred from SurveyMonkey to Microsoft Excel it was analysed in two ways, first with all the participants in a single group and secondly separate into the different "I" and "X" groups. The scale of the survey was rather wide and, due to the grouping, there were too few participants in each group to perform statistical test. Therefore the data were directly converted into percentage values, related to the total numbers of participants in each group.

## 3. Results and discussion

### 3.1 Questionnaire - Introduction part (1-3)

The questionnaire was answered by 42 persons from 9 different countries, 76 % from North America and 24 % from Europe. A position of middle management or higher was occupied by 73 % (Figure 2) and 50 % were authorized for strategic decision-making. 45 % participated in decision-makings. Most were in sales (45 %), followed by R&D 19 %, production 12 % and marketing 10 % (Figure 3). The rest, 14 %, were working across multiple departments or could not be allocated. 42 persons participated this survey and, out of 30.000 to 40.000 possible participants from the LinkedIn groups, this is a representative number reflecting the industries view on VDP and its features within the packaging and printing business.
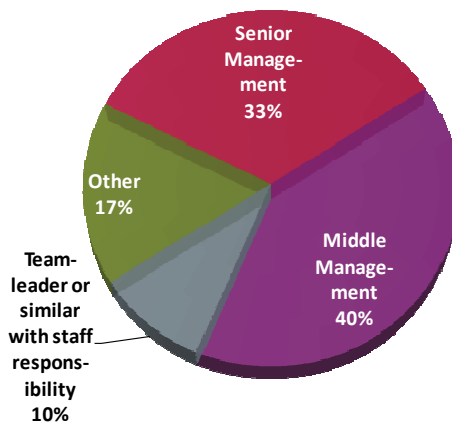


*Figure 2: Position of participant*          *Figure 3: Department affiliation of participant*
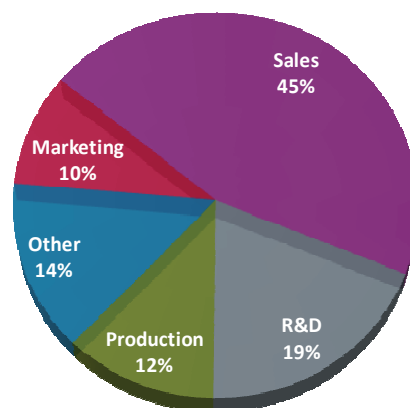
Grouping "I" had an even distribution with 33,3 % in each group. Grouping "X" was less evenly distributed. The choices were substrate, inkjet, flexo, offset, screen and converting (post-press), but the threshold for

inclusion was 50 % involvement in one of these business areas and the groups substrate and screen were excluded from the grouping "X". It was not possible to allocate all participants to a group.

*Table 2: Numbers of participants in each group*

| Total: 42 participants | | | |
|---|---|---|---|
| **Grouping "I"** | | **Grouping "X"** | |
| Group "supplier machinery | 33,3% | Group "inkjet" | 26% |
| Group "producer packaging print" | 33,3% | Group "flexo" | 12% |
| Group "others" | 33,3% | Group "offset" | 26% |
| | | Group "converting (post-press)" | 17% |

Figure 4 shows for each group the extent to which the companies are involved. A large proportion were involved in inkjet and offset print. In the case of flexo printing and converting (post-press), a very high percentage were not involved or the participants were uncertain and gave the answer "unknown". Most of the participants were, however, involved in several sectors, which is evident because the 0-50% fraction is largest in almost all sectors.
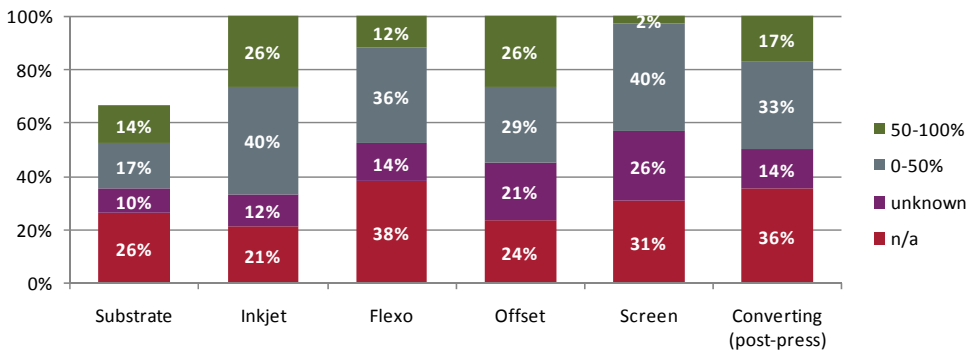


*Figure 4: The business area(s) involved in terms of production*

## 3.2 Questionnaire (part 4-7)

### 3.2.1 Overview all participants

Question 4.2 (Figure 5) asked whether inkjet will be a competitor or a complement to conventional printing in the immediate future. The result was that 43 % believe that it will be a complement, but 52 % consider that it will be a complement but also a competitor.

An inkjet unit can be implemented "in-line" at several locations in the converting process and question 5.1 (Figure 6) asked about applicable locations which can easily be fitted with an inkjet unit without interfering in the production process. It was possible to vote for several units and the folder-gluer received 48 %, although the conventional printing machine, the packer and the die-cutter received between 30 and 40 %. The conveyor, the filling machine, the palletizer, the labelling machine and the logistics and distribution facilities were all mentioned as possible locations for an inkjet unit. All these locations can be considered as serious possibilities.
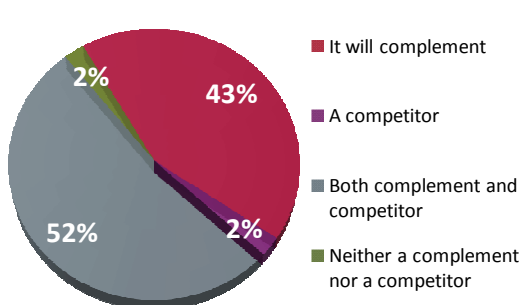


*Figure 5: Question 4.2; inkjet will be a competitor or a complement to conventional printing*
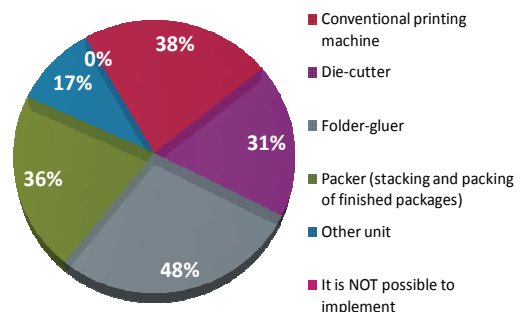


*Figure 6: Question 5.1; possible locations for introducing an inkjet unit into the converting process*

The inclusion of an inkjet unit in the converting of corrugated board or cardboard could raise technical and/or financial issues. Such issues could stop a company from investing in VDP. The participants were asked to rate the issues mentioned in question 5.2. The results are shown in Figure 7 and it is evident that the participants consider the costs for upgrading and for new machines as the most significant factor. New purchases are naturally very dependent on the return on investment.
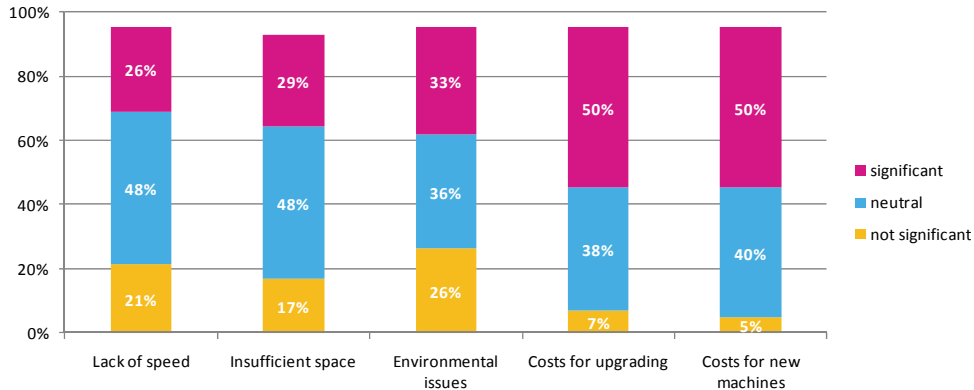


*Figure 7: Question 5.2; the significance of technical and financial issues*

Inkjet print is a so-called non-impact printing (NIP) method and the print head is continuously exposed to the surrounding air. In the cutting, stacking and conveying of fibre-based packaging materials in the converting process, a large amount of dust is generated. This dust is transported through the air around and inkjet nozzles could become blocked with visible print defects as a result. Redundant printing heads could minimize this effect, but the investments would be much higher. However, this environmental issue was considered by 26 % as not significant. The manufacturers of inkjet print heads are, of course, continuously improving their products and systems are becoming available capable of working even in rather dusty environments. The lack of speed and insufficient space were rated as being neutral. The lack of speed can be an issue, especially with inline implementation, but progress is being made and systems like the Kodak Versamark series are capable of printing 300 m/min and even higher if two arrays or more are linked with each other. The lack of space was said to be the least important issue, because inkjet print heads are usually small and the required control unit and ink delivery can be placed outside the converting machine. The participants had the opportunity to add comments, and the most significant ones were that speed and quality together are important for inline VDP such as material handling. Furthermore the problems of inkjet: image quality vs. substrate quality vs. speed and how they interact were mentioned. Other issues mentioned were the costs of consumables and how to convince the management to use VDP because of its great benefits.
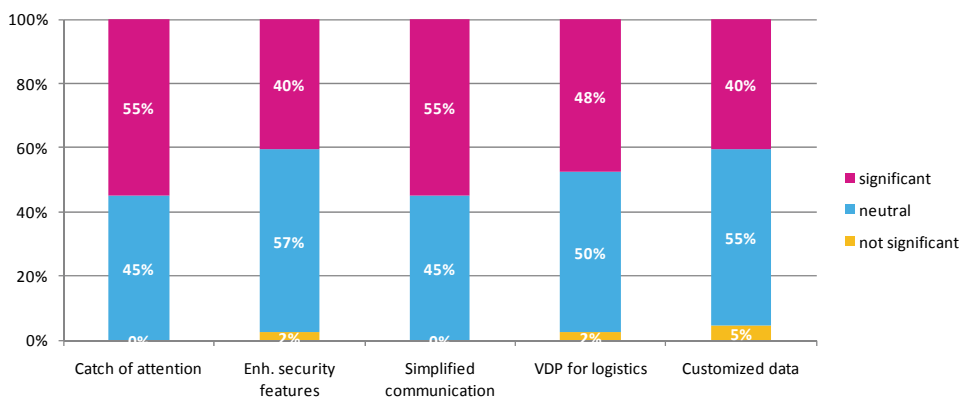


*Figure 8: Question 6.1; the importance of practical VDP features*

In part 6 the participants were confronted with practical VDP features. Three were considered to be only slightly significant. Those considered most significant were catching the attention of the customer and simplifying the communication of information between product and consumer, providing as much information as possible in a short time period. Both shall persuade the consumer to buy this product and not the competing product next to it. The use of customized data to target the consumer directly was considered by the participants to be less important.

Almost half the participants rated the use of VDP for logistics and distribution as a significant factor, even though the application of labels is common practice. The enhanced security feature was rated together with customized data as having the lowest significance, but 40 % is still a very significant number.

The participants were asked to indicate one or two concrete packaging examples, where VDP features could be printed with a hybrid process. The contribution was high even though some examples were related to other examples in the questionnaire and some were also mentioned by other participants. Most participants believed that customized prints with local-related, issue-related or individual-related advertisements have a great market potential. This could be an advertisement of a local athlete on cereal boxes in a local store or an advertisement on a shipped computer for a local retailer selling accessories. Another important feature was that local retailers, service providers or the like could sell products with personalized information. The last quoted example was to use inkjet for personalized marketing of retail shipping packaging, like internet shops to print not only variable but personalized information directly on the package.
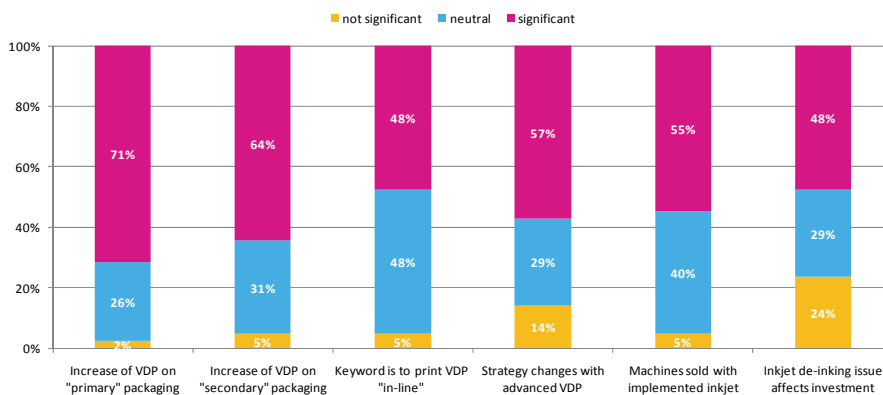


*Figure 9: Question 7.1; the immediate future of inkjet and its applications*

In the last part of the questionnaire the focus was on the future of inkjet and its applications in the printing of fibre-based packaging. The participants were asked to rate six statements. They were first asked if the usage of VDP features on "primary" or on "secondary" packaging will increase with increasing opportunities, assuming that more printers are offering printed products with VDP on a regular basis at a fair price. Primary packaging was rated as more significant with 71 %. Printing VDP features "in-line" in the converting process is important because off-line printing adds extra costs, storage and time. One participant commented that "the ability to easily add functionality to existing equipment without increasing floorspace, manpower, or operating footprint while extending functional life of existing hardware increases the value of integrating inkjet technology". Another commented, however, that "printing "in-line" converting would not utilize the full VDP capabilities without significant system changes", suggesting that upgrading existing machines might be less effective. Only 48 % rated this feature as significant.

The next statement focussed on company strategy and whether it would change with more advanced VDP features available. 57 % of the participants rated it as significant but 14 % as not significant, which suggests that the participants were very aware of their strategy for how to use VDP in the future. The statement regarding machines that will be sold with implemented inkjet units was rated as significant by 55 %. It can be assumed that the participants were aware of other businesses where VDP is a common feature and converting machines are equipped from the beginning or upgraded later with in-line inkjet units. The last statement was devoted to the environment and the de-inking of inkjet prints. The participants had to say whether it would not affect their decision to invest in inkjet technology and its products. 24 % said that it would affect their decision, but for 48 % it is a significant factor. This difference might reflect the different groupings of the participants.

### 3.2.2 Grouping "I": Supplier of machinery, Producer of packaging and print, and Others

The results were further analysed in relation to the different groups in grouping "I". This is not a repeat of the previous overview part, rather a closer examination of conspicuous answers.

In Figure 10 it is evident that the suppliers of machinery rated the folder-gluer machine as the most applicable location in which to implement an inkjet unit. The producers of packaging and printing, however, consider the conventional printing machine as a better solution. The group designated "others" had a neutral point of view.

*Figure 10: Question 5.1, configured for grouping I; possible locations to implement an inkjet unit into the converting process of fibre-based packaging*



*Figure 11: Question 5.2, configured for grouping I; rating of technical and/or financial issues*

With regard to technical and financial issues, Figure 11 shows that the machinery suppliers and others consider lack of speed and environmental issues to be less significant, whereas the producers of packaging and print have the opposite opinion. All groups have the same opinion regarding costs, whether they are related to upgrading or to investment of new machines.
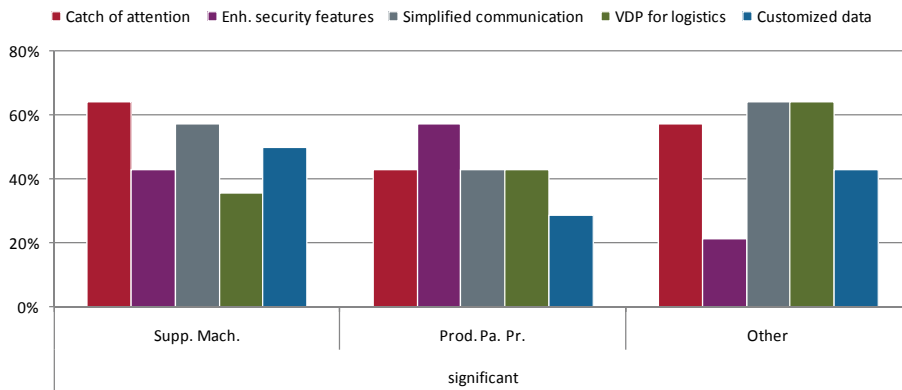


*Figure 12: Question 6.1, configured for grouping I; rating the importance of practical VDP features*

Figure 12, which relates to the importance of certain VDP features, shows only the "significant" votes of the grouped participants. There were few "not significant" votes and this trend was already very well visible in Figure 8. No group favours any particular VDP feature. The enhanced security feature is rated lower by the "others" group, than by the manufacturing groups.

Figure 13 shows that de-inking issues are considered to be insignificant by the suppliers of machinery. All further considerations by the participants in this question 7.1 are not outstanding and due to that not discussed.
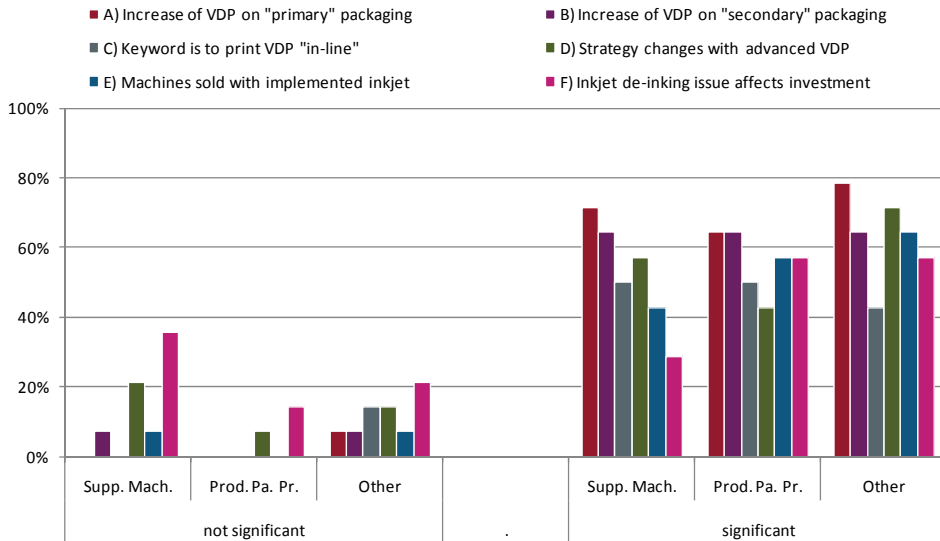
*Figure 13: Question 7.1, configured for grouping I; rating regarding the immediate future of inkjet and its applications*

### 3.2.3 Grouping "X": Inkjet, Flexo, Offset and Converting (post-press)

The question of whether inkjet will complement or compete was not discussed in grouping "I" because there were no significant statements, but it shows interesting differences in grouping "X". Figure 14 shows that 80 % of those mainly working with flexography believe that inkjet will complement conventional printing whereas 64 % of the inkjet group said that it will not only complement but also be a competitor. The other groups voted equally for these two suggestions, and only a very small percentage considered that inkjet will be a competitor.
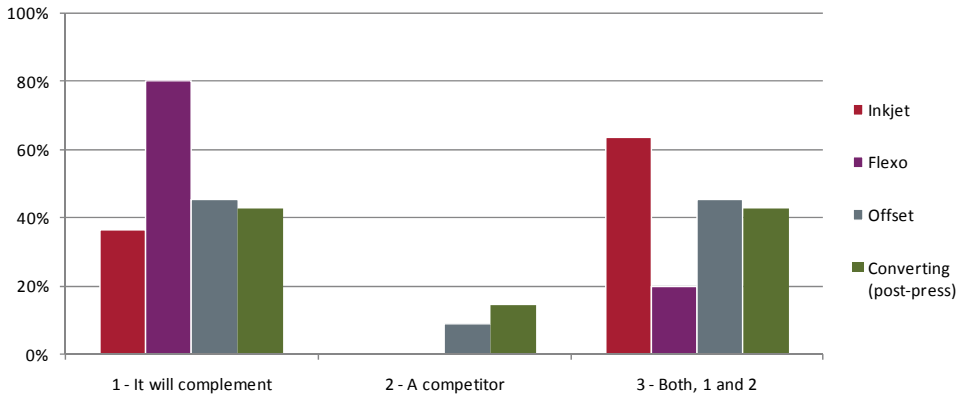


*Figure 14: Question 4.2, configured for grouping X; asking if inkjet print will be a competitor to conventional print or if it will complement it*
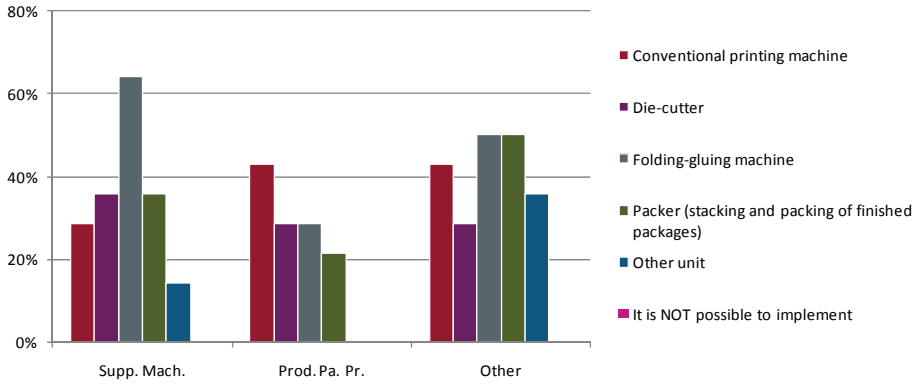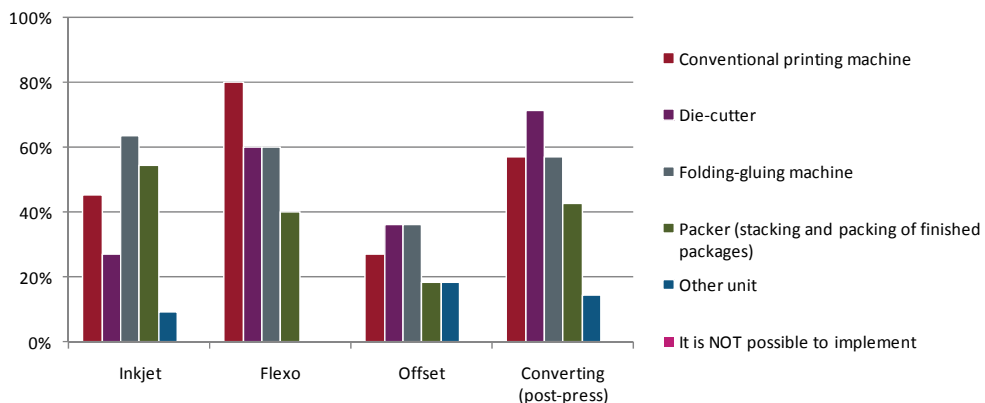


*Figure 15: Question 5.1, configured for grouping X; rating of possible locations to implement an inkjet unit into the converting process of fibre-based packaging*

Figure 15 shows no such clear trend regarding the implementation of an inkjet unit in the converting of fibre-based packaging, but some interesting facts can be read from it. The folder-gluer was favoured most in total, and 50 % in all the groups except offset voted for this location. The conventional printing machine was the second favourite and the flexography group gave it the most votes, perhaps because most flexographic printing machines are most common in the packaging sector and to implement a variable printing unit into such a machine made sense to them. The offset group showed a low interest in any location, and most participants in this group voted for a maximum of two locations. In this question multiple answers were possible and this led to high percentage values.
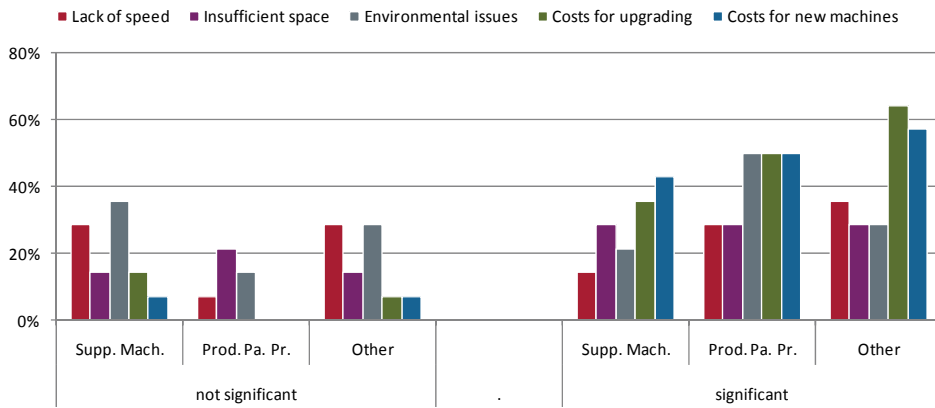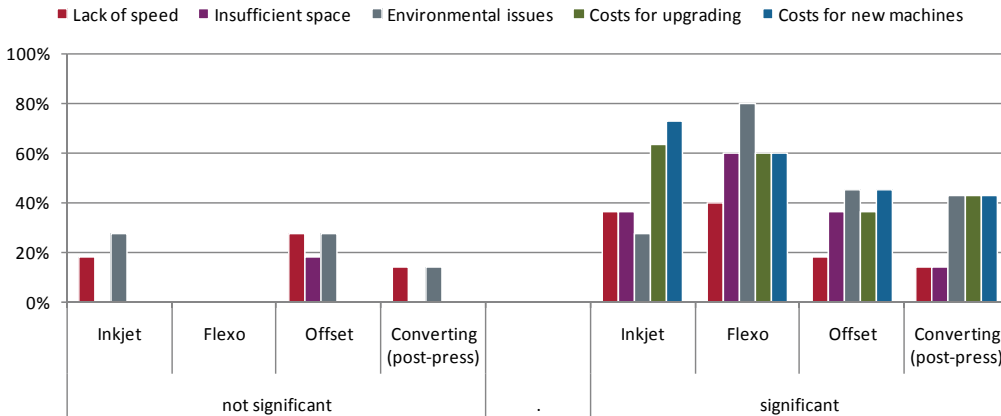


*Figure 16: Question 5.2, configured for grouping X; rating technical and/or financial issues*

With regard to technical and financial issues, Figure 16 shows that the flexo group considered none of the issues to be significant whereas all other groups did, especially the issues "lack of speed" and "environmental issues". To say that "lack of speed" is not significant has a positive effect on the development of inkjet, but the "environmental issues" is very conflicting because the environment is nowadays in any industrial field one of the high priority topics. The offset group had "insufficient space" as an additional issue on the not significant side. On the significant side, the "environmental issue" was rated highest by the flexo group, whereas the inkjet group gave it the fewest votes. All groups, especially inkjet and flexo, gave investments the highest rate. If a company were to invest in variable data print, the space for implementation is a further significant issue and if today's machines have "insufficient space" for integration and the money for new machines is not available, the company has to stop investing in such a technique. This issue was said to be very significant by the printing side whereas the converting (post-press) group had a neutral attitude. Another important issue for integration is the "lack of speed" and the inkjet group together with the flexo group rated this rather highly, but not the other two groups.
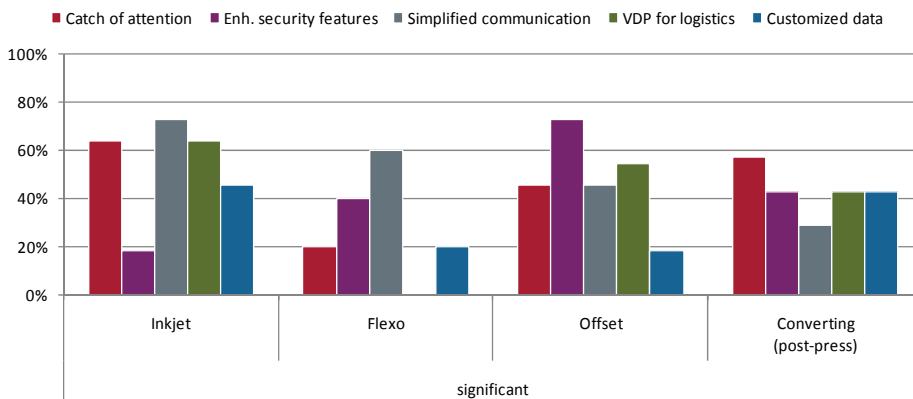


*Figure 17: Question 6.1, configured for grouping X; rating the importance of practical VDP features*

As mentioned before, no one considered any VDP feature as being "not significant" and only the significant ratings are included in Figure 17. There is no consensus within the four groups as to which VDP feature is the most significant. Catching attention is high rated mainly by the inkjet and converting (post-press) group whereas the flexo group rated it as being very neutral. On the other hand, both the flexo group and the inkjet group are highly interested in simplified communication between printed information on the packaging and

the customer. Another feature significantly rated by the inkjet group is to use VDP for logistics. The offset group agreed, but the flexographic group had a neutral attitude. To print enhanced security features with inkjet demands high and stable print quality and the offset group considers this point to be most significant, whereas the inkjet group believes that it is either less problematic to print with inkjet or that fewer applications for inkjet will be found in the future.
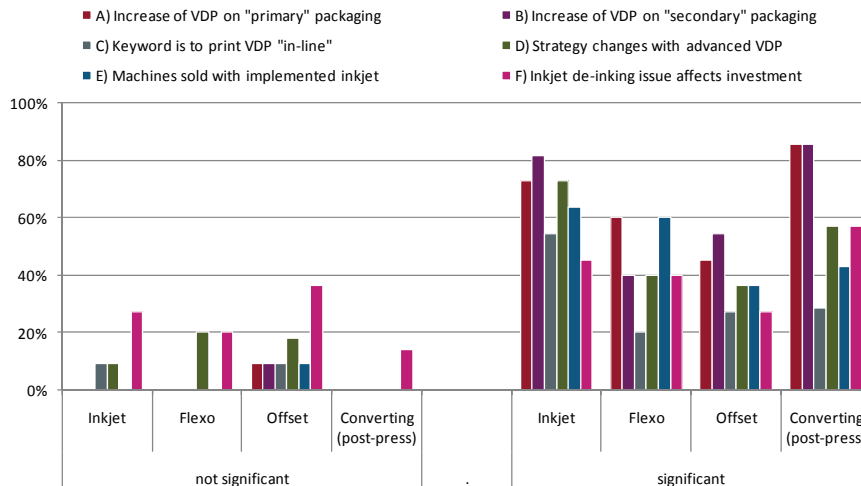


*Figure 18: Question 7.1, configured for grouping X; rating the immediate future of inkjet and its applications*

Figure 18 shows the ratings regarding the immediate future of inkjet and its applications, and the inkjet group rated all statements, except one, as very significant above 50 %. Environmental issues are nowadays a very sensitive topic and many companies have to work hard to minimize the detrimental effects on the environment. For the companies in this survey, however, the decision to invest in ink-jet would be influenced less by the question of the de-inking inkjet-printed substrates. All four groups rated it as not significant. On average, an increase of VDP in primary and secondary packaging was rated high by all four groups, the inkjet and converting (post-press) groups being around 80 %. The statement regarding the in-line implementation was rated only highly by the inkjet group. The other three groups rated it more neutral. Strategy changes due to more advanced VDP features were seen as significant, but less by the flexo and offset groups. The flexo group together with the inkjet group instead rated the statement E) "machine sold with implemented inkjet" very high, because it is very probable that the flexographic press producers will sell their machines with implemented inkjet units.

## 4. Conclusions

In all, 42 persons from both the European and North American printing and packaging markets, participated in this survey. To focus on certain groups and to draw more realistic conclusions, the analysis was done on the total and with two groupings, where the grouping "I" included the groups "supplier of machinery", "producer of packaging print" and "other", and the grouping "X" included "inkjet", "flexo", "offset" and "converting (post-press)". On most questions, all these groups more or less agreed regarding VDP with inkjet implemented in the converting process of fibre-based packaging. Some questions, however, were seen differently by some groups, mostly due to their business interest. A crucial element is to start thinking locally because, with increasing VDP opportunities, the application on primary and / or secondary packaging will also increase according to the participants.

This result can be seen not only in the total, but also in both groupings. The implementation of inkjet "in-line" in the converting process is then an important feature. Otherwise it would be impossible to accomplish large quantities where the static part is printed with conventional printing and the variable data part with inkjet. It is only a matter of time before this can be realized and single-pass inkjet units now print fast enough with sufficiently high resolution to be implemented in-line.

Costs are naturally a crucial factor, because investments in new machinery or upgrades of existing machinery are only made if the cost-benefit ratio is favourable. Upgrading existing machines is in most cases cheaper than investing in new machines and therefore it is important for inkjet to be an easy-to-integrate system.

A factor which was considered to be not significant was the de-inking of inkjet-printed substrates. Nowadays, all environmental issues are very fragile topics and worldwide all companies have to consider detrimental influences on the environment. In the printing business, conventional printed substrates, e.g. with mineral or vegetable-oil ink (offset) or solvent-based ink (gravure), are relatively easily de-inkable by flotation, but water-based inks, as used with inkjet printing, are not. Compared to conventional printed papers, the percentage of inkjet-printed papers, however, is very little and would not significantly influence the waste from the de-inking units. Therefore it can be assumed that for this reason the participants did not consider this issue to be significant.

Both the mentioned VDP features and the future of inkjet and its applications were rated on average as being very significant, and all the participants were very positive regarding inkjet, its applications and VDP features. This trend was also found in each group in the grouping sections. Therefore it cannot be stated that the traditional printing industry with its conventional printing machines has negative thoughts. The inkjet technology has to prove itself first and to increase its technical capability, and the printing industry will then start investing more in this technology and its applications such as VDP.

## Acknowledgements

## References

Ambrose, G., & Harris, P. (2003). *This End Up: Original Approaches to Packaging Design* (abridged ed.): Rotovision.

Anon. (2008). Position Paper - Market Trends and Devlopments (pp. 6): WPO - World Packaging Organization.

Calver, G. (2004). *What is packaging design?* : Rotovision.

Dante, H. M., Karles, G., & Basak, A. (2000). *Digital Printing in Industrial Packaging Applications: Current Status and a Road Map for Success*. Paper presented at the IS&T's NIP 16: International Conference on Digital Printing Technologies, Vancouver, BC.

Davis, H. R. (2010). Profiling Print Markets and Printers Post-Recession. *The Magazine, 2*(1)*,* 10-15.

Löfgren, M. (2006). *The Leader of the Pack - A service perspective on packaging and customer satisfaction*. PhD Doctoral Thesis, Karlstad University, Karlstad.

Mejtoft, T. (2006a). *Strategies for Successful Digital Printing*. Journal of Media Business Studies*,* 3(1), 53-74.

Mejtoft, T. (2006b). *Strategies in the Digital Printing Value System*.  Licentiate Thesis, KTH - Royal Institute of Technology Stockholm, Stockholm, Sweden.

Meyers, H. M., & Lubliner, M. J. (1998). *The marketer's guide to successful package design*: McGraw-Hill Professional.

Olsmats, C. (2002). *The business mission of packaging - Packaging as a strategic tool for business development towards the future*. PhD Doctoral Thesis, Åbo Akademi University, Åbo.

Paine, H. Y. (1992). *A handbook of food packaging* (2, illustrated ed.): Springer.

Rehberger, M., Glasenapp, A. O., & Xiaofan, Z. (2010). *VDP Quality aspects on fibre based packaging - an elementary print quality study on corrugated board liners*. IARIGAI Journal*,* 01(01).

Rehberger, M., Odeberg-Glasenapp, A., & Örtegren, J. (2010). *VDP on packaging - elementary velocity study on inkjet-printed papers for corrugated board production*. Paper presented at the 62nd Annual Technical Conference of TAGA, San Diego, CA, USA.

Shimp, T. A. (2008). *Advertising Promotion, and Other Aspects of Integrated Marketing Communications* (8, revised ed.): Cengage Learning.

Stack, K. (2003). *What you need to know about inkjet*. Print and Paper Europe*,* 15(3), 10-11.

Viström, M. (2008). *Aspects of the Impact of Technology Integration on Agility and Supply Chain Management - the Potential of Digital Packaging Print*.  Doctoral Thesis, Lund University, Lund, Sweden.

Viström, M., & Gidlund, Å. (2006). *Model for Print Quality Evaluation of Hybrid Printed Matter*. Paper presented at the TAGA 2006: Proceedings of the Technical Association of the Graphic Arts, Vancouver, BC.

# The challenges of high-speed inkjet printing in the offset world

*Taina Lamminmäki, Hille Rautkoski, Anna Leena Kokko, John Kettle*

VTT Technical Research Centre of Finland
P. O. Box 1000, FIN-02150 VTT, Espoo, Finland

E-mails: taina.lamminmaki@vtt.fi, hille.rautkoski@vtt.fi, annaleena.kokko@vtt.fi, john.kettle@vtt.fi

**Abstract**

There are increasing expectations to be able to the print the same paper by offset and inkjet printing either during the same printing time, hybrid printing, or to be printed with inkjet after offset printing. In hybrid printing, one-colour printing is quite often utilized to "personalize" the printed product. This certainly puts new challenges on the absorption properties of offset coating paper grades. From the offset printing point of view, the structure should not absorb the oil and resins of the ink too quickly into the paper structure and so raise the splitting forces in the printing nips. However, when considering the inkjet, the really high ink amount, compared to the amount of offset ink, should absorb very quickly into the structure. The absorption volume of coating layer should also be high for use with inkjet. However, in offset printing the pore volume does not need to be high. In both cases the colorant of the ink should stay in the top part of the coating layer. The aim of this work was to clarify how the structure of offset and inkjet coatings affects the print quality of high-speed inkjet printed surface. The results show that offset coatings have too low porosity and too large pore diameters to prevent the colorant of inkjet ink to penetrate too deep into the coating structure. The inkjet dye fixing requires the opposite charges between the ink colorant and the coating layer. It seems that the optimal coating layer structure for the multipurpose printing needs a compromise in the structural properties of nowadays offset and inkjet coatings.

**Keywords**: inkjet printing; offset printing; curtain coating; porosity; permeability; ink penetration

## 1. Introduction

The market share of inkjet printing is increasing all the time. Nowadays, we can find inkjet printed areas in traditionally offset printed products, for example as personalized or targeted information, and this trend becomes more and more common all the time. This puts certainly new challenges for coated paper grades. The paper surface should in offset printing take a couple grams per square meter of oil-based ink and fountain solution whereas in inkjet the ink amount can be several times higher and all this (water or solvent-based), should penetrate into the coating layer very quickly.

The absorption properties of offset and/or inkjet coating layers have been studied a lot in recent year (Sorbie 1995, Donigian 1997, Gane 1999, Schoelkopf 2000, Rousu 2000, Miettinen 2002, Ridgway 2002, Rousu 2005, Fouchet 2006, Desie 2006, Kirmeier 2008, Ström 2008). In the offset area, the interest has concentrated more or less on the different latex types and their amounts and coating pigments as well as how they affect on the absorption and the print quality. In the inkjet area, the focus has been upon the generation of less expensive pigments that produce coated paper with good print quality (Donigian 1997, Ridgway 2005). The coating colour recipes have also been developed by modifying the binder content and type or changing other additives.

### 1.1 Objective

The objective of this work was to understand the performance of offset and inkjet coating formulations to generate curtain coated layers for high-speed inkjet printing and how the differences in coating layer structures affect the formation of inkjet print quality. Observations of the printed surfaces were made on-line and off-line.

## 2. Experimental work

The curtain coater of the pilot plant of Metso (Järvenpää, Finland) was used to produce a three-layer coating structure where the top coating contained clay or calcium carbonate pigment for offset and inkjet coating purpose. In the bottom, there were two inexpensive coating layers. All the coating layers were coated simultaneously. The first coating layer contained HC60 (ground calcium carbonate, GCC) and Capim NP

(clay) and the second coating layer contained HC90 (GCC). The binder was styrene-butadiene (SB) latex. The top coating layer of offset coatings had HC60 and Hydragloss 90 (clay) and the binder was mainly SB latex. HC60 contained pigment particles, which had 60 wt-% of pigment particles below 2 μm diameter and Hydragloss 90 90-100 wt-% below 2 μm. The offset coatings had anionic nature. The top of inkjet coating contained JetCoat 30 (diameter 20-30 nm and the total average at 0.25 μm (measured with NanoSight) and specific surface area 80 $m^2g^{-1}$, PCC) and the binder was a partially hydrolyzed polyvinyl alcohol (PVOH). The coatings had a slightly cationic nature. The coating colours are introduced in Table 1. The coat weight of first coating was 8 $gm^{-2}$ and second layer 2 $gm^{-2}$. The top layer had coat weight of 6 or 8 $gm^{-2}$.

*Table 1: Coating colours*

| Component | Offset, more latex | Offset, less latex | Inkjet |
|---|---|---|---|
| HC60 (GCC) | 40 | 40 | |
| Hydragloss 90 (clay) | 60 | 60 | |
| JetCoat 30 (PCC) | | | 100 |
| Mowiol 4-98 (PVOH) | 0.3 | 1 | |
| DL 966 (SB latex) | 15 | 12 | |
| Mowiol 40-88 (PVOH) | | | 15 |
| Lumiten DF (surfactant) | 0.2 | 0.2 | 0.2 |

The uncalandered coated papers were printed with Versamark VX5000e (Oy Keskuslaboratorio, Finland) which uses aqueous dye-based inks. The printing speeds were 50, 75 and 100 $m \cdot min^{-1}$ and the drying temperature 70°C (both drum and air). During the printing process, on-line imaging with digital camera (Dolphin F145C) and gloss measurements were made. In the optical gloss measurement, the halogen light reflection was detected by voltage measurement. High voltage means high gloss. The papers were printed only in the inkjet press, not by offset. In the discussion part, we shall concentrate on the results of inkjet printed samples and the effects in the offset printing area are discussed based on common knowledge. We have also defined in this study that the inks of inkjet and offset printing locate still in the different areas in the paper surface, not upon each other on the same printed area.

The bulk-density and absorption speed of coated papers were analyzed. The bulk-density was made by following the standard ISO 534:1988. The absorption speed was measured with the DIGAT device which measures the gloss change during the applied ink penetration into the structure (Lamminmäki 2007). The porosity of coating layers was studied with a silicon oil absorption test. During the Si-oil absorption, the pigment cake was left for one hour in Si-oil, and the weight of cake before and after Si-oil saturation was measured. The available porosity for oil absorption is defined as absorbed Si-oil volume in the coating cake divided by the sum of the coating layer volume without oil plus absorbed Si-oil volume, all determined at the normal atmospheric pressure.

The print density of the surface was measured with GretagMacbeth D196. The ink bleeding was analyzed with an Epson Perfection V700 Photo scanner system using a resolution of 2400 dpi. The grey level profile of the line was measured with an image analysis program using a definition of the points A and B. The point A was 15 % brighter than the darkest region and B 15 % darker than a background. The black surface had a grey value of zero and white of 254. Each unprinted paper was adjusted to the value 170. The normal edge width described the bleeding distance of inks. The total width of the line was also measured. It was defined as the distance from the starting of grey value increase in the beginning of black line measurement until the grey value reached again the lightest region (background value). The mottling was analyzed with a scanner system. The printed surface was scanned with an Epson Expression 1680 Pro scanner using resolution 300 dpi. The scanned figure was handled with a wavelet transform (PapEye program). The ink colorant penetration was studied by embedding the printed surface in LR White resin. The embedded sample was placed in a refrigerator to reduce smearing of the dye. The cross-cuts were made with a microtome cutter. The cross-sections were then imaged in a light microscope (Zeiss Axioskope 2 plus).

## 3. Results

The curtain coating succeeded well with the designed coating colours. The coated surfaces were not calendered and therefore the surfaces remained quite rough (Bendtsen roughness about 100 $ml \cdot min^{-1}$). Figure 1 shows how the inkjet coating produced a paper structure which had lower bulk-density and quicker inkjet ink absortion than the offset coatings. However, the abosrption times of 400-500 ms are not yet very high for

the inkjet papers point of view. The porosity (with Si-oil) of offset coating with the higher latex content was 13.7% and with lower 18.3% whereas the inkjet coating had clearly the highest porosity, 40.6%. The plate-structure of clay pigment produces a well packed (low porosity) structure with low liquid permeability which slows down the ink absorption speed into the surface (Figure 1, right side). A little higher bulk-density results in the PVOH containing offset coatings might be expained due to the PVOH pore filling effect. The PVOH fills some of the small size pores. Besides the filling effect, during the ink absorption process, the PVOH swells and it can further close the small pores (Lamminmäki 2009).
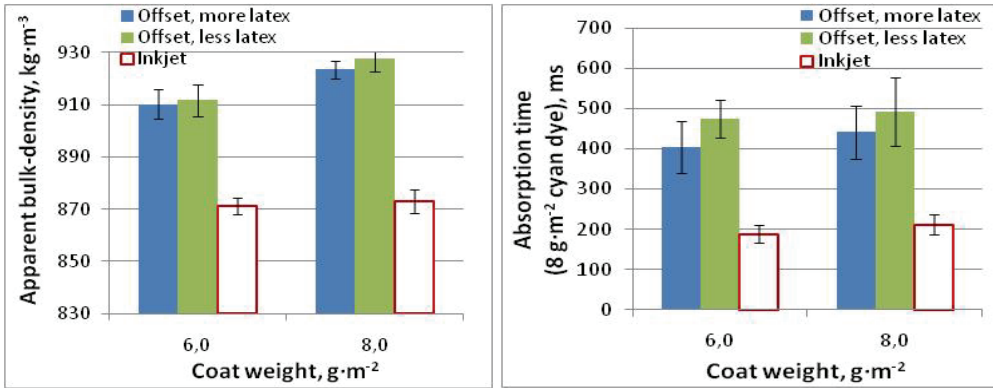


Figure 1: The bulk-density and the ink absorption time (measured with DIGAT device, 8 gm$^{-2}$ of Versamark VX5000e cyan ink)

The inkjet coatings produced a higher print density, a lower print gloss and less mottling than the offset coatings (Figure 2-4). The cationic charge of inkjet coating fixs the anionic dyes effectively in the coating layer. The higher gloss of offset coatings before printing are shown as a higher print gloss. However, the print gloss of offset coatings is still in a low level.
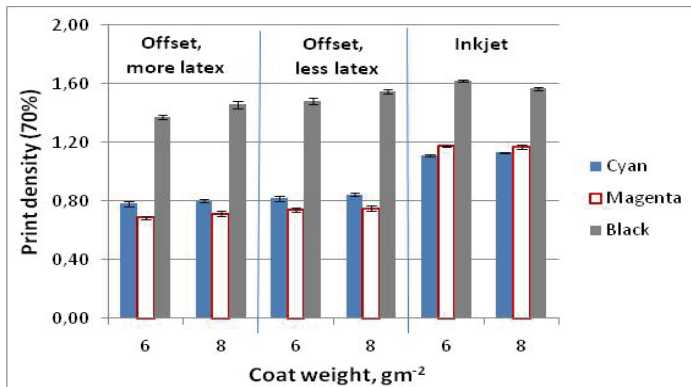


Figure 2: Print density (70% field) of offset and inkjet coating papers. Printed with Versamark VX5000e using 75 m·min$^{-1}$ speed
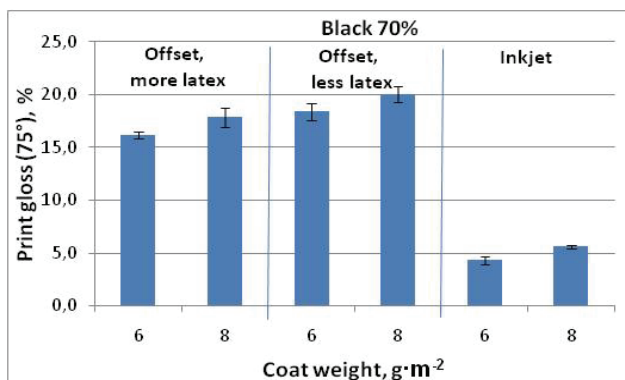


Figure 3: Print gloss (75° measuring angle) of offset and inkjet coating papers. Printing speed was 75 m·min$^{-1}$
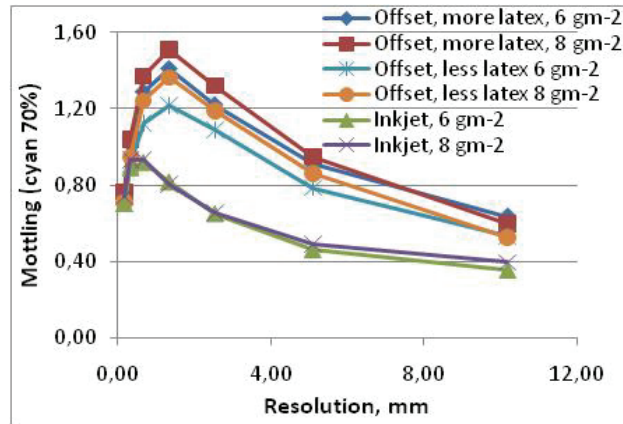
*Figure 4: Mottling (70% half tone dot field) of offset and inkjet coating papers. Printing speed was 75 m·min$^{-1}$.*
*Measured with scanner (PapEye-program)*

The ink bleeding results in Figure 5 and 6 show that on the offset coatings the width of magenta and black lines on the cyan surface were about 650 μm whereas on the inkjet coatings the widths were under 430 μm. The line width in the original image was 169 μm. The bleeding distances (the distance in the edge area of line where the inks have mixed) of inkjet surfaces were narrower than the distances on the offset coatings. The small size PCC pigments produced a structure which had a high porosity and there was a high frequency of narrow pores. This kind of structure had a high ink absorption speed giving less time for inks to mix together. There was also evidence of coating cracking. In the case of offset coatings, the inks stayed longer on the top of coating layer and therefore they have mixed more together.
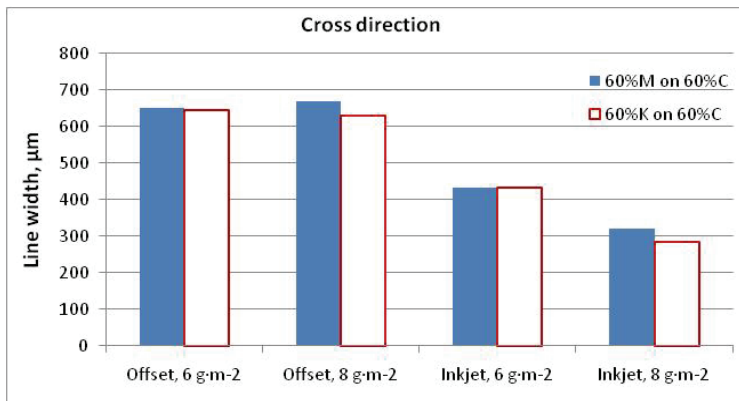


*Figure 5: The magenta and black line width on the cyan surface. The measurements were made*
*from 60% half tone dot surfaces. Printing speed was 75 m·min$^{-1}$*
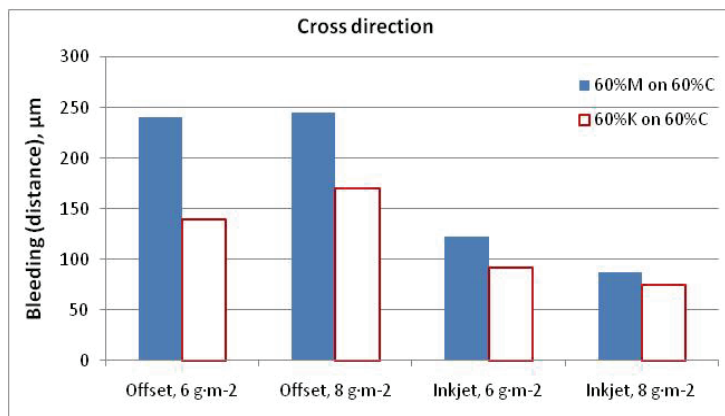


*Figure 6: The bleeding distances of magenta line on cyan surface and black line on cyan surface.*
*The measurements were made from 60% half tone dot surfaces. Printing speed was 75 m·min$^{-1}$*

## 4. Discussion

### 4.1 Effect of pore volume and absorption speed

The on-line figures after 1.09 s (speed 100 m·min$^{-1}$, Figure 7) from the cyan printing nozzles to the on-line imaging show that inkjet coatings had already less bleeding at this moment than the offset coatings. All the surfaces had "cracks" shown by the black ink on the cyan surface but they were shorter on the inkjet coating surfaces. On the offset coatings, the time delay increase from 1.09 s (speed 100 m·min$^{-1}$) to 2.17 s (50 m·min$^{-1}$) increased the bleeding and the width of black line became wider. This indicates that the porosity of offset coating is too low to absorb all the applied ink quickly enough into the coating structure and the longer time has given inks more time to mix and spread on the surface. For the inkjet coatings, this kind of ink mixing difference between these time delays could not be detected. The porosity and absorption speed of coating layer is so high that the first printed cyan ink has penetrated into the structure to such extent that the next printed black ink cannot mix with it. The absorption time of inkjet coatings were 200 ms (Figure 1) and the offset coatings about 400 ms.

If the 100 m·min$^{-1}$ surface had been observed after the same time delay as 50 m·min$^{-1}$ surface, it has probably had similar inks mixing or even higher. On the other hand, the lines of 100 m·min$^{-1}$ printed surfaces show one opportunity for offset coatings in the inkjet world: the colours had not mixed to a similar extent as those printed at low speed. If we could add a dryer very near the print nozzles or have a preheated paper web to speed up the evaporation process of inkjet ink solvent, we could get a better inkjet print quality also with the offset coatings.

|  | 50 m·min$^{-1}$ | 100 m·min$^{-1}$ |
|---|---|---|
| Delay between cyan and black: | 1.09 s | 0.544 s |
| Delay from cyan to on-line video: | 2.17 s | 1.09 s |



Offset, more latex, 8 gm$^{-2}$

Offset, less latex, 8 gm$^{-2}$

Inkjet 8 gm$^{-2}$
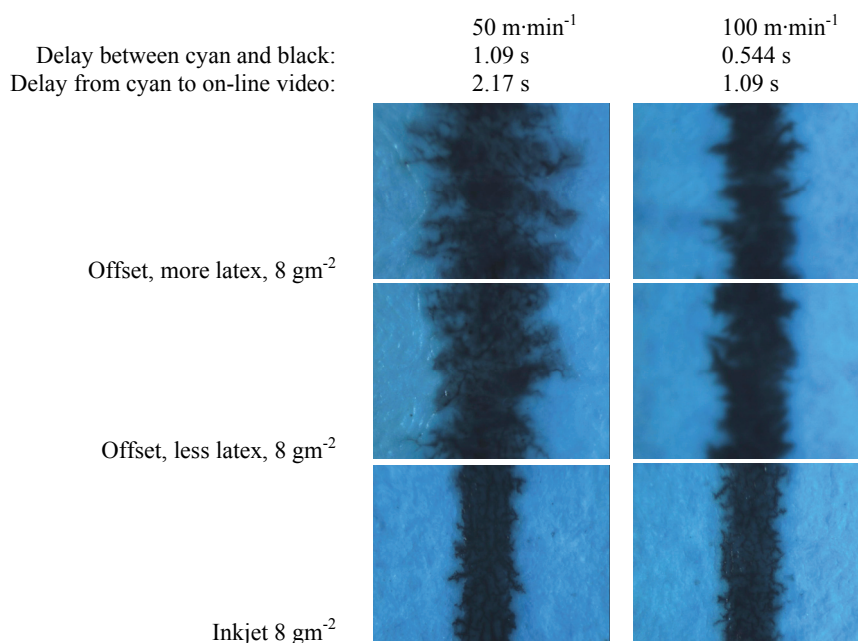
*Figure 7: The on-line figures of offset and inkjet coating papers. Distance from cyan nozzles to imaging was 0.542 m (time delay: 50 m·min$^{-1}$ - 2.17 s and 100 m·min$^{-1}$ - 1.09 s). The delay from cyan nozzles to black nozzles was in the speed 50 m·min$^{-1}$ 1.09 s and speed 100 m·min$^{-1}$ 544 ms*

The on-line gloss measurement shows how the printing speed affects the ink penetration. The distance between the cyan printing nozzles and the on-line gloss measurement was 2.17 m which meant that the time delays between cyan nozzles and the gloss measurement at the speed 50 m·min$^{-1}$ was 2.6 s and at the 100 m·min$^{-1}$ 1.3 s, respectively. Figure 8 shows the results of on-line gloss measurement. Unexpectedly, the gloss of coating layers decreased as ink was applied on the paper surface. It seems that the surfaces became rougher under the influence of ink. A possible explanation can be in the quick penetration of inkjet ink into the structure and water roughens the underlying base paper and lowers the gloss of the coated surface.

Figure 8 illustrates that the offset surfaces produced higher print gloss when a higher speed was used. There was more ink on the top of coating surface when the speed was 100 m·min$^{-1}$ than at the 50 m·min$^{-1}$ speed. The ink has not penetrated into the coating layer to the same extent as in the case of lower speed because of the shorter delay in detection. The figure shows also that the higher ink amount produced the highest gloss, as

expected. However, the gloss of inkjet coatings were very similar independently the speed of printing or studied ink amount. The surface can absorb the ink so quickly (absorption time was 200 ms) that most of the ink has already penetrated into the structure before the gloss measurement. The on-line measurement seems to be useful in the study of inkjet ink absorption and we can assess very well the bleeding tendency of printed surfaces.
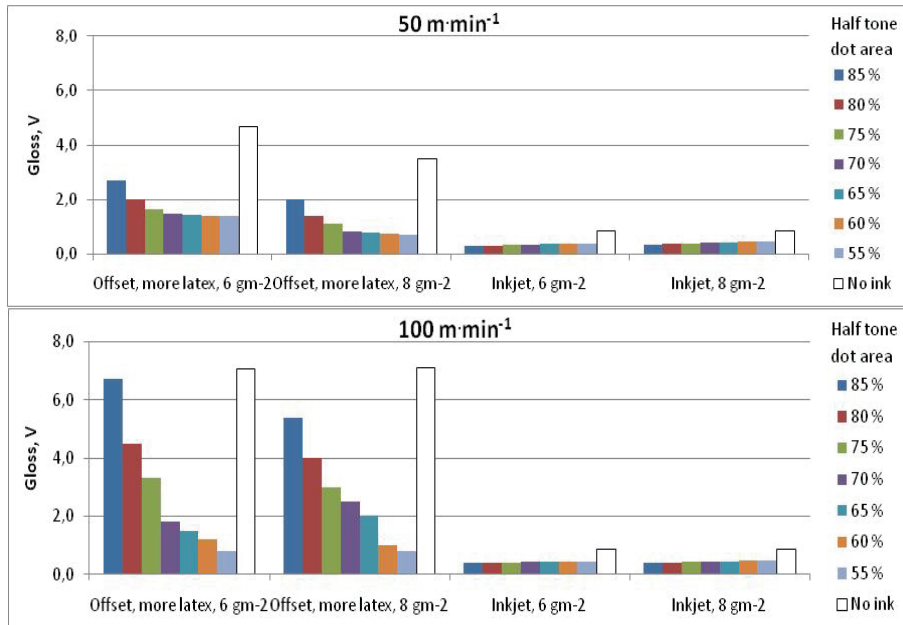


*Figure 8: The on-line gloss results of offset and inkjet coatings. The time delay between cyan and on-line gloss measurements was at 50 m·min$^{-1}$ 2.6 s and 100 m·min$^{-1}$ 1.3 s. The typical error of gloss results is ±0.2 V*

In offset printing, very fast ink setting caused by the high porosity of the substrate with very small pores means that the ink pigments with binder stay on the top of coating layer and the fountain solution penetrates quickly into the structure. The ink pigments form a uniform layer on the surface. However, different picking problems, like dry picking in the first printing unit and wet picking on the later units, can appear because some of the ink oil and resins penetrate too quickly into the coating structure and therefore the splitting forces in the printing nips increase. Wet picking can appear on the printed ink area or on the fountain solution area. In the inkjet coatings, the problem caused by the fountain solution is more obvious because the fountain solution can penetrate more quickly into the coating layer than the ink vehicle. High absorption speed and high pore volume can also mean that the oil with the ink pigments may penetrate too deep in the coating structure and therefore the print quality decreases. The offset printing requires generally higher surface strength, both dry and wet strength, than inkjet. The inkjet printing method does not set any surface strength requirements for coating layer. It is enough that the coating layer stays on the paper surface and does not fail during the inkjet printing process.

## 4.2 Print quality formation

### *Porosity*

The cross-section figures shown in Figure 9 illustrates that the coatings have very different types of structures. The inkjet coating has very small pores and then there are few large pores, cracks. In offset printing, the cracks can cause a partial ink penetration into the coating layer and so the print quality is worsened: the print density decreases, the print-through increases, the print gloss decreases and the mottling becomes higher. The offset coatings seem to have larger pores than the inkjet coating but there are not cracks.

Figure 9 shows how the colorant of dye-based ink has penetrated to the bottom coating of offset surface. This indicates that the offset coatings have had large pores in which the ink had transferred to the bottom part. The colorant location in the bottom of offset coating layer decreases the print density (Figure 2). In the inkjet coating, the colorant remains mainly on the curtain-coating layer. In the offset printing, the colour pigments stay on the top part of the coating layer. In that sense the inkjet coating forms an optimal structure for the offset prints.

Offset, more latex, 8 gm$^{-2}$               Offset, less latex, 8 gm$^{-2}$
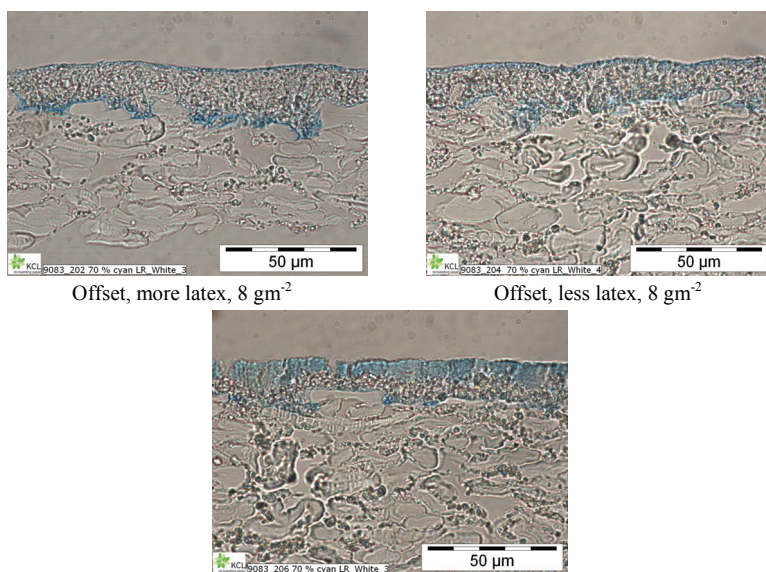
*Figure 9. The cross-section figures of offset and inkjet coatings which had coat weight of 8 gm$^{-2}$. They have been made from cyan 70% field. Printing speed was 75 m·min$^{-1}$ printing*

The on-line figures from the black line on the cyan surface (Figure 7) indicate that the structure of the offset coating is not optimal from the bleeding point of view. There was wider bleeding distance (Figure 6) than on the inkjet coating. It seems that the structure is not suitable in the several-colour inkjet printing. The absorption times were twice as long on the offset coatings than on the inkjet coating, but not so high that they could predict too low absorption speed for the inkjet purpose. The other reason for high bleeding can be in this case in the diameter and the amount of pores. The offset coatings do not have enough small size pores, like 20-60 nm, which could promote the inkjet inks uniform penetration into the structure. The mottling results show as well that the surface penetrated ink unevenly (Figure 4). There are places which could absorb the ink quickly into the structure and others which absorb slowly.

Print gloss is an important property for offset prints. If the target is to use the same coated paper both in the inkjet and offset press, it means that the porosity of coating layer should be optimized. The pores with small diameter produce a coating structure that set the offset ink quickly. Too fast ink setting could produce for example a low print gloss (Donigian 1997). Donigian *et al.* (Donigian 1997) showed that the print gloss of offset prints decreased when the diameter of coating pigment was reduced. Our results show that print gloss of inkjet prints (Figure 3) remains lower when the coating had smaller size pigments. Van Gilder and Purfeerst (Gilder 1994) found out that offset ink set quicker when the coating contains latex binder that absorbs solvent more. So in the very hydrophilic PVOH binder containing coating this could be one reason for low print gloss.

### Colorant fixing

An other aspect of the inkjet print quality formation is the colorant fixing. The anionic latex and dispersing agent produce an anionic nature to the offset coating layer and the anionic inkjet dye can not fix to it. Thus there exist no chemical groups which could fix the colorant. Figure 9 shows how cyan dye has transferred in the bottom part of the offset coating layers. When the coating colour contained a little more PVOH, the ink colorant locates more all over the coating layer and there was less cyan in the bottom coating. The hydrophilic PVOH swells and therefore the colorant can move into the binder film structure and stay there after solvent evaporation. In the inkjet coatings, the colorant stays in the curtain-coating layer. The other thing in inkjet coatings is the cationic dispersion of coating pigments that produces a cationic coating layer. The anionic colorant fixes with electrostatic interactions to the cationic dispersing agent. In the offset printing, the charge of the coating layer must have a less role in the ink setting process. The offset ink contains colour pigments with oils and resins (binder) and the fountain solution with water, isopropyl alcohol and different kind of additives. The oil and resins fix the pigments. We assume that the oil does not have any charge, but the fountain solution has anionic nature. In principle, the cationic nature of inkjet coating attracts the components of fountain solution meaning that those chemicals stay more on the top part of coating layer during the ink setting process and this might have some kind of role in the offset ink bonding because the chemical nature of paper surface has changed.

If the use of inkjet is restricted to a personalization or one colour printing on the offset press, the line spreading seems not to be so large that it would disturb the print quality too much. Figure 10 shows that the black colour line width on the pure paper surface is quite acceptable on the offset surfaces. The interest to use pigment-based inkjet inks can simply further the situation. The pigment-based ink forms a coating cake on the coating surface, similarly as in offset printing ink, and therefore similar ink spreading phenomena as occurs in the case of dye-based inks does not exist.



| Offset, more latex, 8 gm$^{-2}$ | Offset, less latex, 8 gm$^{-2}$ | Inkjet, 8 gm$^{-2}$ |
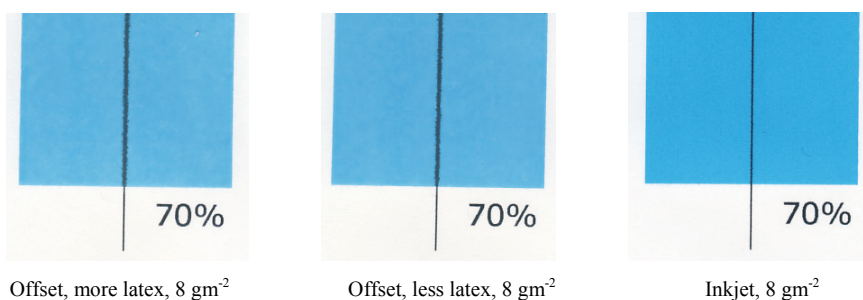
*Figure 10: Printed surfaces. Printing speed was 75 m·min$^{-1}$ printing*

## 5. Conclusions

The offset coating porosity and pore size distribution are not optimal for the inkjet purpose. However, when the printing speed of inkjet nozzles are increasing, there seems to be possibilities to get a better inkjet print quality with offset coating structures, if the drying regime is planned carefully. The offset coating provided an acceptable line width and sharpness for inkjet printing, if there was not another ink colour so near that the different colour inks had a possibility to mix together. Problems occur when more colours are involved in the printing.

Nowadays, the optimal coating layer structure for the multipurpose printing needs always a compromise in the structural properties of coating layer as well as in the chemical nature. The highest challenges for the offset and inkjet printing side come from the absorption properties side. The absorption properties affect the forces in the offset printing nips and fixing of the offset ink pigments. In the inkjet, the absorption affects most of all the colorant location.

## References

Van Gilder, R. L., Purfeerst, R. D. (1994), *Commercial Six-color Press Runnability and the Rate of Ink-tack Build as Related to the Latex Polymer Solubility Parameter*, TAPPI Coating Conference, San Diego, USA, 1994, TAPPI Press, Atlanta, USA, 229-241.

Donigian, D. W., Ishley, J. N., Wise, K. J. (1997), Coating *Pore Structure and Offset Printed Gloss*, TAPPI Journal 80(1997)5, 163-172.

Desie, G., Van Roost, C. (2006), *Validation of Ink Media Interaction Mechanisms for Dye and Pigment-based Aqueous and Solvent Inks*, Journal of Imaging Science and technology 50(2006)3, 294-303.

Fouchet, B., Noirot, P.-A., Desjumaux, D., Van Gilder, R. L. (2006), *Absorption dynamics of offset ink components in thin latex films of different structures and compositions*, J. Pulp Pap. Sci. 32(2006)3, 123-130.

Gane, P. A. C., Schoelkopf, J., Spielmann, D. C., Matthews, G. P., Ridgway, C. J., *Observing fluid transport into porous coating structure: some novel findings*, TAPPI Advanced Coating Fundamentals Symposium, April 29 - May 1, 1999, Toronto, Canada, 213-236.

Kirmeier, M. (2008), *Thoughts about the impact of the absorption properties of paper on printability*, Int. Papierwirtschaft (2008)5, 22, 24.

Lamminmäki, T., Puukko, P. (2007), *New ink absorption method to predict inkjet print quality*, Advances in Printing and Media Technology, 34th International Research Conference of Iarigai, Grenoble, France, September 2007, 231-239 (2007).

Lamminmäki, T., Kettle, J., Puukko, P., Gane, P. A. C., Ridgway, C. (2009): *Inkjet print quality: the role of polyvinyl alcohol upon structural formation of CaCO₃ coatings*, Journal of Pulp and Paper Science 35(2009)3-4, 137-147.

Miettinen, P., Tammi, A.-L. (2002), *Influence of coated paper structure on ink-paper interactions in heat set printing*, 11th International printing and graphic arts conference, Bordeaux, France, 1-3 Oct. 2002, vol. 1, session 6, 14pp.

Ridgway, C. J., Gane, P. A. C., Schoelkopf, J., *Effect of Capillary Element Aspect Ratio on the Dynamic Imbibition within Porous Networks*, Journal of Colloid and Interface Science 252, 373-382 (2002).

Ridgway, C., Gane, P. A. C., *The Impact of Pore Network Structure on the Absorption of Inkjet Inks*, TAPPI Coating Conference, Toronto, Canada, 17-20 April 2005, TAPPI Press, Atlanta, USA, Session 6, 15 pp.

Rousu, S., Gane, P., Spielmann, D., Eklund, D. (2000), *Separation of Offset Ink Components during Absorption into Pigment Coating Structures*, Nordic Pulp and Paper Research Journal 15(2000)5, 527-535.

Rousu, S., Gane, P., Eklund, D. (2005), *Print quality and the distribution of offset ink constituents in paper coatings*, Tappi J. 4(2005) 7, 9-15.

Schoelkopf, J., Ridgway, C. J., Gane, P. A. C., Matthews, G. P., Spielmann, D. C., *Measurement and Network Modelling of Liquid Permeation into Compacted Mineral Blocks*, Journal of Colloid and Interface Science 227(1), 119-131 (2000).

Sorbie, K. S., Wu, Y. Z., McDougall, S. R. (1995), *The Extended Washburn Equation and Its Application to the Oil/Water Pore Doublet Problem*, Journal of Colloid and Interface Science 174(1995), Issue 2, 289-301.

Ström, G .R., Borg, J., Svanholm, E. (2008), *Short-Time Water Absorption by Model Coatings*, TAPPI 10th Advanced Coating Fundamentals Symposium, June 11-13, 2008, Montreal, Canada, Tappi Press, Atlanta, USA, 204-216.

# How to develop a sustainable strategy for a printing organization in a global financial melt down

*Rajendrakumar Anayath, Guenther Keppler, Amrutharaj Harikrishnan, Kiran Prayagi*

Print Media academy-Heidelberg India
333 GST Road, Jameen Pallavaram, Chrompet
IN-600 044 Chennai, India
E-mail: rajendrakumar.anayath@heidelberg.com

**Abstract**

This research paper is a methodical approach to develop a sustainable strategy for a printing/media organization. The first step is to know our self properly by defining "Critical Business Success Factors"( CBSF) and evaluating them to know the organisation's efficiency and competitiveness in all aspects. To know the most appropriate CBSF of an organization, the best way is to do a SWOT analysis (Strength, Weaknesses, Opportunity and Threat) and a PEST analysis (Political, Environmental, Socital,Technical). After performing this, define the respective CBSFs and evaluate the corresponding weightages of each CBSF by answering a number of relevant questions under each CBSF on a 10 point evaluation scale. Then create a profile for the organisation based on the respective weightages assessed .Next step is to prioritise these CBSF as per the defined organisatinal goal. Analysing this way we gain an important information on how and what direction the company should move and plan in the future developmental activities. A special analysis is made further to identify the best product portfolio mix for the organisation. This approach will help to understand the actual situation of the organisation from a bird's eye view. By doing so, the financial and technical health of the organization is maintained and it is easy to develop an appropriate, effective strategy, which is sustainable and certainly help to lift the organisation in to greater heights.

**Keywords**: SWOT analysis; portfolio mix; sustainable strategy, profile development

## 1. The objectives of the research

At the end of year 2007 global printing industry started witnessing tremendous pressures from all angles questioning their sustainability due to the global financial turmoil which even today continues. Many industries closed down and others were not in a position to decide on what to do and how to realign themselves organizationally and technically. The main objective of this paper is to develop a generic methodology to analyze the existing organizational health and then develop the most appropriate sustainable strategy.

## 2. Research methods

### 2.1 Strategy development

To develop an appropriate strategy for a printing organisation the first job is to know our self closely, within a short span of time. The best way to do this is to define the organisations "Critical Business Success Factors" (CBSF). By evaluating these "CBSF" we will come to know the "Organisation's Efficiency" Best way to find out the CBSF are SWOT (Strength, Weaknesses, Opportunity and Threat) & PEST (Political, Environmental, Social, Technical ) Analysis.

In the first step, describe and mark the assessed weightage of each factor on a scale (in this case 10 point scale is adopted) and then create a profile for your organisation's efficiency & competitiveness. In the second step, prioritize these CBSF. From this we gain an important information that how and what direction we should plan for our "Further Developmental Programmes" and the "Right Product Focus" for the future. Also we can identify the best product portfolio mix.

### 2.2 Define Critical Business Success Factors (CBSF) of the organization:
### Eight Critical Business Success Factors are identified

1. *Product Quality*: Means the worth of a product or a service regarding the usability for the customer. This not only applies to "technical" features like resolution, LPI, DPI, AM, FM, HYBRID,MOIRE etc, but also properties such as consistency, reliability and reputability.

2. **Price Flexibility**: This (lowest possible price) shows the company's financial situation to the "outside world" and indicates how far the price of a product can be decreased without making a loss - regardless if it is to be decreased.

3. **Entity Innovations** states how often an enterprise offers new products and services to their customers in an active manner. The higher the frequency, the more services are to be offered on the market. The stronger is this success factor.

4. **Product Portfolio Mix** results from the sum of different products a company offers on the market at a time.

5. **Capability Of Service Offerings** is the sum of all services a company offers on the market at a time - being irrelevant whether these services are charged individually for an item or to the whole product.

6. **Deadline Commitments** shows the company's ability in meeting the deadlines as agreed with the customer. (The short-term ability to deliver quick and unexpected orders is not considered here - unless these are the company's central business.)

7. **Goodwill** or **Corporate Identity** is the company's image and appearance shown internally and externally. The Image creates expectations of competitors and customers towards your enterprise which can have an impact on customer decisions (e.g. on placing orders).

8. **Further Value Additions** concerning special requirements signifies the company's ability to accept those orders which require other services than the specified ones being part of the standard program or product portfolio or in the work order. This includes being ready to guarantee short-term deliveries too.

The below shown table is a typical CBSF "Matrix Form" for analysis:

| CBSF | 1 | 2 | 3 | 4 | 5 | 6 | 7 | 8 | 9 | 10 |
|---|---|---|---|---|---|---|---|---|---|---|
| 1. Product quality | | | | | | | | | | |
| 2. Price flexibility | | | | | | | | | | |
| 3. Entity innovations | | | | | | | | | | |
| 4. Product portfolio mix | | | | | | | | | | |
| 5. Capability of services | | | | | | | | | | |
| 6. Deadline Commitments | | | | | | | | | | |
| 7. Goodwill | | | | | | | | | | |
| 8. Further value additions | | | | | | | | | | |

*(CBSF — 1 TO 10 SCALE)*

## 3. CBSF Analysis step by step

In this stage each CBSF is asked with specific questions and a corresponding weightage is found out. This is posted in the "CBSF-Matrix Form". Each question is created with utmost care so that we will get the most appropriate answer. This is very important while creating the actual profile of the organization. The accuracy of the profile depends up on the truthfulness in answering the questions by the organization in question.

**Question 1**
*Quality means the worth of a product or a service regarding the usability to the customer*
*(Properties such as consistency reliability and reputability*

| Product Quality | | 1 | 2 | 3 | 4 | 5 | 6 | 7 | 8 | 9 | 10 |
|---|---|---|---|---|---|---|---|---|---|---|---|
| 1 | Are there complaints concerning the printing quality? | | | | | | | | | | |
| 2 | Are there complaints concerning quality in the repeat orders? | | | | | | | | | | |
| 3 | How often the jobs are rejected? | | | | | | | | | | |
| 4 | Do you experience any quality deviation on basic raw materials? | | | | | | | | | | |
| 5 | Do you experience deviations between proof and print? | | | | | | | | | | |
| 6 | Do customers demand decrease in price compromising quality? | | | | | | | | | | |
| 7 | Do customers leave you due to quality complaints? | | | | | | | | | | |

*Evaluation: How many out of 10 or 100 orders does the question apply?*
> *Always = 1*
> *Sometimes = 5*
> *Never = 10*

*Total divided by 7*  ☐

**Question 2**     *Price Flexibility*

*The price flexibility (lowest possible price) shows the company's financial strength/situation to the "outside world" and indicates how far the price of a product without making a loss - regardless if it is to be decreased.*

| | Price Flexibility | 1 | 2 | 3 | 4 | 5 | 6 | 7 | 8 | 9 | 10 |
|---|---|---|---|---|---|---|---|---|---|---|---|
| 1 | Whether your price offers are relatively in a higher level to the competetors? | | | | | | | | | | |
| 2 | How rigid are you to decrease your prices? (0-rigid and 10 flexible) | | | | | | | | | | |
| 3 | Do corrections in price lead to poor cost -effectiveness? | | | | | | | | | | |
| 4 | How do you rate your pricing compared to your competetor? | | | | | | | | | | |
| 5 | Do your customers leave you just because of the prices? | | | | | | | | | | |
| 6 | Can orders be gained only by price? | | | | | | | | | | |

*Evaluation: How many out of 10 or 100 (sample size) orders does the question apply?*
　　　　*Always, or inferior = 1*
　　　　*Sometimes, or equal = 5*
　　　　*Never or better = 10*

Total divided by 6 ☐

**Question 3**     *Entity Innovations*

*The amount of product and services innovations states how frequently an enterprise offers new products and service to their customers in an active manner. The higher the frequency and the more services are offered on the market, the stronger this success factor*

| | Entity Innovations | 1 | 2 | 3 | 4 | | |
|---|---|---|---|---|---|---|---|
| 1 | What level your employees are motivated? | | | | | x | 2.5 |
| 2 | Are there any active trainings offered? | | | | | x | 2.5 |
| 3 | How willing is the organisation to experiment to some extent to fulfill market needs? | | | | | x | 2.5 |
| 4 | Do you show any interest in improving processes? | | | | | x | 2.5 |
| 5 | Do you implement trends in to product offers? | | | | | x | 2.5 |
| 6 | How do you rate you interest in new challenges? | | | | | x | 2.5 |
| 7 | Do you have an internal innovation circle? | | | | | x | 2.5 |

*Evaluation: 1="not motivating/existing"*
　　　　*2="little/few"*
　　　　*3="yes, but un systemically"*
　　　　*4="high/large, actively or absolutely yes"*

Total divided by 7 ☐

**Question 4**     *Product Portfolio Mix*

*The product portfolio mix results from the sum of different products a company offers on the market at a time. The product portfolio mix is the complete solution offerings of an organisation to the market.*

| | Product Portfolio Mix | Y | N |
|---|---|---|---|
| 1 | Annual business reports | 1 | 0 |
| 2 | Brochures,flyers | 1 | 0 |
| 3 | Dokumentations/Manuals | 1 | 0 |
| 4 | Posters, Large-format Products | 1 | 0 |
| 5 | Books | 1 | 0 |
| 6 | Packaging material | 1 | 0 |
| 7 | Labels and Security printing | 1 | 0 |
| 8 | Direct Mailing | 1 | 0 |
| 9 | Designing Internet homepages | 1 | 0 |
| 10 | Frameworks for E-business such as Scientific Composition | 1 | 0 |

Total of "yes" ☐

**Question 5**     *Capability of Services*

*The variety of service offerings are the sum of all services a company offers on the market at a time - being irrelevant whether these services are charged for individually or in relation with a product. Generally the wholeness of the services a company offers on the market.*

|    | Capability of Services | Y | N |
|----|------------------------|---|---|
|    | Capability of Services | Y | N |
| 1  | Work related to agencies (Design conceptual work etc) | 1 | 0 |
| 2  | Digitise images and text | 1 | 0 |
| 3  | Page design and make-up | 1 | 0 |
| 4  | Printing with inkjet or similar services for personalisation | 1 | 0 |
| 5  | High-end finishing | 1 | 0 |
| 6  | Converting processes related to bookbinding & packaging | 1 | 0 |
| 7  | Database services | 1 | 0 |
| 8  | Direct marketing services | 1 | 0 |
| 9  | Logistics for customers | 1 | 0 |
| 10 | Internet services | 1 | 0 |

Total of "yes" [   ]

## Question 6    *Deadline Commitment*
*The ability to meet deadlines shows the company's reliability in dealing with the deadlines agreed with the customer (The short-term ability to deliver quick and unexpected order is not considered here - unless are the company's central business)*

|   | Deadine Commitment | 1 | 2 | 3 | 4 |   |     |
|---|--------------------|---|---|---|---|---|-----|
| 1 | Are there any delays in delivery? |   |   |   | x | 2.5 |
| 2 | Do penalties have to be paid often? |   |   |   | x | 2.5 |
| 3 | What is the heighest delay experienced? |   |   |   | x | 2.5 |
| 4 | Do customer pester you due to the inability of meeting deadlines? |   |   |   | x | 2.5 |
| 5 | Is the delay caused by you? |   |   |   | x | 2.5 |

*Evaluation: How many out of 10 or 100 order does this question apply?*
*1=very often/more than 4 days*
*2=2-4 days/often"*
*3="1-2 days/occasionally"*
*4="none/never"*

Total divided by 5 [   ]

## Question 7    *Goodwill*
*The Goodwill or Corporate Identity is a company's image/appearance shown internally and externally. The goodwill creates expectations of competitors towards your organisation, which can have an impact on customer decisions (e.g, on placing orders). The Goodwill is the organisation's Brand Value.*

|    | Goodwill | Y | N |
|----|----------|---|---|
| 1  | Are customers invited to events? | 1 | 0 |
| 2  | Are you certified by any international certification bodies for quality? | 1 | 0 |
| 3  | Does the organisation work with the Internet? | 1 | 0 |
| 4  | Does the Management play an active role in trade associations? | 1 | 0 |
| 5  | Does the Management publish the company`s vision and goals? | 1 | 0 |
| 6  | Does the enterprise advertise their product and service offerings? | 1 | 0 |
| 7  | Does the company have a reputation among experts? | 1 | 0 |
| 8  | Is the company`s name a synonym, for high performance? | 1 | 0 |
| 9  | Are new customers enrolled/acquires every year? | 1 | 0 |
| 10 | Are you referred by you customers? | 1 | 0 |

Total of "yes" [   ]

## Question 8    *Further Value Addition*

|   | Deadline Commitment | 1 | 2 | 3 | 4 |   |     |   |
|---|---------------------|---|---|---|---|---|-----|---|
| 1 | Can the organisation meet all the implied needs of the customer? |   |   |   |   | x | 2.5 |
| 2 | Can the company cop-up with peaks in production? |   |   |   |   | x | 2.5 |
| 3 | Are the employees willing to work overtime? |   |   |   |   | x | 2.5 |
| 4 | Can you arrange working during the overtime? |   |   |   |   | x | 2.5 |
| 5 | Can special requirements be carried out easily? |   |   |   |   | x | 2.5 |
| 6 | Can the company introduce an extra shift if needed? |   |   |   |   | x | 2.5 |

Total divided by 6 [   ]

Below shown table represents a typical profile of an organization created through answering the above questions meticulously. We can create a bar chart or control chart to represent the profile.

*Profile of the organization: (Evaluation result of a typical example)*

| | 1 | 2 | 3 | 4 | 5 | 6 | 7 | 8 | 9 | 10 |
|---|---|---|---|---|---|---|---|---|---|---|
| 1. Product quality | ▨ | ▨ | ▨ | ▨ | ▨ | ▨ | ▨ | ▨ | ▨ | |
| 2. Price flexibility | ▨ | ▨ | | | | | | | | |
| 3. Entity innovations | ▨ | ▨ | ▨ | | | | | | | |
| 4. Product portfolio mix | ▨ | ▨ | | ▨ | ▨ | ▨ | | | | |
| 5. Capability of services | ▨ | ▨ | ▨ | ▨ | | | | | | |
| 6. Deadline Commitments | ▨ | ▨ | | | | | | | | |
| 7. Goodwill | ▨ | ▨ | ▨ | ▨ | | | | | | |
| 8. Further value additions | ▨ | ▨ | ▨ | ▨ | | | | | | |
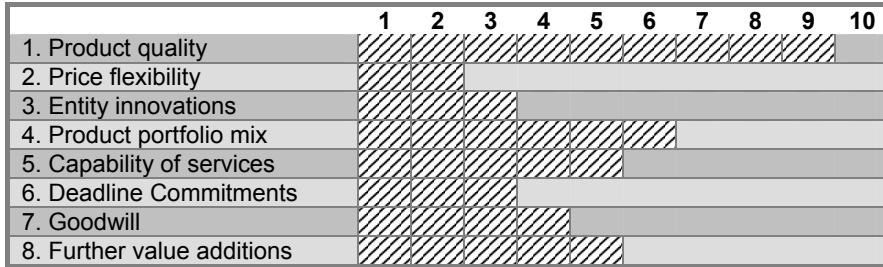
**Prioritize critical business success factors**

From the above bar chart we can decide our priorities. In this case the priority No.1 is "Deadline Commitments" and priority No.2 is "Price Flexibility" and priority No.3 is "Goodwill"

| | 1 | 2 | 3 | 4 | 5 | 6 | 7 | 8 | 9 | 10 |
|---|---|---|---|---|---|---|---|---|---|---|
| 1. Product quality | ▦ | ▦ | ▦ | ▦ | ▦ | ▦ | ▦ | ▦ | ▦ | |
| 2. Price flexibility | **Prio 2** | | | | | | | | | |
| 3. Entity innovations | ▦ | ▦ | ▦ | | | | | | | |
| 4. Product portfolio mix | ▦ | ▦ | ▦ | ▦ | ▦ | ▦ | | | | |
| 5. Capability of services | ▦ | ▦ | ▦ | ▦ | | | | | | |
| 6. Deadline Commitments | **Prio 1** | | | | | | | | | |
| 7. Goodwill | ▦ | ▦ | ▦ | ▦ | | | | | | |
| 8. Further value additions | **Prio 3** | | | | | | | | | |
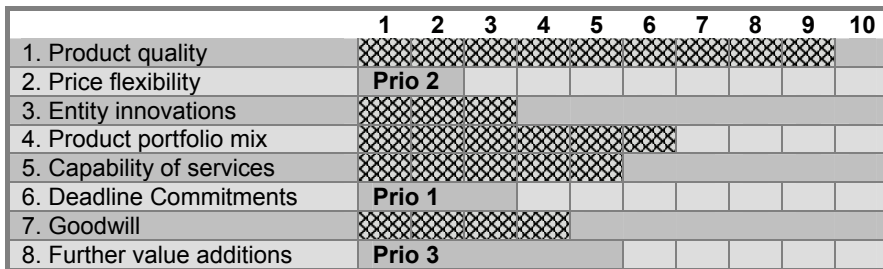
In this case the target point is 10 for the 3 priorities chosen within the next two years. All the necessary programmes are implemented to achieve this goal.

| | 1 | 2 | 3 | 4 | 5 | 6 | 7 | 8 | 9 | 10 |
|---|---|---|---|---|---|---|---|---|---|---|
| 1. Product quality | ▦ | ▦ | ▦ | ▦ | ▦ | ▦ | ▦ | ▦ | ▦ | |
| 2. Price flexibility | **Prio 2** | | | | | | | | ⟶ | ★ |
| 3. Entity innovations | ▦ | ▦ | ▦ | | | | | | | |
| 4. Product portfolio mix | ▦ | ▦ | ▦ | ▦ | ▦ | ▦ | | | | |
| 5. Capability of services | ▦ | ▦ | ▦ | ▦ | | | | | | |
| 6. Deadline Commitments | **Prio 1** | | | | | | | | ⟶ | ★ |
| 7. Goodwill | ▦ | ▦ | ▦ | ▦ | | | | | | |
| 8. Further value additions | **Prio 3** | | | | | | | ⟶ | | ★ |
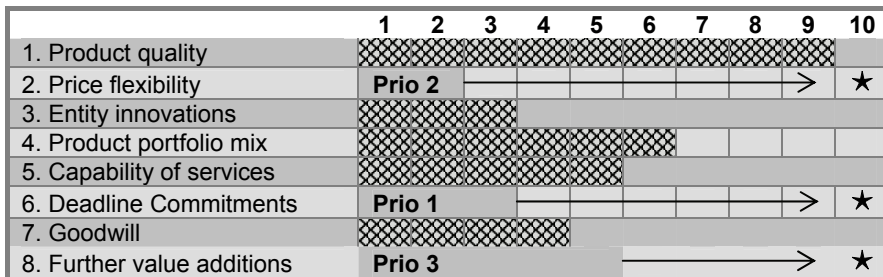
**How to find out the most suitable product port folio mix:**

**Step: 1** Analyze operational contribution to share on total sales turnover: See the below diagram. This analysis will help us to understand the share on sales turn over for each product segments. But at the same time see that shear high percentage on total sales turn over does not contribute in to profit margin. In the below case even though share of the sales turnover of packaging is 43% the contribution margin is - 25%.
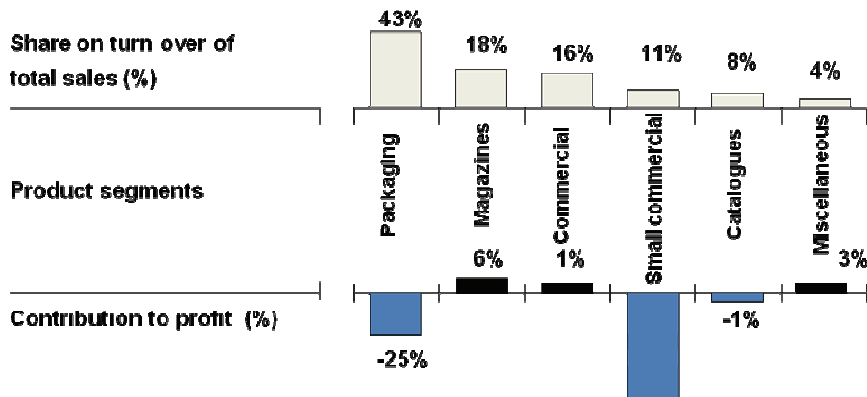
At the same time the Magazine segment's sales contribution is only 18% but contribution to profit margin is 6%.Small commercial is doing in a very unhealthy way with a huge loss of - 64%.What does this mean? It is not the volume but the most effective way doing will bring the profit.

**Step2:** Analyze "Market Attractiveness" to the "Core Competency" This two parameters are considered because market attractiveness of a product decides what product we should do and the core competitiveness in executing the same will decide the profit contribution. To quantify these two factors in a most appropriate way few sub questions are also created with a 5 point scale as below.

| Market Attractiveness | | | | Core Competency Position | | |
|---|---|---|---|---|---|---|
| Market growth? | High | 5 | | Cost situation | Better | 5 |
| | Mid | 3 | | | Equal | 3 |
| | Low | 1 | | | Very bad | 1 |
| Price development | Going up | 5 | | Production competence | Better | 5 |
| | Stable | 3 | | | Equal | 3 |
| | Going down | 1 | | | Very bad | 1 |
| Threat to be substituted | Low | 5 | | Quality of processes | Better | 5 |
| | Mid | 3 | | | Equal | 3 |
| | high | 1 | | | Very bad | 1 |
| Intensity of competition | Low | 5 | | Quality of products | Better | 5 |
| | Mid | 3 | | | Equal | 3 |
| | High | 1 | | | Very bad | 1 |
| Market volume | High | 5 | | Consulting competence | Better | 5 |
| | mid | 3 | | | Equal | 3 |
| | Low | 1 | | | Very bad | 1 |

## Step 3: Portfolio Evaluation

In this stage we will classify the products and set up a strategy. An X-Y quadrant is divided in to 4 segments as below and X- axis is meant for "Core Competency" and Y - axis for "Market Attractiveness". After posting the respective weightings in the different quadrant segments, if the product comes in segment 1, then it means we can invest and produce in our own premises. For segment 2A, produce it in the same premises with the existing facility and for 2B step out and out source with others and watch future trends. For segment 3 step out and give way to others since we are not competentent to do it in the most economical way. Try to identify our blue ocean/niche.
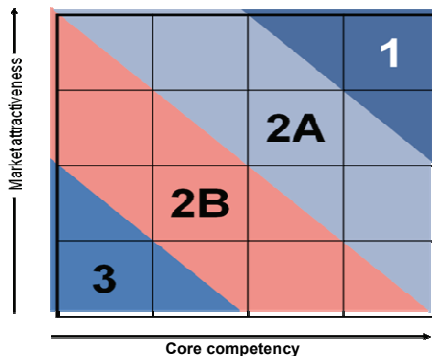


## Step 4: Strategy Building

| | Product segments | Market Attractiveness | Core competency |
|---|---|---|---|
| 1 | Packaging | 3.8 | 3.2 |
| 2 | Magazines | 3.7 | 4.4 |
| 3 | Commercial | 3.7 | 3.6 |
| 4 | Small commercial | 2.3 | 1.4 |
| 5 | Catalogues | 2.0 | 3.2 |
| 6 | Miscellaneous | 1.6 | 2.6 |
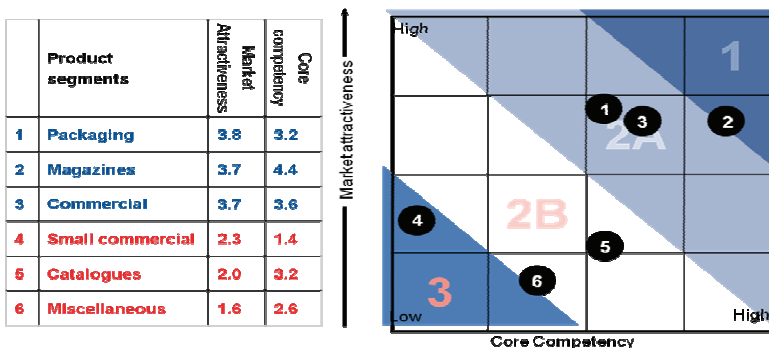
In this case "Magazines" we have both 'core competency' and 'market potential' and we must focus on that but look at "small commercial" which we are doing just for the name sake. It is not bringing any profit. We should leave this business to others because it is not our cup of tea. 'Packaging' and 'Commercial' we can continue to do without investing because our 'Core Competency' is still hold good. At the same time notice that market potential is decreasing.

**Step 5. Analyze and refocus on the product portfolio mix based on their contribution margin:**

*Questions to be answered during this analysis:*

Q1) Do we have the right product portfolio?
Q2) where exactly in the process we lose money?
Q3) Do we have to invest or just change the organizational structure?
Q4) Are we managing and controlling the orders properly? Can we reduce throughput time?
Q5) Do we have an optimized flow of material?
Q6) Can we increase productivity and reduce wastages?
We should also know: How we as the "Print Manufacturer" perceived by our "Print Buyer"

## 4. Summary of Results

Now we have the profile/primary information of the situation existing in our organisation. Further from this result we can take up the optimal measures to lift up our organisational efficiency and prioritising critical business success factors.

Also now we have the best solution to increase the organisations potential opportunities.
Impliment these solutions and take appropriate measures to exploit these potentials the best.
Execute the most suitable improvement programme which will have the greatest impact on the organisations efficiency.

Depending on the analysis result now we know whether to *invest* or *focus on core competency* or *outsource* or *leave way to others*.

## 5. Conclusions

Everyone knows how to create a profile for our "CtP" or for our "Printing machine" but never thought of developing a profile for our organisation. The Profile Development in this research either as a bar chart or control chart will help us to analyse the actual situation of an organisation from a bird's eye view. By doing so we can easily develop an effective strategy which will certainly lift the organisation to greater heights by keeping the organisation very healthy.

**References**

1) Exploring corporate strategy: Text & Cases, By Gerry Johnson, Kevan Scholes, Richard Whittington

2) International Business: The Challenge of Global Competition w/ CESIM access card by Donald Ball, Michael Geringer, Michael Minor, and Jeanne McNett

# Calculating the product carbon footprint in newspaper production

*Ronald Weidel*

University of Applied Sciences Leipzig
POB 30 11 66, D-04251 Leipzig

ronald.weidel@fbm.htwk-leipzig.de

**Abstract**

On the basis of available norms and frameworks the practical conversion of the PCF calculation is examined for newspapers. The aim was to process the available scientific methods in practice and to collect experiences with PCF calculations on the basis of case studies. Critical points were also to be worked out as was the availability of base Life Cycle Inventory Data (LCI Data). The findings of this study are to be entered in a guide for the newspaper branch.

**Keywords:** newspaper production; product carbon footprint; environment; lifecycle assessment; sustainability

## 1. Introduction

Global climate change and countermeasures against the greenhouse effect are currently central subjects of public debate. Companies operating in the graphic industry are therefore required to conduct a critical review of the environmental impact of their products. Increasing public interest in ecological aspects such as "Green Printing" and a rise in the share of ecologically oriented consumers necessitate representative statements. Newspaper publishers and printers in particular are called upon, as new digital media have sprung up and are growing ever further beside the classical paper medium.

One of the more popular approaches in recent years to measure the environmental impact of products and services has been the Product Carbon Footprint (PCF): "*The product carbon footprint ("CO2 footprint") is the outcome of the analysis of greenhouse gas emissions throughout the entire life cycle of a product in a defined application and in relation to a defined functional unit.*" (BMU, UBA, Öko-Institut e.V., 2009). However, it should be noted that the PCF only reports emissions and ignores other environmental factors, e.g. acidification or toxicity. In the past a number of approaches have been developed, but they vary in objectives and methodology. Yet it is aimed to harmonize the available methods with the development of ISO 14067, which is to be published in 2011. A number of studies have already determined the PCFs for newspapers, for instance studies from Scandinavia (Moberg, A. et al, 2007; Nors, M. et al, 2009). With the ongoing development of a harmonized methodology and the growing interest of companies and stakeholders in the subject of PCF numerous projects (THEMA1 et al., 2009) were established to gain more experience of and a comprehensive insight into PCF and LCA techniques.

## 2. Methods

Work started with a literature search to attain a basic overview of the subject of PCF. Available norms and frameworks were evaluated. The following papers were reviewed:

- ISO 14040 / 14044 - "Environmental management - Life cycle assessment" (ISO, 2006)
- BSI, Defra, Carbon Trust - PAS 2050:2008 - "Specification for the assessment of the life cycle greenhouse gas emissions of goods and services" (BSI, 2008)
- WBCSD/WRI - "Product Life Cycle Accounting and Reporting Standard" (WBCSD/WRI, 2009)
- CEPI - "Framework for the development of Carbon Footprints for paper & board products" (CEPI, 2007)

For a better understanding of LCA methodolgy, existing case studies of different media products from Scandinavia (Moberg, A. at al, 2007; Nors, M. et al, 2009) and case studies of different products of the PCF-Pilot-Project Germany (THEMA1 et al, 2009) were evaluated.

In the second phase a system boundary was developed on the basis of PAS 2050:2008 for the subject of newspaper production. According to  the "cradle to grave"- approach a lifecycle of a newspaper was designed. Included are the phases of raw material extraction, production, use, disposal / recycling. The lifecycle is orientated towards paper circulation. Besides, a special focus was placed on the printing plant processes and distribution. In accompanying case studies the functionality of the model was examined. The company data (input/output) of cooperating regional newspapers were used for the case studies. In the case of the suppliers their own PCF were partly used. In addition, the availability of LCI data for the relevant raw and auxiliary materials was evaluated in conversations with suppliers and by searching appropriate data banks.

## 3. Results and Discussion

The following representation will introduce the results that arose by implementing the PCF methodology.. Recommendations have been developed on the basis of the accumulated experiences in the newspaper branch. The newspaper association WAN-IFRA has planned to publish a guide ín autumn 2010.

### 3.1 Methodology

An extensive pool of methods exists given  the norms and frameworks set for this topic. Indeed, there are differences between extent and details of capture. Common to all is the corresponding approach with the LCA technologies defined in the ISO norm 14040/14044 (ISO, in 2006). For the present investigation PAS 2050:2008 (BSI, 2008) was selected for the following reasons:

- specific to the calculation of PCF for  products and services
- reports greenhouse gases (GHG) as CO2-equivalent with a time horizon of 100 years
- uses two different scenarios "business to consumer" and "business to business"
- good documentation and processing for a quick entrance with case studies

Even if some methical recommendations of PAS 2050:2008 are currently being discussed among experts (cf. BMU, UBA, Öko-Institut e.V., 2009),a further examination of this work will prove worthwhile.

Below are presented some single results, which correspond with the recommendations to be given in a guideline for calculating the carbon footprint of newspaper production.

### 3.2 Organizing a PCF study in companies

The introduction of PCF studies as a responsibility of companies brings changes to the organisation of studies. Up to now PCF studies were primarily carried out by independent, scientific institutions or specialized consultants. Mostly a team of scientists and stakeholders worked out the overall process chain, starting with raw material extraction, preproduction, production, usage and ending with disposal.

For the assessment of processes primarily companies and suppliers were interviewed and company data evaluated. Additional data sources from available LCI data banks were also evaluated. To guarantee a consistent quality of data rules were defined and compliance was monitored.

The investigation has shown that organizing a PCF study in an company leads to a change in the basic setup. For a company study it should be assumed that several internal and external partners (customer, suppliers, disposers, cf. guide to PAS 2050:2008, Section I, Engaging Suppliers) contribute information of varying quality and interest. The study showed that detail and depth increases in line with company-internal processes. The used input / output data can be found by exact measurements and calculations and proofing is highly practicable. Uncertainty is very low. However, external processes are less clear for the investigator.
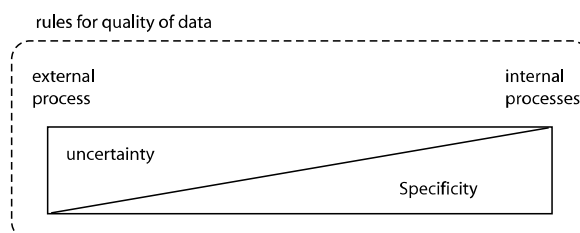


*Figure 1: Quality of data in dependence of source*

At this point the company depends on the co-operation of customers, suppliers and disposer. The level of information decreases and proofing of data becomes more difficult. There is a risk that a badly documented PCF value of the processed raw materials will be delivered. Arranging uniform rules with all partners (figure 1) for data quality should be allocated a central role.

An unexpected critical remark was made by the suppliers. Suppliers worried that their own producted might be wrongly assessed if the PCF data from the suppliers were used without further explanation. This doubt was especially expressed, when the same products were delivered by different suppliers.

### 3.3 Process plan

The process plan plays a central role as the basis of a PCF study. Especially helpful is the formation of process modules. According to PAS 2050:2008 processes should be subdivided to the extent that an allocation can be prevented. This also complies with the recommendations of ISO 14040/14044 (ISO, in 2006). For the newspaper case study the processes were divided into internal and external processes from the point of view of the printer (figure 2). As it was assumed that the PCFs for used fuel, raw and auxiliary materials can be made available by the suppliers the external processes were not carried out in detail. Only one data input for the PCF value was designed, e.g. for the ink production.
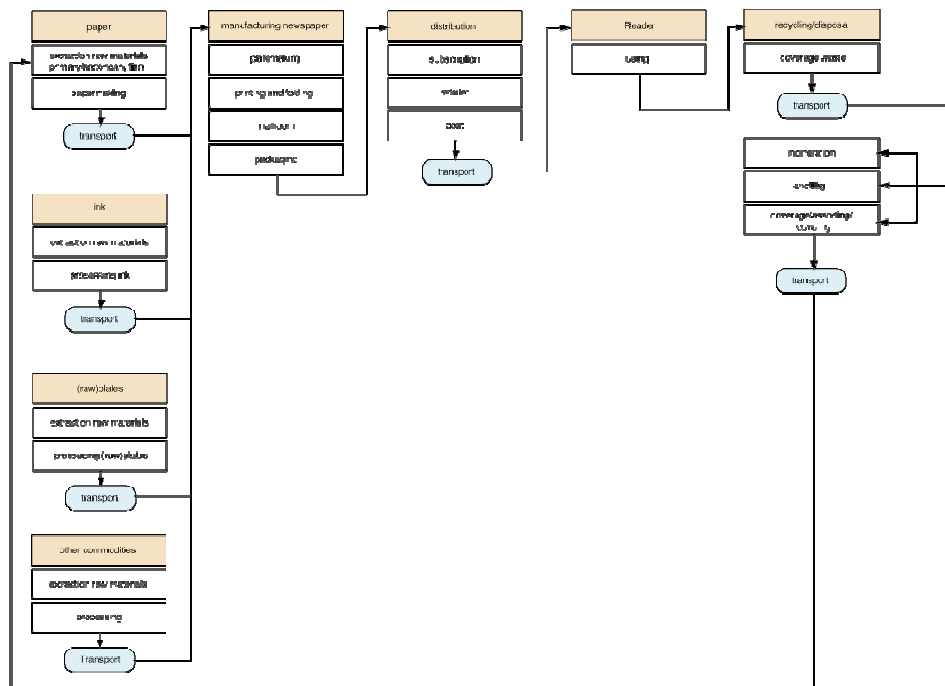


*Figure 2: Process flow chart for calculating the PCF*

A detailed representation was preferred for the internal processes by the newspaper printers, since these processes are directly influenced by the company and the identification of the relevant emissions is of interest. For the printing plant processes were summarized into modules according to the process areas Prepress, Pressing and Postpress. In addition, all supporting processes were summarized into the module infrastructure. This arrangement also corresponds with the operation structure of the surveyed newspaper printers. But for the editorial area there is still no methodical approach in place up to now. This should be an aim when the project is continued.

### 3.4 Distribution process

An important external process in the life of a newspaper is the distribution. A service provider takes over the distribution as a subcontractor or a subsidiary of the publishing house. The transport area can be divided into two areas. Area 1 defines the transport from printing plant to retailer. The transportation chain can be exactly determined with agreed tour plans of the company data to the transported copies, the used transportation means and the distance. In area 2 uncertainty is very high. The delivery of newspapers occurs in multiple ways on foot, by bicycle, motorcycle, car, or by transporter van. No representative data is available at the moment.

## 3.5 Allocations

One of the central problems in LCA studies is the treatment of allocation problems. These occur, for example, when a given process produces by-products. Allocation should be avoided according to ISO 14040/14044 (ISO, 2006). PAS 2050:2008 (BSI, Defra, Carbon Trust, 2008) also makes this recommendation. But in the case of newspaper printers such allocation problems appear only in few places. The following table shows three examples of allocation problems.

*Table 1: Examples of allocation problems*

| process area | allocation problem | solution proposal |
|---|---|---|
| infrastructure | the usage of support equipment such as air pressure, vacuum etc. in different process areas | measurement of consumption according to process area, using volume stream and consumption of electricity |
| processing of old ink | the internal processing of old ink to substitute new ink | measurement of the processed old ink in line with total ink consumption, generate emission credit |
| supplied additions form foreign production | Insertion of supplements to a newspaper which do not belong to the own production, but still affect the weight of transportation. | Measuring the share of weight of supplements and allocation of transportation |

## 3.6 Disposal processes

The disposal processes are very efficient in newspaper production. Over years the large number of circulations has enabled the development of a highly efficient waste disposal process. In the meantime, besides recycling paper, packaging and printing plates, solutions have also been found to process inks or washing agents. This investigation has revealed that waste processes only play a minor part in many PCF studies. The resource consumption can be lowered very effectively at this point. In return, more attention should be spent on on considering the waste processes (figure 3). As in the preproduction processes, the treatment and processing of disposal are highly complicated nowadays. This is made clear by an examined example of the disposal of the prepress chemistry.

Used development chemicals are categorized as special waste, which should be monitored. In Europe it falls under the disposal key 09 01 02 (LANUV, 2010). Old chemicals may be disposed only at a certificated disposer. According to the process the old chemicals contain a water percentage of > 90%. A direct disposal in the form of combustion is not possible. So the water percentage is evaporated first. This process requires energy. At the same time, however, water is also regenerated. Only afterwards the concentrate of a special waste combustion can be supplied. This example shows the investigations of numerous disposal processes and that determining the LCI data is necessary. Using  disposal keys to label the waste processes seems to be helpful from the point of view of the printers.
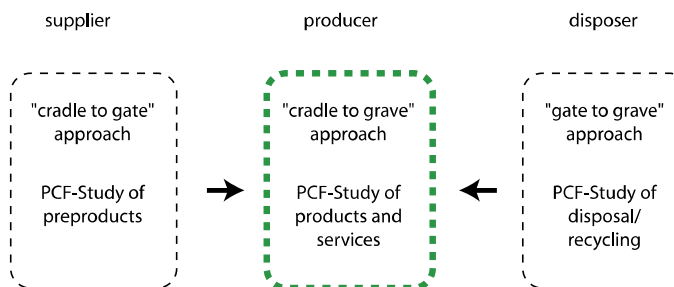


*Figure 3: Integration of suppliers and disposers in PCF studies*

## 3.7 Availability of LCI data

The availability of base data for the calculation varies. The availability of LCI data for paper, printing inks, printing plates and printing chemicals should be pointed out within the study. With regard to the paper suppliers it was found out that extensive data material and detailed documentations are prepared by the manufacturers. Mostly the PCF studies of papermakers are based on CEPI "Framework for the development of carbon footprints for paper & board products" (CEPI, 2007) as well as in June, 2010 by

CEPIPRINT/CEPIFINE published „user a guide to the coach voucher footprint of graphic paper" (CEPIPRINT/CEPIFINE, in 2010). Customers receive on inquiry a concrete PCF value, based on the production of 1t of paper.

The ink manufacturers partly rely on their own case studies. In Germany a study was carried out in 2007 on behalf of the Association of German Printing Ink Manufacturers to calculate the PCF of the production of printing ink. In this study only emissions regarding the consumption of oil, gas and electricity during the production processes were reported.

The printing plate manufacturers have also investigated the PCFs of some products. AGFA has announced the first results for 2010. However, at the time of this report no concrete figures were given yet.

Further data for relevant chemicals were extracted from publicly accessible sources like the PROBAS data base (UBA, 2010). LCI data for assessing the emissions of energy consumption and transportation were also extracted from the PROBAS data basis which is based on the GEMIS database from the Öko-Institut e.V. (Öko-Institut e.V., in 2010). A selection of LCI data for graphic materials is also provided by the Swiss database ecoinvent (Swiss Centre for Lifecycle Inventories, 2010).

## 4. Conclusions

This study has shown that effective PCF calculation requires a uniform method, for example in line with ISO 14067. On the other hand there is also great need of LCI data from different sources. At the moment representative LCI data are absent for many graphic materials. There remain doubts whether the appropriate suppliers of LCI software and databases can provide the required data at short notice. Besides, the rapid changes in technology in the graphic industry will complicate the perpetual updating of datasets. At this point industry associations could and should take up a leading role. The main task is the development and upkeep of uniform calculation bases, for example, in the form of Product Category Rules and in the supply of suitable LCI data for products in their sector. The European paper manufacturers have made a good start here. With the CEPI framework the paper manufacturers have not only positioned themselves clearly on the subject PCF, but have also accelerated the debate on PCF within the sector. As a result, many paper manufacturers are able to present representative LCI data today to their customers.

A more intensive examination of the disposal processes is necessary, because as with the production of preproducts complicated processes have been developed in waste treatment, processing and recycling which require more energy again  In this area there is a lack of effective knowledge as to how credits are to be generated and to be considered in the PCF calculation.

In addition, there is the need to train the staff in companies. The complicated structure of a PCF study requires some expertise, for example to design system boundaries or define cut off-criteria correctly. Working with case studies and practical examples is very helpful here. Showing model processes as flowcharts and presenting calculation examples as well as exemplary documentations seem to be very helpful.

Finally, it should be mentioned that the introduction of PCF calculations can stimulate the optimization of graphic products and processes. However, this can only succeed if work and documentation is done properly and methodically and if the necessary up-to-date knowledge is present in everyone involved.

## Acknowledgements

**References**

ADEME. (2007). *Bilan Carbone - Objectives and Principals for the Counting of Greenhouse Gas Emissions (Version 5.0).* France: ADEME.

BMU, UBA, Öko-Institut e.V. (2009). *Memorandum Product Carbon Footprint.* Berlin: BMU, UBA, Öko-Institut e.V.

BSI, Defra, Carbon Trust. (2008). *Guide to PAS 2050 - How to assess the carbon footprint of goods and services.* United Kingdom: BSI.

BSI, Defra, Carbon Trust. (2008). *PAS 2050:2008 - Specification for the assessment of the life cycle greenhouse gas emissions of goods and services.* United Kingdom: BSI.

CEPI. (2007). *Framework for the development of Carbon Footprints for paper & borad products.* Belgium: CEPI.

CEPI. (2007). *Framework for the development of carbon Footrpints for paper & board products - Appendices.* Belgium: CEPI.

CEPIPRINT/CEPIFINE. (2010). *User Guide to the carbon footprint of graphic paper v1.0.* CEPIPRINT/CEPIFINE.

EPD The International EPD System. (2010). *Draft Product Category Rules - CPC3214 (Processed Paper and Paperboard) Version 0.X.* EPD.

ISO. (2006). *ISO 14040:2006 Environmental management - Life cycle assessment - Principles and framework.* ISO International Organization for Standardization.

ISO. (2006). *ISO 14044:2006 Environmental management - Life cycle assessment- requirements and guidelines.* International Organisation for Standardisation.

Landesamt für Natur, Umwelt und Verbraucherschutz Nordrhein Westphalen (LANUV). (2010). *IPA Informationsportal Abfallbewertung*. Retrieved 06 15, 2010, from Abfallsteckbriefe > 0901 Abfälle aus der fotografischen Industrie: http://www.abfallbewertung.org/repgen.php?report=ipa&char_id=0901_Foto&lang_id=de&avv=&synon=&kapitel=2

Moberg, A. J. (2007). *Screening environmental life cycle assessment of printed, web based and tablet e-paper newspaper.* Stockholm: Reprot from KTH Centre of Sustainable Communication, US-AB.

Nors, M. P. (2009). *Calculation the carbon footprints of a Finnish newspaper and magazine.* VTT Technical Research Centre of Finland.

Öko-Institut - Institute for Applied Ecology, Potsdam Institute for Climate Impact Research (PIK) , THEMA1. (2009). *PCF Pilotprojekt Deutschland, Case Studies*. Retrieved 03 23, 2010, from http://www.pcf-projekt.de/main/results/case-studies/

Öko-Institut e.V. (2010). *Globales Emissions-Modell Integrierter Systeme (GEMIS) Version 4.5*. Retrieved 04 2010, from http://www.oeko.de/service/gemis/de/index.htm

*PRODUCT CARBON FOOTPRINT (PCF) PILOTPROJEKT DEUTSCHLAND.* (2008, 11 18). Retrieved 12 02, 2009, from http://www.pcf-projekt.de: http://www.pcf-projekt.de/files/1227872690/pcf-newsletter-01_komprimiert.pdf

Swiss Centre for Lifecycle Inventories. (2010). *Ecoinvent*. Retrieved 05 2010, from http://www.ecoinvent.ch/

UBA. (2010, 04 12). *Prozessorientierte Datenbank für Umweltmanagement-Instrumente*. Retrieved 05 2010, from http://www.probas.umweltbundesamt.de/php/profisuche.php?

WBCSD/WRI. (2009). *Product Life Cycle Accounting and Reporting Standard.* Switzerland and USA: WBCSD/WRI.

# Environmental impact of Swedish paper magazines and online publications

*Malin Kronqvist[1], Cathrine Löfgren[1], Michael Sturges[2], Anita Teleman[1]*

[1] Innventia AB
  Box 5604, SE-114 86 Stockholm, Sweden
  E-mails: malin.kronqvist@innventia.com, cathrine.lofgren@innventia.com, anita.teleman@innventia.com

[2] Innventia Edge UK
  Box 5604, SE-114 86 Stockholm, Sweden
  E-mail: michael.sturges@innventia.com

**Abstract**

An assessment of the environmental impact of two kinds of media publications, viz. printed magazines and online publications, was made. The study covered all stages of their life cycles, i.e. from cradle to grave. The functional unit for comparison was defined as "the consumption of a magazine for one year by one reader".

Reading a printed magazine that has been subscribed to and reading online for a corresponding period of time generate greenhouse gases in the same order of magnitude. The distribution of the environmental impact across the life cycle of the Swedish paper magazine studied is typical for a printed magazine, with pulp and papermaking usually being the dominant stage in the supply chain. For the online publication, the dominant aspect was the impact associated with the use of a laptop computer, including the manufacturing of a laptop. The printing and distribution of the printed magazine were relevant to the final outcome.

A number of sensitivity scenarios were analysed. The impact of a printed magazine and an online magazine publication can vary considerably, depending on an individual reader's behaviour. In addition, a cleaning gas, $NF_3$, used in the production of computers, contributes significantly to the potential climate impact of online reading.

**Keywords**: carbon footprint; life cycle assessment; printed magazine; web-based magazine

## 1. Introduction

At a time when there is heightened focus on environmental issues, it is important for media and graphic arts industries to understand the environmental profile of their products and services. This is particularly true in a changing market place, where magazine readers have a choice between reading on the Internet and reading the printed copy. A common argument in today's debate is that we should reduce our impact on the environmental by turning to the Internet for information instead of reading printed magazines, assuming that this would reduce the environmental impact. Previous research in newspaper production, carried out at Innventia, showed the two modes of publication to be comparable, from the perspective of impact on the climate (Moberg et al., 2007). Swedish magazine publishers take their responsibility concerning the environment very seriously. They are committed to working very closely with supply chains, in order to reduce carbon dioxide emissions.

Understanding the environmental impacts and factors that drive them will make it possible for us to identify and then propose opportunities for reducing the impact from both forms of media. At present, the magazine supply chain lacks access to independent and systematic data for evaluating the environmental pros and cons of the two media channels and, consequently, it is difficult for perceptions and pre-conceptions to be seen and heard in public debates.

Giving due consideration to the environment is one aspect of sustainable publication. Life cycle assessment is a well developed and widely recognised environmental assessment technique. It has previously been applied to paper magazines (Pajula et al., 2009). However, its application in the field of emerging electronic products and services, e.g. online publishing, has been limited. Its application in this field raises new and difficult questions, such as how to represent the various kinds of online user behaviour, how to allocate the impact of multi-service servers on specific online services, etc. Without such new research and supporting data, the magazine publishing supply chain and its customers are unable to make informed decisions about the relative environmental impact of the different media channels.

Earlier, the Periodical Publishers Association (PPA) launched the *PPA Carbon Footprint Calculator* for magazine publishers. The calculator is based on analysis of production and distribution of real magazines in the UK. However, it only considers climate change impacts rather than wider environmental impacts.

Previous studies (Moberg et al., 2007; Pajula et al., 2009) state that the use of paper (forestry and pulp and paper production) generally gives rise to 30% - 70% of the total impact on the environment from printed paper products. This is consistent with the findings by the PPA concerning carbon footprinting work and other UK-based studies of paper-based information media.

Sörmlands Grafiska (Sweden) carried out a carbon footprint study in 2009 (Enroth 2009a), comparing paper from Sweden and Finland, together with printing in Sweden, Denmark and Poland, to investigate the roles of transportation and distribution. The results showed that distribution was less important than the different sources of energy consumed in the country where the actual printing takes place.

There are hardly any studies available on the impact on the environment from IT, when compared to paper products. Gough (2008) concludes that end-user behaviour is critical of the overall impact of the electronic delivery of scientific journals but, as yet, very limited data exists on this aspect of publishing. Borggren and Moberg (2009) studied the potential impact on the environment from paper books and E-books. They conclude that user behaviour is an important aspect of the environmental impact of the two systems. Enroth (2009b) found that the environmental impact of a web-based electronic teaching aid on global warming is approx. 10 times greater than the environmental impact of a printed textbook. A textbook is used by many users over a long period of time.

The *overall aim* was to describe the potential environmental impact of two separate media publications, viz a printed and a web-based magazine. The scope of the study involved a Swedish magazine produced and distributed in Sweden, in both its physical and electronic formats. The study included all life cycle stages of the magazine, i.e. from cradle to grave. *Another aim* of the study was to identify any knowledge and data gaps and areas, where current and future research efforts should be concentrated.


## 2. Method

### 2.1 LCA

Life Cycle Assessment (LCA) is a technique used to quantify the environmental impact of a product or system, typically from the cradle to the grave i.e. from the procuring and conversion of the raw materials, including mining, forestry and agriculture, through the production of products, their distribution, use, and, finally, to waste management, e.g. disposal to landfill, incineration, recycling or reusing. ISO International Standards, ISO14040:2006 and 14044:2006, define LCA methodology. However, by necessity, these standards are non-prescriptive. They set out a framework to be followed, which ensures that practitioners of LCA identify all the parameters and decisions that need to be made in order to complete a justifiable and transparent study. The methodology consists of four stages, which are goal and scope definition, inventory analysis, impact assessment and interpretation. The whole process is iterative. It is possible and sometimes necessary to alter aim and scope, as a result of findings during the inventory analysis, the impact assessment and/or the interpretation stages. The main impact categories considered in this study are abiotic resource depletion, acidification potential, eutrophication potential, global warming potential (100 years), ozone depletion potential and photochemical ozone formation potential. The modelling was compiled using GaBi 4.3, a commercially available specialist LCA software tool. No external critical review took place in this study.

### 2.2 System boundaries and key parameters

A Swedish monthly magazine was chosen for this study. Two different product systems were studied, viz. a printed magazine and a web-based magazine. The product systems studied are described below. Sensitivity analyses were done. The sensitivity scenarios were a paper magazine with inserts, a paper magazine that is 100% distributed using the postal system, varying the time spent reading online and the number of print-outs for an electronic magazine. The effect of the electricity mix was studied as well.

### 2.1.1 Paper magazine

The physical magazine used in the study was printed in Sweden on paper produced in Sweden and distributed mainly to households in Sweden by post (see Table 1 and Figure 1). It is typical in Sweden for people to subscribe to magazines. The system boundary for the physical magazine is shown in Figure 1. The life cycle

of the paper magazine was studied *from cradle to grave*, i.e. from the wood harvesting to its end use and disposal, to its recycling or archiving. A system expansion was to account for the emissions avoided, due to the recycling and incineration of the magazine. Data concerning the number of readers per copy, the time taken in reading it and its distribution come from a study on the behaviour of a magazine reader in Sweden, conducted by Sveriges Tidskrifter (SMPA). The time taken in reading a magazine does not affect an assessment of its environmental impact, but it is an important aspect when it comes to the benefits of a printed paper magazine.

*Table 1. Description of the printed magazine studied and behaviour of the reader.*

| Parameter | Printed magazine |
|---|---|
| Edition | 12 issues (with nos 2 and 3 combined as one) |
| Size | Total 1,324 pages, including cover (approx. 120 pages per issue) |
| Format | 21.7 cm x 28 cm |
| Basis weight of paper - body | 65 g |
| Paper - body | GraphoCote, LWC paper |
| Basis weight of paper -cover | 150 g |
| Paper - cover | Tom&Otto (LCI data for GraphoCote used) |
| Printing | Heatset web offset (HSWO) 4-colour printed in Sweden |
| Parameter | Behaviour of a reader of paper magazines |
| Number of readers | 3.23 readers per copy |
| Time taken in reading | 40 minutes |
| Distribution | 91% of magazines supplied through the postal system and 9% through newsstands |
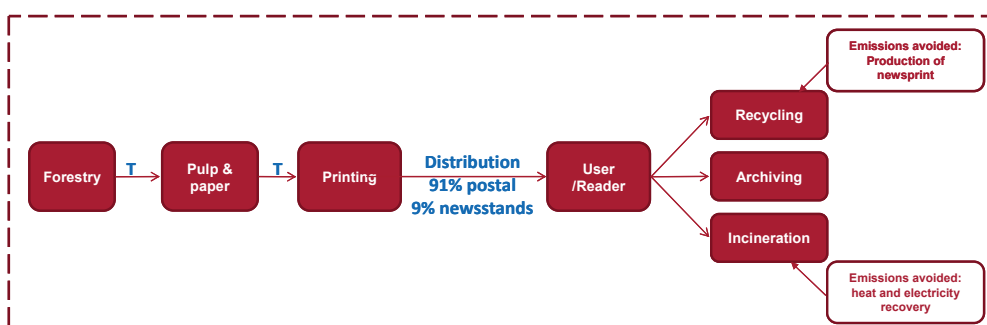


*Figure 1: System boundary and flowchart for basic scenario of a paper magazine*

### 2.1.2 Online publishing

An electronic format is not identical to a physical format. Magazines are generally not published as a full PDF version or any other corresponding format, such as E-magin, on the Internet. The trend is the opposite, that magazines publish additional material, unique to their website. However, the physical and electronic formats are comparable, due to the fact that they both compete for the readers' time. Consequently, this should be reflected in the function / functional unit.

For this study, to provide a starting point for understanding the environmental implications of online publishing, a basic scenario was described and modelled, with some of the parameters being changed. The model consists of the following stages: production of components, data centre (hosting), downloading (i.e. use of the Internet infrastructure to retrieve the materials), use (online reading and printing in the home), waste management and emissions avoided (see Figure 2). Once the electronic content has been prepared, it is uploaded onto a server for storage and online retrieval. The key parameters in the basic scenario are set out in Table 2.

### 2.1.3 Functional unit

The functional unit was established as "*the consumption of a magazine for one year by one reader*".

### 2.1.4 Data

To compile the models, a combination of secondary data (from widely recognised, publically available datasets) and primary data (from participants in the project and their suppliers) were required. The secondary data related primarily to generic materials and processes. The primary data related to operations specific to

the supply chains for the two forms of media that had been identified. The data required was related to the energy and raw materials used and the waste and emissions produced during the operations, relative to the defined functional unit. A questionnaire was developed for each process unit, for which primary data were required. Primary data were collected from conditions during the 2008 calendar year.

### 2.1.5 Electricity mix

"Swedish electricity mix" is used to represent: "SE: electricity, medium voltage, at grid [supply mix]" in the Ecoinvent 2.0 database (Frischknecht et al., 2007). This database differentiates "production mix" from "supply mix", where, in the supply mix, import and export are considered.
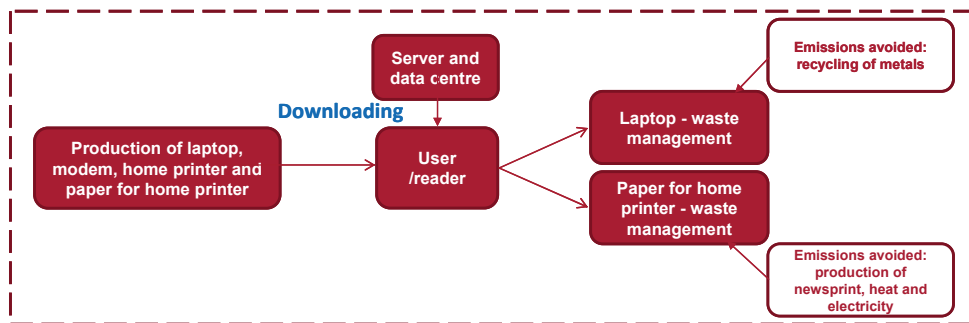


Figure 2: System boundary and flowchart for the basic scenario of online publishing

Table 2: Description of the basic scenario for online publishing

| Parameter | Web magazine |
|---|---|
| Edition | 7 days /week |
| Servers at data centre | 500 W |
| Time taken in reading | 40 minutes/month, divided among 3 visits to the site per month |
| Online reading hardware | Laptop computer, Modem |
| Profile for home laptop and Modem use | For a 24 hour period, laptop is in active/on mode for 5.52 hours; on standby for 1.92 hours; off for 16.56 hours. Impacts associated with standby and off modes are allocated to the active mode. Modem was assumed to be on for 24 hours per day. |
| Geographical location for reading | Online reading in Sweden, using the Swedish electricity supply |
| Print-outs | 2 single-side print-outs per month |

## 3. Results and discussion

### 3.1 Paper magazine - basic scenario

The life cycle system of a paper magazine is well known. Primary data were available from members of the project for many of the life cycle stages. The trend in the results was, as expected, the same as from previous studies carried out on paper magazines. The results are fairly consistent throughout the impact categories, with pulp and paper production being the main contributor, followed by printing or distribution to households. See Figure 3 for the Global Warming Potential (GWP) results and Figure 8 for the other impact categories.

For a single reader for a period of one year, the total GWP impact for the paper magazine is $0.83_7$ kg of $CO_2$ eq., taking emissions from fossil sources into consideration.

The total greenhouse gas emissions associated with the production, distribution and disposal of a typical Swedish magazine are 990 kg of $CO_2$ eq. per ton of the magazines. This is lower than previously reported, considering the carbon footprint of a Finnish magazine, which is 1,140 kg - 1,350 kg of $CO_2$ eq per ton of the magazine (Pajula et al 2009). The item that makes the difference is mainly the electricity mix in the country, viz. the different means used to produce the electricity. The Swedish electricity mix clearly has the lowest impact on climate, since so much electricity in Sweden comes from nuclear and hydroelectric plants. In Finland, 28% of its electricity is produced using coal. Moreover, Pajula et al (2009) assume that there is a 16% landfill in the end-life phase.

The carbon footprint of a copy of the Swedish magazine studied is approx. 245 g of $CO_2$ eq. According to studies at Innventia, the footprint of professional magazines can vary enormously, from as low as 90 g per copy to as high as 550 g per copy, depending on the properties of the publication, such as pagination and choice of paper. A major influence on the footprint of a typical Swedish magazine is the fact that it utilises paper that is both produced and printed in Sweden.

*Recycling*

One advantage of a paper product is that it is recyclable. Recycled fibres from magazine paper can be used as a raw material in the production of newsprint. Furthermore, when paper is incinerated as household waste, electricity and heat are recovered in the incineration plants. To illustrate these advantages in an LCA, a system expansion was applied. The system was expanded to include the production of newsprint, electricity and heat as well. The emissions from these processes were subtracted from the total and a net result was produced. In Sweden 89% of newsprint and magazine paper was recycled in 2008. For the magazine studied, this resulted in a reduction of 0.24 kg of $CO_2$ eq. in emissions per reader and year.
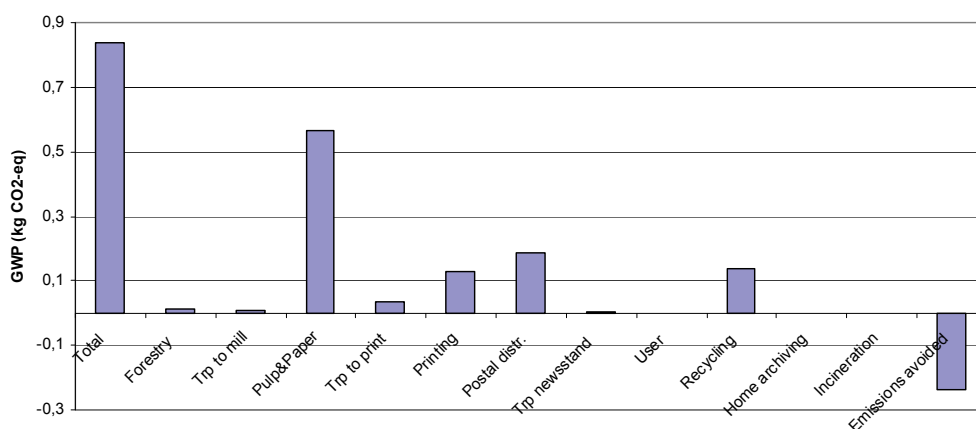


*Figure 3: Basic scenario for a printed magazine. The Global Warming Potential (GWP) for one reader per year. Results are per life cycle stage. The total result is the sum of emissions. The CLM2001 - Dec 07 method was modified to no biogenic $CO_2$ emissions*

## 3.2 Paper magazine - sensitivity analysis

### Distribution and inserts

A somewhat lower GWP impact is observed, when there is a distribution of 100% through the postal system (see Figure 4). This is mainly due to the fact that, in Sweden, 60% of magazines in newsstands are sold, the remainder are returned for recycling to paper mills. To reach the same number of readers, more magazines must be produced if they are to be sold in newsstands. As expected, the GWP impact is greater when the production of inserts and a DVD are included in a magazine. This is mainly due to the resultant increase in weight (see Figure 4).

### Electricity mix

Since emissions from the production of electricity are important for all the impact categories, the basic scenario was tested with two alternative electricity mixes, one based on the mix in the Nordic countries and one based on the average European electricity mix. The results for the GWP impact category are shown in Figure 4. The results of the Swedish electricity mix had the lowest impact, while the Nordic and European mixes were higher. These results indicate the importance of the location of the production, when it comes to energy intensive life cycle stages, such as pulp and paper production and printing. The Swedish electricity mix has a very low carbon footprint, due to the high percentage of hydroelectric power and nuclear power, whereas a large percentage of the electricity produced in Denmark, Finland and European countries utilises fossil resources.

### Number of readers

In the basic scenario, the environmental performance of the printed magazine was related to each individual reader per annum. This means that the environmental impact of the printed magazine was divided among 3.23 readers. The results were therefore different, when the environmental performance per printed issue was studied or when more readers per copy were considered (see Figure 4).
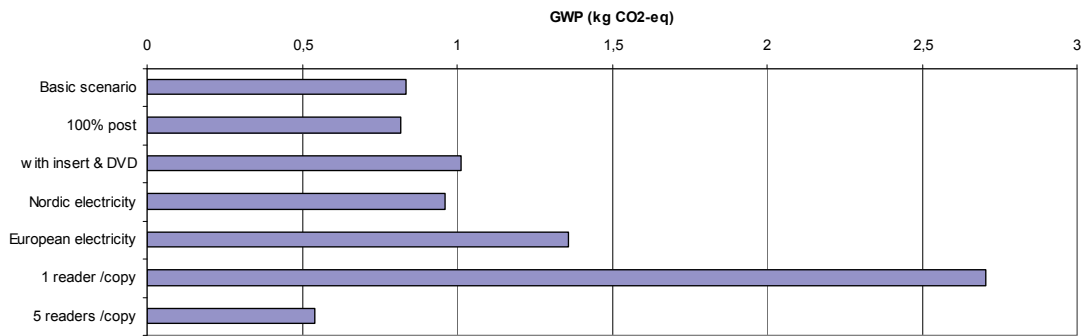
*Figure 4: Sensitivity analysis for a printed magazine. Global Warming Potential (GWP) for one reader per year. The CLM2001 - Dec 07 method was modified to no biogenic $CO_2$ emissions*

### 3.3 Online publishing - basic scenario

Just as every magazine is different, every website is different. Describing the production and use of an average website or online publication to determine the typical environmental impact of online publishing is difficult, since the following parameters can be very different from one website to another and may consequently affect the results achieved and conclusions drawn:

- Number of web pages and type of content, i.e. how much storage space/computing power is required to host the publication and to access/read the publication.

- Number of readers, i.e. the number of users among whom the impact of producing and hosting the website are divided.

- Online time taken in reading and the number of visits made by the reader.

- Equipment used by the reader, e.g. desktop/laptop computer, internet connection, etc.

- Home printing: Does the reader print out any of the materials at home and, if so, what kinds of printing and paper are involved?

Nonetheless, a basic scenario was described and modelled, with some of these parameters being altered. If consideration is given only to emissions coming from fossil resources, the GWP impact for the online publishing was $0.84_4$ kg of $CO_2$ eq., when taking into account the functional unit of one reader for a period of one year. The impact associated with the use of a laptop (incl. laptop production) accounts for approximately 72% of the total GWP impact (see Figure 5). Home printing is the second biggest contributing stage in the life cycle. The use of a modem and of the Internet infrastructure each accounts for approx. 3% - 4% of the total impact. Although the GWP impact of a single data centre may be large, when allocated across the full range of services provided and the end-users, the impact per functional unit becomes very small. Subsequently, the contribution of the impacts that occur from hosting the material in the data centre is less than 1% of the total and is therefore too small for it to appear on the graph.

When it comes to using a laptop computer, three emissions especially dominate the GWP impact, viz. nitrogen trifluoride, carbon dioxide and sulphur hexafluoride. Breaking down the use of a laptop into more detail reveals that the emissions of nitrogen triflouride occur during the assembly of an LCD module that is used in a laptop computer. Nitrogen triflouride ($NF_3$) is a chemical used predominantly for cleaning the chambers used in the high volume production of liquid crystal displays and silicon-based thin film solar cells. In these applications, $NF_3$ is initially broken down *in situ* by plasma. Utilisation by the process of the chemicals applied in the plasma process is typically less than 20%. As a result, some of the $NF_3$ escapes into the atmosphere, although modern gas abatement systems can decrease the levels of emissions. $NF_3$ is a greenhouse gas with a 100 year GWP that is 17,200 times greater than that of $CO_2$. Elemental fluorine was recently introduced as an environmentally preferable replacement for $NF_3$ in the state-of-the-art high volume production of flat panel displays and solar cells. The best available LCI data for manufacturing electronic components was derived from the Ecoinvent database.

However, these data reflect technology and operations from 2001 and, therefore, the GWP impact associated with $NF_3$ emissions in this analysis may be an overestimation, when it comes to the current situation (see Chapter 3.4: Sensitivity analysis).
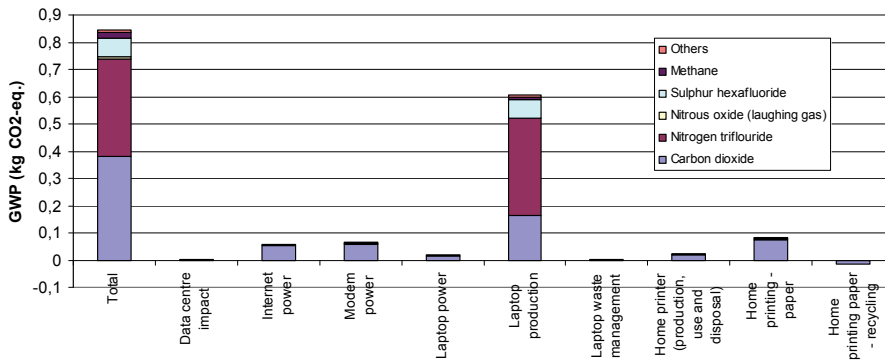
*Figure 5: Basic scenario for online publishing. Global Warming Potential (GWP) for one reader per year. Results per life cycle stage. The total result is the sum of emissions. The CLM2001 – Dec 07 method was modified to no biogenic $CO_2$ emissions*

### 3.4 Online publishing - sensitivity analysis

*Electricity mix*

In the basic scenario, the Swedish electricity mix was considered for the hosting of the website, for powering the Internet infrastructure, for retrieving the web pages and for online reading/printing in the home. Figure 6 shows the effect of the electricity mix on the overall results for the online publishing model. Two sensitivity analysis scenarios were considered: a scenario in which the average European electricity mix was considered and a scenario in which the Nordel energy mix was considered. Clearly, the electricity mix chosen had a significant bearing on the overall results achieved.

*User behaviour*

Undoubtedly, the most important factor determining the scale of the environmental impact that the basic case scenario had was the time spent online by the reader (see Figure 6). This affected (i) the proportion of laptop production allocated to reading the online material and (ii) the energy required for powering the laptop, the modem and the Internet infrastructure. Another important factor was home printing, including the number of pages printed and the choice of paper (see Figure 6).

*$NF_3$ emissions*

The sensitivity analysis considered scenarios with reduced $NF_3$ emissions from the cleaning of the PECVD chamber.  The sensitivity analysis was made on the basic case scenario. Scenario 1 considered a 69% reduction in $NF_3$ emissions, based on an estimate of the proportion of emissions covered by abatement in 2004 (Schottler et al, 2004). Scenario 2 considered a future scenario, where only fluorine is used. It is evident that a reduction in $NF_3$ emissions significantly reduces the GWP impact (see Figure 6).



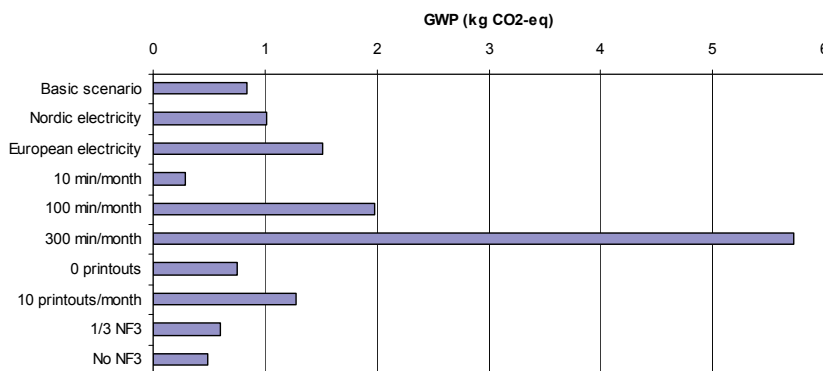*Figure 6: Sensitivity analysis of online publishing. Global Warming Potential (GWP) for one reader per year. The CLM2001 - Dec 07 method was modified to no biogenic $CO_2$ emissions*

### 3.5 Comparison

A comparison of the systems was made. Figure 7 shows how the global warming impact varies according to user behaviour. This shows a crossover in the basic scenario. With little use/few readers, the reading of

materials in a paper format has a greater impact. With greater use/many readers, the reading of online materials has a greater impact.

For the other primary impact categories, the comparison between reading the printed and the online magazine is shown in Figure 8. For the impact categories of abiotic resource depletion, acidification potential, eutrophication potential and photochemical ozone formation potential, there is a tendency towards a somewhat greater impact for reading materials in paper format than for online reading. For the impact category of ozone depletion potential, there is a tendency towards a somewhat lesser impact for reading materials in a paper format than for online reading.
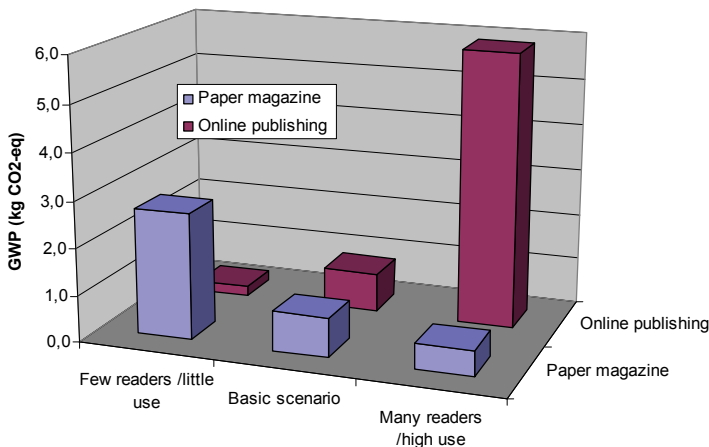


*Figure 7: Global Warming Potential (GWP) for one reader per year, based on different assumptions and choices. Paper magazine: few readers = 1 reader/copy, Basic scenario = 3.23 readers/copy, many readers = 5 readers/copy. Online publishing: little use = 12 min/month and no print-outs, Basic scenario = 40 min/month and 2 print-outs/month, high use = 300 min/month and 10 print-outs/month. The CLM2001 – Dec 07 method was modified to no biogenic $CO_2$ emissions*
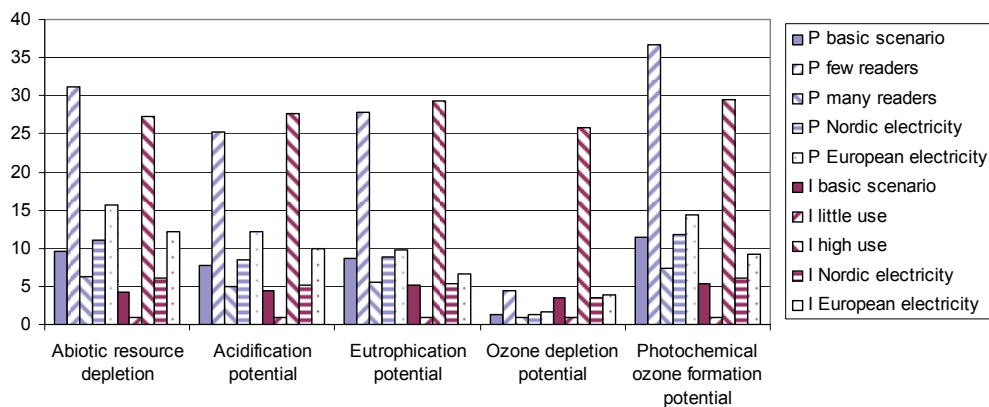


*Figure 8: Comparison of different impact categories for one reader per year, based on different assumptions and choices. Relative unit: for each impact category, the variation with the lowest value was numbered 1 and the other variations have been compared to this. P = Paper magazine; few readers = 1 reader/copy, Basic scenario = 3.23 readers/copy, many readers = 5 readers/copy. O = Online publishing: little use = 12 min/month and no print-outs, Basic scenario = 40 min/month and 2 print-outs/month, high use = 300 min/month and 10 print-outs/month*

## 5. Conclusions

Conclusions can be made, based on this LCA Swedish case study of two media publications, viz. a printed magazine and online magazine publication. In spite of certain uncertainties that occur in the study, the following conclusions can be made:

- Media consumption leads to an impact on the environment, whether on paper or online.
- Reading a printed magazine that has been subscribed to and reading online for a corresponding period of time generate greenhouse gases in the same order of magnitude.
- The impact of a printed magazine and an online magazine publication can vary considerably, depending on individual reader behaviour.

- The results show the importance of the location of the production of energy-intensive operations, such as pulp and paper production and/or the printing.

***The following variables may have a significant effect on the carbon footprint of magazines:***

- Since pulp and paper production typically accounts for the main part of the total carbon footprint of a magazine, the choice of paper obviously has an important effect on the impact. The *national grid electricity mix* available to the mill may have a major influence on the footprint of a particular paper, as can the *fuels* used for any self-generated energy (steam and electricity). The background grid electricity supply in Sweden has a low carbon footprint, when compared to Nordic or European grid electricity. The Swedish grid electricity is mainly produced from renewable resources and nuclear energy, whereas both Nordic and European grid electricity is more reliant on fossil fuels

- *The number of readers per paper magazine* has a major influence on an impact on the environment per individual reader. Since the impact on the environment from a printed magazine is related to production, printing, distribution and waste handling and not to the reading, this means more readers per magazine and less impact on the environment per individual reader.

- *Inserts in a paper magazine* increase their weight and, consequently, the impact on the environment will be greater. The impact per copy is also directly proportional to its pagination.

- *The distribution* of a paper magazine *through newsstands* increases the impact on the environment, when compared to distribution through the postal system.

- For *online* reading, the impact on the environment is directly proportional to the *time taken in reading* per year and reader - the longer the time spent online, the greater the impact on the environment.

- The more *paper pages that are printed out* in connection with reading *online*, the greater the impact on the environment.

- Use of *cleaning gas NF3* in the production of a computer contributes significantly to the potential impact on the environment that comes from reading *online*.

## Acknowledgements

## References from printed sources

Enroth M (2009b), *Environmental impact of printed and electronic teaching aids, a screening study focusing on fossil carbon dioxide emissions*, Advances in Printing and Media Technology, Proceedings of the 36th International Research Conference of iarigai Vol XXXVI: 23-29

ISO, The International Organization for Standardization, (2006) *ISO 14040, Environmental management - Life cycle assessment - Principles and framework*

ISO, The International Organization for Standardization, (2006) *ISO 14044, Environmental management - Life cycle assessment - Requirements and guidelines*

Pajula T, Pihkola H, Nors M (2009), *Challenges in carbon footprint calculation and interpretation - Case Magazine,* Advances in Printing and Media Technology, Proceedings of the 36th International Research Conference of iarigai Vol XXXVI: 15-21

## References from web

Borggren C, Moberg Å (2009), *Pappersbok och elektronisk platta – en jämförande miljöbedömning*, ISSN:1654-479X, KTH, Stockholm, http://www.sustainablecommunications.org/bok/

 "CML 2001 method",  Institute of Environmental Sciences, Leiden University, The Netherlands: Handbook on impact categories "CML 2001", http://www.leidenuniv.nl/cml/ssp/projects/lca2/index.html

Enroth M (2009a), *A general assessment of climate impact from printed matter*, http://www.sormlandsgrafiska.se/documents/Sorml_Grafiska_Klimatpåverkan_090209.pdf

Eriksson E, Karlsson P-E, Hallberg L, Jelse K (2010), *Carbon footprint of cartons in Europe – Carbon footprint methodology and biogenic carbon sequestration*, IVL Report B1924, IVL Svenska Miljöinstitutet, Stockholm

Frischknecht R, Jungbluth N, Althaus H.-J, Doka G, Dones R, Hischier R, Hellweg S, Nemecek T, Rebitzer G and Spielmann M (2007) *Overview and Methodology. Final report ecoinvent data v2.0, No. 1.* , Swiss Centre for Life Cycle Inventories, Dübendorf, CH. Online version www.ecoinvent.ch

Gough M (2008), *Footprinting Study of the Reed Elsevier Journal 'Fuel'*, Best Foot Forward, http://www.reedelsevier.com/corporateresponsibility08/PDFFiles/fuel-footprint-study-exec-sum.pdf

Kajunpää M, Pajula T, Hohenthal C (2009), *Carbon footprint of a forest product – challenges of including biogenic carbon and carbon sequestration in the calculations*, VTT Symposium 262, 27-39 http://www.vtt.fi/publications/index.jsp

Moberg Å, Johansson M, Finnveden G and Jonsson A (2009), *Screening environmental life cycle assessment of printed, web based and tablet e-paper newspaper*, ISSN:1654-479X, KTH, Stockholm, http://www.sustainablecommunications.org/printed-and-tablet-epaper/

Moberg Å, Borggren C, Finnveden G and Tyskeng S (2008), *Effects of a total change from paper invoicing to electronic invoicing in Sweden - A screening life cycle assessment focusing on greenhouse gas emissions and cumulative energy demand*, ISSN:, 1654-479X, KTH, Stockholm, http://www.sustainablecommunications.org

Schottler M, de Wild-Scholten M  (2008), *Carbon footprint of PECVD chamber cleaning,* Photovoltaics International, 2nd edition, November 2008

**2**

*Improving print quality*

# Benchmarking newspaper picture quality

*Fons Put*

Flemish Innovation center for Graphic Communication
Campus Blairon 5, B-2300 Turnhout, Belgium
E-mail: fons.put@vigc.be

**Abstract**

Newspaper publishers today are interested in the quality of the printed pictures. Nice colorful pictures can help to attract new markets and customers. Question is what is good picture quality? In the publishing company itself there is mostly no general agreement on this topic. Different department show different opinions. This ambiguity makes it difficult for the management to take proper actions for improvement. In this research we try to develop an objective evaluation method on the perceived picture quality.

This quality evaluation can than be used to keep track of the progress in the picture quality level.

**Keywords:** ISO 12647-3; newspaper printing; standardization; perception; quality

## 1. Introduction

Newspapers today have still a strong position in the media landcape. The number of sold copies in Nord-America still beats the number of television viewers on top sports events. But newspaper publishers have several points of concern: circulation, advertisement rates and new media competitors showing up. The production of nice colorfull pages, filled with pictures, can be a great support in attracting new readers.

In order to achieve this goal, you can notice differences in the methods publishers use to achieve these type of printed pictures: manual and automatic photo-correction, advanced screening types, new print techniques (conventional versus waterless offset) and press controls (graybalance, camera-based press controls, manual measurements). As a result the look and feel of the pictures can be very different between the newspaper titles. The companies themselves have noticed this and are interested to see how they perform compared to their competitors.

Consultation of the different departments in a typical newspaper publisher lead to following opinions:

Editorial/commercial departments are focused on the printed result: How do I, from a readers viewpoint, evaluate our printed pictures compared to my competitors? These departments are less interested in technical numbers and parameters.

Production departments focus on their production settings: They occupy themselves with settings for automated picture correction, screening type and resolutions, print performance. Production departments typically tend to make more personal judgements on print quality, rather than evaluating from the readers viewpoint.

In this battlefield lies the cause and motivation for this research. The goals can be defined as:

- How to objectively evaluate the picture quality compared to competitors?
- How to objectively evaluate the influence of production settings to picture quality?
- How to improve the communication between production and commercial departments in case of picture quality?

*The objectives of the research presented in this paper are:*

- Developing and testing a method to characterize the quality of printed pictures
- Collecting information on the perception of quality of printed pictures
- Examine relationships between the characterization and perceptual data

## 2. Methods

In order to evaluate the picture quality between the different newspaper titles following questions emerges: What kind of data can be collected to describe picture quality? And secondly, are there relationships with the quality-perception by the consumers/readers?

We proposed following methods to gather useful information on picture quality in newspapers:

- Gathering of characterization data of printed pictures. This involves an indication of dynamic range, median, contrast, color chroma, sharpness and smoothness of a printed picture.

- Gathering of consumer perception related properties. How does a reference group judge the picture quality? In this project the reference group consists of high school graphical students.

### 2.1 Picture characterization data

In this approach we look for a method to compare image properties of the printed product. It is the printed product that will be evaluated (not digital files). The basis of the quality-comparison between the printed pictures is making digital photographs of these printed products.



*Figure 1: Camera setup for making digital photographs of the printed pictures*

The digital photographs of the printed samples are produced on the following manner:

- Preparation of the samples. The newspaper pictures are placed on a black background to minimize the show-through effect.

- Photographing the printed samples:
  - High-end digital camera
  - Fixed D50 light conditions (Gretag light booth)
  - Fixed settings for diaphragm/exposure
  - Fixed geometry that resembles reading a newspaper (light incident at 45°, viewing at 0°)
  - RAW shooting and conversion with fixed RAW/RGB settings (AdobeRGB)

Color management is not used during the shooting: We are not looking for color reproduction, but we are interested if differences: For example does picture A shows higher color chroma than picture B? Is picture A sharper than picture B?

- Cropping of the digital pictures so that they consist of identical content.

- Extracting of characterization data by suited image processing algorithms. The selected algorithms describe following image parameters:
  - Dynamic range.
    Calculated as the luminance difference of the lightest ands darkest point. The measured dynamic range will be influenced by the brightness of the paper and the darkness (lightness) of the maximum inkfilmthickness.

- Median

    Calculated as the median of the luminance histogram. The median can help in comparing the gradation of identical pictures between different titles.

- Contrast

    Contrast is in this project defined as the sum of local luminance maps. This method is described by Alessando Rizzi in CGIV2004: The Second European Conference on Colour Graphics, Imaging and Vision). The original image is resampled and transformed to CIElab color space. In this resampled image local contrast maps are formed and the luminance difference is calculated. The sum of all the calculated local maps serves as a reference number for the picture contrast.

- Color content

    The image is coded in an AdobeRGB color space with according CIELAB values. After down sampling the average and maximum chroma of the different pixels are calculated. On basis of the maximum chroma only pictures that reaches a threshold level of color chroma are selected for chroma comparison.

- Sharpness

    Calculated as the black level frequency of the image distribution after passing through an edge-filter algorithm.

- Smoothness

    Calculated as the median of the image distribution after passing through an edge-filter algorithm.

## 2.2 Consumer perception

The perception of the reader is an important factor in the comparison of the printed images in the different newspapers. The methodology for this perception is found in the Study (2007/2009) of the RIT Printing Industry Centre: "Evaluating the Image Quality of Digital Print Technology relative to Traditional Offset Lithography". In our research people are asked how much money they are prepared to pay for a published newsprint image, compared to the reference image. If the selected reference image costs 1 EUR, how much are you willing to pay for the other print?

After analysis of the perception scores, the average awarded value for a picture and the spreading of the awarded value of a picture are calculated.

## 2.3 Picture selection

Two types of printed pictures in newspapers are selected for analysis:

- Identical advertisement pictures in different publications. Each publisher start with a print-ready PDF in CMYK color space. The evaluation results will give information about the plate making and printing.

- Identical editorial pictures in different publications. Each publisher starts with an RGB-coded digital picture. Before plate making and printing this type of picture is corrected before plate making. The evaluation results will give information of the picture handling, plate making and printing.

Notice that to benchmark the quality identical pictures are needed. The detection parameters are image specific: picture contrast can only be evaluated by comparing it with the contrast of the same picture in other publications.

## 2.4 Reporting

In order to make the results clearly understandable for the different departments, every parameter is scaled in the range 0 to 100. The maximum score of 100 points is set at the highest recorded value on a parameter. The zero-reference (lowest possible score) is at the recorded value of the image with the maximum score after adding a fixed amount of image degradation. This scaling gives us the advantage that communication can easily be understood: The picture with the highest color chroma scores 100 points. If the same picture printed in another publication scores 95 points, it is almost as colorful as the high-score. If it scores 10 points, it has clearly a lower color chroma compared to the high-score picture.

- Color
    - Maximum score (100pt) for the high color image with the highest chroma
    - Minimum score (0pt) for the high score image after a fixed amount of desaturation

- Sharpness
  - Maximum score (100pt) for the image with the highest recorded sharpness
  - Minimum score (0pt) for the high score image after a fixed amount of Gaussian blurring
- Smoothness
  - Maximum score (100pt) for the image with the highest recorded smoothness
  - Minimum score (0pt) for the high score image after adding a fixed amount of noise

# 3. Results

## 3.1 Advertisement pictures

In case of advertisement 3 different titles, with 4 different editions for title 3 are used in the benchmark.
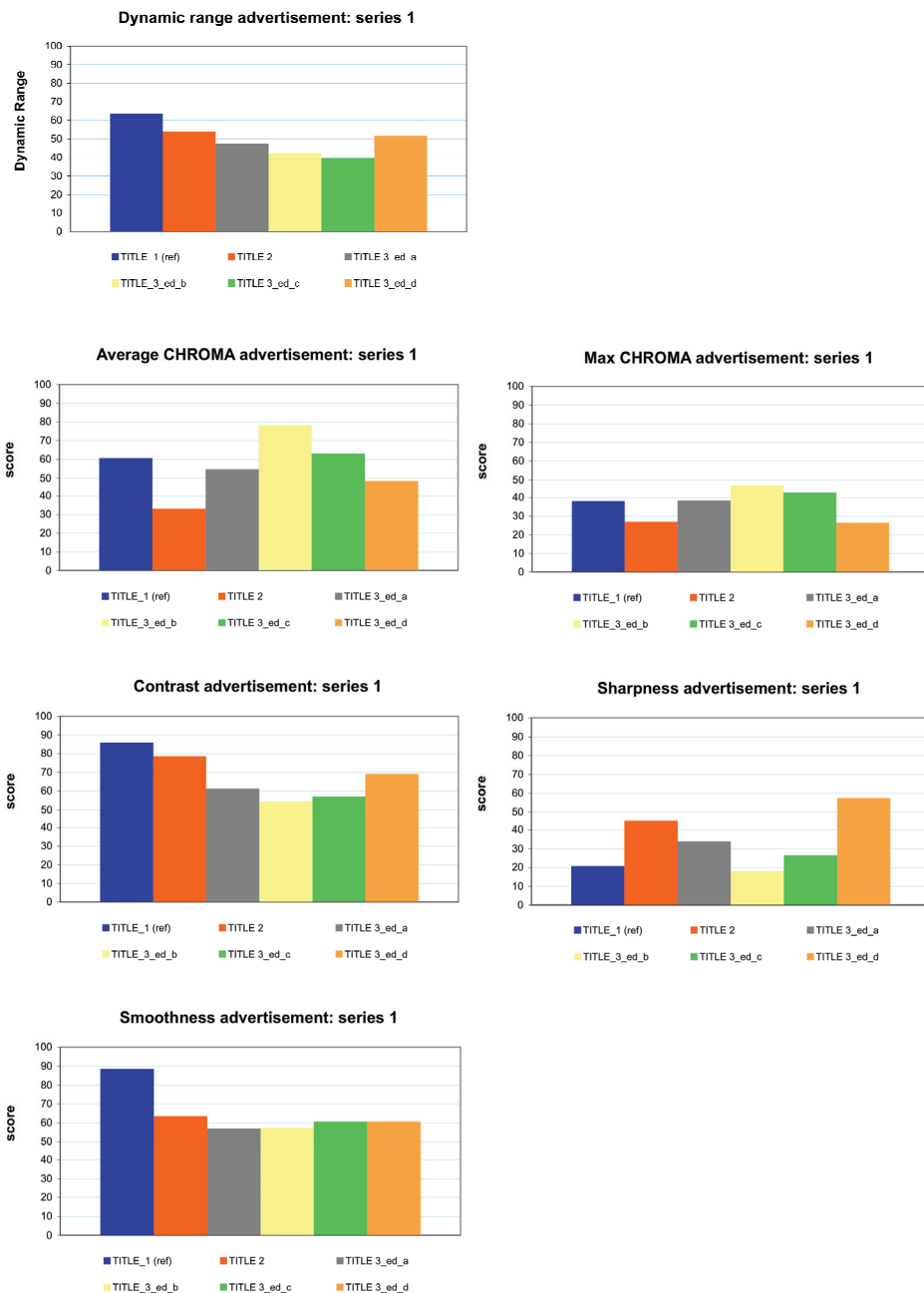
Figure 2: Scores of the advertisement pictures on basis of the picture characterization data

## 3.2 Editorial

For the editorial benchmark 2 titles are selected. These titles use totally different workflows and are printed on different presses and materials.
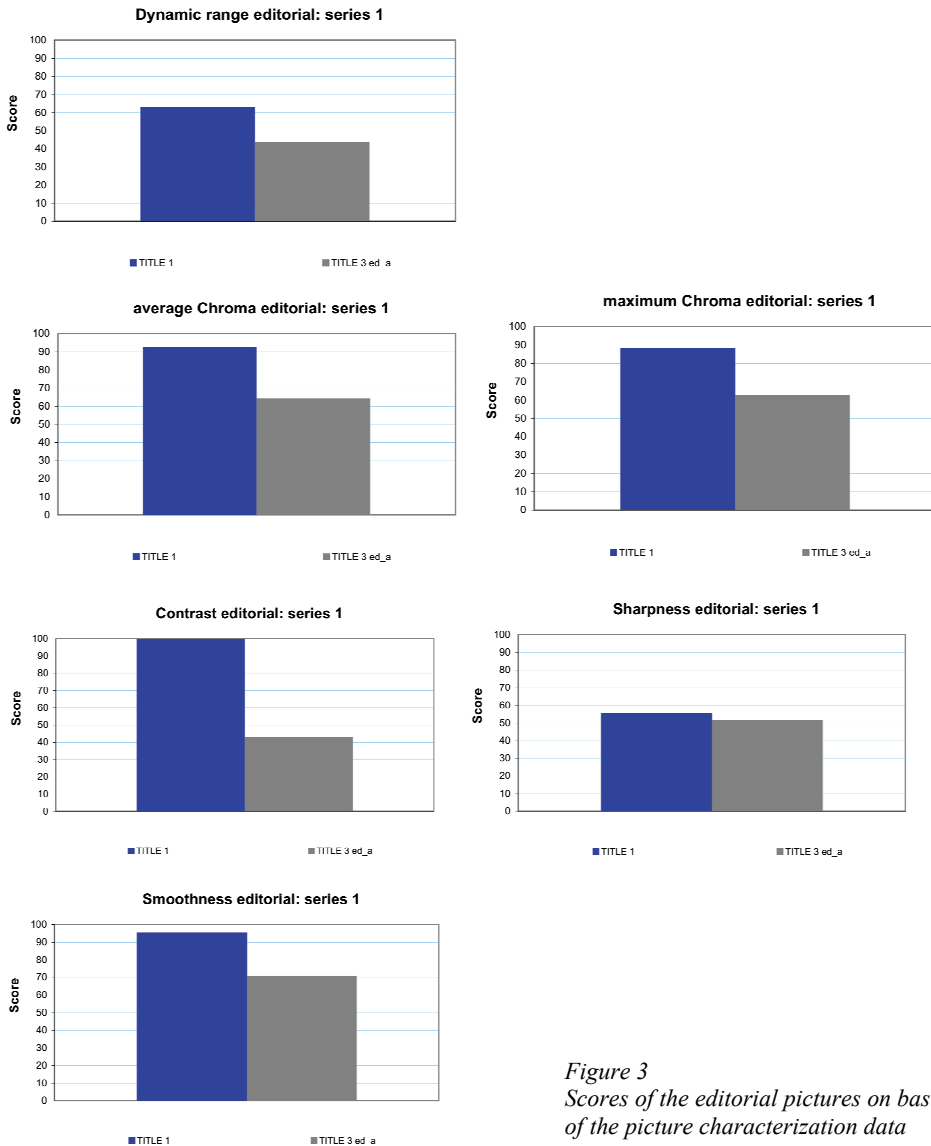


*Figure 3*
*Scores of the editorial pictures on basis of the picture characterization data*

## 3.3 Perceptual scores

A selection of the measured samples was presented to a reference group for perceptual evaluation. The reference groep consist of graphic highschool students. These reference group conducted 228 scores an advertisement samples and 82 for editorial pictures.
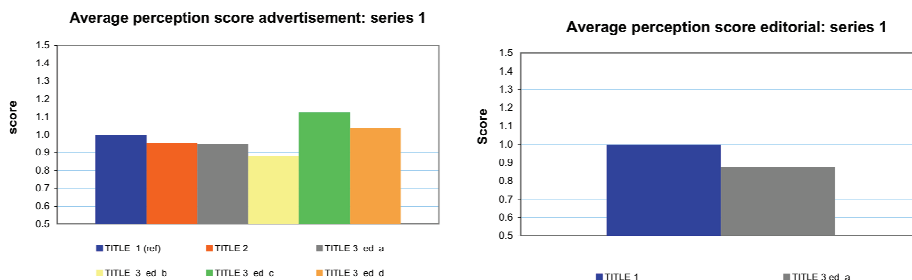


*Figure 4: Average perceptual scores of editorial and advertisement pictures*

## 3.4 Individual reports

To examine and evaluate relationships between the measured properties and perception score indivual reports are made of each sample set. These serve as basis for discussion between the different departments.
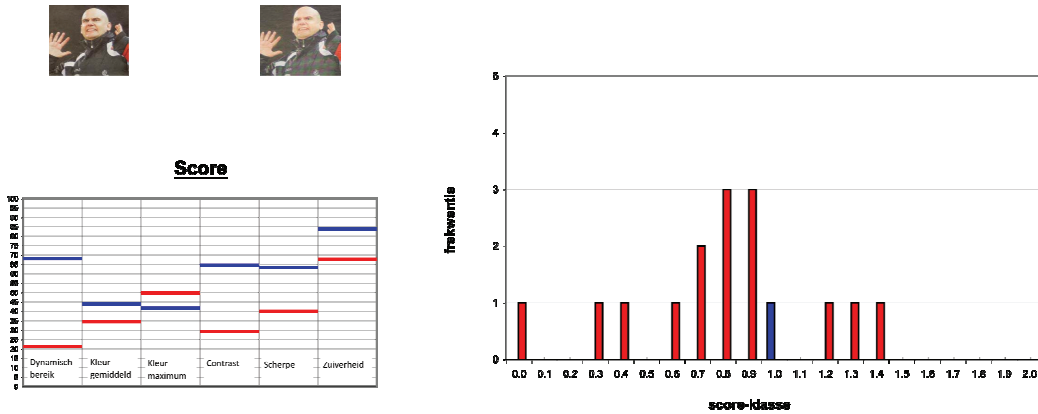


*Figure 5: Example of an indivual picture report*

## 4. Conclusions

- Title 1 shows a significantly higher dynamic range compared to the other titles. This is caused by slightly higher ink gloss of title 1. Gloss-measurement shows 14 TAPPI-units for Title 1 and 6 TAPPI-units for title 3.



*Figure 6: Differences in perceived dynamic range as a result of ink-gloss. The pictures on the first row are top-lighted and recording under 45°. The pictures on the second row are tilted under 45° (newspaper are often read in this way)*

- Title 1 uses significantly higher contrast in editorial pictures. This is often perceived as higher quality (perceptual reports). The lower contrast of Title 3 is caused by the settings of the image optimization software. This was guided on holding maximum detail in the dark and light region. After adjustment of these settings a second set of samples has been prepared and run through the evaluation procedure.



*Figure 7: After adjustment of image optimization settings, Title 3 reaches the same contrast level as Title 1*

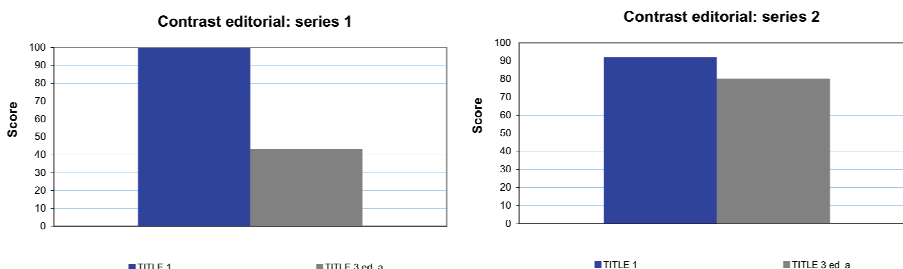- The chroma of the color of the advertisement is significantly higher than for editorial pictures. The cause of this can be found in the printers' attention for correct adjustment of ink-settings for advertisement and editorial pictures: ink setting is first made for advertisement and only if these are finished the printer switches to the editorial pages. The perceptual scores also confirm the lack of color. This information made the publisher to decide in investing in closed loop color control for all printed color pages.

- Caution with using picture with low-resolution. Publishing editorial pictures with too low resolution for the used dimension has consequences: sharpness scores is zero and the reference group rates these types of pictures very low.
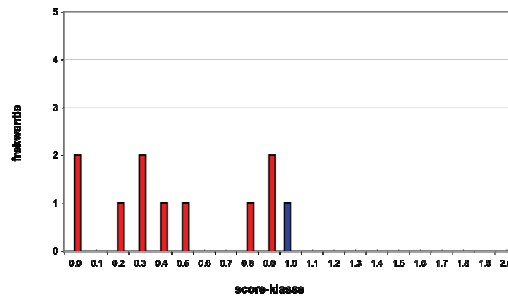


*Figure 8: Perceptual scores of a low-resolution picture printed on a large format and smaller format*

- Perceptual evaluation correlate with the characterization data. Title 3 has significantly higher scores on printed advertisement than on editorial pictures (higher chroma). The perceptual scores also confirm this trend.

- Median. Individual reports of advertisement comparison show significantly higher median value for 2 newspapers. After examining the phenomenon it came out that these 2 titles used a different (older) compensations in plate exposure that were not suited for the standardized 26% dot gain.
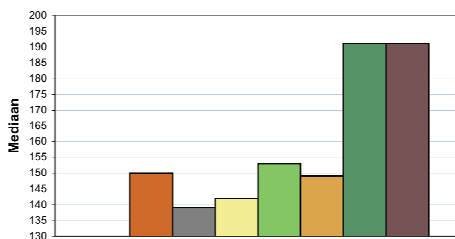


*Figure 9*
*The 2 newspapers on the right shows a higher median value compared to others. This was caused by unadjusted plate-compensation curves*

### References

1. IFRA PRINT SUMMIT 2010, *Salzburg*

2. Study (2007/2009) of the RIT Printing Industry Centre: "Evaluating the Image Quality of Digital Print Technologie relative to Traditional Offset Lithography".

3. DIS/ISO 12647-3:2004, Newspaper offset (coldset) and proof printing on standard newsprint

4. A proposal for Contrast Measure in Digital Image, Alessando Rizzi, Thomas Algeri, Giuseppe Medeghini, Daniele Marini (presented at CGIV2004: The Second European Conference on Colour Graphics, Imaging and Vision).

5. Quality prediction of printed photographs using computational and instrumental methods, Raisa Halonen, Tuomas Leisti, Pirkko Oittinen.

# Quality measurements in anti-counterfeit offset print production

*Slavtcho Bonev[1], Rainer Gebhardt[2],*
*Stoyan Maleshliyski[3], Reinhold Günter[3] and Bernhard Wirnitzer[3]*

[1] Epyxs GmbH
Richard-Wagner-Str. 29, 68156 Mannheim, Germany
E-mail: s.bonev@epyxs.com

[2] manroland AG, Print Technology Center
Borsigstrasse 16, 63165 Mühlheim am Main, Germany
E-mail: rainer.gebhardt@manroland.com

[3] Mannheim University of Applied Sciences
Paul-Wittsack-Strasse 10, 68163 Mannheim, Germany
E-mails: s.maleshliyski@hs-mannheim.de, r.guenter@hs-mannheim.de, b.wirnitzer@hs-mannheim.de

**Abstract**

The realization of an effective and low-cost product protection concept is an important step in the fight against product piracy. Using high-volume offset printing, the high-density printed data storage **DataGrid** was applied to packaging and labels for reliable product identification and its individual fingerprint **EpiCode**, resulting from the physical interaction between paper and ink, was used for authentication of products. The recognition quality was estimated and improved by means of biometric evaluation methodology, the influence of different substrates (paper material and surface roughness), printing techniques (offset, digital) as well as inventions, such as **Cluster Code** - the printing plate fingerprint and **NanoGrid** - an embedded copy detection pattern, were described.

In this paper the practical aspects of anti-counterfeit print production are discussed and an overall product security concept is presented. The main advantages of this new approach are: adaptable security level, easy integration into the production chain, verification with and without access to a data base and the interoperability with existing track-and-trace solutions.

**Keywords:** security features; paper-and-print fingerprint; production quality control; scanning devices; overall security printing concept

## 1. Introduction

A product protection concept based on identification and authentication can be built on the simple fact, that each printed matrix code has its individual non-replicable characteristics (Figure 1). If the code is applied on the secondary package, its contents are used to identify the product. Its unique fingerprint, resulting from the physical interaction between medium and substrate during the printing process, can be used to identify whether the product is original or not.



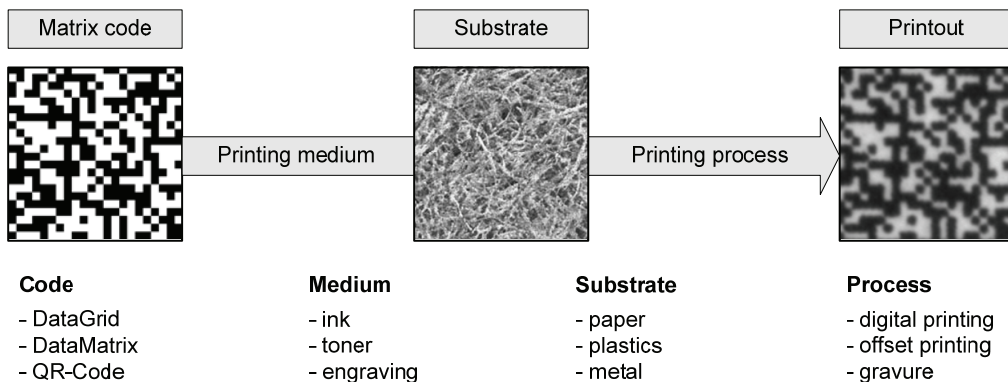| Code | Medium | Substrate | Process |
|------|--------|-----------|---------|
| - DataGrid | - ink | - paper | - digital printing |
| - DataMatrix | - toner | - plastics | - offset printing |
| - QR-Code | - engraving | - metal | - gravure |

*Figure 1: Basic technology for product identification and authentication*

To realize a low-cost effective anti-counterfeit marking of packages and labels a high-volume printing method and a proprietary matrix code as well as algorithms for extraction and processing of "fingerprints" were suggested (Bon, 2008). Further, the influence of some components of the printing process, such as printing technique, paper roughness or dot gain, on the code readability and the achieved recognition quality, was investigated (Bon, 2009).

A comprehensive theoretical and experimental study was conducted within the three-year cooperative research project O-PUR (Opu, 2008), which is in its final phase. The aim of the project was the industrial implementation of the presented technology, including the realization of a scalable security concept, the achievement of the lowest production costs using conventional materials, the easy integration into the production chain, the usage of standard scanning devices and the interoperability with other existing track-and-trace solutions.

By the O-PUR project the industrial production of security features using sheet-fed and reel-fed offset presses, digital printers and also direct marking methods were demonstrated successfully. Besides the initial costs for fingerprint capturing modules only minimal variable costs were incurred. The use of standard matrix codes and improved internet applications makes an implementation in track-and-trace or inventory management systems also conceivable. The protection concept was demonstrated on boxes and labels, and first pilot applications were realized with confirmed benefits for customers and consumers.

The protection concept is subdivided into production and examination of the security mark as presented in Figure 2. The proprietary matrix code DataGrid contains encrypted product data and the embedded copy detect pattern NanoGrid, which is treated as an artificial fingerprint and used for authentication (copy detection) without database access. After printing the code on a package or label, the unique fingerprint EpiCode naturally occurs as a result of the interaction between paper and ink. If an offset printing process is used, the characteristic signature of the printing plate ClusterCode appears as an additional individual feature. EpiCode and ClusterCode can be used for authentication in the supply chain only if captured and stored in a database during the production process.
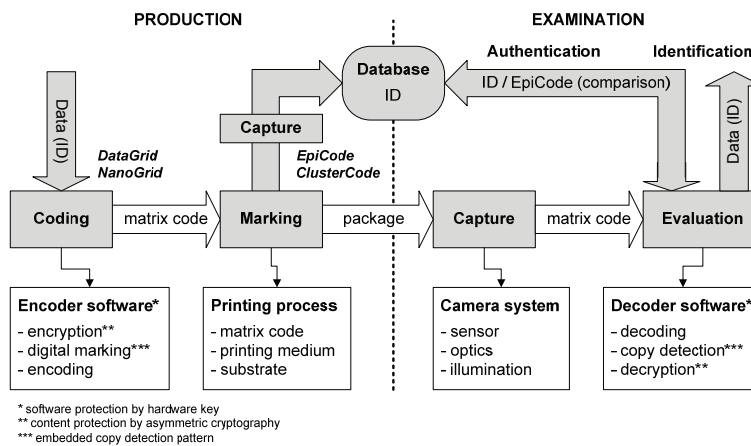


*Figure 2: Overall security concept for product protection based on identification and authentication*

The basic technology was firstly[first] developed at the Mannheim University of Applied Sciences. The methods for digital data storage (Wir, 2001, 2002, 2004), fingerprint extraction (Wir, 2003, 2007) and printed product marking (Wal, 2007) were patented. Under the guidance of manroland AG the research project O-PUR was initiated and performed in collaboration with different technology partners with specific know-how, as listed in Table 1, to cover all aspects of the realization of the protection concept. Pilot customers, mainly printing houses as contractors of big industrial companies, were appointed and associated with the project to prove the feasibility of the approach. An accompanying project EpiCode-3D was established to investigate the adoption of alternative direct marking techniques.

O-PUR is a part of the production research initiative of the German Federal Ministry of Education and Research (Bmb, 2008) against product piracy in order to find effective prevention and protection mechanisms and make them available to companies at risk. Some of the main objectives are (i) the development of cost-

effective and forgery-proof tagging and authentication procedures for both products and processes and (ii) the creation of comprehensive protection concepts by combining individual technological, organizational and legal options.

*Table 1: List of participants on the cooperative research project O-PUR*

| Nr. | Project partner | Contribution to the research project |
|---|---|---|
| 1 | manroland printing machines AG (project coordinator) | Offset printing machines, packaging printing |
| 2 | Mannheim University of Applied Sciences | Image proc., basic technologies, security concept |
| 3 | Fraunhofer Institute for Physical Measurement Tech. | Fast image capturing, ring light module |
| 4 | Epyxs GmbH | Basic technologies, encoding/decoding software |
| 5 | EINS GmbH | Databases, secure connections, communications |
| 6 | PEPPERL+FUCHS, Omnitron AG | Scanning device, embedded hardware platform |
| 7 | GEWA Etiketten GmbH (associated partner) | Label printing for the vineyard industry |

## 2. Methods

The authentication concept is based on measured fingerprints - in our case these are the EpiCodes extracted from printed DataGrids. In principle, the EpiCodes are calculated from the error signal of a decision feedback equalizer (DFE) described in (Wir, 2002) and compared with the reference values from the database. The comparison results are processed using biometrical evaluation methodology (Gar, 2006; Dau, 1999). For the authentication quality check of a used printing technique a small batch of a single digital test sheet is printed. Then a reference scan (database) and an authentication scan (probe) are made, usually by different scan devices used for production and examination, respectively. Depending on the code constellation on the test sheet, there are five different groups of comparison pairs as depicted in Figure 3 with corresponding comparison results (cross correlation coefficients) presented in Figure 4:

- (1) original: same code [$\mu_1 = 0.69$]
- (2) cluster (short-term): copies on consecutive sheets created by the same plate region [$\mu_2 = 0.57$]
- (3) cluster (long-term): copies on distant sheets (dist.$\geq$100) created by the same plate region [$\mu_3 = 0.51$]
- (4) copy: copies created by different plate regions [$\mu_4 = 0.24$]
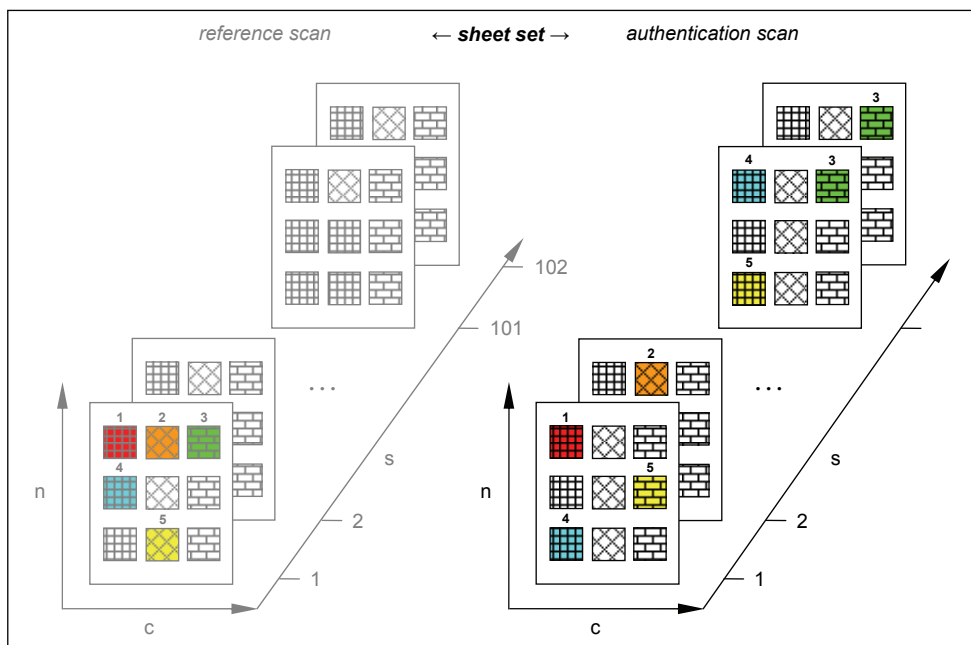- (5) false match: codes with different information [$\mu_5 = 0.02$]



*Figure 3: Experimental concept: n - code number (N=8), c - code info (C=4), s - sheet number (S=20)*
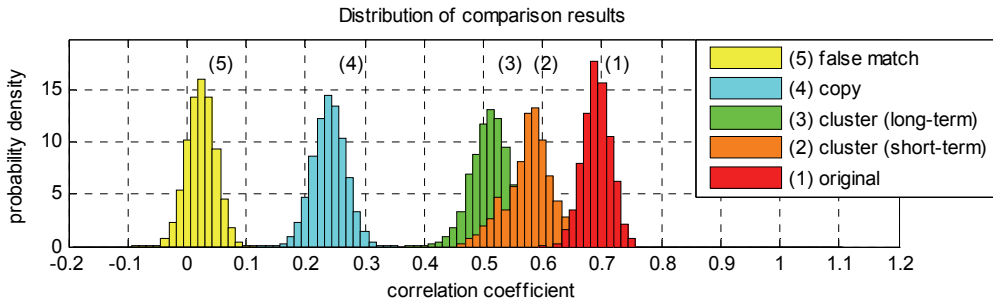
*Figure 4: Comparison results. Groups 2 and 3 represent the short-term and long-term ClusterCode results.
They occur only if an offset printing technique is used for the creation of the sheet set*

The group *false match* (codes with different information) is evaluated to confirm the expected zero mean distribution and is not used for further calculation of recognition performance. Important are the groups *original* and *copy* which occur for each applied printing technique, offset or digital printing (Bon, 2008). They allow a clear discrimination between originals and copies of the same matrix code. The groups *cluster (short- and long term)* result also from impressions of the same code and occur - only if offset printing technique is used - caused by the common characteristics of the printing plate. As the ClusterCode was proposed, but not proved, to remain constant for a batch of sheets (approximately $\geq 100$) and to be used for their recognition, the group *short-term cluster* (comparison results for consecutive sheets) was removed from the calculation approach. EpiCode and ClusterCode are extracted from printed DataGrid codes - usually at a proper stage of the production chain - and are stored in a database for authentication. Experimental details are given in the next section.
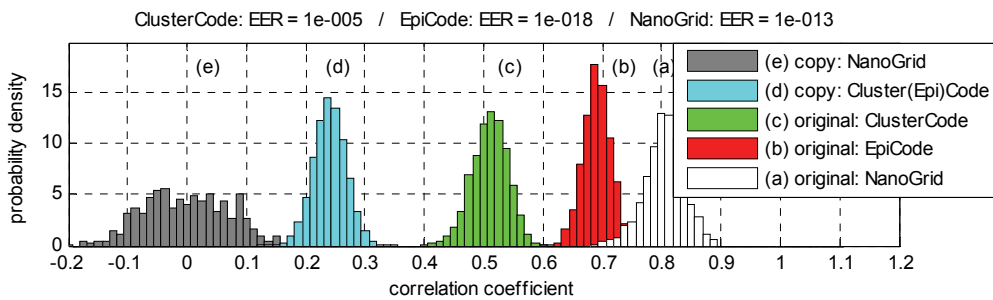


*Figure 5: Full set of comparison results (including NanoGrid) used in the authentication approach*

If a reference scan is not made at production or an access to a database cannot be granted at examination, authentication would not be possible. To solve this problem, the digital mark NanoGrid is embedded in the DataGrid code and used as a copy detection pattern. In the context of authentication NanoGrid can be interpreted as an artificial fingerprint with a reference signal originating from the digital data stored in the code.
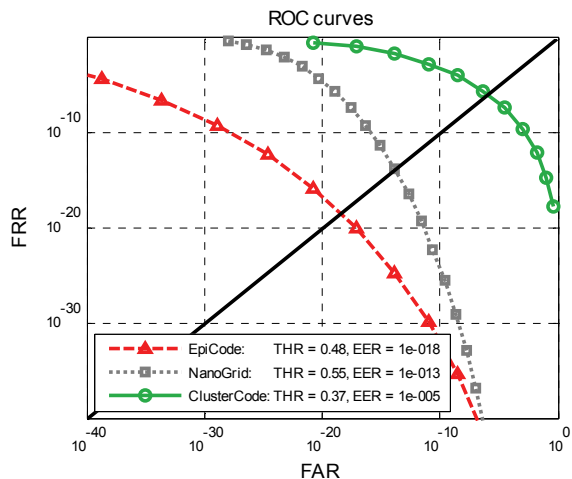


*Figure 6
Estimated recognition performances of EpiCode,
NanoGrid and ClusterCode based on DataGrid*

For each pair of distributions (copy, original) the receiver operating characteristic (ROC) and the corresponding equal error rate (EER) are estimated empirically, as presented in Figure 6. To this end, the mutual overlap of two distributions is evaluated by calculation of the false acceptance rate (FAR) and false rejection rate (FRR) at variable discrimination levels assuming normal distributions. The estimated EER are used as a measure of the recognition performance. The authentication concept is also implemented for standard codes, e.g. DataMatrix or QR-Code, and the resulting EER are used in the same manner to estimate the recognition performance (Gün, 2010).

## 3. Experimental results

### 3.1 Production

To investigate the influence of the applied printing ink and different matrix codes on the recognition performance, the test prints shown in Figure 7 are produced using the same substrate and printing machine.
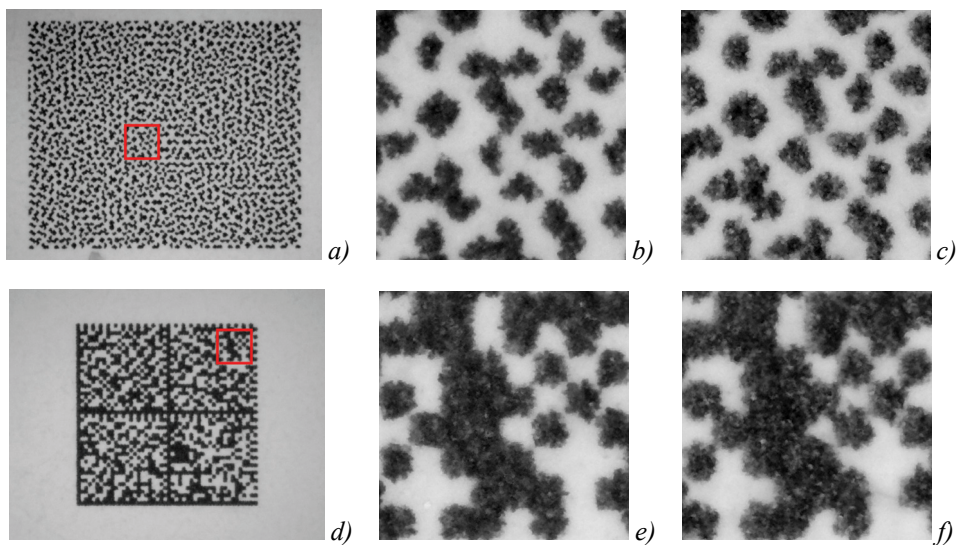


*Figure 7: DataGrid (a, 4.1 x 3.8 mm, payload up to 180 Bytes) and DataMatrix (d, 3.1 x 3.1 mm, payload 174 Bytes) with similar data densities printed with conventional (b,e) and UV-curable (c,f) inks at a printing resolution of 2400 dpi. The high-resolution scans are made using the KEYENCE VH-M100 digital microscope*

Due to different flowing and drying behavior of conventional and UV-curable inks a higher distortion of code details is observed for the UV-curable ink. A comparison of the resulting EER values presented in Table 2 shows better results for conventional ink (Nr. 2, 3). Using DataGrid a better recognition performance based on EpiCode then for DataMatrix is achieved due to the higher spatial detail content of the code (Nr. 2, 4). Fast drying inks are found to better preserve the printing plate characteristic ClusterCode, which is an expected result (Nr. 1, 2, 3) due to faster freezing of the impression from the plate onto the substrate. Also, sheet-fed printing shows better results for ClusterCode than reel-fed printing at equal results for EpiCode (Nr. 2, 5). More accurate substrate guidance is supposed to be the reason for this. The EER values estimated for NanoGrid are comparable to those for EpiCode and confirm the usability of this feature for authentication purposes.

In an intermediate summary, DataGrid shows permanently better EER values than the standard code DataMatrix and is more convenient for authentication applications. EpiCode and NanoGrid are reliable authenticating features due to achieved EER values below $10^{-8}$. Sheet-fed printing combined with fast drying inks shows the highest achievable EER values.

To produce readable codes an indicator of the print quality has been recommended. The quality parameter QP (Bon, 2009) is equal to the carrier-to-noise ratio CNR, well known from the theory of digital communications, measured at decoding. Investigating the influence of the dot area DA on the code readability, a clear relationship between QP and DA was found. Considering this, a complementary method for print quality monitoring without the usage of a decoding device was suggested. It allows printing houses to control

the production quality of DataGrid e.g. by observing the halftone 30% field. The results presented in Figure 8 prove finally that DataGrid is very robust against print quality distortions due to the special design of the used code symbols. NanoGrid could be verified for the codes in Figure 8a, 8b and 8c.

*Table 2: Experimental data and results of recognition quality measurements*
*for sheet-fed (Roland 706 LV) and reel-fed (Gallus RCS-330) offset printing*

| Nr. | Matrix code | Paper grade (substrate) | Ink type (medium) | Paper feed type | EER EpiCode | EER ClusterCode | EER NanoGrid |
|---|---|---|---|---|---|---|---|
| 1 | DataGrid | Zanders Mega gloss | conventional fast drying | sheet-fed | $10^{-28}$ | $10^{-7}$ | - |
| 2 | DataGrid | Sappi Mega gloss | conventional | sheet-fed | $10^{-18}$ | $10^{-5}$ | $10^{-13}$ |
| 3 | DataGrid | Sappi Mega gloss | UV curable | sheet-fed | $10^{-16}$ | $10^{-3}$ | $10^{-12}$ |
| 4 | DataMatrix | Sappi Mega gloss | conventional | sheet-fed | $10^{-8}$ | $10^{-1}$ | - |
| 5 | DataGrid | Adestor Soria Plus | conventional | reel-fed | $10^{-18}$ | $10^{-2}$ | - |
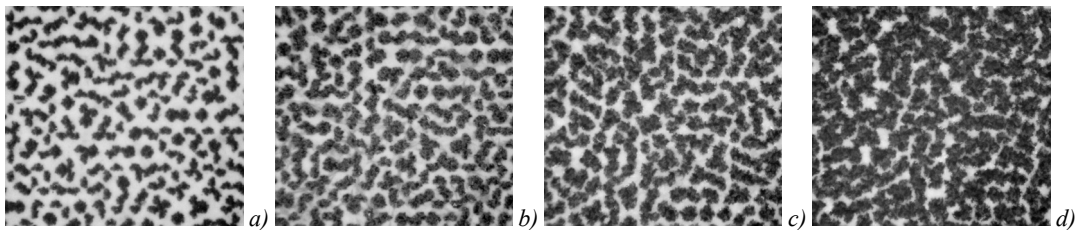


*Figure 8: Readable DataGrid codes at different print qualities. The measured value pairs of quality parameter and dot area QP [DA] are 7.8 [56%] (a), 4.8 [68%] (b), 3.2 [80%] (c) and 2.2 [90%] (d). DA is measured by reflection densitometer GretagMacbeth D196. The DA of the digital halftone image of DataGrid is 33%*

The short-term stability of the ClusterCode was confirmed by observations of the correlations coefficients in all clusters shown in Figure 9, expressed by the (high) values in the secondary diagonal which correspond to group 2 in Figure 4. Only minor changes in code expressions on consecutive sheets occur, which is an expected result. Long-term stabile ClusterCode was observed only for a group of 800 sheets using DataGrid and conventional ink (Figure 9, center). The comparisons of sheet pair (801,802) to all other sheet pairs have shown outlier values corresponding to copies, removed from group 3 in Figure 4.
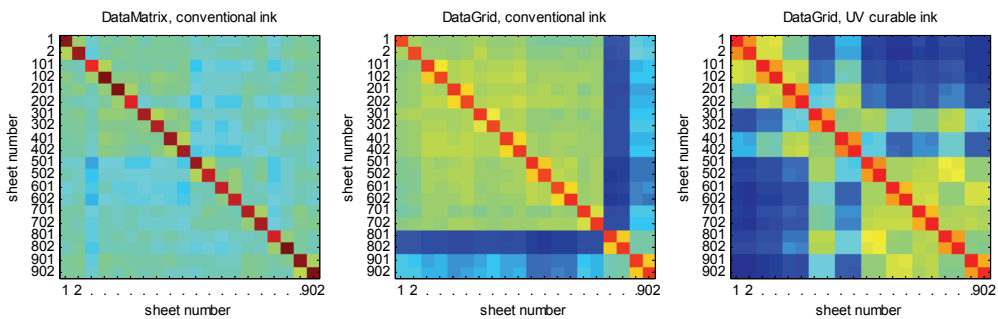


*Figure 9: Evaluation of the behavior of ClusterCode during the print run by extraction of 10 consecutive sheet pairs in an interval of 100 sheets (observation over 1000 sheets). Each matrix element represents the mean correlation coefficient (color coded) of 32 EpiCode pairs according to Figure 3*
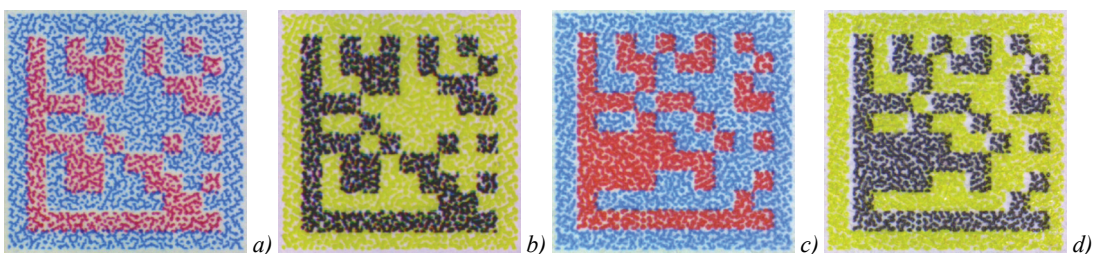


*Figure 10: DataGrid with implemented DataMatrix code in the color layer printed on sheet-fed Roland 706 LV (a,b) and reel-fed Gallus RCS-330 (c,d) offset printing machines*

Using multicolor mixed codes additional individual properties, e.g. the spatial shift between different plates of the color printing units and the hue distance between the process colors as depicted in Figure 10, were extracted and applied to enhance the recognition performance (Mal, 2009, 2010).

## 3.2 Examination

For quality control of DataGrid and measuring of EpiCode during the production of packaging or labels, image capturing and processing devices were inserted in the production chain as shown in Figure 11. The decrease of the product throughput at each subsequent chain link is considered in the concept. Therefore image capturing for the item level measuring and registering of EpiCodes in the database is recommended to take place in the last stage. Nevertheless, scanning for quality control at the highest production speeds was also implemented at early production stages to assure the functionality of the authentication feature.



*Figure 11: Production chain of packaging/labels and recommended positions of image capturing/processing devices*

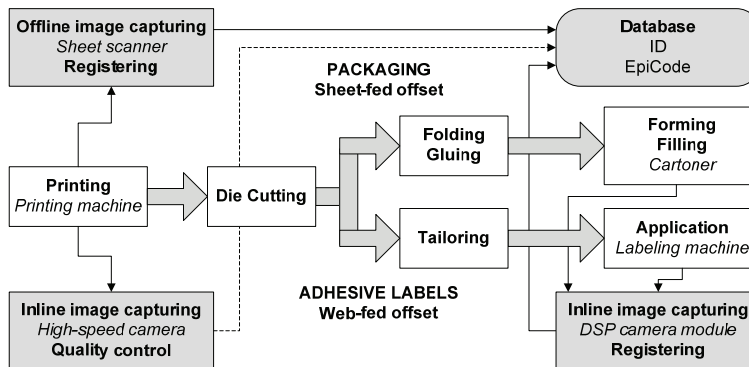To demonstrate the image capturing, different production machines (Figure 12) were equipped with high-end scanning devices consisting of an illumination unit, objective and digital camera. The required scanning resolution is 2400 dpi. Telecentric objectives with fixed working distance and high focus depth were used to enhance the system robustness by avoiding defocusing during the measurement. The decoder was implemented on PC (offline processing) and on the VC4468 smart camera (inline processing) where decoding times (including code detection, code reading and fingerprint extraction) of 100 ms were achieved. In the conducted experimental run on a labeling machine, a roll with 2500 labels was processed within 10 minutes which corresponds to a processing speed of 4-5 labels per second. Using a sheet scanner, 12 packaging copies on a single sheet were processed within 2 minutes. In this constellation a control sheet was analyzed for each 500 printed sheets at a printing speed of 15.000 sheets per hour. Thus, a fully developed technology for examination in the production chain was demonstrated.
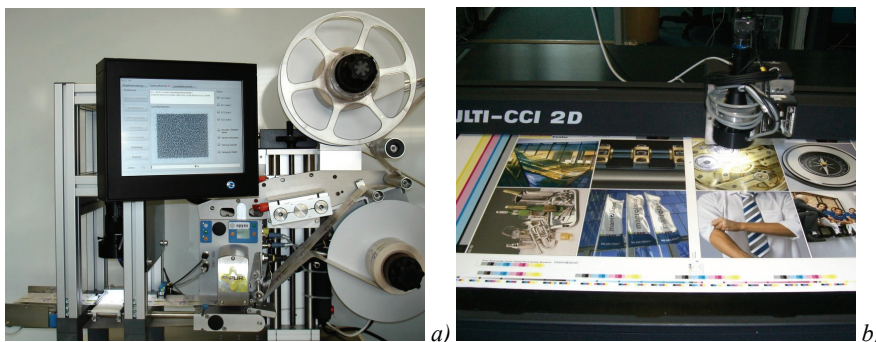


*Figure 12: Labeling machine HERMA 400 (a) equipped with a smart camera and control PC and sheet scanner MULTI-CCI 2D (b) equipped with an USB camera with mounted telecentric lens*

For inline scanning in offset printing machines, where the substrate speed can exceed 10 m/s, a special solution presented in Figure 13 was developed to avoid motion blur. Since the shortest CCD camera shutter times are in the range of 5-10 μs, stroboscopic illumination with light pulses of less than 1 microsecond is indispensable. The achieved production speed for a maximum allowed substrate shift of 20 μm during the light pulse of 1 μs is 20 m/s.
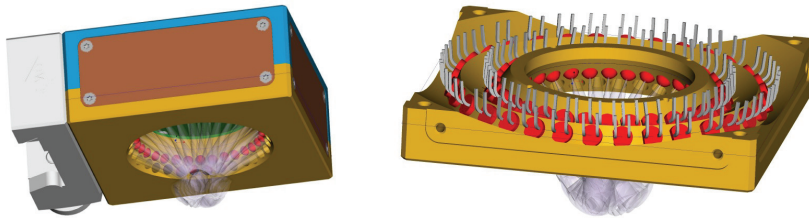
*Figure 13: Ring light module (64 LED) with control logic for microsecond light pulses developed by Fraunhofer Institute for Physical Measurement Techniques used for inline print quality control at production speed up to 20 m/s*

To enable easy examination and widely spread the technology among all end-users, conventional mobile devices with cameras were targeted for product authentication based on printed matrix codes. A high-end solution (Figure 14) was developed to realize suitable scanning using a wide range of camera phones.
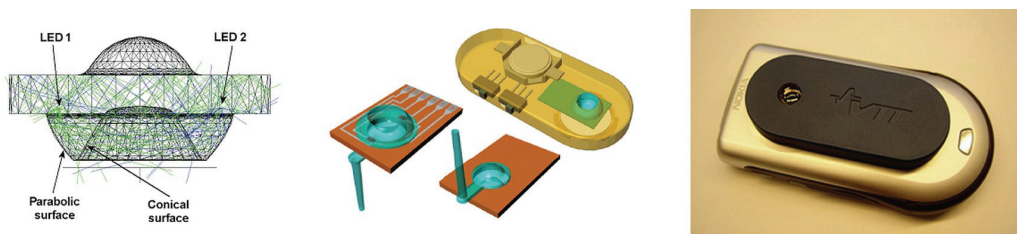


*Figure 14: Additional optics developed by the VTT Technical Research Centre of Finland used with Nokia 6630 mobile phone camera for authentication check*

Additional optical elements as well as conventional and embedded devices (Figure 15) were used by advanced users and consumers to examine product packaging or labels in the field. The platform independent decoding software was implemented in portable devices with an imaging unit and is also available as an internet application.



*Figure 15: Used optics and scanning devices: Jelly Lens$^{TM}$ Close-Up and PEAK magnifier loupes (a), digital microscope dnt DigiMicro 1.3 (b), code scanning device Omnitron MAH300 (c), camera phone Samsung Omnia 900i with Windows Mobile OS (d) and the personal digital assistant (PDA) Pidion BIP-6000*
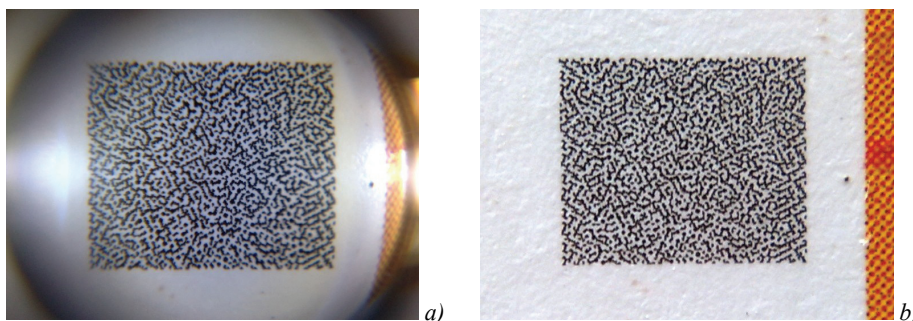


*Figure 16: Images of a DataGrid using VTT optics (a) and Jelly Lens$^{TM}$ (b) made by Nokia 6220c mobile phone camera. The examination delivered results in the interval [-0.01, 0.08] for copies and [0.41, 0.45] for originals*

The connectivity options of the mobile devices allow image upload via wireless LAN, MMS etc. Successful authentication checks were performed using different scanning approaches (Figure 16). The numerous developed scanning solutions afford flexible design of any user-defined application for the security feature examination introduced here.

## 4. Discussion

The presented protection concept is based on the robust printed product identifier DataGrid and its authenticating features NanoGrid, ClusterCode and EpiCode which are also applicable for standard matrix codes. The security level of a realized product protection solution can be adjusted according to the requirements of the customer concerning implementation and maintenance costs. Establishing a free verification procedure will also allow consumers to participate actively in the fight against product piracy.

Similar security printing technologies rely on the uniqueness of the substrate surface for authentication or use matrix codes as copy detection patterns as shown in Figure 17. ProteXXion® (Bay, 2007) is based on LSA® - Laser Surface Authentication (Ing, 2005) and uses laser light for capturing the individual surface structure and unequivocal recognition of each object. Difficulties at implementation level may arise by the need of additional synchronisation patterns to recover the area of interest for authenticity check, the problems with surface capturing for glossy/coated papers or plastics, and the usage of costly scanning devices. In practice, additional 2D code is printed near the area of interest to serve as a product identifier and eventually as a link to a database. A novel proposal of LSA® uses the individuality of printed matrix codes (Ger, 2008) similar to the concept discussed in this paper.



*Figure 17: Basic elements used by the technologies ProteXXion® (a), Seal Vector® (b) and BitSecure® (c)*

Seal Vector® (Adv, 2006) and BitSecure® (Sch, 2009) rely on the error detecting property of the forward error correcting mechanism (FEC) used in special printed matrix codes. Copying or a reprint of the codes will lead to an increase of bit errors and - if the error level exceeds a certain threshold - to copy detection. Both technologies have the great advantage of not using a database, but the quality control is obligatory during production to avoid self-created copies; the data amount stored in the code is possibly limited.

## 5. Conclusions

It was shown, that conventional offset printing can provide anti-counterfeit marking for mass production. The main features of the presented product authenticating system are (i) adaptable security level, (ii) easy integration into the production chain, (iii) easy offline and online verification with and without access to a database and (iv) the interoperability with existing track-and-trace solutions.

## References

Advanced Track & Trace®, (2006), *Seal Vector®, http://www.att-fr.com/solutions_english.php*

Bayer Technology Services, (2007), *ProteXXion®, http://www.protexxion.de*

BMBF, (2008), *Research campaign against product piracy (project O-PUR), http://www.bmbf.de/en/12095.php, Research at Universities of Applied Sciences (project EpiCode-3D), http://www.bmbf.de/en/864.php, Federal Ministry of Education and Research (BMBF), Germany*

Bonev S., Wirnitzer B., (2009), *Security printing for product packaging in industrial printing applications, Advances in Printing and Media Technology, Vol. 35, No. 3, P. 307-312, ISBN 978-3-9812704-0-2*

Bonev S., (2009), *High volume security printing using sheet-fed offset press, Advances in Printing and Media Technology, Vol. 36, No. 4, P. 449-455, ISBN 978-3-9812704-1-9*

Bonev S., Günter R., Maleshliyski S. and Wirnitzer B., (2010), *New Forensic Features in Secure Offset Printing, 7th Pan European High Security Printing Conference, 13-15 April 2010, Berlin, Germany*

ConImit, (2008), *Contra Imitatio - Platform for preventive IP protection against product piracy, www.conimit.de*

Daugman J., (1999), *Recognizing Persons by Their Iris Patterns, Advances in Biometric Person Authentication, Vol. 3338/2005, P. 783-814, ISBN 978-3-540-24029-7*

EFPIA, (2010), *Coding & Identification, European Federation of Pharm. Industries and Associations, www.efpia.org*

Garris M. D., Tabassi E. and Wilson C. L., (2006), *NIST Fingerprint Evaluations and Developments, IEEE Proceedings, Vol. 94, No. 11, P. 1915-1926*

Gerigk, M., Borchers, W., Brüll, L., Friedrich, M., Focke, J., Vougioukas, S., Joa, W., Klein, R., Moers, M., (2008), *Authentifizierung von Objekten mittels Bilderkennung, DE102008016803A1, Deutsches Patentamt, München*

Günter R., Maleshliyski S. and Bonev S., (2010), *A 2D Fractionally Spaced Output DFE for Anti-counterfeiting Applications of Printed Matrix Codes, IADIS Multi Conference on Computer Science and Information Systems, 26-31 July 2010, Freiburg, Germany*

Ingenia Technology Limited, (2005), *LSA® - Laser Surface Authentication, http://www.ingeniatechnology.com*

ISO 12647-2(1):2004, *Graphic technology - Process control for the production of half-tone color separations, proof and production prints - Part 2: Offset lithographic processes (Part 1: Parameters and measurement methods), ISO*

Maleshliyski S., García F., (2009), *Integration of Anti-counterfeiting Features into Conventional 2D Barcodes for Mobile Tagging, TAGA 61st Annual Technical Conference, New Orleans, USA, ISBN 978-1-935185-01-7*

Maleshliyski S., Günter R., (2010), *Security printing techniques based on substrate and print-process individualities, TAGA 62nd Annual Technical Conference, 14-17 March 2010, San Diego, USA*

O-PUR, (2008), *Original Product Protection and Track-and-Trace Strategy, www.opur-secure.de*

Schreiner Group GmbH & Co. KG, (2009), *BitSecure®, http://www.schreiner-bitsecure.de*

Walther T., Wirnitzer B., Hochschule Mannheim, manroland AG, (2007), *Apparatus method and process for the stochastic marking and tracking of printed products, DE102007050691, PCT/EP2007/009089, WO2008/049550*

Wirnitzer, B., Spraggon-Hernandez, T., (2002), *Deconvolution in line scanners using a priori information, Proceedings of SPIE - Image Reconstruction from Incomplete Data II, Volume 4792, P. 156-163, Seattle, WA, USA*

Wirnitzer, B., (2003), *Datenträger mit Kopierschutz und Verf. zum Erzeugen eines Sicherungscodes, DE10345669*

Wirnitzer B., Bonev. S., (2004), *Method for encoding data via matrix print data storage, DE102004036809, PCT/EP2005/008097, WO/2006/013037*

Wirnitzer B., Maleshliyski S., (2007), *Verfahren zur Erzeugung eines Sicherungscodes für einen Rasterdruckdatenspeicher und Gegenstand mit Farbrasterdruckdatenspeicher, DE102008025785*

# Influence of UVC treatment on sheetfed offset print quality

*Roger Bollström, Anni Määttänen, Petri Ihalainen, Jouko Peltonen, Martti Toivakka*

Åbo Akademi University, Laboratory of Paper Coating and Converting
Centre for Functional Materials
Porthaninkatu 3, FIN-20500 Turku, Finland
E-mail: Roger.Bollstrom@abo.fi

**Abstract**

The influence of using UVC irradiation as a post treatment method on pigment coated papers was studied. The germicidal wavelength ($\lambda_{max}$ = 254 nm) is known for breaking chemical bonds in organic material and has commonly been used for cleaning of surfaces. Pigment coated paper was treated under UVC irradiation and the influence on roughness, coating structure and wettability was analyzed. No change in roughness could be observed but wettability of water could be increased which indicates an increased polarity. Offset printability regarding print density, gloss, picking and ink setting was further studied as a function of different treatment parameters. In addition to changes in ink setting, a reduced picking tendency on low surface strength papers could be observed. The change in surface wetting is believed to arise from organic materials such as dispersing agents on the outermost surface being degraded by the UVC irradiation.

**Keywords:** UVC treatment; surface chemical properties; printability; print quality

## 1. Introduction

Paper can be coated or sized with aqueous mineral pigment suspension in order to improve its printability. Properties, such as hydrophilicity or hydrophobicity, are required in a variety of applications. Surface energy and chemistry have in several studies been shown to influence both dampening water absorption and ink setting in offset printing process (Pykönen 2010, Liu et al. 2008). The structure of the pores in the coating and the type and amount of binder used play important roles as well (Gane 2004, Ström 2005 and Preston et al. 2001). Rousu (2001) compared dispersed and undispersed calcium carbonate pigment in order to evaluate the influence of surface energy on ink setting. A high polar component of surface energy due to use of polyacrylate dispersants increased separation of polar linseed and non-polar mineral oils during ink oil absorption.

UV light has been used for curing of inks, cleaning of surfaces as well as for modifying surface energy of polymer films and rubber (Romero-Sanchez et al. 2005 and 2007). Surface energy of polymer films has been increased by use of UV-irradiation of wavelength 185 nm and 254 nm, where the 185 nm wavelength is known to form ozone and therefore attach oxygen to the surface which leads to the surface energy increase (Romero-Sanchez et al. 2005 and 2007). An alternative method for tuning the wetting properties of paper is to use a germicidal wavelength of 254 nm that conventionally has been used for cleaning and removing of organic material (Määttänen et al. 2010). The UVC irradiation process is fast, dry, clean, and easily controllable. No chemical treatment is needed and the effects are limited to organic compounds such as dispersing agents on the surface. Topography of the paper surface is not affected by the UVC treatment; therefore modifying surface chemistry without changing surface topography allows ink setting studies from a new perspective. The objective of the current work is to understand the influence of UVC irradiation on the surface chemical properties of pigment coated paper and related changes in the offset printability.

## 2. Materials and methods

### 2.1 The coating and calendering procedures

The three papers used in the experiments were double pigment coated on both sides on a woodfree basepaper. The pre-coating was done with coarse ground Calcium Carbonate (GCC) (Imerys Carbital 60). The top coating formulations are given in table 1. A jet applicator with stiff blade metering and rigid loading was used during the pilot scale coatings. The coat weight target was 10g/m$^2$ for each side for precoat and topcoat. Drying was done using both IR-dryers and hot-air dryers. The calendering was performed using an off-line supercalender with 7 nips.

*Table 1: Coating colour formulations for the topcoat*

|   | PCC | GCC | Kaolin | SB latex | Starch | PVOH |
|---|-----|-----|--------|----------|--------|------|
| **A** |     | 70  | 30     | 9        |        | 0,7  |
| **B** | 100 |     |        | 9        |        |      |
| **C** | 100 |     |        | 4        | 2,5    |      |

The pigments used were fine glossing clay (KaMin LLC Hydragloss 90), fine GCC (Imerys Carbital 95) and aragonite precipitated Calcium Carbonate (PCC) (Specialty Minerals Opacarb A 40). Other chemicals used in the coating formulations were polyvinyl alcohol (PVOH), low viscosity corn starch, a cross linker, and carboxy methyl cellulose (CMC) for adjusting of the viscosity. Styrene-butadiene latex (DOW) with a glass transition temperature of 20°C was used as binder. The target solids content was 67% and pH 8,5.

## 2.2 Laboratory scale printing

Two commercial sheetfed offset inks supplied by Siegwerk Finland Oy were used in the study. One containing both mineral and linseed oil, Tempo Max Soft (TMS) and one purely linseed oil based, Tempo Perfect (TP). The printings were performed both as dry and with predampening. The fountain solution contained 87 % water, 10 % isopropanol and 3% additives. An IGT GST2 printability tester was used for the print trials and for the wet repellence measurements. The ink-surface interaction tester (ISIT) was used to measure the paper tack versus time. The dry pick measurements were performed with an IGT AIC-2 at a set maximum speed of 1,5 m/s. All printings were performed at 23° C and 50 % relative humidity conditions.

## 2.3 UV-treatment

A germicidal ozone free UVC lamp ($\lambda_{max}$ 254 nm) supplied by Heraeus was used for the UV-treatment. The effect of the lamp is 30W at 254 nm wavelength, and the intensity can be adjusted by varying the distance between the lamp and substrate. The irradiation intensities used were 30, 50 and 70 mW/cm² at 254 nm wavelength. A UVA lamp supplied by Hönle UV Technology was used as a reference and tested at the same intensities as the UVC, but measured at 370 nm wavelength. Influence of treatment time was also investigated.

## 2.4 Contact angle

The contact angles of water as a function of time were measured using a CAM 200 contact angle goniometer (KSV Instruments Ltd). The contact angles for linseed and mineral oil were measured using a Citius Imaging high speed video camera and analysed with ImageJ and Drop Shape Analysis (Stalder et al. 2005).

## 3. Results

### 3.1 Paper whiteness

The UVC treatment slightly decreased the whiteness of the coated papers. Figure 1 shows the changes in whiteness after different treatment times. The difference is obvious on the paper containing GCC and Kaolin combined with 9 pph of SB latex (A), also on the PCC coated paper containing 9 pph of latex (B) a difference can be seen but on the paper containing only 4 pph of SB latex (C) only a small difference in whiteness can be seen. Shorter exposure times of 2-10 s at a higher intensity did not show any difference in whiteness for any of the papers. This suggest latex being affected by a long treatment time, however the reason for decreasing whiteness after a long treatment might also be because of temperature, since especially SB latex is known to decrease in whiteness due to temperature and light. The temperature increased during a long exposure since the substrates were treated in a batch process and the lamp temperature reached almost 100°C at a close distance. This might at least partly explain the difference between 50 mW/cm² and 70 mW/cm² after 120 seconds of treatment time. During an exposure time of 1-10 seconds the temperature did not noticeably increase from room temperature.

### 3.2 Roughness and porosity

PPS roughness and Gurley air permeance were measured in order to detect possible changes in surface topography or structure. No changes in roughness or porosity could be detected (Table 2). This supports earlier results where no change in topography could be detected by AFM (Määttänen et al. 2010). Mercury porosimetry was further performed on the samples, both as treated and untreated (fig. 2).
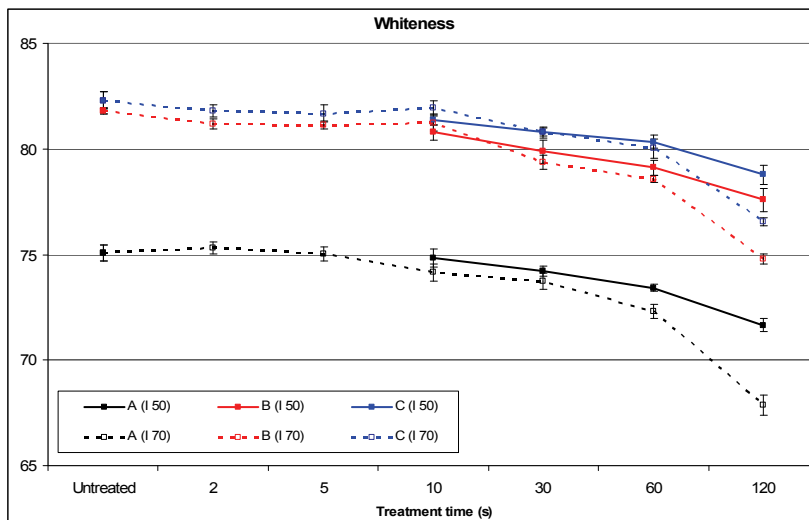
*Figure 1: Whiteness of the papers as a function of different treatment intensity (I) in mW/cm² and treatment time*

*Table 2: Roughness and air permeance for the papers, both as treated (UVC) and untreated (UT)*

| | PPS roughness (µm) | | | | Gurley air permeance (s) | | | |
|---|---|---|---|---|---|---|---|---|
| | UT | | UVC | | UT | | UVC | |
| | Avg. | St. Dev. | Avg. | St. Dev. | Avg. | St. Dev. | Avg. | St. Dev. |
| **A** | 0,77 | 0,02 | 0,78 | 0,01 | 15333 | 351 | 15100 | 100 |
| **B** | 0,60 | 0,01 | 0,61 | 0,02 | 10900 | 265 | 10900 | 300 |
| **C** | 0,74 | 0,01 | 0,74 | 0,03 | 7210 | 50 | 7217 | 120 |
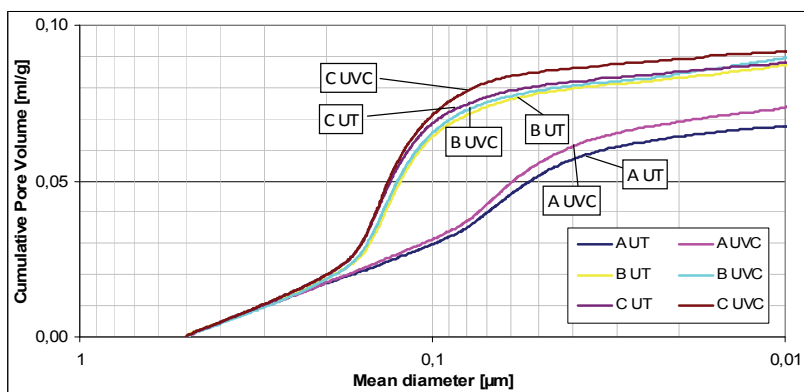


*Figure 2: Cumulative pore size distribution measured by mercury porosimetry*
*Results show a 5 % increase in porosity for paper A and C. The measurements were performed*
*with a Pascal 140/440 series porosimeter. (No parallel measurements)*

A slight increase in porosity of approximately 5 % in the 50 nm pore diameter region could be observed for paper A and C after the UVC treatment. Whether this is a real increase or only noise, requires further investigation. The possible increase in porosity cannot be explained by differences in coating formulations, nor is it reflected in the printing results.

### 3.3 Contact angle

The water contact angles were measured for the untreated, UVC and UVA treated papers. The irradiations were done using an intensity of 50 mW/cm² and treatment time of 30 s. The PCC coated papers (B and C), show a higher initial contact angle than paper A containing a blend of GCC and kaolin. As shown in Figure 3, the UVC irradiation decreased the contact angles for all the papers by an average of 10°. In contrary, the UVA treatment did not considerably affect the contact angle, which suggests that the effect is specific to the UVC wavelength. The UVC treatment makes the paper more hydrophilic, which has a potential to affect the ink setting both when printed as dry and when using predampening. Since no changes in topography were detected, the UVC enhanced surface wetting is most probably related to changes in surface chemical

properties. The contact angles versus time for both polar linseed oil and non-polar mineral oil were measured, but no changes can be observed (fig. 4). Usually an increased polarity of a surface also increases wetting by polar linseed oil, however, the higher viscosity of the linseed oil might have reduced the effect on the contact angle when compared to water.
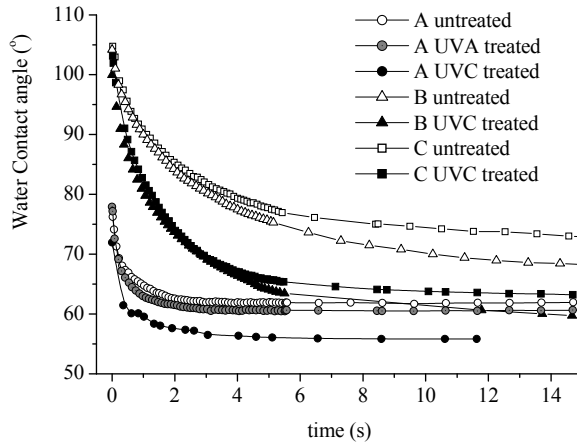


*Figure 3: Contact angle of water as a function of time for the untreated and treated paper samples. As a reference, paper A treated with UVA light was also analyzed*
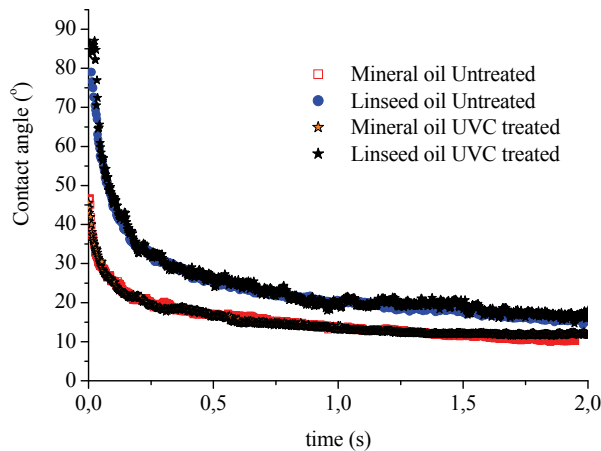


*Figure 4: Contact angle of polar linseed oil and non-polar mineral oil as a function of time on paper C for the untreated and treated paper samples. No change in contact angles versus time can be observed*

### 3.4 Treatment effect and stability

The treatment effect was studied both as a function of treatment time and as a function of intensity. When the decrease in contact angle on a PCC coated substrate is plotted as a function of the product of both (energy per unit area), a linear relationship is observed (fig. 5)
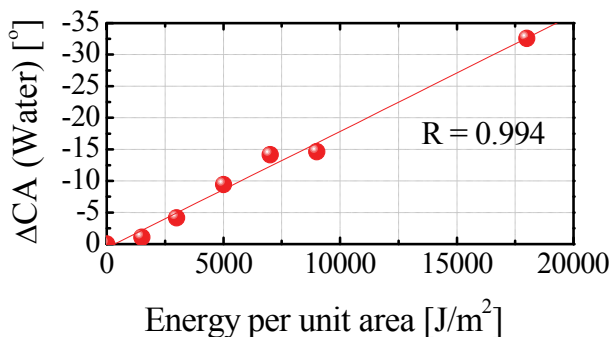


*Figure 5*
*Decrease in water contact angle versus applied energy per unit area of paper*

For scaling up to a reel to reel process the required intensity can therefore easily be extrapolated. The stability was tested by measuring contact angles for water versus time after treatment. The contact angle for water remained the same for at least half a year after the treatment.

## 3.5 Zeta potential

XPS measurements in an earlier work (Määttänen et al. 2010) showed UVC irradiation affecting the thin overlay of NaPA on PCC on coated paper. In the current study a new approach by studying the effect on Zeta potential was taken. Pigments in powder form were treated with UVC light and the Zeta potential was measured with a Malvern Zetasizer Nano ZS instrument (fig. 6). A change in Zeta potential might be an indication of the surrounding polymer layer of dispersing agents being degraded by the UVC treatment. The Zeta potential of calcium carbonate pigments is a function of the amount of adsorbed sodium polyacrylate. At a zero dosage the Zeta potential is ca -20 mV according to K. R. Rogan et al. (1994). By adding of sodium polyacrylate the Zeta potential reaches its minimum value of ca -55 mV at an amount of 5 mg / g calcite. The Zeta potential after the UVC treatment is shifted towards that of the pure mineral as shown in Figure 6. While the measurement of Zeta potential is most reliable on round pigments such as GCC, the same measurement was also carried out for the platy kaolin. For the kaolin the change in Zeta potential was the opposite, potentially because the dispersing agent attaches to the kaolin particle edges. The Zeta potential was measured at pH = 9, at which pH the kaolin particle edges are negatively charged.
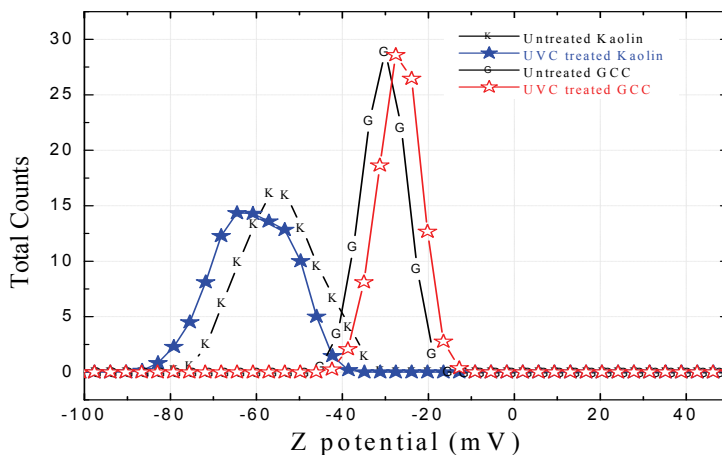


Figure 6: Zeta potential of treated and untreated GCC and kaolin pigments. The pigment particle (GCC) is surrounded by a polymeric layer (NaPA) which is partly degraded by the UVC radiation

## 3.6 Ink setting

The ink setting rate was quantified using the Ink Surface Interaction Tester (ISIT), which measures the tack of an ink on paper versus time. Immediately after printing the ink film is wet and tack is therefore low, but as the ink sets by oil absorption into the coating layer, the tack increases and reaches its maximum point. After this point, the tack decreases as the ink film solidifies. The time it takes to reach the maximum point and the slope of the tack rise indicates the ink setting rate (Gane et al. 2003, Saari et al. 2009). Differences between the ink containing both linseed and mineral oil (TMS) and only linseed oil based ink (TP) could be observed both in maximum tack and ink setting rate. For the mineral oil containing ink the maximum tack was reduced by ca 1 N on the treated surfaces regardless of paper and surface strength. This could be observed as a slight reduction in picking on the scanned ISIT stripes. When using the linseed oil based ink an obvious decrease in picking could be observed on the low surface strength paper (C) from the scanned stripes. At the same time, the maximum tack remained the same (fig. 7), which suggests that the adhesion between the ink and the pigments is lower after treatment while the cohesion in the ink film remains the same. Without the treatment the adhesion between the ink and pigments is higher than the cohesion in the ink meaning the weakest point is between the pigments, which leads to picking. IGT dry pick was also measured and results show the UVC treatment slightly decreasing the picking speed: on paper B from 0,58 to 0,56 m/s and on paper C from 0,46 to 0,38 m/s. The surface strength of the coated paper is an important factor in offset printing where highly viscous and tacky inks are used. The surface strength is normally ensured by addition of latex, however the recent trend has been to develop inexpensive paper grades for which the latex is partly replaced by starch. Paper C in this study contained only 4 pph latex and showed as untreated a clear tendency for picking. The papers containing 9 pph latex as binder (A and B) had a surface strength high enough that hardly any picking

could be detected. The main advantage of the treatment could therefore be observed on paper C where the tendency for picking was noticeably reduced. The same test was performed both immediately after the treatment and one week later, which showed that the UVC treatment was stable over time.
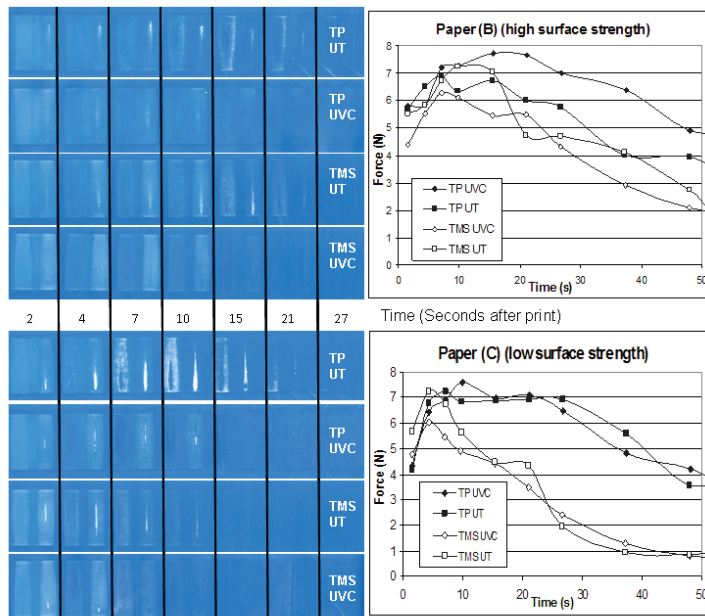


*Figure 7: ISIT curves and scanned test stripes on paper B and C with linseed oil based ink (TP) and both mineral and linseed oil containing ink (TMS) on both UVC treated (UVC) and untreated (UT). UVC-treatment appears to reduce the picking tendency. Two parallel measurements were performed for each sample*

### 3.7 Print density and gloss

All the papers were printed with both inks both using dampening solution and as dry following the IGT standard method for measuring of wet repellence. The print density and gloss were measured. Print density increased with 2-8% on the UVC treated papers when printed as dry, but when dampening solution was used there was no difference on paper A and B. Paper C, containing starch however showed a significant decrease in print density, indicating wet repellence when dampening solution was used. This might be due to the change in polarity of the surface caused by degradation of organic material. However, as shown in Figure 3 the contact angles with water were approximately the same for paper B and C after UVC treatment. UVC treatment increased the hydrophilicity of the surfaces, and water could have spread on the surface of the paper rather than penetrate into the pores. The water forms a weak boundary layer, which leads to rejection of the ink, and low print density and gloss. It seems that an increase in hydrophilicity also increased ink rejection (Figures 8 and 9).
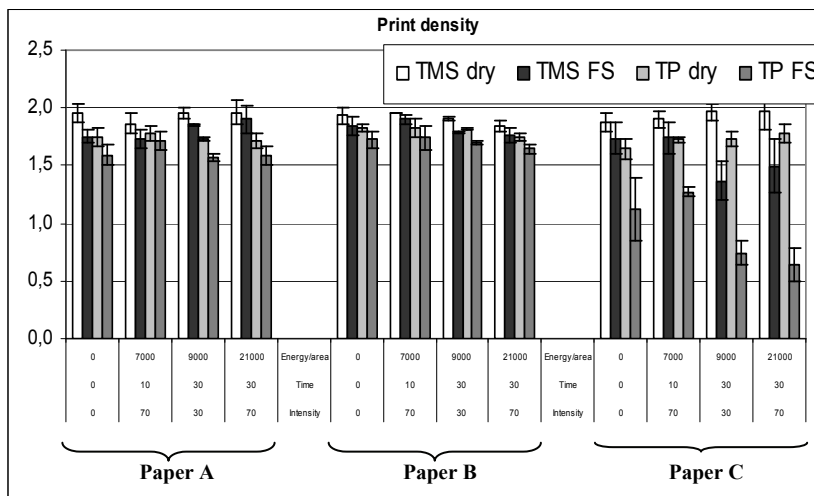


*Figure 8: Print density of the different papers with both inks, both with and without use of fountain solution (FS) Time (s), Intensity (mW/cm²) and Energy per unit area (J/m²)*
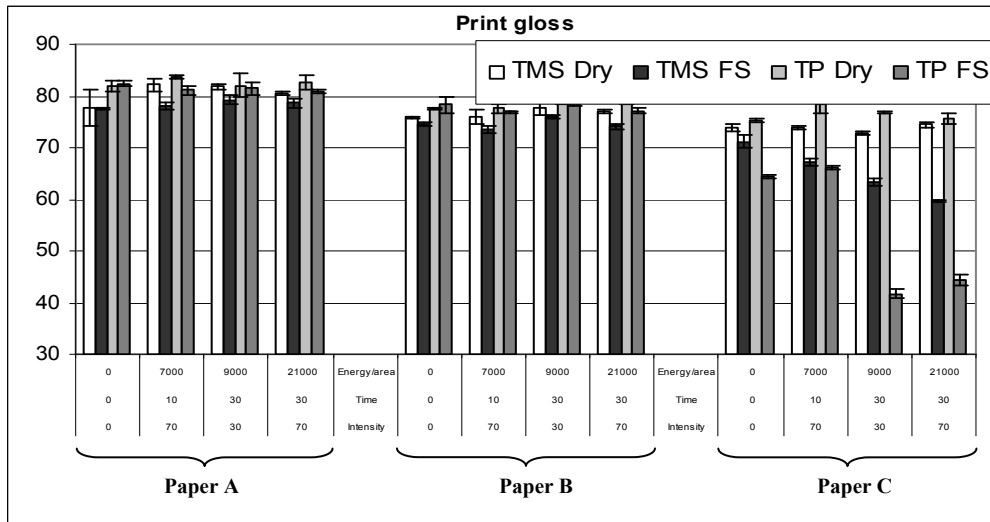
*Figure 9: Print gloss of the different papers with both inks, both with and without use of fountain solution (FS). Time (s), Intensity (mW/cm²) and Energy per unit area (J/m²)*

UVC has in an earlier work (Määttänen et al. 2010) been shown to affect the dispersing agent surrounding the pigment particles causing a polarity change in the surface of the paper. The effect was larger when using polar linseed oil based ink compared to the ink also containing nonpolar mineral oil. The treatment time seems to play an important role compared to the intensity. A short treatment time of only 10 s did not induce changes in the wet repellence, but when printed as dry, there was an increase of approximately 0,1 units in print density for the UVC treated samples. The increase in print density when printed as dry can be related to increased ink - pigment surface adhesion. By degrading the sodium polyacrylate dispersant, the UVC treatment can reduce the weak boundary layer that is formed by adsorbed water on pigment surfaces. Adhesion failure related to the presence of excess dispersant has been studied by Kamal et al. 2010. A longer treatment time of 30 s clearly shows a high wet repellence on the starch containing paper, but on the other papers no differences can be observed. The change in wettability by water is related to the applied energy per unit area but when it comes to the optical properties and the printability, a high intensity in combination with a short treatment time is favourable.

## 4. Conclusions

1. The UVC wavelength at 254 nm is known for its cleaning effects and is limited only to the outermost surface, causing degradation of organic compounds. UVC treatment can therefore be used for adjusting wettability as a post treatment method without affecting the structure of the paper surface.

2. The ink setting mechanism and ink tack build up can be affected by increased polarity of coating surface, however a detailed study using well defined model inks is necessary for drawing further conclusions.

3. Printability on low surface strength paper could be improved by reduced picking tendency and higher print density in waterless offset.

## References

Gane P. A. C., (2004), Absorption Properties of Coatings: *A Selected Overview of Absorption Criteria Derived from Recent Pore Network Modelling*, Journal of Dispersion Science and Technology 25

Gane P. A. C., Matthews G. P. Schoelkopf J, (2003), *Offset ink tack and rheology correlation part 1: ink rheology as a function of concentration ,* TAPPI JOURNAL, Vol. 2(6)

Gane P. A. C., Matthews G. P. Schoelkopf J, (2003), *Offset ink tack and rheology correlation part 2: determining in real time the solids content of ink-on-paper using the ink tack force-time integral*, TAPPI JOURNAL, Vol. 2(7)

Kamal H., Ström G., Schoelkopf J., Gane, P. A. C., (2010), *Characterization of Ink-Paper Coating Adhesion Failure: Effect of Pre-dampening of Carbonate Containing Coatings*, Journal of Adhesion Science and Technology, Vol. 24, Nr. 3

Liu F, Shen W, Parker I, (2008) *The distribution of ink emulsion component in papers of different surface energy*, Journal of Pulp and Paper Science 34

Määttänen A., Ihalainen P., Bollström R., Wang, S. Toivakka M., Peltonen J, (2010), *UVC-enhanced surface wetting of pigment coated papers*, Industrial & Engineering Chemistry Research (under review)

Preston J. S., Elton N.J., Legrix A. and Nutbeem C., (2001), *The role of pore density in the setting of offset printing ink on coated paper,* TAPPI Advanced Coating Fundamentals

Pykönen M, (2010), *Influence of plasma modification on surface properties and offset printability of coated paper*, Doctoral thesis, Åbo Akademi University

Rogan K. R., Bentham A. C:, George I.A., and Skuse D.R., (1994), *Colloidal stability of calcite dispersion treated with sodium polyacrylate*, Colloid Polym Sci 272

Romero-Sanchez M. D., Mercedes Pastor-Blasa M., Martin-Martineza J.M., Walzakb M.J., (2005), *Addition of ozone in the UV radiation treatment of a synthetic styrene-butadiene-styrene (SBS) rubber,* International Journal of Adhesion & Adhesives 25

Romero-Sanchez M. D., Walzakb M.J., Torregrosa-Macia R, Martin-Martineza J. M., (2007), *Surface modifications and adhesion of SBS rubber containing calcium carbonate filler by treatment with UV radiation,* International Journal of Adhesion & Adhesives 27

Rousu, S., (2002), *Differential Absorption of offset Ink Constituents on Coated Paper.* Doctoral thesis, Åbo Akademi University

Saari J., Bollström R., Mueller K., Toivakka M., (2009), *Ink formulation with the new multi-phase ink model*, Advances in Printing and Media Technology Proceedings, volume 36, Iarigai

Stalder A. F., Kulik G., Sage D., Barbieri L., Hoffmann P., (2005), *A snake-based approach to accurate determination of both contact points and contact angles*, Colloids and Surfaces A: Physicochem. Eng. Aspects 286

Ström, G., (2005), *Interaction between Offset Ink and Coated Paper - A Review of the Present Understanding,* 13th Fundamental Research Symposium, Cambridge

# Quality and efficiency enhancement in heatset web-offset drying by adopting thermally designed paper coatings

*Philip Gerstner*[1]*, Teemu Grönblom*[2]*, Patrick A. C. Gane*[1, 3]

[1] Aalto University, School of Science and Technology
  Faculty of Chemistry and Materials Sciences, Department of Forest Products Technology
  P. O. Box 16300, FIN-00076 Aalto, Finland
  E-mail: philip.gerstner@tkk.fi

[2] Forest Pilot Center (FPC)
  Kerrolankatu 2, FIN-21200 Raisio, Finland
  E-mail: teemu.gronblom@fpc.fi

[3] Omya Development AG
  CH-4665 Oftringen, Switzerland
  E-mail: patrick.gane@omya.com

**Abstract**

For print quality and efficiency out of the drying section in heatset web-offset (HSWO) printing, the four components of dryer design/setting, substrate, inks and fountain solution play a combined role. This work analyses the effect of coated substrate, particularly the impact of the coating layer design, on print quality parameters like printed gloss, roughness and waviness. Since waviness is to a certain degree due to an uneven moisture profile, it is investigated how thermal barrier coatings might be used to reduce the waving (fluting) tendency by shielding the basepaper from the heat of the dryer. Two thermally insulating paper coating constructions are formed using precoatings consisting of either platy mica or a blend containing a highly porous modified calcium carbonate (MCC). Both coating concepts have a comparable topcoating formulation applied and are compared to two references, one consisting of a double coating 100 % calcium carbonate formulation concept and the second a single coating of comparable coat weight based on a typical commercial calcium carbonate-rich coating formulation. The mica precoated paper was shown to exhibit lowest waving tendency. The mica precoating can reduce waving effects even more effectively at high moisture contents and high drying temperatures. By studying the liquid permeability of the mica layer, it is found that the tortuous precoating layer formed by the mica platelets acts to combine a liquid and thermal barrier, such that both quality and efficiency enhancements, due to reduced fountain solution and ink vehicle permeation, can be achieved. However, the lower brightness of the mica pigment studied, compared to calcium carbonate pigments remains a drawback in practice.

**Keywords:** heatset web-offset; drying, energy efficienc; waving, flutin; blisterin; thermal propertie; printability

## 1. General

Because of the increasing cost pressure as well as gaining focus on sustainable print production, more and more attention is being paid to the specific energy consumption of printed products. In heatset web-offset (HSWO), a significant amount of the total energy consumption is used for drying. However, it is known that only ~2 % of the drying energy is utilised for the evaporation of the ink solvent, i.e. the actual ink setting [Frank, 1996; Wendt, 1982]. This creates an open opportunity for possible improvements in the energy efficiency, and resulting quality control, of the HSWO drying process. In general, the drying process, and, thus, both efficiency and print quality, are defined by the design of four components: the dryer, in particular its hot air nozzles, the substrate, the ink and the fountain solution. Koivumäki and Hellén [2009] showed that all of these components need to be considered to optimise drying. Figure 1 illustrates how each element is part of a "chain" contributing to the efficiency. The work of Gane *et al.* [2004], and Gane and Koivunen [2010] also show the importance of limiting the penetration of liquid components, such as ink oil and fountain solution, if heat transfer to the surface of the coating is to provide maximum drying efficiency.

At first, the dryer is responsible for the transfer of thermal energy to the substrate. Avcı and Can [1999] discussed the ink drying process from the perspective of the nozzle design, and evaluated the energy consumption based on the heat transfer coefficient of the dryer. Part of the boundary layer, the stagnant film, behaves in a manner so viscous that heat is merely transported by conduction, and thus it forms the main

resistance to heat transfer as air itself is a poor conductor of heat. Avcı *et al.* [2001] have further shown from a theoretical perspective for the drying of thin films of ink that the coupled effects of heat and mass transfer are a result of jet velocity and temperature and can effectively be influenced by these design criteria. There is also a large number of publications discussing the impingement heat transfer coefficient in hot air dryers, e.g. [Heikkilä and Milosavljevic, 2002; Dano *et al.*, 2005]. It is therefore evident that the dryer design has a significant impact on the overall drying efficiency. This significance is reflected in the continuous development of dryer designs.

As the thermal energy is transported to the substrate, the transient temperature response throughout the substrate is a result of the effective thermal properties in each layer of the substrate. Gerstner and Gane [2008] showed that a thermally insulating coating layer leads to a faster temperature rise on the surface. They further showed [2009] that this can result in increased energy efficiency in case of thermally designed coated papers for the toner adhesion development in electrophotography. They also emphasised that print quality, e.g. print gloss, may benefit as well. A similar effect might apply for ink setting in HSWO.

The final element in the drying "chain" is the ink itself, i.e. the material that is required to be dried. However, fountain solution is additionally present. It is a water-based component and itself requires latent heat to vaporise before the local temperature can be raised sufficiently to vaporise ink oil components. Limiting its transport into the substrate is, therefore, also an important priority. After the heat has been transferred to the substrate, its thermal properties in combination with the liquids present in its pore structure determine the temperature response. The local temperature rise causes the ink solvent to evaporate. In this process, the vapour pressure range of the solvent used has the main effect, but also interactions of solvent and binder resin (in the ink layer) as well as solvent and substrate structure (within the substrate) play a role [Hartus and Oittinen, 1996; Avcı and Can 1999; Rousu *et al.* 2002].
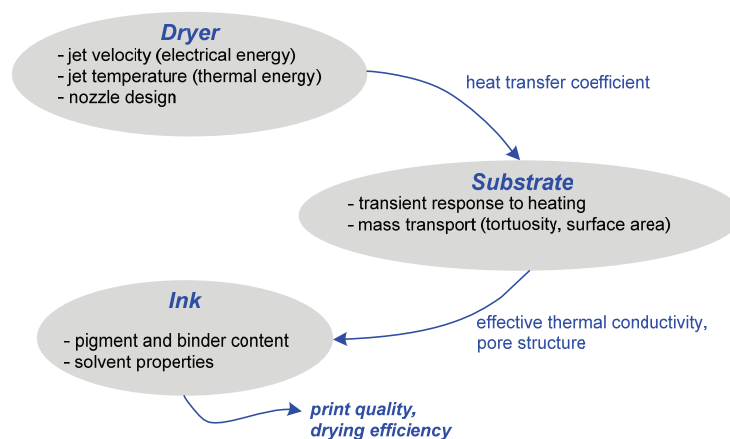


*Figure 1: Elements responsible for quality and efficiency in HSWO drying*

This work focuses on the effects of the substrate, primarily its coating, on the print quality, and, thus, aims also to improve the overall process efficiency. Printed gloss, roughness and waviness, also known as fluting, are examples of such print quality parameters in HSWO that are related to the thermal response of the substrate in relation to the ink and liquid phase present. Fluting is often a cause for complaints in HSWO printed papers [Weigl and Weigl, 2008]. To outline the aspects of this work in more detail, we first take a closer look at theoretical considerations in respect to the possible thermal and liquid transport mechanisms and how they affect print quality and ink setting in a double coated paper.

## 2. Theoretical considerations

On the one hand, waving is considered to be, at least in part, a systematic issue of the web-offset printing process. Due to the strain of the web in the machine direction throughout the press, there is an inevitable cross-dimensional shrinkage. On the other hand, the paper quality itself can have an influence on how susceptible the paper is to waving. For instance, high degrees of fibre orientation lead to more cross-directional shrinkage and thus increase the waving tendency. Low basis weight papers and high initial moisture contents are also known to increase the waving tendency. Furthermore, waving is promoted by an

uneven moisture profile caused by printed and unprinted areas (Figure 2.a), i.e. areas poor and rich in fountain solution moisture, respectively. This affects local fibre shrinkage in the dryer and can further increase the waving tendency [FOGRA, 2010; Weigl and Weigl, 2008].

Based on the mechanism that waving is due to the formation of an uneven moisture profile in the base paper expressed during drying of the web, one can introduce a precoating to act as a liquid barrier layer in order to shield the basepaper from moisture changes caused by ink and fountain solution and thus help to keep the moisture profile in the basepaper even. The topcoating would then be responsible for the printability, i.e. ink absorption. Such a concept, however, would normally make the printing paper more susceptible to blistering. Blistering occurs if the base paper moisture cannot escape fast enough during drying, and thus water vapour pressure causes the base paper structure to rupture (Figure 2.b). It has been found, therefore, that sealing the base paper with a moisture barrier promotes blistering [Weigl and Schachtl, 1995]. However, it is here envisioned that if the liquid barrier would at the same time act as a thermal barrier, the basepaper would be shielded from excessive heating. Thus the temperature would rise slower, thus effectively reducing the risk for blistering while also maintaining an even moisture profile in the basepaper due to its liquid barrier properties (Figure 2.c).
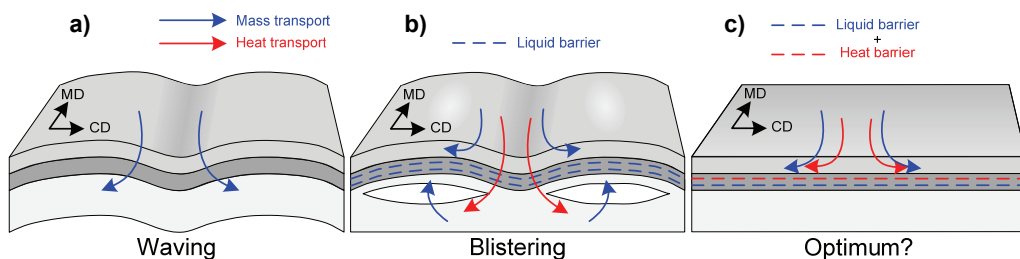


*Figure 2: a) Increased waving tendency cased by uneven moisture profile in the basepaper. b) A liquid barrier could shield the initially even moisture in the basepaper, but alone this would increase the risk of blistering. c) Having a combined liquid and heat barrier could keep the moisture profile even and reduce the risk of blistering*

We now examine the concept of introducing first a thermal barrier in order to improve the drying efficiency and minimize fluting at the same time. Two thermally designed coatings are studied: a precoat consisting of either a modified calcium carbonate (MCC[3]), that is insulating because of its highly porous structure but permeable and absorptive to liquid, or, secondly, an intrinsically insulating platy mica barrier coating, which is also largely impermeable to liquid if laid down correctly with ordered platelet orientation. Further studies are then reported, which compare the thermal barrier properties of the mica precoating layer to a commercial calcium carbonate based coating formulation, both having similar topcoatings applied. This enables a discussion regarding the effect of moisture transport and the thermal response of the substrate in the dryer. Print quality parameters will be discussed as well, and thus suggestions for the thermal optimisation of the drying process from the substrate point of view can be formulated.

## 2. Materials and methods

### 2.1 Materials

In the first part of this study, two thermally designed coating concepts are studied and compared to a reference. The first concept uses a platy mica[1] pigment precoating. The thermal conductivity of the mica as a solid homogeneous mineral is less than one fifth that of calcium carbonate [Landolt-Börnstein, 1980]. A topcoating of fine, narrow particle size distribution ground calcium carbonate[2] is applied on the mica layer for good printability. The second coating concept consists of a porous modified calcium carbonate precoating (MCC[3]). To provide sufficient internal cohesion of the MCC coating layer for offset printability, it was used in blend combination with a broad particle size distribution ground calcium carbonate (bfGCC[4]). The MCC coating concept had a comparable top-coating formulation applied, as was used in the mica concept.

---

[1] Mica SFG 40 (Mica), Aspanger
[2] Covercarb 75 (nfGCC), Omya AG
[3] MCC564, 5 μm, 64 $m^2g^{-1}$ (MCC), supplied as an experimental product by Omya Development AG
[4] Hydrocarb 90 (bfGCC), Omya AG

*Table 1: Coating formulations and coating methods used for the comparison of thermally engineered layers with a reference*

| Precoat | Reference | Mica | MCC |
|---|---|---|---|
| Method | Blade | Blade | Film |
| Pigment(s) | 80 nfGCC[2] | 100 Mica[1] | 80 bfGCC[4] |
| | 20 Clay[5] | | 20 MCC[3] |
| Binder | 11 w/w%, SA[6] | 9 w/w%, SA-R[7] | 12 w/w%, SA[6] |
| **Topcoat** | * | **Top I** | **Top II** |
| Method | | Film | Blade |
| Pigment(s) | | 100 nfGCC | 100 nfGCC |
| Binder | | 6 w/w%, SA[6] | 10 w/w%, SA[6] |
| | | 4 w/w%, Starch | |

*single coating layer

Table 1 provides a summary of the coating formulations and the corresponding coating method used. All the coatings had a similar target total coat weight of ca. 12 gm$^{-2}$ per side and were coated on an industrial scale pilot coating machine[8]. After coating, the web was calendered to a target gloss of 33-35 % and a target moisture content of ca. 4.5 %.

In a subsequent part, the mica precoat is compared to a commercial coating formulation. The commercial coating colours, both a precoat (Com. A) and topcoat (Com. B), are calcium carbonate based. Like the experimental coatings, the commercial formulations were also coated on the pilot coater for better comparability. Since a high base paper moisture content is known to increase the waving tendency (see discussion above), the effect of the substrate moisture content was studied for two different levels of 4.5 % and 6.5 % moisture targeted in the calendering.

The printing of the papers for both parts of this study was done on an HSWO machine[9] using standard ink[10]. In the sampling phase, the machine was running at a speed of 5.6 ms$^{-1}$. The drying temperatures were adjusted to both low (115 °C) and high web temperatures (130 °C and 150 °C). The length of the dryer was 8 m, which results in a residence time of 1.43 s. Even at low drying temperature, no ink smearing was observed. Table 2 summarises both parts of this study.

*Table 2: Two parts of this study comparing the objectives and trial parameters*

| | Part 1 | | | Part 2 | |
|---|---|---|---|---|---|
| **Objective** | Comparison of thermally designed coatings to that of a reference | | | Comparison of Mica precoated paper to a commercial formulation | |
| **Coatings** | | | | | |
| Precoat | Ref | Mica | MCC | Com. A | Mica |
| Topcoat | Ref | Top I | Top II | Com. B | Com. B |
| **Calendering** | | | | | |
| Target gloss | 33-35 % | | | 40-43 % | |
| Moisture | 4.5 % | | | 4.5 % | |
| | | | | 6.5 % | |
| **Printing** | | | | | |
| Speed | 5.6 ms$^{-1}$ | | | 5.6 ms$^{-1}$ | |
| Drying (web-temp.) | 115 °C | | | 115 °C | |
| | 130 °C | | | 150 °C | |

## 2.2 Measurement of waving

In order to quantify the resultant waviness in the printed paper, without the bias of the human eye in relation to the printed image, a laser scanning method was used to create a three dimensional surface topographic image of the printed sheet. The printed sample is laid out flat on the measurement table (Figure 3.1). A laser scans in the paper cross machine (CD) direction of the sample while moving along in the web (machine) direction (MD) (Figure 3.2) and transfers the data to an acquisition system (Figure 3.3). The measurement is done on a 10 cm x 10 cm green printed area (C100, Y100) of the test pattern. Figure 4 shows such a collected

---

[5] Hydragloss 90, Kamin (formerly Huber Engineered Materials)
[6] Latexia 203, Ciba
[7] Latexia 211, Ciba
[8] FPC – Forest Pilot Center Oy, Raisio, Finland
[9] Heidelberg Web-8
[10] Sun Topgloss, Sun Chemical

surface topography of a coated paper. The topography data are then transformed into the frequency domain and the amplitude in the 15-30 mm wavelength interval was used to characterise waving. The camera records the surface height deviations with an in-plane resolution of ca. 100 $\mu m^{-1}$ and an out of plane resolution of 50 $\mu m^{-1}$.
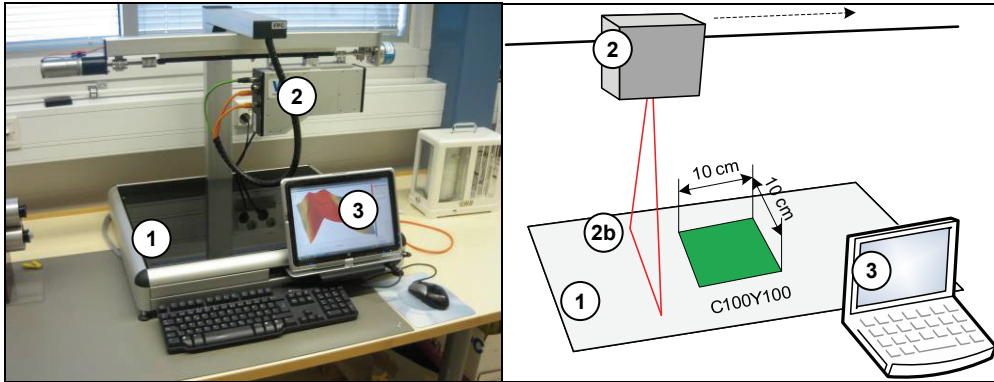


Figure 3: Photo (left) and schematic of the waving measurement device. 1)Measurement table, the measurement area is a 10 x10 cm green printed area. 2) Laser profilometer. 2b) Scanning laser beam. 3) Data acquisition
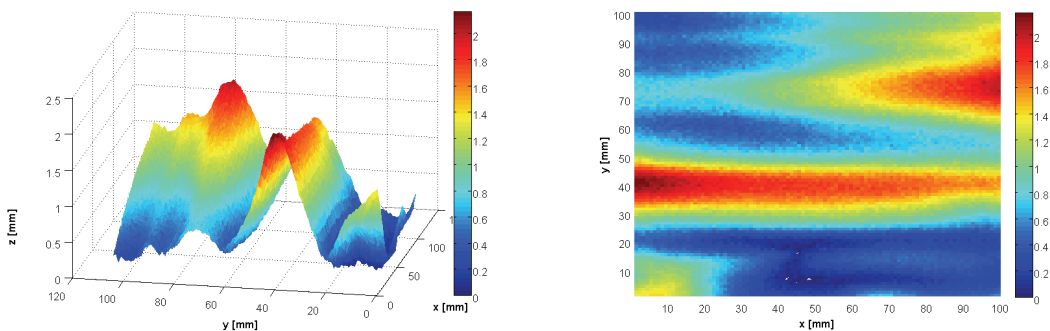


Figure 4: Surface topography of a green (C 100, Y 100) printed area on the print test pattern. The waviness is characterised by the amplitude in the 15-30 mm wavelength region

## 2.3 Liquid permeability

For the characterisation of the liquid barrier properties, the permeability was measured adopting the method of Ridgway *et al.* [2003]. In this method a stack of (ca. 200) small sample sheets is embedded round its edges in resin (Figure 5). An advantage of this technique is, therefore, that it is not susceptible to local defects, e.g. pinholes, in the individual sample sheets. The embedded sample sheets are saturated with hexadecane, which does not interact with either the fibres of the basepaper or the binders used in the coating layer(s).
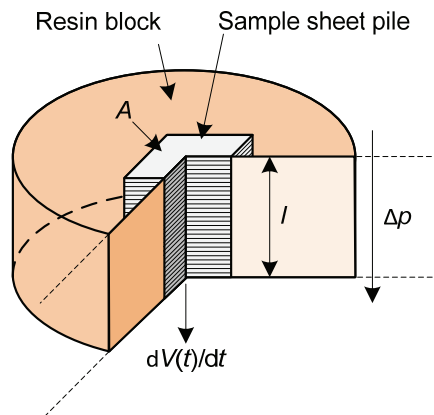


Figure 5: Schematic cut through the resin block with embedded sample sheet pile. Adapted from Ridgway et al. (2003)

The saturated sample block is then placed in a pressure cell. Gas over-pressure pushes excess hexadecane though the sample stack and an electronic scale records the permeated liquid mass flow rate. For the given density of the hexadecane, the volume flow rate of the hexadecane through the sample pile can be used in the Darcy equation to determine the permeability $\kappa$:

$$\frac{\mathrm{d}V(t)}{\mathrm{d}t} = \frac{-\kappa A \Delta p}{\eta l} \qquad (1)$$

where: $V$    is the volume of permeated hexadecane,

$A$    is the cross-sectional permeable area,

$\Delta p$    the applied pressure difference,

$\eta$    the viscosity of the hexadecane and

$l$    the effective pile thickness (calculated by the number of individual sheets).

## 2.4 Ink-surface interaction (ISIT)

The ink tack force development was measured with the ISIT apparatus [Gane and Seyler, 1994] where a tack disk is brought in contact with the sample a certain time interval after the print. The tack disk pulls away from the printed sample and measures the tack force $F_T(t)$. The tack force development, repeatedly measured, each from a fresh surface of the print as a function of time, can generally be divided into three stages. In the first stage, the tack rises to a maximum. This tack rise time describes the initial ink vehicle imbibition defined by the finest pores. The maximum tack force (second stage) is a measure of the ink cohesion increase in competition with adhesion to the surface, and is a function of surface microsmoothness and the nature of the ink-surface adhesion energy, respectively. In the third stage the tack decays at a rate depending on the available pore volume and surface area taking part in absorption.

The ink tack development curves will help to evaluate whether the experimental barrier coating layer will have a detrimental effect on the ink absorption behaviour, i.e. the printability, in comparison with the commercial coating formulation.

## 3. Results and Discussion

### 3.1 Basic properties

Figure 6 shows the printed gloss (Tappi 75°) and the printed roughness (Parker Print Surf (PPS)) of the two thermally designed formulations as well as for the reference coating. It should be kept in mind that the topcoatings used are comparable to each other. Therefore, the effects will be primarily due to the precoating layer. It can be seen that both in terms of print gloss and, to a smaller extent, also for roughness, the MCC concept is favourable. This is because of the compressibility of the porous MCC pigment particles aiding smoothing in the calender. Also the mica precoated paper showed a slightly higher print gloss compared to the reference. This might be related to the platy nature (high aspect ratio) of the mica pigment improving physical basepaper coverage.
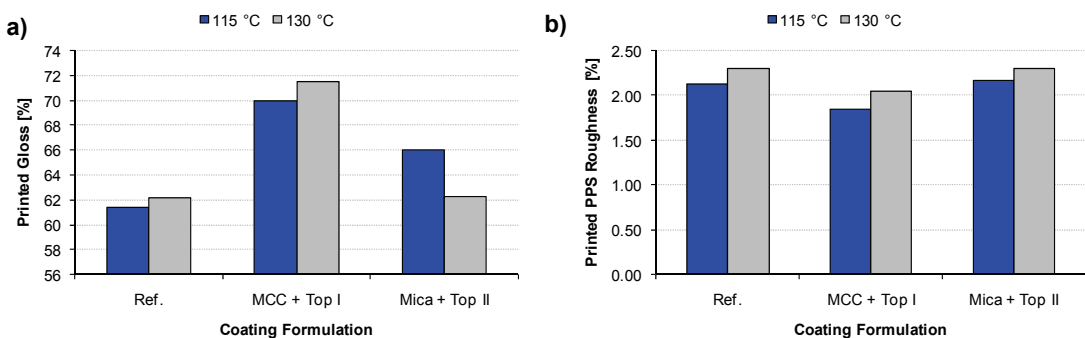


*Figure 6: Printed gloss a), and printed PPS roughness b), for the thermally designed coating formulations including MCC and Mica experimental precoats, respectively, as well as for the reference coating, observed after low and high temperature drying*

When comparing the mica precoating with the commercial precoating, both using the very same topcoating formulation, one can see that the print gloss level (Figure 7.a) is also distinctly higher, which is a positive side effect of the mica pigment barrier coating. Figure 7.b shows that this is due to the higher delta gloss.
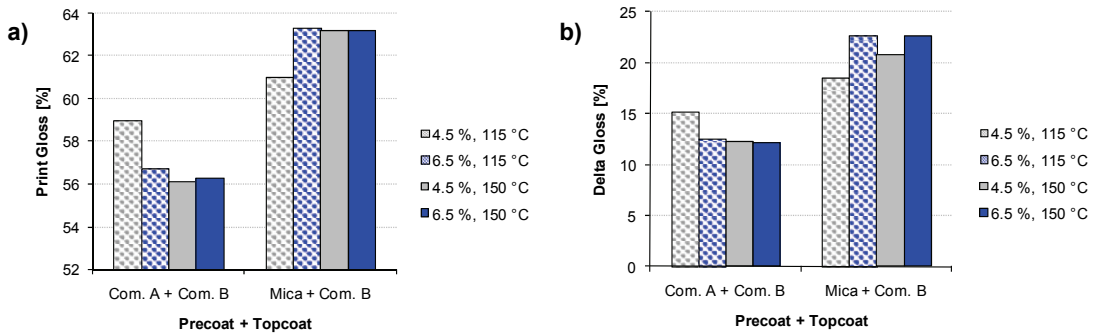


*Figure 7: Printed gloss a), and delta gloss b), for the commercial formulations and the formulation with the mica precoat*

However, the lower final ISO brightness of the mica precoated sample studied (85.4 %) compared to calcium carbonate pigment coatings (89.2 %) poses a potential drawback in practice. Further work would, therefore, be needed to develop a higher brightness permeation barrier and insulating layer.

## 3.2 Waving

There is a clear advantage in the result of the waving measurement in the case where a mica precoat is used (Figure 8.a). While it is often difficult to assess waving visually, because of the bias of the human eye to brightness and gloss, nonetheless these results reflect the visual impression of the printed sheets very well.
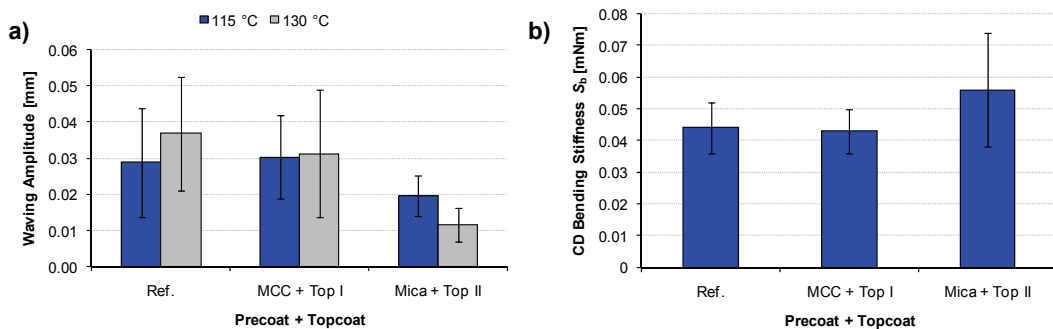


*Figure 8: a) Waving for the reference and the thermally designed coatings. b) CD Bending stiffness of the unprinted papers*

The advantage of less waving for the mica coating concept can be at least in part due to the thermal barrier properties of the mica precoating and/or in part due to the liquid/moisture barrier properties because of the platy pigment structure and the self-swelling rotogravure latex used as binder. Additionally, there may a small stiffness increase associated with the mica precoat adding rigidity to the planar structure (Figure 8.b). However, given small differences and the standard deviation of the bending stiffness, it is unlikely that it is a decisive factor for the lower waving tendency of the mica. We, therefore, differentiate these mechanisms further by looking at different paper moisture levels, and also study how the mica performs in comparison with the commercial formulation. To do so, the mica precoat formulation is used in combination with the commercial topcoat formulation (Com. B).

Figure 9 shows the waving results of commercial precoat and topcoat as well as for mica precoat and commercial topcoat for different moisture levels and different drying temperatures. It can be seen that at low drying temperatures there is generally little waving, even at the high moisture level, and the mica formulation is definitely comparable to the commercial formulation, given the standard deviation in the results. The combination of high moisture content and high drying temperature leads to strong waving. This was to be expected based on the assumed underlying mechanisms of waving [FOGRA, 2010; Weigl and Schachtl, 1995]. However, the mica precoat continues to show a clear advantage over the commercial formulation under these extreme conditions. As pointed out earlier, this difference could not be directly related to the mechanical
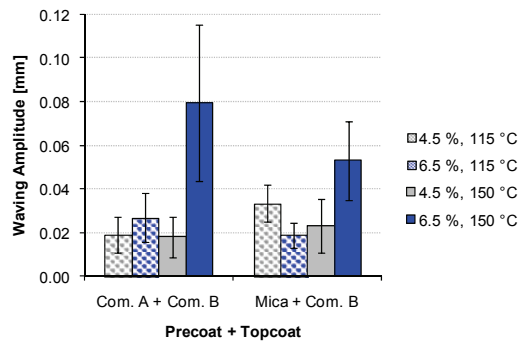
*Figure 9*
*Waving for the commercial formulations in comparison with the mica formulation*

property of bending stiffness. The cross-machine directional bending stiffness is 0.07 mNm and 0.06 mNm for the double coated papers with the commercial precoating and the mica precoating, respectively. It is more likely that despite the high web temperature, the platy and thermally insulating mica can shield the moisture in the base paper to some extent and prevent stronger waving. It was observed that neither the commercial formulation nor the mica formulation showed blistering. The ink level was 200 % and 300 % on each side of the paper, respectively. The absence of blistering could on the one hand indicate that the basepaper is largely blister resistant up to the web temperature of 150 °C, but on the other hand it could also support the theory that in addition to the liquid barrier, the mica precoating also creates a thermal barrier that compensates for an increased risk of blistering expected when using a less permeable precoat. The discussion, therefore, now goes on to take a special look at the liquid barrier properties of the mica layer and evaluate whether that has an influence on the printability.

## 3.3 Barrier properties and ink interaction

Figure 10 and Figure 11 show SEM cross-sectional images of the coated papers with the commercial formulation and the mica precoating formulation, respectively. It can be seen in Figure 10 that the commercial precoating (Com. A) is somewhat "coarser" than the topcoating, but there is generally little visual difference between the precoating and the topcoating (Com. B).



*Figure 10: SEM cross-section images of the commercial double coated (Com. A + Com. B) calendered paper. a) 250x*



*Figure 11: SEM cross-section images of the mica precoated, commercial topcoated (Mica + Com. B), calendered paper. a) 250x and b) 1000x*

In contrast, Figure 11 shows the mica precoating with the commercial topcoating. The platy mica pigment is readily visible. However, it is questionable to say based on the SEM cross-section how much the mica layercan contribute to forming a liquid barrier. It is, therefore, necessary to quantify the liquid permeability for further discussion.
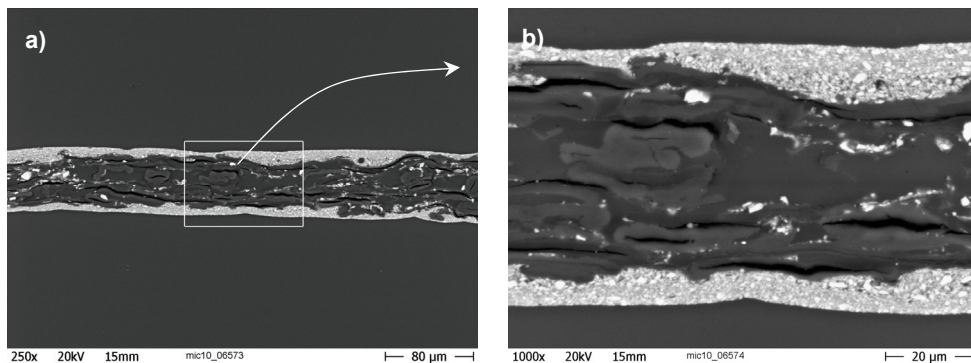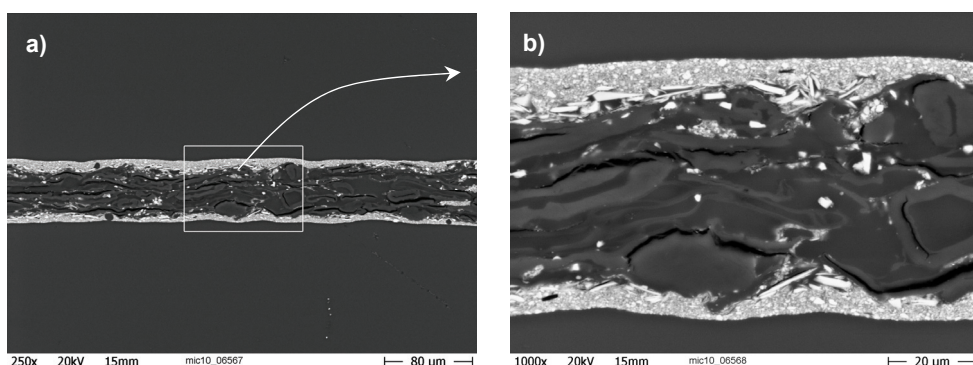
Figure 12.a shows the measured permeabilities for the basepaper only and proceeds with the permeabilites of the respective precoated papers, the double coated papers and the calendered papers, respectively. The only difference in the bars of each step in Figure 12.a is the precoating formulation (Mica versus Com. A). In general, it is seen that both coating and calendering lowers the liquid permeability roughly one order of magnitude. The difference between the mica precoating and the commercial precoating seems rather small on this logarithmic scale. However, if one takes the actual ratio of both, one can see that for commercial precoating the permeability is in fact more than twice as high. This relation of both concepts is not notably changed by the application of the identical topcoating or the calendaring, emphasising the dominant role of the mica precoat in reducing permeability. Table 3 summarises the permeability data and also provides the ratios of permeability of commercial versus mica and the calendered grades versus the basepaper.

Based on the permeability measurement, it is clear that there is a notable difference in the mass transport rate though the precoating layer. However, for optimum ink setting behaviour some mass transport into the coating is required. The following question arises, therefore, whether the ink setting is affected by the mass transport barrier of the mica layer. This can be studied by looking at the dynamic tack force response.

It is seen (Figure 12.b) that the coatings are comparable in terms if the initial tack increase behaviour. This confirms the identical nature of the top surface microstructure of both papers. However, the tack decrease from the maximum shows a dual porosity step in the curve for the case of the two commercial coating layers, illustrating a potential interlayer phenomenon. The overall tack decrease rate, though, which is describing the available pore volume, can nonetheless be regarded as similar. It is known that the tack response is primarily dependent on the top coating layer [Klosse et al., 2001]. This means, in turn, that the beneficial effect of the mica coating layer in reducing waving (see Figure 9) is not primarily due to the ability to shield the basepaper from ink vehicle oil transported by capillarity, but, rather, due to the ability to keep an even moisture profile within the basepaper by reduced permeation, as well as its thermally insulating behaviour. This explains the particular advantage of mica in the reduction of waving for high moisture contents in combination with high drying temperatures.
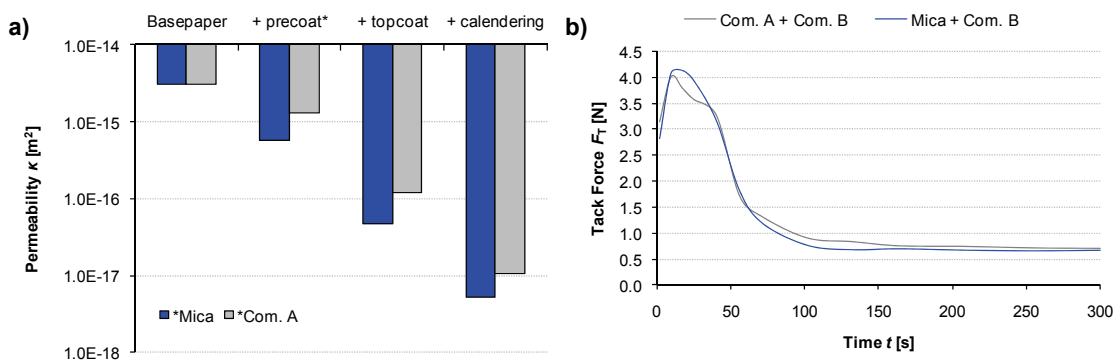


Figure 12: a) Measured permeabilities of the base paper, the precoated papers with Com. A and Mica, respectively, as well as the respective permeabilites of the double coated and the final calendered papers. b) Comparison of the tack force development for the commercial pre- and topcoated paper with the mica precoated and commercial topcoated paper. Both papers have the same topcoating formulation

Table 3: Coating formulations and methods used for the comparison of thermally engineered layers with a reference

| Permeability κ [m²] | Com. A* | Mica* | Ratio (Com. vs. Mica) |
|---|---|---|---|
| Basepaper | 3.04E-15 | 3.04E-15 | |
| + precoating | 1.32E-15 | 5.67E-16 | 2.33 |
| + topcoating (Com. B) | 1.22E-16 | 4.75E-17 | 2.56 |
| + calendering | 1.06E-17 | 5.17E-18 | 2.06 |
| *Ratio (Base vs. Calendered)* | 285.77 | 587.33 | |

*precoating formulation

## 4. Conclusions

Porous MCC and platy mica precoatings were applied in combination with topcoating formulations for studying HSWO printability and fluting tendency. While the MCC coating concept showed high gloss values, a property due to the compressible pigment and its excellent bulking coverage, the mica coating layer showed advantages in terms of a low waving tendency. This was, therefore, further investigated by comparing the mica precoating formulation directly to a commercial formulation, both having the very same topcoat. It was observed that the mica precoating can reduce waving effects particularly present at high moisture contents and high drying temperatures. This reduction was accounted for by the thermal and/or liquid/moisture barrier properties. To distinguish the barrier effects, the liquid barrier properties were measured by means of permeability. It was shown that the mica precoating reduces the permeability by a factor of two in respect to the commercial formulation. This helps in maintaining an even moisture profile in the basepaper. In spite of the increased moisture barrier, no blistering was observed, even at high temperatures, which supports the action of mica in terms of thermal insulation, which results in a slower temperature rise in the basepaper. In turn, the thermal energy is more focused on the drying of the ink and moisture removal from the topcoating only. A disadvantage of the mica pigment, seen in this study, is its low brightness. In order to compete successfully with the typically used high brightness carbonate coatings an alternative pigment or pigment beneficiation would have to be found. Nonetheless, this study showed, in principle, that by combining the concept of a liquid barrier and a thermal barrier, both quality and efficiency enhancements in the HSWO process can be achieved.

### Acknowledgments

### References

1.  E. Frank. Trocknung im Rollenoffset: Neue technologische und ökologische Erkenntnisse. *Dtsch. Drucker*. **32**(25):w2-w10, 1996.

2.  P. Wendt. Trocknung, Abluftentsorgung und Energiekreislauf an Rollenoffsetmaschinen heute. *Dtsch. Drucker*. **18**(4):6-13, 1982.

3.  K. Koivumäki and E. K. O. Hellén. Drying in heatset web offset printing. **Advances in Printing and Media Technology. Volume 36**. N. Enlund and M. Lovreček (ed.), Iarigai, Darmstadt, 2009, pp. 267-271.

4.  P. A. C. Gane, C. J. Ridgway and J. Schölkopf. Absorption rate and volume dependency on the complexity of the porous network structures. *Transp. Porous Med.* **54**(1):79-106, 2004.

5.  P. A. C. Gane and K. Koivunen. Relating liquid location as a function of contact time within a porous coating structure to optical reflectance. *Transp. Porous Med.* In the press, DOI: 10.1007/s11242-009-9523-x

6.  A. Avcı and M. Can. The analysis of the drying process on unsteady forced convection in thin films of ink. *Appl. Therm. Eng*. **19**(6):641-657, 1999.

7.  A. Avcı, M. Can and A.B. Etemoğlu. Theoretical approach to the drying process of thin film layers. *Appl. Therm. Eng*. **21**(4):465-479, 2001.

8.  P. Heikkilä and N. Milosavljevic. Investigation of impingement heat transfer coefficient at high temperatures. *Drying Tech*. **20**(1):221-222, 2002.

9.  B. P. E. Dano, J.A. Liburdy and K. Kanokjaruvijit. Flow characteristics and heat transfer of a semi-confined impinging of jets: effect of nozzle geometry. *Int. J. Heat Mass Trans*. **48**(3-4):691-701, 2005.

10. P. Gerstner and P. A. C. Gane. Considerations for Thermally Engineered Coated Printing Papers: focus on electrophotography. **Advances in Printing and Media Technology. Volume 35**. N. Enlund and M. Lovreček (ed.), Iarigai, Darmstadt, 2008, pp. 249-261.

11. P. Gerstner and P. A. C. Gane. Fusing of Electrophotographic Toner on Thermally Engineered Coated Paper. **Advances in Printing and Media Technology. Volume 36**. N. Enlund and M. Lovreček (ed.), Iarigai, Darmstadt, 2009, pp. 391-400.

12. T. Hartus and P. Oittinen. Characterisation of the drying properties of heatset inks by thermal methods. *Graphic Arts in Finland*. **25**(1):9-15, 1996. Available online at: http://media.tkk.fi/GTTS/GAiF/GAiF_artikkelit/gaif96_1.pdf [cited: 19.05.2010]

13. S. Rousu, M. Lindstöm, P. A. C. Gane, A. Pfau, V. Schädler, T. Wirth and D. Eklund. Influence of latex-oil interaction on offset ink setting and ink oil distributions in coated paper. *J. Graphic Technol*. **1**(2):45-46, 2002.

14. C. Weigl and J. Weigl. Mechanismen von Reklamationsfällen durch hohe Trocknungstemperaturen im Heatsetdruck. *Wochenblatt für Papierfabrikation*. **136**(1-2):20-23, 2008.

15. FOGRA. [online] Wellenbildung im Rollenoffset. Online Fehlerkatalog. Available online at: http://www.fogra.org/DB/_fogra/index.htm [cited: 17.05.2010]

16. J. Weigl and M. Schachtl. Blasenbildung bei doppelt gestrichenen Rollenoffset-Druckpapieren. *Wochenblatt für Papierfabrikation*. **123**(8):332-345, 1995.

17. Landolt-Börnstein. **Zahlenwerte und Funktionen**. Band IV Technik, 4. Wärmetechnik b, 6. Auflage, Heidelberg, 1980.

18. C. J. Ridgway, J. Schoelkopf and P. A. C. Gane. A new method for measuring the liquid permeability of coated and uncoated papers and boards. *Nord. Pulp Paper Res. J.* **18**(4):377-381, 2003.

19. P. A. C. Gane and E. N. Seyler. Some novel aspects of ink/paper interactions in offset printing. Proc. *International Printing and Graphic Arts Conference*, Halifax, Nova Scotia, TAPPI press, Atlanta, GA, 1994, pp. 209-228.

20. J. Kosse, P. A. C. Gane, D. C. Spielmann, C. Naydowski and S. Kleeman. Auswirkung der Pigmentfeinheit auf die Porenstruktur der Strichoberfläche. *Münchner Papier-Seminare*, Tagung der Fachschule München, März 28, 2001

# Light stability of thermochromic prints

*Mojca Friškovec*[1]*, Rahela Kulčar*[2]*, Marta Klanjšek Gunde*[3]

[1] Cetis, Graphic and Documentation Services
  Čopova 24, Celje, Slovenia
  E-mail: mojca.friskovec@cetis.si

[2] University of Zagreb, Faculty of Graphic Arts
  Getaldićeva 2, Zagreb, Croatia
  E-mail: rkulcar@grf.hr

[3] National Institute of Chemistry
  Hajdrihova 19, Ljubljana, Slovenia
  E-mail: marta.k.gunde@ki.si

## Abstract

Light with larger photon energy has a detrimental effect on colour and appearance of prints over longer periods of time. Conventional printing inks usually have an acceptable lightfastness, mainly because of the high stability of applied pigments. On the contrary, novel smart printing inks have more sophisticated pigments which, in most cases, are not crystalline and therefore have a low resistance to light and also to high temperatures and some chemicals, thus needing additional protection.

Our work is based on protection of thermochromic printing inks against UV light. Such inks have micro-encapsulated thermochromic composite (leuco dye, developer, solvent). Three different commercial inks were tested. Two different lacquers were applied over printed samples as a protective layer. The dynamic colour of protected theromochromic layers was compared with the properties of the corresponding unprotected samples. Physical properties of samples were analysed by SEM micrographs of differently etched sample surfaces.

**Keywords:** thermochromic inks; protective lacquers; UV protection; artificial weathering; total colour difference

## 1. Introduction

Most frequently applied thermochromic (TC) printing inks are based on organic composite which is protected in pigment capsules from unwanted reactions with their surroundings [Seeboth & Lötzsch, 2008, Seeboth et al., 2007]. The capsule is hard, non-polar, thermally very stable and relatively impermeable [Small, 1996]. The TC composite usually consists of a colour former (leuco dye), a colour developer and a solvent. The reaction between dye and developer prevails at lower temperatures and gives rise to coloured complexes. At higher temperatures the solvent melts, making the solvent-developer interaction dominant, and colour complexes are destroyed [Seeboth & Lötzsch, 2008, Seeboth et al., 2007, White & LeBlanc, 1999]. The colour of samples printed with such ink depends on temperature and on thermal history – the effect is described by colour hysteresis [Kulčar et al., 2009]. Dynamic colour may be described by the area of colour hysteresis in 3D colour space or, alternatively, by four characteristic temperatures of the hysteresis loop [Kulčar et al., 2010].

Leuco dye-based TC inks have short pot life, poor lightfastness, low resistivity to high temperatures and many chemicals. Polymer envelopes are much more stable than the polymer binder in TC ink [Kulčar et al., 2010]. However, lightfastness and chemical stability of TC capsules in the applied vehicle were considered to be the origin of poor stability of TC inks [Small, 1996].

The lightfastness of leuco dye-based TC samples might be increased simply by applying a protective layer. For this reason, two transparent lacquers were tested. Special commercial TC ink with intrinsically improved lightfastness (the so-called UV-protected ink) was used without protective layer as a comparison. The effect was evaluated by total colour differences between exposed and unexposed samples and by the total colour contrast between fully coloured and totally discoloured states.

## 2. Experimental

Three commercially available TC inks with red colour shade were considered here, two UV-curing and one air-drying, which is announced to be UV protected (Table 1). Two transparent lacquers were applied. The PK 70/36 (Coates Screen, Germany) is a solvent-based top coat ink, recommended to improve weather resistance of graphic art products. The UV absorbing lacquer WPT325 (Siltech Ltd, England) is a water based lacquer for flexographic and gravure printing, designated for UV protection.

*Table 1: Selected data of applied inks: drying method, activation temperature ($T_A$), the size of the largest pigment particles (grindometer value), and specular gloss evaluated at 60° (gloss units, GU)*

| sample | drying method | $T_A$ (°C) | grindometer value (μm) | gloss (GU) |
|--------|---------------|------------|------------------------|------------|
| UV31 | UV curing | 31 | 11 | 35 |
| UV33 | UV curing | 33 | 1,5 | 63 |
| AD15 | air drying | 15 | 1 | 5 |

The three inks were screen printed using a flatprinting SD 05 machine (RokuPrint, Germany) over OBA-free gloss coated paper (150 g/m$^2$) employing SEFAR® PET 1500 monofilament polyester mesh 120/34Y. The samples were cured with energy ~ 400 mJ/cm$^2$. The two lacquers were applied over dried TC layers using bar film applicator with gap clearance of 100 μm.

Spectral reflectance was measured using Lambda 950 UV-VIS-NIR spectrophotometer (Perkin-Elmer) using 150 mm integrating sphere with (8°:di) measuring geometry. The fully coloured state was measured at 5 °C and completely discoloured at 50 °C. The temperature of the sample was regulated by circulation of thermostatically controlled water through copper base of water block (EK Water Blocks, EKWB d.o.o. Slovenia).

The CIELAB values were calculated using D50 illuminant and 2° standard observer. The total colour differences were calculated according to the CIEDE2000 colour difference equation [CIE Publication, 2004]. Spectral transmittance of the lacquers was measured in collimated beam over UV and visible spectral region. The samples were applied over fused silica wafer (Corning 7980).

The samples were exposed to quartz-filtered Xenon Arc Radiation (Suntest XLS+, Atlas Material Testing Technology) for 1.5, 6 and 24 hours, corresponding to radiation dose of 2700, 10800 and 43200 kJ/m$^2$, respectively.

The sample surfaces were monitored using a Karl Zeiss Supra 35 field emission SEM. More particles were made visible when the topmost layer of the binder was selectively etched by weakly ionised highly dissociated oxygen plasma. For this purpose the oxygen plasma was created in a glass Pyrex tube with an inductively coupled RF generator operating at 27l12 MHz and 200 W output. The oxygen pressure was about 75 Pa. Selective etching is a consequence of different oxidation probability of the binder and TC pigment. The removal of the highest layer of the binder was attained in a couple of minutes.

## 3. Results and discussion

Light stability was studied through the optical properties in the UV and visible spectral regions. Colour differences appearing on samples due to UV exposure were measured. Colorimetric characterisation of dynamic colour was expressed by the total colour contrast, i.e. the colour difference between the completely coloured and discoloured phases of the same sample. The light stability of TC prints was studied by this colour contrast in dependence on exposure to UV light. TC prints were also analysed by the stability to selective oxygen plasma etching.

### 3.1 Optical properties

Transmittance of the two protective lacquers is shown in Figure 1. They are both highly transparent over the entire visible spectral region. The weather resistant lacquer blocks UV light below 360 nm whereas the UV protective blocks almost all radiation below 400 nm.
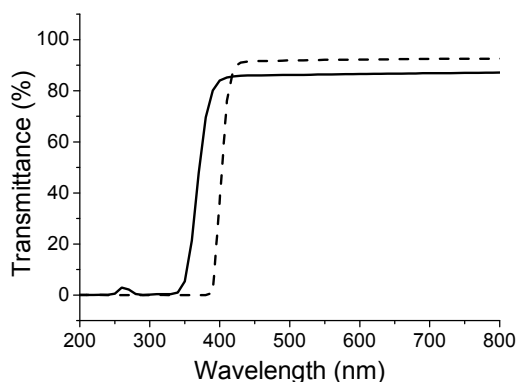
*Figure 1: Transmittance of weather resistant (solid line) and UV protective (dashed line) lacquers*
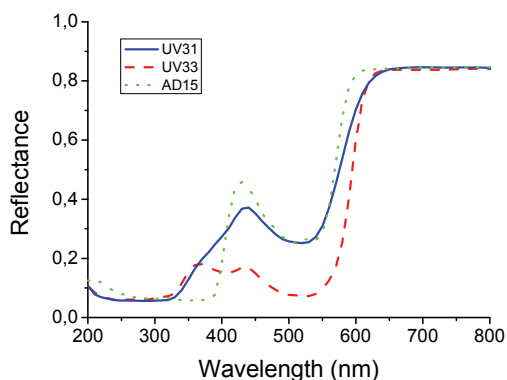


*Figure 2: Reflectance of the applied TC samples in fully coloured form (no protective layer)*

The applied TC inks have similar spectral reflectance for the red light (above 600 nm) but different in the blue and UV spectral region (Figure 2). The AD15 sample absorbs practically all UV light whereas the other two inks reflect some part of UV light with longest wavelengths, between 340 and 400 nm.

The lacquer layer increases the specular gloss of samples. The effect is larger for UV protective lacquer (above 88 GU) and smaller for weather resistant one (73-81 GU). Only very little change in gloss was observed after exposure to radiation up to 24 hours.

### 3.2 Colorimetric properties

The exposure to radiation influences the colour of all samples. The colour difference between the unexposed and exposed sample in fully coloured and totally discoloured state increases with exposure time, more rapidly for unprotected layers (Figure 3). Effect is the largest for UV33 and similar for UV31 and AD15 inks. The results show that application of a protective layer has a large influence, which is higher when UV protective lacquer was applied.
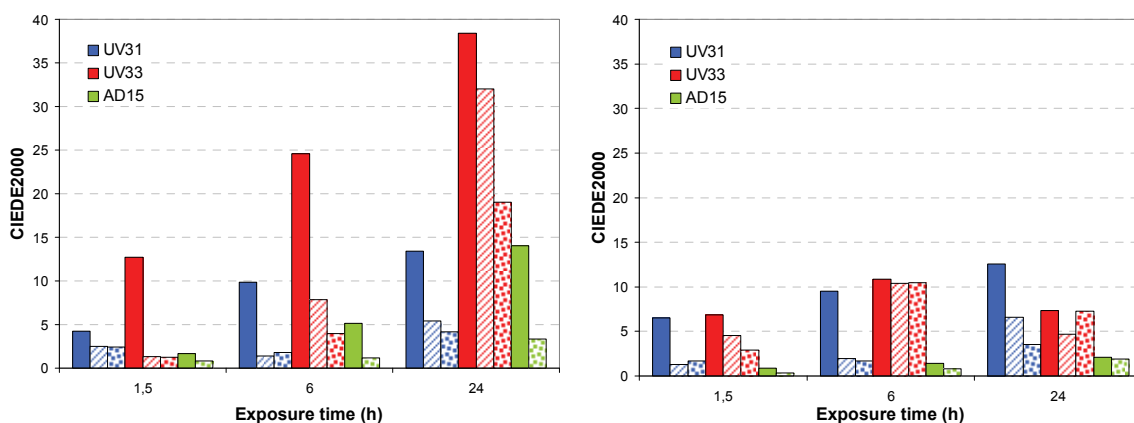


*Figure 3: The total colour difference between unexposed and exposed samples in dependence on exposure time for fully coloured (left) and totally discoloured state (right). Unprotected samples are represented in solid colour, samples protected with PK lacquer in diagonal lines and with WPT325 lacquer in dots*

A TC sample is considered to work properly if the total colour contrast between the fully coloured and totally discoloured state is clearly recognizable. The total colour difference between the two states for the unexposed and exposed samples is shown in Figure 4.

After 24 hours of exposure it completely vanishes in unprotected UV33 sample and drops below 5 CIELAB units for unprotected UV31 sample but remains above 10 CIELAB units for unprotected AD15 sample. Protective layers give great benefit to the operating ability of samples.
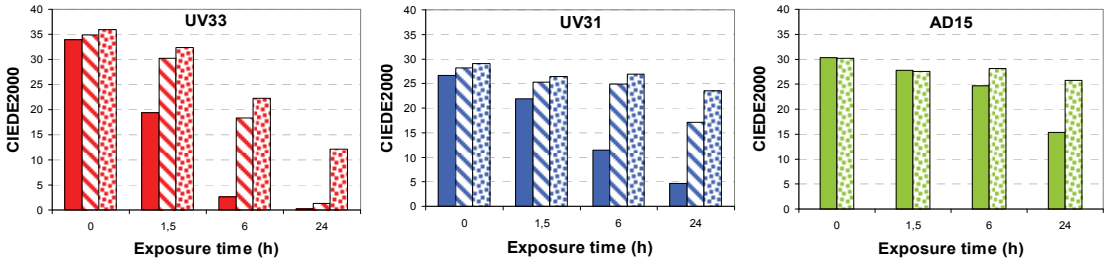
*Figure 4: The total colour contrast between fully coloured and totally discoloured states of unprotected samples (solid colour), samples protected with PK lacquer (diagonal lines) and protected with WPT325 lacquer (dots) in dependence on exposure time*

Photographs of protected and unprotected samples in fully coloured state after different exposure times were taken. UV31 and UV33 were photographed at 17 °C and AD15 at 5 °C. Samples in coloured state are shown on Figures 5, 6 and 7.
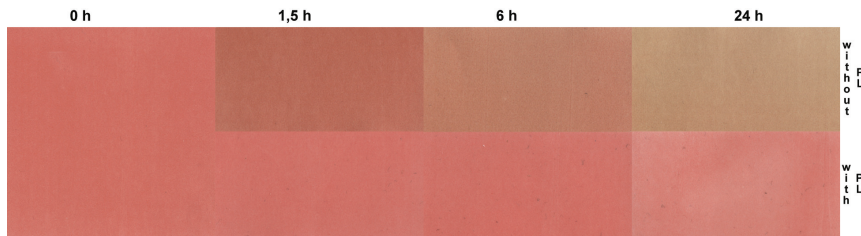


*Figure 5: UV31 sample with (lower row) and without (upper row) a protective layer (WPT325 lacquer), exposed for different times*
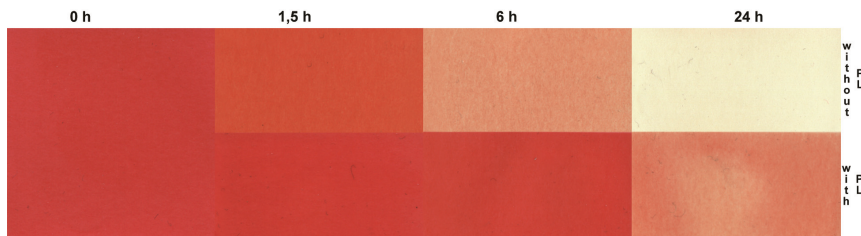


*Figure 6: UV33 sample with (lower row) and without (upper row) a protective layer (WPT325 lacquer), exposed for different times*
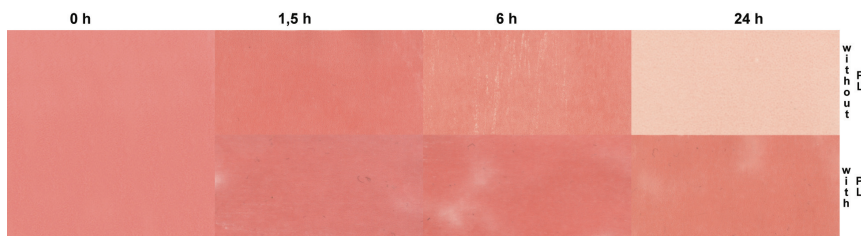


*Figure 7: AD15 sample with (lower row) and without (upper row) a protective layer (WPT325 lacquer), exposed for different times*

It can be seen from the Figures 5, 6 and 7 that the application of a protective layer is effective, as the difference between protected and unprotected samples is more than obvious. The best results were obtained for the AD15, slightly worse for the UV31 and the worst for the UV33. Without protection, UV33 loses all of its colour after 24 hour exposure to UV.

The colour of thermochromic samples does not depend only on their temperature but also on thermal history - they show colour hysteresis. Samples become discoloured during heating and coloured again during cooling. The process is illustrated by the change of lightness L* as a function of temperature. Hysteresis loops for unexposed samples, exposed unprotected and exposed protected samples are shown on Figure 8.
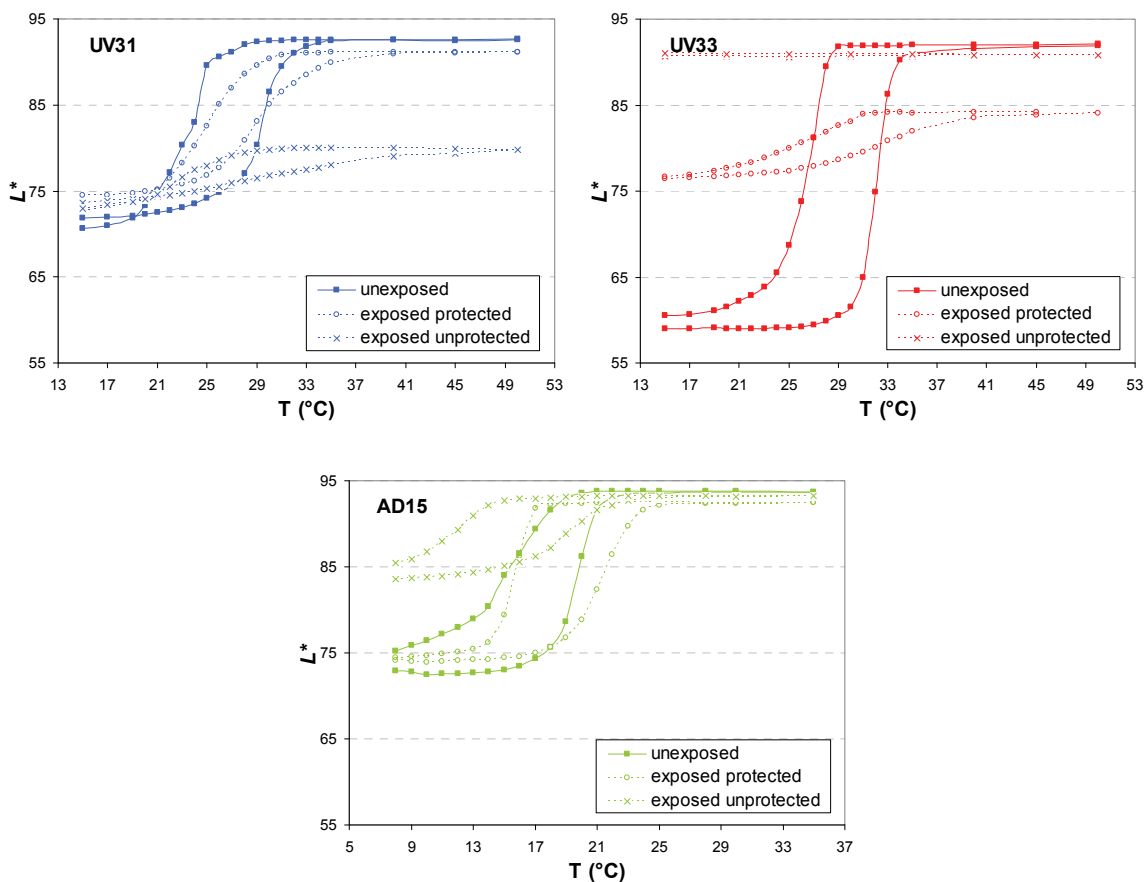
*Figure 8: Hysteresis loops of all three samples; solid lines (unexposed), dashed lines (exposed to UV light for 24 h)*

All hysteresis loops get smaller and their slopes become gradual after 24 hours of UV exposure. The best results were obtained for the AD15 sample and the worst for the UV33. The latter sample in exposed and unprotected state exhibits no colour and therefore has no dynamic colour properties.

### 3.3. Physical properties

SEM micrographs of a sample without plasma etching may show only pigment particles located at the very top of the layer, but they are usually covered by the binder and therefore could hardly be observed very clearly. More particles become visible when the topmost layer of the binder is removed by selective etching in oxygen plasma. By longer etching time more and more material is etched away, quicker the one with higher oxidation probability.

The SEM micrographs of sample surfaces are shown in Figure 9 where the surfaces of unexposed and exposed UV31 samples are shown at different etching times. The unetched surfaces look almost the same, independently on UV exposure. After 120 s of etching a large difference in the binder is observed. On the UV-exposed sample surface the binder was completely etched away, but large surface regions remain covered by the binder on the unexposed one. By further etching, the top binder etched further and the top TC pigment capsules become almost completely visible after 180 s of etching.

At the same conditions on the UV-exposed sample it was not only the binder that was removed further but also a large amount of pigment capsules were damaged. Such a sample irreversibly loses its functional properties - the top TC capsules do not protect the TC composite from the environment therefore their dynamic colour change is not guaranteed any more. Similar results were obtained on the other two samples.

These results show that the polymer envelopes are more stable against oxidation in oxygen plasma than the binder. Exposure to UV light diminish the stability of the binder, therefore the topmost layer of the binder was etched away after shorter exposure.
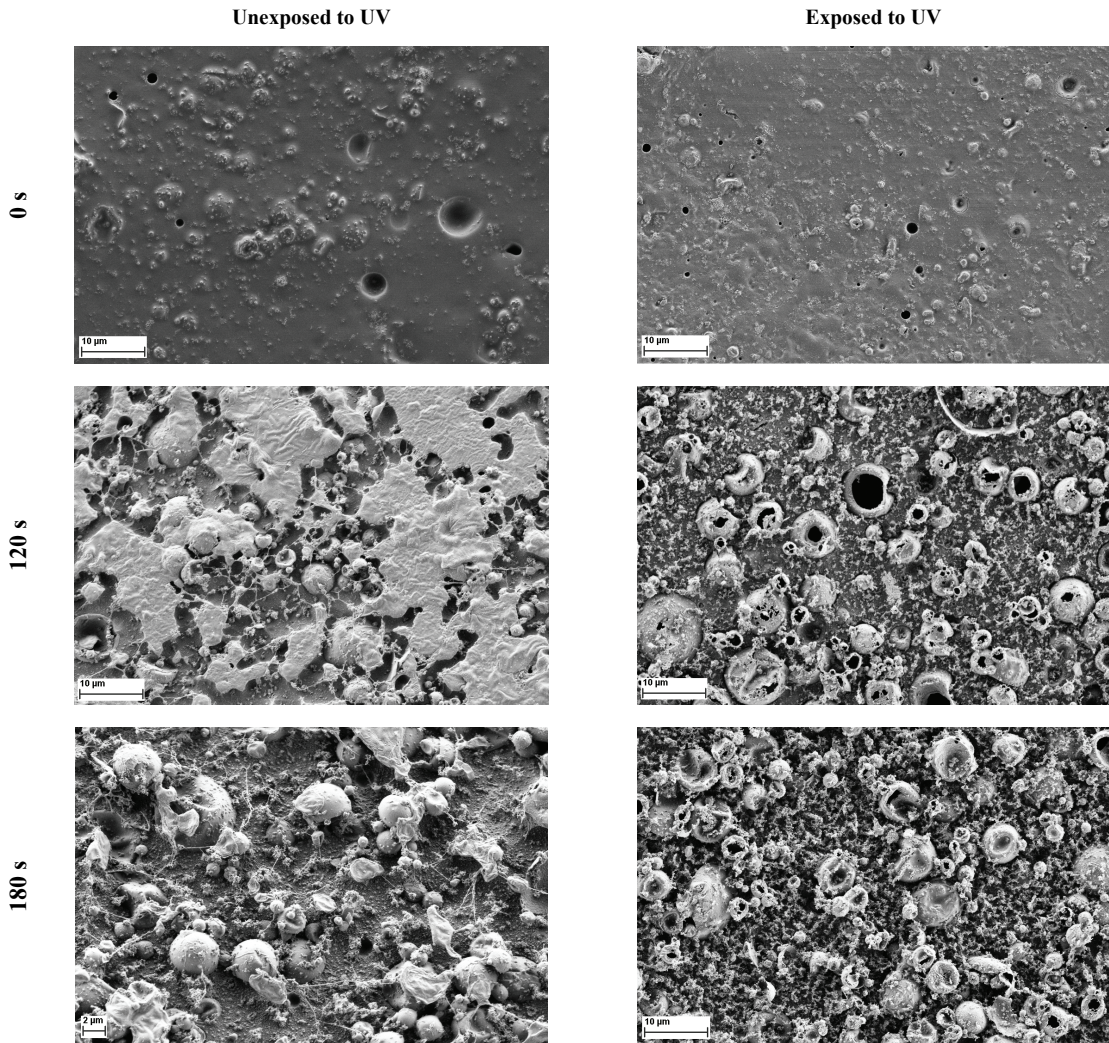
*Figure 9: SEM micrographs of the UV31 samples; unexposed (left column) and exposed to UV light (right coloumn), in untreated form (first row), after exposure to oxygen plasma for 120 s (middle row) and 180 s (last row)*

## 4. Conclusions

Lightfastness of TC printing inks is poorer than that of conventional ones. TC pigment particles consist entirely of organic compounds with different stability, which are generally lower than inorganic. The envelopes are much more stable than the vehicle however TC colour change might have quite lower UV stability than supposed.

The influence of light radiation for the two extreme colour states of samples was analysed here, the fully coloured and totally discoloured ones. Three TC printing inks in red colour shade were examined; one of them is announced by a producer to have increased UV-stability. The lightfastness was evaluated by three total colour differences:

  (a) between unexposed and exposed samples in the fully coloured state,
  (b) between unexposed and exposed samples in the totally discoloured state and
  (c) between fully coloured and totally discoloured states of the same sample

as a function of exposure time. In general, the first two values increase with light exposure but the last one decreases. Degradation of colour is larger for the two inks with no UV protection and considerably smaller for the ink with improved UV stability. The colour contrast (c) of the improved ink diminishes to 50 % of the initial value after 24 hours of exposure. This property was gradually improved with protective layer. Two

transparent lacquers with high UV absorption were tested. The best results were obtained for the lacquer which absorbs larger amount of UV radiation: it helps retain the operation colour properties for at least 30 % of initial value after 24 hour of exposure.

UV exposure has an effect on hysteresis loops of all three samples. Compared to unexposed samples, the loops of exposed samples reduced gradually. For the larger exposures there may be no loops at all, i.e. practically no dynamic colour.

When the binder covers all the TC pigment capsules, it is able to protect them from the light for a certain extent. UV light reduces stability of the binder against oxidation. This was confirmed by the higher oxidation probability, seen by selective oxygen plasma etching. This effect could be one of the reasons for poor light stability of the TC samples. Another reason could be poor stability of the TC composite inside capsules. Nevertheless, the protection of the functional material in pigment capsules by a good polymer envelope and with a well-stable binder could give better stability of TC printing inks.

Further research is needed to understand the degradation processes that are taking part in all components of the TC printed layer and protective cover layers. The chemistry of the degradation process of TC composite inside capsules, polymer envelope, binder system and the ability of the protective lacquers to filtrate away the detrimental UV light should be analysed in more details.

## Acknowledgements

## References

1. CIE Publication x015:2004, (2004), Colorimetry, 3rd ed. Vienna: CIE Central Buerau

2. Kulčar, R., Friškovec, M., Knešaurek, N., Sušin, B., Klanjšek Gunde, M.,(2009) *Colour changes of UV-curing thermochromic inks, Advances in printing and media technology. Vol. 36. Darmstadt: International Association of Research Organizations for the Information, Media and Graphic Arts Industries, pp. 429-434*

3. Kulčar, R., Friškovec, M., Hauptman, N., Vesel, A., Klanjšek Gunde, M., (2010), *Colorimetric properties of reversible thermochromic printing inks, Dyes and Pigments, Vol. 86, Iss. 3, pp. 271-277* doi:10.1016/j.dyepig.2010.01.014

4. Seeboth, A. & Lötzsch, D., (2008), *Thermochromic Phenomena in Polymers. Shawbury: Smithers Rapra Technology Limited, Shawbury, UK, pp. 98*

5. Seeboth, A., Klukowska, R., Ruhmann, R. & Lötzsch, D., (2007), *Thermochromic polymer materials, Chinese Journal of Polymer Science, Vol. 25, Iss. 2, pp. 123-135*

6. Small, L. D., & Highberger, G., (1996), *US Patent; WO 96/10385, Thermochromic ink formulations, Nail lacquer and methods of use*

7. White, M. A., & LeBlanc, M., (1999*), Thermochromism in commercial products, Journal of Chemical Education, Vol. 76, Iss. 9, pp. 1201-1205*

# Color matching in inkjet proofing using spectral methods

*Arash Ataeian and Abhay Sharma*

School of Graphic Communications Management, Ryerson University
350 Victoria street, Toronto, ON, Canada M5B 2K3

E-mails: arash.ataeian@ryerson.ca and sharma@ryerson.ca

**Abstract**

Color matching of images from one process to another is an important requirement in color management. Matching an offset press sheet on an inkjet proofer is one such practical application. The match, in most color management systems, is based on minimizing the color difference in terms of tristimulus colorimetric values, CIE L*a*b* or CIE XYZ. Colorimetric matches however, may match under a specific lighting condition, but are not guaranteed to match if there is a change in illumination, a phenomenon known as metamerism. As an alternative to colorimetric matching, this paper examines different color mixing models and spectral matching algorithms in order to create an inkjet proof that decreases the likelihood of metamerism - increases the robustness of the color match. This research uses an Epson Stylus Pro 4800 inkjet printer. The ColorBurst RIP is used to ensure control of the individual C, M, Y and K ink channels. Spectral measurement data from print samples was used to create matrix-based, algorithmic solutions that were programmed and evaluated in MATLAB. The conceptual framework for the algorithms is based on the Kubelka-Munk color mixing model using inks and paper substrates.

**Keywords:** spectral color matching; inkjet proofing; Kubelka-Munk theory

## 1. Introduction

There are many situations where we need to create or re-create the color of a given sample on a different imaging media or reproduction system. In a paint store we may seek to match a customer's color swatch, in the printing industry we often seek to create on an inkjet printer, a color accurate proof of an offset press sheet. Color reproduction and color matching in these situations, can be based on heuristic techniques using the experience of a colorist or, more commonly today, by means of an algorithmic/numerical solution based on appropriate theoretical assumptions (R. S. Berns, 2000).

One methodology for color matching between disparate imaging media is provided by the ICC architecture and framework (ICC, 2004). The ICC color management architecture is now well established. In the color characterization process we obtain data by printing and measuring CMYK (subtractive color model) ink combinations, followed by suitable modelling and fitting algorithms, and implemented via a series of 1-dimensional and multi-dimensional lookup tables (A. Sharma, 2007). In the ICC approach, regression analysis and higher order polynomial fitting may be used, but the content of the lookup table is based primarily on empirically derived data (P. Green, 2010). For color reproduction on CRT monitors (additive color model), where we have an additive and linear system, and it is now well established to use a linear mixing model that consists of a 3x3 matrix in conjunction with 1-dimensional tone curves (R. S. Berns, 1993).

In this research we used an Epson Stylus Pro 4800 inkjet printer. A Color Burst RIP was used to ensure control of the individual C, M, Y and K ink channels. In general this research is based on the explanation of Allen (E. Allen, 1980) and seeks to model optical and physical combination of thin layers of ink on opaque paper using the Kubelka-Munk theory, by considering CMYK dot percentages and assuming the printed test patch colors, exhibit total reflectance. We did not premix inks before printing and it is therefore not necessary to provide a full cover printed area as modelled by Kang in his 1991 study (H. R. Kang, 1991).

### Kubelka-Munk Theory (Single constant and two constant)

The goal of color matching models is computing the concentration or relative proportions of colorants (dyes, paints, pigments or inks) to match the color of samples or targets (R. S. Berns, 2000). The most widely used theory in color matching algorithms, Kubelka-Munk, characterizes the scattering and absorption behavior of colorants (R. S. Berns, 2000) (E. Walowit, 1987 & 1988). If they have negligible scattering property, single-constant, most often for textile and dyed paper, and otherwise two-constant model, most often for paints and inks, is applied to formulation (R. S. Berns, 2000 & 2007) (E. Allen. 1980). In this research we use the single constant theory where we substitute the coefficients of the single constant theory concentrations with digital (CMYK) values.

*Colorimetric and spectral color matching*

Spectrophotometric and colorimetric models are two major computing approaches (B. Sluban, 1993). In general, the literature describes approaches for colorimetric matching where we relate device-dependent pixel values (RGB, CMYK), with colorimetric values (CIEXYZ, CIELAB). The mapping is done via mutli-dimensional look-up tables with values extracted from analytical expressions or for monitor displays, for example, using linear (matrix) and non-linear (1-dimensional) lookup tables (G. Sharma, 2003). In spectral color matching, one seeks to match the reflectance of two samples, i.e. reduce the difference between the spectral distribution function at each wavelength. This may be expressed mathematically as

$$\sum_i (\Delta R_i)^2 \rightarrow 0 \qquad\qquad\qquad (1)$$

where i typically is from 400 – 700 nm, and we square the values to ensure only positive numbers. Some studies have suggested weighted fitting due to different importance of various wavelengths on visual perceptions (A. Karbasi, 2008),

$$\sum_i W_i (\Delta R_i)^2 \rightarrow 0 \qquad\qquad\qquad (2)$$

where $W_i$ is weighting function that represents the importance of wavelength based on visual perception. It is relevant to note that in tristimulus or colorimetric matching strategy the spectral distribution between two samples may be *different*, but due to the averaging effect of the human observer (color matching functions) and the illuminant, the samples may *appear* to match. This situation, however, allows for the possibility of metamerism. Two samples with always match, under different illuminants, only if their spectral power distribution is similar. This is why tristimulus or colorimetric matching attempts to predict zero color difference for a specified illuminant, it is normal to assume D50, (equation 3). In other words light source relative energy distribution is used in the computation, so a large color difference under another light source is always a possibility.

$$(\Delta X, \Delta Y, \Delta Z)_{D50} \rightarrow (0, 0, 0) \qquad\qquad\qquad (3)$$

In practice it may be the norm to offer iteration should be performed usually to attain better color agreement between target and match in desired accuracy (A. Karbasi, 2008). The general accuracy of different approaches for commercial solutions has been determined for ICC-based solutions and ranges from 1-4 for printer profiles (A. Sharma, 2006). The goal of this approach is reach to zero color difference without evaluation of color. Although in practice it's not possible to find a complete agreement between reflectance curves, but balanced color difference under different light sources could be an advantage of this method.

## 2. Methods

In this research, we used an Epson Stylus Pro 4800 inkjet printer with an 8 channel print head, controlled by a Color Burst RIP v5.0. This printer has light inks for better color reproduction; there are for example, cyan and light cyan cartridges. In normal operation the light cyan is effective during the lower (lighter) tone values and drops off from the 50% tone value and simultaneously, the normal cyan ink kicks in. The RIP configuration was altered to direct all cyan pixel information to the cyan cartridge only and not to use any light cyan ink, Figure 1. The printer was controlled via the RIP and this system was used to print with only the normal inks and to not direct any pixel values to the light ink cartridges. All light inks were set at 0% and all "normal" CMYK inks were set to a linear response. This process reduced the number of active colorants from 8 to 4.
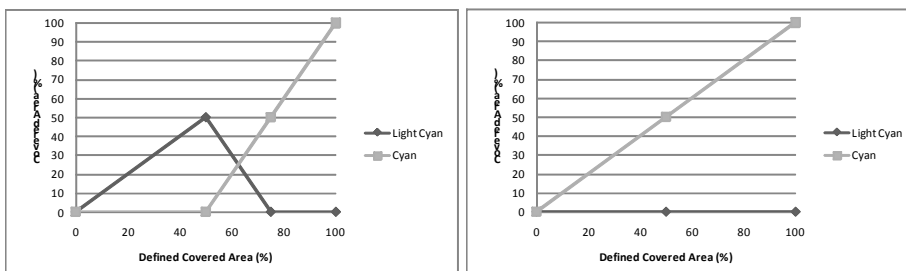


*Figure 1: Left-Cyan and Light Cyan Ink delivery system before channel control, Right-Cyan and Light Cyan Ink delivery system after channel control*

X-Rite's Color Port 1.5.4 was used to create test targets. The simple ramp test target (Figure 2) consists of 40 patches of 4 inks from 10% to 100% coverage. This target was printed on HP Bright White Inkjet paper (containing optical brightening agents, #1), FABRIANO TIZIANO 26 PERLA (grey shade, #3), and FABRIANO TIZIANO 31 NERO (black shade, #4).



*Figure 2: Simple ramp test target that used simple C, M, Y and K, 10 step ramps*
*from 10% to 100% at 10% intervals*

We utilized the DTP70 spectrophotometer along with Measure Tool 5.0 software, both from X-Rite to measure printed samples in reflectance and color (UV excluded and included). Resulted spectral measurement data was used to investigate the influence of substrate on reflectance factor and color of substrate. Kubelka-Munk theory and Complex-Subtractive mixing model for opaque material were used to model inkjet colorants response. Digital values of C, M, Y, K (%) assumed as colorant concentration in well-known Kubelka-Munk formulation (Equation 4).

$$(k/s)_\lambda = (k_{sub} + cc\,k_c + cm\,k_m + cy\,k_y + ck\,k_k) / (s_{sub} + cc\,s_c + cm\,s_m + cy\,s_y + ck\,s_k) \qquad (4)$$

where k, s, cc, cm, cy, ck are reflectance, absorption coefficient, scattering coefficient, covered area of cyan, magenta, yellow and black respectively. Subscripts λ, sub, c, m, y, k indicate wavelength, substrate, cyan, magenta, yellow and black respectively. Due to ink scattering negligibility in relation to the substrate, the result of first part i.e. influence of substrate on color of printed samples, equation 4 was simplified as follows(Equations 5 and 6). Only one parameter i.e. unit "k over s" is considered instead of two parameter, k and s.

$$(k/s)_\lambda = (k_{sub} + cc\,k_c + cm\,k_m + cy\,k_y + ck\,k_k)/(s_{sub}) \qquad (5)$$
$$(k/s)_\lambda = (k/s)_{sub} + cc(k/s)_{unit\,c,\,\lambda} + cm(k/s)_{unit\,m,\,\lambda} + cy(k/s)_{unit\,y,\,\lambda} + ck(k/s)_{unit\,k,\,\lambda} \qquad (6)$$

A characterization test target consists of 60 simple and overprints patches (Figure 3) was created and printed on paper #1 (Characterized media).
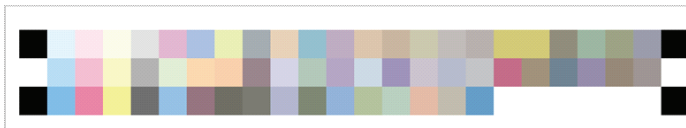


*Figure 3: Characterization test target with 60 color patches including various overprint combinations*
*of C, M, Y and K*

Matrix algorithm was created to compute unit (k/s) or (k/s)$_{unit}$ at each wavelength, using the reflectance data of characterization test target(Equations 7 and 8).

$$(k/s)_\lambda = (1-R_\lambda)^2 / (2R_\lambda) \qquad (7)$$
$$KOVERS_{n\times1} = inv(KSCOEF'_{n\times m} \times KSCOEF_{m\times n}) \times KSCOEF'_{n\times m} \times OBS_{m\times1} \qquad (8)$$

Where R is the reflectance factor, n is the number of inks and m is the number of mixtures of inks are provided to make a database or characterization test target , KOVERS is the matrix of unit (k/s) , KSCOEF is the matrix of covered area and OBS is the matrix of $[(k/s)_\lambda - (k/s)_{sub}]$.

The adequacy and performance of model was tested by performing a spectral color matching process; a sample target with 10 color patches (Figure 4) was printed on different media (COPYPRINT Weyerhaeuser paper, #2) and measured in reflectance and color.
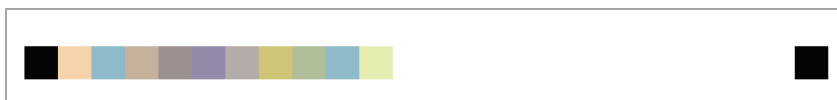


*Figure 4: Sample target with 10 color patches in different hues and combinations of C, M, Y, K*

Resulted spectral measurement data was used in algorithmic spectral matching model in MATLAB R2010a (Equation 9). This algorithm computes the covered area of inks (dot %) to match the reflectance of a sample.

$$C_{n \times 1} = inv (P'_{n \times q} \times P_{q \times n}) \times P_{n \times q} \times (T_{q \times 1} - A_{q \times 1}) \qquad (9)$$

Where n is the number of inks, q is the number of wavelengths which applied spectrophotometer has measured reflectance at them. P is the matrix of unit (k/s) for inks at several wavelengths. T is the matrix of target (k/s) and A is the substrate (k/s). CMYK values that seek to re-create the sample target reflectance were printed on characterized paper, followed by reflectance and color measurement. Then we performed a colorimetric correction (Equations 10 and 11) and new CMYK values were printed on characterized paper, followed by new reflectance and color measurement.

$$C_{ac} = C_{bc} + \Delta C \qquad (10)$$
$$\Delta C = inv (TED\Phi) \times \Delta t \qquad and \ (11)$$

where   C = covered area, ac is after correction, bc is before correction
TE = normalized 31×31 matrix (Color matching functions for $2^o$ observer × Power distribution of $D_{50}$)
D = diagonal matrix for derivative function $[dR/d(K/S)] = [2R^2/(R^2-1)]$ , a 31×31 matrix
R = reflectance of target per wavelengths from 380-730nm at 10nm interval,
$\Phi$ is the matrix of unit (k/s) for Cyan, Magenta, Yellow and Black inks per wavelengths from 380-730nm at 10nm interval, a 31×4 matrix and $\Delta t$ represents the differences in tristimulus values between target sample and matched sample, a 3×1 matrix $[\Delta X; \Delta Y; \Delta Z]$ .We note that the inverse function could be replaced by pseudo-inverse when TED$\Phi$ matrix is not square. The reflectance of new printed sample (after correction) was compared to the sample target again.

## 3. Results

A number of results are presented here that - support the assumptions and derivations of equations in the Section Experimental; demonstrate the effect of the substrate on the reflectance spectra; and provide numerical values for accuracy of the color matching process (Delta E).

*Basic Optical Behaviour* of Chosen Substrates
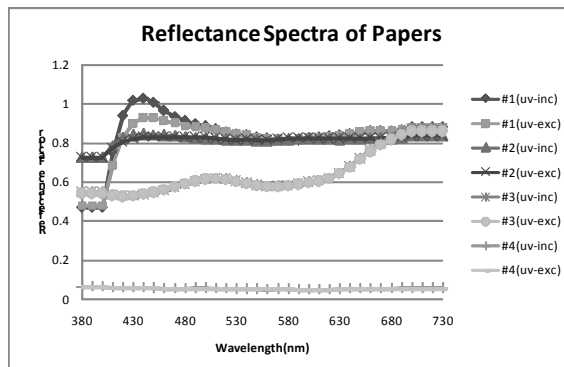


*Figure 5: Reflectance Spectra of papers within the range of 380-730nm*

*Table 1: Tristimulus and Uniform Color Space Values of papers (XYZ and L\*a\*b\**
*Observer angle: $2^0$, Illumination: D50)*

| Paper # | X | Y | Z | L* | a* | b* |
|---------|-------|-------|-------|-------|------|-------|
| 1(UV-inc) | 81.84 | 83.81 | 79.3 | 93.37 | 2.00 | -8.82 |
| 1(UV-exc) | 80.42 | 83.09 | 73.52 | 93.05 | 0.60 | -4.44 |
| 2(UV-inc ) | 78.99 | 81.58 | 68.72 | 92.39 | 0.65 | -1.31 |
| 2(UV-exc) | 78.91 | 81.62 | 67.87 | 92.41 | 0.42 | -0.5 |
| 3(UV-inc) | 57.96 | 59.65 | 45.61 | 81.65 | 1.08 | 4.21 |
| 3(UV-exc) | 58.07 | 59.77 | 45.78 | 81.71 | 1.07 | 4.11 |
| 4(UV-inc) | 4.83 | 5.00 | 4.54 | 26.73 | 0.08 | -2.38 |
| 4(UV-exc) | 4.83 | 5.00 | 4.54 | 26.75 | 0.08 | -2.35 |

As it is shown in the Figure 5 and Table 1, there is some color difference between sample target substrate (#2) and matched substrate (#1). It is clear that paper #1 contains optical brighteners – absorption of UV radiation and emission in the blue part of the spectrum. The reflectance factor at some shorter wavelengths (blue spectrum) is greater than 1, as shown by measurement in UV mode. These values cannot be adequately modelled by equation 7. In the present work, the process for spectral color matching was performed using UV-excluded measurements.
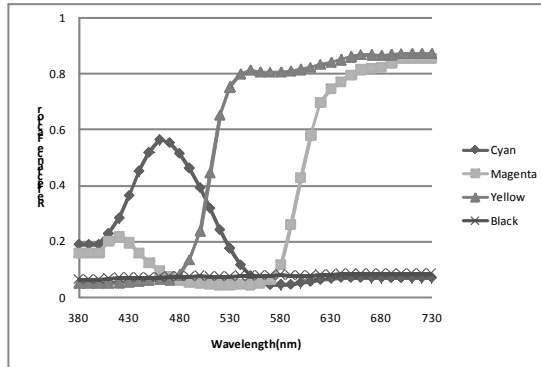


*Figure 6: Reflectance spectra of 4 printed samples by individual inks in 100% covered area on paper #1 (UV-exclude mode)*

Figure 6 shows the reflectance spectra of the CMYK inkjet inks on substrate #1, based on this figure we determine the maximum absorption (minimum reflectance) of inks occurs at wavelengths as shown in Table 2.

*Table 2: Maximum absorption wavelength for C, M, Y, and K at 100% dot percentage on paper #1*

| Ink | Cyan | Magenta | Yellow | Black |
|---|---|---|---|---|
| Wavelength(nm) | 580 | 520 | 410 | 380 |
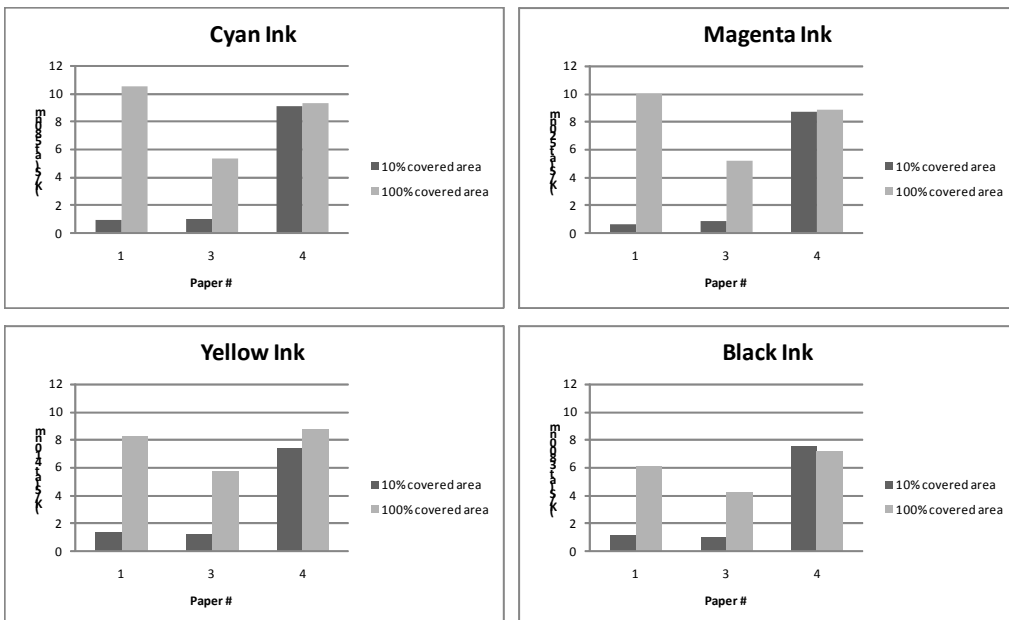


*Figure 7: (K/S) variance for 10% and 100% covered area for Cyan, Magenta, Yellow and Black Inks at the wavelength of maximum absorption*

Figure 7 shows that (K/S) has a significant change from 10% to 100% covered area for papers #1(white) and #3(Light Gray). This alteration could not be found on the black paper substrate (#4). In this case, (K/S) values are close together. It should be noted that physical properties of paper as well its color influence the total reflectance of a printed sample. This is why in this research we involved paper #3 in the (K/S) investigation, due to its physical similarity to paper #4. Paper #2 was only used for printing the sample target

and is therefore not shown in these figures. To further investigate the influence of substrate on the reflectance spectra, lightness (L*) values of printed samples were plotted versus covered area percentage (Figure 8).
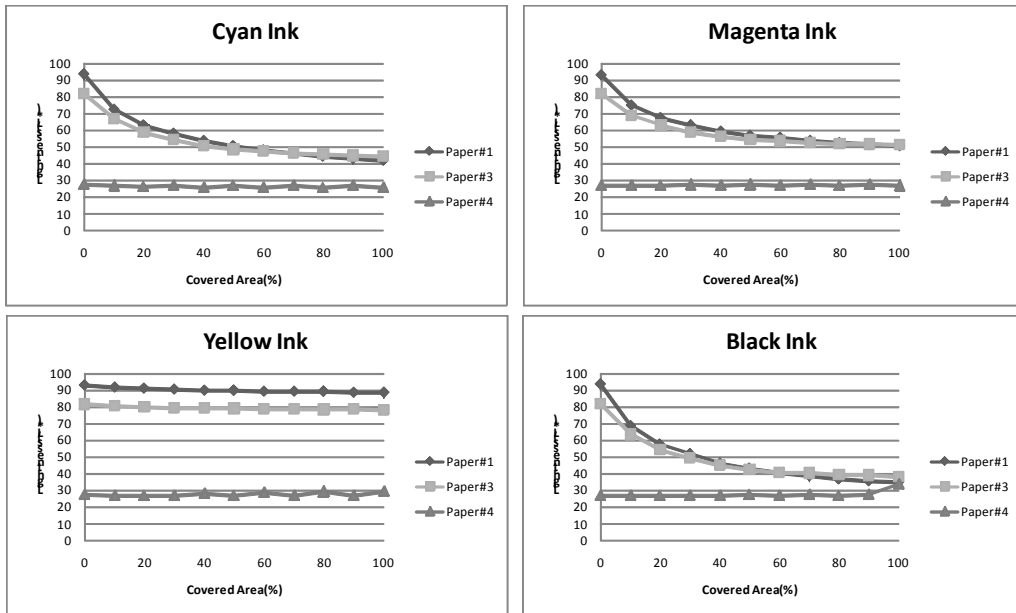


*Figure 8: Lightness of printed samples at diverse covered area for Cyan, Magenta, Yellow and Black*

We expect, that for an opaque material there is a direct relation between L* and total reflectance factor. This relation should be an inverse relation between L* and (K/S), i.e. a decrease in L* or reflectance factor due to increase of colorant concentration, causes an increase in (K/S). Consider Figures 7 and 8, this trend is obvious and can be seen in papers #1 and 3. This phenomenon could be arising from absorption strength of inks that is evident on substrates like papers #1 and 3. Significant change in L* cannot be seen for printed samples on black paper (#4). In this case, light passing through the thin transparent layer of ink is absorbed by the substrate. On the other hand, scattering power of ink is negligible, and even if 100% of substrate is covered by ink, an obvious diffuse reflectance is not expected. Considering this result, i.e. most scattering effect comes from the substrate; we simplified equation 4 and attained equations 5 and 6 respectively. Ink covered area or dot percentage assumed concentration coefficient in the Kubelka-Munk single constant theory. This approach is almost the same as dyed textiles, but in textiles, the weight of applied colorant as a percentage of textile weight is expressed as concentration; in textiles, scattering predominates and dyes have negligible contribution (R. S. Berns, 2007). As mentioned before, decreasing of L* as ink covered area increases on a white (#1) or light gray substrate (#3) shows absorption strength of inks. Due to characteristics of yellow color, the increase in covered area causes a small decrease in L* even on light papers (#1 and 3). In contrast with L*, b* is expected to present a greater change (Figure 9). This figure shows considerable changes in b* for papers #1 and 3 but negligible for #4 i.e. yellowness on black paper cannot be seen.



*Figure 9: b* of printed samples at diverse covered area for Yellow*

*Numerical Results for Spectral Color Matching*

In Table 3, C, M, Y and K digital values of sample target that was printed on the paper #2 are shown.

*Table 3: C M Y K values (%) of sample target patches printed on paper #2, and computed C M Y K values (%) for spectral color matching to create this color on paper #1, before and after correction*

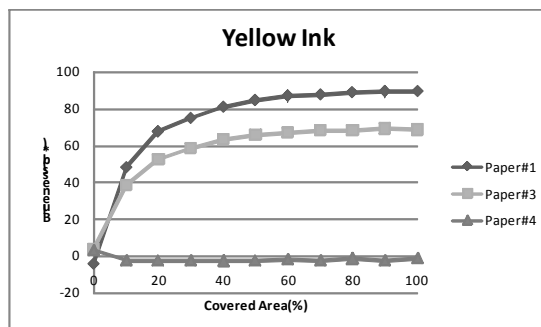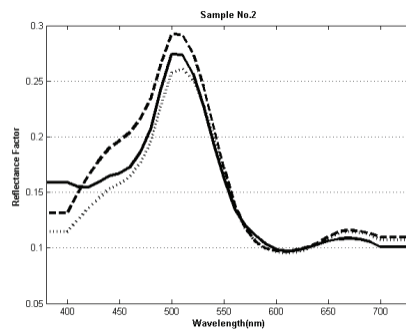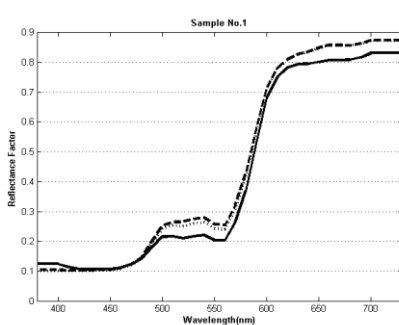| Sample target patch# | Sample target C, M, Y, K values(%) printed on paper #2 | | | | Computed C, M, Y, K values(%) for spectral color matching of sample target on paper #1 (before correction) | | | | Computed C, M, Y, K values(%) for spectral color matching of sample target on paper #1 (after correction) | | | |
|---|---|---|---|---|---|---|---|---|---|---|---|---|
| | C | M | Y | K | C | M | Y | K | C | M | Y | K |
| 1 | 0 | 20 | 35 | 0 | 0 | 14.87 | 26.02 | 0 | 0 | 14.92 | 25.99 | 0 |
| 2 | 45 | 0 | 15 | 10 | 25.47 | 0 | 7.88 | 12.08 | 24.16 | 0 | 10.39 | 14.65 |
| 3 | 10 | 20 | 30 | 15 | 5.87 | 8.56 | 13.47 | 18.69 | 7.11 | 9.51 | 13.34 | 19.54 |
| 4 | 25 | 25 | 25 | 25 | 8.54 | 3.13 | 3.88 | 30.9 | 8.85 | 4.08 | 6.79 | 32.82 |
| 5 | 40 | 40 | 10 | 10 | 17.06 | 10.89 | 0 | 20.18 | 12.09 | 9.32 | 0 | 28.45 |
| 6 | 20 | 20 | 20 | 15 | 9.36 | 4.62 | 5.49 | 25.36 | 9.68 | 5.69 | 8.14 | 27.22 |
| 7 | 10 | 10 | 70 | 10 | 4.53 | 2.47 | 26.31 | 17.04 | 6.22 | 2.95 | 25.86 | 17.66 |
| 8 | 35 | 15 | 50 | 0 | 15.1 | 0 | 14.99 | 18.04 | 14.59 | 0 | 14.62 | 20.61 |
| 9 | 45 | 0 | 15 | 10 | 25.47 | 0 | 7.88 | 12.08 | 24.26 | 0 | 10.47 | 14.49 |
| 10 | 10 | 0 | 45 | 0 | 7.76 | 0 | 32.66 | 1.75 | 12.38 | 0 | 34.19 | 0.41 |

There is a significant difference between the sample target CMYK values printed on paper #2 and the computed/predicted values required to create a match of these colors on paper #1. This illustrate a well-known principle in color management, that is, to achieve the same visual color on different substrates, it is often necessary to use different CMYK inking instructions in each instance. The influence of optical and physical behavior of inks and substrate on total reflectance and color is the main reason for this difference. Inspection of the data in Table 4 shows that some inks are replaced by another or even totally eliminated. For example, four inks are originally used to make patch #5 but one of them i.e. yellow is eliminated when creating the new color match. In another example, black ink in combination with cyan and yellow is replaced for magenta in patch #8. Computed CMYK pixel values were called "before correction" recipes. In Table 5 color differences of sample target patches and matched samples are shown. Color differences (Delta E, 1976) in four patches are less than 1 after correction and this difference is less than 2 for eight patches.

*Table 4: Color differences (DE, 1976) between sample target patches and matched sample before and after correction*

| Sample target patch# | 1 | 2 | 3 | 4 | 5 | 6 | 7 | 8 | 9 | 10 |
|---|---|---|---|---|---|---|---|---|---|---|
| Color difference(DE,1976) before correction | 8.01 | 3.83 | 2.23 | 2.19 | 4.97 | 2.14 | 3.51 | 1.68 | 3.79 | 10.06 |
| Color difference(DE, 1976) after correction | 6.62 | 1.89 | 0.42 | 0.99 | 1.97 | 1.18 | 0.68 | 0.5 | 1.75 | 3.80 |

Some part of these differences comes from unwanted errors such as inherent process errors including printer repeatability errors and instrument repeatability. Also note that "negative" colorants were ignored in the formulation. Color gamut limitations may also contribute to the error, due to spectral reflectance and color differences of the different papers, they may not have the same color gamut (E. Perales, 2009), thus there could be colors that are out of gamut and gamut clipping or compression can contribute to the observed color differences. It could be a reason for bigger color differences for patches #1 and 10 in comparison to the others. The appearance of spectral reflectance curves and color difference values in Table 5 suggests that the method has been able to match spectral reflectances accurately; also that the correction process improves the agreement between the target curves and the matched samples.
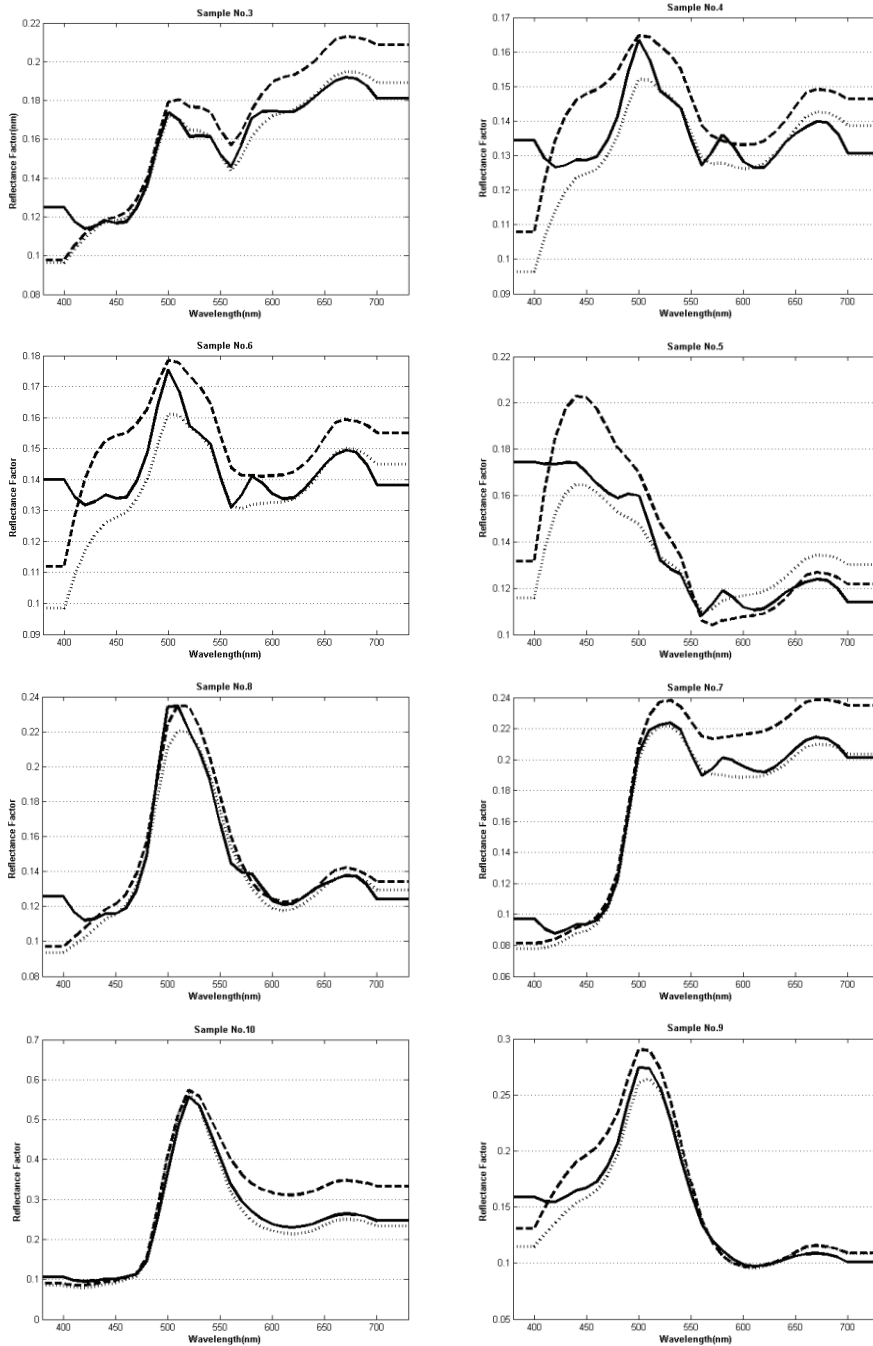
*Figures series 10: Line curves (Spectral Reflectance of sample target patches printed on paper #2), Dashed curves (Spectral Reflectance of samples matched on #1 before correction), and Dotted curves (Spectral Reflectance of matched samples after correction)*

## Conclusion

Spectral color matching based on Kubelka-Munk single constant theory and least square method matrix-algorithm was tested in inkjet printing. Studying the color behavior of Inkjet inks on substrates in different shade directed us to use single constant theory. The relation between color digital pixel values (CMYK) and spectral data of samples on a characterized media was found. We could properly match a sample target containing 10 different CMYK color patches. For some sample target patches we could reach a color difference of 0.5. The creation of spectral match increases the robustness of a color match by decreasing the probability of metamerism.

## References

A. Karbasi, S. Moradian, and S. Asiaban, Improving the performance of computer color matching procedures, *J. Opt. Soc. Am*. **25(9)**, 2251-2262 (2008)

A. Sharma, Methodology for Evaluating the Quality of ICC Profiles-Scanners, Monitor, and Printer, *J. Imaging Sci. Technol.* **50(5)**, 469-480 (2006)

A. Sharma, *ICC Color Management: Architecture and Implementation*, Chapter in R. Lukac, K. N. Plataniotis, *Color Image Processing - Methods and Applications,* CRC Press, Taylor and Francis Group, LLC, 2007

B. Sluban, Comparison of Colorimetric and Spectrophotometric Algorithms for Computer Match Prediction, *Color Res. Appl.* **18(2)**, 74-79 (1993)

E. Allen, *Colorant formulation and shading,* Chapter in F. Grum and C.J. Bartleson, *Optical Radiation Measurements*, Vol.2, Academic Press, NY, 1980

E. Perales and et al., Comparison of Color Gamuts Among Several Types of Paper with the Same Printing Technology, *Color Res. Appl.* **34(6)**, 330-336 (2009)

E. Walowit, C. J. McCarthy, and R. S. Berns, An Algorithm for the optimization of Kubelka-Munk and Scattering Coefficients, *Color Res. Appl.* **12(6)**, 340-343( 1987)

E. Walowit, C. J. McCarthy, and R. S. Berns, Spectrophotometric Color Matching Based on Two-Constant Kubelka-Munk Theory, *Color Res. Appl.* **13(6)**, 358-382 (1988)

G. Sharma, *Digital Color Imaging Handbook*,  CRC Press LLC, 2003

Henry R. Kang, Kubelka-Munk Modelling of Ink Jet Ink Mixing, *J. Imaging Tech.* **17(2)**,76-83 (1991)

International Color Consortium, *Specification ICC.1:2004-10 (Profile version 4.2.0.0) Image technology colour management-Architecture, profile format, and data structure,* 2004

P. Green, *Color Management: Understanding and Using ICC Profiles,* John Wiley & Sons, 2010

R. S. Berns, *BILLMEYER and SALTZMAN'S, Principles of Color Technology*, 3$^{rd}$ Edition, JOHN WILEY and SONS, INC, 2000

R. S. Berns, R. J. Motta, and M. E. Grozynski, CRT colorimetry, PART 1: Theory and Practice, *Color Res. Appl.* **18(5)**, 229-314 (1993c)

R. S. Berns, M. Mohammadi, Single-Constant Simplification of Kubelka-Munk Turbid-Media Theory for Paint Systems-A Review, *Color Res. Appl.* **32(3)**, 201-207 (2007)

# Evaluation of gray balance and G7 in inkjet proofing of GRACoL and SWOP printing

*Martin Habekost and Rebecca Dykopf*

Ryerson University, School of Graphic Communications Management
350 Victoria Street, Toronto, Ontario, M5B 2K3, Canada
E-mail: mhabekos@ryerson.ca, rdykopf@ryerson.ca

**Abstract**

The printing industry uses inkjet proofing systems to match and predict the result of offset printing. Most often when generating proofs these results are represented by GRACoL, SWOP#3 and SWOP#5 reference printing conditions. Traditionally, the measure of how well a system matches an offset reference printing condition is based on a Delta E measure, averaged over measurements of an IT8.7/4 test target (1617 patches). This research seeks to determine if the new IDEAlliance ISO 12647-7 Digital Control Strip 2009, with only 54 patches can provide the same or similar verification, for everyday, practical situations. Another variable in offset printing and inkjet proofing is G7 gray balance. The G7 process is being implemented by many printers in the North American print industry. This research seeks to measure G7 gray balance in inkjet proofs and analyze the relationship between G7 and match to a reference printing condition as calculated by measuring the IT8.7/4 target.

The data for this study was gathered as part of the IPA Technical Conference in 2009, and considers 21 proofs from 8 different suppliers, as well as 32 proofs from the end user community.

**Keywords:** inkjet proofing; gray balance; GRACoL; SWOP; G7; ISO 12647

## 1. Introduction

Inkjet proofing has become the de facto standard in proofing technology in the printing industry. These proofing systems are used to match and predict the result of offset printing. Most often the proofs are generated to match GRACoL, SWOP#3 and SWOP#5 reference printing conditions. The accuracy of how well a proofing system matches one of the reference printing conditions has been measured with an IT8.7/4 test target containing 1617 test colors. Once measured, this data was compared with the reference data. The difference between the measured data and the reference data was expressed in Delta $E_{ab}$ as an average over all test patches. It has been proven at numerous occasions (IPA, 2007 & 2009) that proofing system suppliers have no problems matching the reference printing conditions.

Since the IT8.7/4 target is quite large in size, printers need a more convenient way of assessment to see if their proofing device is still operating within an allowable tolerance to the reference printing condition without printing the entire IT8/7.4 target. This assessment, or "control strip" should be able to fit onto the same page as any proof, so it is possible to conduct a daily test of proofing accuracy. This lead to the development of the IDEAlliance proofing control strip, which contains a subset of color patches found in the IT8.7/4 target. This control strip was introduced in 2007 and an updated version was made available in 2009 (IDEAlliance, 2010). The difference between both iterations of the control strip is the size and the colors that are used to separate the test patches from each other, so that either a handheld or an automated device can distinguish between the test patches.

The P2P target has been developed for the G7 gray balance control process. This test target contains screen tints of the four process colors plus tints of three-color grey and grey made from black only. The P2P target can be measured with the DTP70 or iSis measuring device and the gathered data is analyzed with the IDEAlink Curves software to check if the proof matches the criteria of the being in control in relation to the G7 process. A proof should be meeting the G7 gray balance criteria if it matches the Neutral Print Density Curve. P2P targets were also measured from all the supplied proofs.

The above mentioned test targets were all on one test sheet together with some other test elements in order to see if the overall umbrella of meeting a reference printing condition ensures that all the other test targets meet also their criteria. An image of the test sheet can be seen below.
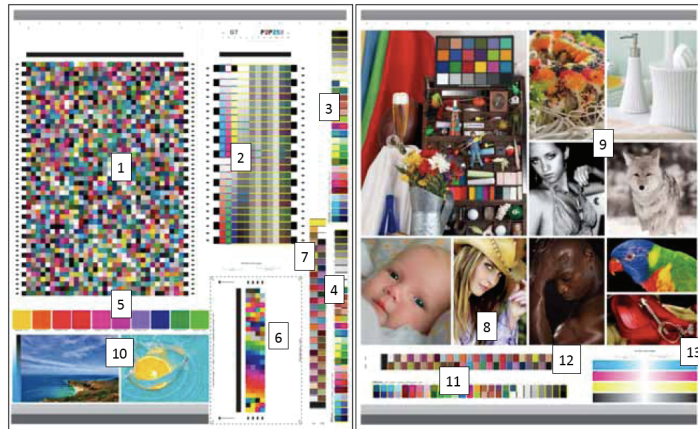
*Figure 1: Test sheet used for the evaluation of the various test targets*

There were 13 main elements in the test form. They are numbered in the example above:

1. The IT8.7/4 target with DTP70 and iSis tracks
2. This target contains 1617 patches was used to check compliance to characterization data sets
3. The Hutchcolor G7 P2P 25x target
4. This target is used to evaluate G7 compliance
5. 2007 IDEAlliance Control Strip
6. 2009 IDEAlliance Control Strip
7. PANTONE chips in visual form
8. 104 PANTONE and PANTONE Goe patches in machine readable format
9. Dynamic wedge
10. A target containing 53 patches, created from colors that were selected from the photographs on the test form
11. Images with skin tones
12. High key images
13. Images with cyan content
14. Repeat of 4 from page 1
15. Repeat of 7 from page 1
16. Scale markings

The results gathered from the test sheet will be grouped by the reference printing conditions the proofs were generated under. The data for this study was gathered as part of the IPA Technical Conference in 2009, and considers 21 proofs from 8 different suppliers, as well as 32 proofs from the end user marketplace community.

## 2. IPA Proofing RoundUP

The IPA proofing RoundUP took place in May and June 2009 as part of the IPA Annual Technical conference. Vendors and users were asked to supply proofs of the above shown test form for one or more of the three reference printing conditions. The reference data for the test targets and ICC profiles for the three reference printing conditions were made available to prospective participants on the website that accompanied the technical conference. The reference data and the ICC profiles were also available through the IDEAlliance website.

## 3. Results

The measurements were conducted at Ryerson University using the following X-Rite instruments: iSis, i1iO, and 939. Measuretool from ProfileMaker 5.0.9 and Toolcrib were used to record the data. The tolerances used for the evaluation of the IT8.7/4 target were taken from ISO 12647-7 and IDEAlliance and the color differences are reported in $DE_{ab}$. Many researchers use now newer Delta E equations, but the $DE_{ab}$ is the metric currently used in specifications and standards. Newer metrics have been calculated for all the data presented here.

For the IT8.7/4 target the tolerances listed in table 1 below were used.

*Table 1: Proofing RoundUP Certificate criteria*
*\*Note: the tolerance for all patches of the IT8/7.4 target according to the IDEAlliance Proofing Certificate Program is 1.5ΔE. Throughout this report when the IDEAlliance Proofing Program is referenced it will refer to the tolerance of 1.5ΔE*

| Row | IDEAlliance Proofing Certificate Program (2008) | | | Tolerances |
|---|---|---|---|---|
| 1 | IT8/7.4 - Average All Patches | | Pass/Fail | $\Delta E_{ab}$ 1.5* |
| 2 | IT8/7.4 - 95th Percentile | | Pass/Fail | $\Delta E_{ab} \leq 6$ |
| 3 | Solid | Cyan | Pass/Fail | $\Delta E_{ab} \leq 5$ |
| 4 | | Magenta | Pass/Fail | |
| 5 | | Yellow | Pass/Fail | |
| 6 | | Black | Pass/Fail | |
| 7 | Overprints | Red | Pass/Fail | |
| 8 | | Green | Pass/Fail | |
| 9 | | Blue | Pass/Fail | |
| 10 | 50/40/40 Neutral Gray | | Pass/Fail | $\Delta E_{ab} \leq 1.5$ |
| 11 | Paper White | L* | Pass/Fail | $\Delta L^* \leq 2$ |
| 12 | | a* | Pass/Fail | $\Delta a^* \leq 1$ |
| 13 | | b* | Pass/Fail | $\Delta b^* \leq 2$ |
| 14 | Sheet-to-Sheet Variation | Control Strip | Pass/Fail | $\Delta E_{ab}$ difference $\leq 1.5$ |
| 15 | | Dynamic Wedge | Pass/Fail | |
| | ISO 12647-7 | | | |
| 16 | IT8/7.4 - Average All patches | | Pass/Fail | $\Delta E_{ab} \leq 4$ |
| 17 | IT8/7.4 - 95th Percentile | | Pass/Fail | $\Delta E_{ab} \leq 6$ |
| 18 | Outer Gamut | | Pass/Fail | Average $\Delta E_{ab} \leq 4$ |
| 19 | 50/40/40 Neutral Gray | | Pass/Fail | $\Delta H_{ab} \leq 1.5$ |
| 20 | Paper White | | Pass/Fail | $\Delta E_{ab} \leq 3$ |
| | IDEAlliance Control Strip | | | |
| 21 | All patches | | Pass/Fail | Average $\Delta E_{ab} \leq 3$ |
| 22 | | | Pass/Fail | Maximum $\Delta E_{ab} \leq 6$ |
| 23 | 50/40/40 Neutral Gray | | Pass/Fail | $\Delta H_{ab} \leq 1.5$ |
| 24 | Paper White | | Pass/Fail | $\Delta E_{ab} \leq 3$ |

The results are grouped per reference printing condition.

## 3.1. Matching GRACoL

### 3.1.1. IT8.7/4 target

The results for the results from the IT8.7/4 target can be seen in figure 2 below.
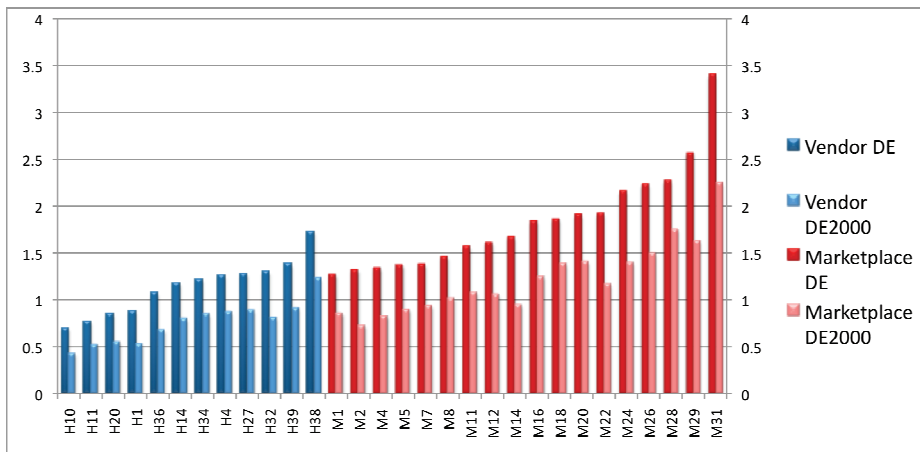


*Figure 2: Average DE of the IT8.7/4 target for GRACoL printing conditions. M denotes submissions from users and H denotes submissions from hardware suppliers*

The average DE for vendors was 1.14 and 1.83 for the user submissions. Note: All systems are under the ISO tolerance of 4 DE, but one vendor and most user submissions did not fall under the IDEAlliance certification tolerance of 1.5 DE.

### 3.2 Matching SWOP #3

For the SWOP#3 reference printing conditions the same stringent set of rules as listed in table 1 were applied. The results for the SWOP #3 submissions can be seen in figure 3.
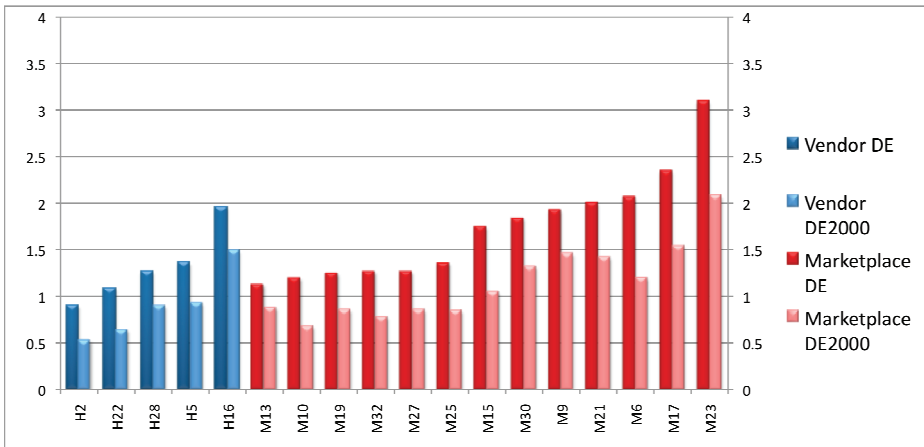


*Figure 3: Average DE of the IT8.7/4 target for SWOP #3 printing conditions. M denotes submissions from users and H denotes submissions from hardware suppliers*

The average DE for vendors was 1.32 and 1.73 for the user submissions. Note: All systems are under the ISO tolerance of 4 DE, but a few marketplace submissions and one vendor submission did not fall under the IDEAlliance certification tolerance of 1.5 DE.

### 3.3 Matching SWOP #5

For the SWOP#5 reference printing conditions the same set of rules as listed in table 1 were applied. The results for the SWOP #5 submissions can be seen in figure 4.
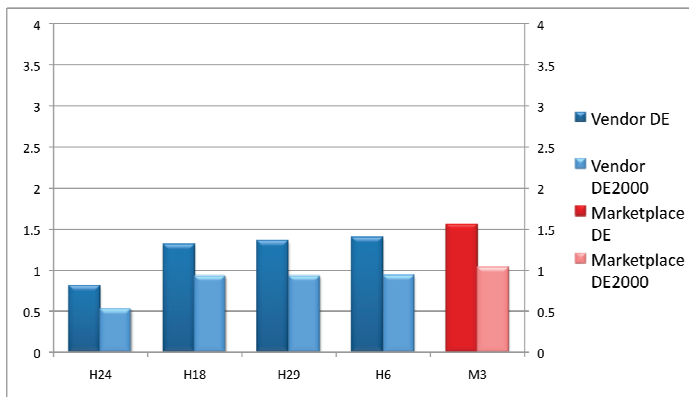


*Figure 4: Average DE of the IT8.7/4 target for SWOP #5 printing conditions. M denotes submissions from users and H denotes submissions from hardware suppliers*

The average DE for the vendors was 1.22 DE. The user submission is just a bit over the IDEAlliance certification tolerance of 1.5 DE, while all of the vendor submissions are bellow.

### 3.4 Results from the IDEAlliance control strip

The IDEAlliance control strip, was created as a quick-check measure, to ensure that the proof meets the reference printing conditions. It is much smaller than the IT8.7/4 test target and can usually be placed outside of the actual job on the proof sheet. The IDEAlliance control strip contains a subset of the color patches from the IT8.7/4 target.

The IDEAlliance control strip was measured only on the vendor-submitted proofs due to time constrains. The GRACoL proof control strips had an average DE of 1.26. SWOP #3 and SWOP #5 had averages of 1.62 DE and 1.57 DE respectively. All proofs measured fell within the ISO tolerance of 3 DE.

The 2009 strip from the first page of the test forms was compared to the IT8/7.4 target of the same page. The differences between the IT8/7.4 and control strip averages were computed for each proof. The GRACoL proofs had an average difference of 0.26 DE, SWOP #3 had an average difference of 0.31DE, and SWOP #5 had an average difference of 0.4 DE. Most proofs had a higher average DE from the control strip rather than the IT8/.4. When compared to the IT8/7.4, the values between the two targets were very similar in most cases, with only one supplier having a difference of more than 0.75 DE. Figure 5 shows a comparison of the IT8/7.4 and IDEAlliance Control Strip results for each proof. The systems which fall between the two black lines have a difference between the IT8/7.4 and control strip averages of less than 0.5 DE. These results show that most systems print the IDEAlliance control strip very close to or give the same DE average as the IT8/7.4 target.
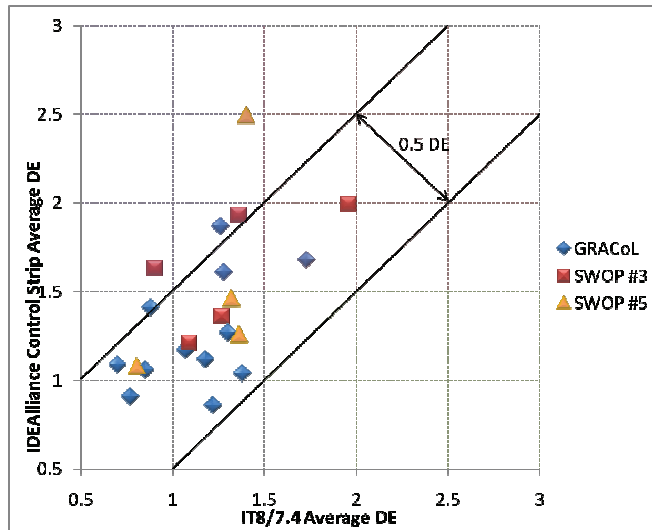


*Figure 5: A comparison of the control strip and IT8/7.4 results for each proof. The proofs which fall between the two black lines had a difference of less than 0.5 DE between the two targets. The proofs in the red area were above a DE of 1.5 for both the IT8/7.4 and the control strip. Those in the purple area were above 1.5 DE for the control strip but below 1.5 DE on the IT8/7.4*

There are no systems that fell into the green area of Figure 5. If a system were in the green area then it would be above 1.5 DE on the IT8/7.4 but below 1.5 DE on the IDEAlliance Control Strip. There are two systems which fell into the red area which means that they were above 1.5 DE on the IT8.7/4 and the control strip. The systems which fell within the purple area have DE values above 1.5 on the control strip but below 1.5 on the IT8/7.4. This would mean that, using 1.5 DE as an example tolerance, five systems would "fail" the IDEAlliance Control Strip while "passing" the IT8/7.4. This type of analysis is important because these results lead to the suggestion that the IDEAlliance Control Strip is a suitable "quick check" to ensure a system is within tolerance when the entire IT8.7/4 cannot be printed on the sheet. Since most systems are producing higher DE readings in the control strip a looser tolerance may be needed for the control strip if its purpose it to represent the status of an IT8/7.4 target.

## 3.5 Results from the G7-P2P test target

The IDEAlink Curve software was set-up to give suggested dot size changes for each system at 10% intervals. According to the software these changes, if implemented, will result in gray balance. The suggested changes for the 10% to 90% dot area for each color were averaged and are shown in the figure below. This test was performed on both the supplier and the marketplace proofs. The average suggested change for vendors were absolute 1% for GRACoL, 1.26% for SWOP#3 and 1.25% for SWOP #5. For the user/marketplace submissions the averages were absolute 1.21% for GRACoL and 1.25% for SWOP#3. When looking at the figure below one should keep in mind that these are the average changes suggested for each color which means, that some dot sizes within each color needed more changes and some less.

This relationship between the IT8/7.4 and P2P targets is explored further in Figure 6. Figure 6 shows a more clear measure of whether or not there is a direct link between the DE-value and the suggested dot size change. The questions these graphs are attempting to answer is whether or not a system which can produce a proof with accurate color according to the IT8/7.4 target will also automatically produce gray balanced color according to G7.
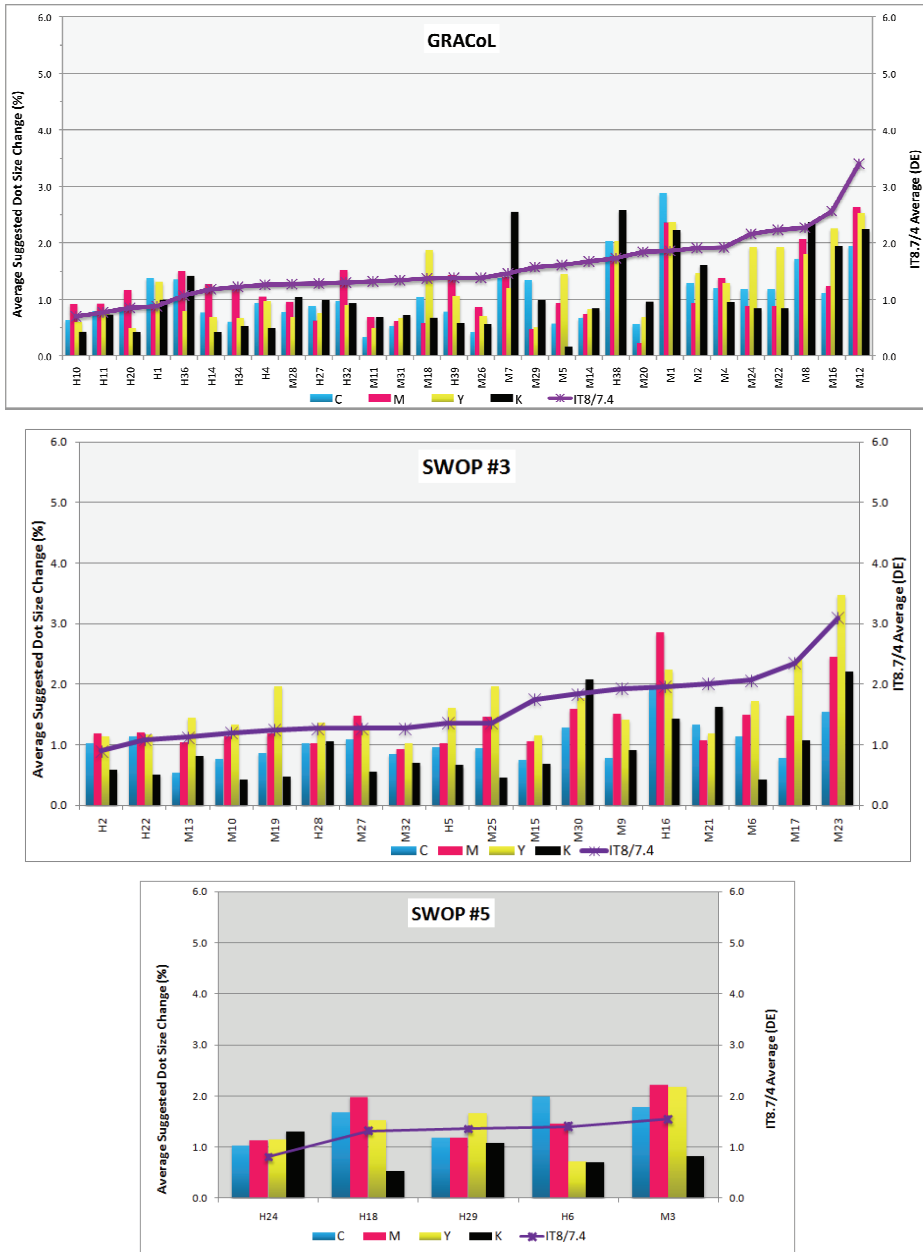
*Figure 6: The average dot size changes from the IDEALink Curve software for each system. The suggested change for 10 - 90% dots have been averaged for each color. Systems starting with an H denote a vendor submission. The grey shaded areas denote changes of less than 1%*

While analyzing the results presented in figure 6 it can be seen that many submissions had averages below or around 1%. These are probably not changes which would be made since a change of 1% or less could be attributed to normal fluctuations, and a change of 1% does not significantly affect colour. Figure 6 also shows a comparison of results from the IT8/7.4 target alongside the average suggested dot size change from the P2P target. From figure 6 a pattern, in some cases, can be distinguished. There is a trend with some of the systems where a lower DE average from the IT8/7.4 is paired with a low average from the P2P target. However there are a few user submissions that give quite a low average suggested dot size change, but had an relatively higher readings from the IT8/7.4 target, such as M11 and M20.

In the following graphs the average DE-values of the IT8.7/4 target for the three reference printing conditions has been compared with the 95th percentile of the suggested dot size changes shown in figure 6. The 95th percentile was chosen, since it is closer representation of the largest percent screen changes that were suggested by the IDEALink Curve software and it was seen as a more accurate capture of the overall suggestions of the software.
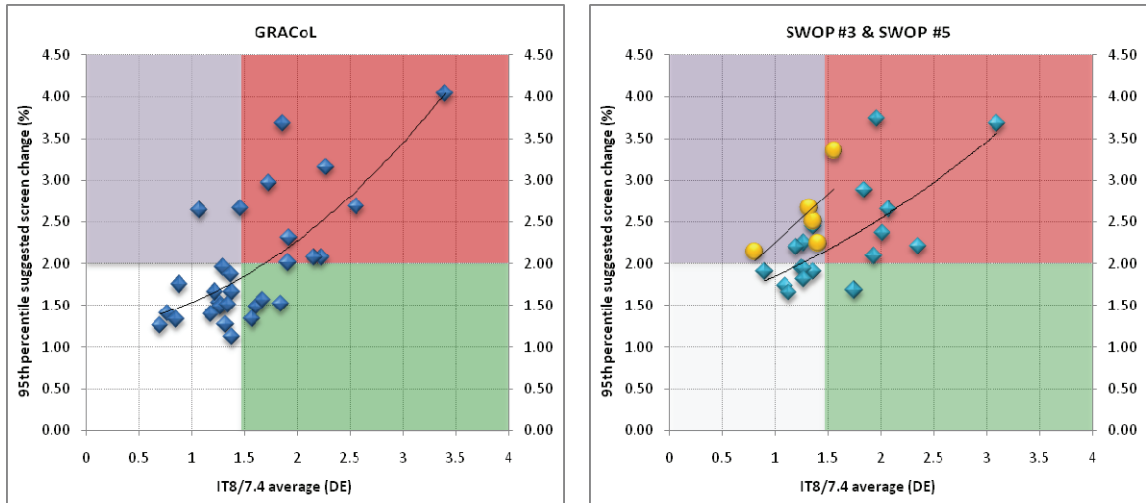
*Figure 7: Average DE-values from IT8.7/4 versus the 95th percentile of the suggested screen size changes for all three reference printing conditions. The yellow dots in the lower graph represent values for SWOP #5*

From Figure 7 it can be seen that there is not really a clear correlation between the average DE value from the IT8.7/4 target and the 95th percentile of the suggested screen change from the analysis of the P2P target. For all three proofing conditions the white square represent an average DE-value of under 1.5 and suggest screen value change of under 2 %. Quite a few of the measured proofs fall into this quadrant. This means that a low DE-value from the IT8.7/4 target results also in a grey-balanced proof that will meet the G7 requirements. Those proofs which fall in the red quadrant of the graph have both high DE values and high suggested changes from the P2P target. There are a number of systems which fall into the purple area of the graphs. These systems have a accurate colour according to the IT8/7.4 target, but had higher suggested dot size changes from the P2P target. Overall, the $r^2$-values for the trendline produced when comparing the 2 measurements is approximately 0.51, which means that there is a 50% correlation between the IT8.7/4 average DE-value and the suggested screen change values from the measurements of the P2P-target. Similar to what can seen in Figure 6, Figure 7 shows that there is 50% likelihood that a system will have accurate colour according to G7 if it has accurate colour according to the IT8/7.4, and vice versa.

## 4. Conclusions

The results from the Proofing RoundUP showed that not only proofing equipment vendors can generate proofs that match the reference printing conditions very well, but also that users are very well capable of producing proofs that deviate only a little from the reference printing conditions. This was established by measuring the IT8.7/4 test target. Since this test target is quite large it is not practical to print this target on every proof and measure it to see if the reference printing conditions is being met. For this purpose IDEAlliance came up with the proofing control strip that contains around 50 test colors that are a subset of the test colors of the IT8.7/4 target. The average DE-values for the IDEAlliance proofing control strip were found to be usually no more than 0.5 DE higher or lower than the average DE-values of an IT8.7/4 target form the same proof. This shows that the IDEAlliance Control Strip is a suitable "quick check" which will be able to closely represent the results of the more elaborate IT8/7.4 target, without taking as much space on paper or time to measure.

Another question that was answered was, if a proof matches the reference printing conditions will it also meets the G7 requirements as it was determined by measuring the P2P target, which was printed on the same sheet as the IT8.7/4 target. This was measured by analyzing how the IT8.7/4 average DE-values correspond with the suggested screen size changes from the IDEALink Curve software. It was found that the averages of the 95th percentile of the absolute values of the suggested screen value changes for all process colors did not have a clear relationship with the DE-value from the IT8.7/4 target. This shows that a system will not automatically have proper G7 gray balance if it has accurate color according the IT8/7.4 target or vice versa.

After all this it can only be repeated again that it is absolutely essential to keep a well maintained proofing system that deviates as little as possible from the reference printing conditions. The necessary measurements should be taken on a regular basis, and adjustments made as necessary.

## Acknowledgements

## References

IDEAlliance, http://www.idealliance.org, 2010

IPA 2007, Proofing RoundUP, An independent study of proofing technologies

IPA 2009, Proofing RoundUP, An independent study of proofing technologies

ISO, 2008, ISO/CD 12647-7.2 Graphic technology - Process control for the production of half-tone color separations, proof and production prints - Part 7: Off-press proofing processes working directly from digital data, Date of document 2008-05-23

# Overprinting of spot colors for flexo packaging

*Alexandra Pekarovicova*[1], *Veronika Lovell*[2], *Sangmeshwar L. Sangmule*[1],
*Paul D. Fleming III*[1] *and Timothy Pietrack*[1]

[1] Center for Ink and Printability, Western Michigan University
  A-231 Parkview, Kalamazoo, MI 49008, United States
  E-mail:a.pekarovicova@wmich.edu

[2] SUN Chemical Corporation
  30110 S Wixom Rd.
  Wixom, MI 48393, United States
  E-mail: veronika.lovell@sunchemical.com

**Abstract**

The correctness of the overprint models included in several different pre-press proofing applications based on the digitally generated color design was evaluated. Color proofs were compared to the real ink on paper reproduction from a flexo printing press. The substrate used in the press run was SBS board. The CIE L*a*b* values of printed test charts were measured using MeasureTool software with an X-Rite i1-iO scanning spectrophotometer. The spot colors were proofed on a semi-matte substrate printed from two different Epson Stylus Pro printers, using different prepress and color management software: SmartColour[TM] iVue plugin, Adobe Photoshop, and two different technology based RIP solutions. CIE L*a*b* values for the press and digital printed test chart were compared and ΔE values were calculated, which showed that the proofing of the spot colors and its reproduction through SmartColour[TM] iVue and one of the RIP software produced better results than the other technology based RIP and Adobe Photoshop. The 3-color overprints yield the worst color agreement between the real press proof and the predicted overprint on the digital proof. UV curable spot color inks were found to have better color stability than solvent based ones, and were found easier to work with. Digital proofing of both ink chemistries resulted in similar results in terms of ΔE values.

**Keywords:** spot colors; flexography; solvent based; UV curable ink; digital proofing

## 1. Introduction

Key reasons for the success of flexography lies in its ability to print on virtually any substrate, such as corrugated, flexible packaging, shrink sleeve films, labels, folding cartons, or cans. Large scales of materials, ranging from thin extensible and flexible materials, through rough and tough corrugated boards, can be flexo printed. Inline finishing makes the turnaround and set-up time of print orders less costly than other processes. The possibility of using digital plates improves the sharpness and quality of the printed image. Flexo ink quality has improved dramatically over the past decade, and it can use variable chemistries, such as water, solvent, or UV and EB curable ink systems [Hayes, 2009]. Especially UV flexo inks are gaining popularity because of much sharper graphics, vibrant colors, higher opacity and very high gloss [Kerchiss, 2009; Savastano, 2008]. UV curable inks are mainly used for printing labels, shrink sleeves, and light weight cartons [Atkinson, 2010; Hammer, 2008], and their huge advantage is that they do not produce any volatile organic compounds. A large share of flexo printing is in packaging, compared to other markets, where the spot colors have wide application, in order to assure colorful design and extended color gamut, helping to more efficiently stimulate brand name recognition [Tolliver-Nigro, 2007].

Package printing will have steady growth. About 40% of packaging jobs are printed by flexo, 30% by offset lithography, 22% by rotogravure and 8% by digital and other printing processes [Pekarovicova, 2007]. Printing processes with master image carriers will dominate, and flexography will be a leading process in the next 10 years, followed by rotogravure and lithography. Future growth of flexo markets is forecast in film, film labels and flexible packaging. There will be labels for highly shaped containers and opportunities for flexible labels, wraparound labels, pressure-sensitive shrink labels, wet-glue labels, die-cut labels, stretch labels and in mold labels [Duncan, 2008]. Growth in container printing and packaging will mirror population growth [Pekarovicova, 2008]. The flexo advantage definitely is, and will be, that it can print on all of these substrates. To keep the packaging segment attractive, the colorfulness of print job is a must, and it can definitely be improved with spot color usage, new technologies, blending of digital and flexo presses [Hole, 2009].

Spot colors can be printed by using specially formulated spot color inks, containing single or multiple colorants, such as Coca-Cola red and many other inks mixed e.g. according to Pantone Formula Guides. Many other spot color libraries, with a multitude of custom colors, are available for the spot color printing industry. It is desirable that spot color inks are as close as possible to being opaque. Another possibility is to arrive at a particular color by blending transparent process color inks, because the light needs to pass through all overprinted ink films and then light, reflected from it forms final the color sensation. Transparency or opacity as a function of the ink strength is given by particle size of pigment particles in the ink formulation [Thompson, 1998]. Due to advancements in pre-media software, instead of using a single opaque spot color, the trend of overprinting of spot color is increasing [Pekarovicova, 2009; Chung, 2009; Suchy, 2005; Wu, 2007; Sangmule, 2010]. The void in knowledge concerning overprint of spot colors was previously recognized by Chung, and therefore work on two custom ink overprints at 100 and 50% tone was done, which confirmed importance and lack of knowledge in this area [Chung, 2009].

The goal of our work was to evaluate the correctness of the overprint models included in several different pre-press proofing applications, based on the color design produced before the press run. The obtained color proofs were compared to the real ink on paper reproduction from a flexo printing press. The substrate used in the press run was deliberately chosen to be SBS board, often used in flexible packaging. A further goal was to observe and evaluate the color differences when using different ink chemistry, such as solvent-based, or UV-curable on the flexo press.

## 2. Methods

### 2.1 Solvent based trial setup

Four different spot colors were chosen in Adobe Photoshop at the designer phase. These four colors, Pink, Blue, Green, and Orange, represent a different color space and could be found in the product packaging on the store shelves. The CIELAB values were defined for all colors for D50/2° illuminant/observer combination. Figure 1 shows four chosen spot color and their corresponding CIELAB values.
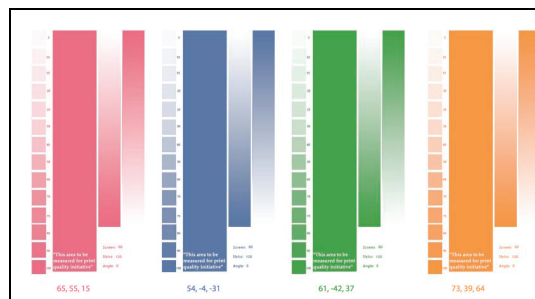


*Figure 1: Four spot color standards for the overprint test*

The spot color specifications, such as base line, viscosity, color coordinates together with the press and substrate information provided by WMU pilot plant, where the press run took place were forwarded to an ink manufacturer. Inks were delivered for the test run and adjusted accordingly for the proper color based on the press conditions.

### 2.2 Spot color overprint chart design

A test chart containing 264 patches was created. The test chart was designed for three ink colors and has patches of the solid and its tone scale in a 10% increment for each color. It also contains different overprints of different intensity from highlights to shadows of chosen three spot inks. Out of the four inks chosen for this test, four different combinations of three inks were used to create four overprint test charts as shown in Figure 2. These charts were named based on the print order of the inks on the press as follows: GOP, BOP, BOG, and GBP. Each test chart contained 76 of 1-color patches, 65 of 2-color overprint patches and 123 of 3-color overprint patches.

For proofing purposes, the Epson Semi Matte substrate was used for both the printers, i.e. Epson Pro Stylus 9800 and the Epson Pro Stylus 7900. The printers differ in number of colors employed, Epson Pro Stylus 9800 uses C,c,M,m,Y,K,LK, and Llk (Cyan, light Cyan, Magenta, light Magenta, Yellow, Black, light Black, and Light light black) inks, the Epson Pro Stylus 7900 uses the same set plus G and O (Green and Orange).
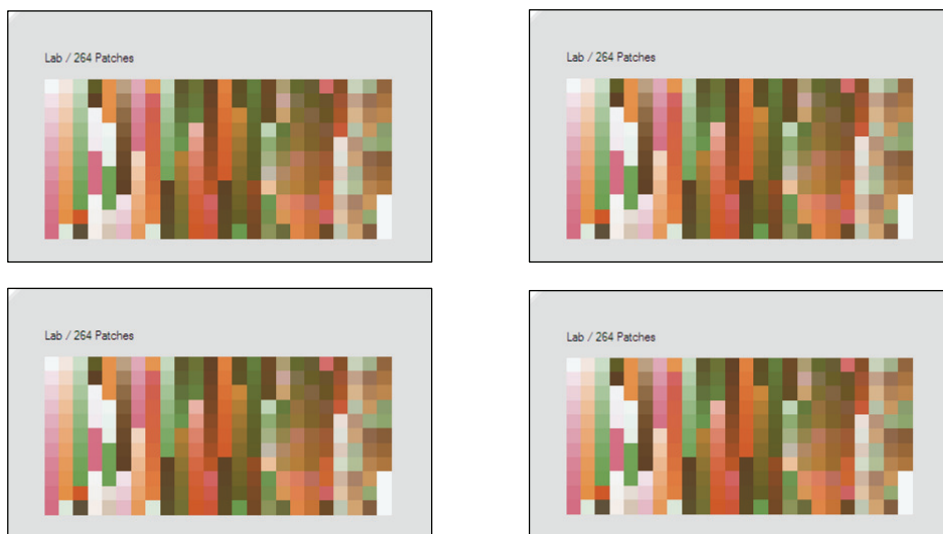
*Figure 2: Overprint test charts - Four combinations of three spot colors; GOP, BOP, BOG, and GBP*

The overprint testcharts were sent to the digital printers through different proofing workflows; color managed Adobe Photoshop, Adobe Photoshop with SmartColour iVue Plugin, RIP #1, and RIP #2. Adobe Creative Suite serves as a great designer tool with its solution of InDesign, Illustrator and Photoshop. It is well established software used in almost all prepress and designer houses around the world. Sun Chemical's SmartColour iVue plug-in can be installed as an option in Adobe Photoshop and Illustrator and provide an access to the Sun Chemical's Global Shade Library, which has various color shades and were developed by previously proofed, printed, and measured inks for particular substrates and printing processes. The software serves as the plugin that allows previewing and proofing from the regular Adobe application and addresses the printer through the color managed workflow. The main advantage of the iVue software is to enable one to predict how the job will look like on the press with a specific substrate and with a specific printing process. The Raster Imaging Processor (RIP) based workflows are used in two other proofing solutions tested in this paper. The RIP workflows are usually CMYK or CMYK+spot color workflows. In order to have predictable and repeatable results through the printer, most of the RIPs also have functions of device calibration and linearization processes. The use of built-in color management functions helps in defining the color space in software at pre-press and RIPing stage, which contributes to attaining the optimal end result. Some RIP workflows use color matching features that are based on integrating third-party ICC profiling techniques while other RIP workflows totally ignore the ICC workflow and work on their well established approaches. Both types of the RIP workflow systems are tested here.

The tone value increase (dot gain values) measured from the Comco Commander flexo press run were applied in all the tested workflows. All of the proofing solutions have an option to input the tone value increase data. In most cases, the overall number is applied to all present channels. In SmartColour iVue plugin, it is possible to set the dot gain values per channel to achieve more accurate and consistent color reproduction. The opacities of each ink were calculated from the X, Y, Z values measured from the proof, which were made by printing the colors over the BYKO charts on a K-proofer, with a spectrophotometer with $45^o/0^o$ geometry and with no filter applied These calculated opacities of inks were entered into Photoshop and in the RIP software. SmartColour iVue applies opacity based on the information plugged in when a certain ink system is chosen. In the case of the RIP software, the printers were linearized and calibrated with the built-in tool provided by the software. RIP#1 is based on non-ICC technology while RIP#2 supports the ICC workflow. ICC profiles, both for RGB and CMYK workflow, were created for the printers.

## 2.3 Flexo press run

Flexographic photopolymer plates with the 150 lpi resolution were designed to include the registration marks, vignettes and other print components to better assess the printability during the press run. Anilox screen rulings of 800 lpi were used to print the test charts, with the solvent based and UV curable inks, on the Comco Commander narrow web flexo press in the WMU Printing Pilot Plant. The substrate used was SBS board. The viscosity of the inks was kept constant at 22 seconds on a #2 Zahn cup over the period of the press run. The speed of the press was set to 50 feet/min.

## 3. Results and discussion

### 3.1 Proofing results for solid spot colors

All solutions were used to proof the solid spot colors in order to asses the ability to provide accurate solid spot color representation. The CIELAB values were measured using MeasureTool software and an X-Rite scanning spectrophotometer with $45^o/0^o$ geometry and with no UV filter applied. The level of accuracy for solid spot color matching was computed in terms of color differences $\Delta E$, between the originally assigned CIELAB values and the flexo press proof (see Figure 1). $\Delta E_{cmc\,(2:1)}$ resulting values are displayed in Figure 3. The reproduction of the spot colors by the Epson Stylus Pro 7900 printer was slightly better compared to that by the Epson Stylus Pro 9800. The better color reproduction capability of the Epson 7900 is very likely due to the HDR ink technology, with the two additional colors - Orange and Green. This is the main reason the $\Delta E$ values were lower in both cases, irrespective of the software used for proofing purpose.
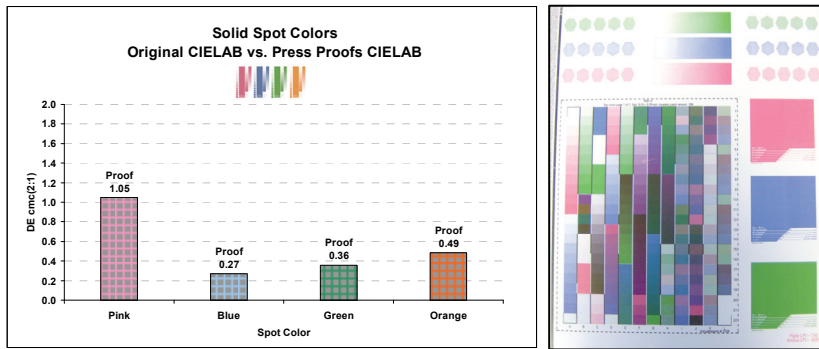


*Figure 3: Graphic representation of $\Delta E_{cmc(2:1)}$ color differences for solid spot colors between the original CIELAB values and the flexo press sheet (right)*

Figure 4 shows the graphical results of the average $\Delta E_{cmc\,(2:1)}$ values that were obtained between the flexo press proof CIELAB values and the digital proofs that were produced through the tested proofing solutions on the Epson 7900.
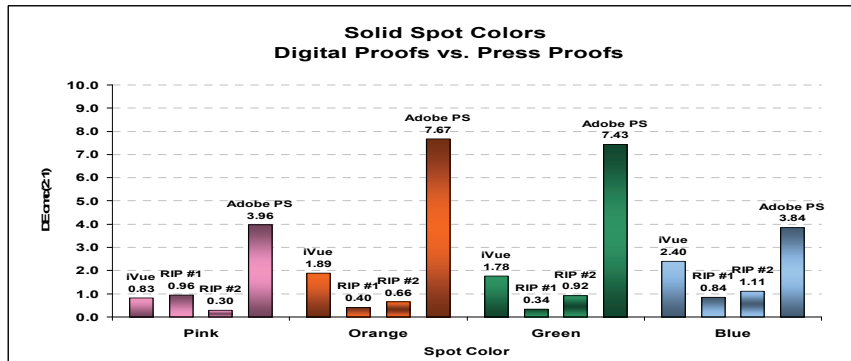


*Figure 4: Graphic representation of $\Delta E_{cmc(2:1)}$ color differences for solid spot colors between the flexo press sheet CIELAB values and proofing CIELAB values*

The spot colors produced on the flexo press proof are in very good agreement to the requested CIELAB data. It is evident from the graphical illustration that both RIP solutions provided excellent results in terms of matching the solid spot colors. These solutions usually provide some kind of tool where iteration is used in order to achieve better color match to assigned CIELAB values. The SmartColour iVue plugin provides worse results than these, due to the fact that the color tweaking is not allowed. The SmartColour plugin is able to access the well established library, where data are set to a specific CIELAB value based on the real press proofed ink on paper.

### 3.2 Proofing results for overprints of spot colors

The overprint testcharts were produced with all four proofing solutions with two different printers and the CIELAB values from the proof results were compared to the values gathered from the press sheets. In this case, the reference CIELAB values were set to be those from the press sheet.

Again, the final ΔE values show better color agreement when digital proofing is carried on the Epson 7900 printer. The level of accuracy for overprints of spot colors was computed in terms of color differences ΔE calculations, using formulae $\Delta E_{ab}$ and $\Delta E_{cmc\,(2:1)}$. The results were split into three categories: 1-color patches, which include solid colors and the tones steps, 2-color overprints of different levels of tones steps, and 3-color overprints of different levels of tone steps. The graphs below show the resulting ΔE values for 1-color, 2-color and 3-color patches as well as the overall average of all 264 patches included on the test chart.
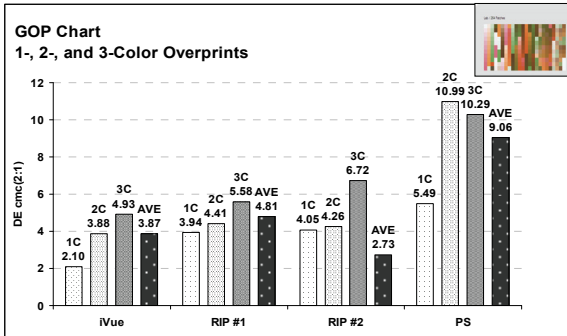


Figure 5a: $\Delta E_{cmc(2:1)}$ values for 1-color, 2-color and 3-color overprint patches and the overall average of all 264 patches on the GOP test chart comparing the press sheet to the digital proof
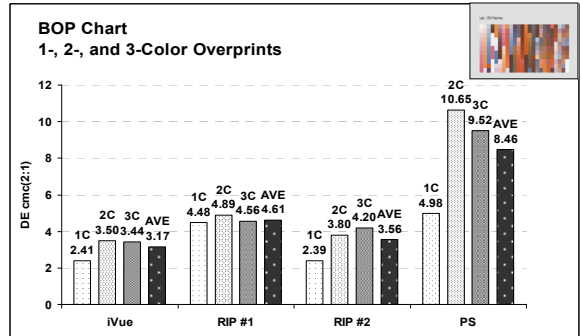


Figure 5b: $\Delta E_{cmc(2:1)}$ values for 1-color, 2-color and 3-color patches and the overall average of all 264 patches on the BOP test chart comparing the press sheet to the digital proofs
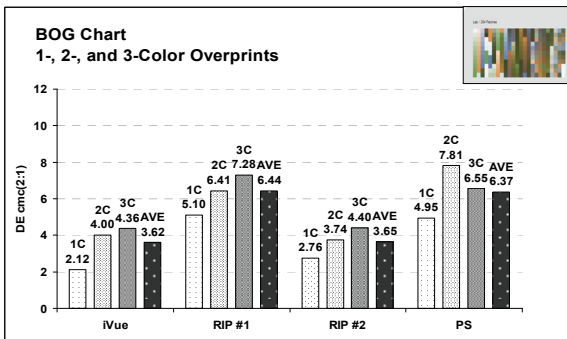


Figure 5c: $\Delta E_{cmc(2:1)}$ values for 1-color, 2-color and 3-color patches and the overall average of all 264 patches on the BOG test chart comparing the press sheet to the digital proofs
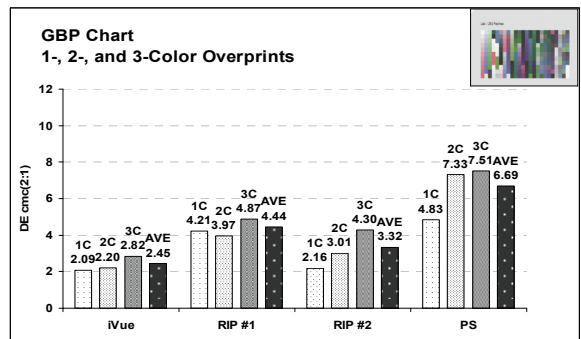


Figure 5d: $\Delta E_{cmc(2:1)}$ values for 1-color, 2-color and 3-color patches and the overall average of all 264 patches on the GBP test chart comparing the press sheet to the digital proofs

Table 1 shows consolidated results for all tested patches (264), of 1-, 2-, and 3-color overprints in terms of $\Delta E_{ab}$ and $\Delta E_{cmc\,(2:1)}$ for each proofing solution for four charts. The overall average values are also reported.

Table 1: Overall color difference results for four different test chart based on different proofing software and average color difference per proofing solution that covers all tested charts

| | iVue | | RIP #1 | | RIP #2 | | Adobe PS | |
|---|---|---|---|---|---|---|---|---|
| **Chart** | $\Delta E_{ab}$ | $\Delta E_{cmc(2:1)}$ | $\Delta E_{ab}$ | $\Delta E_{cmc(2:1)}$ | $\Delta E_{ab}$ | $\Delta E_{cmc(2:1)}$ | $\Delta E_{ab}$ | $\Delta E_{cmc(2:1)}$ |
| **GOP** | 6.97 | 3.87 | 8.50 | 4.81 | 4.73 | 2.73 | 15.09 | 9.06 |
| **BOP** | 5.48 | 3.17 | 9.89 | 4.61 | 5.54 | 3.56 | 11.44 | 8.46 |
| **BOG** | 4.80 | 3.62 | 7.67 | 6.44 | 4.87 | 3.65 | 13.12 | 6.37 |
| **GBP** | 3.81 | 2.45 | 7.01 | 4.44 | 4.49 | 3.32 | 11.72 | 6.69 |
| **Average** | **5.26** | **3.28** | **8.27** | **5.08** | **4.90** | **3.31** | **12.84** | **7.64** |

## 4.1 UV trial setup

The two systems of the inks, solvent based and UV based, were then compared in terms of color stability on press, overprint capabilities, drying time and its effects, and dot gain achieved on press.

Both spot color ink systems were adjusted to desired CIE L*a*b* values by adding necessary color dispersions. With the green color, for UV ink the 1000 lpi anilox was used instead of 800 lpi, because the L value was too low for the 800 lpi (i.e. too much ink transfer). The spot orange UV ink had 15% (20 parts) warm red added to achieve the proper CIE L*a*b* values, matched to average CIE L*a*b*values of solvent based ink systems. While running the acetate inks, solvent was evaporating, and therefore numerous viscosity adjustments had to be made throughout the runs to keep the CIE L*a*b* values in the desired range. For UV inks, no adjustments of viscosity were needed on press during the entirety of the run. There were no problems with the UV ink drying neither into the features of the plate, nor cells of the anilox, which was one of the obvious advantages when comparing solvent based and UV curable ink. This great press stability of UV ink resulted in much greater color stability of UV ink printed sheets. Printed samples were taken from various points throughout the press run and CIE L*a*b* values on solids were measured and averaged (Table 2). $\Delta E_{ab}$ was then calculated.

*Table 2: Average ΔE variation throughout press run for solvent based, and UV curable inks*

| Ink | $\Delta E_{ab}$ | | |
|---|---|---|---|
| | **Orange** | **Green** | **Blue** |
| **Solvent Based** | 2.26 | 5.36 | 2.66 |
| **UV Curable** | 0.36 | 2.81 | 0.27 |

Table 2 shows that the UV ink had less color variation when compared to the acetate based inks. UV curable orange and blue spot colors had ΔE values below 0.5 while the green spot color had a ΔE value below 3. ΔE values of the acetate inks are approximately nine times that of the UV spot colors. These measurements show that UV inks are much more color stable than acetate based inks. In solvent based inks, the increase of the viscosity due to solvent flash off can drastically change the color of the solvent based ink prints.

Tone value increase was measured on blue ink tone curve. However, it is not entirely correct to use spectrodensitometer with its process filters to measure tone value increase of a spot color, but it was assumed that the blue spot ink will give the most reasonable results, using the red filter. Results are given it the Figure 6. Because of the fact that UV inks are cured instantaneously when UV light is applied to the ink film, there is little possibility of increase in dot size due to spreading. Solvent based inks typically dry slower, because the solvent has to flash off for the ink to dry onto the substrate. This slower drying process gives the ink a chance to spread, which results into the TVI increase.



*Figure 6*
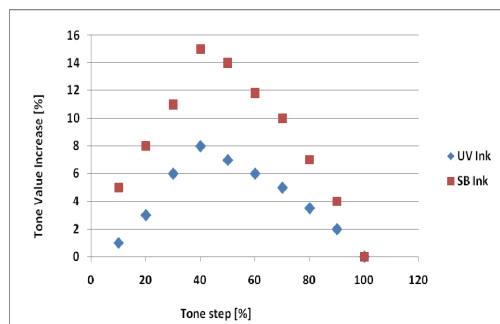*Tone value increase for solvent based and UV curable inks*

Figure 6 shows that the TVI for the acetate inks was much larger than UV curable inks, thus UV curable inks have sharper dots. Also, specular gloss was much better on UV curable (50-70 %) than the solvent based (20-30%) inks, as illustrated in Figure 7.
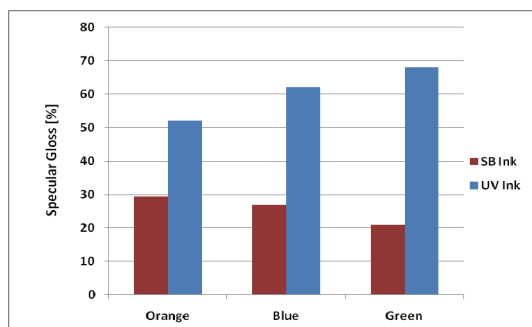


*Figure 7*
*Specular gloss of solvent based and UV curable inks at 60 degree geometry*

Only one combination of 3 UV spot colors was chosen to be proofed on a digital proofing device. The Epson 7900 was used, together with the best performing proofing solution which was set to be RIP #2.

Figure 8 shows the graphical results of the average $\Delta E_{cmc\ (2:1)}$ values that were obtained between the flexo press UV proof CIELAB values and the digital proofs that were produced through the best performing proofing solutions RIP #2 on the Epson 7900. $\Delta E_{cmc\ (2:1)}$ values are slightly higher, but comparable to those obtained for solvent based ink set (Figure 4).
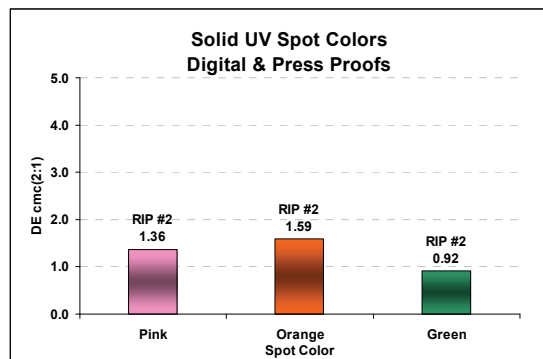


*Figure 8: Graphic representation of $\Delta E_{cmc(2:1)}$ color differences for UV solid spot colors between the flexo press sheet CIELAB values and the RIP #2, the best tested proofing CIELAB values*

The overprint testchart was produced on the best performing proofing solution and the CIELAB values from the proof results were compared to the values gathered from the UV ink press sheets. In this case the reference CIELAB values were set to be those from the press sheet. Average $\Delta E_{cmc\ (2:1)}$ value for 1-, 2- and 3 color overprint produced with RIP#2 was 3.72 (Figure 9), which was almost the same as one reached for solvent based ink system and RIP #2 (Figure 5c), equaling 3.65. This confirms that RIP #2 is the digital solution that is able to visually match both solvent based and UV curable flexo ink chemistries.
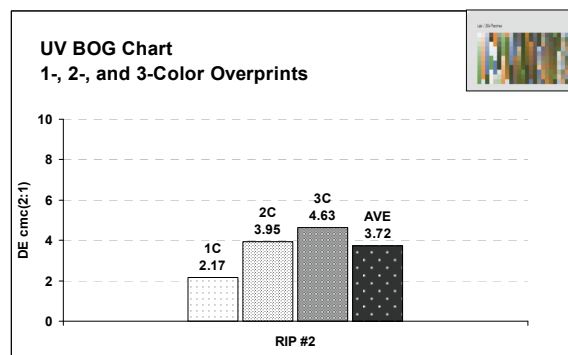


*Figure 9: $\Delta E_{cmc(2:1)}$ values for 1-color, 2-color and 3-color patches and the overall average of all 264 patches on the BOG test chart comparing the press sheet to RIP #2 digital proof*

## 4. Conclusions

The goal of this work was to evaluate the correctness of the overprint models that are included in several different pre-press proofing applications based on the color design produced before the press run. The color proofs obtained were compared to the real ink on paper reproduction from a flexo printing press. The substrate used in the press run was deliberately chosen to be SBS board, which is often used in packaging. Another goal was to evaluate the color differences when using different ink chemistry, such as solvent-based, or UV-curable on the flexo press. It was found that the SmartColour iVue plugin and the RIP #2 solutions produced the best proofing results with almost the same level of color agreement in the terms of $\Delta E$. The RIP #2 with its proofing abilities for the solid spot color, which were notably better than those in iVue and its built-in overprinting model, is considered more rewarding in this case. The RIP #1 solution performed next to the best and Adobe Photoshop was the least accurate proofing option when handling spot colors. In all cases, the iVue plugin provided the best results for the single color channels, these include tints and solid patches.

This finding is interesting due to the fact that the single solid color patches produced the $3^{rd}$ from the highest ΔE numbers compared to other proofing solutions. The 3-color overprints usually yield the worst color agreement between the real press proof and the digital proof. This is expected considering the complexity of the process and the differences in color creation between the analog and digital color production. Although the 3-color patches have the worst ΔE values, they are still remarkably low numbers. The substrate simulation was found to be the best solution when working with the iVue plugin, which is built in individual ink libraries. UV curable ink set had better color stability and lower color variation on flexo press than solvent based ink.

## Acknowledgements

## References

Atkinson, D., (2010), Press and substrate rule, OK! FlexoTech, Issue 109, 3, 22-23.

Chung R., Riordan M., Prakhya S., (2009), Predictability of spot color overprints, Advances in Printing and Media Technology, Ed. Edlund N., Lovrecek M., Vol. XXXV, Darmstadt, 373-380.

Duncan G., (2008),The future outlook for shrink labels, $11^{th}$ PLGA Annual Operational Conference, Miami FL.

Hammer, T., Olsson, N., (2008), UV Ink for shrink: Make the right choice challenging sleeve applications, Flexo, Volume 33, Issue 9, 34-38.

Hayes, R., (2009), Flexibility and versatility is key to flexo, Flexo Tech, Issue 107, 12, 17-19.

Hole, I., (2009), Label them digital flexo shops consciously & courageously move product across print methods, Flexo Vol. 34, 9, 36-41.

Kerchiss T., (2000), Product testing & development, Polymers Paint Colour Journal, Vol.199, Issue 4542, 9, p. 40.

Pekarovicova A., (2007), Emerging Pigment Dispersion Technologies, IntertechPira, Leatherhead, UK, $1^{st}$ Ed., 17pp.

Pekarovicova A., Chovancova-Lovell V., Sangmule S.L, Fleming P.D., Yu Ju Wu, and Guillot B., (2009), Rotogravure Spot Color Proofing for Decorative Laminates Using Smartcolor iVue Software, $36^{th}$ IARIGAI Conference, Stockholm, Sweden.

Pekarovicova A., Pekarovic J., (2008), Ten-Year Forecast in Disruptive Technologies in the Inks and Pigment Industries, Pira International Ltd., Leatherhead, UK, $1^{st}$ Ed., 80 pp.

Sangmule S. L., Lovell V., Pekarovicova A., Fleming P. D., (2010), Digital Proofing of Spot Colors for Flexo Packaging, TAGA Conference, San Diego, March 14-17.

Savastano D., (2008), The flexo ink market, Ink World, Vol. 14, Issue 3, 27-28.

Suchy, M., Fleming, P. D. & Sharma, A., (2005), Spot Color Reproduction with Digital Printing, Proceedings of the IS&T NIP21: International Conference on Digital Printing Technologies, Baltimore, Maryland, 93-97.

Thompson B., (1998), Printing materials, Science and Technology, PIRA International, Leatherhead, UK, $1^{st}$ Ed., 567 pp.

Tolliver-Nigro H., (2007), Flexo: A market transition, Ink Maker, 85, 4, 14-18.

Wu, Y. J., Fleming, P. D., and Pekarovicova, A., (2007), Color Matching Capability of Digital Printers, Proceeding of NIP $23^{nd}$ International Conference on Digital Printing Technologies, Anchorage, Alaska, 414-418.

# UV-sensitive printing ink based on photocatalitically active materials

*Andrijana Sever Škapin*[1]*, Raša Urbas*[2]*, Marta Klanjšek Gunde*[3]

[1] Slovenian National Building and Civil Engineering Institute
  Dimičeva 12, SI-1000 Ljubljana, Slovenia

  E-mail: andrijana.skapin@zag.si

[2] University of Ljubljana, Faculty of Natural Sciences and Engineering
  Snežniška 5, SI-1000 Ljubljana, Slovenia

  E-mail: rasa.urbas@ntf.uni-lj.si

[3] National Institute of Chemistry
  Hajdrihova 19, SI-1000 Ljubljana, Slovenia

  E-mail: marta.k.gunde@ki.si

**Abstract**

A simple indicator of UV-dose exposure based on photocatalytically active materials was prepared. Its colour irreversibly changes in dependence to UV-exposure time. Water-born photocatalytically active functional printing inks were prepared using UV indicator dye, photocatalyst, cellulose base and some additives. Two indicator dyes were examined, Resazurin and Rhodamine B. They were combined with different amounts of nanocatalyst and suitable reducent materials to obtain controllable photocatalytic reaction in which colour of the applied dye irreversibly changed. Several formulations were prepared to achieve acceptable properties of wet ink. They were applied onto paper cards, dried and exposed to UV light. The colour differences between exposed and unexposed samples were measured as a function of UV exposure. Optimal samples provide distinctly visible colour changes after 3 hours of UV exposure, which could reach in some formulations almost 80 CIELAB units. Another formulation of functional printing ink appears to be suitable as a longer-term exposure indicator because it reaches such colour difference after 17 hours.

**Keywords:** functional printing ink; photocatalytically active materials; UV indicator dye; photocatalyst; colorimetry

## 1. Introduction

Modern graphic art products tend to provide more information that is important to customers. These are so-called smart elements that provide useful features and can be printed on different products such as commercials, newspapers, tall-tale labels. Such printed feature can represent an important element of smart packaging that is likely to emerge as one of the key elements in the future. One such piece of information is also the amount of ultraviolet (UV) radiation gathered by exposure of the product to sunlight or some artificial source of light.

UV radiation plays an important role in the environment and affects all living organisms. Some effects are helpful whereas the others can cause considerable harm. The detrimental effects have been observed more seriously after marked increase in incidence of skin cancer since the early 1970s[1]. Optical hazards associated with sunlight as well as with artificial sources initiated introduction of evaluation tools such as Global Solar UV index[2] and several ways of measuring radiation hazards associated with various lamps and lamp systems[3]. These standards require special equipment for measuring the radiation and suitable calculation procedures to evaluate the radiation dose and to compare it with the highest safely recognized level. Such information appears in the form of a number with distinct meaning, which becomes more-or-less inconvenient or practically useless in several everyday situations. Simple indicators that undergo irreversible colour change due to the exposure to UV light would therefore be more suitable. One of the most useful solutions could be application of functional printing ink in a desired shape that changes colour irreversibly upon UV exposure.

Photocatalytically active materials are a special class of materials in which exposure to UV light initiates photocatalysis, a process that may lead to decomposition of chemically stable organic molecules. Such reaction is enabled by a photocatalyst, material which is able to create electron-hole pairs under exposure to

the light with suitable photon energy. Free electron-hole pairs generate reactive species which trigger reduction-oxidation reactions within which a degradation of organic substances may also happen. If an organic dye is involved, its colour may change. Suitable photocatalytically active materials could therefore be combined to get UV sensitive printing ink. Such ink, in principle, would be able to change the colour continuously and irreversibly from the initial up to the final stage where the dye is completely destroyed.

Photocatalytically active material may consist of a photocatalyst, UV indicator dye, suitable base material and some additives. Its photocatalytic activity depends on UV exposure and on several other factors, most importantly on the type and dimension of photocatalyst, and its concentration. Other compositions of functional composite are also important for the final material to be effective[4-7]. All components must withstand photo-induced degradation process and should not react with the indicator dye. The colour change of the dye must be clearly visible in a suitable time period of the UV exposure.

Some results of our research are shown here in order to illustrate how to prepare suitable functional printing ink based on photocatalytically active materials. Such ink could detect the time for which the sample was exposed to UV light. Our aim was for exposure times to range from a couple of hours up to a couple of days while simulating the outdoor exposure to sunny sky. The rather simple ink could be used to prepare printed indicator of exposure to sunlight or artificial UV lights with similar UV dose. Such product could be applied as a smart tag on packaging, magazines and clothing to provide real-time dosimeter for UV light, easily recognized also by non-skilled laymen.

## 2. Experimental

Colloidal dispersion of nano-dimensional titanium dioxide in anatase crystal form, the nanostructured $TiO_2$ was applied as a photocatalyst. The Hombikat XXS 700 (Sachtleben, Germany) was used for this purpose. It is almost transparent sol containing 11.8% of $TiO_2$ with particle sizes 1-100 nm and some organic additives that stabilize the dispersion.

Two dyes that change the colour in a photocatalytic chemical reaction were tested, Resazurin and Rhodamine B. Resazurin is a blue dye used as an oxidation-reduction indicator in several biological applications. When it is illuminated with UV light in presence of a reductive component (e.g. glycerol), it easily and irreversibly reduces into Resorufin, which has a pink colour. Under further influence of UV light, Resorufin transforms to Dihydroresorufin, which is colourless. This reaction is reversible and pink coloration may return if the photobleached ink is left in the dark[3].

Rhodamine B (CI Basic Violet 10: CI No. 45170) is bright magenta red dye with yellow fluorescence, soluble in water, alcohol, and glycol ethers[8]. Due to fluorescence it can be easily detected and inexpensively with instruments called fluorometers. It is often used as tracer dye in water to determine the rate and direction of flow and transport. Another application is in biotechnology for fluorescence microscopy, flow cytometry, and fluorescence correlation spectroscopy. It is being tested for use as a biomarker for wildlife.

The other materials used for photocatalytically active functional printing ink were hydroxyethyl cellulose, glycerol and some suitable additives. Water was added as a solvent.

Several compositions of functional printing inks were prepared with different amounts of photocatalyst, indicator dye, additives and base material. The inks were applied on Leneta WM plain white cardboard (300 g/m$^2$). This is one-side coated colour retentive, non-fluorescent white card (i.e. without optical brighteners) that provides solvent-resistant, non migrating surface. A cube film applicator with 200 μm gap clearance was applied, giving wet layer thickness of about 200 μm (Byk-Gardner, Germany). Such application is regarded to be a good simulation for screen printed samples. All prepared samples were dried in a dark at room temperature for one day.

Dry samples were exposed to UV light for different period of time. Two parallel Osram Eversun lamps (40 W), developed for use in solariums and sunbeds, were used for this purpose. The lamps give continuous spectral power distribution from 300 up to 400 nm with the maximum at approximately 355 nm. In this measuring geometry the sample is illuminated by the total power of 23 W/m$^2$ irradiated in UV spectral region. This corresponds well to the total UV power of 28 W/m$^2$ as measured outdoor on a horizontal surface in Ljubljana on a clear day (April 21$^{th}$, 2010 at 12:45). Thus UV dose from the exposure to the applied lamps is comparable to the outdoor dose from the Sun obtained at Ljubljana latitudes (46° 03' North).

Half of each sample was covered by aluminium foil to be protected from the light. This way a quick visual comparison of the colour change due to UV light was assured. The colour of samples was measured in dependence on exposure time. The colorimeter KonicaMinolta CR-331c was used for this purpose. It has 45/0 measuring geometry and 25 mm sample aperture. All measurements were accomplished in CIELAB colour space applying D65 illuminant and 2° standard observer.

## 3. Results ad discussion

### 3.1. Resazurin-based functional printing inks

The total colour change ($\Delta$E) of Resazurin-based functional printing inks in dependence on time of UV exposure is shown in Figures 1 and 2. When ink is applied onto coated side of cardboard (Figure 1), $\Delta$E strongly depends on the amount of photocatalyst and reaches the maximum of $\Delta$E=80 for sample with 0.5 wt.% of $TiO_2$ after 3 h of UV exposure. When the same ink was applied on the non-coated side, much smaller colour difference was obtained and the quantity of $TiO_2$ has no influence on it (Figure 2). After 3 h of UV exposure $\Delta$E=20 was obtained. The effect of the amount of photocatalyst and the substrate on colour change of Resazurin-based functional printing inks after 2.5 h of UV exposure is clearly shown in Figure 3, while the continuous change of colour in relation to time of UV exposure of the sample with 0.3% of $TiO_2$ is illustrated by Figure 4.



*Figure 1: The CIELAB colour change of Resazurin-based functional printing ink applied on coated side of cardboard in dependence of UV exposure (left) and the corresponding colour in the (a\*,b\*) plane (right). The samples were prepared applying 0% (black), 0.1% (blue), 0.3% (red) and 0,5% (green) of TiO2.*



*Figure 2: The CIELAB colour change of Resazurin-based functional printing ink applied on uncoated side of cardboard in dependence of UV exposure (left) and the corresponding colour in the (a\*,b\*) plane (right). The samples were prepared applying 0% (black), 0.1% (blue), 0.3% (red) and 0.5% (green) of TiO2.*



*Figure 3: Resazurin-based functional printing ink layers having different amounts of photocatalyst (denoted on picture) applied on (a) coated and (b) non-coated sides of cardboard after 2.5 h of UV exposure - upper-half of samples was covered by aluminium foil to protect them from light*

*Figure 4: The continuous change of colour in relation to time of UV exposure of the Resazurin-based sample with 0.3% of TiO$_2$ applied on coated side of cardboard*

### 3.2. Rhodamine B-based functional printing inks

Rhodamine B-based functional printing inks changes due to UV exposure from magenta red to orange colour shade. However, larger exposures are required as compared to Resazurin-based samples for similar colour difference. The Rhodamine B samples prepared on coated side of cardboard after 3 hours of UV exposure exhibit ΔE up to 40, and reach steady value ΔE=92 after 17 hours of UV exposure (Figure 5). The effect of the amount of photocatalyst on colour changes of Rhodamine B-based functional printing inks is insignificant (Figure 5). The effect is different when the same ink was applied on the uncoated substrate (Figure 6). After 17 h of UV exposure ΔE of up to 40 was reached. The direction of colour change in the CIELAB colour space depends on the substrate – if the ink is applied on coated or non-coated sides of cardboard (compare Figures 5 and 6). The effect of the amount of photocatalyst and the substrate on colour change of Rhodamine B-based functional printing inks after 17 h of UV exposure is shown in Figure 7, while the continuous change of colour in relation to time of UV exposure of the sample with 3% of TiO$_2$ is illustrated by Figure 8.
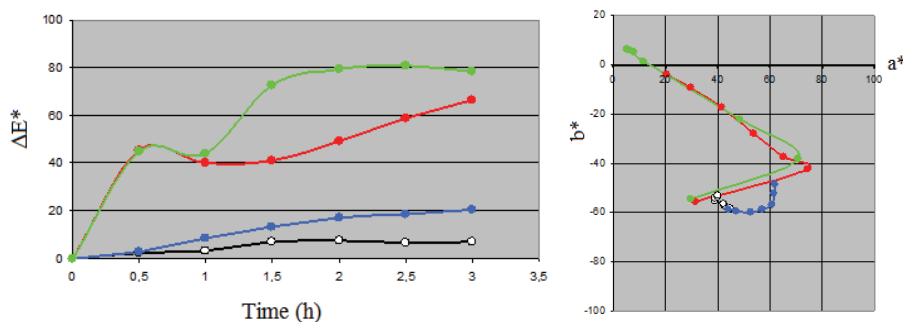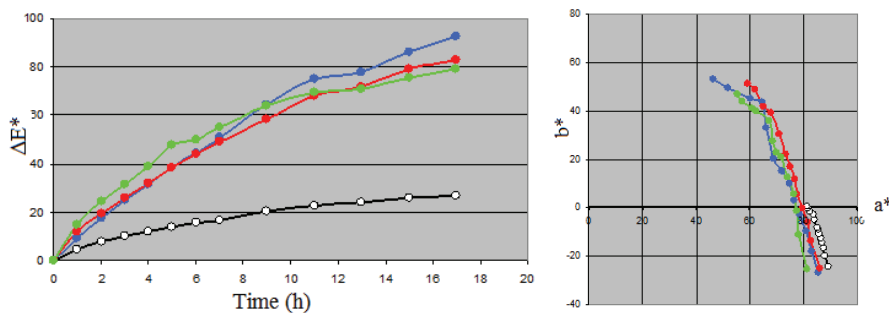


*Figure 5: The CIELAB colour change of Rhodamine-B-based functional printing ink applied on coated side of cardboard in dependence of UV exposure (left) and the corresponding colour in the (a\*,b\*) plane (right). The samples were prepared adding 0% (black), 1% (blue), 2% (red) and 3% (green) of TiO$_2$.*
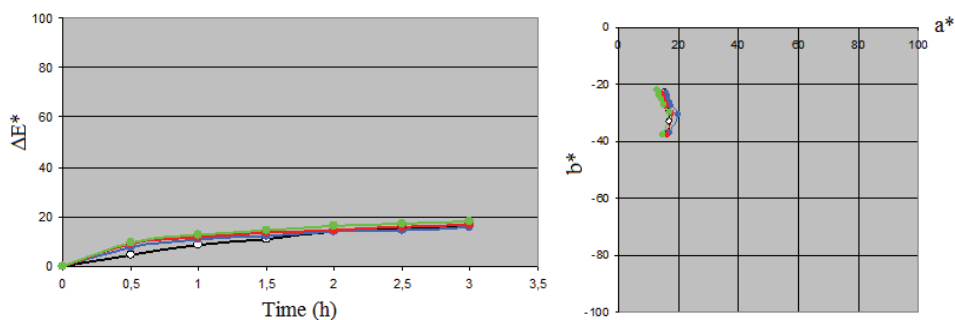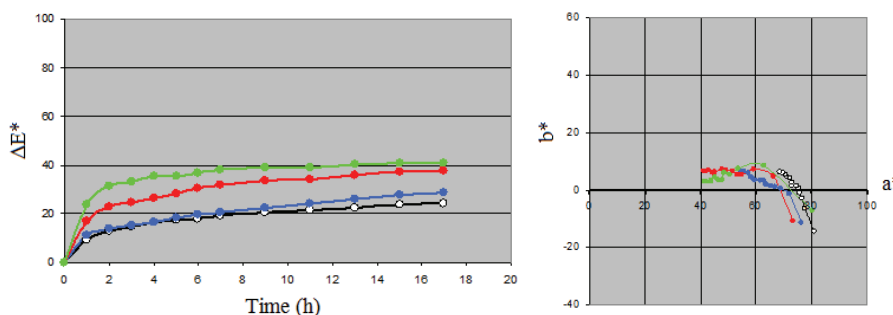


*Figure 6: The CIELAB colour change of Rhodamine B-based functional printing ink applied on uncoated side of cardboard in dependence of UV exposure (left) and the corresponding colour in the (a\*,b\*) plane (right). The samples were prepared adding 0% (black), 1% (blue), 2% (red) and 3% (green) of TiO$_2$*
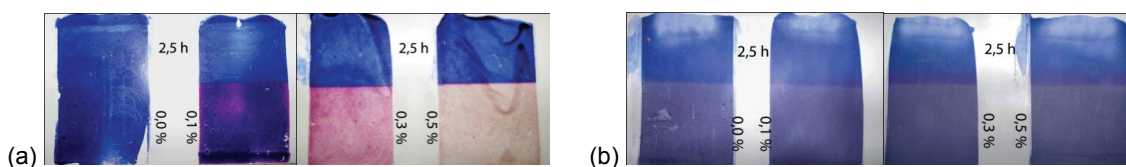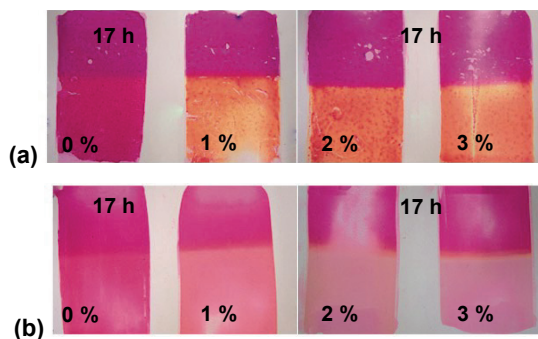
*Figure 7: Rhodamine B-based functional printing inks samples with different amounts of photocatalyst
(denoted on picture) applied on (a) coated and (b) non-coated sides of cardboard after 17 h of UV exposure.
Upper part of samples was covered by aluminium foil to protect them from light.*
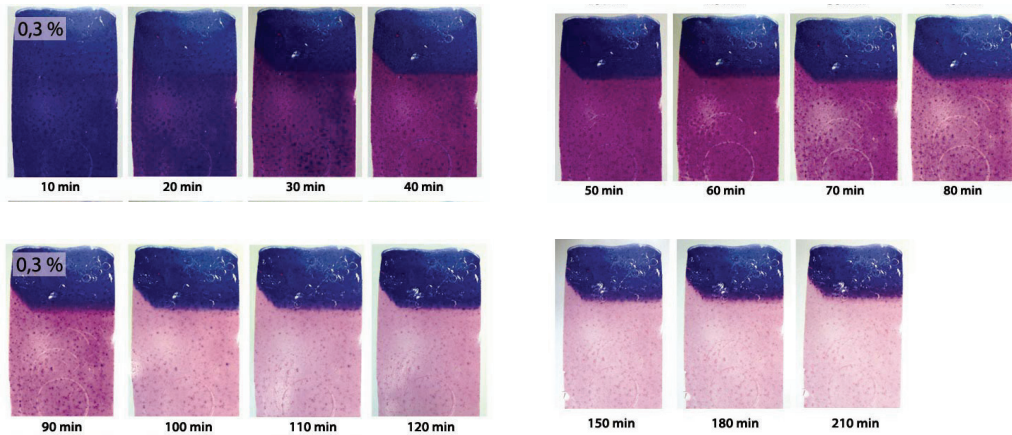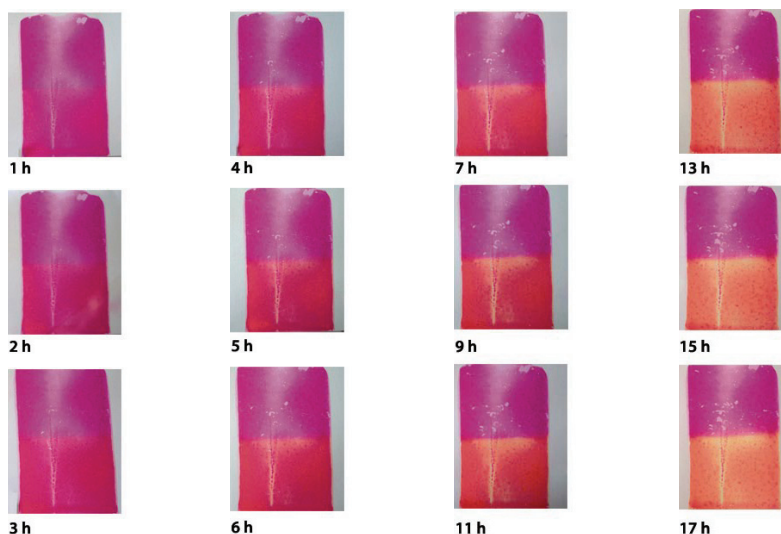


*Figure 8: The continuous change of colour in relation to time of UV exposure of the Rhodamine B-based sample
with 3% of TiO$_2$ applied on coated side of cardboard*

## 4. Conclusions

Both dyes tested in this research have been found to be appropriate for application in functional printing ink that could be applied as a good UV-indicator offering easily recognized information. Under constant irradiation (3 h under UV exposure), the biggest colour change ($\Delta E=80$) was obtained in the Resazurin-based ink with 0.5 wt.% of nanocatalyst TiO$_2$ when spread on the coated side of the substrate. When applied onto the uncoated side, the corresponding photocatalytic reaction did not take place. It produced much smaller colour change, occurring in a different direction of the CIELAB colour space. Analysing the colour route that a sample undergoes in the (a\*, b\*) plane during UV exposure, the presence/absence of photocatalytic reaction can be observed. If a non-characteristic route appears, photocatalytic reaction loses in competition with some other dye-changing reactions. In the case of the uncoated substrate shown here, such reactions occur between the ink constituents and the substrate. Rhodamine B-based functional printing inks require much higher amount of nanocatalysts to obtain suitably visible colour change upon UV exposure. The biggest change of colour ($\Delta E=92$) was observed at the highest TiO$_2$ loading used (3 wt.%), again when the ink was applied on the coated side of cardboard. However, the corresponding exposure time (17 h) had to be much longer than in the case of Resazurin (3 h). Similarly as before, the effect on the non-coated side was much smaller and different colour route in the CIELAB took place during UV exposure.

Our research confirms that it is possible to prepare functional printing ink by adding photocatalytically active materials. When such ink is applied onto a suitable substrate, its colour irreversibly changes when exposed to UV light. We show here that Resazurin-based inks could be suitable for printing simple UV-indicators for short-time exposure (a couple of hours), while Rhodamine B-based inks may be more appropriate as long-term exposure indicators (a couple of sunny days).

**References**

1. D .J. Leffell, D. E. Brash, "Sunlight and skin cancer", Scientific American, July 1996, 38-43.

2. Global Solar UV index - A practical guide. United Nations Environment Programme. http://www.unep.org/Documents.Multilingual/Default.asp?DocumentID=468&ArticleID=3944&l=en

3. Photobiological safety of lamp and lamp systems, CIE S 009/E:2002. CIE Central Bureau Vienna 2002.

4. A. Fujishima, T. N. Rao, D. A. Tryk, "Titanium dioxide photocatalysis", Journal of Photochemistry and Photobiology C: Photochemistry Reviews 1 (2000) 1-21.

5. A. Mills, M. McFarlane, "Current and possible future methods of assessing the activities of photocatalyst films", Catalysis Today 129 (2007) 22-28.

6. A. Mills, J. Wang, M. McGrady, "Method of rapid assessment of photocatalytic activities of self-cleaning films", Journal of Physical Chemistry 110 (2006) 18324-18331.

7. J. Zita, J. Krysa, A. Mills, "Correlation of oxidative and reductive dye bleaching on $TiO_2$ photocatalyst films", Journal of Photochemistry and Photobiology A : Chemistry 203 (2009) 119-124.

8. The Printing Ink Manual, Fifth edition, Ed. R. H. Leach and R. J. Pierce, Springer Science + Business media B.V. 2008.

# High speed UV inkjet - impact of speed and substrates on print quality

*Marianne Klaman[1], Per-Åke Johansson[1], Jon Lofthus[1], Erik Blohm[1], Ingo Reinhold[2]*

[1] Innventia AB
  Box 5604, SE-114 86 Stockholm, Sweden
  E-mails: marianne.klaman@innventia.com, erake.johansson@innventia.com,
       jon.lofthus@innventia.com, erik.blohm@innventia.com

[2] XaarJet AB
  Box 516, SE-175 26 Järfalla, Sweden
  E-mail: ingo.reinhold@xaar.se

**Abstract**

Up to very recently, high speed inkjet meant high speed but low print quality. The trend today is that a new generation of high speed inkjet printing heads/presses, able to produce higher quality, begins to appear. It is therefore of increased interest to evaluate what impact the speed has on the final print quality due to the interactions between print head, ink and the substrate. Also what effect different substrates have on the print quality.

The results here presented emanate from a project concerning high quality inkjet at higher speeds, performed at Innventia together with industrial partners. The work has been carried out in cooperation with the printhead manufacturer Xaar, as well as paper and ink producers.

The inkjet research platform has been integrated into a universally useful reel-to-reel machine for the dynamic evaluation of paper and other substrate's mechanical as well as printability properties at the institute. The set-up is described as well as the chosen inkjet technology. Results from the print trials are presented and measures for print density, gloss, print mottle and dot shape are given. Ink penetration on different paper grades and UV curing efficiency are analysed as well.

**Keywords:** high speed inkjet printing; impact of speed on print quality;
        impact of substrates on print quality; UV curing

## 1. Introduction

Up to very recently, high speed inkjet meant high speed but low print quality. The trend today is that a new generation of high speed inkjet printing heads/presses, able to produce higher quality, begins to appear. One of them, Kodak, has recently launched a print machine in this category with their Stream technology in the Prosper Production Platform (Cleary, 2009). This machine allows speeds up to 200 m/min. Kodak showed the prototype at Drupa 2008 and now the first machines are sold. UV curing systems are the fastest growing technology seen over the past 10 years, and are thought to dominate the market with its quality, productivity and versatility (Morgan, 2010). Development efforts are on the way with cationic UV-curable inks, which are more favourable in for instance reduced smell. However, they still have a drawback having a tendency to be affected by moisture (Tomotake, 2008).

With improved performance of high speed inkjet, competition with offset for mainstream printing may be in the offing. It is therefore of increased interest to evaluate what impact the speed has on the final print quality due to the interactions between print head, ink and the substrate. The impact of the substrate on the final quality is of crucial importance when choosing the accurate material for the product. The results here presented emanate from a project concerning high speed, high quality inkjet carried out at our institute together with industrial partners. In cooperation with the printhead manufacturer Xaar, as well as paper and ink producers, we are aiming towards higher speeds without loosing dot rendering and print quality.

The objectives of the work here presented were:

- Development of high speed UV inkjet printing.
- Analyses of the impact of speed on print quality.
- Analyses of substrate influence on print quality.

## 2. Research methods - the research platform

### 2.1 The research platform

The strategy has been to use the Innventia reel-to-reel Linda machine for the development of an inkjet research platform. It is a universally useful set-up for the dynamic evaluation of paper and other substrate's mechanical as well as printability properties. It was anticipated that due to its very stable construction, it is well suited to study rapid processes. In the project, the integrated inkjet platform has been used for the print trials in order to evaluate the effects of speed, different substrates and inks, in combination with the capability of the inkjet print heads. In Table 1 the specifications for the Linda machine can be seen.

*Table : Specifications for the Linda machine*

| Web width | 260-400 mm |
|---|---|
| Speed | 10-300 m/min (0.2-5 m/s) |
| Web tension | 100-500 N/m |
| Maximal paper roll diameter | 1200 mm |

### 2.2. System overview

The machine is built to be versatile while still stable and consists of a 7 m long lathe bed with place for measurement modules freely placed along the prisms, see Figure 1. In each end paper rolls and bobbins are mounted. They are directly connected to the web tension motors which are run in torque mode and are balanced to give the set web tension at any speed. The web movement is controlled by a speed regulated nip (NIP 1 in the figure).
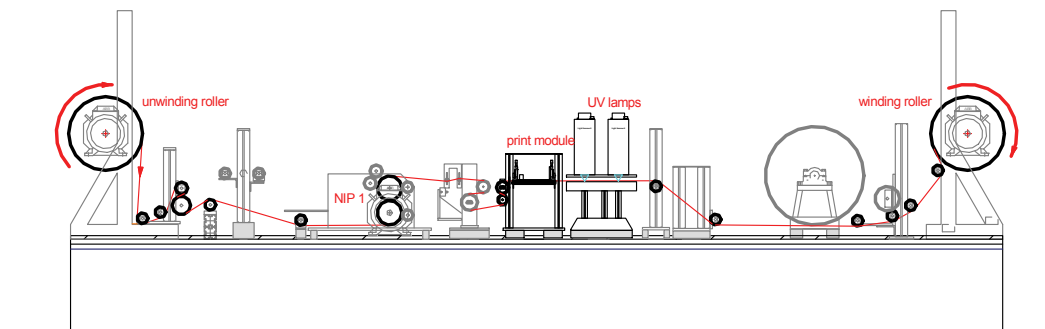


*Figure 1: The **Linda** machine with print module and UV-curing module*

### 2.3 Print module

#### 2.3.1 Construction

The main frame is made from rigid aluminium profiles on which the encoder roller, the print head assembly with height adjustment and the support plate for the substrate are mounted, see Figure 2.

#### 2.3.2 Pulse encoder and resolution

The encoder roller is synchronizing the printing in relation to the web movement and is mounted close to the heads to prevent web tensions to show up as misplaced dots. The inertia of the roller is low and the wrap angle is large to ascertain a minimum of slip between roller and substrate. The 2 µm/pulse quadrature signal is fed to the control logic where it is decoded to suit the 360 dpi print resolution.

#### 2.3.3 Print heads

The chosen inkjet technology for this particular project was Xaar's hybrid sideshooter printhead, Xaar1001. The parameters of operation include Xaar's multipulse binary greyscale technology to generate droplets of up to 42 pL with increments of 6 pL with a print frequency of up to 6 kHz. At its natural resolution of 360 x 360 dpi this results in print speeds of about 0.42 m/s, with an apparent resolution due to the variable droplet size of approximately 1000 dpi.

This printhead differs strongly from previous concepts applied in piezoelectrically driven actuators, as it does not use the commonly anticipated *endshooter* principle, where the nozzle is the terminal end of the ink path, but ejects ink perpendicular to the direction of travel of the acoustic wave in the channel. This form of ejection
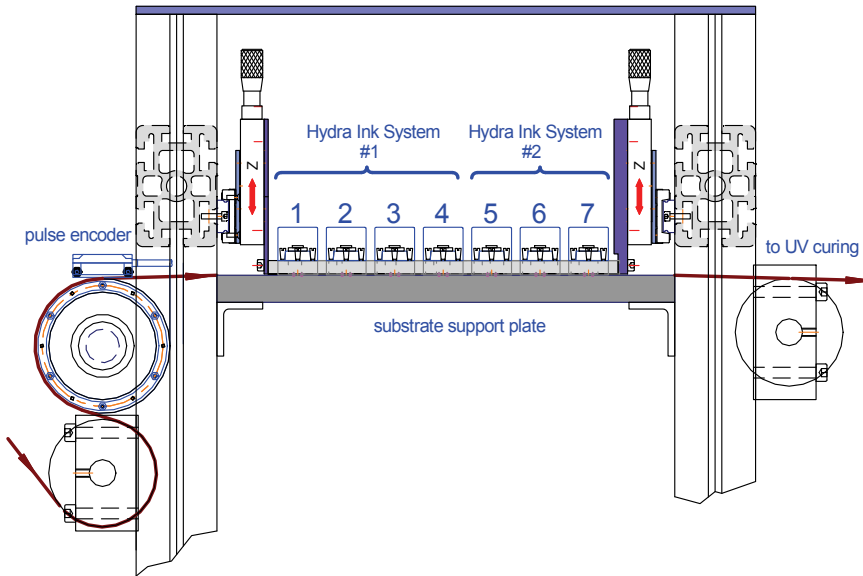
*Figure 2: Seven print heads assembly with encoder roller for synchronisation*

results in the possibility of continual through flow through the channel and therefore self-recovery after air or particle ingestion. The continuous flow furthermore offers the advantage of temperature stability of the head, as temperature generated from energy dissipation due to actuation voltages as well as electronics is carried away from the printhead and equilibrated by the large volume of the ink supply.

Using a ganging approach, with n printheads in a series, to overcome the restrictions posed on a single printhead by the shared-wall principle, an *n*-fold increase in print speed may be accomplished. However, due to the special design of Xaar's printheads only a certain combination of printheads allows for 360 x 360 dpi operation and needs careful redesign of the print patterns to yield desired results. Proprietary software has been developed to accommodate preprocessing of 8 bit print masters for multiple combinations of printheads and firing schemes.

### 2.3.4 Print head fixture

The print heads are mounted on a plate with slots for up to seven ganged print heads. Each head's transversal position and angle, relative the print direction, can be adjusted, see Figure 3. The plate's height above the support plate can be adjusted with micrometer translation units to assure an accurate and consistent distance from the substrate. The whole assembly is supported on linear rails to allow for positioning over the full paper width. It can also be retracted outside the paper edge when cleaning or inspection is required.



*Figure 3: The seven print head assembly with conical adjustment screws. The green printed circuit boards are the head driver cards and the two boxes over the heads at the ends, contain ink temperature and meniscus pressure sensors*

### 2.3.5 UV light source

To cure the ink supplied by SunJet a UV light source is placed immediately after the print heads. It consists of two high energy microwave UV lamps (Light Hammer 6 from *Fusion UV Systems, Inc.*[®]), see Figure 4, standing on an enclosure with slits to allow for the web passage.
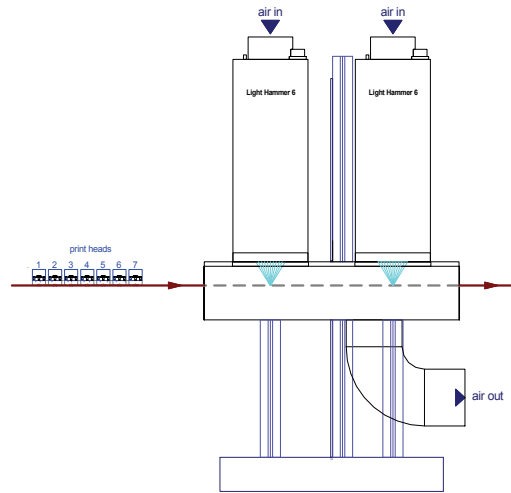
*Figure 4: The UV light source*

The lamps require a rather high amount of cooling air (recommended 3,7 m³/min) which is released into the enclosure. As the laboratory has a controlled atmosphere, the cooling air is evacuated from the enclosure at a slightly higher rate to minimise the heating and the smell from the ink and ozone. The web inside the UV housing is mechanically stabilized with a support plate to avoid tension variations caused by the air turbulences. The irradiator tubes emit a maximum of 184 W/cm and are 15,2 cm long, giving 2,8 kW each. As the irradiated width is 15,2 cm and the printed width is 7 cm, the construction is made to allow for an individual rotation of the lamp houses to increase the curing energy to the substrate as can be seen in Figure 5.
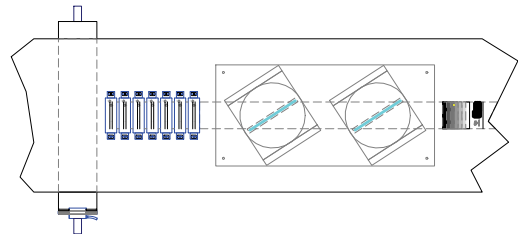


*Figure 5*
*Showing a top view of the UV-source assembly.*
*By rotating the UV lamps, the curing energy*
*to the printed area can be doubled.*

The two UV sources are both based on mercury emission spectrum but have been doped to give their energy peeks at somewhat different wavelengths, see Figure 6.
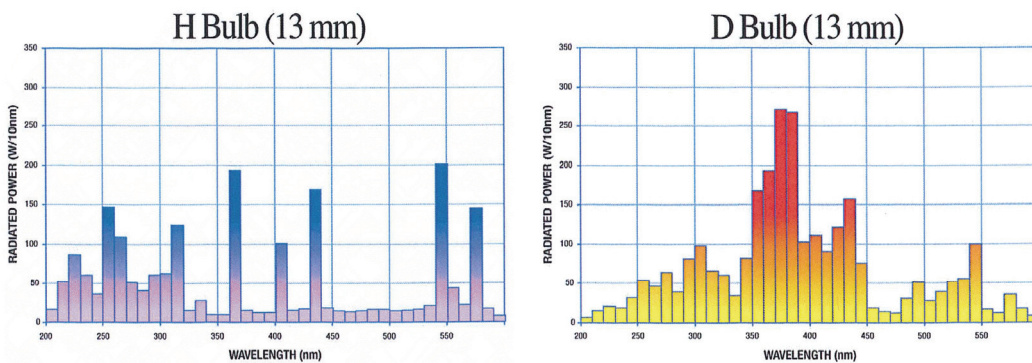


*Figure 6:Spectrum for the two UV-lamps. Fusion UV Systems, Inc.*[®]

As can be seen, the H-lamp has a higher short wavelength UV energy content than the D-lamp. As the order in which the different wavelengths work on the ink may be important, the lamp order can easily be changed. Some experiments to investigate this have been made but no significant difference was seen in the print results.

## 2.4 Limiting factors for successful achievement of high speed

Heading for the highest possible print speed, one will eventually reach limiting factors concerning paper handling or print quality that prohibit further increase of speed. These limiting factors can be of different character e.g.:

### 2.4.1 Mechanical paper handling problems giving unstable paper transport and positioning

The prerequisite of stable paper transport is fulfilled by our existing roll-to-roll paper web test machine, in which an inkjet platform has been integrated. The construction is very stable and different drive parameters can be changed while running. It thus is very suitable for high speed trials and its maximal web speed of 300 m/min is clearly above the speed aimed at in the present project, 150 m/min.

#### 2.4.1.1 Web speed and tension variations
Slow speed variations are normally not a problem as the synchronisation pulses follow the speed and the system calculates the correct dot placement from the pulses. If, however, a variation in web tension causes the web to stretch, the encoder cannot detect this elongation and the dots will hit the wrong place.

#### 2.4.1.2 Transversal web movements
Slow changes in web placement in cross direction (CD) are seldom a problem if the wavelength of movement is considerably longer than the length of the head array. The wavelength however is strongly dependent of the paper dimensional stability and the web tension. The calibration of the rollers is of course crucial as any misalignment will cause the web to wander.

### 2.4.2 Ink droplet firing frequency limits and timing precision

The maximal ink droplet firing frequency of a printhead sets a limit for the printing speed, but spreading the print image over several synchronized printheads increases the possible speed. However, this calls for a very precise positioning and synchronization of the heads. Any failure in this will lead to unsharp edges and moiré patterns in halftones. The extra speed/resolution benefit offered by the variable drop technique was also utilized.

### 2.4.3 Too little time or power available for successful curing to avoid smearing

The system used is based on UV curable inks. The prerequisite of avoided smearing requires UV energy enough to cure the ink during the short passage under the UV source. The installed UV sources of 2 x 3 kW LightHammer™6 from Fusion UV Systems Inc. proved to deliver ample power.


## 3 Research methods - print quality evaluation

**Print Density:** Measured with a conventional spectrophotometric densitometer Techkon Spectrodens A 801023 Premium. Black channel, ISO-E setting with polarizer and paper white reference.

**Gloss:** Measured with a Zehntner ZLR 1050 Lab-Glossmeter at 20°, 60° and 75° (ISO 8254, Tappi T480)

**Raggedness:** Using a QEA Personal IAS system adopting the ISO 13660 print quality standard for Raggedness and Blurriness

**Mottling: Epson** scanner and STFI Mottling Expert Software.

**Dot shape + satellites:** Visually judged from microscope images.

**Ink penetration:** Ink deposition was studied by light microscopy of embedded sheet sections as well as by 3D X-ray micro tomography of sheets.

**UV curing:** The curing was measured as set-off density on a receiving paper. The rub-off test was performed in a K&N wipe test equipment Wennberg Type 49. The rub-off test was performed shortly after the curing moment. The set-off density was measured with a Techkon Spectrodens A 801023 Premium.

*Table 2: Specification of substrates used for the trials*

| Specifications of paper |
|---|
| *Gloss coated paper: GL*<br>Gloss Coated Wood Free paper 100 g/m$^2$. |
| *Silk coated paper: SI*<br>Semi-Matt Silk Coated Wood Free paper 100 g/m$^2$ |
| *Uncoated paper: UC*<br>Uncoated Wood Free paper 100 g/m$^2$. |

A set of papers, see Table 2, were chosen in order to cover a typical range of printing surface structures including uncoated, silk matt coated and glossy coated. The ink used was a black UV curing grade from Sunjet division of Sun Chemical.

## 4. Results

### 4.1 Print density

Print density is increased by the amount of ink transferred, the forming of a homogenous, well covering ink film, and that the final deposition of cured ink is on top of the surface rather than penetrated into the substrate.
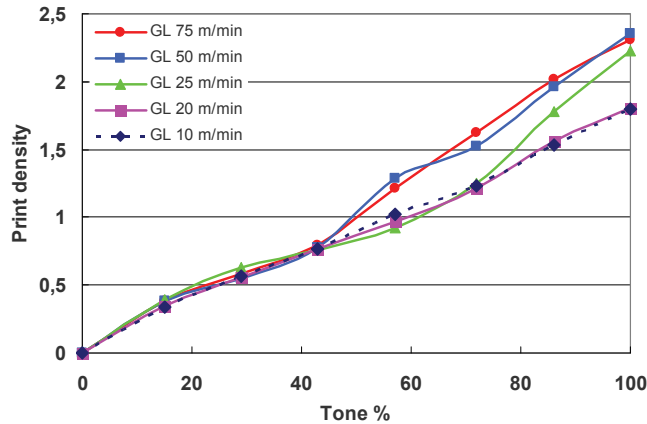


*Figure 7: Print density on glossy coated paper (GL) increases with printing speed from 10 to 75 m/min (see legend) especially for tone values above 60%.*

Figure 7 shows print density results from trials at speeds from 10 to 75 m/min on the glossy paper. Interestingly, the print density increases with printing speed especially for tone values larger than 60%. The reason might be that the shorter time span from ink impact to curing at higher speeds results in a more superficial deposition of the ink, thus yielding better optical efficiency. Time span from ink impact to curing position is 3 s at 10 m/min and 0.6 s at 50 m/min in our equipment.

### 4.2 Gloss

Indications in the same direction come from gloss data, see Figure 8, where gloss measured on uncoated papers printed at 10, 20 and 25 m/min is represented. The gloss rises with increased printing speed especially on the uncoated paper, where the risk of ink penetration is especially high. This can be seen as yet another example of usefulness of high speed within the studied range. Similar but weaker tendencies to higher gloss at higher speeds were found also on gloss coated papers where the gloss level however is high already on unprinted papers.
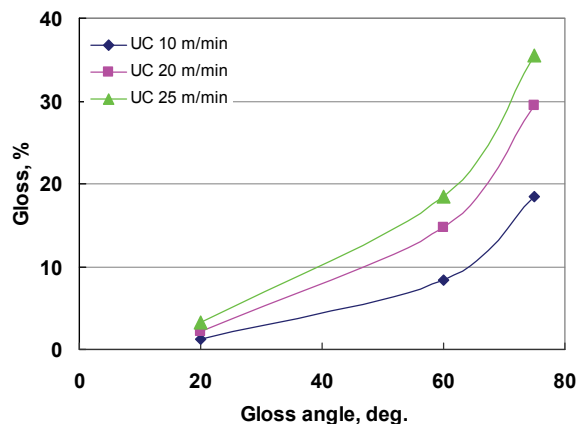


*Figure 8: Print gloss on an uncoated paper (UC) increases with printing speed from 10 m/min to 25 m/min (see legend)*

## 4.3 Print mottle

Smooth reflectance of printed halftones relies on equally sized and regularly placed printed dots. Varying interactions ink-paper as well as bad synchronization or nozzle alignment can lead to random or ordered mottle patterns. Such effects can be speed dependent, but the print mottle results in Figure 9 show no measurable speed dependence. There is however a distinct influence from the paper surface with the tendency towards worse mottling on smoother paper. This perhaps surprising tendency is explained by the sharp dot formation on smooth coated paper which reveals any misplacement of droplets. On the uncoated paper on the other hand, the droplets tend to spread in the structure which creates a kind of smoothing filter effect that blurs out mottling tendencies.
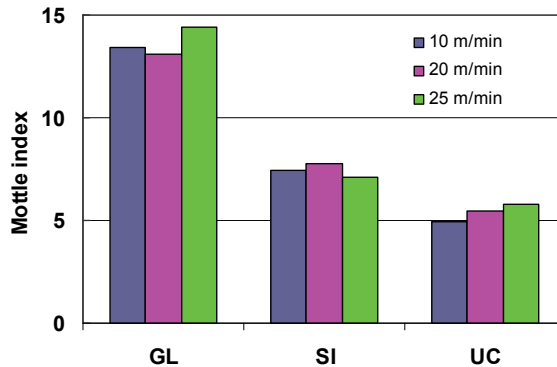


*Figure 9: Print mottle index (1-8 mm wavelength) is highest on the gloss coated paper (GL), lower on silk (SI) and lowest on the rougher uncoated paper (UC). No systematic dependence on printing speed is seen from 10 m/min to 25 m/min*

## 4.4 Line sharpness

The line raggedness measured as contour deviations from a straight line show the expected dependence on surface smoothness, i.e. more ragged contours on rough uncoated paper on which ink spreads more easily. Lines perpendicular to the print direction generally has higher raggedness since synchronization errors here add to the common ink spreading phenomenon.

## 4.5 Dot shape

As seen in Figure 10, the individual print dots are not smeared out or markedly deformed in any other way when the print speed is increased from 10 to 150 m/min. Thus, dot deformation seems not to be a speed limiting factor here. The satellite droplets however seem to be more intense at high speed.



GL 10 m/min                                          GL 150 m/min
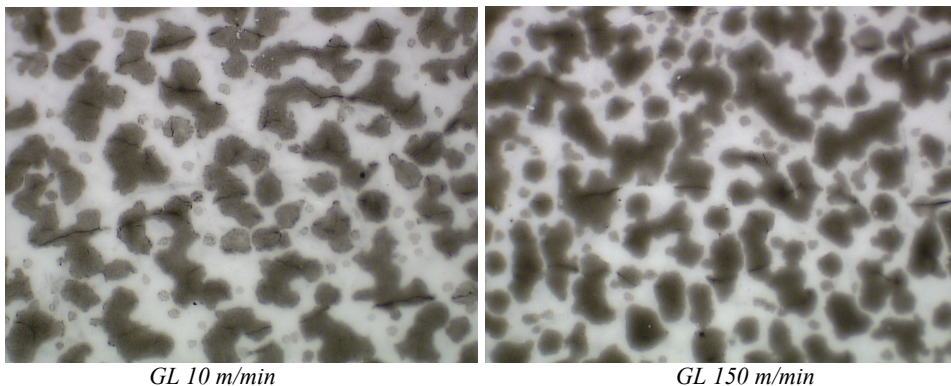
*Figure 10: Screen tone printed on glossy paper GL at 10 m/min and 150 m/min respectively. The dots are not markedly deformed by the higher print speed.*

## 4.6 Ink penetration

Figures 11 and 12 show the radical difference in ink deposition between papers with and without mineral coating. This difference has consequences for the optical effects (print density and gloss) as well as for the curing and set-off behaviour. The anticipated effect of more shallow ink deposition at higher speeds was hard to detect due to the strong variation in local penetration in the images. Subjectively a tendency to such behaviour was however experienced.

What could also be seen in 12 was that the gloss variations in the uncoated surface could be explained by the differences between the deeper penetration in certain parts, causing a more matte surface and the more shallow penetration with ink staying on the surface giving clearly glossier parts.

The X-ray 3D image volumes gave the opportunity to virtually scan through the bulk of the sheet, but getting a quantitative value of penetration proved even harder than for the optical sections due to weak image contrast between ink and fibre material.
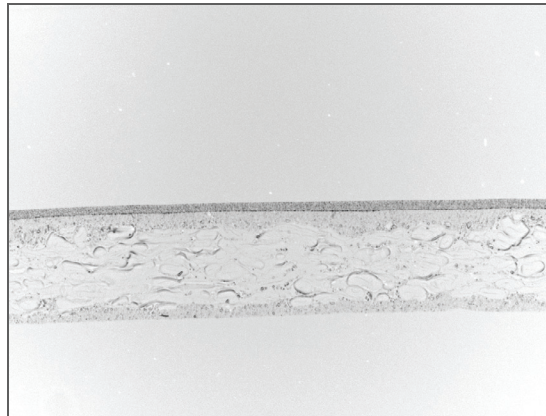


*Figure 11: Light microscopy section image of Glossy paper GL printed with a full tone ink patch at 25 m/min speed. The 36 μm thick paper has a very homogenous 6 μm ink film on top of its coating on one side*

### 4.6 UV curing

With a limited UV power available this will obviously lead to a speed limit at which the ink becomes insufficiently cured and starts to smear against other sheets or objects.

Results from tests with measured set-off as a function of UV power shows, as can be seen in Figure 13, that there is a "knee" at a certain level of power for all grades except for the uncoated. A power level above that is enough for total curing. For the uncoated paper the set-off is on a very low level already at low power, but it is not further reduced at higher power to the same low level as for the other grades. The mechanism for curing is obviously different on uncoated paper, probably due to a stronger penetration of ink into the paper structure.
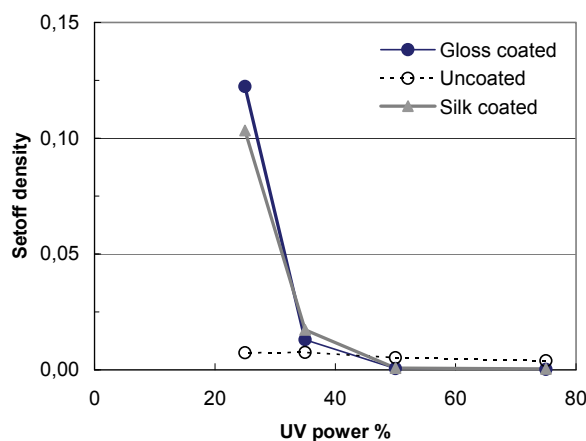


*Figure 13: Set-off density on a receiving paper rubbed against fresh prints after curing with a given percentage of the full UV power 2 x 3kW. Gloss coated (GL), silk coated (SI) and uncoated (UC) paper. Printing speed: 25 m/min*

The curing efficiency at higher printing speeds was evaluated. The reverse side set-off density on GL paper grade after curing with 100% UV power was evaluated. The printing speeds were 150 m/min and 175 m/min. A slight speed dependence was found, the printing ink was not totally cured. This lead to the conclusion that the curing lamps at full speed have to be rotated in order to achieve power concentration and full curing, as seen in Figure 5.

## 5. Discussion and conclusions

The printed dots showed no severe speed induced shape deterioration within the studied speed range. The number of satellites increased with increasing speeds, which indicates yet imperfect driving waveforms and therefore, incomplete cancellation of the preceding acoustic pulses. As a result of this residual energy, longer tails are formed during the ejection, which, depending on the ink's characteristics, may translate into higher satellite counts. A reiteration of the driving waveform and/or the ink may produce better results.

The highest speed gave the highest print density, which indicates that the speed limit is not yet reached, and the gloss measurements showed the same tendency. The reason for the increased values might be that the shorter time span from ink impact to curing at higher speeds results in a more superficial deposition of the ink, thus yielding better optical efficiency. The ejected amount of ink at higher substrate velocities has not been studied so far, we however believe that the amount is in the range of +10% in volume due to not fully damped preceding actuations.

Print mottle stayed constant without speed dependence. It was noted that uncoated grades can achieve an extra smooth mottle-free appearance due to a structural filtering effect where small print imperfections are blurred out.

Results from tests with measured set-off as a function of UV power showed that there is a "knee" at a certain level of power for all coated grades. A power level above that is enough for total curing. For the uncoated paper the set-off is on a very low level already at low power, but it is not further reduced at higher power to the same low level as for the coated grades. The different mechanism for curing on uncoated paper could well be explained by the stronger penetration of ink into the paper structure.

From the ink deposition studies the radical difference in ink deposition between papers with and without mineral coating was experienced and this difference gives explanation for the optical effects (print density and gloss) as well as for the curing and set-off behaviour. The penetration into uncoated paper could be estimated, at least in several cases, to half the paper thickness. For the gloss coated paper the ink remained on top of the surface.

The anticipated effect of more shallow ink deposition at higher speeds on uncoated paper was hard to detect due to the strong variation in local penetration in the images but subjectively a tendency to this behaviour was experienced.

The gloss variations on uncoated printed surfaces could be explained by the differences between the deeper penetration in certain parts, causing a more matte surface and the more shallow penetration with ink staying on the surface giving clearly glossier parts.

When the very precise positioning and synchronization of the heads is achieved and maintained during printing, and if misalignments causing the web to wander can be avoided, the results so far show a promising potential for achieving high quality UV inkjet prints at high speeds.

### References

Cleary, N., *The heart of a new machine: trends in inkjet printing technologies*, Digit. Print., no 24, July-Aug. 2009, pp 12-13.

Morgan, T., *The future of UV inks; perspectives and opportunities,* PrePress, vol. 18, no. 12, Dec 2009, pp 38-39

Tomotake, A., Sasa, N., Nakajima, A., Takabayashi, T., Kida, S., *Development of a cationic UV curable inkjet ink: formulation effect on curing behaviour*, NIP24, 24th international conference on digital printing technologies, 2008, pp 532-534.

# Influence of atmospheric plasma treatment on surface properties and inkjet printability of lpastic packaging film

*Johanna Lahti*[1], *Kim Eiroma*[2], *Tiia-Maria Tenhunen*[3], *Maiju Pykönen*[4] *and Martti Toivakka*[4]

[1] Tampere University of Technology, Department of Energy and Process Engineering
Paper Converting and Packaging Technology
P.O. Box 541, FI-33101Tampere, Finland
E-mail: johanna.lahti@tut.fi

[2] VTT Technical Research Centre of Finland, Printed Functional Solutions
PL 1000, FI-02044 VTT (Espoo), Finland
E-mail: kim.eiroma@vtt.fi

[3] VTT Technical Research Centre of Finland, Functional Fibre Products
PL 1000, FI-02044 VTT (Espoo), Finland
E-mail: tiia-maria.tenhunen@vtt.fi

[4] Åbo Akademi University, Laboratory of Paper Coating and Converting and Center for Functional Materials
Porthaninkatu 3, FI-20500 Turku, Finland
E-mails: mpykonen@abo.fi, martti.toivakka@abo.fi

**Abstract**

Plastic films are used in various flexible packages, such as wrappings, pouches and bags. In packages, the most important function of a packaging material is to shield the product inside the package. Plastic films give a barrier against water, water vapor, aroma, grease, oxygen, etc. In addition to barrier properties, printability is an important property in packaging applications, and especially in labels. In inkjet printing, the controlled spreading of the low viscosity ink on the substrate is essential for satisfactory print quality. This requires suitable absorption properties and controlled surface chemistry. From the point of view of printing, the dense and impervious structure of plastic film is challenging: printing inks do not penetrate into the substrate. When polymer surfaces, like plastic films, are printed, adhesion of the printing ink is essential. Durability of the printed image is important, because the image must withstand various converting operations when the package is constructed. Also the end-use of the material (label or package) requires both durability and high visual print quality.

Surface treatments are used in order to produce special functional groups at the surface for special interactions with other functional groups and to increase the surface energy. The objective in this study was to compare traditional corona treatment to a novel roll-to-roll atmospheric plasma treatment (APT). The APT process offers unique advantages over existing technologies for surface treatment such as corona including more uniform and longer lasting treatment. Plasma treatment activates the surfaces without affecting the reverse sides of the substrates. Plasma also allows tailored surface activation by using different process gases, like helium and argon. Furthermore, the aim was to evaluate the effect of surface treatments on the surface properties and inkjet printability of polypropylene (PP) film.

**Keywords:** atmospheric plasma treatment; corona treatment; inkjet printing; packaging; plastic film

## 1. Introduction

Plastic films are used besides in labels, also in various flexible packages, such as wrappings, pouches and bags. In packages, the most important function of a packaging material is to shield the product inside the package. Plastic films give a barrier against water, water vapor, aroma, grease, oxygen, etc. In addition to barrier properties, printability is an important property in packaging applications, and especially in labels. From the point of view of printing, the dense and impervious structure of plastic film is challenging: printing inks do not penetrate into the substrate. Durability of the printed image is important, because the image must withstand various converting operations when the package is constructed. Also the end-use of the material (label or package) requires both durability and high visual print quality.

In inkjet printing, the controlled spreading of the low viscosity ink on the substrate is essential for satisfactory print quality. This requires suitable absorption properties and controlled surface chemistry. Dense

and smooth polymeric surfaces very often do not possess such surface properties, because of low surface energy, incompatibility, chemical inertness, or the presence of contaminants and weak boundary layers. When polymer surfaces, like plastic films, are printed, adhesion of the printing ink is essential. Surface treatments are used in order to produce special functional groups at the surface for special interactions with other functional groups, increase the surface energy, introduce surface cross-linking, modify the surface morphology by increasing or decreasing surface crystallinity or roughness, and to remove contaminants or weak boundary layers. Many processes have been developed to modify polymeric surfaces, including flame, corona and plasma treatment. These processes generally alter physical or chemical properties of a thin surface layer without affecting bulk properties. These treatments increase the surface energy and also provide polar molecular groups necessary for good bonds between ink and polymer molecules. [1-8]

The objective in this study was to compare traditional corona treatment to a novel roll-to-roll atmospheric plasma treatment (APT). The APT process offers unique advantages over existing technologies for surface treatment such as corona including more uniform and longer lasting treatment. With plastic films, the most important advantage is the lack of backside treatment, because in plasma treatment there are no breakdowns through the material. Plasma treatment activates the surfaces without affecting the reverse sides of the substrates. Plasma also allows tailored surface activation by using different process gases, like helium, argon and nitrogen. [3, 5-8]

Furthermore, the aim was to evaluate the effect of surface treatments on the surface properties and inkjet printability of polypropylene (PP) film. The influence of corona and plasma on the surface energy of PP film has been evaluated with contact angle measurements. In addition, the effects of the surface treatments on the surface chemical composition of the polymeric surfaces have been evaluated with XPS. The effect of plasma activation on inkjet print quality was studied by using UV curable inks with controlled surface tension levels and PP plastic film substrates. The positive effects of plasma treatment compared to corona treatment such as uniformity of treatment, better bonding potential resulting in improved ink adhesion, and permanence of treatment were expected to translate into improvements in parameters typically representative of print quality.

## 2. Materials and methods

The surface of multilayer polypropylene (PP) film (thickness 50 μm) from UPM Raflatac Oy was surface treated in the coating pilot line at Tampere University of Technology (TUT). Roll-to-roll corona and atmospheric plasma treatments (Vetaphone A/S) were used to modify the surface of the PP film (Table 1, Figure 1). Helium and argon were used as process gases in the plasma treatment. The efficiency value E (Wmin/m$^2$) of corona and plasma treatment is evaluated with the following formula:

$$E = \frac{P}{l \cdot v}$$

$$(1)$$

where P (W) is the output of corona power supply or power of flame , l (m) is the width of the electrodes (corona) or burner (flame) and v (m/min) is the line speed.

*Table 1: Surface treatment parameters*

|                | Power  | Line speed | Treat.width | Efficiency value        | Gas feed | Frequency |
|----------------|--------|------------|-------------|-------------------------|----------|-----------|
| **Corona**     | 1300 W | 50 m/min   | 500 mm      | 52.2 Wmin/m$^2$         | –        | 24.8 kHz  |
| **Helium plasma** | 1020 W | 50 m/min   | 380 mm      | 53.7 Wmin/m$^2$         | 90 l/min | 28.1 kHz  |
| **Argon plasma**  | 915 W  | 50 m/min   | 380 mm      | 48.2 Wmin/m$^2$         | 30 l/min | 28.6 kHz  |

Surface energy levels of the samples were defined by measuring the contact angle of water on the substrate surface. The measurements were made with a KSV CAM 200 Optical Contact Angle Meter. The samples were stored in a constant laboratory environment (23°C, 50% RH).  Changes in chemical composition of the substrate surfaces due to treatments were determined with x-ray photoelectron spectroscopy (XPS) using a Physical Electronics Quantum 2000 ESCA instrument, equipped with a monochromatic Al Kα x-ray source, operated at 25 W of power. Three different spots were measured in each sample. The pass energy for the survey spectra was 184 eV, and the measurement time was five minutes.
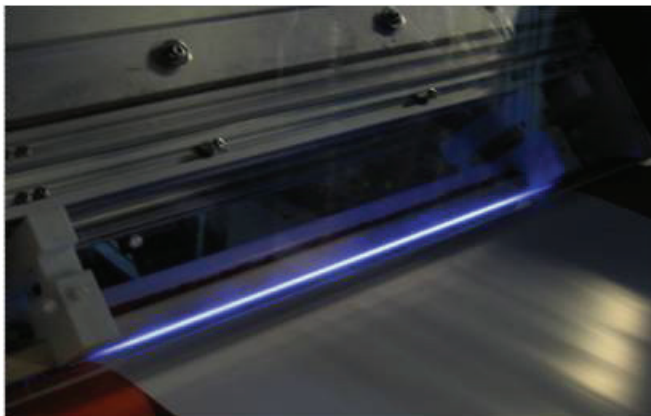
*Figure1: Atmospheric plasma treatment unit at TUT pilot line*

Inkjet printing parameters, such as resolution, printhead, printing speed and UV-curing, were set up to simulate an industrial printing situation as well as possible. A FUJIFILM Dimatix Apollo II PSK/iTi XY MDS2.0 printer driving a FUJIFILM Dimatix SL-128 printhead with a drop volume of 80 pL and native resolution of 50 dpi was used. UV curable model inks with varying surface active monomer and surfactant content, prepared by Sun Chemical Ltd., were used. An inline UV curing device from Integration Technology (Vzero 085) was used to cure the ink. The printed test image contained 100% coverage areas and 1 pixel lines, which allowed for studying of the ink-substrate interaction, such as how much the ink spreads (line width) and how uniformly the spreading occurs (line edge raggedness) before immobilization by UV curing. Measurements were carried out using a QEA Scanner IAS image analysis system, which uses algorithms based on the ISO-13660 print quality standard. Ink adhesion was evaluated by means of a tape test, where the results were quantified based on a subjective visual inspection of the tested samples. Conventional mottling/graininess analysis was also anticipated to give an indication of how homogeneous the effect of the plasma surface treatment is.

## 3. Results and Discussion

### 3.1 Treatments' effect on substrate

The treatments' effects on the substrate surfaces were characterized by XPS analysis and contact angle measurements. According to the contact angle measurements, all treatments increase the surface energy of the PP film (i.e. decrease the contact angle of water) (Figure 2). As can be seen in surface chemical composition analysis made by XPS (Figure 3), the argon plasma increases the O/C ratio the most, while corona treatment oxidizes the surface to a lesser extent. The helium plasma increased the O/C ratio least. This result did not correlate with the contact angle results. However, the changes between the treated samples were minimal. No oxygen was observed on the untreated substrates. In previous studies [1, 9, 10] it has been observed that corona treatment produces a less uniform treatment effect compared to plasma treatments.
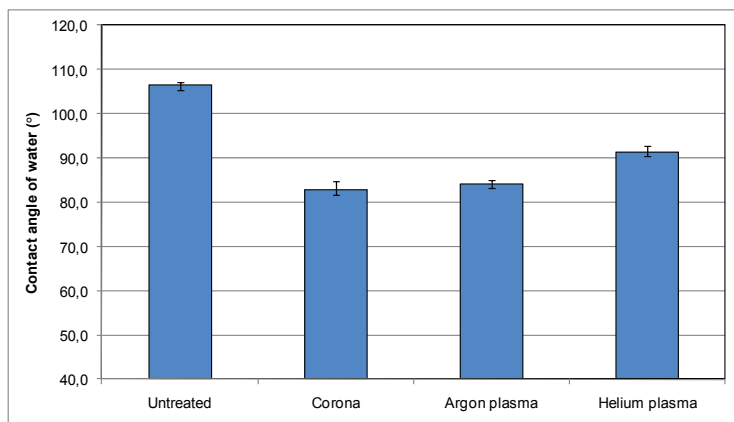


*Figure 2: Contact angles of water for corona and plasma treated surfaces*
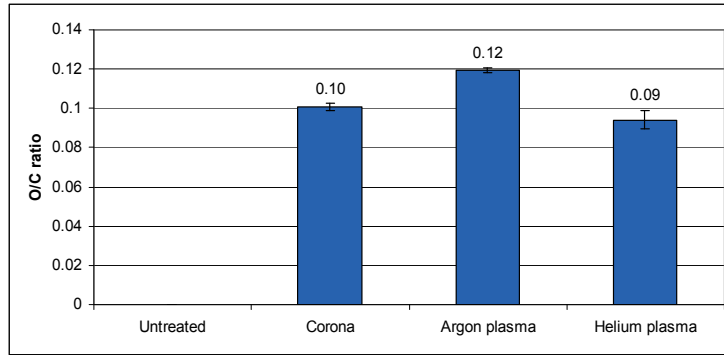
*Figure 3: O/C-ratio of corona and plasma treated surfaces*

## 3.2 Print uniformity

The 1 pixel print process direction lines (Figure 4) scanned at 1600 dpi, printed with the lower surface tension (26 mN/m) ink on untreated, corona and argon plasma treated substrates, clearly show that argon plasma treatment enhances ink wetting and uniformity of the printed lines.



*PP film / 1 pixel line width / 300 dpi /*
*UV ink with decreased surface tension*

*Figure 4: UV-inkjet printing on corona and plasma treated surfaces*

These visual observations were supported by image analysis data, as argon plasma treatment's strong effect on surface chemical uniformity was evident in line edge raggedness data (Figure 5), which shows a clear decreasing trend from untreated to corona and argon plasma treated substrates, with both inks showing similar behavior. Edge raggedness levels are lowest for the lower surface tension ink. An increase in O/C ratio from corona to argon plasma treated substrates, as shown in Figure 3, leads to a decrease in line edge raggedness. In addition to the O/C ratio being highest for argon plasma treated substrates, O/C ratio deviation is also lower for argon plasma than for corona treated substrates, which again indicates better uniformity of argon plasma treatment. Mottling/graininess analysis was not successful due to a strong banding effect in full coverage printed areas, which was a result of the multiple pass scanning type printing done by the XY printer.
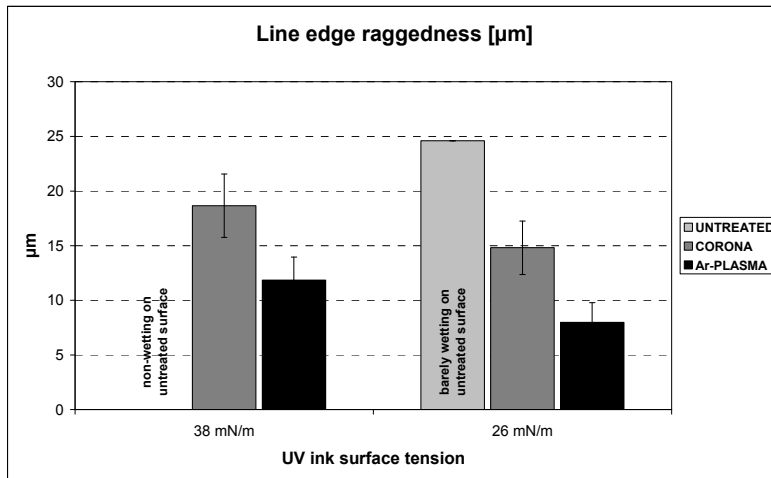
*Figure 5: Line edge raggedness values for substrate treatments using UV curable inks with different surface tension levels*

Line width results in Figure 6 show the enhanced wetting effect of the corona and argon plasma treatments. On the untreated substrate, the lower surface tension ink just barely wets the substrate enough to form a uniform continuous line, the higher surface tension ink being completely non-wetting. However, line edge raggedness remains high, indicating that in any case there is a need for enhanced uniformity of ink wetting. As expected, line width increases as a result of corona and argon plasma treatment, due to an increase in surface energy. However, based on the contact angle measurements (Figure 2), wetting and spreading (i.e. line width) of the corona and argon plasma treated substrates was expected to be roughly at the same level. For the ink with lower surface tension, the difference is indeed almost within standard deviation, but for the higher surface tension ink, the difference is more distinct. Line width standard deviation values for argon plasma treated substrates compared to corona treated substrates are slightly lower, also supporting the hypothesis of a more homogeneous treatment effect with argon plasma activation over corona treatment.
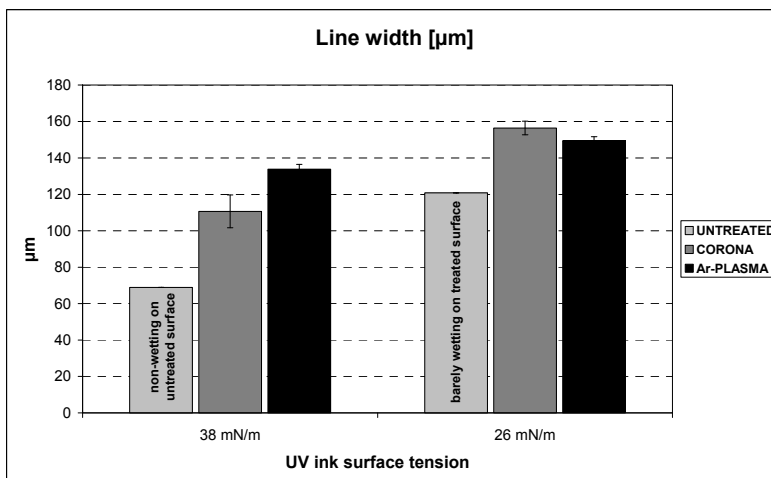


*Figure 6: Line width values for substrate treatments using UV curable inks with different surface tension levels*

## 3.3 Ink adhesion

Adhesion results are in line with O/C ratio measurements, indicating that argon plasma treated substrates may give slightly better ink adhesion than corona treated substrates through increased bonding potential. In Figure 7, the lowest score indicates the best adhesion. Although the ink having higher surface tension shows slightly better adhesion overall, for both inks, surface treatment is essential and argon plasma activation is slightly more effective than corona treatment. It must be taken into consideration that adhesion is also strongly influenced by the degree of curing. Detailed analysis on the optimum UV dosage required for the two inks was not done. However, the curing dosage which was based on an industrial process and similar inks did ensure complete curing of both ink layers.
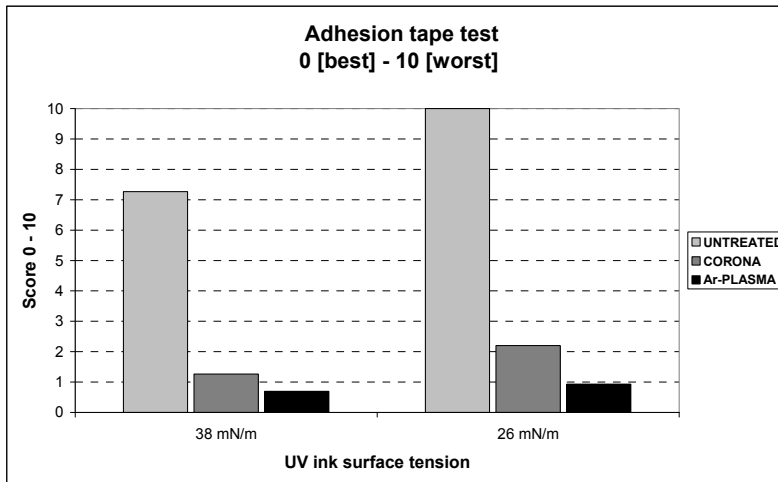
*Figure 7: Adhesion values for substrate treatments using UV curable inks with different surface tension levels*

## 4. Conclusions

Converting processes and end-use of packaging films set quite high demands for polymeric surfaces and printed images. Adequate ink adhesion and visual print quality are important elements in various packaging applications. High enough surface energy and functional chemical groups are necessary for uniform print quality and ink adhesion. Some polymeric surfaces have suitable surface properties without any surface treatments, but for example low surface energy surfaces, like PP, need surface modification in order to succeed in the ink jet printing process and to produce good print quality.

This study demonstrates that the surface treatments clearly increase surface energy (i.e. decrease the water contact angle) of PP film by introducing oxygen-containing molecular groups on the surface. As a more novel knowledge, this paper presents the atmospheric plasma treatment as a roll-to-roll process and the benefits of this treatment over corona. Surface analysis with XPS shows that argon plasma oxidizes PP surface more than corona and thus, it is the most effective treatment for PP. With UV-curable inks, argon plasma activation had a positive effect on both visual print quality and ink-substrate adhesion:

→ Improved print uniformity over corona treatment through improved surface chemical uniformity
→ Improved ink adhesion over corona treatment through improved bonding potential.

### Acknowledgements

### References

[1] J. Lahti, Dry Toner-Based Electrophotographic Printing on Extrusion Coated Paperboard, PhD Thesis, Tampere University of Technology, Tampere, Finland (2005).

[2] C. S. Leech, Screen Printing Magazine. January, 52-55 (1991).

[3] J. Kuusipalo (Ed.), Paper and Paperboard Converting, Book 12, 2nd Edition. Gummerus Printing, Jyväskylä, Finland (2008).

[4] K. L. Mittal (Ed.), Contact Angle, Wettability and Adhesion, Vol. 4, VSP-An Imprint of Brill (2007).

[5] C. M. Chan, Polymer surface modification and characterization. Carl Hanser Verlag, Munich, Vienna, New York (1994).

[6] L. Černaková, P. St´ahel, D. Kováčik. D. Johansson. M. Černak, in: TAPPI European Place Conference, Turku, Finland (2006).

[7] M. C. Coen, G.Dietler, S. Kasas, P. Gröning, Applied Surface Science. 103 (1996) 27-34.

[8] J. B. Lynch, P. D. Spence, D. E. Baker, A. Postlethwaite, Journal of Applied Polymer Science, 71 (1999) 319-331.

[9] J. Lahti, M. Tuominen, 2009 TAPPI European Polymers, Laminations and Coatings Conference Proceedings, Budapest, TAPPI PRESS, Atlanta, Georgia, 2009, pp. 1-17.

[10] M. Tuominen, J. Lahti, J. Lavonen, J. Räsänen, T. Penttinen, J. Kuusipalo, Journal of Adhesion Science and Technology 24(2010) 471-492.

**3**

*Improving the
printing process*

# Tailored magazines distribution workflow and data communication between a publisher, a printing house and distribution organisation(s)

*Olli Kuusisto*

VTT Technical Research Centre of Finland
P.O. Box 1000, FIN-02044 VTT, Finland
E-mail: olli.kuusisto@vtt.fi

**Abstract**

This paper describes the work done in a project which focused on compiling inventory of data needs in operational networks for the distribution of tailored magazines production process, defining new demands for control, and developing a demonstration system for the data communication in the distribution of tailored magazines The project extended previous work done in workflow control between a publisher and a printer.

Characteristics of modern supply chain management include the different activities and their functions to be described, and that the systems involved communicate with each other in desired extent thus making the operation transparent to participating parties. This is not the case in the magazine supply chain. Data is communicated between publisher, printing house and delivery organisations. However, despite that the data can mainly be found from the various systems involved the data communication occurs mainly manually and the supply chain is not transparent.

**Keywords:** magazine workflow; tailored magazines; publishing; printing; distribution; JDF

## 1. Introduction

The main parties of magazine supply chain are publishers, printing houses and distribution organisations. In a previous project the workflow and mainly manual data communication between a publisher and a printer was examined and a data communication demonstration system using JDF specification was set up. The project showed that there is much development potential in data communication and automatisation between the parties. The demonstration system covered information from the product structure and production to delivery from the printing house to distribution organisations. During that project it was discovered that some of the same information - and more - is needed in especially postal distribution of the magazines, and that there might be opportunities for better data communication and getting control of the whole supply chain.

Edition versions and delivery lots having different cover and body versions together with tailored inserts leading into several edition versions and delivery lots can be specified and a corresponding JDF-file printed. There may be more delivery lots than edition versions.

Tailoring ie. different magazine versions are mostly based on specific target groups advertisers want to reach, but sometimes also editorial content is tailored. Tailored magazines increase delivery lots in subscription edition if different versions cannot be bundled selectively so that one bundle contains different versions. This in return increases distribution costs which are commonly based on the amount of delivery lots, delivery lot size and the extent of needed sorting, which has lead into low usage of versioning. There is a need to develop the distribution process with timely and precise data communication along with developing new operations models.

There are following trends to be taken into account in efficient supply chain management:
- Communicating between organisations and systems must be enabled.
- The share of agile services will grow.
- The share of embedded technology and systems will grow.
- Data collection and communication will be automated which will increase the transparency of the supply chain.

Supply chain development demands partners to have a comprehensive view of the whole supply chain and that the information is as real-time as possible. Only then can the different actors optimize their operations.

Besides common grammar, syntax, communication between information systems needs uniform vocabularies. There are eg. over 500 different branch-specific vocabularies built on XML-language. JDF (Job Definition Format) is an XML-based vocabulary designed to simplify information exchange between different applications and systems in and around the graphic arts industry. The vocabulary ensures standardized integration, where JDF-based information about the product and production can be communicated between different systems. CIP4 organization is responsible for the creation and development of the JDF specification.

## 2. Implementation

### 2.1 Magazine distribution workflow

Magazine publication planning is made in long term, usually yearly, cycles. Typically this includes information such as the number of issues, format, paper grades and binding types together with estimated print runs, number of pages and issue dates. This information acts as basis for both printing houses and distribution organisations as they allocate resources for the job. The process is scheduled backwards from the issue date of the publication and usually issue-specific schedules are made both for distribution and printing of the job. Magazine publishers agree the delivery times and other things concerning the distribution of magazines in advance. Publishers are responsible of communicating updated information about the upcoming issues.
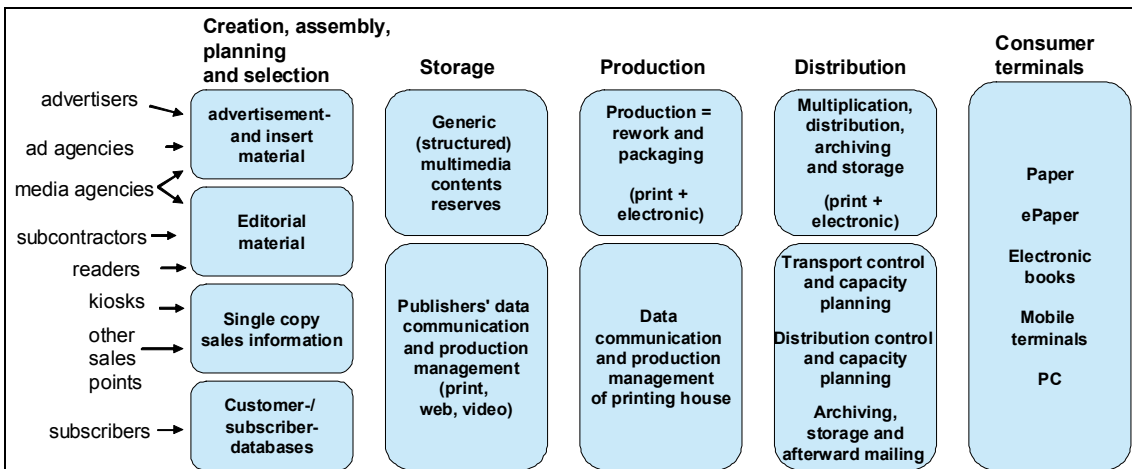


*Figure 1: A simplified generic and print-based model of magazine production and distribution*

Distribution of magazines can be divided into three categories: subscription-based, single-copy and other distribution, the latter meaning distribution for own organisation, exhibitions etc. This paper handles the subscription-based ie. postal distribution which is more complicated process than the others, especially concerning tailored magazines. In postal distribution it must be ensured that each subscriber gets his or her own copy, being also right version if the magazine is tailored. In this paper postal distribution consists - in addition to the actual home delivery to subscribers - of transports and sortings, which both may occur in several steps eg. main and local transports, bundle and magazine sorting.

Especially postal distribution organisations need information about possible changes in the print run, the amount of pages, and tailoring, as these affect the resources needed to transport, sort and deliver magazines to subscribers. Tailoring can cause significant changes which may add up - changes coming from various customers - to major reallocations of workload. Postal distribution organisations have company-specific practices in regard to bundling and unitizing (packing bundles into transport units), marking them and communicating data about delivery lots. In practice, it is often the printing house or other mailer, which communicates the realized amounts and other data about delivery lots to postal distribution organisations.

In Finland, Itella is at present the only daily mail service provider, but the situation may change when EU's postal opening is implemented. Within Itella's process different delivery lots form several transport units/bundles to be carried to the same area with different products inside, eg. with or without an insert. This leads into increased amount of sorting of bundles and magazine copies. One aim is to do as much sorting as early in the process as possible, preferably already at the printing house. In any case, delivery lot data is ne-

eded at postal distribution organisation(s). Itella's general process regarding magazine distribution functions as presented in figure 2.
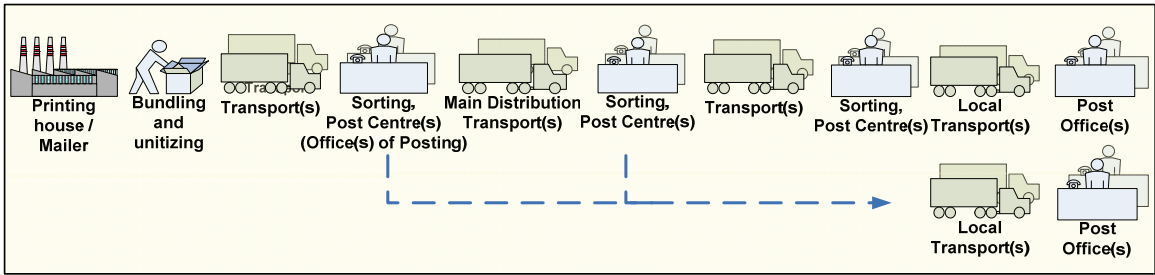


*Figure 2: General presentation of magazine distribution process at Itella from printing house to Post office(s)*

In bundling and unitization the aim is to produce as many transport units and bundles as possible to go directly as far as possible before sorting. The bundle size is affected by the unit weight, thickness and the paper types of the main product in addition to different inserts, their thickness, weight and form. The bundling and unitization work which is done at printing houses is sorting prework which reduces work of distribution organisation.

## 2.2 Needs for development

The present state and needs for development were analyzed. Based on visits and discussions in the participating companies, the main development potential lies in data communication between parties.

The budgeted information about an issue may change considerably during the year depending on the amount of subscribers, advertisers' campaigns, and special numbers. As the information becomes more precise, it should be communicated to printing house and postal distribution organisation(s). This - besides bilateral agreements on major changes - ensures that enough resources are available for printing, transport and distribution of the issue. In practice changes are seldom communicated to postal distribution organisation(s) as also printing houses often lack that information. Main reason for this is that the information is scattered to many systems and departments at the publisher, and informing demands extra work for first getting all relevant data and then communicating it manually to both printing house and postal distribution organisation(s). All parties also have several contact persons. At Itella, information from the long-term contract is fed into their internet sales system and issue-specific electronic dispatch lists are made. The publisher can update this information through web interface while the printing house / mailer enters the realized data into Itella's system when mailing the delivery lots.
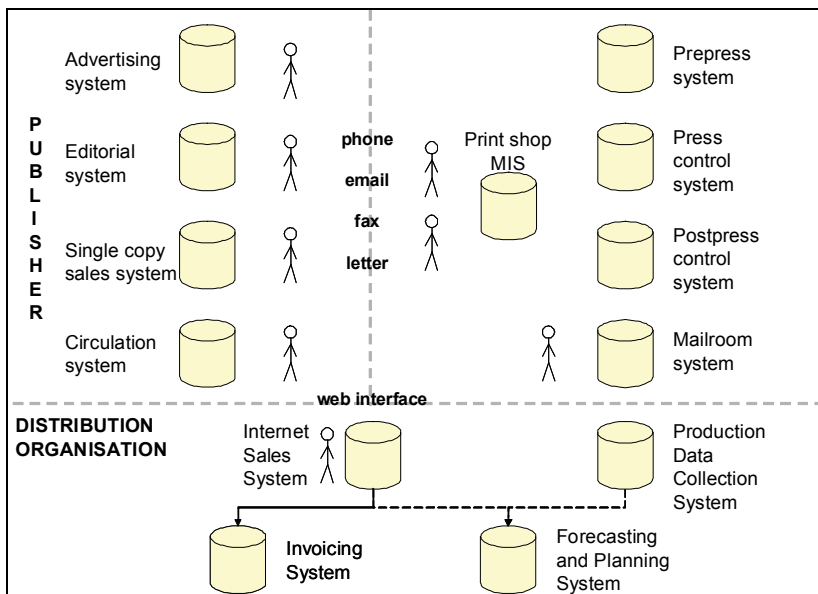


*Figure 3: The present communication methods between publisher / printing house and distribution organisation*

In short, the present information exchange includes manual phases, is mostly unidirectional and electronic data communication practices are not specified. Communication to postal distribution organisation(s) takes place mostly manually before the realized distribution information is fed into the system of distribution organisation by the printing house. As stated before, all changes are not communicated at all, not even to the printing house.

Hence, the progress in supply chain is not transparent and none of the parties has a clear view of it. This is emphasized especially when changes or deficiencies occur.

## 3. The applicability of JDF vocabulary in magazine distribution

JDF is an industry standard designed to simplify information exchange between different applications and systems in and around the graphic arts industry (figure 4). It is a comprehensive XML-based file format and proposed industry standard for end-to-end job ticket specifications combined with a message description standard and message interchange protocol. JDF is designed to streamline information exchange between different applications and systems thus allowing integration of heterogeneous products from diverse vendors to create seamless workflow solutions. It is intended to enable the entire industry, including media, design, graphic arts, on-demand and e-commerce companies, to implement and work with individual workflow solutions. (CIP4)

JDF contains delivery information from the printing house to distribution organisation(s). It does not support further distribution process and information required for it, which postal distribution organisations require.
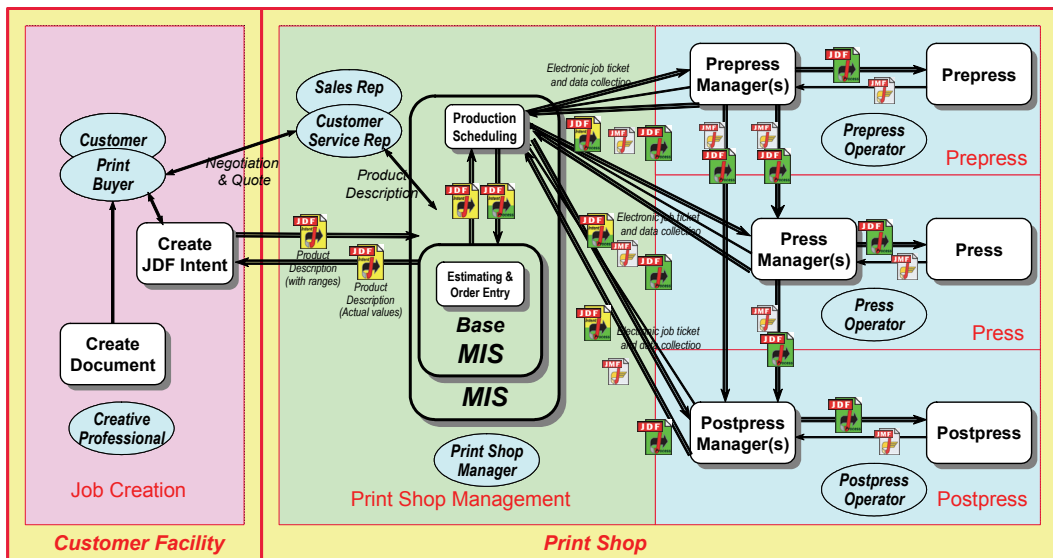


*Figure 4: CIP4 Reference model*

A general data communication model based on the information needed for magazine distribution was made along with an Itella-specific more extensive model. The information in the former one could be described using JDF while the additional information needed by Itella demanded the use of own JDF-extensions. Another option in the future is the use of UPU's (Universal Postal Union coordinating worldwide postal) EPPML-standard (Extensible XML-based Postal Product Description Model and Language) which is in the making.

## 4. Demonstration system (Results)

### 4.1 Setting up the demonstration system

General information about postal distribution can be described with JDF using DeliveryIntent resource when coming from the publisher, the mailer (printing house) may use also JDF process resources instead of intent resources.

A small-scale web-based demonstration system applying JDF specification for communicating the postal information needed for distribution of a specific issue of magazine was set up. In the demonstration system, all information is fed manually, but a requirement specification for a productional system was made. This system can act as stand-alone system (users being publishers and printing houses) or it can be integrated to the previous demonstration system for communicating product structure and production data.

Two versions of postal distribution information data were constructed. The generic distribution data for a generic postal operator includes basic data. The more detailed information needed by national post operator Itella includes - besides the general model data - following information for each delivery lot:

```
- <Component Class="Quantity" ComponentType="FinalProduct" DescriptiveName="Final Product"
      ID="ID_FinalProduct" PartIDKeys="Edition" Status="Unavailable">
    <Component DescriptiveName="Tilaajapainos 1" Edition="TP1" ResourceWeight="30" />
    <Component DescriptiveName="Tilaajapainos 2" Edition="TP2" ResourceWeight="35" />
    <Component DescriptiveName="Tilaajapainos 3" Edition="TP3" ResourceWeight="40" />
  </Component>
- <DeliveryIntent Class="Intent" ID="ID_DeliveryIntent" PartIDKeys="Edition" Status="Available">
    - <DropIntent>
    <Method DataType="NameSpan" Preferred="BestWay" />
    <Required DataType="TimeSpan" Preferred="T00:00:00+02:00" />
      - <DropItemIntent Amount="10000">
            - <ComponentRef rRef="ID_FinalProduct">
            <Part Edition="TP1" />
            </ComponentRef>
      </DropItemIntent>
    - <Comment ID="ID_C_DropIntent_1">
    <itellaext:LineIdentifier>1</itellaext:LineIdentifier>
    <itellaext:ProductIdentifier />
    - <itellaext:AdditionalProducts>
    <itellaext:AdditionalProductCode />
    <itellaext:AdditionalSubProductCode />
    </itellaext:AdditionalProducts>
    <itellaext:ProductNameText />
    <itellaext:InformationCode />
    <itellaext:BatchIdentifier />
    <itellaext:ZoneCode />
   <itellaext:UsageCode />
    <itellaext:AbcSortingCode />
    <itellaext:DeliveryIdentifier />
    <itellaext:Directions />
    <itellaext:UnitSize />
    <itellaext:LocalDelivery />
    <itellaext:InfoserviceUsage />
    </Comment>
  </DropIntent>
</DeliveryIntent>
```

## 4.2 Feedback and comments of the demonstration system

The validity of the JDF-file created by the demonstration system has been checked with CheckJDF Server of CIP4. The demonstration system made by the requests by participating companies has been introduced to them in the end of June 2010. Feedback has not yet been received.

Internally, following remarks have been made to be taken account with a production system:

- permitted values should be specified in advance for all information (besides the type eg. an integer or decimal number, also rational min and max limits with alert in order to minimize human errors
- there should be more automation eg. in calculating the amounts of the editions
- after final confirmation the distribution data should be locked
- there should be proactive alerts based on the agreed schedule of communicating the information to distribution organisation
- the access right management should be implemented regarding to seeing and sending the information
- the user interface should be made based on the access rights, ie. the user should see only the information that is relevant to him/her in order to minimize the amount of human errors

## 5. Results

The tailored magazine distribution process was modelled and the information needed for the distribution of a magazine issue was determined in co-operation with the participating companies. The appropriate general JDF counterparts were documented with extensions for Itella-case which - in future - could be substituted by UPU's EPPML-standard which is in preparation. The general distribution data of tailored magazines turned out to be fairly easy to define with JDF. The more important matter is to get the whole supply chain integrated so that data communication is bidirectional. This way the costs of retrospectively disentangling unclarities in the process can be avoided and flexible operations models adopted. Development suggestions for JDF specification were not made as postal operations belong more to UPU's field of activities.

A web-based application was set up to demonstrate the determination and communication of the distribution data of tailored magazines with various delivery organisations. The general version uses standard JDF while Itella-specific implementation has own extensions.

The demonstrated system would probably not be feasible as a stand-alone system but would greatly benefit as part of publishers product control and procurement system which was demonstrated in a previous iarigai paper (Kuusisto et al, 2008), as the process would be transparent and controllable. Furthermore, the communication should be bidirectional so that the publisher would be able get real-time data of the progress of distribution in addition to quality data of the performance.

During the project an alternative method - sorting service -  was developed and tested by Itella. It is based on the fact that much of the information is specific to delivery organisation - mainly information about the distribution structure, which makes it more difficult to flexibly change the structures based on demand. Sorting service accepts basic information about delivery lots and communicates bundling and unitization data in return. This way the mailer (here: the publisher) doesn't have to know about the distribution structure and delivery organisation can flexibly adjust the structure and resources according to demand. Furthermore, a preliminary solution for selective posting was developed to be tested. Both alternative models require also data communication.

## 6. Conclusions

Efficient networked operation between organisations needs new operations models and information technology solutions. In order to overall ensure efficient and agile operations the whole supply chain needs be to be managed. This emphasizes the importance of information systems as digitalisation of information accelerates the versatile exploitation and supply chain transparency in the network. In the future, networks will operate more and more with other networks which will demand for compatible technological solutions.

Characteristics of modern supply chain management include the different activities and their functions to be described, and that the systems involved communicate with each other in desired extent thus making the operation transparent to participating parties. This is not the case in the magazine supply chain. Data is communicated between publisher, printing house and delivery organisations. However, despite that the data can mainly be found  from the various systems involved the data communication occurs mainly manually and the supply chain is not transparent.

At present the information needed for the postal distribution of a magazine issue is a) situated scattered in the various software systems of the publisher and b) stored at the systems at the delivery organisation. This leads into a situation where the publisher does not communicate neither receive data about the postal distribution, and eventual verifications need to be settled manually. With present systems and communication methods between the publisher, the printing house and the postal operator, the distribution data might be inconsistent.

The small-scale demonstration indicated that needed postal distribution data can be composed by using JDF. The parties have the basic information based on long-term contracts. When that information changes, the publisher can send JDF files about more defined information.

The next step would be to implement the demonstrated system in practice to communicate the postal distribution data together with previously demonstrated publisher's product control and procurement data system.

## Acknowledgements

## References

CIP4, JDF Specification, www.cip4.org.

Kuusisto, Olli; Antikainen, Hannele; Pajukanta, Janne, (2008). Magazine product structure and workflow control between a publisher and a printing house. Advances in Printing and Media Technology, Vol. XXXV, Proceedings of the 35th International Research Conference of iarigai, pp. 91-100. Darmstadt 2008.

# Implementing ISO12646 standards for soft proofing in a standardized printing workflow according to PSO

*Aditya Sole, Peter Nussbaum and Jon Yngve Hardeberg*

The Norwegian Color Research Laboratory
Dept. of Computer Science and Media Technology
Gjøvik University College, Norway

E-mails: aditya.sole@hig.no, peter.nussbaum@hig.no, jon.hardeberg@hig.no

**Abstract**

This paper defines one of the many ways to setup a soft proofing workstation comprising of a monitor display and viewing booth in a printing workflow as per the Function 4 requirements of PSO certification. Soft proofing requirements defined by ISO 12646 are explained and are implemented in this paper.

Nec SpectraView LCD2180WG LED display along with Just colorCommunicator 2 viewing booth and X-rite EyeOne Pro spectrophotometer are used in this setup. Display monitor colour gamut is checked for its ability to simulate the ISO standard printer profile (ISOcoated_v2_300_eci.icc) as per the ISO 12646 requirements. Methods and procedures to perform ambient light measurements and viewing booth measurements using EyeOne Pro spectrophotometer are explained. Adobe Photoshop CS4 software is used to simulate the printer profile on to the monitor display, while, Nec SpectraView Profiler software is used to calibrate and characterize the display and also to perform ambient light and viewing booth measurements and adjustments.

**Keywords:** colour measurement; colour management; process control standards; soft proofing; display calibration; display characterisation

## 1. Introduction

To reduce expensive and time consuming iterations in standardized printing workflow soft proofing has become unimportant concept in predicting the final print product. Soft proofing can be defined as 'the ability to match colour images displayed on colour monitors to the images produced when the same digital file is rendered by proofing and printing systems' (ISO12646 2008). However, although the concept soft proofing is not new and the task may sound rather simple, in practical applications the colour appearance between two different medias (e.g. softcopy simulation of a hardcopy) can differ a lot due to unsuitable type of devices, incorrect use of parameters and inaccurate device calibration and characterization or inappropriate measurement methods. In the past a number of studies and research work have addressed the issue of soft proofing. For more details see the work of (Gatt et al. 2004) and (Gatt et al. 2005).

ISO 12646 defines parameters for monitor and viewing booth condition setup for soft proofing environment. The practical methods to implement these standards as per the job requirements are not been clearly defined. This paper therefore is aiming for to describe in details one of the ways to setup an appropriate soft proofing station (comprising of a monitor and a viewing booth with the appropriate ambient lighting conditions) according to ISO 12646 standards for soft copy and hard copy proof comparison in the graphic arts industry and evaluate the performance of the entire soft proof set up according to ISO 12646. This is also in accordance with soft proofing in a standardized printing workflow according to PSO (UGRA 2009).

In this work the current standards and the appropriate parameters for soft proofing are reported before proposing the method of implementing these standards.

## 2. Methods

### 2.1 Standards for soft proofing (specifications)

ISO 12646 specify the soft proofing standards. This standard describes two scenarios. The first scenario consists of comparing a soft copy directly with a hard copy while the second scenario consists of viewing soft copy images on a display independently of any hard copy images. This paper primarily focuses on the first scenario where soft copy is directly compared with the hard copy.

The technical requirements defined by ISO 12646 for scenario 1 i.e. comparing a soft copy with a hard copy are as follows:

### Ambient illumination, surroundings and environment

The level of ambient illumination should be sufficiently low. The standards recommend for "luminance of a perfectly reflecting diffuser placed at position of the faceplate of the monitor, with the monitor switched off, shall not be greater than ¼ of the monitor white point luminance and should not be greater than 1/8 of the monitor white point luminance" (ISO 12646, sec 4.7.2)

The colour temperature of the ambient light, such as room light, should be within ± 200°k of the colour temperature of the illumination used in the viewing booth. The conditions within the viewing booth shall conform to viewing condition P2 of (ISO3664 2009)(ISO 12646, sec 4.7.2). P2 viewing conditions are defined as the conditions for practical appraisal of prints, including routine inspection.

The luminance of the area surrounding the monitor shall not exceed 1/10 of the luminance of the monitor showing a white screen. Extraneous light, whether from light source or reflected by objects, shall be baffled from view and from illuminating the print or other image being compared (ISO 12646, sec 4.7.2). The surround and backing shall be neutral and matt (ISO 3664, sec 4.3.4). The surround shall have a luminous reflectance between 10% and 60% with the specific value being selected to be consistent with practical viewing.

### Chromaticity, luminance of the white and black points

The black point of the display shall have a luminance that is less than 1% of the maximum luminance of the display (ISO 12646, sec 4.8.1).

The conditions within the viewing booth shall conform to viewing condition P2 of ISO 3664 (ISO 12646, sec 4.8.2). P2 viewing conditions specify conditions applicable for the appraisal of tone reproduction of individual images, photographic image inspection or the judgement of prints. The illumination of the plane of viewing shall approximate that of CIE standard illuminant D50. It shall have $u'_{10}$, $v'_{10}$ chromaticity co-ordinates within the radius of 0.005 from $u'_{10} = 0.2102$, $v'_{10} = 0.4889$ in the CIE 1976 Uniform Chromaticity Scale (UCS) diagram (calculations using the 10° observer angle). The illuminance at the centre of the viewing surface shall be (500 ± 125 lux). The illumination uniformity should be such that for a viewing area up to $1m^2$, the illuminance at any point within the illuminated area shall not be less than 75% of the illumance measured at the centre of the illuminated viewing surface area. The uniformity should be evaluated by measuring at least 9 points equally distributed on the viewing surface (ISO 3664, sec 4.3.3).

The luminance of the white displayed on the monitor shall be at least 80 $cd/m^2$ but preferably 160 $cd/m^2$ in order to match an unprinted sheet of white paper located close to monitor having an illuminance of 500 lux, as specified in ISO 3664 for viewing condition P2 (ISO 12646, sec 4.8.2).

ISO 12646 recommends D50 as white point for the soft proofing display (as the white point in the viewing booth is D50); namely $u'=0.2092$, $v'=0.4881$, as specified in CIE Publication 15 (CIE15 2004). The chromaticity obtained, for the white point chosen shall be within a circle of radius 0.005 from this point (ISO 12646, sec 4.8.2).

### Colorimetric accuracy and grey balance of the display

Tristimulus values shall be measured for at least 10 neutral colours (R=G=B). For each neutral colour the colour difference, $\Delta E^*_c = \sqrt{(\Delta a^2 + \Delta b^2)}$, where $\Delta a$ is the difference for the CIELAB (red-green) co-ordinate and $\Delta b$ is the difference for the CIELAB (yellow-blue) co-ordinate, shall be calculated between these measured CIELAB values and the CIELAB values which are intended to be displayed by the software characterizing the display. The average deviation shall not exceed $\Delta E^*_c = 3$ and preferably not $\Delta E_c = 2$ (ISO 12646, sec 4.10).

The average of the $\Delta E^*_{ab}$ between the measured CIELAB values and the CIELAB values intended to be displayed by the *.icc monitor profile shall not exceed $\Delta E^*_{ab}$ 5 and preferably not $\Delta E^*_{ab}$ 2 units respectively.

### Uniformity of display luminance

The display should be visually uniform when displaying flat white, grey and black images. All the measured luminance values should be within 5% of the luminance of the centre and shall be within 10% of it (ISO 12646, sec 4.4).

Table 1 below summarizes the specification and tolerances defined by ISO 12646 standards for soft proofing.

*Table 1: Specification and tolerances according to ISO 12646 standards for soft proofing*

| Parameters | Target | | | | |
|---|---|---|---|---|---|
| | Colour Temp | Intensity | Chromaticity | Uniformity | Black point |
| **Ambient light** | 5000°K | ¼ monitor white point | | Uniformly diffuse | -NA- |
| **Surround** | Neutral and matt with luminous reflectance between 10% and 60% | | | | |
| **Display** | 5000°K | >80 cd/m$^2$ | u'= 0.2092 v'= 0.4881 | 10% within the centre measurement | Luminance < 1% of max luminance |
| **Viewing booth** | 5000°K | 500lux ± 125lux | u'$_{10}$ = 0.2102 v'$_{10}$ = 0.4889 | for 1m$^2$ area, luminance = >75% luminance at the centre | -NA- |

## 2.2 Procedure followed for implementing the conditions/specifications mentioned above

In this section methods and procedures are proposed for implementing the specifications mentioned previously. To setup the soft proofing station and the ambient light condition following apparatus was used:

### *Hardware*
- NEC SpectraView LCD 2180WG LED display
- Apple MAC PRO 10.4
- Just Normlicht ColorCommunicator 2 viewing booth
- X-Rite EyeOne Pro spectrophotometer including ambient light measurement adaptor.
- OSRAM L58W/950, LUMLUX de LUXE, Daylight tubes for ambient light

### *Software*
- SpectraView Profiler Version 4.1 (NEC SpectraView monitor calibration and profiling software)
- UDACT (UGRA Display Analysis Certification Tool) monitor certifying software by UGRA.
- Adobe Photoshop CS4

Nec SpectraView LCD 2180EG LED display was used as the display monitor to display the soft copy images. Nec LCD 2180WG LED is a high end display which features individual high power red, green and blue LEDs (Light Emitting diodes) as a backlight light source for the LCD, instead of the typical CCFL (Cold Cathode Fluorescent Lamp) (NEC 2005). LED backlight results in a wide output colour gamut of the display. Hardware calibration can be performed on this display using its own calibration and profiling software. Hardware calibration lets the user adjust the brightness and gradation properties of each RGB primary within the monitor compared to the software calibration were the monitor's primaries are measured and the difference between the measured values and the target values is corrected by adjusting the output of the video card. Software calibration method can create problems like greyscale banding, decline in appearance of colours in greyscale images. Hardware calibration eliminates the need to correct the RGB output for smooth, accurate display of greyscale images.

Nec SpectraView Profiler software calibrates and profiles the Nec LCD 2180WG LED display monitor (NEC 2008). The software allows custom target calibrations that can be preset or can be defined by the user. The user can define the white point, light intensity, gamma curves, black point, etc. At the end it also profiles the display and generates a *.icc colour profile. Target and measured results are analysed and displayed, showing information like measured colour, colour difference, gamut etc. (NEC 2005).

Just colorCommunicator 2 viewing booth was used for the soft proofing station along with the NEC SpectraView monitor display. Just colorCommunicator 2 can be connected to the system by an USB interface. The light intensity of the viewing booth can therefore be adjusted via software to match the light intensity of the display for soft proofing (JUST 2008). NEC SpectraView Profile software has a facility to communicate with the Just colorCommunicator 2 to adjust the light intensity of the viewing booth as per the ISO 12646 soft proofing standards.

To perform the measurements of light intensity, white point, colour rendering on the monitor display and on the hard proofing a number of different measuring instruments can be used. To perform the measurement of

colour on the monitor display either a colorimeter or a spectrophotometer can be used. While to perform ambient light measurements a light meter, colorimeter or a spectrophotometer with ambient light adaptor can be used.

To avoid inter-instrument uncertainty and reproducibility issue only one instrument has been used for the measurements (Nussbaum et al. 2009). For this setup, a X-Rite EyeOne Pro spectrophotometer was used to perform the measurements on monitor display and hard copy and also to perform the ambient light measurements using the ambient light adaptor.

### Monitor Calibration and viewing booth adjustment

To calibrate the monitor and adjust the viewing booth following procedure was followed:

The viewing booth and the monitor display were turned on half an hour before any measurements/adjustments were made in order to properly warm and stabilize the performance of the devices. The viewing booth was connected to the system via UBS cable connection.

X-rite EyeOne Pro was connected to the system and the emission measurement mode chosen. Consequently the LCD display profiling test chart (with 99 colour patches) was measured using the ProfileMaker Pro MeasureTool software to warm up the measurement instrument.

NEC SpectraView Profiler Version 4.1 software was used to calibrate, to characterize and to adjust the viewing booth according to ISO 12646 standards parameter for soft proofing. This software communicates with the viewing booth via the USB cable connection (NEC 2008). P2 viewing conditions defined in ISO 3664 were setup in the viewing booth according to ISO 12646 specifications (ISO 12646, sec 4.8.2).

NEC SpectraView Profiler software asks the user to define the parameters white point, light intensity, gamma, etc to perform the calibration according to the defined parameters. It also has a specific calibration targets for which the monitor can be calibrated. It contains a target for soft proofing according to ISO 12646 and ISO 3664 standards where the target for calibration parameters is in accordance with the specifications of the ISO 12646 standards. Table 2 shows the parameters selected for the calibration and characterization of the monitor display.

*Table 2: Preset target settings in NEC SpectraView Profiler software*

| | |
|---|---|
| Display Type | LCD |
| Calibration method | Hardware calibration (monitor LUTs) |
| Calibration settings | ISO3664 and ISO 12646 |
| Profile settings | LUT based (accurate) |
| CIE Daylight standard | D50 |
| Tonal response Curve | L* (recommended) |
| Specify | White and black luminance |
| White | 160 cd/m$^2$ |
| Black | Minimum neutral |
| Profile type | 16 bit LUT based |
| Chromatic adaptation | CAT02 |

After selecting the target the software asks for a monitor profile name and consequently the measurement process were started. According to the defined parameters the software (SpectraView Profiler) projects colour patches with certain RGB values that are measured using the X-rite EyeOne Pro spectrophotometer. Depending on the measurement data appropriate adjustments are made automatically until the difference between the measured parameters and the target parameters is achieved minimum. Consequently, an ICC monitor profile is created at the last stage of the calibration process defining device independent values (CIEXYZ) that correspond to a given set of device dependent numbers and vice versa. After calibrating and creating the monitor profile, the profile was validated in order to check the objective quality of the generated profile in terms of calculating $\Delta E^*_{ab}$ colour difference between given reference values and the corresponding measured values. After successfully validating, the $\Delta E^*_{ab}$ colour difference is shown in form of a bar graph and the profile is automatically applied as the system profile. Subsequently, the viewing booth settings were checked. 'Check viewing booth' option was selected in the review column 'Viewing booth and monitor comparison' and measurements were performed.
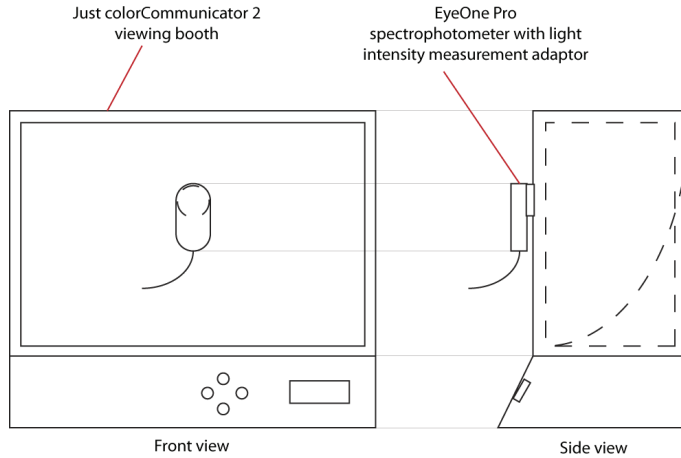
*Figure 1: Schematic diagram of the position of the measuring instrument for viewing booth measurement*

To record the measurements, the measuring instrument was held parallel to the viewing booth facing towards the plane of viewing as shown in Figure 1. Instructions on the screen were followed. Viewing booth conditions were checked against the P2 viewing condition mentioned in ISO 3664. In order to reduce the difference between the measured values and the target values 'Adjust viewing booth' tab was selected to make the necessary adjustments. In the 'Adjust viewing booth' tab, for ISO reference values, 'viewing booth and monitor comparison' was selected. It performs the necessary adjustments in the viewing booth (for light intensity, etc) to match the ISO 3664 P2 viewing condition requirements. The viewing booth measurements were performed using X-rite EyeOne Pro with the ambient light adaptor.

### Ambient light condition setup and adjustment
The room used for the soft proof setup has a neutral and matt colour according to ISO 3664 (sec 4.3.4). To setup the ambient lighting conditions according to ISO 12646 standards for soft proofing, daylight tubes named 'OSRAM L58W/950, LUMLUX de LUXE, Daylight' were setup in the room. These tubes simulate Illuminant D50 and the light intensity can be varied as per the requirements. Therefore, in order to vary the intensity of these tubes a varying knob facility was introduced in the room with which the ambient light intensity in the room could be controlled.

SpectraView Profiler software was used to perform the ambient light measurements. 'Ambient light' option was selected in the review column and measurements were performed as per the instructions given by the software. To perform the measurements, X-rite EyeOne Pro spectrophotometer with the ambient light adaptor was used for measuring the ambient light in the room. The measurement instrument was held straight parallel to the display facing towards the room, with the monitor switched off. Furthermore, Figure 2 illustrates the schematic diagram of the position of the spectrophotometer to perform the ambient light measurements.
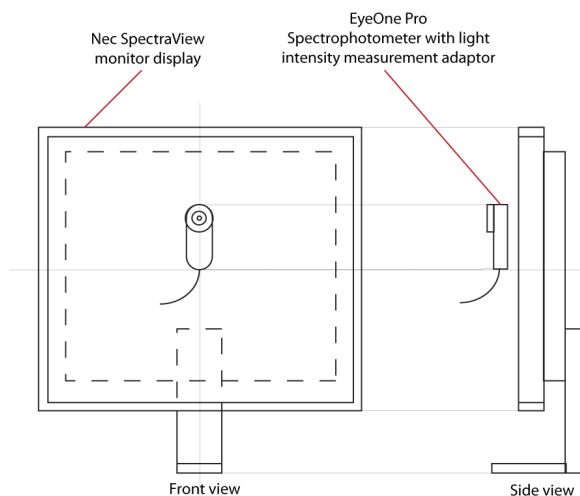


*Figure 2: Schematic diagram of the position of the measuring instrument for ambient light measurement*

Notice, the geometry of the measurement device is very critical in terms of the measured values. Small changes of the measurement instrument angle or distance to the light source can change the measurement results dramatically. The ambient light was measured for light intensity and colour temperature. Depending upon the measurements obtained the light intensity was adjusted using the varying knob facility to be within the tolerance defined by ISO 12646 standards for soft proofing conditions.

After varying the knob to change the light intensity, measurements were again conducted with a gap of 30 minutes (time required for the tubes to stabilize after adjusting the light intensity). This procedure was followed till the time appropriate light intensity was achieved to be within the ISO 12646 standards for soft proofing.

As an alternative a number of software's like BabelColor CT&A, UDACT, etc can be used to perform ambient light measurements. BabelColor CT&A uses its Spectral Tool feature with EyeOne Pro spectrophotometer to measure and evaluate the ambient light conditions. This software, upon measurements, shows a small graph of u', v' co-ordinates which tells if the measured colour temperature is within the ISO 12646 defined tolerance. BabelColor CT&A also provide values for Colour rendering index (CRI) and Metamerism index (MI) of the measured light for P1 condition of measurements. According to ISO 3664: 2009 CRI and MI are more important parameters to determine the quality of the illumination.

## 3. Results and discussions

### 3.1 Monitor display

To analyse and evaluate the display for soft proofing environment the UDACT certifying software was used. UDACT enables objective, quality oriented and comparable evaluation for an individual soft proofing display (UGRA 2008).

X-rite EyeOne Pro spectrophotometer was connected to the UDACT software. Instructions on the screen were followed. UDACT then shows 102 colour patches on the screen of which measurement values are recorded using the connected spectrophotometer. The measurements include 21 patches to verify the gray balance. To determine the profile quality 35 patches are measured. Finally, UDACT analyses the display for the specifications according to ISO 12646 standards for soft proofing measuring the 46 patches of the Ugra/Fogra Media Wedge. UDACT records the measurements and generates a report at the end that shows all the details of evaluation. ISO 12646 standards for soft proofing addresses the factors 'white point and black point', 'gray balance', colour gamut' and 'uniformity of luminance' determining the performance of the monitor display. In the following chapter, the results of the monitor display analysis will be presented.

### *White point and black point*
According to ISO 12646, white point of the display should be as close as possible to the calibration target. Table 3 below presents the target and the measured values for white and black point.

*Table 3: White and black point of the NEC display*

|             | Target                | Measured                | Difference            |
|-------------|-----------------------|-------------------------|-----------------------|
| **White point** | 5000 °K           | 4991°K                  | 0.5 $\Delta E_{ab}$   |
| **Luminance**   | 160 cd/m$^2$      | 159.5 cd/m$^2$          |                       |
| **Black point** | <1.6 cd/m$^2$     | 0.5 cd/m$^2$            |                       |

The comparisons between the measured values and the target values in terms of white point, black point and luminance show acceptable results.

### *Gray balance*
The maximum allowed deviation shall not exceed max $\Delta C^*_{ab}$ 3 unit and preferably not max $\Delta C^*_{ab}$ 2 unit (ISO 12646, sec 4.10). For further details on calculating $\Delta C^*_{ab}$ and a general overview of CIE colorimetry see (Hunt 1998)). Table 4 shows the 21 patches for the gray balance measurement and the performances of the monitor display in terms of the corresponding measurement and the $\Delta C^*_{ab}$ deviation. It can be seen that although, the max $\Delta C^*_{ab}$ is 2.35 units, it is still within the given tolerance. Flare light could be considered influencing the measurement on dark colours (e.g. 0%, 5%, 10% and 15%).

*Table 4: Gray balance measurements performed and reported by UDACT*

| % | CIELAB (calculated) | | | CIELAB (measured) | | | $\Delta C^*_{ab}$ |
|---|---|---|---|---|---|---|---|
| | L | a | b | L | a | b | |
| 100 (white) | 100 | 0 | 0 | 100.00 | 0.41 | -0.22 | 0.47 |
| 0 (black) | 5.01 | 1.47 | 0.8 | 2.72 | -0.07 | -0.17 | 1.82 |
| 5 | 9.59 | 0.85 | 0.46 | 7.02 | -1.41 | -0.20 | 2.35 |
| 10 | 13.53 | 0.29 | 0.14 | 11.69 | -1.39 | -0.79 | 1.92 |
| 15 | 17.63 | 0 | 0 | 16.13 | -0.98 | -0.93 | 1.35 |
| 20 | 22.06 | 0 | 0 | 20.96 | -0.59 | -0.61 | 0.85 |
| 25 | 26.35 | 0 | 0 | 25.57 | -0.40 | -0.61 | 0.73 |
| 30 | 31.09 | 0 | 0 | 30.39 | -0.37 | -0.52 | 0.64 |
| 35 | 35.94 | 0 | 0 | 35.43 | -0.23 | -0.37 | 0.44 |
| 40 | 40.84 | 0 | 0 | 40.31 | 0.06 | -0.78 | 0.78 |
| 45 | 45.41 | 0 | 0 | 45.23 | 0.04 | -0.29 | 0.29 |
| 50 | 50.37 | 0 | 0 | 50.29 | 0.15 | -0.42 | 0.45 |
| 55 | 55.37 | 0 | 0 | 55.37 | 0.06 | -0.22 | 0.23 |
| 60 | 60.38 | 0 | 0 | 60.40 | 0.28 | -0.36 | 0.45 |
| 65 | 65.03 | 0 | 0 | 64.99 | 0.52 | -0.55 | 0.76 |
| 70 | 70.05 | 0 | 0 | 70.13 | 0.13 | -0.20 | 0.24 |
| 75 | 75.10 | 0 | 0 | 75.06 | 0.39 | -0.31 | 0.50 |
| 80 | 80.15 | 0 | 0 | 80.17 | 0.54 | -0.39 | 0.67 |
| 85 | 84.82 | 0 | 0 | 84.82 | 0.37 | -0.49 | 0.62 |
| 90 | 89.87 | 0 | 0 | 89.81 | 0.54 | -0.53 | 0.76 |
| 95 | 94.93 | 0 | 0 | 94.95 | 0.23 | -0.33 | 0.40 |
| Average | | | | | | | 0.80 |
| Max | | | | | | | 2.35 |

## Colour gamut

The colour gamut of the display should be such that it totally encloses the colour gamut produced by the inks specified in the appropriate part of ISO 12647 for which the display is required to provide a proof (ISO 12646, sec A.2). UDACT checks for the colour gamut by measuring the Ugra/Fogra Media Wedge 2.0 on the display simulating the ISOcoated_v2_300_eci.icc profile. The 46 Ugra/Fogra Media Wedge patches are visualized using the system profile and the corresponding measurements are recorded and compared with the reference values. The average colour difference between the reference values and the measurement values is $\Delta E^*_{ab}$ 0.8 units. The max $\Delta E^*_{ab}$ 2.8 and related to black (16 0 0) which is not unexpected due to the results of the gray balance task which show the largest colour differences in dark colours. The entire table including the reference values, measurement values and the calculated colour difference are provided in the appendix. For illustration purposes Figure 3 shows the top down projection of the colour gamut of the monitor profile (wireframe) and the ISOcoated_v2_300_eci.icc profile (solid) in the CIELAB colour space. In this presentation it can be seen that the boundary of the ISOcoated_v2_300_eci.icc colour gamut is clearly within the gamut of the monitor profile.
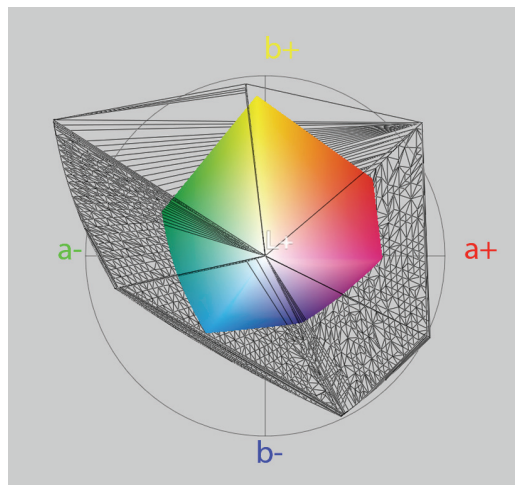


*Figure 3: Top down projection of the colour gamut of the monitor profile (wireframe) and the ISOcoated_v2_300_eci.icc profile (solid) in the CIELAB colour space*

On the other hand, Figure 4 illustrates the horizontal projection view of the four CIELAB planes a+, a-, b+ and b- (clockwise) of colour gamut of the monitor profile (wireframe) and ISOcoated_v2_300_eci.icc profile (solid). It can be clearly observed that the monitor colour gamut is big enough to simulate the ISO coated printer profile.
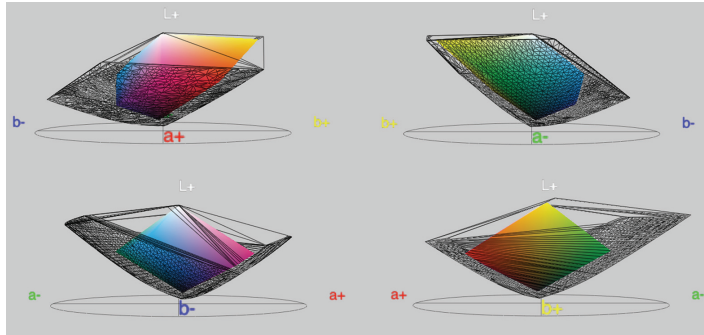


*Figure 4: Horizontal projection view of the four CIELAB planes a+, a-, b+ and b- (clockwise) of colour gamut of the monitor profile (wireframe) and ISOcoated_v2_300_eci.icc profile (solid)*

### *Uniformity of luminance*

Finally the results of the uniformity of the luminance are presented. As previously mentioned the uniformity will be determined displaying white, grey and black images each filled the entire screen. Minimum 9 points of the image area of the screen shall be measured, for each level (Figure 4). According to the ISO 12646 standard requirement the white image consist of the maximum value in each channel Red, Green and Blue (255 for 8 bit). Then the grey image should have about half of the maximum value in each channel (127 for 8 bit), and finally the black should consist of approximately a quarter of the maximum value in each channel (which is e.g. 63 for 8 bit) but shall be greater than 10 % of the maximum digital code value (which is 26 for 8 bit). Table 5 shows the uniformity of luminance measurements performed on the display.
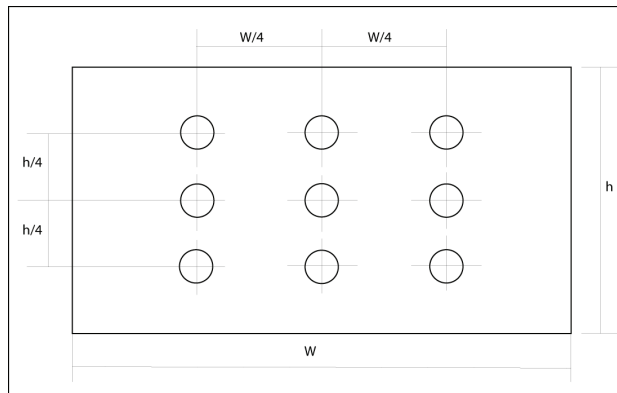


*Figure 5: Measurement positions on the monitor display*

*Table 5: Luminance measurements performed on the display at 9 different positions*

|  | Luminance measured in cd/m$^2$ | | |
|---|---|---|---|
|  | **Position 1** | **Position 2** | **Position 3** |
| **White** | 158.21 | 156.94 | 154.07 |
| **Grey** | 30.14 | 30.22 | 31 |
| **Dark Grey** | 7.28 | 7.34 | 7.66 |
|  | **Position 4** | **Position 5** | **Position 6** |
| **White** | 161.75 | 159.29 | 155.23 |
| **Grey** | 30.72 | 30.88 | 30.77 |
| **Dark Grey** | 7.52 | 7.5 | 7.6 |
|  | **Position 7** | **Position 8** | **Position 9** |
| **White** | 173.18 | 166.46 | 166.97 |
| **Grey** | 32.8 | 32.15 | 32.91 |
| **Dark Grey** | 7.97 | 7.84 | 8.17 |

Figure 6, Figure 7 and Figure 8 show the result of the uniformity check for white, grey and dark grey neutrals according to ISO 12646 standards for soft proofing. According to ISO 12646, sec 4.4, the luminance of the display (measured at 9 different locations figure 10) shall be within 10% of the luminance of the measurement made at the centre of the display. Position 5 (on X-axis) in the graphs below is the centre of the display.
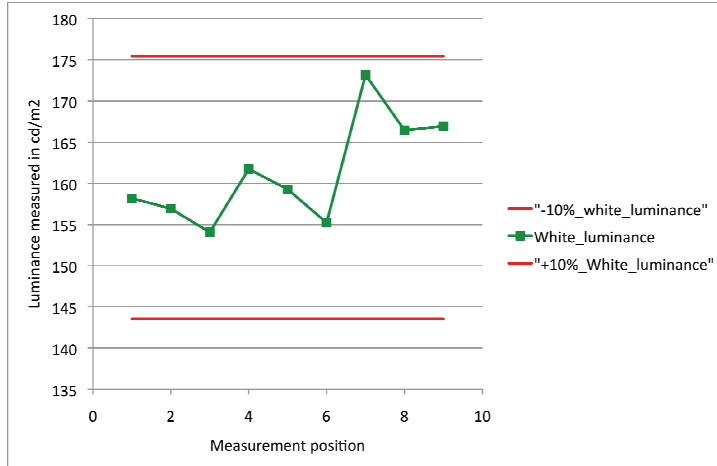


*Figure 6: Uniformity of the display for white neutral*
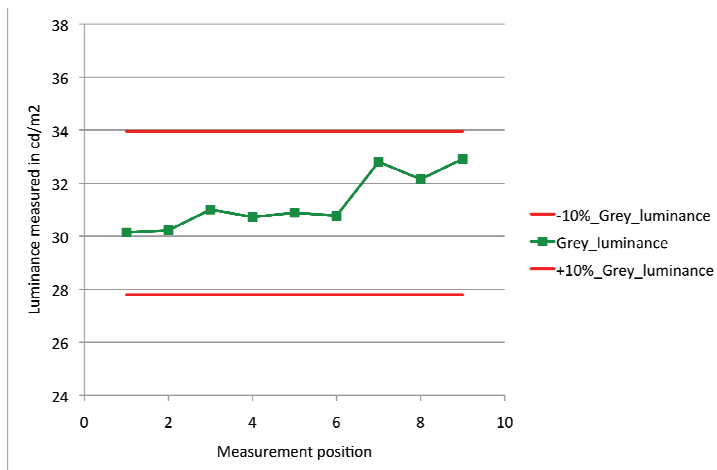


*Figure 7: Uniformity of the display for grey neutral*
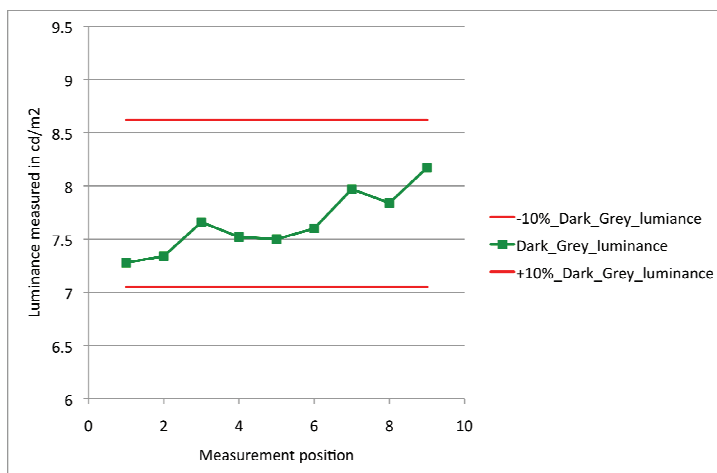


*Figure 8: Uniformity of display for dark grey neutral*

From the graphs it can be observed that the luminance values varies at 9 different positions on the display. It can be noticed that the luminance at position 7, 8 and 9 (lower part of the monitor display) gives the highest values. However, all the measurements are within the 10% tolerance defined by ISO 12646 standards.

## 3.2 Viewing booth and ambient lighting conditions

To analyse and evaluate the viewing booth and ambient lighting conditions, measurements were performed using the X-rite EyeOne Pro spectrophotometer with the ambient light adaptor. The measured value was then compared against the P2 viewing conditions defined in ISO 3664:2009 standards. Table 6 and Table 7 show the target and measured viewing booth and ambient light conditions.

*Table 6: Viewing booth target and the measured values*

| Viewing Booth | Illuminant | | Illuminance lux |
|---|---|---|---|
| | Colour Temperature | Chromaticity Tolerance (u'v') | |
| **Target** | 5000 °K | $\leq 0.005$ | $500 \pm 125$ |
| **Measured** | 4995 °K | 0.00203 | 480 |

*Table 7: Ambient light condition target and measured values*

| Ambient light condition | Illuminant | Illuminance |
|---|---|---|
| | Colour Temperature | |
| **Target** | 5000 °K | ¼ monitor white point luminance |
| **Measured** | 4853 °K | 103 lux |

## 3.3 Soft proofing image data

Implementation of the ISO standard 12646 alone does not guarantee that a displayed (soft copy) image will match the colour of the same image produced on the hard copy in the viewing booth (ISO 12646). To obtain a colour match, colour transformation is required to convert the colour data format from the printer colour space to the display colour space. This transformation is mainly done by means of a colour management system using the appropriate ICC profiles. ICC profiles define the relationship between the device specific colour space and the profile connection space (PCS) (ISO 12646:Annex A.1). Therefore, to obtain a colour match between hard copy and soft copy proofs using ICC colour management, the soft proof is obtained by applying the image data, the combination of the device to PCS transforms of the print output profile and the PCS to device transforms of the display profile.

In this study, Adobe Photoshop CS4 software was used to perform the colour transformation. Visual Print reference (VPR) images were applied to simulate the ISOcoated_v2_300_eci.icc profile. These images were compared to evaluate the visual match between the VPR hard copy in the viewing booth and the soft copy on the display. To apply necessary simulation profiles a VPR image was opened in Photoshop and the menu 'View > Proof setup > Custom' selected. In the 'Customize Proof Condition' window the appropriate simulating profile was selected. In this case, simulating profile was the CMYK output profile that needed to be soft proofed (ISOcoated_v2_300_eci.icc profile). Image background was selected as neutral gray (similar to the viewing booth background). 'Simulate paper white' option was tick marked to simulate the paper white and the images were then compared with the hard copy in the viewing booth.

For the soft proofing task Adobe Acrobat Pro software can also be used to display the soft copy image on the monitor display to compare with the corresponding hard copy image in the viewing booth.

## 4. Conclusion

In this paper methods and procedures to setup a soft proofing station are discussed. ISO 12646 standards for soft proofing were successfully implemented. The NEC LCD2180WG-LED monitor display used in this paper has a very wide colour gamut and is performing visually uniform. The appropriate calibration and characterization procedure has been applied. Gamut plots in Figure 3 and Figure 4 showed that the monitor display is able to simulate printer profile colours. This was verified further by measuring the UGRA/FOGRA step wedge simulated with ISO coated printer profile on the display using the EyeOne Pro spectrophotometer. The maximum colour difference obtained was $\Delta E_{ab} = 2.8$.

Measurement procedures to measure ambient light using an EyeOne Pro spectrophotometer with ambient light adaptor are implemented and discussed in this work. NEC SpectraView Profiler software was used to perform the ambient light measurements. A number of different software's can be used to perform ambient light, viewing booth and display measurements. As an alternative to NEC SpectraView profiler, Babel Color CT&A software can be used to perform these measurements.

ISO 12646 standards were successfully implemented, as, all the measurements obtained were within the tolerance level defined. UDACT software was used to evaluate the display for soft proofing and printer profile simulation according to these soft proofing standards.

ISO 12646 define a wide range of tolerance for ambient light and viewing booth light intensity measurements. It was observed that, in spite of being within the ISO 12646 standards tolerance level the two images (soft copy image on the display and the corresponding hard copy image in the viewing booth) might not show an exact visual match. Therefore, the ambient light intensity and the viewing booth light intensity can be adjusted (within the tolerances defined by ISO 12646) as per different job requirements to get the closest possible visual match between the soft copy on the display and the corresponding hard copy in the viewing booth.

Finally, it is of interest to consider other potential directions for further work in the field soft proofing. Firstly, to verify the monitor display measurement results of dark colours a spectroradiometer could be used. Furthermore, colour measurements of the monitor display and the viewing booth could be conducted with a spectroradiometer to confirm the appropriate set up. Moreover, a psychophysical experiment could evaluate the magnitude of visual differences between the soft proofed image on the monitor display and the hard copy in the viewing booth in terms of perceptibility and acceptability threshold. Factors and their magnitude affecting the appearance on the monitor display and the viewing booth could be investigated.

Nevertheless, using more than one measurement instrument in the soft proofing workflow the inter-instrument reproducibility has to be considered.

**References**

CIE15 (2004), 'Colorimetry', *3rd ed* (CIE Central Bureau, Vienna).

Gatt, A, Westland, S, and Bala, R (2004), 'Testing the softproofing paradigm', *12th Color Imaging Conference,* p. 187-192.

Gatt, A, et al. (2005), 'Testing the Softproofing Paradigm II', *10th Congress of the International Colour Association,* p. 1243-1246.

Hunt, RWG (1998), *Measuring colour* (3 ed.: Fountain Press).

ISO 3664 (2009), 'Graphic technology and photography - Viewing conditions', third ed.: Geneva: ISO [www. iso. org].

ISO12646 (2008), 'Graphic technology - Displays for colour proofing - Characteristics and viewing conditions', Geneva: ISO [www. iso. org].

JUST (2008), 'Normlicht, Color communicator, Help manual'.

NEC (2005) LCD2180WG-LED technical background and feature overview', *Display Solution* <http://www.necdisplay.com/ >, accessed 2. July 2010.

NEC (2008), 'SpectraView Profiler Version 4.1, User's manual'.

Nussbaum, P, Sole, A., and Hardeberg, Jon Y. (2009), 'Consequences of using a number of different color measurement instruments in a color managed printing workflow', *TAGA Proceedings*.

UGRA (2008), 'UDACT – Ugra display analysis and certification tool, Help manual'.

UGRA (2009), 'PSO certification', <http://www.ugra.ch/pso-certification.phtml>, accessed 6. July 2010.

# Appendix

*Measurements performed and recorded by UDACT for colour gamut*

|    | Reference | | | Measured | | | $\Delta E_{ab}$ |
|----|------|-------|-------|------|-------|-------|------|
|    | L    | a     | b     | L    | a     | B     |      |
| 1  | 55   | -37   | -50   | 55.4 | -36.1 | -50.2 | 1    |
| 2  | 66.9 | -24.7 | -37.1 | 66.8 | -24.3 | -37.2 | 0.5  |
| 3  | 79.7 | -12.5 | -21.8 | 79.8 | -12.4 | -21.7 | 0,1  |
| 4  | 48   | 74    | -3.0  | 48   | 73.6  | -3.7  | 0.8  |
| 5  | 60.8 | 50.6  | -6.7  | 60.7 | 49.8  | -6.8  | 0.8  |
| 6  | 76.4 | 25.8  | -6.9  | 76.4 | 25.5  | -6.7  | 0.3  |
| 7  | 89   | -5    | 93    | 88.5 | -4    | 92.5  | 1.2  |
| 8  | 90.3 | -4.7  | 62.6  | 90   | -3.9  | 62    | 1.1  |
| 9  | 92.2 | -3.5  | 31.1  | 92   | -3.2  | 31.3  | 0.4  |
| 10 | 53.1 | 37.7  | 28.9  | 53.2 | 36.7  | 29    | 1    |
| 11 | 41.5 | 22.7  | 16.8  | 41.6 | 22.3  | 17.1  | 0.5  |
| 12 | 31.9 | 40    | 24    | 31.8 | 40.6  | 24.4  | 0.8  |
| 13 | 32.5 | 44.5  | -1.8  | 32.3 | 44.7  | -1.9  | 0.4  |
| 14 | 51.3 | 1.3   | 44.5  | 51   | 0.9   | 44.6  | 0.5  |
| 15 | 34.6 | -36.4 | 13.9  | 33.9 | -38   | 13.5  | 1.7  |
| 16 | 36   | -26.2 | -20.9 | 35.3 | -27.1 | -22.6 | 2.1  |
| 17 | 20.9 | 9.6   | -23.6 | 19.9 | 9.1   | -25.2 | 1.9  |
| 18 | 89   | 0     | -1.9  | 89   | -0.3  | -2    | 0.3  |
| 19 | 82.8 | 0     | -1.7  | 82.8 | 0     | -2.1  | 0.5  |
| 20 | 69.3 | 0     | -1.4  | 69.2 | -0.6  | -1.3  | 0.6  |
| 21 | 54.1 | 0     | -1.0  | 54.2 | -0.6  | -1.3  | 0.7  |
| 22 | 36.6 | 0     | -0.5  | 36.2 | -0.6  | -1    | 0.9  |
| 23 | 16   | 0     | 0     | 14.2 | -1.4  | -1.5  | 2.8  |
| 24 | 24   | 22    | -46   | 23.1 | 21.7  | -47.8 | 2    |
| 25 | 40.9 | 17.9  | -36.6 | 40.6 | 17.8  | -37.6 | 1.1  |
| 26 | 63.7 | 10.3  | -23.8 | 63.8 | 10.2  | -23.9 | 0.2  |
| 27 | 47   | 68    | 48    | 47   | 67.7  | 48    | 0.3  |
| 28 | 58.5 | 47.1  | 37.9  | 58.5 | 46.4  | 37.9  | 0.7  |
| 29 | 74.2 | 22.9  | 21.4  | 74.1 | 22.3  | 21.2  | 0.6  |
| 30 | 50   | -65   | 27    | 49.9 | -66.2 | 26.6  | 1.3  |
| 31 | 62.1 | -39.8 | 21    | 62.1 | -39.5 | 20.9  | 0.4  |
| 32 | 77   | -19.1 | 11    | 77.1 | -18.9 | 10.9  | 0.2  |
| 33 | 71.2 | 18.9  | 17.2  | 71   | 19.1  | 17.2  | 0.4  |
| 34 | 71.2 | 22.1  | 73.1  | 70.8 | 22.4  | 72.5  | 0.8  |
| 35 | 47.7 | 71.2  | 16.2  | 47.7 | 71    | 16.3  | 0.2  |
| 36 | 38   | 55.4  | -20.9 | 38.1 | 55.6  | -21.1 | 0.3  |
| 37 | 73.7 | -22.8 | 67.6  | 73.2 | -22.3 | 67.1  | 0.8  |
| 38 | 52.3 | -52.3 | -20.1 | 52.5 | -53.3 | -20.7 | 1.2  |
| 39 | 43.3 | -17   | -48.6 | 43.1 | -17.3 | -49.9 | 1.3  |
| 40 | 95   | 0     | -2    | 94.9 | -0.3  | -1.9  | 0.3  |
| 41 | 88.5 | -0.4  | -3.1  | 88.6 | -0.6  | -3.4  | 0.3  |
| 42 | 82   | -0.9  | -4.1  | 81.9 | -1    | -4.1  | 0.1  |
| 43 | 67.7 | -2    | -4.4  | 67.8 | -2.3  | -4.2  | 0.4  |
| 44 | 52.2 | -2.5  | -3.5  | 52.3 | -2.4  | -3.9  | 0.4  |
| 45 | 37.5 | -3.9  | -3.1  | 37.1 | -4.3  | -3.6  | 0.8  |
| 46 | 26.3 | -6.8  | -3.4  | 25.4 | -8.2  | -4.3  | 1.9  |
|    |      |       |       |      |       | Avg   | 0.8  |

# Ink mist formation in roller trains

*Tim C. Claypole, Georgios Vlachopoulos, David C. Bould*

Welsh Centre for Printing and Coating, Swansea University
Singleton Park, Swansea SA2 8PP UK
Email: t.c.claypole@swansea.ac.uk

**Abstract**

Misting occurs during ink film splitting when filaments are ruptured in multiple points giving rise to droplets of ink that detach from the roller train. A laboratory based physical simulation uses trapping techniques on a tack-tester was developed to enable the investigation of misting mechanisms under controlled conditions. The trapped mist was analysed both in terms of the location combined with the size distribution of the droplets. This provides unique information on the origin of the misting droplets which can be related to local dynamic nip and roller conditions.

The origin of misting can be traced to the ink film splitting mechanisms at the exit to the printing nip. The film splits into ribs and then ligaments. These extend at increasing speed as the rollers separate. Under the action of viscoelastic forces these ligaments of ink can split to form both satellite droplets and larger droplets attached by a ligament of ink to one roller. The interaction between the centripetal forces and the visco-elastic forces can cause either the ink to collapse back onto the roller, leading to a rib or for the ink to accumulate at the outer end eventually leading to a large breakaway droplet.

**Keywords:** offset; ink transfer; film splitting; misting

## 1. Introduction

Misting occurs during ink film splitting when filaments are ruptured in multiple points giving rise to droplets of ink that detach from the roller train. This is of particular issue for high speed offset printing presses, such as used in newspapers and packaging. The droplets can cause a loss of the product quality, as well as being ink lost and an environmental hazard. The majority of previous work has tended to be qualitative. Sjobal (1949) used photographic techniques to observe misting generated due to filament break-up. Voet (1952-56) focused on the study of misting phenomena of rotary news letterpress. He found misting was affected by rotation speed, ink additives and fluid properties, film thickness and the presence of moisture in the system. The decrease of ink viscosity increased misting in his study and it also increased with the ink film thickness. However, Voet based his study on letterpress system and inks. Bisset et al (1979) argued that smaller roller diameter and higher ink film thickness tends to increase misting on distribution systems. These results were confirmed by others such as Christiansen (1995), and McKay (1994). Others found that misting also increases with temperature (Evans 1995 and Traber et al 1992). Blayo et al (1998) used a tack-o-scope tester to study misting phenomena. They used aluminium foil to cover the tester in order to trap the misting ink. The weighted the samples to carry out the amount of ink that been lost from the distribution rollers. They concluded that misting was increased by decrease of tack and viscosity. Their work carried out the average amount of ink that been lost from the system and they did not calculated distribution system transits or variations of the droplets profile with the changes into viscosity or tack. Owens (2005) studied misting mechanisms of Newtonian and polymer solutions. He used an aerodynamic sizing system to measure and count the amount of droplets generated at the nip exit. His study focused on viscoelastic fluid properties in an extremely narrow area of the roller nip exit without establishing relations and variations by the printing parameters.

This paper presents an investigation of the effect of process parameters on misting. Unlike the previous studies that have tended to focus the filament break up mechanism at one point in the nip or on the overall quantity of mist produce, the work reported in this paper, analyses the trapped mist both in terms of the location combined with the size distribution of the droplets. This provides unique information on the origin of the misting droplets which can be related to local dynamic nip and roller conditions, thus making the study relevant to the impact of uneven ink film distributions such as caused by ribbing or image ghosting. There are practical difficulties in investigating misting in printing presses such as the narrow roller gaps, the high printing speed, the thin ink film thickness and the process noise. This is coupled with the dynamics of the

printing press caused by the ink transients when the supply and removal of ink do not matched. Therefore, a laboratory based physical simulation uses trapping techniques on a tack-tester was developed to enable the investigation of misting mechanisms under controlled conditions.

## 2. Experimental methodology

An IGT Tack tester was used as a short closed loop ink distribution system consisting of three rollers. Such a system eliminates the dynamic effects of incoming and outgoing ink volume. Trapping techniques were developed to collect misting droplets and to establish variations in the misting phenomena. The misting trap comprised a smooth flexible substrate whose geometry was varied according to the aspect to be studied. A flat misting trap was used to determine average misting effects and film thickness profile on the rollers (Figure 1). A curved trap was used to determine the misting effects of the individual rollers nip (Figure 2). In the latter cases, the roller that was not being studied was disengaged from the motor roller contact area and so a single nip was formed.
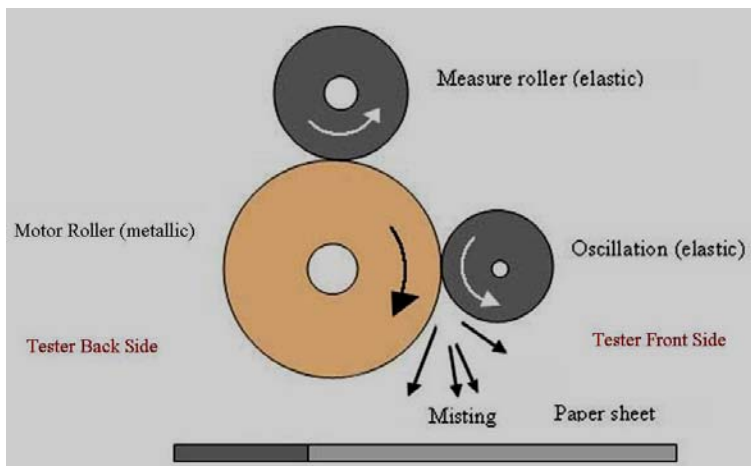


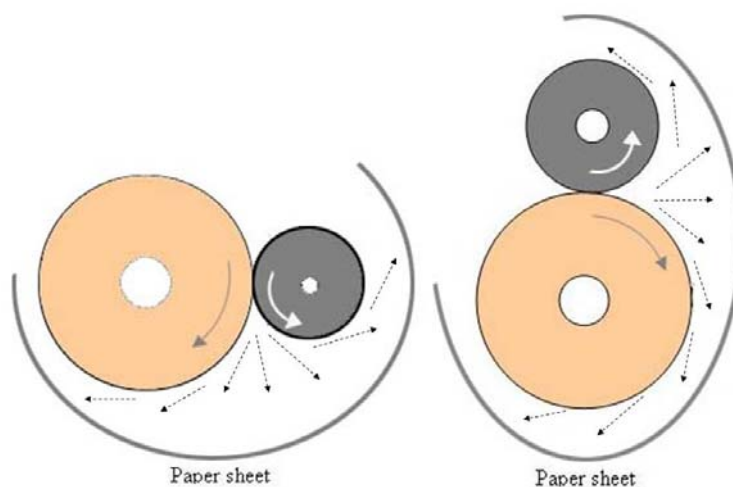*Figure 1: Flat misting trap at the bottom side of the IGT tack tester*



*Figure 2: Misting trap, curved configuration surrounding each independent nip - arrows indicate directions of the expecting misting*

The surface quality of the substrate is important in terms of absorption and drying of dispersed droplets. Highly porous substrates produce an increased absorption and droplets appear with increased area. However, coated substrates have an extended drying time of several days before they can be used for contact

measurements. The substrate with best qualities was determined to be a velvet quality paper which provided high contrast and good droplets shape. The low porosity of the velvet substrate does not absorb the ink and droplets are presented in profile on the paper surface.

The misting traps were analysed with a scanning spectro-densitometry, flat bed scanner, white light inteferometry and digital microscope, to obtain both the macro distribution of misting and the local micro characteristics such as droplet size, size distribution and total surface coverage.

A Gretag Spectrolino scanning spectrophotometer was used to scan misting samples at a low and high resolution which produce 1 and 4 measurements per square centimetre respectively. The density values were averaged across the length and across the width to generate misting profile trends, while L*a*b* ΔE values were used to create a topographic analysis of the misting trap (Figure 3).

An Epson flatbed scanner was used to produce a higher resolution analysis of the misting traps. The whole sheets were scanned at 350dpi to obtain the macro distribution and at 1200dpi for analysis of the individual droplets. The white paper surface of the misting trap was measured prior to it being used for the experiment and the misting density calculated relative to this profile to avoid any influence of paper or variation in light intensity in the scanner. The droplet sizes and distribution were also calculated. The images were transformed into 8-bit image that generated high contrast between substrate and droplets. Intensity threshold was used to highlight the ink droplets and eliminated the substrate grey values. The individual droplets were analysed using the particles analysis macro of the ImageJ software. The analysis summarises coverage area, number of droplets and average droplet surface.
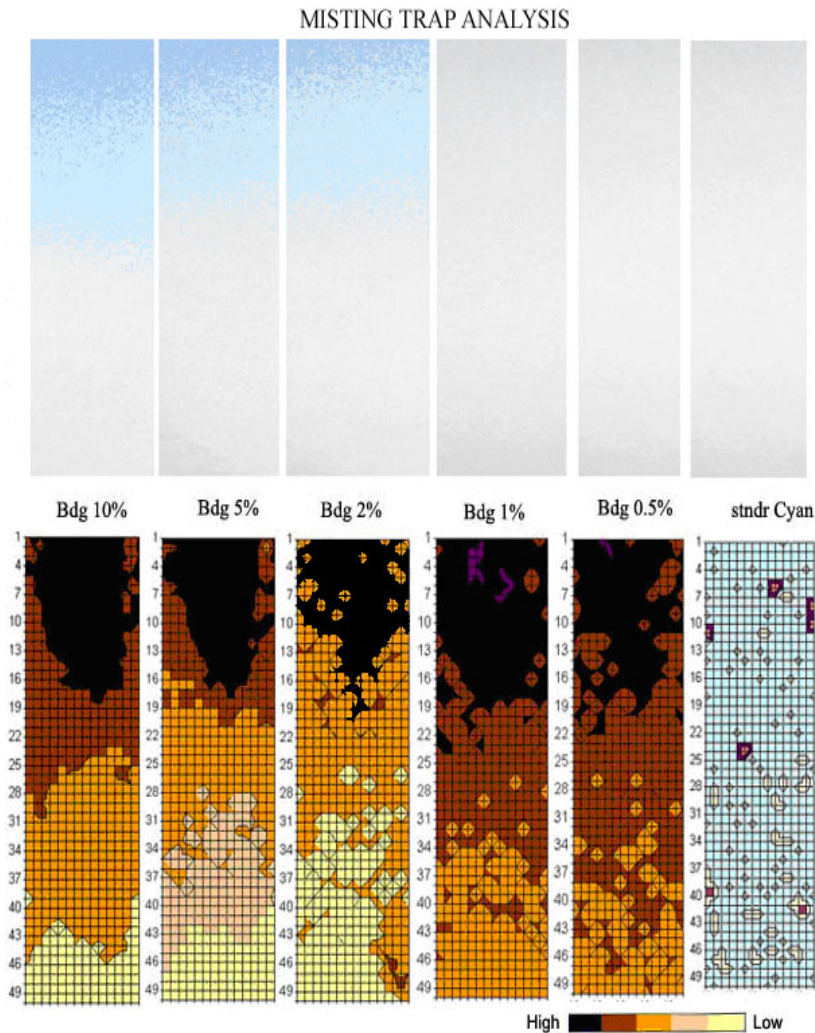


*Figure 3: Distribution of ink on misting traps for varying levels of dilution*

The Leica image analysis microscope was also used to capture selected parts of the misting image throughout the length of the trap for higher accuracy and verification of scanning and measured droplets geometries results.

White light interferometer was used to measure the droplets volume. The ink droplets sat on the surface of the misting trap. The low volume droplets (less than 20 microns) produced a variation in height which was comparable with the substrate roughness and were therefore difficult to locate and measure. However, the higher volume droplets (more than 20 microns) were easily located and the volume calculated (Figure 4).
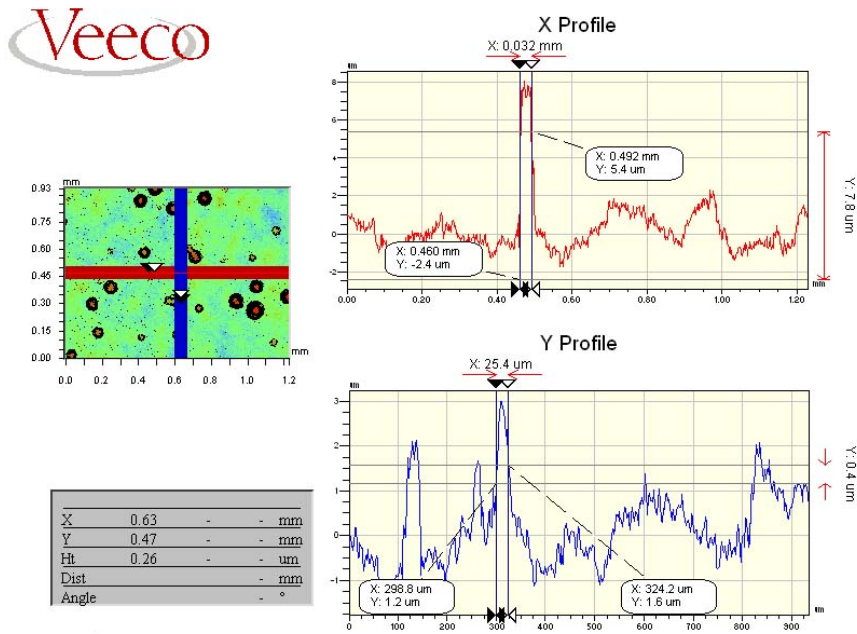
*Figure 4: Analysis of ink droplets on misting trap using white light interferometer*

## 3. Results and discussion

Misting was investigated with respect to the ink rheology, the distribution speed and the ink film thickness. The viscosity of cyan ink was varied by dilution with Butyl-Diglycol (Table 1). The distribution speed was varied set to 50, 150 and 450 m/min. Ink film thicknesses of 3.9 μm and 7.8 μm were used.

*Table 1: Rheological characteristics of the inks*

| Dilution | Shear Viscosity | Extension Viscosity | Hysteresis Loop Area | Tack | Printing Density | Surface Tension |
|----------|-----------------|---------------------|----------------------|------|------------------|-----------------|
| ND Cyan | 22.75 | 9.89E+02 | 2.67E+04 | 115 | 1.08 | 33 |
| 0.5%BDG | 22.06 | 6.60E+02 | 2.52E+04 | 111 | 1.12 | 32 |
| 1%BDG | 21.86 | 1.45E+02 | 2.03E+04 | 105 | 1.11 | 32 |
| 2%BDG | 17.03 | 9.31E+01 | 1.49E+04 | 82 | 1.10 | 27 |
| 5%BDG | 9.28 | 5.47E+01 | 9.76E+03 | 72 | 1.10 | 25 |
| 10%BDG | 4.524 | 9.72E+01 | 4.94E+03 | 41 | 1.14 | 23 |
| 20%BDG | 1.728 | 4.61E+01 | 1.66E+03 | 34 | 1.06 | 17 |

There is an interaction between the ink film thickness and the rheometric characteristics of the ink (Figure 5). Whilst the low film thickness produces a consistent misting density, the misting increases with reducing viscosity with the thicker ink film.

There is a significant interaction of speed and rheology on misting (Figure 6). At the lowest speed there is not significant misting for the higher viscosity fluids of less than 2% dilution. The decrease in viscosity leads the lower speed to generate similar misting rates to the higher viscosity fluid at higher speed. However, at the highest speed there is a clear relationship between rheology and quantity of misting.
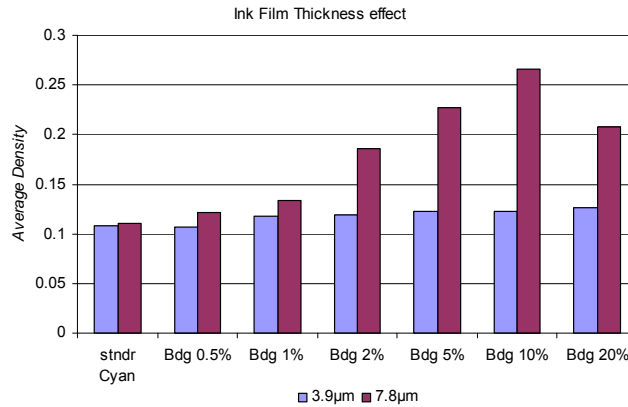
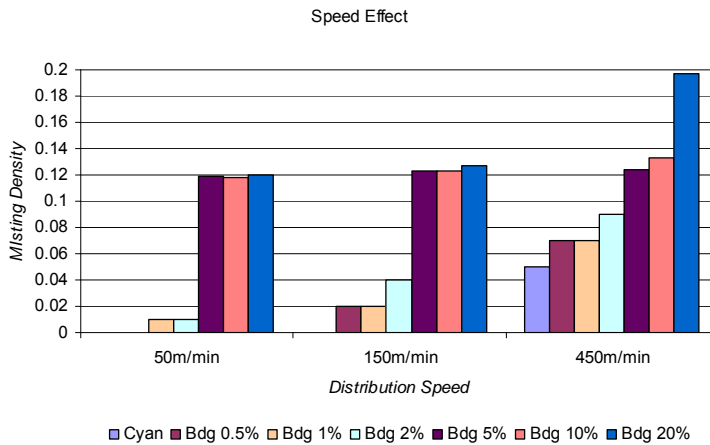*Figure 5: Misting effects for varying ink film thickness and dilutions.*



*Figure 6: Misting density for varying speed and dilution*

The misting trap topographic analysis visualises the misting distribution (Figure 7). Misting spreading dominates at the motor roller area on the left versus the oscillator area. The same trends are seen regardless of ink film thickness or rheology (Figure 3).
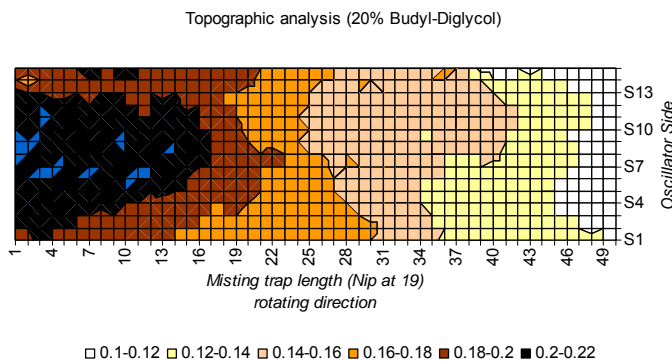


*Figure 7: Topographic analysis of the misting trap surface*

The range of droplet volume, measured by white light interferometer, does not vary significantly with ink film thickness. The whole range of ink viscosities generates droplets between $4.5\mu m^2$ to $130\mu m^2$ on the misting trap. Droplets of $4.5\mu m^2$ occur evenly across the misting trap regardless of the experimental conditions. Thus, the average droplet volume reflects the increase in larger droplets. The number of the larger droplets increase with decreasing viscosity (Figure 8). It is also increases with ink film thickness but effect

becomes significant with decrease in viscosity. Decrease of viscoelasticity forces produces shorter filaments with increases the effect on satellite droplets due to high speed elongation of the ink body. The elongation rate is a function of speed ratio depended on rollers size and rollers speed (Owens 2005).
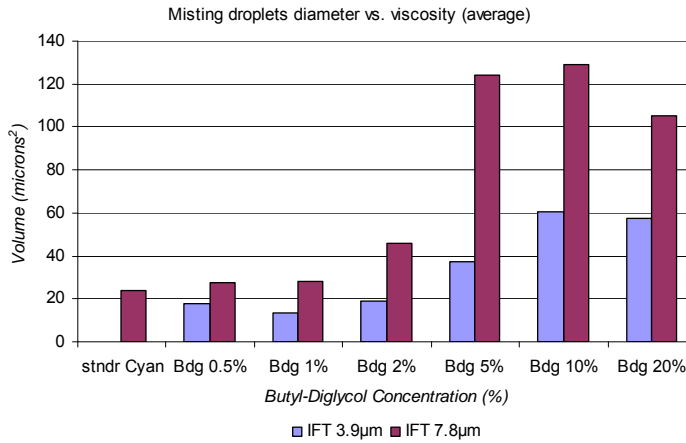


*Figure 8: Average droplet volumes for varying dilution and ink film thickness*

The average volume does not describe completely the misting effects and it is also important to identify the variation of droplets that are formed. The average is affected by the number of droplets variations. The difference between maximum and minimum volume gives the same rates with maximum volume because minimum is constant with $4.5\mu m^2$. Maximum to minimum volume difference does not illustrate significant difference when there is no much difference in viscosity. Standard deviation calculates the average difference between the droplets volume variations and so provides higher accuracy of droplets variation (Figure 9). The increase in ink film thickness allows more ink to flow away. Decrease in tack and viscoelasticity decreases dynamics of polymers network and so lower ink volumes are affected more by the rollers speed and so misting effects increase with an increase in droplets volume. The increased misting indicates high droplets volume variations due to droplets overlapping on the misting trap. The variation increases with the misting effects and indicates a linear effect between droplets variations and misting rates.
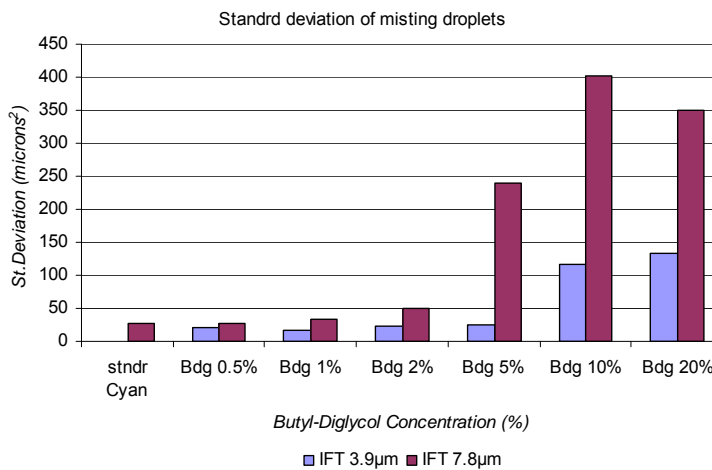


*Figure 9 Standard deviation of the droplets surface area for varying ink film thickness and dilution*

The misting effect was calculated as a function of the misting characteristics. The misting occurrence was the number of droplets versus the average droplets size. Therefore, the misting effect was calculated as the ratio of occurrence to the characteristic viscosity of the ink dilution.

Misting effect = $(Nd/Sv)/\eta*$

where Nd is the number of droplets, Sv is the average droplets size, and $\eta*$
is thecharacteristic viscosity at $147/sec^{-1}$ shear rate.

The misting increases with increased ink film thickness and decreased viscosity. The number of misting droplets also increases with the viscosity decrease and surface tension. This indicates an effect of capillary number which decreases with Butyl-Diglycol concentration (Figure 10). This indicates that the misting becomes critical as the Capillary number is reduced. The ink filaments tend to split unequally and aggregated ink parts are forced to extend and finally to flow away due to centrifugal forces.
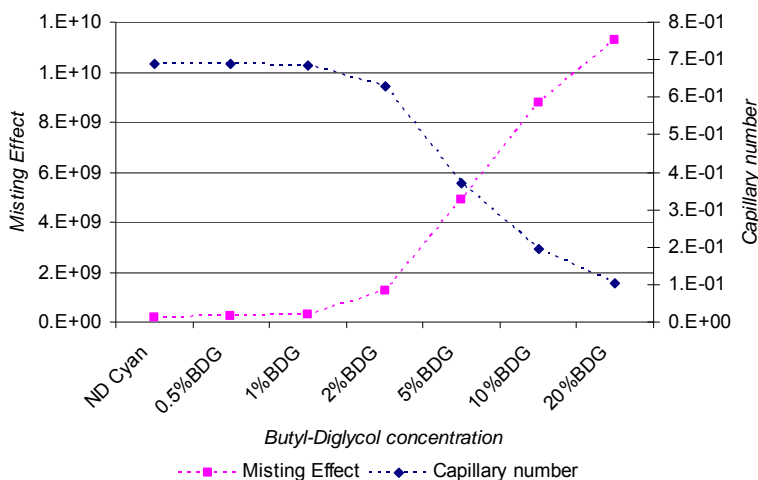


*Figure 10: Effect of dilution with Butyl-Diglycol on capillary number and misting effect*

## 4. Conclusions

An experimental methodology has been established which will allow the study of the formation and distribution of misting during the ink film splitting process. It has the potential to examine the formation of droplets in the nip and those formed by the rotational motion of the rolls. This will allow a better understanding of the mechanisms which effect misting.

Decreasing viscosity, which also alters the capillary number and increasing speed both increase misting. This affects misting droplets volume, spreading rates and droplet size range. There is a strong influence of ink film thickness which interacts with these parameters. The misting is related to the ink film thickness.

Misting increases with speed as the tensile forces generate instabilities leading to filaments failure and formation of satellite droplets. High viscoelasticity and adhesive dynamics allow the ink to extend in extremely thin filaments that break-up in multiple points across the length. The fine droplets are formed at the nip exit, which tend to follow the air flow.

However, in some cases there will be a significant volume of ink which remains attached to one of the rollers via a filament of ink. Aggregation occurs due to surface tension as a function of the ink film thickness or filaments width and extension rate. Those aggregate parts generate instabilities in the ink filaments with increased volume at the filaments neck. The filaments split unequally at the thinner area of the filament, sometimes giving rise to further satellite drops while a high volume ink droplet remains attached by the thicker filament to a roller. The roller surfaces accelerate away from each with rotation. If the drop is small, then the elastic forces will cause it to be drawn to the roller and the continuing changing direction of acceleration will cause it to fall back onto the surface. This mechanism is an integral part of rib formation. However, if the appended drop is large enough, the centripetal forces will overcome the elastic forces, the filament will extend and fail, leaving a larger volume droplet whose direction is dependent on it's velocity at the time of separation and whose trajectory is affected by gravity with little aerodynamic effects until it impacts on the mist trap. This produces large drops with characteristic tear drop shapes. This is could also be referred to as splashing or spitting.

## References

Bisset D. E., Goodacre C., Idle H. A., Leach R. H., Williams C. H., 1979, "The printing ink manual", Third edition, Chapters 3 and 10, Northwood Books, U.K.

Blayo A., Fang Waig Sandrine, Gandini A., Le Nest J. F., 1997, "Study of ink misting phenomena", TAGA Conference Proceedings

Christiansen S., 1995, "Resins are Gaining Weight", American Ink Maker 73, No. 101.

McKay R., 1994, "Effectiveness of pigments in suppression of misting of lithographic printing inks", FATIPEC Congress Vol. 22.

Owens M. S., 2005, "Misting in forward roll coating, Structure-Property-Processing Relationships", PhD Thesis, University of Minnesota, U.S.A

Sjodahl L. H., 1949, "Ink flow on rotating rollers", American Ink Maker Vol.29

Voet A., 1956, "Ink misting and its prevention", American Ink Maker 34, No. 2.

# A laboratory method to characterize and predict ink misting

*Saeid Savarmand*[1]*, Douglas Bousfield*[2]*, Richard R. Durand Jr.*[1]*, Robert Warren*[3]

[1] Sun Chemical Corporation, Material & Characterization Science
  631 Central Avenue, Carlstadt, NJ 07072, USA

  E-mails: saeid.savarmand@sunchemical.com, richard.durand@sunchemical.com

[2] University of Maine, Department Chemical & Biological Engineering
  Orono, ME 04469, USA

  E-mail: dbousfield@umche.maine.edu

[3] Sun Chemical Ltd, Rheology & Print Science
  Cray Avenue, St Mary Cray
  Orpington, Kent BR5 3PP, England

  E-mail: bob.warren@sunchemical.com

**Abstract**

Mistingis a common issue for high speed offset press operation. A laboratory device is used to characterize misting. Computer controlled drives turn rolls at known speeds. A flush mounted pressure transducer is used to record the pressure distribution during operation. Plastic strips, placed under the nip, capture mist generated. Several inks were characterized with a stress-controlled rheometer. Proposed dimensionless numbers consolidate the results for the inks studies in this work. A model of fluid slinging from a roll is proposed. The amount of misting inversely correlates with the pressure peak generated in the nip and directly increases with increasing the Reynolds number. The slinging model predicts that centrifugal forces can pull fluid into defects to enlarge filaments that can lead to slinging, but this mechanism only explains the results at high speeds. Misting at low speeds must come from a filament breakup pattern driven by surface tension.

**Keywords:** misting; filaments; rheology

## 1. Introduction

Ink misting during the distribution of inks on rolls and during printing has been a long standing issue for trouble free operation of presses. As press speeds increase to drive down costs, misting often increases. Misting is also an issue in the operation of size presses and metered size presses when coating paper: high misting conditions limit the coat weight range that can be obtained and operational speeds. A good fundamental understanding of misting is still lacking in the literature.

Many scientists have published on the roll coating flows in an effort to better understand the process and its flow instabilities. A number of studies have been performed for Newtonian liquids and two rigid rolls with a fixed gap. Pitts and Greiller (1961), Savage (1982), Coyle (1992), Benjamin *et al.* (1995) and Coyle (1986, 1988) studied the flow in a narrow, fixed gap between two rigid rolls. The fluid experiences an increase in pressure as it is pulled into the nip in front of the rolls. After the maximum pressure, the pressure drops, even below atmospheric, as the fluid exits the roll nip geometry. Decre *et al.* (1995) measured the meniscus profiles in asymmetric forward rigid roll coating of Newtonian fluids using laser sheet technique to provide an extensive database of more than 100 meniscus profiles. Gaskell *et al.* (1998) experimentally explored the detailed fluid mechanics of meniscus rigid roll coating of Newtonian fluids in which inlets are starved and flow rates are small. The key features of their findings were two large eddies in the forward mode and a single larger eddy consisting of two sub-eddies in the reverse mode. Others have looked at the ink film split mechanism, such as Hintermaier and White (1965) and Taylor and Zettlemoyer (1958). Pressure at the exit of the nip is able to drop to low levels, even below the vapor pressure of the fluid. This is thought to cause cavitation that provides a non-uniform film split and filaments at the nip exit. These filaments are stretched and break at short times. However, recent work with paper coatings by Lecuyer *et al.* ( 2009) indicates that cavitation is not a necessary condition for misting.

The amount of misting obtained for a loaded nip system was reported by Owen (2005). The mist was pulled into a device that quantified the drop size and number. A misting number was proposed to correlate the

results. However, the use of this misting number and the method to set the amount of fluid on the roll surface was not clear. These results were also limited to rolls in contact.

In this work, an experimental device is used to generate mist. This device is set up in such a way as to resemble the non-contact nip between the first (ink fountain) roller and second (engraved) roller on a typical web-offset (newspaper) press. One roll is loaded by pressure against a stop that is adjusted to give a known gap between a steel and rubber covered roll. The amount of misting, for a known number of revolutions, is obtained by weighing plastic strips placed near the nip exit. The pressure pulse in the nip is measured and correlated with the misting amount. Dimensional analysis gives some an initial correlation between the misting rate and the Reynolds number. A model is proposed that describes the centrifugal flow into potential fluid slings. A model is proposed that describes the centrifugal flow into potential fluid slings.

## 2. Experimental

A laboratory device is used to characterize misting is shown in Figure 1. Computer controlled drives turn rolls at known speeds. One roll is on a mount that slides to open or close the nip. By loading this mount against a stop, a set gap is established between the roll surfaces. The gap is adjusted by a 100 μm thick plastic film. The roll diameter and length are 127 and 235 mm, respectively. A flush mounted pressure transducer is used to record the pressure distribution during operation. Plastic strips, placed under the nip, captures mist generated. A digital camera records the filament formation in the nip and the behavior of the filaments after the nip. Details of the measuring system and the dimensions of the device are given in Johnson (2003).

Six inks were characterized in a controlled stress rheometer AR-G2 from TA Instruments with a parallel plate geometry of 40 mm at a gap of 500 μm. Both steady and oscillatory tests were completed, but the oscillatory were used for characteristic viscosity data. Table 1 shows the dynamic viscosity of the inks at 1 Hz and 30°C as they were found to result in relationships once employed in the corresponding dimensionless numbers.

3.0 mL of the ink sample is distributed on the roll surfaces at low speeds for five minutes. The rolls are stopped. Five plastic strips, around 20 x 5 cm, are placed next to each other in the cross machine direction on the base of the device near the nip exit. The rolls are rotated 25 revolutions at the speeds of interest. The weight increase of the plastic strips characterizes the amount of misting.
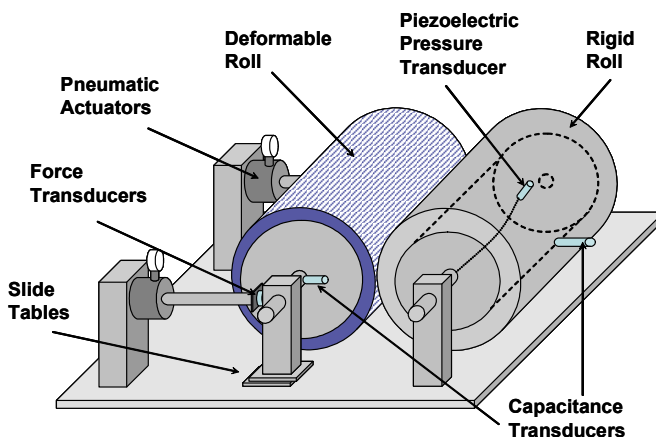


*Figure 1: Experimental device for ink misting*

*Table 1: Dynamic viscosity at 1 Hz and 30 °C for the six inks*

| Ink ID | Viscosity (Pa.s) |
|--------|------------------|
| A | 13.6 |
| B | 59.3 |
| C | 11.8 |
| D | 41.5 |
| E | 8.7 |
| F | 7.8 |

Figure 2 shows a typical pressure distribution of the ink for both roll surfaces turning at 1 m/s and a gap between roll surfaces of around 100 μm. As the ink is pulled into the nip, the pressure increases. At the exit of the nip, the pressure is sub-ambient This pressure behavior is typical of what others have reported such as by Zang, et al. (1991).
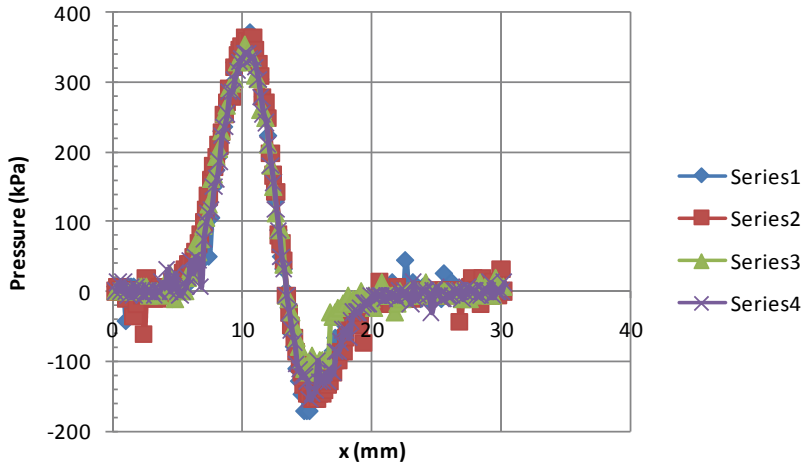


*Figure 2: Pressure pulse for ink A with roll speeds of 1 and 1 m/s. Different series are the same ink but repeated passes through the nip*

Figure 3 shows the filamentation of the ink well away from the nip exit for ink A. Some filaments break, ejecting a small drop of ink. All inks show a significant amount of filamentation for these conditions because of the large gap. In normal printing, filaments are also known to form, but these filaments are much smaller and hard to image.
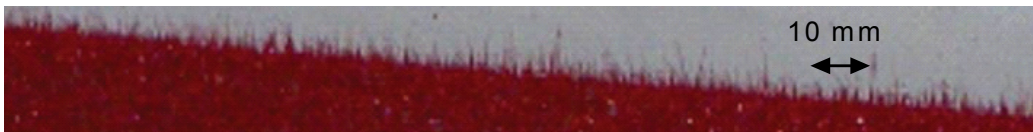


*Figure 3: Surface of roll for conditions in Fig. 2*

The model of Roper, et al. (1997) is modified to describe the flow of inks into filaments due to centrifugal forces. Development of the equations are in Appendix A. The surface evolution of an ink film subject to a variation in thickness and centrifugal forces is shown in Figure 4. Surface tension forces work to keep the film level while the centrifugal forces act to pull the ink into a filament. This filament has the potential to eject a drop at some speed.

Through a linear stability analysis, a velocity criteria for defect growth gives:

$$U > \sqrt{\frac{4\pi^2 \sigma R}{\lambda^2 \rho}}$$

(1)

where σ is surface tension, $R$ is the roll radius, λ is the length scale between filaments, and ρ is density. The non-linear calculation gives slightly higher velocities, but this is a approximation. Also, the non-linear calculation shows that large disturbances such as what is often seen at the exit of a printing nip, can grow at lower speeds than above and grow rapidly.

The only uncertain factor in this equation is the length scale between filaments λ. A figure that describes the geometry is located in the appendix. The filaments in Fig. 3 seem to be less than 0.5 mm apart, but the side view is capturing several filaments that are not in the same plane. If we select 2 mm as the length scale between filaments, and a surface tension of 30 mN/m, a density of 1000 kg/m³, and a roll radius of 60 mm, the critical speed is around 4 m/s. The event or factors that determine the spacing between filaments is not well understood at present. In the experiments, a small amount of misting is seen at 0.5 m/s.
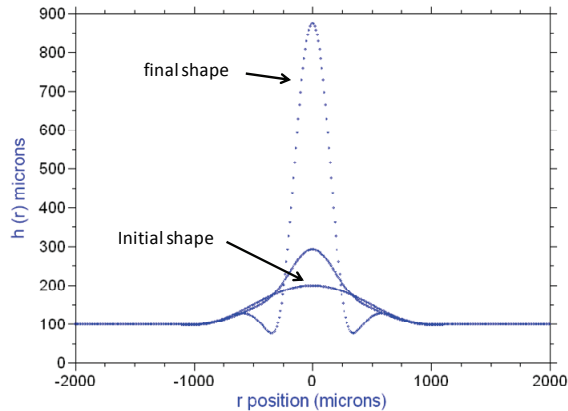
*Figure 4: Growth of a non-uniform film thickness due to centrifugal forces. At r=0, a small disturbance grows by pulling ink from other locations*

Another condition needs to be met before the filament will "sling" out a drop: the event must be rapid enough before the roll surface sees the nip again. For the laboratory device, the time scale is *2πR/U*. At 10 m/s, this is on the order of 40 ms. High viscosity inks will slow down the event, but thick films will speed it up. Figures 5 and 6 show the growth of a filament on a roll surface for parameters as noted.
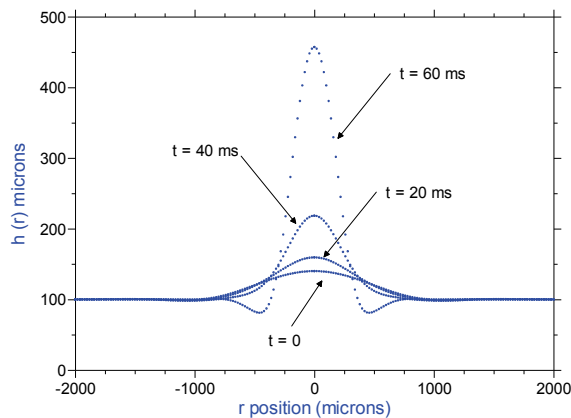


*Figure 5: Growth of a disturbance into a filament for a film thickness of 100 μm, a speed of 10 m/s, viscosity of 1 Pas, an initial disturbance of 50 μm, a surface tension of 30 mN/m, and roll radius of 0.1 m for a total elapsed time of 60 ms*
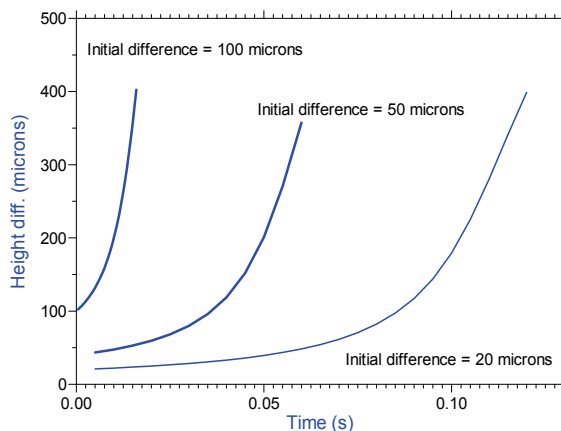


*Figure 6: The difference in height between the highest and lowest points of the film for conditions in Fig. 5 but for different initial disturbances*

Figure 6 demonstrates that a small initial disturbance, while it is unstable and grows, does not have enough time to sling fluid from the roll surface before the fluid would see the nip again. A large initial disturbance, one that is close to the film thickness, easily has time to sling fluid.

## 4. Results

After distribution of the inks on the roll surfaces, even at the lowest speeds tested of 0.5 m/s, misting is seen on the plastic strips. The amount of misting is small at 0.5 m/s. Speeds of up to 14 m/s were also tested even though the pressure distribution in the nip was not possible to record at these speeds. As expected, at speeds larger than 5 m/s, the amount of misting is significant. However, for some inks, the amount of misting is much less than other inks at the same speeds. Some cases were run when the roll speeds are not the same, but those results are not reported here. Most of the mist falls on the strip of plastic straight across from the nip, but mist is also seen on other strips that are on both sides of the center strip.

Different inks generate different pressure pulses in the nip. Figure 7 compares inks A and B when the roll surface speed is 2 m/s. Ink B does have a higher steady shear and complex viscosity. Therefore, it is expected that the pressure builds to a higher level with ink B compared to A as the ink passes through the nip of a set gap. For these inks, the pressure at the exit is well below atmospheric and even an absolute zero pressure. This result indicates that the ink is behaving as a solid and is able to withstand a tensile force. For the cases when the two rolls are loaded into contact with a set force, the pressure pulse is always the same even for different viscosity fluids Devisetti and Bousfield (2010).
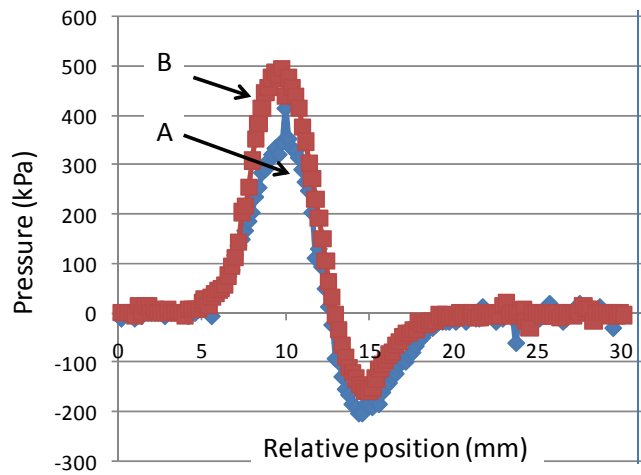


*Figure 7: Pressure pulses for inks A and B for roll speeds of 2 m/s. Gap between rolls is fixed near 100 μm*

There appears a correlation between the amount of misting, and the peak pressure recorded in the nip. Figure 8 shows this correlation using dimensionless misting and dimensionless pressure numbers defined as following.

$$N_m = \frac{M_m}{2\pi R N_{Rev}\,\rho W h} \tag{2}$$

$$N_{\Delta P} = \frac{(h/D)\Delta P}{\frac{1}{2}\rho U^2} \tag{3}$$

where   $M_m$ denotes the total misting mass measured on all the strips to collect mists and slings,
$U$ is the average surface roll speed,
$W$ is the width of the roll,
$h$ is the gap between the roll surfaces,
$D$ and $R$ are the roll diameter and radius, respectively.

Similar trend was found by Ascanio *et al*. (2003) where misting decreased as the pressure increased. This result may be due to the resistance of the ink to flow: a high resistance to be pulled into the nip may relate to the resistance of the ink to misting. In the model presented here, a high viscosity will slow down the slinging event. High viscosities are also known to reduce the formation of satellite drops during the breakup of jets, such as reported by Bousfield et al. (1990).
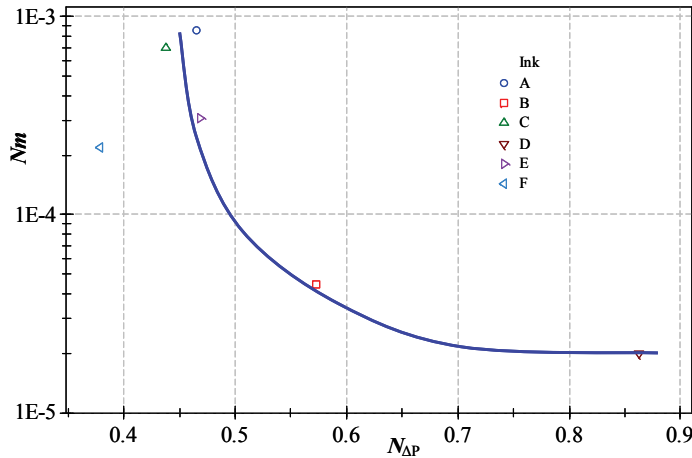
*Figure 8: Peak pressure vs. and the amount of misting for the six inks at roll surface speed of 1.4 m/s.*
*The line is to guide the eye*

Other dimensionless groups were also used to correlate the data and reduce the complexity of the problem. A Reynolds number, speed ratio, dimensionless roll radius and Capillary number can be defined as follows, where ρ is density, η is a characteristic viscosity, $U_1$ and $U_2$ are the velocities of each roll, $R$ is the roll radius, and σ is the surface tension of the ink. In this work, the dynamic viscosity obtained at 1 Hz and 30 °C is used.

$$Re = \frac{\rho h U}{\eta}; \quad U^* = U_1/U_2; \quad R^* = R/h; \quad Ca = \frac{\eta U}{\sigma} \qquad (4)$$

By using these dimensionless groups, the results for different inks tend to collapse onto a single line. Figure 9 shows how six inks, that have different misting behavior, tend to follow a single relationship. For a larger group of inks, this general correlation still exists but requires more ink parameters to obtain good correlation coefficients.
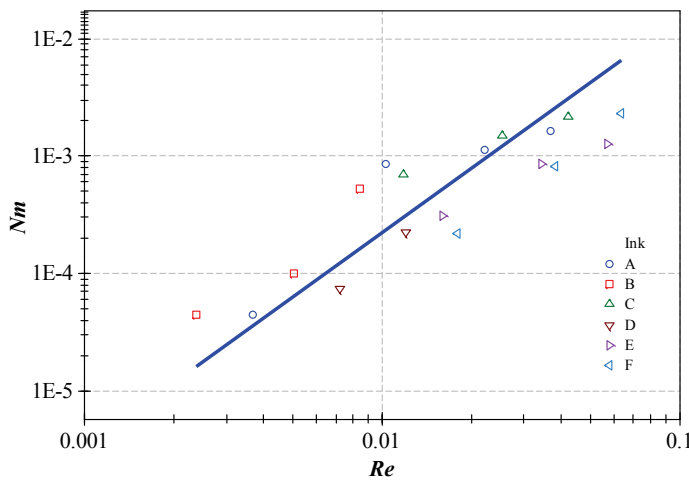


*Figure 9: Mist number as a function of Reynolds number. The data is for six inks at three different speeds*

Ink A has a measurable amount of misting even at speeds of 1.4 m/s. The model predicts that the length scale between filaments would need to be 6 mm to allow filaments to grow; this length scale is λ in Eq. (1). This length scale is larger than what is seen in Fig. 2. In addition, the time scale for these larger spacing of filaments to grow is slow compared to the time for the roll to rotate once. Therefore, most of the misting that occurs at this lower speed must be from the splitting of filaments to generate "satellite" drops, and not the slinging of ink from centrifugal forces. This finding is similar to what is discussed in Roper *et al.* (1997) with regard to misting for a metered size press. However, more modeling work is possible that would clarify the fate of attached filaments right after they exit the nip and move around the roll surface. A well-defined filament has the time to grow and become unstable, as Fig. 6 demonstrates.

## 5. Conclusions

Misting for six inks was characterized with a laboratory rolling nip device. The results are with a fixed gap that duplicates a nip on an offset press. The procedure described here can also be used to characterize misting for different speed ratios, inks that contain emulsified fountain solution, and for nips that are loaded into contact. The amount of misting inversely correlated with the pressure peak generated in the nip. Dimensional numbers are proposed to correlate the results; a preliminary result is that misting increases as Reynolds number increases. A model is developed to predict the slinging of a fluid from a roll surface; this model predicts misting only for higher speeds for filaments that are separated from each other by a couple millimeters. The misting at moderate speeds must come from filament breakup patterns described in the literature related to satellite drop formation during the breakup of jets.

## References

Ascanio, G., Carreau, P. J. and Tanguy, P. A., "Non-Newtonian effects on forward deformable roll coating at high speed," Paprican University Report 833, 1-28, (Nov. 2003).

Benjamin, D. F., Anderson, T. J., and Scriven, L. E. Multiple roll systems: steady-state operation. AIChE Journal. 1995; 41(5):1045-1060.

Bousfield, D. W., I.H. Stockel, and C. K. Nanivadekar, "The Breakup of Viscous Jets with Large Velocity Modulations", J. Fluid Mech., 218:601-617(1990).

Coyle, D. J.; Macosko, C.W., and Scriven, L. E. Film-splitting Flows in Forward Roll Coating. Journal of Fluid Mechanics. 1986; 171:183-207.

Coyle, D. J. Forward roll coating with deformable rolls: a simple one-dimensional elasto-hydrodynamic model. Chemical Engineering Science. 1988; 43(10):2673-2684.

Coyle, D. J. Roll coating. In Modern Coating and Drying Technology (ed. E. D. Cohen & E. B.Guto), VCH Publishers, New York. 1992; 3:63-115.

Decre, M., Gailly, E. and Buchlin, J.-M. Meniscus shape experiments in forward roll coating. Physics of Fluids 1995; 7(3):458-467.

Devisetti S. K. and D. W. Bousfield, "Fluid absorption during forward roll coating of porous webs", Chem. Eng. Sci., (2010) 65: 3528-3537.

Gaskell, P. H.; Innes, G.:Savage, M. D. An Experimental Investigation of Meniscus Roll Coating. Journal of Fluid Mechanics. 1998; 355: 17-44.

Hintermaier, J. C. and White, R. E. The Splitting of a Water Film Between Rotating Rolls. TAPPI Journal. 1965; 48(11):617-625.

Johnson M., Viscoelastic roll coating flows, PhD thesis, University of Maine, 2003.

Lecuyer H. A., J. P. Mmbaga, R. E. Hayes, F. H. Bertrand, and P.A. Tanguy, "Modeling of forward roll coating flows with a deformable roll: Application to non-Newtonian industrial coating formulations", Computers and Chem. Eng., 2009; 33:1427-1437.

Owen M. S., "Misting in forward roll coating: structure-property-processing relationships", PhD Thesis, University of Minnesota, 2005.

Pitts, E. and Greiller, J. The flow of thin liquid films between rollers. Journal of Fluid Mechanics. 1961; 11:33-50.

Roper III, J. A., Bousfield, D. W., Urscheler, R. and Salminen, P., "Observations and proposed mechanisms of misting on high-speed metered size press coaters," Proc. Tappi Coating Conf., Atlanta, GA, 1-14 (1997).

Savage, M. D. Mathematical models for coating process. Journal of Fluid Mechanics. 1982; 117:443.

Taylor, J. H. and Zettlemoyer, A. C. Hypothesis on the mechanism of ink splitting during printing. TAPPI Journal. 1958; 41(12):749-757.

Zang, Y. H., Aspler, J. S., Boluk, M. Y. and De Grace, J. H., "Direct measurement of tensile stress ("tack") in thin ink films," J. Rheol., **35,** 345-361 (1991).

# Dynamic analysis of temporal moisture profiles in heatset printing studied with near-infrared spectroscopy

*Carl-Mikael Tåg*[1]*, Maunu Toiviainen*[2]*, Mikko Juuti*[2]*, Patrick Gane*[3, 4]

[1] Forest Pilot Center Oy, FI-21200 Raisio, Finland
  E-mail: mikael.tag@fpc.fi

[2] VTT Technical Research Centre of Finland
  P. O B. 1199, FIN-70211 Kuopio, Finland
  E-mails: maunu.toiviainen@vtt.fi; mikko.juuti@vtt.fi

[3] School of Science and Technology, Faculty of Chemistry and Materials Sciences
  Department of Forest Products Technology, Aalto University
  P.O. Box 16300, FIN-00076 Aalto, Finland

[4] Research and Development, Omya Development AG
  CH-4665 Oftringen, Switzerland
  E-mail: patrick.gane@omya.com

### Abstract

Dynamic analysis of the water transfer onto uncoated paper, and its permeation and absorption into the porous structure were studied online in a full-scale heatset web offset printing environment. The moisture content of the paper was investigated at five different positions during the printing process. Changes in moisture content of the paper were studied as a function of web temperature and printing speed. Additionally, the influence of fountain solution composition on the pick-up by the paper was investigated. The water content of fountain solution transferred to the paper from the printing units was observed as changes in near-infrared absorbance. A calibration data set enabled the subsequent quantification of the dynamic moisture content of the paper at the studied locations. An increase in the printing speed reduced the water transfer to the paper and an increase in web temperature resulted in a reduction in the moisture content. Differences in the drying strategy resulted in different moisture profiles depending on the type of fountain solution used. As a conclusion, the near-infrared signal provides an effective way to characterize the moisture dynamics online at different press units.

**Keywords**: evaporation; moisture content; fountain solution transfer; heatset printing; water uptake

## 1. Introduction

Although exemplifying paper as the porous medium in this work, the generalisation to dynamic liquid transfer onto the surface, including permeation and absorption into porous media, is of importance to many industrial and naturally occurring environmental processes. In offset printing the image is transferred from the plate cylinder via a rubber blanket to the paper, thus transferring water from the printing plate non-image area, ink from the image area and an ink-water emulsion developed during equilibration on the press to the paper. The evaporation and emulsification properties of the fountain solution in the ink are important in order not to interfere with the ink transfer (Kipphan, 2001). One of the reasons to study the transfer of water to the paper is that water governs the expansion of paper causing dimensional changes, e.g. misregister, decreased strength of the paper, an increase in surface roughness and a decrease in gloss (Enomae and Lepoutre, 1997). Accurate measurement of predominantly water-containing fountain solution picked up by the ink and the paper has been a missing link in the evaluation of the behaviour of paper on the printing press, and is required for understanding the mechanism of the interaction between fountain solution, ink and paper.

In the literature, there is a broad interpretation of how much water is transferred to the paper. Despite its large impact, the amount of fountain solution picked up by the paper is a very small quantity in absolute terms, though significant in reference to the mass, pore volume and thickness of paper. Gravimetric methods, therefore, cannot be expected to provide the accuracy which is required, especially since fountain solution is lost in the delivery system and in roller trains through spillage and evaporation. It has been pointed out in previous studies that in some cases more fountain solution is transferred to the printed areas of the paper by the water-ink emulsion than in the unprinted areas (Lim *et al.,* 1996). Trollsås and Larsson (1987) found,

using a gravimetric method, that the moisture uptake in newsprint is 0.3 - 0.5 gm$^{-2}$ per side per printing unit. Hansen (1997) measured the uptake with a micro-wave based method and found that the uptake in newsprint is 0.4 - 0.7 gm$^{-2}$. Results reported for a single nip coldset offset press vary from 0.20 gm$^{-2}$ (Trollsås, 1995) to 0.68 gm$^{-2}$ (Hansen, 1997). The fact that ink carries most of the solution has been established (MacPhee, 1985; Lindquist *et al*., 1981) but quantitative information on the amount of the solution carried by the ink and the paper has not been firmly reported so far. A number of measurement principles to quantify water content can be adapted to on-press applications, based on, for example, infrared (Rosenberg, 1985; Thormählen, 1988) and radioactive trace element detection (Säynevirta and Karttunen, 1973). However, knowledge of the emulsified state and the amount of the transferred water and how much is transferred with the ink to the paper and to the unprinted parts is lacking. This study focuses on using near-infrared (NIR) spectroscopy in determining absolute and relative moisture levels in-line in a heatset web offset printing process. Due to the strong absorption bands of water near 1 450 and 1 940 nm, NIR spectroscopy is very sensitive to moisture. The NIR spectra of wet paper clearly exhibit visible characteristics which are related to its moisture content. NIR diffuse reflectance spectroscopy provides a fast and robust method for measuring both chemical and physical attributes of a wide variety of materials. In coating applications, the moisture content and *z*-directional moisture profiles of paper coatings have been studied (Paaso, 2007, Keränen, 2009).

The absorption and evaporation of liquid mixtures applied as droplets on porous pigmented tablet structures have been studied by combining total liquid weight loss and the corresponding NIR absorbance, showing the behaviour in which liquid water and moisture are transported in different stages of absorption and evaporation (Tåg *et al.,* 2010). The primary findings in this current work relate the observations previously made on the idealised coating pigment tablet structures to observations of how the dynamic printing process is delivering moisture to an uncoated, highly mineral filled supercalendered paper. This study suggests that NIR diffuse reflectance spectroscopy can be used as a moisture sensitive system and to provide accurate online qualitative indicators, but, also, when accurately calibrated, can provide quantification of moisture levels, moisture distribution and dynamic moisture transfer. The NIR signal provides a way to follow relatively easily the dynamics online at different press units.

## 2. Methods

The printing trials were performed at the Forest Pilot Center Oy, Raisio, Finland, on a Heidelberg Web-8 heatset printing machine with five over five printing units, i.e. with application potential for 5 colours applied to each side of the paper web. The press room conditions were constant, maintained at 50 % RH (relative humidity) and temperature, $T$ = 23 °C. The width of the paper web was 500 mm. Two types of fountain solution were used. Each fountain solution is proprietary and primarily based on the given proportions of isopropyl alcohol (IPA). Commercial fountain solutions are known to contain small amounts of further emulsion stabilisers and cleaning agents. Fount 1, supplied by KTA (KTA-yhtiöt Oy, FIN-02630 Espoo, Finland) contained 6 % IPA and 3.5 % of an additive (Vegra 3232Zi, VEGRA Gesellschaft für Herstellung und Vertrieb von Produkten für die grafische Industrie mbH, 84544 Aschau am Inn / Germany). Fount 2, supplied by Hostmann Steinberg, contained 3 % IPA and 3 % of an additive supplied by Hostmann Steinberg (Redufix AF, Hostmann Steinberg, Bremer Weg 125, Celle D-29223, Germany). The temperature of the fountain solutions in the circulation was 10 °C, the pH 5.2 and the conductivity 1 100 µS. The paper was printed only on one side with the upper printing units using Flint Premoterm 6000 (Flint Group, 26b, Boulevard Royal, L-2449 Luxembourg) low tack inks.

In Table 1, the trial program is presented. The printing speed and the web temperature in the drying unit were varied. The silicone applied after the oven before folding was Rollosil CXT 35, Fujifilm Hunt Chemicals Europe NV Zwaluwbeekstraat 14 - 9150 Kruibeke, Belgium. The silicone concentration in the aqueous solution was 6 %. Silicone is used in the printing process to ensure better runnability in the folding unit, i.e. crack prevention, rub resistance, and to provide additional reduction in the levels of static electricity and friction.

The studied paper was a lightweight uncoated (LWU) paper with a basis weight of 60 gm$^{-2}$. The paper was stored under 50 % RH and $T$ = 23 °C conditions for 12 months before the trial, thus providing fully stabilized humidity inside the reel at a level of 5.5 % by weight. The measurement positions in respect to the width were located 5 cm from the front side edge of the web and placed 25 cm from the printing nips (probe 2 and 3). The moisture content of the paper was determined from an unprinted and a fulltone (100 %) cyan strip along the paper sheet. In addition, the moisture content from a fulltone yellow strip was measured in a separate trial.

| Fount 1 (KTA) | Fount 2 (Hostmann Steinberg) | Printing speed [rph*] | Printing speed [ms⁻¹] | Web temperature [°C] |
|---|---|---|---|---|
| tp1 | tp7 | 22 000 | 3.9 | 120 |
| tp2 | tp8 | 22 000 | 3.9 | 120 |
| tp3 | tp9 | 32 000 | 5.6 | 120 |
| tp4 | tp10 | 32 000 | 5.6 | 120 |
| tp5 | tp11 | 22 000 | 3.9 | 150 |
| tp6 | tp12 | 32 000 | 5.6 | 150 |

## 2.1 NIR measurement setup

The multipoint NIR instrument utilized in this work is designed to perform diffuse reflectance measurements over a full NIR wavelength range simultaneously at multiple locations. It consists of a halogen lamp as light source and an NIR spectral camera (SWIR Spectral Camera, Specim Ltd., Oulu, Finland) as spectrometer. Multipoint in-line measurements are facilitated by several diffuse reflectance probes which are connected to both the light source and the spectrometer with optical fibres. The light source contains a high power (~50 W) halogen lamp from which the radiation is collected into multiple illumination output fibres accessible through Straight-Tip connectors at the front panel of the device. The custom-made fibre-optic hub of the camera/spectrometer permits the simultaneous use of 112 detection channels accessible through Miniature Unit connectors. The measurement probes include mirror-optics which project the illuminating light from the source fibre onto the sample and, conversely, collect the back-scattered light into the detection fibre. To permit a true noncontact measurement, the sample-to-probe distance is optimized to be 165 mm, although the variation of ± 5 mm is permitted which makes the instrument robust against the vibrations of the paper web in the $z$-direction in the current application. The illumination spot has an elliptical shape of the size 4 mm x 7 mm (minor and major axis) on the sample surface, and the elliptical detection spot of the size 1 mm x 3 mm resides within the larger illumination spot. Using a spectrograph, the polychromatic light from a single detection fibre is dispersed into a full spectrum in the wavelength range 1000 – 2500 nm onto a column of the 256 x 320-pixel MCT detector matrix. Due to the low transmission of the utilized quartz optical fibres at long wavelengths, the effective wavelength range is limited to 1000-2100 nm. The illumination and detection fibres were 400 μm and 90 μm in diameter, respectively, and varied between 3 - 20 m in length depending on the measurement position.

The probes were mounted with adjustable mounting parts (CVI Melles Griot, Albuquerque, USA) and mechanics to five positions in the printing process. A schematic figure of the measurement positions is shown in Figure 1. Probe 1 was located at the unwinder in order to detect moisture variations in the unprinted reel. Probe 2 was placed after the first printing unit, where only fountain solution (FS) was applied (no image) with the aim to detect water transfer to paper after one printing unit. Probe 3 was positioned after the last printing unit with the purpose of studying the water pick-up by the paper from all 5 printing units. Probe
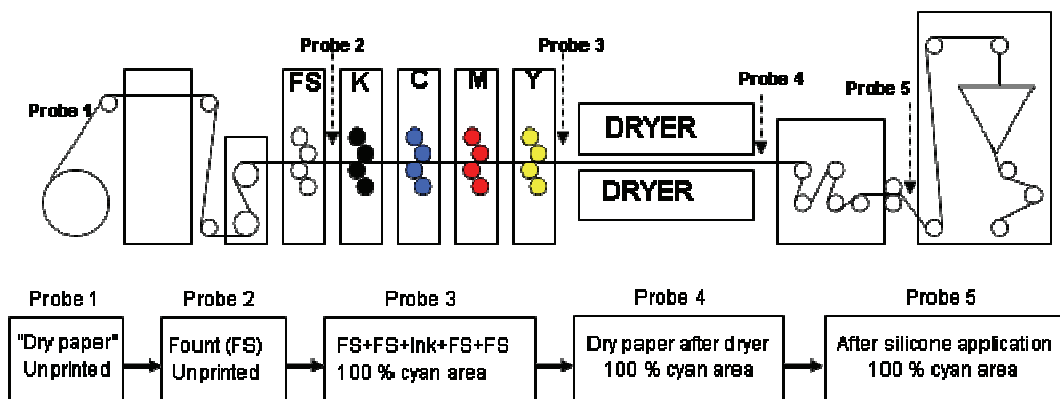


*Figure 1: The measuring spots in chronological order: Probe 1 at the unwinder, Probe 2 after the first printing unit (only fountain solution application), Probe 3 after the last printing unit, Probe 4 after heatset dryer, Probe 5 after the silicone application unit*

4, positioned after the dryer, gave information on the effect of the heatset dryer on moisture removal, and probe 5 on the influence of silicone application on the re-moistening of the paper. In addition, the web temperature was measured at each of the 5 positions during the moisture measurements with a noncontact laser thermometer (Raytek, ST$^{tm}$ 20 Pro, Raytek Corporation, 1201 Shaffer Rd. PO Box 1820, Santa Cruz, CA 95061 - 1820 USA).

Conventionally, the linearity of measured spectral data is enhanced by subjecting them to the $\log(1/R)$ transform, where the reflectance, $R$, at the wavelength $\lambda$ is given by

$$R(\lambda) = \frac{I(\lambda) - D(\lambda)}{W(\lambda) - D(\lambda)} \tag{1}$$

and this transform was utilized in this study, as well. The numerator in Eq. (1) consists of the raw signal $I(\lambda)$ corrected for the instrumental dark current $D(\lambda)$, whereas the denominator contains the instrumental response, i.e. the white reference $W(\lambda)$ after dark-correction. The white reference is usually measured with a non-absorbing material, such as optical Teflon, which scatters light strongly and has no absorption bands in the NIR wavelengths. In this study, the instrumental response was measured using a white reflectance standard (1.5-mm thick Optical Diffuse Material, Gigahertz-Optik, Germany) at the beginning and at the end of the trial day, and the dark current was measured hourly. The integration time of the detector was set to 7 ms and the frame rate to 100 Hz. The amount of data was reduced and signal quality was improved by averaging 100 consecutive spectra to obtain one spectrum per second. The experiments involved the collection of data at both static and dynamic printing process conditions. The single moisture levels of the static trial points were obtained by averaging all spectra of the corresponding measurement and subsequently calculating the moisture level with the constructed calibration model.

## 2.2 Calibration setup and measurements

To obtain quantitative moisture profiles for the experiments conducted at the printing press, the measured NIR data should be related to absolute moisture values. This is accomplished with the use of a calibration model which requires that a calibration data set be measured offline in laboratory conditions. The calibration measurements were conducted using the commonly known loss-on-drying method, in which a wetted paper sample was dried on a microbalance (MS-70, Dosetec, Finland), so that its NIR spectrum and weight were measured simultaneously. First, the NIR spectrum and weight of the sample were measured prior to wetting at room temperature. Second, the paper samples were held in a humid chamber for the duration of 30 - 40 min so that their moisture levels were raised up to 8 - 12 % (w/w) before they were placed on the microbalance and the drying process was started. The paper samples were then dried in room temperature and 20 % RH, and their NIR spectra and weight were measured simultaneously 10-20 times until a stable condition with regard to the paper mass was achieved. Third, the paper sample was heated with a halogen lamp at 105°C until its weight reached a minimum level. This value was interpreted as the dry weight of the paper and its NIR spectrum was paired with zero moisture level.

The moisture percentages of the calibration samples were then calculated using the equation,

$$Moisture\ (\%) = 100 \times \frac{m_{wet} - m_{dry}}{m_{wet}} \tag{2}$$

where $m_{wet}$ is the weight of wet paper, at each stage of drying, and $m_{dry}$ is its dry weight. To mitigate the effect of measurement error, the loss-on-drying measurement was repeated five times with different paper samples, each having a dry mass between 200-400 mg.

The calibration procedure was performed by estimating the bias and slope coefficients, i.e. the coefficients a and b, in the linear equation,

$$\boldsymbol{y} = a + b\boldsymbol{a} + \boldsymbol{e} \tag{3}$$

using least-squares (LS) regression. Here, the elements of the vector $\boldsymbol{y}$ contain the moisture percentages of the calibration samples calculated using Eq. (2). The vector $\boldsymbol{a}$ contains the areas of the water absorption peak calculated for each spectrum as the area between the linear line and the NIR spectrum as illustrated in Fig. 2. The linear line (Fig. 2, left) is fitted between two points which are calculated as the average $\log(1/R)$ values in the wavelength ranges coloured in light grey. The vector $\boldsymbol{e}$ contains the model errors which are here

minimized in LS sense. The calibration set is visualized in Fig. 2 (right-hand image). The actual moisture percent values on the horizontal axis were calculated using Eq. (2), whereas the moisture values on the vertical axis were estimated for the same samples using the linear model of Eq. (3). Ideally, in the absence of noise and measurement errors, the dots should be located on the solid diagonal line drawn in the figure. However, due to the random nature of the measurement, they exhibit variance around the diagonal. Prior to calibration and prediction, the spectral noise was reduced by smoothing all spectra with the Whittaker smoother (Eilers, 2003).

As opposed to using multivariate calibration models with the whole effective range of 1 000 - 2 100 nm, the wavelength range of interest was reduced to cover the water peak area between 1 850 - 2 050 nm in the quantitative analysis of moisture content. The chosen calibration technique was robust against any changes in the offset and curvature of the spectral baseline and other interfering spectral features occurring outside the range of interest which might result from the drift of electronics, the vibration of the paper track and the use of several measurement probes. Based on separate laboratory studies, it was concluded that the use of siliconization, yellow and cyan ink, did not have a significant effect on the NIR spectra of paper in the wavelength range of interest (results presented in Figure 7). The siliconized and printed paper samples did not, e. g., exhibit varying light scattering properties manifested as multiplicative error in the spectral amplitude. Multiplicative correction of the spectral signal via, e. g., the use of a ratio model was thus not needed (Osborne, 1993). With the current instrumentation, the chosen simple calibration technique yielded stable temporal moisture signals, and it was thus preferred over other ratio models and multivariate calibration techniques. All paper samples utilized in the calibration were unprinted and no silicone was applied.
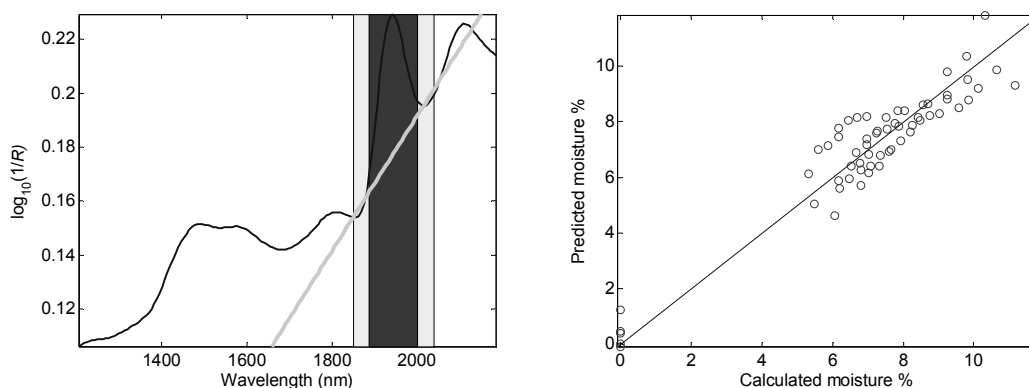


*Figure 2: Visualization of the water peak area calculation (left); calculated and predicted moisture percentages of the calibration set (right)*

## 3. Results

### 3.1 Water transfer under dynamic conditions

In Figure 3, the moisture contents at the different measurement positions are exemplified. The error bars were calculated as standard deviations of the moisture profiles from a single run, and they thus reflect the stability of the process. One has to take into account that Probes 1 and 2 measure the moisture from an unprinted area and Probes 3 - 5 from a 100 % cyan printed area. The good correlation between the NIR signal in Probe 1 and the moisture content reported by the paper manufacturer is evident. In the first printing unit, fountain solution is applied on the paper (recorded by the difference between Probe 1 and Probe 2). At the second printing unit (black) fount is transferred to the areas without black ink and in the third unit, cyan ink is applied, and after that again fountain solution from the two remaining units (See also Figure 1). The results clearly and logically show that:

1) the more printing nips the paper web passes, the more liquid water is transferred to the paper,
2) the dryer dries the paper, and
3) application of silicone acts to re-moisten the paper after the dryer.

The moisture content is seen to increase by approximately 12 % after the first unit, and with additionally ~ 1 % after all subsequent printing units, the initial uptake therefore being somewhat larger. The figure also gives the relative response of liquid transferred to the paper by capillarity and permeability in the first units and

pressure permeation primarily in the latter units. The dryer reduces the moisture content by 74.2 %, and by application of silicone the paper picks up additional moisture.
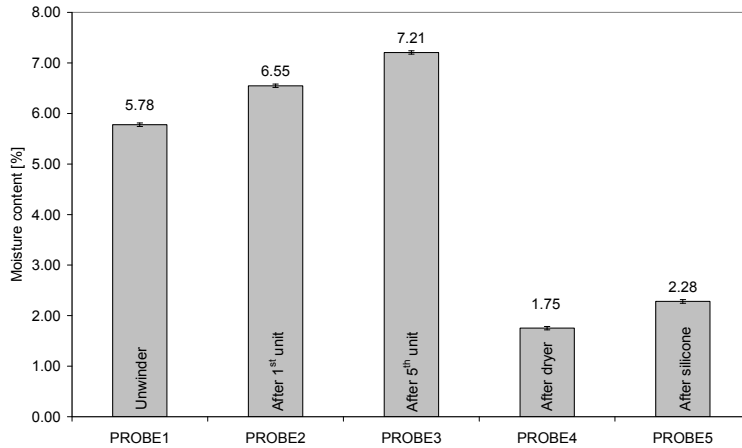


*Figure 3: Moisture contents of the paper during the printing process for tp4. Probe 1 = unwinder, Probe 2 = after 1st printing unit with only fountain solution application, Probe 3 = after 5th printing unit, Probe 4 = after dryer, Probe 5 = after silicone application. The printing speed was 32 000 rph (5.6 ms⁻¹) and the web temperature 120 ℃ (paper web temperature measured inside the dryer)*

Figure 4 exemplifies how the paper web speed influences the uptake of the fountain solution by the paper. The figure describes the residence time dependence in the printing nip of the rate parameters of water sorption. It needs to be highlighted that when the machine speed increases, the water ductor roller speed also increases linearly. Hence, the fount demand to avoid toning (ink drying on printing plates) is compensated for the changes in printing speed, and, as seen in Figure 4, the NIR measurements were able to detect the changes in fount uptake by the paper as a function of unit speed. The results state that an increase in the web speed decreases the liquid uptake by 0.61 % for Fount 1 and 0.20 % for Fount 2. However, since the delivery conditions are not analysed here it would be premature to consider this finding as universal. The differences in liquid uptake by the paper between the two founts are partly due to the fast evaporating IPA, which concentration is lower for Fount 2.
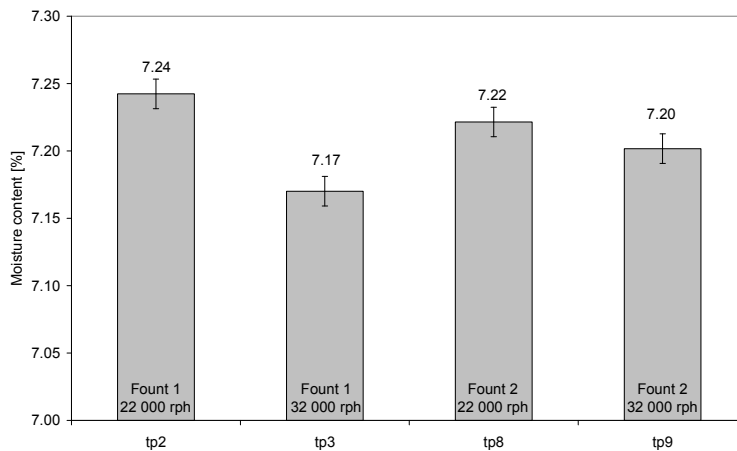


*Figure 4: The influence of paper web speed on the fountain solution uptake by the paper. The printing speed was 22 000 rph (3.9 ms⁻¹) vs. 32 000 rph (5.6 ms⁻¹), respectively. The web temperature in the NIR measurement spot (Probe 3) measured with the noncontact laser thermometer was 24.8 °C for Fount 1 and 24.4 °C for Fount 2*

As exemplified in Figure 5, the web temperature affects the drying of the paper differently. An increase in web temperature reduces the moisture content of the paper by 61.2 % for Fount 1 and 65.4 % for Fount 2. A higher web speed results in a higher moisture content of the paper, especially as the web temperature is lower. Hence, it can be concluded that both printing speed and web temperature affects the moisture content of the paper, partly by the printing speed which affects the amount of liquid uptake by the paper and partly by the drying efficiency.
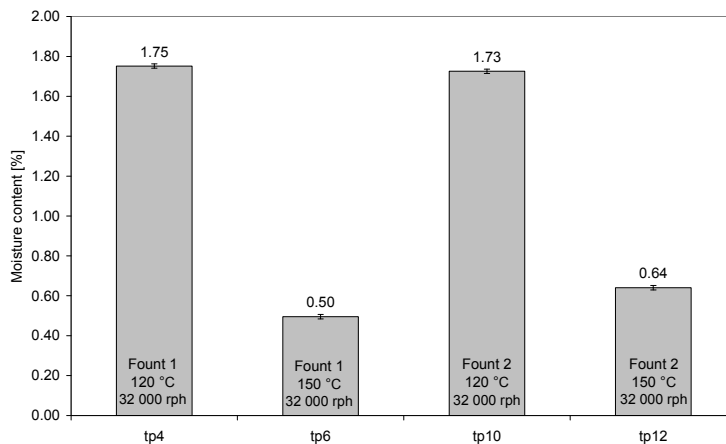
*Figure 5: The influence of web temperature in the dryer on the drying of the paper. The web temperatures were achieved by setting the blowing temperature in the dryer to 167.0 °C and 207.0 °C generating the web temperatures 120 °C and 150 °C, respectively*

In Figure 6, dynamic measurements were performed from a normal printing situation for the studied paper and the fountain solution dosage was gradually increased with time to its maximum level, keeping the printing speed constant. The paper moisture content was determined from an unprinted, a 100 % cyan and a 100 % yellow printed area. It can be seen that more fountain solution is transferred to the unprinted parts of the paper compared to the area printed with cyan and yellow as delivered fount amount increases. The areas printed with yellow also generated higher moisture content compared with cyan. When printing cyan, two layers of fount were applied before the ink and two layers on top of the ink (See Figure 1). The presence of cyan ink decreases the amount of moisture detected by the NIR method by 2 % when compared to unprinted paper. The ink layer obviously acts as a barrier, closing the surface pores and refuses thus to take up the fount applied from the two last units. In the case of the yellow printed area, 4 layers of fount were applied under the ink, hence resulting in a higher moisture content after which the surface is sealed by the ink. The data also suggest that yellow ink might emulsify more fountain solution than cyan, which can be related to its lower tack level. It can thus be concluded that the relative amounts of fount from (a) image and (b) non-image areas depend on the equilibrium ink emulsification power above a threshold fount dosage for (a), relative to the fount dosage for (b).
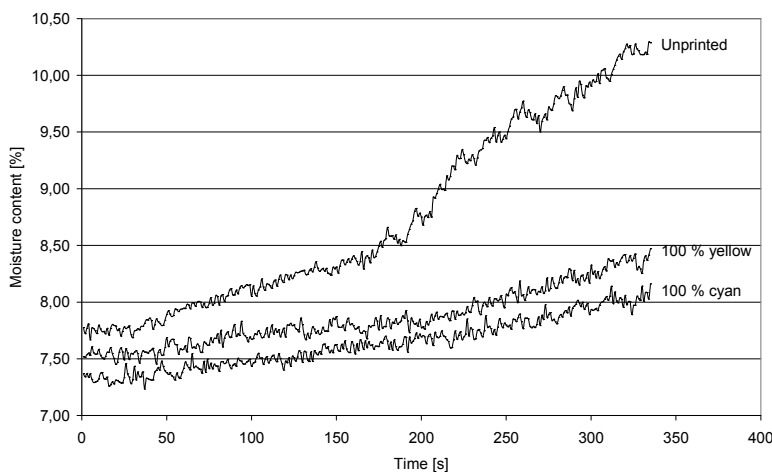


*Figure 6: Paper moisture determination from an unprinted area (fountain solution (FS) application from 5 units), a 100 % cyan (application order: FS + FS + ink + FS + FS) and a 100 % yellow (application order: FS + FS + FS + FS + ink) printed area (Probe 3) as the fount dosage level was increased to its maximum*

## 4. Discussion

Online moisture determination has been conducted on a 5 / 5 colour heatset offset printing machine using NIR diffuse reflectance measurements. Online information about moisture profiles was obtained at different

locations along the printing line. The dynamic measurements revealed information about the relative uptake of fountain solution in image and non-image area combinations, how the printing speed influences the fountain solution uptake by the paper and how the web temperature influences the drying capability in relation to volatile component and total moisture. Quantitative moisture contents were determined at different locations along the printing line applying an offline calibration technique. The calibration model is simple and robust as it eliminates the spectral baseline effects caused by varying sample-to-probe distance induced, for example, by the flapping of the paper web. It is also intuitively direct as it links the water content with the magnitude of the major water absorption band at 1 940 nm.

The study clearly showed that an increased web temperature reduced the moisture content significantly. The speed increase in the Heidelberg Web-8 printing machine increases both the ink ductor roller speed as well as the fount ductor roller speed 1:1 for compensation of the ink-water demand in the printing process. The linear increase of the roller speeds leads us to conclude that running faster should deliver practically the similar amount of fount per unit area to the blanket and to the paper at the proportionally increased rate. However, an increased printing process speed resulted in an apparently lower moisture content of the web, indicating that the residence time in the nip could be the issue of decisive importance. Thus, the fount pickup by the paper might not be dependent solely on the physical and chemical structure of the paper but more on the nip dynamics presenting the liquid to that structure. A decrease in moisture content of a paper should then indicate that for similar dynamic capillary pressure and the capillary transport velocity, defined by the paper structure, the pressure-absorption-time integral in the nip defines the volume being transferred. If the water sorption is diffusion controlled, as with, for example, extremely dense paper, the water transport rate is increased by diminishing moisture content. Salminen (1988) has shown that during pressure penetration in uncoated paper, the effect of capillary forces is minimized, and the transport rate is independent of the moisture content.

As illustrated in Fig. 7, the NIR absorption of the cyan and yellow ink is relatively low at the location of the water absorption band near 1 940 nm. As stated above, it was verified in separate measurements that printing has negligible effect on the NIR spectra of paper in the wavelength range of interest. Furthermore, the NIR spectra of the aqueous fountain solutions are virtually identical with the spectrum of pure water. Thus, in a spectroscopic sense, all fountain solutions may be treated as water from the perspective of the measurement. It is thus assumed that the spectral signals of the other components, i.e. the inks, the fountain solutions and the silicone fluid, do not interfere with the signal of interest, namely the strong absorption spectrum of water. The presence of IPA, however, has an influence on the amount of moisture the paper is able to pick up, and the relative evaporative loss. Furthermore, the presence of ink also has an influence on how much moisture the paper picks up, as shown in this study. The effect of silicone application can also be detected with the NIR method as an increase in the moisture level. This is expected since the silicone fluid is mostly water.
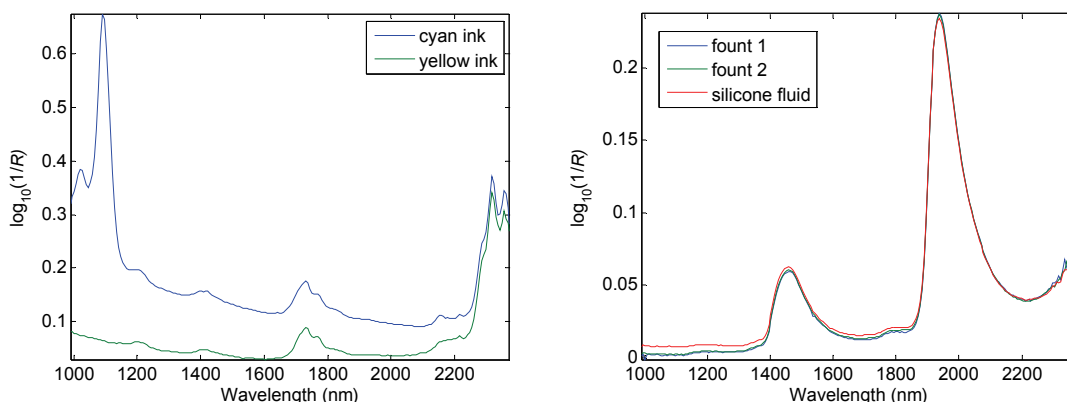


*Figure 7: NIR spectra of cyan and yellow inks (left), as used in the printing trial. NIR spectra of the two different fountain solutions and the silicone-izing liquid (right). The spectra were measured in diffuse transflectance*

The online moisture determining technique provides a tool to examine more closely the interactive nature of liquids with porous substrate media exposed to capillary forces and pressure permeation. For example, in comparing the uptake of fountain solution from the first unit (non-image press) with that of uptake from later units (cyan image unit plus further non-image units applied to the prior full tone (100 %) cyan image area) we see that the initial uptake into unprinted paper is greater than that delivered on average by subsequent non-image units applying fountain solution to the prior printed area. This finding enables us to begin to draw

conclusions concerning the relative effects of capillarity versus pressure-driven permeation and the competitive nature of fountain solution versus ink oil within the pore structure of paper. The initial application of a water film is made under pressure to a relatively dry paper displaying an effectively empty pore volume. This empty pore volume at the paper surface can exhibit capillarity, filling the finest pores initially. Concurrently, the pressure pulse applied to the water film in the printing nip forces water into larger pores and acts to transmit water through the permeable part of the pore structure, depending primarily on pore size and connectivity. At subsequent units, the capillary action is greatly diminished as the surface fine pores are already saturated and ink oil competes within those fine pores for capillary absorption capacity and wetting. Unfilled fine pores within the paper bulk then have to draw liquid through the resistive structure of already filled fine pores at the surface and the now ever present ink layer. Thus, in subsequent print units, permeation under external pressure takes the dominant role in accessing the bulk structure of the paper. Using this technique, the relative magnitudes between the three forces, capillarity, liquid exchange competition and permeation can in principle be identified. The observed reduced fountain solution uptake as a function of speed provides a further tool to conclude the comparison of these forces. Higher speed translates into reduced residence time. This means that the pressure pulse amplitude increases but the integral of force over time may either increase or decrease depending on the deformation properties of the blanket and paper. Furthermore, the observation that increasing fountain dosage impacts non-image areas more than image areas suggests that the capacity of ink to emulsify fountain solution and the permeability of the ink layer are the limiting factors in the case of the image area water pickup, whereas increased dosage in the non-image area provides a rapid response to the wet film thickness, and hence pressure pulse, in the printing nip at the non-image contact area.

## 5. Conclusions

Information about local moisture content of paper during printing, exemplified in a heatset web offset press, and the evolution of moisture distribution during drying has been provided by the application of near-infrared spectroscopy. The process parameters evaluated on-line led to initial findings of practical importance, namely:

- fountain solution uptake by the paper is decreased as the web speed was increased partly due to changing press nip conditions,
- different drying properties of the paper can be identified depending on the type of fountain solution used as the web temperature was increased, and
- re-moistening of the paper can be evaluated, exemplified by silicone solution applied onto the paper after the drying section.

The moisture content determined from a yellow printed area was higher than that of cyan, showing the emulsification properties of the different process colours and also the phenomena of capillarity, pressure driven permeation and film splitting.

The study gives insight into the moisture distribution at different process steps, and thus helps to identify the reasons for possible uneven moisture profiles in the paper. Additional potential for using the NIR probe technique in studying detailed liquid-porous substrate interactions in real time has been identified.

### References

Eilers P H C (2003) A Perfect Smoother Anal. Chem. 75 3631-3636.

Enomae T and LePoutre P (1997) Gloss relaxation processes: surface roughening by water J. Pulp Paper Sci. 23 34-39.

Hansen Å (1997) Water absorption and dimensional changes of newsprint during offset printing, 23rd research conference of IARIGAI: Advances in printing science and technology Paris France (UK: Wiley 1997).

Keränen J T, Paaso J, Timofeev O and Kiiskinen H (2009) Moisture and Temperature Measurement of Paper in the Thickness Direction, Appita Journal 62 308-313.

Kipphan H (2001) Handbook of print media - Technologies and production methods ISBN 3-540-67326-1 Springer-Verlag Berlin Heidelberg New York.

Lim P Y W, Daniels C J and Sandholzer R E (1996) Determination of the fountain solution picked up by the paper and ink in offset printing, International Printing and Arts conference, Minneapolis, USA 83-87.

Lindquist U, Karttunen S and Virtanen J (1981) New models for offset lithography, Advances in printing science and technology 16 67-96.

MacPhee J (1985) Further insight into the lithographic process-with special emphasis on where the water goes TAGA Proceedings 269-297.

Paaso J (2007) Moisture depth profiling in paper using near-infrared spectroscopy, Doctoral thesis, University of Oulu.

Osborne B G, Fearn T and Hindle P H (1993) Practical NIR Spectroscopy with Applications in Food and Beverage Industry, Chapter 6, Longman Scientific and Technical, Essex, England.

Rosenberg A (1985) What part play surface water and emulsified water in the lithographic process, TAGA Proc. 264-282.

Salminen P (1988) Studies of water transport in paper during short contact times, Doctoral thesis, Åbo Akademi, Department of paper chemistry, Turku, Finland.

Säynevirta T and Karttunen S (1973) New fountain solution for offset newspapers, Graphic Arts in Finland 2 1-12.

Thormählen I (1988) Testing the lithographic behaviour of printing ink in printing presses and in the laboratory, TAGA Proc. 220-226.

Trollsås P E and Larsson L O (1987) Vattenupptagning och dimensionsförändringar hos tidningspapper vid tryckning i offsetförfarande Tidningspappersbrukens forsknings-laboratorium, rapport nr. 4:6, Stockholm.

Trollsås P E (1995) Water uptake in newsprint during offset printing Tappi J. 78 155-160.

Tåg C - M, Juuti M, Koivunen K and Gane P A C (2010) Dynamic water transport in a pigmented porous coating medium: novel study of droplet absorption and evaporation by near infra-red probe spectroscopy, Ind. Eng. Chem. Res. 49 4181-4189.

# Surface and structural properties of EPDM and NBR rubber blankets

*Gorazd Golob*[1]*, Mladen Lovreček*[2]*, Miran Mozetič*[3]*, Alenka Vesel*[3]*, Odon Planinšek*[4]*,*
*Marta Klanjšek Gunde*[5]*, Vilibald Bukošek*[1]

[1] University of Ljubljana, Faculty of Natural Sciences and Engineering, Slovenia
  E-mails: gorazd.golob@ntf.uni-lj.si, vilibald.bukosek@a.ntf.uni-lj.si

[2] University of Zagreb, Faculty of Graphic Arts, Croatia
  E-mail: mlovrece@grf.hr

[3] "Jožef Stefan" Institute, Ljubljana, Slovenia
  E-mails: miran.mozetic@guest.arnes.si, alenka.vesel@guest.arnes.si

[4] University of Ljubljana, Faculty of Pharmacy, Slovenia
  E-mail: Odon.Planinsek@ffa.uni-lj.si

[5] National Institute of Chemistry Slovenia, Ljubljana, Slovenia
  E-mail: marta.k.gunde@KI.si

**Abstract**

During our research work we studied surface properties of lithographic offset rubber blankets based on polar NBR/TM and non-polar EPDM elastomer blends, modification of surface free energy using oxygen plasma treatment and defunctionalization of surface properties using IR and UV high power laser devices.

Results of defunctionalization or modification of blanket surface properties using proper IR or UV laser are presented in this paper. Our investigation includes surface free energy determination using contact angle measurements with different liquids and calculation method by Owens Wendt, chemical analysis of the surface using FTIR ATR spectra measurement and analysis using KnowItAll software with database and dynamic mechanical (structural) analysis of elastomer samples. We studied properties of untreated and plasma or laser treated elastomer material as a basis for the improvements and understanding of new functionality of rubber blankets with discrete hydrophilic/oleophobic and hydrophobic/oleophilic areas.

After treatment with oxygen plasma we achieved higher level of total surface free energy and polarity with NBR/TM compared to EPDM rubber. The ratio of surface cleaning effect compared to chemical modification during oxidation process is still unknown but it seems that surface cleaning or ablation effect using oxygen plasma has stronger impact on surface free energy compared to oxidation.

After additional IR and UV laser treatment of the same the values of surface free energy did not return to the former state of untreated samples, as we expected. We are able to reach about half of water contact angle value differences only at EPDM sample.

**Keywords:** NBR rubber; EPDM rubber; oxygen plasma treatment; laser treatment; FTIR ATR spectroscopy; dynamic mechanical analysis

## 1. Introduction

During our research work we studied surface properties of lithographic offset rubber blankets based on polar NBR/TM and non-polar EPDM elastomer blends, modification of surface free energy using oxygen plasma treatment and defunctionalization of surface properties using IR and UV high power laser devices.

We studied surface properties of untreated and plasma or laser treated elastomer material as a basis for the improvements and understanding of new functionality of rubber blankets with discrete hydrophilic/oleophobic and hydrophobic/oleophilic areas. First results of plasma treatment were already presented at IARIGAI and other international research conferences (Golob et al, IARIGAI 2009, SGA 2009, Tiskarstvo 2010). Results of defunctionalization or modification of blanket surface properties using proper IR or UV laser are presented in this paper.

## 2. Research methods

Our investigation included surface free energy determination using contact angle measurements with different liquids, chemical analysis of the surface using FTIR-ATR spectroscopy and dynamic mechanical (structural) analysis of elastomer samples to find correlations between surface and bulk properties of rubber samples. According to our experience during investigation we performed sample treatment and measurements within 24 hours to avoid degradation of achieved surface changes. Presented results are mean value of 10 or more measurements of contact angles, IR spectra were measured at least twice for each sample. Dynamic mechanical analysis (DMA) were performed only once per sample.

### 2.1 Materials

Four different blankets, commercial products of Savatech, Kranj, were used:

- Advantage UV Red - EPDM rubber for UV printing, non-polar, silica filler (RED)
- Advantage UV Black - EPDM rubber for UV printing, non-polar, soot/carbon conductive filler (BLACK)
- Advantage DUAL - NBR/TM (90/10) blend rubber for conventional printing, polar, silica filler, stronger cured (BLUE)
- Advantage Expression - NBR/TM (90/10) blend rubber for conventional printing, polar, silica filler (LIGHT BLUE)

In this paper only results of two typical rubber blankets, RED and BLUE, are presented in detail. For DMA, special rubber plates consisting of blanket surface layer only, were prepared.

### 2.2 Oxygen plasma treatment

For oxygen plasma treatment (Mozetič, 2003, 2006) of the samples we used a lab plasma reactor with a vacuum pump and an inductively coupled RF generator at the power of approximately 200 W. Each sample was exposed to oxygen plasma with the neutral atom density of $5x10^{21}$ m$^{-3}$, the electron density of $8x10^{15}$ m$^{-3}$ and the electron temperature of 35 000 K for 27 s. The samples were kept at floating potential of -15V.

### 2.3 Defunctionalization by laser treatment

Defunctionalization of oxydized hydrophilic rubber surface, described in literature, is achieved with warming at high temperature for long time. In our case our intention was to get hydrophobic stage on different types of plasma treated rubbers using proper laser source for heating.

Professional IR laser (1050 nm) device, built by LPKF for marking, ablation and cutting systems with power from 1 W to 12 W in pulsed or CW mode gave us good results on all samples with exception of BLACK sample, where strong ablation occurred. High power UV laser (355 nm) in range from 0.17 W to 3.80 W gave us acceptable results, but different comparing to IR laser.

### 2.4 Surface free energy

During most of our research work we used Young and other equations based on contact angle measurements of sessile drop with polar and non-polar liquids: water, diiodomethane and formamide. For calculations of surface free energy we used Owens-Wendt method (geometric mean equation), Wu method (harmonic mean equation) and acid-base calculation by Lewis (Erbil, 2006).

For surface free energy measurements we used Krüss DSA100 apparatus with software and test liquids database for calculations.

### 2.5 FTIR-ATR Spectrometry

FTIR-ATR (Fourier Transform Infrared - Attenuated Total Reflectance) spectroscopy is an established method for analysis of solids and other samples. In ATR, the sample is placed in contact with a high refractive index crystal. The IR beam enters the crystal and rays at or beyond a critical angle to the sample interface are reflected. The beam penetrates into the sample up to a few μm, most of reflection is from the surface layer of the sample. Typical peaks of absorption spectra give us information of chemical elements, chemical groups or bonds at the surface.

We used Perkin Elmer FTIR-ATR spectrometer type Spectrum GX1 in mid IR area (wavenumber 500 - 4000 cm$^{-1}$) to get IR spectra of untreated and treated samples. Analysis of spectra was performed using KnowItAll software with spectral database.

## 2.6 Dynamic mechanical analysis

$T_g$ (glass transition temperature) is a property of only the amorphous portion of a semi-crystalline solid depends on the cooling rate, molecular weight distribution and could be influenced by additives. At a low temperature the amorphous regions of a polymer are in the glassy state. If the polymer is heated the molecules can start to wiggle around and polymer reach its rubbery state. Tan δ is a measure of elastomer dampening and ratio of loss to storage modulus (Brady, 2003).

We used TA Instruments Q800 DMA (Dynamic Mechanical Analyzer) with GCA (Gas Cooling Accessory) for cooling up to -80 ºC for measurements of $T_g$, tan δ and other bulk material properties.

## 3 Results

Results of surface free energy (total, disperse and polar part) calculated using Owen Wendt method, are presented in Figure 1.
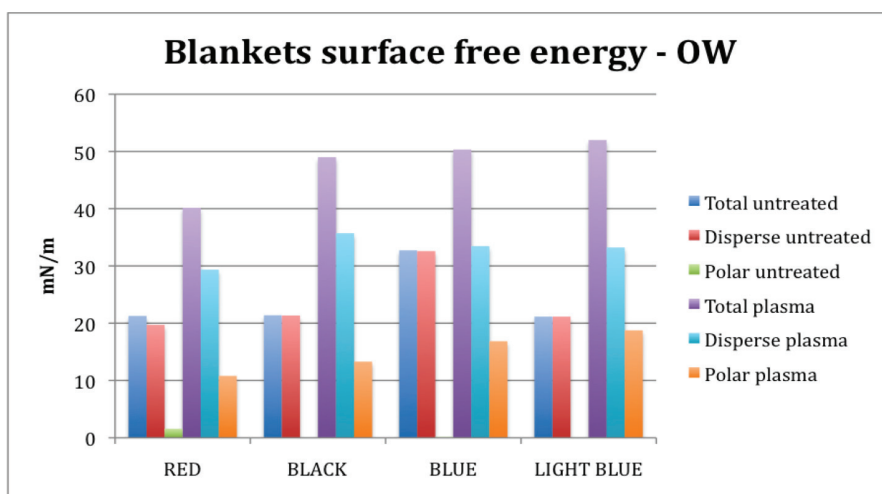


Figure 1: Surface free energy of rubber blankets with their polar and disperse parts

Figure 2 shows contact angles for water of untreated, oxygen plasma treated and laser treated rubber blanket for all four samples.
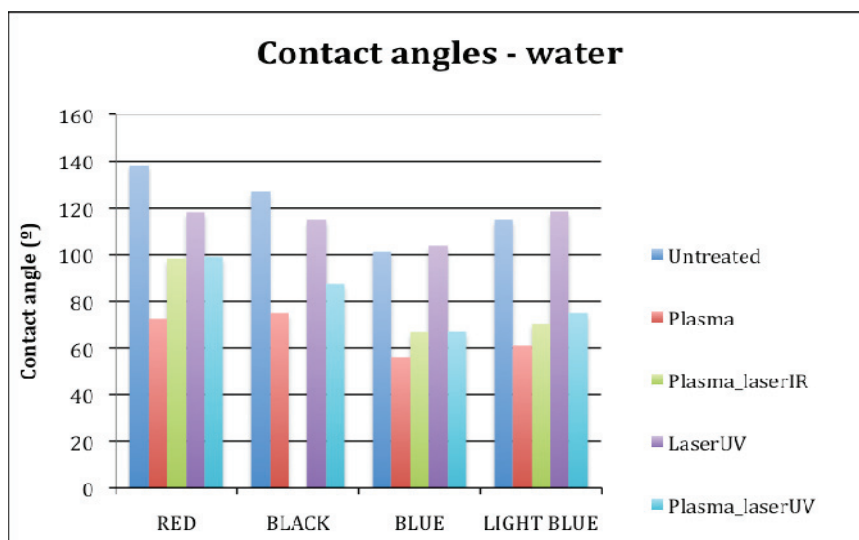


Figure 2: Contact angles of untreated, plasma and laser treated rubber blanket samples

Figures 3, 4 and 5 show FTIR ATR absorption spectra of untreated, plasma and laser treated RED samples.
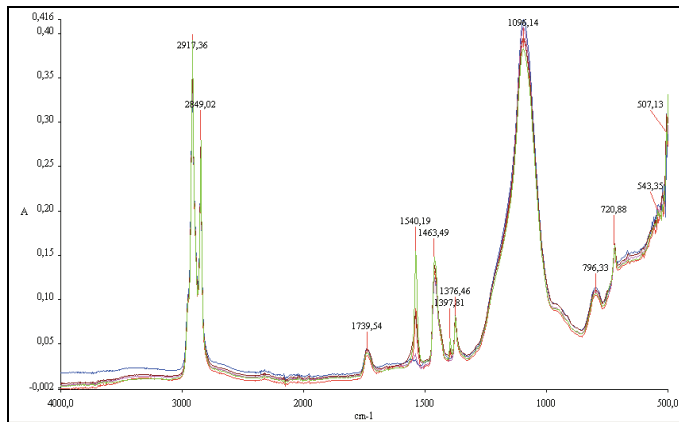
*Figure 3: Absorption spectra of RED rubber blanket spectra -(green - no treatment, red - oxygen plasma treatment, blue - oxygen plasma and IR laser treatment, violet - oxygen plasma and UV laser treatment, brown - UV laser treatment)*
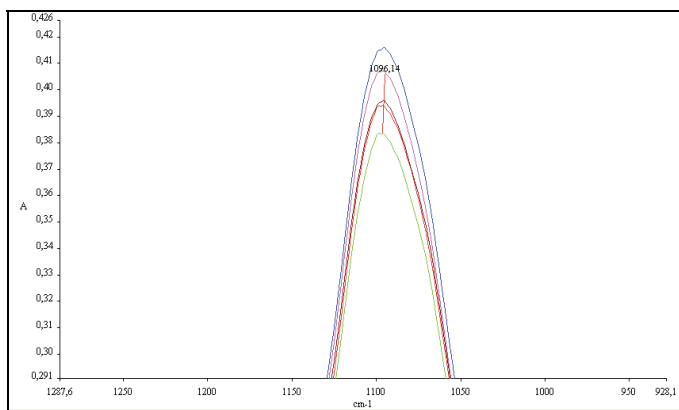


*Figure 4: Zoomed part of absorption spectra of RED rubber blanket spectra with significant peak at 1096.14 cm$^{-1}$*
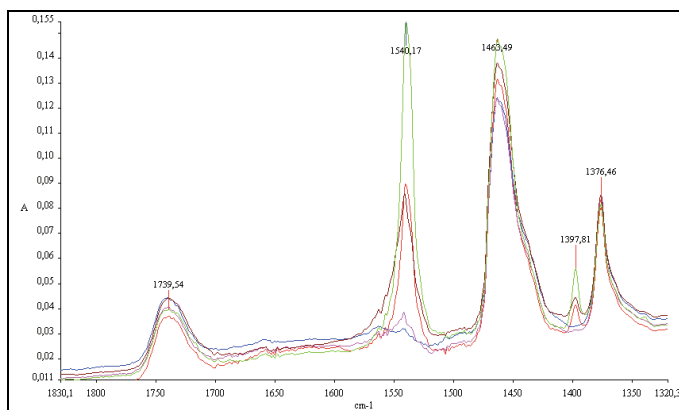


*Figure 5: Zoomed part of absorption spectra of RED rubber blanket spectra with significant peaks at 1397.81 cm$^{-1}$, 1463.49 cm$^{-1}$ and 1540.17 cm$^{-1}$*

Significant changes between untreated and plasma treated RED samples were achieved at 1096.14, 1397.81, 1463.49 and 1540.19 cm$^{-1}$.

1096.14 cm$^{-1}$ is characteristic strong peak for alcohols (C-O), anhydrides (C-O-C), ethers (C-O-C), silicons (Si-Ph) and medium strong peak for sulfur (C=S). At this peak lowest absorption is achieved for untreated sample and highest for oxygen plasma combined with IR laser treated sample. 1397.81 cm$^{-1}$ is characteristic strong peak for sulfur (SO$_2$). 1463.49 cm$^{-1}$ is characteristic medium strong peak for many alkanes (CH), amides (N-H), aromatic (ring) chemical groups and some impurities - water vapor (OH). 1540.19 cm$^{-1}$ is characteristic for amides (CNH), nitro (NO$_2$) groups with strong and ureas (NH) with medium peak. At this

peaks the highest absorption was achieved at untreated samples and lowest at plasma combined with IR or UV laser treated samples. Figures 6 and 7 show us spectra of BLUE samples after same treatment with oxygen plasma, IR and UV lasers.
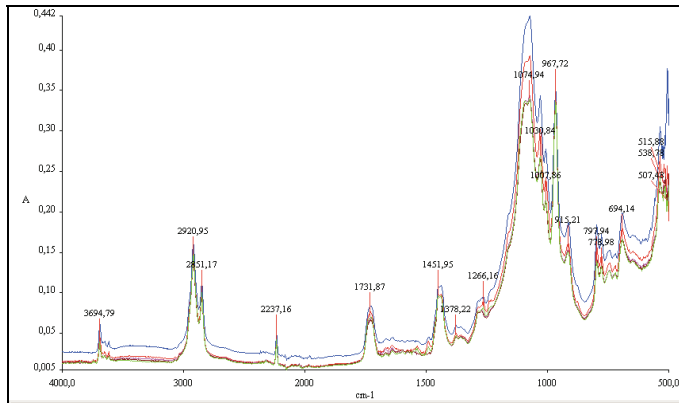


Figure 6: Absorption spectra of BLUE rubber blanket spectra (green - no treatment, red - oxygen plasma treatment, blue - oxygen plasma and IR laser treatment, violet - oxygen plasma and UV laser treatment, brown - UV laser treatment)
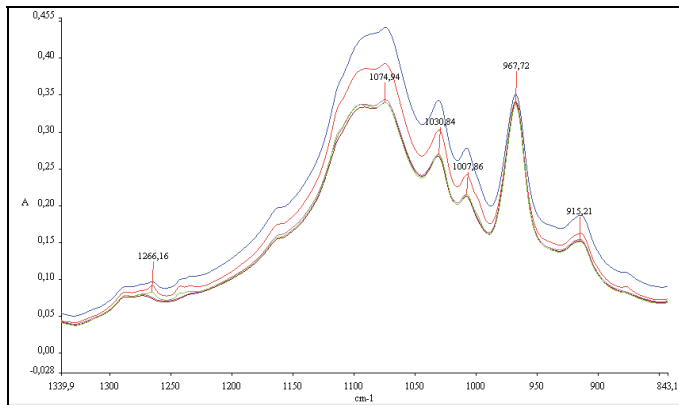


Figure 7: Zoomed part of absorption spectra of BLUE rubber blanket spectra with significant peak at 1074.94 cm$^{-1}$

Significant changes between untreated and plasma treated BLUE samples were achieved at 1074.94 cm$^{-1}$. This is characteristic peak for anhydrides (C-O-C), ethers at 1103 cm$^{-1}$ (C-O-C), 5 ring ethers (C-O-C), silicons (Si-O-Si), sulfur (S=O) with strong peaks and some other chemical groups with weak peaks. Highest absorption is achieved at oxygen plasma treated and oxygen plasma treated combined with IR laser treated samples. Figures 8 and 9 show the results of dynamic mechanical analysis.



Figure 8: DMA analysis of RED sample, indicating $T_g$ = -32.92° C and tan δ with one peak at -22.84° C

*Figure 8: DMA analysis of BLUE sample, indicating $T_g$ = -18.75° C and tan δ with two peaks at -8.97° C and 5.57° C*

## 4. Conclusions

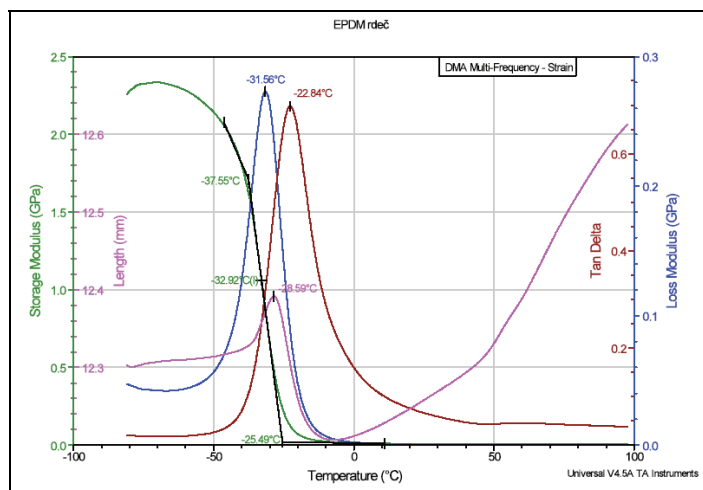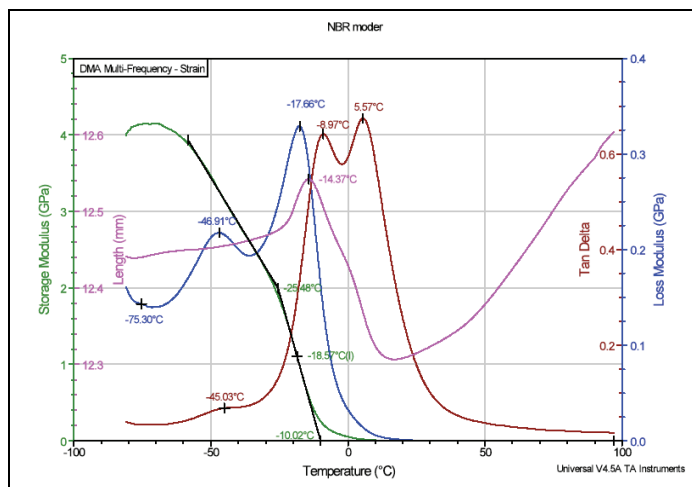After treatment with oxygen plasma we achieved higher level of total surface free energy and polarity with BLUE compared to RED rubber. The ratio of surface cleaning effect compared to chemical modification during oxidation process is still unknown but it seems that surface cleaning or ablation effect using oxygen plasma has stronger impact on surface free energy compared to oxidation. To avoid influence of impurities at the surface of untreated samples they were wiped with ethanol five minutes before measurements and/or plasma treatment but obviously this treatment was not enough efficient comparing to plasma treatment. Contact angle measurement and surface free energy calculation of untreated samples compared to oxygen plasma treated samples show us significant differences between samples. After additional IR and UV laser treatment of the same the values of surface free energy did not return to the former state of untreated samples, as expected. We were able to reach about half of water contact angle value differences only at RED sample. Treatment using only UV laser gives us lower contact angle for water at RED and BLACK samples, but slightly higher for BLUE and LIGHT BLUE samples. Obviously UV laser treatment gives us different results for EPDM and NBR types of rubber. We intend to continue our research of plasma and laser treatment of rubber blanket surface in the future to find out their highest possible differences of surface free energy and polarity.

Surface free energy measurements and FTIR-ATR spectra measurement and analysis of chemical structure are not sufficient to determine hydrophilic/hydrophobic or oleophilic/oleophobic character of the surface before and after oxygen plasma and/or IR or UV laser treatment. Comparing spectra analysis of BLUE and RED we see that significant changes of spectra peaks are at different wavenumber. At BLUE sample after oxygen plasma treatment, amount of chemical groups with bonded oxygen and sulfur were higher (higher peak). At RED sample spectra peaks after plasma treatment were lower, changes occurred on NO2, SO2 with bonded oxygen and other chemical groups without oxygen. There were no additional peaks formed by new chemical groups. In general spectral curve of BLUE and RED samples treated with oxygen plasma and IR laser was positioned slightly higher compared to untreated sample perhaps due to higher roughness of treated samples. Apparently chemical changes during plasma and laser treatment were not significant but they are different for EPDM and NBR type of rubber. During our further investigation we will try to find out other possible reasons for significant changes of surface free energy and polarity after plasma treatment like roughness, porosity and heterogeneous composition of the surface.

DMA analysis is a method for material bulk analysis. It gives us opportunity to compare surface properties with internal structure of rubber blankets, determined by glass transition temperature and dampening. Glass transition temperature difference between RED and BLUE samples gives us basic information about macromolecular structure of both elastomers. Tan δ with double peak at BLUE sample confirmed that a blend of two crude rubbers is a basic raw material in this case.

### Acknowledgements

## References

Brady, Robert: *Comprehensive Desk Reference of Polymer Characterization and Analysis*, Oxford University Press, 2003, ISBN 0 8412 3665 8.

Erbil, H. Yildrim: *Surface Chemistry of Solid and Liquid Interfaces*, Blackwell Publishing, 2006, ISBN 1 4051 1968 3.

Gorazd Golob, Miran Mozetič, Kristina Eleršič, Ita Junkar, Dejana Đorđević, Mladen Lovreček: *Rubber blanket surface energy modification using oxygen plasma treatment*, 36th International Resarch Conference IARIGAI, Stockholm, 2009.

Gorazd Golob, Miran Mozetič, Mladen Lovreček: *Rubber raw material surface energy modification using oxygen plasma treatment,* SGA Pardubice, 2009.

Gorazd Golob, Mladen Lovreček, Miran Mozetič, Alenka Vesel, Odon Planinšek, Marta Klanjšek Gunde, Diana Gregor Svetec: *Determination of surface free energy and chemical modifications of plasma treated elastomer surface*, Tiskarstvo 2010, Stubičke Toplice.

Mozetič Miran, Alenka Vesel, Cvelbar Uroš: *Method and device for local functionalization of polymer materials, international patent WO 2006/130122*.

Mozetič, Miran: *Controlled oxidation of organic compounds in oxygen plasma*. Vacuum. [Print ed.], 2003, vol. 71, p. 237-240.

# Plate performance affects offset blanket piling

*Kaisa Vehmas, Soile Passoja, Asko Sneck, Eija Kenttä, Antti Peltosaari, Jani Kiuru*

VTT Technical Research Centre of Finland
P.O. Box 1000, FI-02044 VTT, Finland
E-mail: kaisa.vehmas@vtt.fi

**Abstract**

Non-image area piling on blanket is considered as a process property of offset printing, which influence on print quality and press runnability. There is not a single reason for piling - it is always a combination of press settings and all the materials used in printing. In this study the role of the printing plates and fountain solution purity on piling build-up was clarified.

It was found out that piling formation is sensitive to plate characteristics; different plates produced different kind and amount of piling on blanket surface. Ink spread to the non-image area of the plate as spots or tails and ended up on the non-image area of the blanket. The main reason for the non-image area piling was found to be the poor emulsion stability on the plate. The fountain solution itself did not cause non-image area piling on the blanket but it affected the mechanism of piling by interacting with the ink. With fresh fountain solution, the ink spread mainly as tails from the back edges of the dots, while with used fountain solution mostly ink spots were noted on the plate non-image area.

**Key words:** heatset offset printing; thermal plate; CtP plate; piling

## 1. Introduction

In heatset printing high productivity and good cost efficiency are nowadays essential. This has lead to requirements of exquisite runnability of the press and lower consumption of the printing materials and chemicals. The main runnability problem in heatset printing is piling on blankets. Non-image area piling on blanket is considered as an unavoidable process property of offset printing, which during longer print runs lowers both print quality and press runnability. The build-up varies with time and materials used. There is not a single reason for piling formation - it is always the combination of press settings and all the materials used in printing. Several studies have shown that all printing materials (fountain solution, ink, paper, plate and blanket) and press adjustments affect piling tendency (Swan 1973 and Aspler et al. 1991). In addition to materials, press parameters like temperature, screening technologies (Bohan 2006), speed and fountain solution feed affect piling formation.

In IARIGAI conference 2007 the results of blanket piling were presented. New on-line microscopic imaging system showed how the piling occurs around the halftone dots or all over the non-image area (Passoja et al., 2007). The blanket properties have an effect on where the piling is located (either around dots or on whole non-image area). According to Bohan (2006) some blankets seem to be more insensitive to non-image piling than others. Certain blankets are insensitive to changes in paper grade, while other blankets show a large difference. Also, ink has significant effect on piling tendency.

Kiuru et al. (2010) showed that the fountain solution purity affects piling; with used fountain solution the piling layer cover the blanket more evenly and the halftone dots are smaller than with fresh fountain solution. Chemical impurities in fountain solution cycle are mainly due to dissolution of ink. This is noted during printing in terms of increased concentration of aluminium and calcium in the fountain solution cycle. The increased amount of ink particles in the fountain solution cycle increases the conductivity of the fountain solution.

Passoja et al. (2007) noted that piling formation varies according to paper grade. The main difference in piling formation is noted in the dot areas: the dots are clean with the coated paper as the dots are having fibrous material after printing the uncoated paper. The piling problems are most severe with coated grades, most likely due to the sharp edge between the dot and accumulated material.

The main focus of this study was to clarify the role of the printing plates on piling build-up on blanket and the mechanism behind it. In addition, the effect of fountain solution purity on piling formation was studied.

## 2. Methods

Different thermal CtP (Computer to Plate) plates were tested during this study. Thermal plates were chosen because most of the heatset printers worldwide use thermal CtP printing plates instead of photopolymer or silver CtP plates. Plates were characterized in laboratory. Plate roughness was measured using NanoFocus µScan laser profilometer to estimate the fountain solution carrying properties of the plates. Rougher plate is expected to carry more fountain solution than the smoother one. The wetting ability of the plate was also predicted with the contact angle and surface energy measurements. The measurements were carried out with Fibro DAT 1100 device.

Plate performance was studied during heatset printing trials. Trials were performed at KCL's heatset web offset press, Albert-Frankenthal A 101 S. The speed of the press was 5 m/s. Commercial magenta ink was printed on commercial WFC paper together with non-alcoholic fountain solution having 4% dosage of additive. Ink transfer unit was observed. Fountain solution was applied also from previous units. Pressmen controlled the ink and fountain solution feed on the basis of target density and print quality. Trials were run in normal press conditions. The effect of fountain solution feed on piling tendency was observed by decreasing fountain solution ductor speed 10% from the normal level.

Plate performance and piling build-up on blanket were studied using triggered micro cameras during the trials. The system consisted of a colour CCD-camera with a high resolution zoom lens. The field of view was about 1.3 mm x 1.7 mm. Imaging system captured on-line still images. A high speed and intensive gas-discharge illumination system was used for "freezing" the magnified image of the rolling blanket. The microscopic imaging was done from the 15% magenta halftone area both from the plate and the blanket surfaces.

## 3. Results

### 3.1 Surface characteristics of the plates

Five different thermal CtP plates were characterized in laboratory. Surface roughness values varied between the plates, see Figure 1. Plates A and C were the rougher ones and were expected to carry more fountain solution on the plate surface e.g. compared to plate B. These differences can be seen very well also on images examined using scanning electron microscope (SEM).
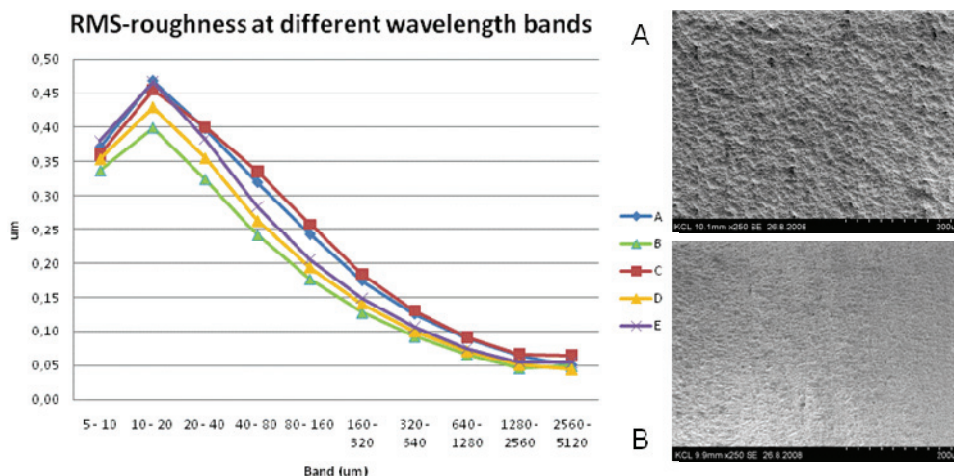


*Figure 1: RMS-roughness of the plates measured by laserprofilometer. SEM images from the non-image areas of the plates A and B (scale bar 200 µm)*

According to high magnification SEM images, plate B seemed to have more details on the plate surface in micro scale and this could influence on specific surface area of the plate, see Figure 2. It is thought that the increased specific surface area is capable of holding more fountain solution on the plate surface during printing. The water surface renews when the plate cylinder is rotating during printing, but the amount of water inside the plate surface capillaries remains constant.

*Figure 2: SEM images from the non-image areas of the plates A and B in 10000x magnification (scale bar 5 μm)*

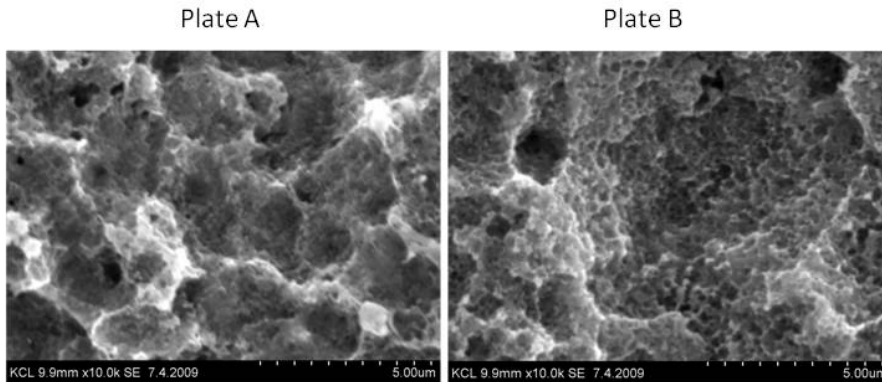The wetting ability of the plate was also predicted with the contact angle and surface energy measurements (Figure 3). There were no significant differences in water contact angles on non-image areas between the plates B, C, D and E. Plate A had slightly higher water contact angle compared to other thermal plates. The changes in surface energy values were not remarkable varying between 65 and 73 mJ/m$^2$. Rougher plate A had higher water contact angle and lower surface energy compared to smoother plate B. Therefore, it can be expected that fountain solution spread more easily on the non-image area of the plate B with lower water contact angle, but because of smoother surface, the amount of fountain solution was lower on plate B.
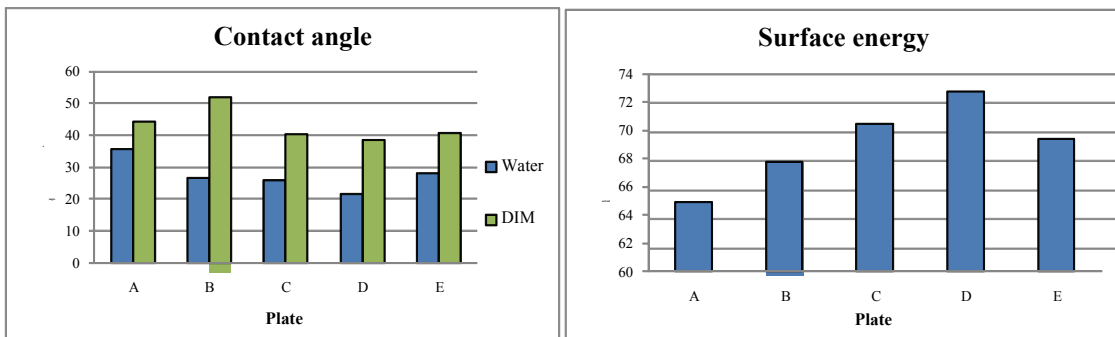


*Figure 3: Contact angle and surface energy of the plate non-image areas measured by Fibro DAT 1100*

The effect of plates A and B on piling tendency is compared more in detailed in this paper since they showed the biggest differences in wetting ability.

### 3.2 Mechanisms of piling formation on the non-image area

According to micro images ink particles spread to the non-image area of the plate and ended up on the non-image area of the blanket. The main reason for the non-image area piling seemed to be the poor ink stability on the plate. There were two different reasons for this: ink spots and tails (see Figure 4).

Ink spots are defined as small ink particles seen on the non-image area of the plate due to the chemical interactions between plate, ink, and fountain solution. High amounts of cations (dissolved impurities) in fountain solution might separate ink particles to the fountain solution cycle and to the non-image area of the plate in nip contact with the inking roller. This was seen as ink spots on the non-image area of the plate. The separation was sensitive to plate characteristics such as surface energy. The formation of spots occurred despite the uniform fountain solution layer on the plate surface.

Ink tails means ink spreading from the halftone dots or compact area edges to the non-image area of the plate. This was caused by ink filamentation in the ink transfer nip and centrifugal forces of the plate cylinder. Rosenberg (1999) has shown that ink splitting takes place in the ink transfer nip causing filamentation. Fountain solution quality, emulsification and the surface properties of the plate affect formation of ink tails. Also, the speed of the inking rollers affects formation of filaments. Higher speed causes ink splitting closer to the nip but centrifugal forces tilt the filaments over the back edges of the dots. It is also possible that, after

emulsification, the inner cohesion of ink decreases and the ink spreads more easily to the non-image area of the plate. Ink tails can also be caused by the centrifugal forces of the plate cylinder exceeding the surface tension of the ink droplet.
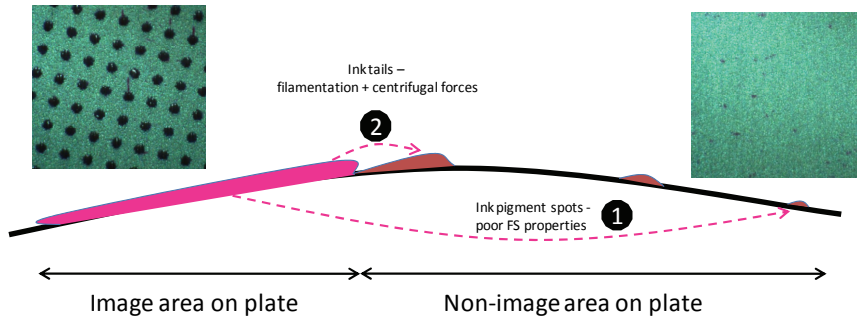


*Figure 4: Piling originates from plate, two mechanisms*

It was noticed that ink tails started to form at a certain press speed and it was depended on the plate properties. With a smoother plate ink tails started to form at lower speed and more ink tails were formed compared to rougher plate. One explanation for this can be that a smoother plate carried less fountain solution on the non-image area and more readily caused formation of ink tails. The appearance of ink tails decreased with an increased fountain solution feed, but they did not disappear totally.

Both the ink spots and tails appeared on random locations and disappeared during the next revolution of the plate cylinder, so they were transferred from plate non-image area to the blanket surface causing piling. Particles from ink and paper accumulated on the blanket surface. It can be concluded that the role of the printing plate is essential in piling formation on blanket; piling originates from plate conditions.

### 3.3 Fountain solution purity determines piling mechanism

There were more ink tails when using fresh fountain solution compared to a used one. For fresh fountain solution, the ink spread as tails from the dots and there were just a few ink spots on non-image areas, see Figure 5. For used fountain solution ink spots were noted on the non-image area. The used fountain solution contains high amounts of multivalent cations such as calcium and aluminium (Kiuru et al., 2010). These cations easily adsorb on the surface of negatively charged particles which are present in ink and in fountain solution. This "unstable" state can cause ink particles to spread as spots to the non-image area. For fresh fountain solution conditions are more "stable" and ink remains more easily in the halftone dots - or they just slightly spread as tails. The fountain solution itself did not cause any non-image area piling on the blanket but it affected the mechanism of piling by disturbing the emulsification.
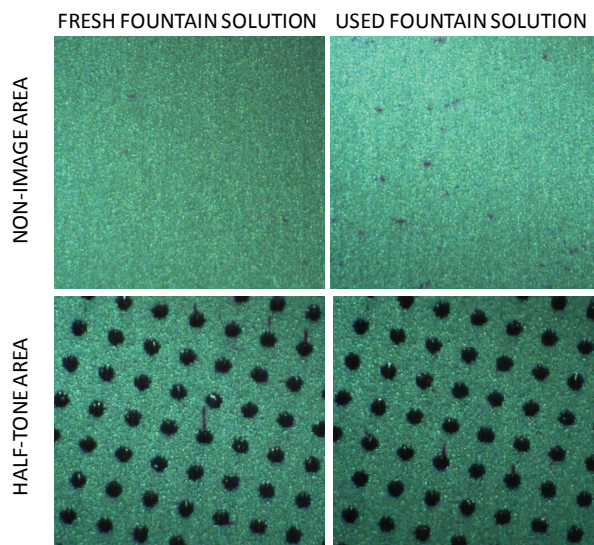


*Figure 5: Effect of fountain solution purity on formation of ink tails and spots on the plate surface*

### 3.4 Plates affect piling formation on blanket

When the press conditions were kept constant, plates seemed to cause different amounts of piling on the blanket surface, see Figure 6. According to images taken from the blanket surface after 20 000 printed copies, plate A had the lower amount of piling compared to plate B in different fountain solution feed levels. Piling on the blanket surface consisted of ink and paper coating pigment particles already after two minutes printing. In that time piling was mainly formed around the halftone dots and did not yet cover the whole blanket surface.

Small differences in surface properties of the plates made it difficult to point out the dominating properties of the plates. For instance, the differences between plates A and B clearly caused differences in plate performance. Plate A had higher roughness and it kept fountain solution in the plate structure and therefore caused less accumulation, even it had higher water contact angle value. It is also possible, that the higher surface energy value on the non-image area of the plate B might induce higher attachment of ink spots on the plate non-image area. This could result in higher ink transfer on the blanket non-image area.

Under selected conditions plate A performed better, but most likely by changing the ink and/or fountain solution, plate B would perform better with some other material combination.
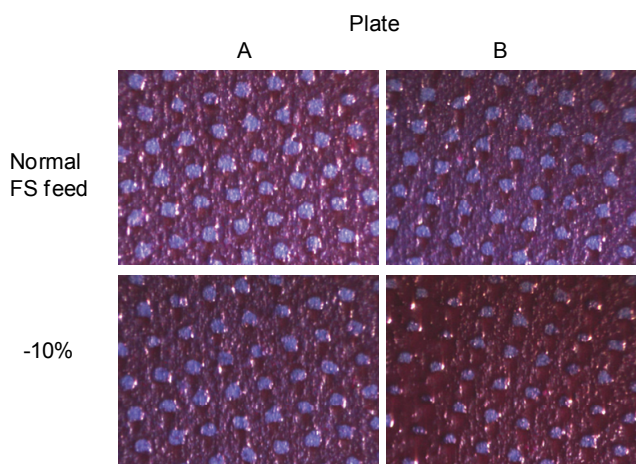


*Figure 6: Blanket images after switching off the ink feed with different fountain solution feed levels after 20000 copies*

## 4. Discussion

In this study the piling mechanism was clarified by performing full scale heatset trials with one printing unit. In this paper so called used fountain solution was used in KCL's press during two trial days. In commercial printing houses normal fountain solution circulation is from two to four weeks. It is expected to reach higher concentrations of the fountain solution impurities in the commercial printing houses when using fountain solution at least 14 hours per day. Therefore, it is likely that ink spot formation is more critical in piling at commercial presses and can cause significant problems with print quality, runnability and productivity during printing.

The plate is a very crucial component in printing since the ink and fountain solution is mixed on it and it is also responsible for transferring the unwanted ink tails and spots to the blanket and further to the paper. Surface properties of the plates such as surface energy and roughness describe the wetting ability of the plate. There were differences in piling formation between the plates due to the different plate performance. Results indicate that higher surface roughness and lower surface energy of the plate were beneficial for reducing piling formation on blanket. It was, however, impossible to state which one of these properties affected more. In addition, SEM images indicated that plates have differences in specific surface area, but we could not measure these differences due to lack of proper method.

The mechanism of ink tail and spot formation indicates that piling is due to the unstable emulsion. Emulsion stability is defined by the relation between ink's inner cohesion and its adhesion on the plate. Emulsification

lowers the cohesion causing easier spreading of ink to the non-image area of the plate. The emulsion was not studied more in detailed in this study, but it was seen that fountain solution's role in emulsification is a critical when adhesion properties are concerned. In the future, it would be interesting to concentrate more precisely on emulsion formation and the state of emulsion during printing.

Since the piling is a consequence of a complex dynamic printing process with several variables it is not possible to point out a single reason for piling. The reason is always a combination between press conditions and materials used. In the future it would be interesting to follow up the piling formation in commercial printing house where for example the extended printing time, four colour printing and actual printing conditions give a more realistic picture about the process and its challenges.

## 5. Conclusions

Non-image area piling is a process property of offset printing and there is not a single reason for piling formation. The heatset printing trials with different plates and fountain solutions revealed that piling on blanket originates from the plate. Two different mechanisms on the plate control piling formation on the blanket and explain instability of ink-fountain solution emulsion: ink spots and tails. Ink spots are mainly formed with used fountain solution. Ink tails are thin ink filaments at the back edges of the dots and compact areas. More ink tails are noted with fresh fountain solution. It was noticed that ink tails started to form at a certain printing speed and the speed was dependent on the plate properties. Both ink spots and tails are formed at random locations on the plate, transferred to the blanket and further to the paper.

Surface properties of the plates affect plate performance in the press. Different plates had different kind of response to fountain solution feed levels. Both plate roughness and contact angle affect plate performance in the press, but it is not possible to say that one of these properties is a more remarkable factor. Plates affect more the speed of piling formation compared to fountain solution impurity. These results can be applied also to other plate types, like silver halide CtP plates or conventional plates because there are similarities in plate surface structure. However, the role of ink and ink-fountain solution emulsion on piling tendency is more remarkable than the effect of the plates. Piling on blanket contains particles both from ink and paper.

More sophisticated plate characterization is needed to better understand the role of plate in printing performance. For example the specific surface area of the plates can have an effect on piling, but there was not any proper method available to characterize the specific surface area from the plates during this work. Also, the studies related to emulsion formation and behavior would be useful to continue in the future.

### References

Swan, A., (1973), Carry-over piling on litho presses, Printing Equipment and Materials, no.8, pp. 32-33.

Aspler, J. S., LePoutre, P., (1991), The transfer and setting of ink on coated paper: a review, TAPPI/CPPA Symposium on Papercoating Fundamentals, p. 77-98.

Passoja, S. et al., (2007), Mechanisms of non-image area piling in heatset web offset, IARIGAI conference.

Bohan, M., (2006), An evaluation of piling on press, Ink Maker July/August 2006, pp. 21-24.

Kiuru, J. et al., (2010), Effects of ink - fountain solution interactions on piling formation in heatset web offset printing, TAGA conference.

Rosenberg, A., (1999), A closer look to ink splitting. FOGRA research report, 1999, 10p.
Advances in Printing and Media Technology, Vol. XXXII. Zagreb 2006, p. 11-16.

# Effect of blanket properties on web tension in offset printing

*Merja Kariniemi*[1]*, Markku Parola*[1]*, Artem Kulachenko*[2]*, Joonas Sorvari*[1]*, Leo von Hertzen*[1]

[1] VTT Technical Research Centre of Finland, PL 1000, FI-02044 VTT, Finland
  E-mail: name.lastname@vtt.fi

[2] KTH Kungliga Tekniska Högskolan, SE-100 44 Stockholm, Sweden
  E-mail: artem@kth.se

**Abstract**

VTT and KCL together with several companies in the printing value chain have studied how to control web tension in different parts of a printing press. Extensive trials on printing presses, at pilot scale and at laboratory scale have yielded data for modeling work. Modeling was carried out with statistical methods and by finite element method (FEM). Results show the extent to which paper and printing blankets affect tension formation in a printing press. The main emphasis of this paper is on the effect different printing blanket types have on web tension.

It was found that printing blankets have a clear effect on web tension. The degree of tension change is affected by the type of blanket, nip pressure, distances between the blankets, moisture, paper properties and the combination of blanket types in different printing units. Depending on their feeding properties and their effect on web tension, in general, the blankets can be distinguished as negative, neutral and positive. Also the blanket's effect on web tension is influenced strongly by the type of adjacent blankets. The interactions of fountain solution, ink, nip, blanket and paper had also an effect on the tension formation. The paper experiences a very high rate of strain inside the printing nips, which can affect the paper's response and therefore tension after the nips. Results suggest that tension cannot be solely predicted with the elastic paper properties measured by conventional methods.

**Key words:** offset printing; web tension; runnability; printing blanket; paper

## 1. Introduction

The most important runnability disturbances in newspaper offset printing are register errors, web breaks, web instability, wrinkles, dusting and linting. These phenomena are caused partly by paper and partly by the printing press and how the press is operated. Previous studies have shown (Paukku 2004, Parola 2000, Linna 2001) that web tension has an effect on web breaks, printed waste and a web's lateral movements. Both too high web tension and too low web tension led to these problems.

In newspaper printing, where several webs are printed simultaneously and combined in the former, web tension variations can trigger serious runnability problems. A single web's tension can be controlled mainly by an infeed unit. Drag rollers after printing units are normally only for fine tuning, as this control affects opposite way to upstream and to downstream web tension. To improve press runnability and production economy a better understanding of the dynamic interactions between paper web and press is necessary, including the effects of printing and press components as well as the impacts of paper properties. There has been a lot of discussion but no results about the effect of different printing blanket properties on web tension.

## 2. Methods

To find out the influence of different paper, press and blanket properties on runnability, several different tests were made. Trials were carried out in printing presses as well as in pilot printing presses. An extensive number of paper and blanket tests were carried out in laboratory. The results were utilized in modeling and simulations.

The main goal of the trials carried out with the pilot press at KCL was to find out the effect of blankets with different feeding properties on web tension. In addition, the effect of paper properties was studied with eight different paper grades. An extensive number of test runs were performed on KCL's Albert-Frankenthal A 101 S, heatset offset printing press. Measurements on the press included tension measurements by weighing rollers installed between every printing unit and before and after printing units. Speed difference was measu-

red by rollers attached to the infeed unit and to the chilling roller. Nip load profiles of all printing nips were measured off-line. The amount of transferred fountain solution was measured with lithium tracer.

Three different types of blankets delivered by ContiTech were tested in the KCL trials: very negative, negative and neutral. The delta value ($\delta$) of the feeding properties varied between -0.3 and -2. Printing units two and three were the test units where the blankets were changed during the trials. In the first and the fourth printing units standard negative blankets were used.

The feeding properties of the blankets were measured by two cylinders, one that has a blanket on it and the other is rigid. One of the cylinders is driven by a motor with a prescribed velocity. The other is driven by the friction between the cylinders (Figure 1).
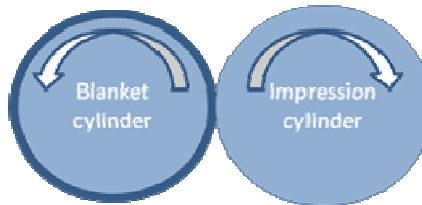


*Figure 1: Schematic view of the measurement of blanket feeding properties.*

By monitoring the surface speed of the blanket cylinder and impression cylinder, the blanket feeding properties can be characterized by the following equation (Scaschek 2001)

$$\delta = \frac{V_{\text{imp}} - V_{\text{blanket}}}{V_{\text{blanket}}} \times 1000 \tag{1}$$

where $V_{\text{imp}}$ is the surface speed of the impression cylinder and $V_{\text{blanket}}$ is the surface speed of the blanket cylinder. The blanket is called positive when $\delta > 0$, negative when $\delta < 0$ and neutral when $\delta \approx 0$.

Trial runs and long term studies were performed in two four color newspaper printing presses, one press had blanket to blanket units in four towers. The other press had satellite units in six printing towers and one tower consisted of blanket to blanket units. The main task of trials was to study web tension formation in a production scale press. Web tensions were measured at the infeed unit, just after the last printing unit and before the folder. Nip load profiles were measured off-line from every printing nip. Also several other measurements and control signals were collected on round-the-clock basis in data bases. These included for example all draws (control values) from reel stand to folder affecting tension, fountain solution feed, press speed, amount of paper waste. Thousands of paper reels were measured in the long term study.

Printing trials generate a lot of valuable data from direct measurements. It is, however, difficult to sort out the influence of individual printing parameters such as paper grade, blanket, printing nip configuration etc. Numerical modeling offers a unique and inexpensive possibility to separate the impact of each parameter by making systematic changes in the model. Rolling contact is a well investigated area (Kalker 1990). Rolling contact considering multilayered cylinders has been reported with a focus on the strains and stresses in the nip area (Hallbäck et.al 2006, Holmval & Uesaka 2007, Wiberg 1999, Diehl et al 1995 and Hinge et al 1998). We adopted the main principles used in the previous studies and also considered the impact of the nip on the paper under tension.

We used a 2-D, plain strain finite element model to describe the nip region (Figure 2). The nip model was implemented in a commercial finite element software ANSYS. The Lagrangian description of motion was used. The blankets are represented as a two layer structure with a thin hyperelastic rubber layer and thicker foam layer. We used a three parameter Mooney-Rivlin hyperelastic material (Tussman & Bathe 1987) to represent the outer, rubber layer of the blanket. The compressible layer was represented by Ogden compressible foam (Ogden 1984). With 4 nips placed in a row, this model mimics a four color printing system. The tension was set to be constant before the first nip and velocity controlled conditions were used after the last nip by introducing the rigid winding roll (Figure 3). Normally the nip is not fully orthogonal to the direction of the web movement. Figure 4 shows an example of such configuration which is implemented in the pilot printing press.
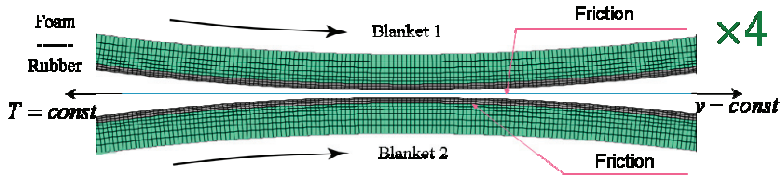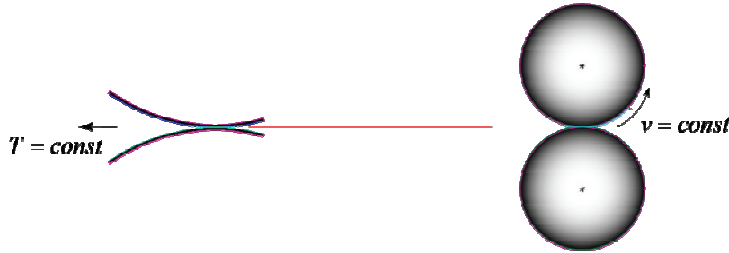
*Figure 2: Finite element model of the nip region*



*Figure 3: Finite element model with one nip and one winding unit*



*Figure 4: Tilted nip configuration (before and after nip closure)*

In addition to the nip model, a paper model was created by finite element method (FEM). Equations 2-5 describe a paper web's tension formation and were utilized in modeling work, which is reported in more detail in (Parola 2001). The web tension in a printing press is dependent on a number of factors, but basically it can be expressed as follows:

$$T = E\varepsilon_{el}h = K\varepsilon_{el}$$

*(2)*

where $E$ is the elastic modulus of paper, $h$ the thickness and $\varepsilon_{el}$ is the elastic strain, $K$ is the tensile stiffness that is often used since thickness measurements are rather difficult with paper. The elastic strain is a part of the total strain $\varepsilon_{tot}$

$$\varepsilon_{el} = \varepsilon_{tot} - \varepsilon_{in} - \varepsilon_{hyg}$$

*(3)*

where $\varepsilon_{in}$ is inelastic strain (due to creep or plasticity, for example) and $\varepsilon_{hyg}$ is the hygroexpansion strain. The total strain is controlled by the speed difference in the following way:

$$\varepsilon_{tot} = \varepsilon_o + \frac{v_2 - v_1}{v_1}$$

*(4)*

where $\varepsilon_0$ is the pre-strain and $v_1$ and $v_2$ are the velocities at the entrance and exit of the span. Now to consider the several effects of increased moisture on web tension. First, it reduces the elastic modulus $E$ (Equation (2)), second, it causes hygroexpansion strains $\varepsilon_{hyg}$ (Equation (3)) and finally, it accelerates the inelastic deformations $\varepsilon_{in}$ (Equation (3)). The blankets affect the pre-strain $\varepsilon_0$ and velocities before and after the nip (Equation (4)).

The effect of moisture on tensile stiffness was calculated using equation 5:

$$E = E_0 e^{-\gamma mc}$$

*(5)*

Where mc is moisture content and $\gamma$ is an exponential factor, value 0,05 was used based on literature (Niskanen 1998).

Hygroexpansion of paper was measured with KCL Vesikko and creep with KCL Elviira. The effects of printing nips on paper elongation (plastic elongation) were estimated values calculated from dry web deformation due to nip pressure in the cross-direction. It was presumed that the elongation in machine direction due to nip pressure obeys the same ratio as hygroexpansion ratio (MD/CD). Mechanical elongation was calculated from the speed difference between the infeed unit and the drag roller. The effects of blankets were considered negligible as neutral blankets were used in measurements.

## 3. Results

The results are divided into three categories. First the main results of how the blanket properties affect the web tension are presented. Second we consider how the paper properties affect the web tension. Finally we describe the press related factors that influence the web tension formation.

### 3.1 Effect of blanket properties on web tension

In this section we will discuss the difference between negative and positive blankets. The feeding property of the blanket is dependent on its layered structure. In fact, if the blanket has only one layer, it will always be positive. Figures 5a and 6a show the differences between negative and positive blankets in terms of local straining in the printing nip area. The positive blanket causes positive straining (extension) in the nip region, the negative blanket causes compression. It means that paper web will have a tension peak inside the nip with the positive blanket and tension drop with the negative one. Figures 5b and 6b show the differences in velocity profile. The positive blanket accelerates in the nip region while the negative blanket slows down. This behavior has a direct impact on the feeding properties of the blanket. The velocity profile is not symmetric since the material is being pushed out from the nip during rotation.
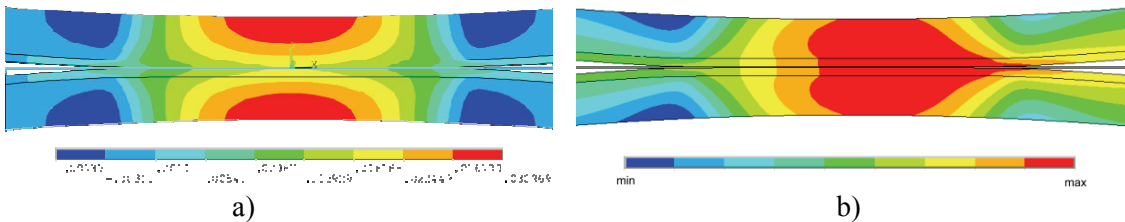


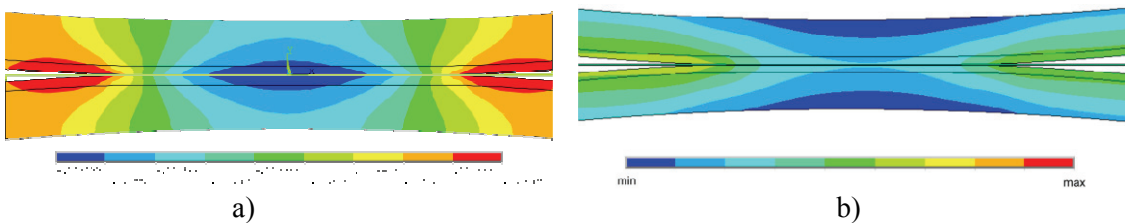*Figure 5: Positive blankets a) Machine directional (MD) (X) strains b) total velocity*



*Figure 6: Negative blanket a) Machine directional (MD) (X) strains b) total velocity*

The effect of the printing nip on web tension in a case with a single nip is demonstrated in figure 3. There is only one negative nip (negative blankets), constant tension on the left side (mimicking the infeed unit) and a rigid winding unit on the right side rotating with a constant speed. There is no rotational speed difference between the nip cylinder and the winding unit. The web is elastic and hygroexpansion and inelastic deformations are not included in the model. Figure 7a shows how the web speed changes as the web passes the nip and enters the free span (open draw) in a steady state regime when all the velocity components are settled.

The computations started when the nip was open and initially the velocity was constant and equal to 10 m/s along the entire web length. Then the nip was closed and consequently the negative blanket feeds less paper on the right hand side than it is given from the infeed. Since the mass flow should be constant, this eventually translates into speed difference along the open draw between the nip and the rigid cylinder. The velocity before the nip decreases, while the same tension is maintained (similar to the way the infeed operates). In the steady state regime, the feeding imbalance is fully compensated by the velocity difference (Equation (4)).
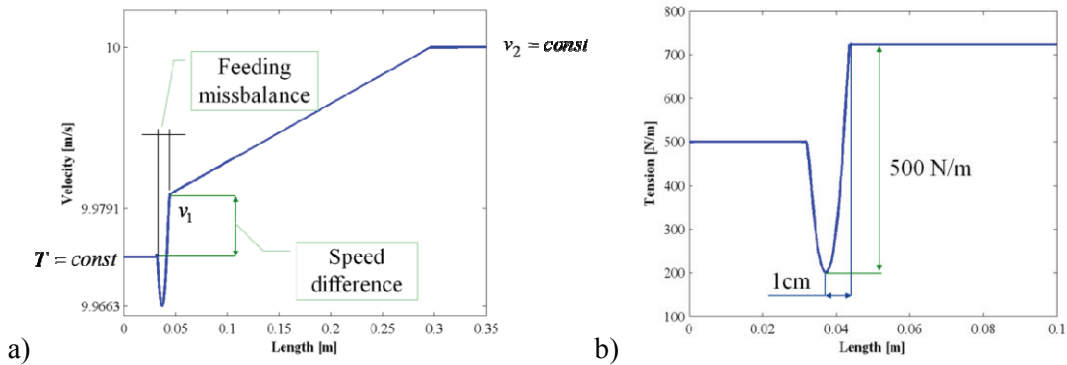
*Figure 7: a) Speed difference introduced by the printing nip, negative blanket. b) Tension change through the nip in case of negative blanket, nip length 2 cm*

The velocity difference occurring along the open draw contributes to increased tension. Figure 7b shows how the tension changes in the nip region. As the web passes the nip region, the tension first decreases considerably because of local compressive strain introduced by the negative blankets. After passing the middle of the nip, the tension increases dramatically along a 1 cm distance. This causes a very high straining rate (around 200%/s), far higher than that normally used during lab testing. The tension then remains constant along the open draw. A feeding imbalance with the positive blankets leads to an opposite effect than with the negative blankets, i.e. the speed difference in the open draw decreases, and tension decreases after the nip.

Lets consider the situation in which four equally positive and negative blankets are placed in a row. Figure 8a shows a modeling result of web tension change as the web passes the blankets. (In the figures, the letter P denotes a positive blanket and the letter N a negative, so PPPP means four positive blankets in a row.) Note, the distances between the blankets are rather short (about 20 cm). With absolutely neutral blankets the tension remains the same through the printing units.
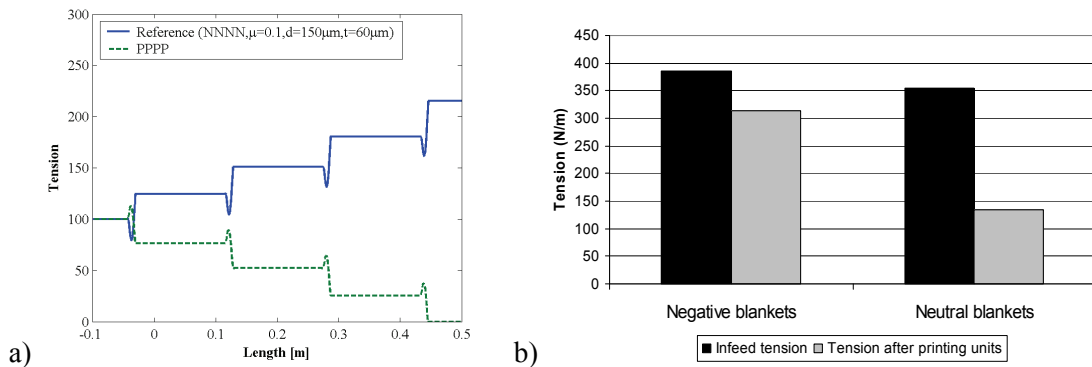


*Figure 8: a) Simulated effect of four positive and four negative blankets on web tension b) Measured web tension in newspaper production trials for negative and neutral blankets*

The nip modeling results show that each nip changes the tension equally. The effect depends on the feeding properties: negative blankets increase tension, positive blankets decrease it. The same type of phenomena were observed in the pilot printing trial, where negative blankets created higher tension than neutral ones. Furthermore, web tensions were also measured in a production scale press with negative and neutral blankets in all printing units. Figure 9b presents the results and negative blankets created much higher tension after the printing units than neutral ones. Tension after the units was measured just after the last printing nip. In this case the effects of fountain solution and inelastic paper properties also affect web tension.

In a numerical test we introduced an isolated nip with reverse feeding properties into the line of blankets. Figure 9 shows that significant tension changes are created around the isolated nip. The reason is that the preceding and following nips exert opposite feedings, i.e. if the negative nip feeds less paper to the span, the next positive nip demands more amplifying the effect from the previous blanket. Thus, mixing blankets of different types can lead to sudden tension changes.
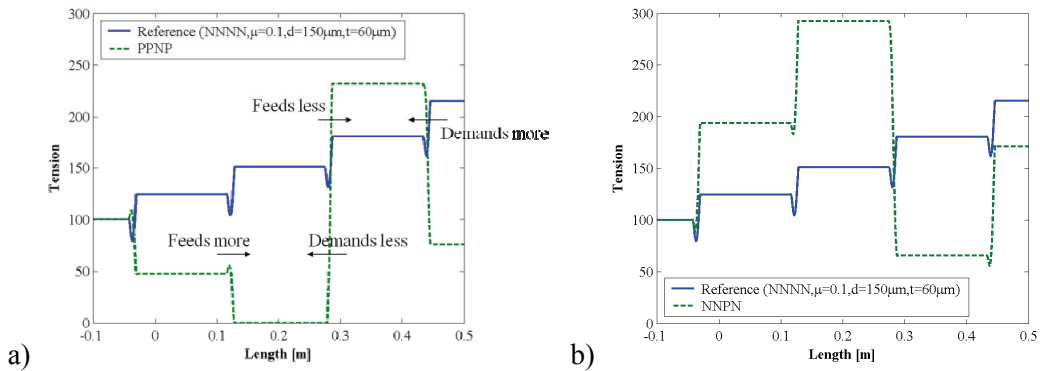
Figure 9: Simulated effect of isolated nip a) negative b) positive to web tension.

One of the questions that arose during the pilot printing trials was why the negative blankets, which are supposed to increase tension, had the opposite effect. In that case, blankets with different degrees of negativity were mixed together. The simulation results showed that when the second and third blankets (denoted with small "n" in the figures) had lower negativity than the first and fourth blankets, these blankets behaved as positive, i.e. decreased the tension (Figure 10). This implies that negative blankets can behave as positive when used in combination with more negative blankets. The same conclusion can be applied to positive blankets.  Figure 11 presents results obtained with similar blanket combinations (NnnN) in pilot printing trials. The measured results correlated well with simulation results. The effect of paper's tensile stiffness on web tension can be seen from the figure and it will be discussed in the following section.



Figure 10: Simulated effect from combination of blankets with different degrees of negativity to web tension



Figure 11: Web tensions measured in pilot trials with blanket combination NnnN with five different papers having different elastic modulus. N-highly negative n-less negative blanket

### 3.2 Effect of paper properties

According to Equation 2, tension change is proportional to the elastic modulus of paper. Figure 12a shows the results from varying elas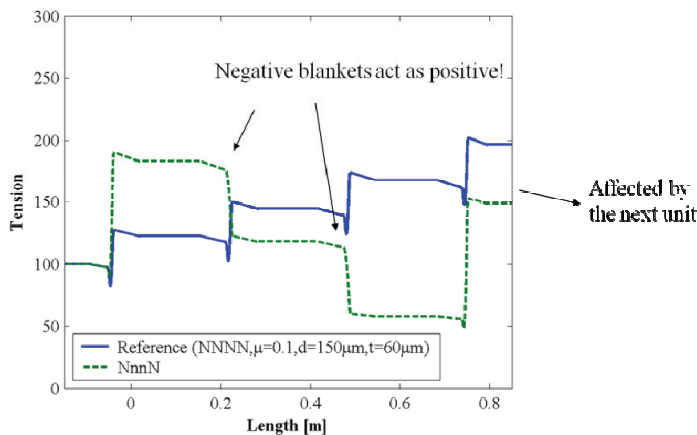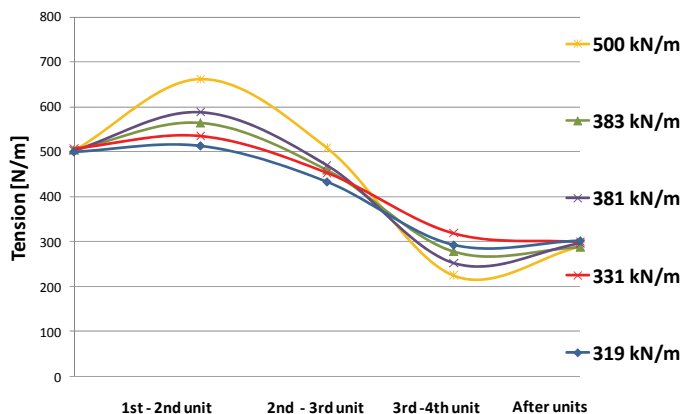tic modulus of the web in the nip model. The nip affects the strain and it is reflected in tension after it proportionally to the elastic modulus. Note that the model used considers paper as an elastic material and inelastic effects are not included in the model. Similar linear effects were observed with changed web thickness. This means that any changes introduced by the nip will be proportional to the tensile stiffness of paper in the machine direction. This was confirmed in the printing trials figure 12b, where higher tensile stiffness created higher tension after the first negative blanket.
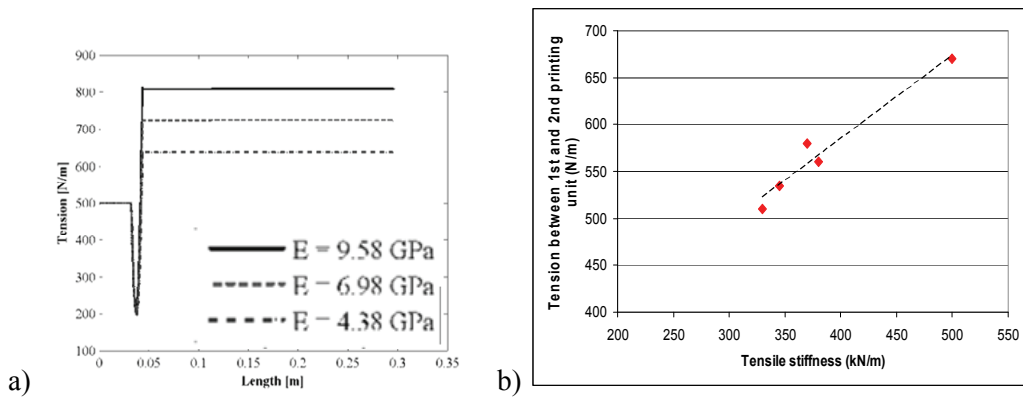


*Figure 12: a) Simulated effect of elastic modulus to web tension b) Effect of paper tensile stiffness on web tension in pilot press trial after first negative blanket*

When different blankets are mixed, the combined effect of several blankets is difficult to predict intuitively. The nip model results and measurements suggest that tension changes between printing nips are strongly dependent on web velocity differences caused by blanket properties as discussed earlier. This means that a paper with a higher elastic modulus can create high or low web tension depending on the blanket combination used as can be seen in figure 11, where the paper with the highest elastic modulus gives highest tension between the first and second printing unit but gives the lowest tension between the third and fourth printing unit. So, one cannot predict the web tension throughout the printing press only by comparing paper tensile stiffnesses.

The tensions were measured in a printing press for two papers (A and B) at the infeed and just after the printing units. Figure 13 presents measured values of web tension in the press (left side) and modeled web tension from the paper model (right side). When the paper model included only tensile stiffness, it predicted much higher tension than was measured. When including hygroexpansion, creep and plastic strain the paper model gave a much bigger decrease in tension and the model correlated well with measured ones. Hygroexpansion had the biggest effect on tension drop in this case. Results here and earlier in this paper suggest that a paper web's tension in a printing press can be predicted only if blanket properties, tensile stiffness, paper hygroexpansion, and inelastic properties of paper (creep, plastic elongation) are known. It must be noted that there are also several other paper parameters, e.g. grammage and pulp mix which have an effect on web tension.
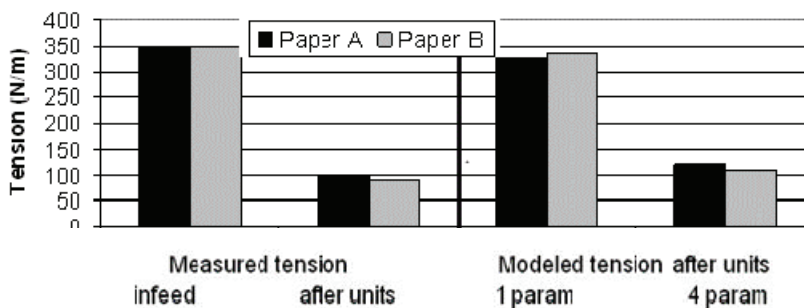


*Figure 13: Effect of paper properties on web tension with neutral blankets. In modeled tensions 1 parameter was tensile stiffness, 4 parameters included tensile stiffness, hygroexpansion, creep, and plastic strain*

## 3.3 Effect of other properties on web tension

The nip model was also used to examine the effect of infeed tension, nip pressure, nip tilt and open draw length on web tension formation.

If the paper is elastic, the infeed tension was found to have a negligible effect on the tension difference introduced by the nip in the simulation results. Increases in the infeed tension level increased the tension level after printing nips, but did not affect the absolute tension difference between printing units. Similarly, during the printing trial the infeed tension was increased by 200 N/m and this difference appeared in all tension measurements between the printing units.

The effect of nip pressure was studied by changing nip indentation in the nip model (Figure 14). The increased nip pressure increased the friction force but also changes the nip width and deformed the shape of the blanket. The increased nip indentation somewhat increased the tension change, which means that the negativity and positivity of the blankets were increased by the pressure. Pressure deforms the blanket and redistributes the material in the nip, which explains the changes in feeding characteristics.
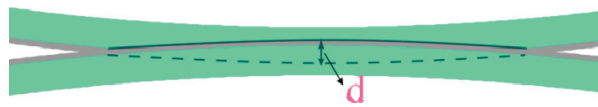


*Figure 14: Nip indentation (d)*

Normally the printing nip is not fully orthogonal to the direction of the web movement. Figure 4 showed an example of such a configuration. The web passing through such a nip experiences additional bending stresses. The contact region with the nip is enlarged (Figure 15). Numerical results show that the effect on the tension in such a configuration is quite similar to that in the straight configuration. The strains however are different and that is the reason for the small change in line shape in Figure 10. Due to the bending the paper may experience even large strain gradients along the thickness.
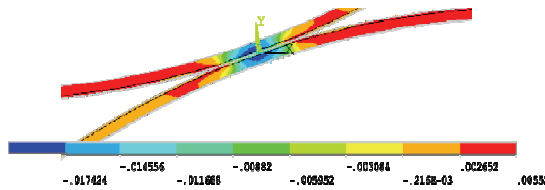


*Figure 15: Machine directional (X) strains in tilted configuration*

Figure 16 shows how the tension is affected in the simulation by the distance of the printing units. It shows that the tension change is inversely proportional to the length of the open draw. The effect of the distance between printing units was also studied by measurements in the pilot press. It was found out that the longer the distance between printing units, the smaller the effect of blankets is on tension. This effect can be explained as follows. The nip affects the tension by introducing a feeding imbalance, which has to be compensated for by the velocity difference. The feeding imbalance is a blanket characteristic and it does not depend on the open draw length. The incremental strain, however, is equal to the feeding imbalance divided by the open draw length. Thus, the longer the span, the lower the effect of the blanket becomes. Trials in the pilot press were carried out by closing printing nips one at a time. Results agreed well with the modeling data.
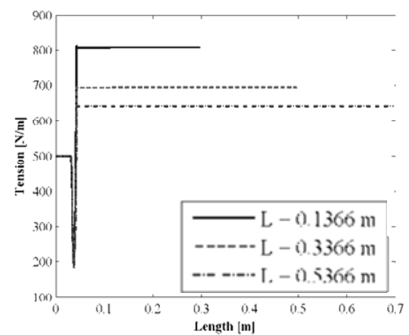


*Figure 16*
*Simulated effect of the open draw length on web tension*

## 4. Discussion

The results for this paper are based on simulations as well as trial runs on a pilot press and printing presses. In the nip model the paper web is considered as an elastic material. This allowed us to separate the impact of each blanket or press parameter by making systematic changes in the model. With a separate paper model we studied the effects of paper and applied moisture on web tension.

Earlier on, there have been speculations but no evidence as to how different blanket types affect web tension. With this study we have been able to understand where the different feeding properties of the blanket originate from and also how feeding properties affect the web tension.

The simulations gave an understanding of the different forces that are applied to the web. How the paper web reacts to all of these forces is not yet clear. This study utilized two different models. The next logical step would be to combine these models so that the tension formation through a printing press could be modeled and simulated. The real life interactions of paper - ink - blanket - fountain solution - nip all have an effect on the web tension.

## 5. Conclusions

This study shows that the printing nip phenomena is influenced by several variables at the same time. The interactions in the nip have a strong effect on web tension.

It was found that printing blankets have a clear effect on web tension. The degree of tension change is affected by the type of blanket, nip pressure, distances between the blankets, moisture, paper properties and the combination of the blanket types in different printing units. It was found that a blanket's effect on web tension is influenced strongly by the type of adjacent blankets. Also other parameters such as infeed tension and nip geometry affect web tension.

Also paper properties and applied fountain solution have a strong influence on web tension. Results suggest that tension cannot be solely predicted with the elastic paper properties measured by conventional methods. Paper hygroexpansion, creep and plastic strains are needed to understand web tension formation in printing. Furthermore the results suggest that with certain blanket combinations a paper having higher elastic modulus will give lower tension than a paper having lower elastic modulus. This means that one cannot predict tension in a press without knowing the blanket properties.

How the printer uses the press is critical to web tension. The infeed and other tension controls are naturally dominant parameters. However this study suggests that printer needs to know the feeding properties of all blankets to use them the right way. If blankets with different feeding properties are mixed in the printing units, the web tension can change significantly and lead to runnability problems. Printer can use the results of this paper to gain better control of web tension through the printing units.

According the results, the paper web experiences very high strain rate inside the printing nips, which can affect the tension after the nips. Further studies are needed to find out interaction mechanisms inside the nip area in dynamic conditions. The interactions of ink, fountain solution, blanket and paper web under nip load needs to be studied in more detail.

## References

Diehl et al (1995) - Diehl, T., K. D. Stack, and B. R. C. A study of three-dimensional nonlinear nip mechanics. 2nd International Conference on Web Handling. 1995. Oklahoma State University.

Hallbäck et al (2006) - Hallbäck, N., O. Girlanda, and J. Tryding, Finite element analysis of ink-tack delamination of paperboard. International Journal of Solids and Structures, 2006. 43(5): p. 899-912.

Hinge et. al (1998) - Hinge, K. C., J. C. Wilson, and M. A. M., Model of steady rolling contact between layered rolls with thin media in the nip. Engineering Computations, 1998. 15(7): p. 956-976.

Holmvall & Uesaka (2007) - Holmvall, M. and T. Uesaka, Nip mechanics of flexo post-printing on corrugated board. Journal of Composite Materials, 2007. 41(17): p. 2129-2145.

Kalker (1990) - Kalker, J. J., Three-dimensional elastic bodies in rolling contact. Solid mechanics and its applications, ed. G.M. Gladwell. Vol. 2. 1990: Springer. 344.

Linna et al (2001) - Linna, H., Parola, M. and Virtanen, J. Better productivity by measuring web tension profile, Proc. 55th Appita Annual General Conf. (Hobart), pp. 323-329, 2001.

Niskanen et al (1998), Paper making science and technology, book 16 on "Paper physics", ed K. Niskanen. FAPET, 1998, chapters 8 and 9.

Ogden (1984) - Ogden, R. W., Nonlinear Elastic Deformations, Dover Publications, Inc. (1984).

Parola et al (2001) - M. Parola, S. Vuorinen, H. Linna, T. Kaljunen, N. Beletski, Modelling the web tension profile in a paper machine. Transactions of the 12th Fundamental Research Symposium, vol. 2, ed. C. F. Baker, Oxford (2001) 759 - 781.

Parola et al (2000) - Parola, M., Sundell, H., Virtanen, J. and Lang, D. Web tension profile and gravure press runnability, Pulp & Paper Canada, Vol. 101, no. 2, pp. 35-39.

Paukku (2004) - J. Paukku, M. Parola, S. Vuorinen. Web Widening and Lateral Movements of Paper Web in a Printing Press. International Printing and Graphic Arts Conference, October 2004, Vancouver, British Columbia, Canada. IPGAC preprints (2004), 245 - 249.

Schaschek et al (2001) - Schaschek, K., R. Christel, et al. The effect of printing blankets on the rolling conditions of printing cylinders. in TAGA. 2001. San Diego, CA.

Tussman & Bathe (1987) - T. Tussman, K-J Bathe, "A Finite Element Formulation for Nonlinear Incompressible Elastic and Inelastic Analysis", Computers and Structures, Vol. 26 Nos 1/2, 1987, pp. 357-409.

Wiberg (1999) - Wiberg, A., Rolling contact of a paper web between layered cylinders with implications to offset printing, in Department of Solid Mechanics. 1999, Royal Institute of Technology: Stockholm. p. 90.

# The effect of surface properties on the printability of flexographic printing plates

*David Galton[1], David Bould [2] and Tim Claypole[2]*

[1] Asahi Photoproducts (UK) Ltd
 1 Prospect Way
 Hutton Industrial Estate
 Shenfield, Essex CM13 1XA, United Kingdom
 E-mail: dg@asahi-photoproducts.co.uk

[2] Welsh Centre for Printing and Coating
 School of Engineering, Swansea University
 Singleton Park
 Swansea, SA2 8PP, United Kingdom
 E- mails: d.c.bould@swansea.ac.uk, t.c.claypole@swansea.ac.uk

**Abstract**

The move to environmentally friendly, water-washable flexographic printing plates has resulted in a variation in the surface properties of the plate, compared to plates processed traditionally, using solvent. In order to assess the impact on printability, a trial has been performed, to compare the two plate chemistries. The objective of the investigation was to compare the printing performance of the two types of material and to quantify the results in terms of tone value increase, physical dot area and solid density. Two plate materials were selected, one conventionally processed, using solvents to wash the plate, and a water washable plate. Large differences were observed in the printing characteristics of the two plates and it was concluded that the higher contact angle of the water washable plate resulted in the ink being pinned on the surface of the halftone dot, during ink transfer, rather than being squeezed down the dot shoulder.

**Keywords**: environmental; flexography; surface energy

## 1. Introduction

The move to environmentally friendly, water-washable flexographic printing plates has resulted in a variation in the surface properties of the plate, compared to plates processed traditionally, using solvent. In order to assess the impact on printability, a trial has been performed, to compare the two plate chemistries. The objective of the investigation was to compare the printing performance of the two types of material and to quantify the results in terms of tone value increase, physical dot area and solid density. Two plate materials were selected, one conventionally processed, using solvents to wash the plate, and a water washable plate. Both plates were manufactured by Asahi Photoproducts and were processed digitally, with no need for a separate negative.

The trial was performed at Swansea University, using the Timsons T-Flex 508 Flexographic printing press. The trial conditions are outlined in Table 1. A banded anilox roll was used for the trial, with each band engraved at a different line ruling. However, the cell volume for each band remained constant at $4 cm^3 m^{-2}$. The current investigation presents details for two anilox cell bands only.

*Table 1: Trial details*

| | |
|---|---|
| Press Speed | 100m/min |
| Ink system | Cyan UV cured ink |
| Anilox line ruling | 500lpi and 1200lpi |
| Anilox volume | $4 cm^3/m^2$ (constant for both line rulings) |
| Plate line ruling | 150lpi and 175lpi |
| Mounting tape hardness | Soft and Hard |
| Anilox to plate pressure | Low and High |

The investigation was performed as a full factorial trial, where the full range of parameter settings was considered. A test image was generated and a plate manufactured using both types of plate material. The image comprised seven discrete bands, to align with the seven bands of the anilox roll. The same test image was repeated in each band (Figure 1). The designations of the two plate types are shown in Table 1. Each plate was imaged under the same conditions, with no tonal correction apart from in the highlight region, where 'bump-up' was applied, to allow the highlight dots to be produced.
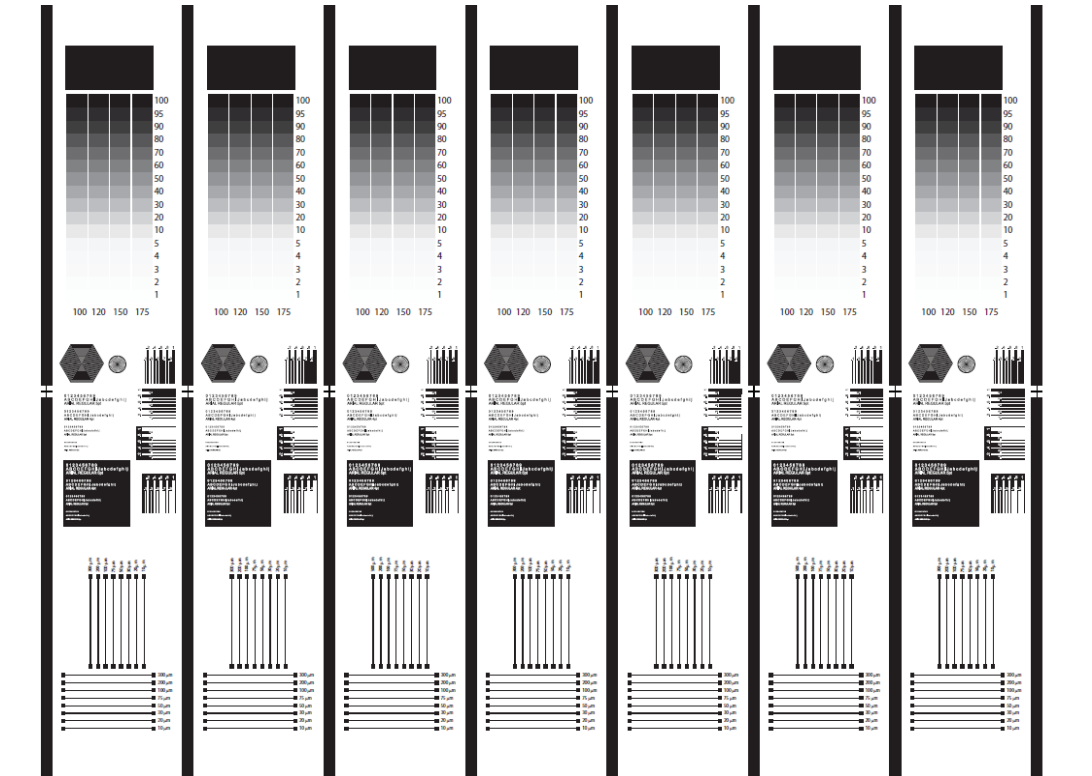


*Figure 1: Plate image for trials*

*Table 2: Designations for two plate types*

|         | Plate type                    |
|---------|-------------------------------|
| Plate A | Conventionally processed plate |
| Plate B | Water-washable plate          |

The print run for each trial condition was 2500m. This was to compare the printing performance at the start and end of each print run, allowing any dot growth, due to ink build up on the dot shoulder to be quantified. A summary of the individual trial conditions is shown in Table 3. Print quality was assessed in terms of density, tone value increase and physical dot growth.

*Table 3:Trial conditions*

| Expt No | Plate type | Tape hardness | Anilox-plate pressure |
|---------|------------|---------------|-----------------------|
| 1       | Plate A    | Soft          | Low                   |
| 2       | Plate A    | Soft          | High                  |
| 3       | Plate A    | Hard          | Low                   |
| 4       | Plate A    | Hard          | High                  |
| 5       | Plate B    | Soft          | Low                   |
| 6       | Plate B    | Soft          | High                  |
| 7       | Plate B    | Hard          | Low                   |
| 8       | Plate B    | Hard          | High                  |

## 2. Results

A comparison of Figures 2 and 3 shows that Plate B exhibits lower dot gain characteristics, compared to Plate A. This will produce better print contrast for Plate B. For both Plate A and Plate B, little difference was observed in dot gain between the start and the end of the print run. However, the high tonal values for Plate A highlight coverages suggests that by the time the 'Start' sample was taken, the shoulders of the highlight dots were already inked, and the long print run did not result in further inking of the shoulder. Plate B did not exhibit high dot gain in the highlight region, suggesting that this plate was less prone to build up of ink on the shoulders.
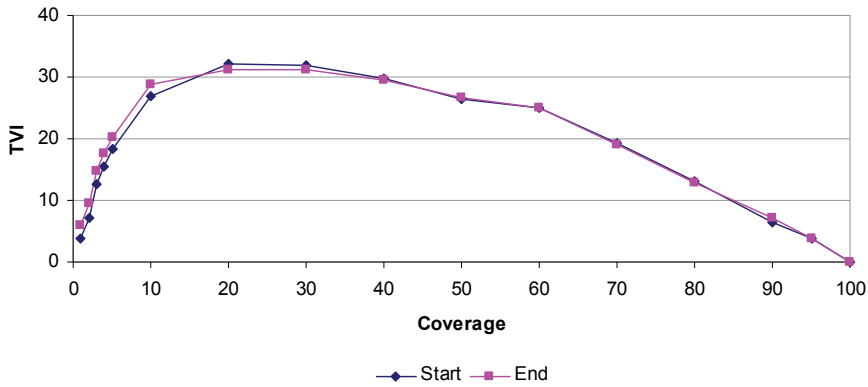


*Figure 2: Plate A Soft Tape - Low Anilox pressure - 500lpi(anilox) / 150lpi (plate)*
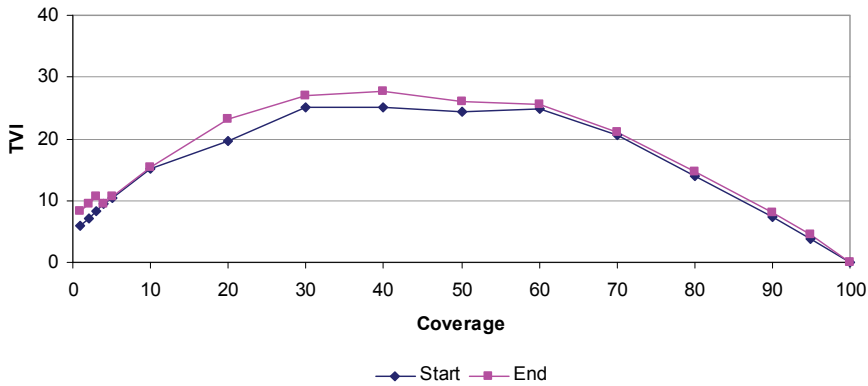


*Figure 3: Plate B Soft Tape - Low Anilox pressure - 500lpi(anilox) / 150lpi (plate)*

A comparison of the solid densities for the low anilox pressure, using the soft mounting tape is shown in Figure 4. The graph shows lower solid density for Plate B compared to Plate A. In both cases, a slightly lower solid density was observed at the end of the print run, compared to the start of the run.
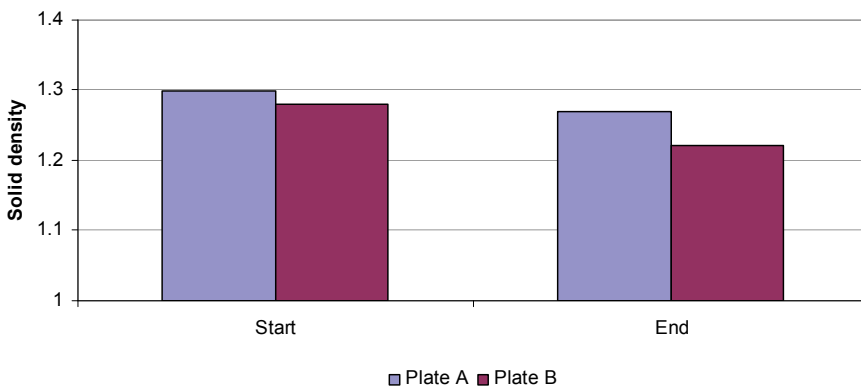


*Figure 4: Solid density comparison for Soft tape at low anilox pressure*

Measurement of the physical dot area, obtained using image processing is displayed in Figure 5, for the 10% halftone dot. The data shows that the dots on Plate B are much closer to nominal value of the tone. Little difference was observed between the 'Start' and 'End' samples.
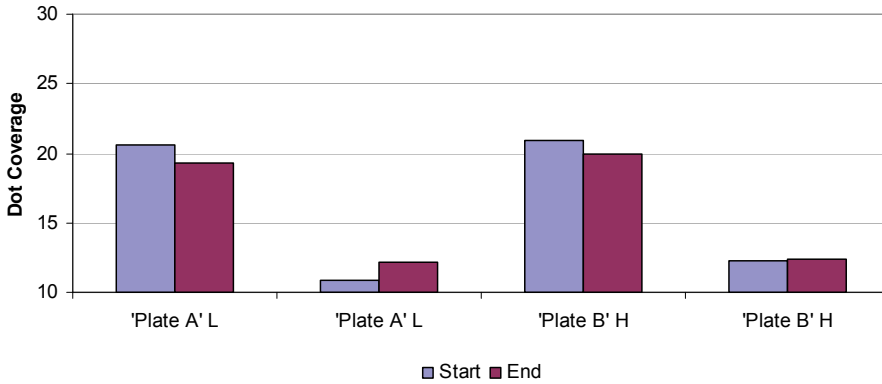


*Figure 5: Image processing data for 10% tone, soft tape, 500 lpi anilox, 175 lpi plate*

Figure 6 shows images of the printed 1% tones for both plate types, on the soft mounting tapes, at low and high anilox pressures. For the low anilox pressure images, no doughnuts were observed in the dots, for either plate type. However, at the higher anilox pressures, doughnuts were observed in the dots for Plate A, but not for Plate B. Therefore Plate B produces cleaner printed highlight dots, over a broader range of print conditions, compared to Plate A.



*Plate A low anilox pressure*



*Plate B low anilox pressure*



*Plate A high anilox pressure*



*Plate B high anilox pressure*
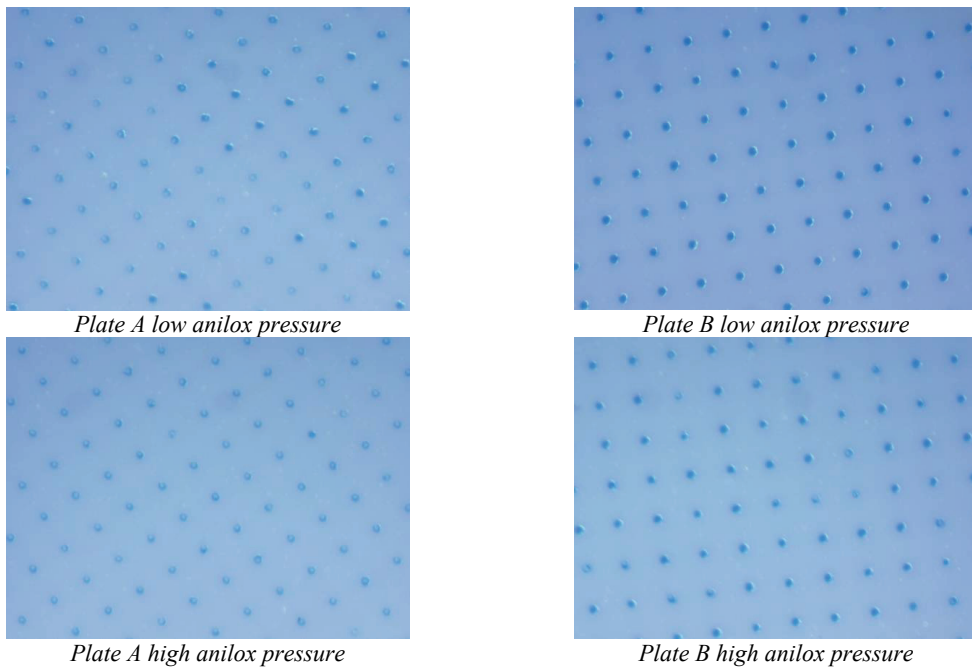
*Figure 6: 1% tone images, soft tape*

In order to understand the differences in print quality resulting from the two plate types, droplets of ink were deposited onto the plate surface and the contact angle was measured, using a FibroSystems DAT1100. The contact angle results for the average of 5 droplets on each plate material are presented in Table 4.

*Table 4: Contact angle results for UV ink on two plate materials*

|         | Ink Contact Angle |
|---------|-------------------|
| Plate A | 34°±2             |
| Plate B | 53°±2             |

The higher contact angle for Plate B implies a higher droplet volume per area coverage. As a result, it can be concluded that Plate B has the ability to carry more ink. However, exactly how the ink sits on top of a halftone dot will also be a function of how the contact angle is pinned at the interface of the dot shoulder and top surface.

## 3. Discussion

This investigation has focused on the comparison of printability characteristics of two plate systems; a traditionally processed plate and a water-washable plate. The data from the investigation suggests two mechanisms of ink lay on the dots, which is dependent on plate material. For Plate A, there is a migration of ink down the dot shoulder during printing (Figure 7). However, for Plate B, the ink does not travel down the dot shoulder, instead remaining on the dot surface. This suggests that Plate B releases more ink to the substrate, than Plate A.
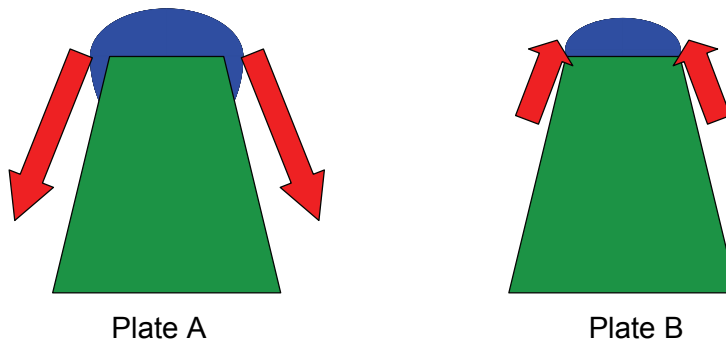


*Figure 7: Schematic representation of ink on halftone dots during printing*

The results have shown that there is little difference in solid density between Plate A and Plate B. This is due to both plate types receiving the same quantity of ink from the anilox, and therefore transferring the same volume of ink to the substrate in the solid regions. However, visual analysis of the prints have shown that the solid areas area more consistent for Plate B than for Plate A. This is in part due to the lower coefficient of friction for Plate B. A fluid on a material with a low coefficient of friction is more likely to have a higher contact angle, as it will be able to coalesce more easily. For Plate B, ink is able to spread more evenly over the surface of the plate, reducing mottle and pinholes. However, this effect would also be a consequence of higher surface energy (manifested as a higher contact angle) causing the ink to join and tend to form a circular dot.
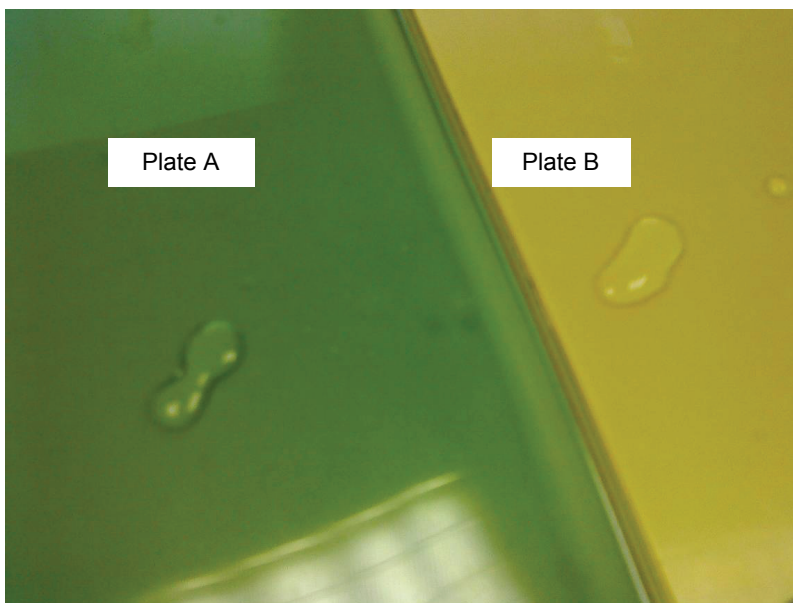


*Figure 8: Surface energy effects differences between Plate A and Plate B*

This is demonstrated in Figure 8, where two droplets of water have been deposited side by side on both Plate A and Plate B. For Plate A, although the two droplets have joined together, the forms of the original drops remain discernable. However, for Plate B, the two droplets have merged together to form a much more coherent single drop, and little distinction between the two original drops can be made. Therefore, when ink flows out of the discrete cells of the anilox roll onto the plate, it is more inclined to flow together to form a continuous film on the solid regions of Plate B than for Plate A, producing an even solid. The lower coefficient of friction for Plate B may be attributed to parameters, including surface roughness, or the different chemical composition of the photopolymer material.

## 4. Conclusions

As a result of the investigation, the following conclusions have been drawn:

- Ink transfer from the anilox to the plate is not affected by the plate material, as once the plate has been inked, it is an ink on ink contact, not ink on plate.
- Differences between the two plate materials were observed when the contact angle of a droplet of ink was deposited on the plate surface. The plate which exhibited the higher contact angle enabled the ink to be pined on the top of the halftone dot, as the ink is squeezed in the nip. For the plate with the lower contact angle, no pinning occurred and the ink travels down the dot shoulder, resulting in growth of the printed halftone dot
- Where the ink in pinned on the dot surface, due to the high contact angle, ink will not build-up in the recesses between dots, over the course of a long print run. This will result in the reduced ink spitting and therefore fewer press stops to clean the plate.
- Reduced friction of the plate surface allows ink to flow together more freely, once it has been transferred from the anilox roll. This was observed as an improved appearance of the printed solids, compared to the plate with a higher surface friction.

# Influence of gravure process on ink lifting efficiency

*Soile Passoja, Asko Sneck, Yingfeng Shen, Jorma Koskinen, Robert Roozeman*

VTT Technical Research Centre of Finland
P. O. Box 1000, FIN-02044 VTT, Finland

E-mails: soile.passoja@vtt.fi, asko.sneck@vtt.fi, yingfeng.shen@vtt.fi,
        jorma.t.koskinen@vtt.fi, robert.roozeman@vtt.fi

**Abstract**

This work is a continuation study of electric field assisted ink transfer in gravure presented earlier. We studied the influence of the shape and the size of the engraved cell on ink transfer both experimentally and theoretically. As well, the effect of the ink properties and ESA (electric field assistance) levels on ink lifting height from the cells was observed and studied. Furthermore, the relevance of these was verified with the full-scale gravure printings.

The study showed that the engraved cell shape affects strongly gravure ink lifting. With traditional diamond shaped cells the ink lifting in electric field occurs near the cell edges and an ink meniscus is quite easily formed inside the cell. If the ink is mainly transferred from the edges of the cell to the substrate doughnut shaped dots are printed. With more rounds shaped cell the ink is lifted faster and more evenly. This predicts also more stable ink transfer. Developed simulation model provides excellent possibilities to study the influence of the process parameters on gravure ink lifting. With the model the critical parameters affecting ink lifting efficiency can easily be detected. Furthermore, the model offers enhanced possibilities to optimize the printing performance of the certain printing processes with the printing parameters used.

**Keywords**: gravure; ink transfer; ESA; cell geometry; doughnut dot

## 1. Introduction

In gravure printing efficient ink transfer defines print quality. The ink transfer is secured when ink–substrate contact is formed in the printing nip. This contact formation is enhanced by electrostatic assisted (ESA) ink lifting. However, quite often unsatisfactory ink transfer is noted especially in light tone areas as non-uniform dot shapes. This has led to the development of differently shaped engraved cells. Gravure ink transfer and factors affecting it have been widely studied. Already in 1965 Weidemann was able to monitor the location of ink in the cells before and after ink transfer. Bery (1985) studied emptying mechanisms of the cells and imaged the ink-substrate contact through cellophane. These earlier studies were carried out without ESA. Serafano et al. (1998) made a study about the optimal level of ESA to improve ink transfer. Experimental studies relating to liquid release from grooves and cells have been published by Yin et al. (2006). Modelling has also been used to explain the liquid movements e.g. by Piette et al. (2002) and Powell et al. (2002). Apart from these liquid movement related studies the effect of electromechanically and laser engraved cells on missing dots frequency has been compared by Rong et al. (2007).

This work is a continuation study of work on electric field assisted ink transfer in gravure presented at IARIGAI 2009 (Passoja et al.). The objective of this work was to study the influence of cell shapes on gravure ink lifting. Also the effect of ESA levels on ink lifting speed and height was studied. Two approaches were selected: numerical simulation and experimental studies for verification. Simulation was used to achieve a deeper understanding of the phenomena involved in ink lifting. Experimental studies were used to capture the physical ink movement in a nip while applying an electric field. The relevance of these studies was verified through pilot scale printings using both electromechanically engraved and laser etched cylinders with identical layouts.

## 2. Methods

A static 2D ink lifting model was developed to illustrate ink movements in a cell approaching the nip. This model was used to simulate the influence of cell shapes and ESA levels on the ink lifting efficiency. The implementation of the model is based on OpenFOAM (Open Field Operation and Manipulation), which is an open source CFD package (Computational Fluid Dynamics). The standard multiphase solver from Open FOAM was extended with the effect of electric field. The basic geometry used is described in Figure 1.
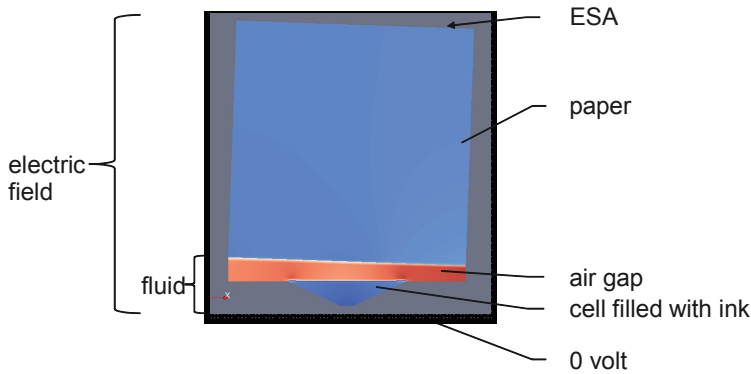
*Figure 1: Geometry used in the 2D ink lifting model*

From the modeling point of view, the ink lifting is a coupled multiphysics process. It includes the physics of fluid flow and the physics of electric field, which interact through the dielectrophoretic force. As shown in Figure 1, the fluid field includes the cell and the air gap between substrate and cylinder surface. The electric field includes the fluid domain and the paper. Mathematically, two systems have to be solved sequentially over a very short time interval.

The properties of a gravure ink (viscosity, surface tension, permittivity) and paper (thickness, permittivity) were used as parameters in this model. Simulations were carried out using the dimensions of both electromechanically engraved V cells and laser etched U cells in slightly tilted (2˚) plate geometry that mimics the impression roller approaching the nip. The simulation was made under static nip conditions using a 5 µm nip gap. The diameter of the cell was set to 30 µm. With the V cell the bottom angle was 130°. With U cells both the diameter and the depth of the cell could be varied, in the reference case the diameter of the cell was 30 µm and the depth was 7 µm. The ink lifting speed and height were the simulation output.

The influence of the cell shape on the electric field assisted ink lifting was initially studied using scaled-up V- and U-shaped grooves. An experimental set-up was arranged with an engraved aluminum plate and a metal cylinder depicting the gravure cylinder and the impression roller, respectively (Figure 2). A nip voltage of -800 V was used. The arrangements allowed side view monitoring of the nip phenomena. The same arrangement was used in the previous gravure study presented at IARIGAI 2009 (Passoja, et al.).
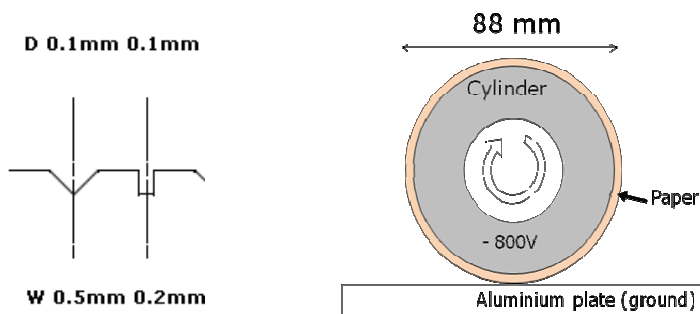


*Figure 2: Sketch of V and U shaped grooves (left). Side view test arrangement of electric field assisted ink lifting studies with machined grooves on aluminium plate (right)*

Electric field assisted ink lifting was subsequently studied with a set-up including a transparent impression glass slide. The main objective was to capture the actual ink lifting and contact formation in the nip. This set-up was based on a gravure hand-proofing device cylinder and a conductive glass plate. A glass slide under the cylinder simulates the impression roller. The slide was made conductive by an ITO-coating. A 20 µm thin transparent PET film was used as the substrate enabling monitoring ink movement in the nip area. A CCD camera and a light source were installed under the glass slide to record the ink movements. Ink lifting was monitored on both electromechanically and laser etched hand-proofing cylinders. The electromechanically engraved cells had square shape while the laser etched cells had round shape. Studies were carried out with gravure ink. The ink viscosity was 15 s (measured with a DIN4 cup). Figure 3 shows the technical arrangements of this setup in detail.
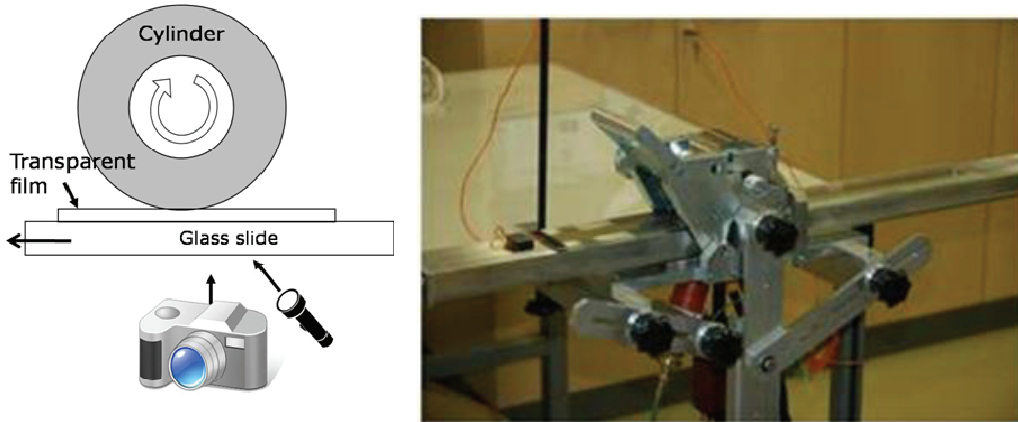
*Figure 3: Study of ink lifting and contact formation through transparent glass slide.*
*Schematic of apparatus (left), imaging setup (right)*

A small amount of ink was applied to the hand-proofing device and the excess ink was wiped away with the doctor blade. The glass slide was connected to a power source and the ink lifting was monitored at nip voltage of 0 V, -800 V and -1200 V. During the experiments the glass slide was moving making the fixed cylinder rotate. The printing speed was 30 to 40 cm/s. The ink lifting was monitored through the glass slide using a colour CCD camera with high resolution zoom lens. A high speed (100 ns) gas discharge illumination was used. The camera was set perpendicular to the cylinder. The angle between the light source and the camera was 20°. The actual size of the image area was 2.1 mm x 2.8 mm.

## 3. Results

The simulations show that with both V and U cells, the ink first moves towards the "approaching" plate indicating that the effect of the electric field is the strongest at the cell side which is closest to the charged plate. Ink is slightly spreading over the cell edge while being lifted. As the influence of the electric field at the trailing edge of the cell increases the ink is also lifted from that side and an ink meniscus is formed inside the cell, Figure 4.
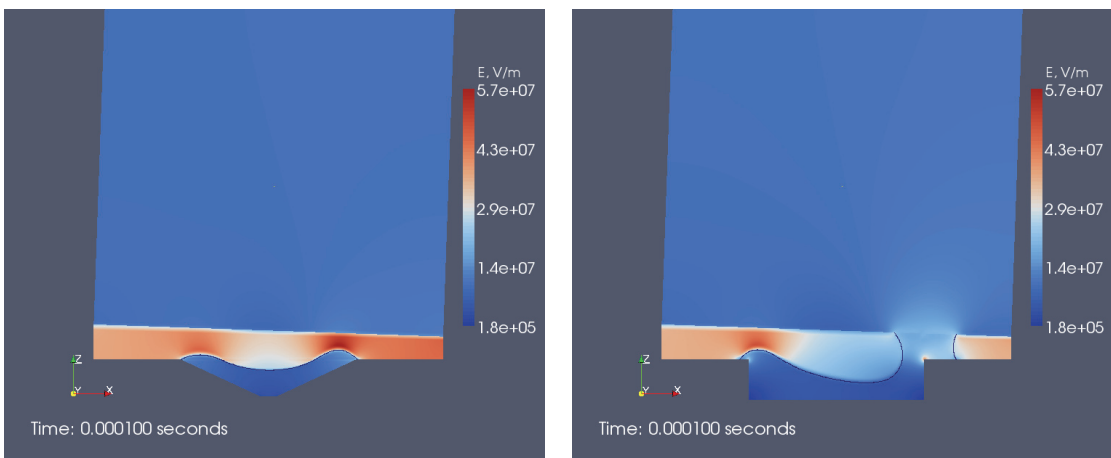


*Figure 4: Simulated ink lifting from V and U shaped cells, ink lifting after 100 µs. Simulation case: ESA= -800V,*
$\varepsilon_{r,ink}$=4.8, $\mu_{ink}$=20mPas, $\gamma_{ink}$=27mN/m, $\Delta h_{paper}$=60µm, $\varepsilon_{r,paper}$=4, $gap_{min}$ 5µm, tilt angle 2°, cell width 30µm,
*cell depth 7µm*

With the selected boundary conditions of the model and with the chosen values of materials and process the ink lifting occurs faster from U cells than from V cells when the cells are having the same diameter and depth, Figure 4. This means however that the ink volumes in the cells are not comparable; thus areas with different print densities are compared. When decreasing the cell diameter or increasing cell depth the U cells show slower lifting, Figure 5.
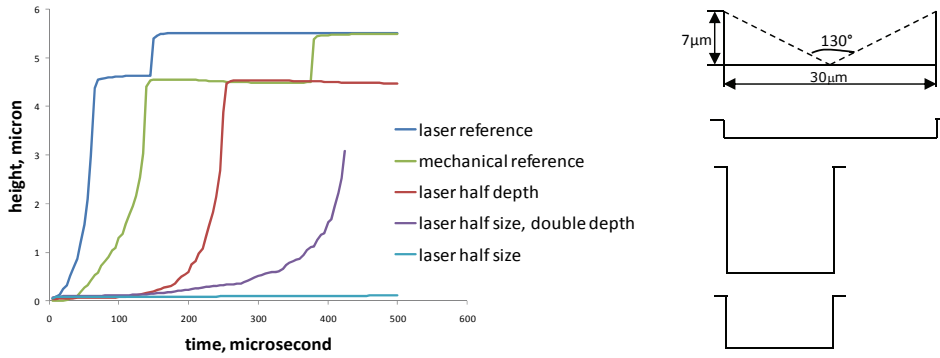
*Figure 5: Influence of cell shape on ink lifting (left), compared cell dimensions (right).*
*Simulation case: ESA=-800V, $\varepsilon_{r,ink}$=4.8, $\mu_{ink}$=20mPas, $\gamma_{ink}$=27mN/m, $\Delta h_{paper}$=60µm, $\varepsilon_{r,paper}$=4,*
*$gap_{min}$ 5µm, tilt angle 2°, cell width 30µm, cell depth 7µm*

The simulations describe the ink lifting from the cell across a nip gap of 4.5 µm (leading) to 5.5 µm (trailing edge). Normally, ink is lifted faster close to the edge where the air gap is the smallest. After the ink surface has reached the substrate, the surface height remains at 4.5 µm until the ink at the other edge is lifted above that height. This stepwise ink lifting is a result from the boundary conditions used in the model. In a real gravure nip there obviously is no need to lift the ink from the cell to this height since the engraved cylinder is continuously rotating so that the nip contact is achieved earlier.

The influence of the ESA level on the ink lifting speed and height was simulated using both V and U cell geometries. According to Figure 6 the nip voltage should be approximately -600 V or more to lift the ink from the cell in time when the gap between cylinder surface and paper is 5 µm. A higher voltage considerably increases the ink lifting speed. According to this comparison, ink lifting is easier from U cells than from a V cells when the ESA level is kept constant. At a nip voltage of -1000 V the ink is lifted the fastest, but in real printing this may lead to whiskering or other high ESA level induced problems.
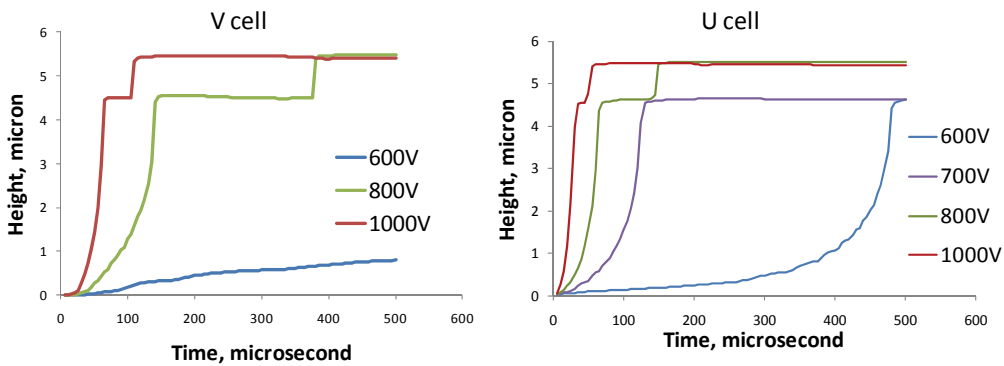


*Figure 6: Influence of (negative) ESA level on ink lifting height, simulation result. V cell (left), U cell (right)*
*Case: $\varepsilon_{r,ink}$=4.8, $\mu_{ink}$=20mPas, $\gamma_{ink}$=27mN/m, $\Delta h_{paper}$=60µm, $\varepsilon_{r,paper}$=4, $gap_{min}$ 5µm, tilt angle 2°,*
*cell width 30µm, cell depth 7µm*

The side view monitoring of the electric field assisted ink lifting shows the difference of ink lifting with grooves of different shape, Figure 7. With a V groove the ink is first lifted from the leading edge of the groove as the roller approaches the nip. As the roller moves on, similar ink lifting takes place at the trailing edge of the groove. This two sided ink lifting increases the concavity of the ink surface in the groove resulting in stronger ink lifting mainly at the edges of the groove. These observations from the V groove support the simulated ink movements.

With a U groove ink is lifted more evenly (Figure 7): initially, ink is lifted only from the leading edge of the groove. The rotational movement of the roller pushes the lifted ink ahead in the cell thereby filling the slightly concave ink surface. This leads to more evenly distributed ink in the cell and, further, to complete contact between ink and paper in the nip. Thus, the contact between ink and paper is promoted. This also partly confirms the simulated ink lifting in a U cell.
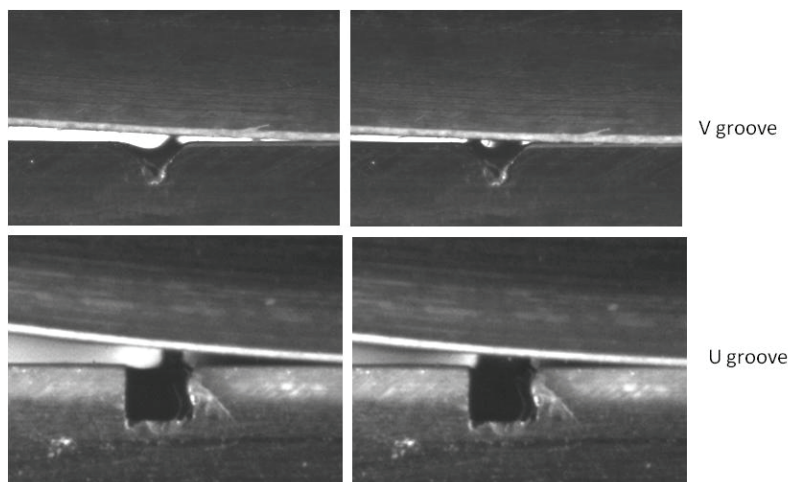
*Figure 7: Side view monitoring of electric field assisted ink lifting from V (upper images) and U groove (lower images). ESA -800 V, scale: 1cm=1000µm*

The studies with the transparent impression glass slide show how ink is lifted near the cell edges before the nip and how the lifted ink first contacts the transparent film at the leading edge of the cells, Figure 8. Furthermore, the ink–film contact is formed all around the cell edges. At the same time the centre of the cell is darker which indicates the formation of an ink meniscus. This indicates that ink is lifted more efficiently near the cell edges so that contact with the substrate starts there, predicting printed doughnut dots if the ink meniscus is not totally lifted from the cell. Similar ring shaped ink lifting was noticed with both V and U cells.
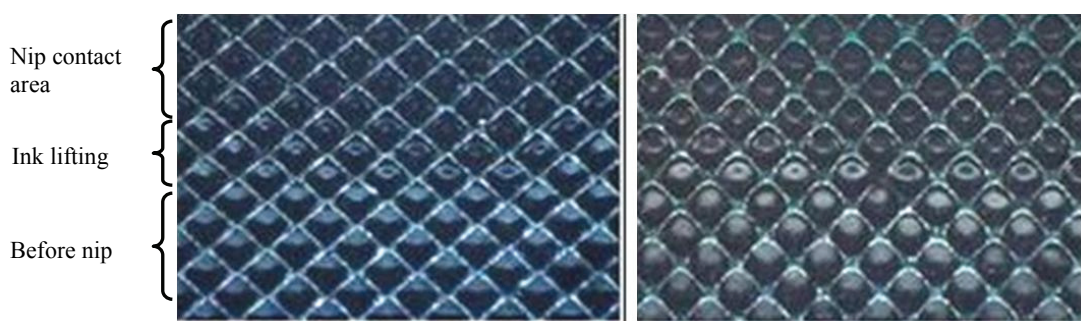


*Figure 8: Ink lifting from electromechanically and laser etched cells, transparent glass slide arrangement. Three stages of ink lifting: before the nip (bottom), ink lifting (middle), nip contact area (upper part of the images)*

The influence of ESA level on ink lifting is shown in Figure 9. Without ESA the ink stays in the cells until the physical nip contact is formed. When using -800 V the ink starts to lift before nip contact often leading to a ring shaped feature near the contact line. Thus a dougnut shaped contact area is formed between the cell edges. With -1200 V ESA the ink lifting starts earlier and the effect is stronger. At high ESA level the formation of ring shape can also be seen more often in the cells.
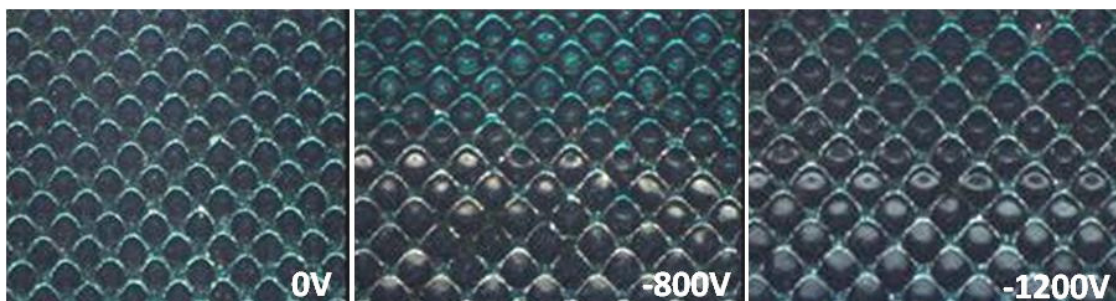


*Figure 9: Ink lifting with ESA level 0 V, -800 V and -1200 V from laser etched cells, transparent glass slide arrangement. Three stages of ink lifting: before the nip (bottom), ink lifting (middle), nip contact area (upper part of the images)*

## 4. Discussion

In this work modelling was used to gain an insight of the influence of the cell dimensions and ESA levels on ink lifting. Simplification of complex nip phenomena offers a possibility to clarify the ink movements in the nip when an electric field is applied between the gravure cylinder and the impression roller. The real values of printing materials and process variables can be used in the model. In addition, it provides possibilities to find out the limits for each process variable in order to optimize it. In this work the ink transfer from cells of the same diameter but different volumes were compared. This way the effect of the electric field and the ink contact was measured over a comparable area. The drawback of this approach was that, due to the different geometries, identical surface area implies different ink volumes: whereas the V cells have a triangular shape, the U cells have an almost rectangular crosscut. The weakness of this way of comparing therefore lies in the fact that with the fixed ink properties cells of different print density are compared. On the other hand, both simulation and experimental studies showed how ink is lifted more evenly from U cells resulting more evenly formed printed dots (Figure 10).

2D ink lifting simulations were verified with transparent impression glass slide studies showing the ink–film contact in the nip. Both V and U shaped cells offered a ring shape ink lifting near the cell edges. Studies also showed that the concave ink meniscus in the centre of the cell was deeper when higher levels of ESA were used. This is known to lead to printing of incomplete dots if the contact is not totally achieved. This too was supported by the simulations.

When comparing the simulated ink lifting in a static nip to the real gravure process one should keep in mind that when the simulated sequence lasts 0.5 ms the actual web moves 5 mm (assuming a web speed of 10 m/s). The side view ink lifting and transparent impression glass slide imaging showed how the rotational movement of the roller actually promotes ink transfer from U groove and cell. As the charged roller approaches the ink is lifted from the leading edge of the groove or a cell. The rotational movement of the roller pushes the ink ahead thereby filling the slightly concave ink surface. This causes ink bridging over the concave ink surface resulting in better ink-substrate contact in the nip. The situation is different in V groove or cells where the electric field causes almost simultaneous ink lifting from both edges where the ink amount is smaller and a deeper concave ink meniscus is formed in the middle of the groove or cell. This two sided ink lifting is so strong that the rotational movement of the roller is not able to fill up the missing ink volume in the centre of the cell therefore more probably leading to incomplete printed dots. This was in fact seen from the printed halftone areas using two differently engraved cylinders having the same layout with fine black cells (Figure 10). The only difference between the cells was the cross sectional shape of the engraved cells: triangular in electromechanically engraved cells or rectangular in laser etched cells. Based on these printed samples one could say that a more evenly distributed ink in the cell also provides more even ink transfer.



Gravure cell dimensions
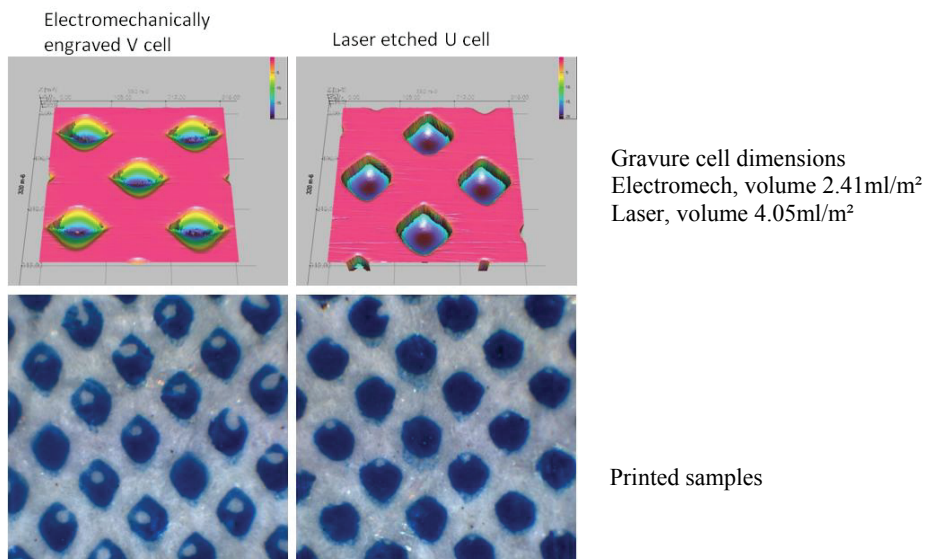Electromech, volume 2.41ml/m²
Laser, volume 4.05ml/m²

Printed samples

*Figure 10: Upper images: Measurement of the gravure cell dimensions, 40% halftone area (Heimann 3D-volume Measuring system µ-surf-mobile). Lower images: Printed with ESA, 40% halftone area. Electromechanically engraved V cells (left), laser etched U cells (right). Trailing edge at the bottom of the images*

The ink lifting model is prepared to study a static nip configuration meaning that the effect of rotational movement of the cylinder and the speed of the press are not taken into account. In large cells, ink transfer improves with increasing speed but in smaller cells the ink transfer efficiency is lowered. As the engraved cylinder is rotating faster, the centrifugal forces and the capillary forces of the substrate increase the emptying of the large cells. With small cells, the cohesive-viscous forces of the ink keep the ink more steadily in the cell. Furthermore, the solvent evaporation has a stronger effect on the small ink amounts in smaller cells resulting in faster drying of the ink in these cells. Therefore, the higher the speed, the lower the emptying rate of the small cells. Based on these considerations we suggest that the effect of centrifugal forces and shearing forces of doctor blade and nip pressure should be further studied.

The experimental arrangements in the ink lifting studies may raise a question of how relevant these studies are to real gravure nip conditions. One could criticize the scale of the experimental groove set-up: the engraved grooves were bigger than the actual engraved cells of a gravure cylinder. The groove set-up and the bigger dimensions of the engravings were selected mainly to visualize the effect of the electric field in ink lifting. Furthermore, the set-up provided a possibility to monitor the ink movements in nip conditions. The side view ink lifting observations were supported by the transparent glass slide ink lifting studies where the actual engraved cells were used for ink lifting. These smaller cells showed similar ink lifting near the cell edges and formation of the ink meniscus in the cells. In addition, similar ink movements were noted in simulations so that the experimental observations can well be used to explain ink lifting in actual engraved cells.

In publication printing the typical value of nip voltage is -800 V. According to simulation, ESA level -800 V provides ink lifting above the cylinder surface within 120 μs. This is sufficient to secure the contact between ink and substrate in the nip. On the other hand, with such a high nip voltage, a concave ink meniscus is formed in the cell. This is more obvious with V cells and increases the possibility of incomplete printed dots. However, this ink lifting speed should secure the ink transfer since in publication printing the nip contact lasts from 1 ms to 2 ms.

## Conclusions

In this work the influence of cell dimensions, electromechanically engraved V cells and laser etched U cells, as well as ESA levels on ink lifting speed and height was studied. The dimensions of the cell strongly affect ink lifting in electric field. When the cells have same diameter and depth, and other process parameters are the same, the ink lifting occurs faster from U cells than from V cells. This means however that the ink volumes in the cells are not comparable. With ESA ink is lifted in a ring shape near the cell edges inside the cells. Minor ink spreading over the cell edge is noted when the nip contact is approaching. This ring shaped ink lifting is noticed with both triangular V cell and rectangular U cell. Higher ESA level induces stronger ring shaped ink lifting in the cells providing faster ink lifting.

The rotation of the cylinders promotes ink transfer in the nip especially with U cells. As the charged roller approaches ink is lifted from the cell and pushed forward in the cell thus thereby filling the slightly concave ink surface resulting in better contact in the nip. The situation is different in triangular V cells where the electric field causes two sided ink lifting from the cell edges and a deeper concave ink meniscus is formed in the middle of the cell. This two sided ink lifting is so strong that the rotational movement of the roller is not able to fill up the missing ink volume thereby increasing the probability of incomplete printed dots.

The developed 2D static nip model provides excellent possibilities to study the influence of the process parameters on gravure ink lifting and, in general, liquid movements in electric field. With this model the critical parameters affecting ink lifting efficiency can easily be detected. Furthermore, the model offers enhanced possibilities to optimize the printing performance and materials of certain printing processes with the parameters used.

## References

Weidemann, K., (1965) *What happens in high speed ink transfer, Gravure February 1965, pp. 34-38.*

Bery, Y. A., (1985), *Mechanisms governing gravure printing, Proceedings of TAPPI 1985 Coating Conference, pp. 149-159.*

Serafano, J., Triantafillopoulos, N., (1998), *Optimizing ESA To Improve Ink Transfer, Ink World, 5, pp. 22-25, 67.*

Yin, X., Kumar, S., (2006), *Flow visualization of the liquid-emptying process in scaled-up gravure grooves and cells, Chemical Engineering Science, 61, pp. 1146-1156.*

Piette, P., Trehoult, C., (2002), *Ink transfer theory in Rotogravure Printing, International Printing and Graphics Arts Conference, Bordeaux, p. 5.*

Powell, C. A., Savage, M. D., Guthrie, J. T., (2002), *Computational simulation of the printing of the Newtonian liquid from trapezoidal cavity. Methods for Heat & Fluid Flow, 12, 4, pp. 338-355.*

Rong, X., Pekarovicova, A., (2007) *The study of Missing Dots of Electromechanical and Laser Engraved Cylinders, TAGA Proceedings 2007, pp. 596-604.*

Passoja,S., Koskinen, J., Roozeman, R., Sneck, A., (2009), *Electric field assisted ink lifting in gravure. 36th IARIGAI Proceedings 2009, pp. 201-205.*

# Using microwave drying systems in the graphic arts.
# Modern solutions for environmental industrial applications

*Marios Tsigonias*[1,2,3]*, Eugenia Ploumi* [1,2]*, Anastasios Politis*[2,3] *and George Vekinis*[1]

[1] National Centre of Scientific Research Demokritos
  Terma Patriarchou Grigoriou & Neapoleos, GR-15310, Ag. Paraskevi, Greece

[2] Technological Educational Institute of Athens
  Dept. of Graphic Arts Technology, Ag. Spiridonos, GR-12210, Egaleo, Greece

[3] Hellenic Open University, School of Applied Arts
  18, Parodos Aristotelous St., GR-26 335, Patra, Greece

  E-mails: mtsigon@chem.demokritos.gr, pl.eugenia@gmail.com,
        politisresearch@techlink.gr gvekinis@ims.demokritos.gr

**Abstract**

A large share of the cost of production in the Graphic Arts industry corresponds to the energy consumed. This is estimated at roughly 10% of total cost of the production.

The present study is a first-order investigation of the potential amount of energy that can be recovered from the replacement of conventional drying methods with microwave (MW) drying. Ambient drying methods, infrared radiation or other hot air drying methods, require a long drying period and large amounts of energy. Besides that, conventional drying mechanisms lead to, in certain cases, insufficient drying which results in misprints and added cost. On the other hand, with the use of microwaves it is possible to achieve satisfactory drying of various materials since microwaves have the ability to interact with polar molecules such as water and penetrate non-conductive materials to some depth heating any contained water. Because of this ability, microwaves are used in various industrial applications that require drying or desiccation. Several applications can be mentioned, such as the ceramic materials industry (hi-tech applications, bricks and porcelains), dried fruits and other foods, in the desiccation of by-products of biological waste treatment, thermal inertification of asbestos and other.

Microwave drying systems have the potential to work with all the existing printing technologies and produce a very good printing result. Additionally, they offer two important comparative advantages: energy efficiency and the effective use with water-based inks and varnishes. These potential capabilities make microwaves ideal candidates for new applications towards more environmental sustainability in printing.

**Keywords**: microwave drying; energy efficiency; water based inks; polar solvent based inks;
        green graphic arts industry

## 1. Introduction

### 1.1 Drying systems in printing - the existing situation

Drying of the printed substrates is an important issue for the printing industry. Many alternative drying systems are currently in operation both off and online with the printing machines and processes, such as thermal devices that rely on gas combustion or infrared radiation. These systems speed up the drying procedure by assisting the solvents' evaporation. Penetration of a printing ink is faster if the viscosity is low. Viscosity decreases when the temperature is raised so, the transferred ink film can be heated up together with the substrate by using a thermal gas combustion or IR radiation source.

Chemical drying processes (e.g. oxidation, catalitic assisted drying) following the physical drying process are also accelerated by a heating. Such processes are found in almost any kind of solvent-based oleophilic ink (Kipphan et al., 2001).

In newspaper offset printing, the printing ink dries on the paper substrate by partial absorption or penetration into the paper fibber body (coldset method). In commercial printing, the printing ink on coated papers, that have a lower adsorption capacity, also needs to be dried by thermally evaporating the solvent (heatset method). Long extended hot air drying is used to blow hot air over both sides of the fresh print via nozzles.

Combinations of hot-air dryers and infrared dryers are also in use. Infrared dryers are used in newspaper printing only to stimulate ink adsorption, thereby facilitating printing with higher ink density, that is, with higher ink application. Nowadays UV radiation dryers are hardly ever used, due to their limited quality (they don't give the "ink melting effect" which offers brilliance) and to the high printing ink costs they incur in web offset. For the same reason, electrobeam dryers or ink curing systems have not come to be generally accepted in practical operation, although they have efficient drying properties (Kipphan et al., 2001; Todd, 1997 & Stanganellis, 1995).

The ink used for rotogravure and flexographic printing has a low viscosity so that the ink in the cells can run out properly and be transferred onto the paper. This low viscosity is principally achieved by using a high proportion of low boiling point solvent with the ink. To dry the printed ink, the solvent must evaporate in a high velocity air dryer after leaving the printing nip. Counter flow/parallel flow drying systems and heating drums are no longer used. Instead, high-velocity nozzle dryers are used. Radial fans route the air in pipes fitted closely above the web and equipped with circular or slot nozzles. The air hits the web vertically, and thus the fresh print. The effect of the impact is to turn the air around by 180° which returns between the pipes, back to the radial fans, to be fed back into the nozzle pipes. In front of the radial fans, part of the circulated air is branched off and routed into a solvent recovery unit in order to prevent uncontrolled increase in the solvent concentration in the ambient air. The solvent (usually Toluene) must be recovered for environmental and financial reasons. The proportion of air removed thereby is automatically replaced by fresh air or ventilation air. Since not only the speed at which the air emerges from the nozzles, but also the length of the dryer plays a decisive role in determining the effectiveness of drying and therefore the maximum production speed (typically 5-15 m/s) of the gravure or flexographic printing press, the dryers are placed on both sides and surround the entire printing unit. Depending on the type of solvent used, shorter drying units, which do not surround the entire printing unit, are sometimes sufficient. (Tsimi, 2010; Kipphan et al., 2001; Thompson, 1995; Nomikos, 1998)

The solvent recovery unit consists of large vessels that are filled with activated carbon and through which the air charged with solvent is routed. In this process the solvent settles down on the activated carbon, whereby the air is freed from the solvent and simultaneously cleaned in an environmentally sound way. In order to release the solvent from the activated carbon for re-use, steam is sent through the activated carbon vessels in the "reversal process," which washes out the solvent. Since the solvent has a lower specific gravity compared to water, it can be easily separated from condensed steam, as it separates itself from the mixture onto the surface. (Tsimi, 2010; Kipphan et al., 2001)

Alternative recovery units use several columns of hollow fiber filters that may separate the different solvents during their flow through. This separation is happening in the volatile state of the solvent (VOCs) and deliquescence with the use of special distillers is the process that follows. (Tsimi, 2010)

### 1.2 Microwaves (MWs) in various drying applications

MWs have been used in the past for many industrial applications. In the food industry, besides the well known heating, MWs can be used for the desiccation of foods like carrots, fish, peach, biscuit and many other foodstuffs. (Zheng-Wei Cui et al., 2004; Tao Wu et al., 2008; Jun Wang & Kuichuan Sheng, 2006)

MW processing of ceramic materials is another novel industrial application with MWs offering superior drying efficiencies and increases in production of existing or new factories. Even high tech materials have been successfully treated with MW processing. (Sutton, 1989)

Many interesting environmental applications are also reported. Biological waste treatment and thermal inertification of asbestos with MW irradiation constitute just two of the environmental MW applications. (Martin et al., 2005; Leonelli et al., 2006) Hundreds of other industrial MW applications are mentioned in the international bibliography.

## 2. The use of MWs for ink drying

In the present study, MW drying of ink has been evaluated for potential use in printing drying systems. For this purpose the drying effectiveness of a group of inks used in the printing industry (offset, rotogravure, flexography and screen printing) was studied with the use of drying systems based on MWs in comparison with ambient drying, drying in hot air environment and infrared radiation drying. (Ploumi, 2009)

Two types of paper (plain uncoated paper and illustration paper - both of 90g/m$^2$) were used as printed substrates for this study. A large variety of inks were tested for their drying attitudes with different drying systems [ambient drying, thermal drying system (1.4 KW), IR drying system (1.0 KW) and MW drying system (1.2 KW)].

*Table1. Offset ink drying process with different systems*

| Type of ink | Solvent | Drying system | Drying Yes/No | Drying time |
|---|---|---|---|---|
| Offset printed ink Fresco/stabile Spirit-alcohol | Several organic solvents | IR | Yes | 35 sec |
| | | Ambient drying | Yes | 2 h (aprox.) |
| | | Thermal treatment | Yes | 60 sec |
| | | MW | No | N/A |

Printed substrate weight decrease was correlated to the drying process that was used each time. Ambient drying's printed substrate change of weight was used as the basis for the calculation of the efficiency of the other drying methods. The printed substrate (with flexographic water-based ink) weight's decrease is plotted in figure 1 for all four drying processes used. Similar diagrams were constructed for all inks (Tables 1-3) that were tested for this study. We present an estimate of the necessary time for each drying method in order to get the same weight loss to the ambient drying process. These estimations where used for the calculation of the total energy consumption for each drying method (E=P·t where E is the consumed energy in kWh, P is the power in kW and t is the necessary time for the drying system to produce the same weight loss to the corresponding ambient drying). Energy consumption data are referred on the Tables 2 and 3 regarding flexographic and screen printing inks.
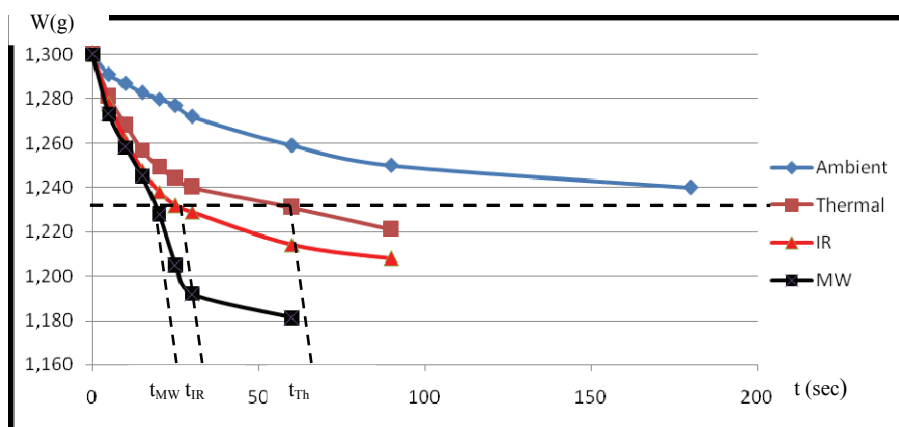


*Figure 1: Printed substrate weight decrease during different drying processes (water based flexographic ink)*

Energy consumption estimations of the most popular drying techniques in comparison with the MW-assisted drying system energy consumption were also carried out with the aim of evaluating their comparative cost. Water-based inks were examined in greater depth regarding their printing quality and drying effectiveness with the MW drying systems (Tables 2 & 3).

*Table 2: Flexographic water based ink drying process with different systems*

| Type of ink | Solvent | Drying system used | Drying Yes/No | Drying time | Consumed Energy (kWh) |
|---|---|---|---|---|---|
| Aqua base plus TP-1902 Van Son Liquids B.L. | Water | IR | Yes | 30 sec | 0,0083 |
| | | Ambient drying | Yes | 30 min | N/A |
| | | Thermal treatment | Yes | 60 sec | 0,0238 |
| | | MW | Yes | **20 sec** | **0,0067** |

*Table 3. Screen printing inks drying process with different systems*

| Type of ink | Solvent | Drying system used | Drying Yes/No | Drying time | Consumed Energy (kWh) |
|---|---|---|---|---|---|
| MV32 MATT VINYL Apollo-colours Limited | G.V. (gloss vinyl) Thinner R33 | IR | Yes | 30 sec | 0,0083 |
| | | Ambient drying | Yes | 30 min | N/A |
| | | Thermal treatment | Yes | 60 sec | 0,0238 |
| | | MW | No | N/A | N/A |
| SIO87 (for metals) Apollo | - | IR | Yes | 30 sec | 0,0083 |
| | | Ambient drying | Yes | 1,25 h | N/A |
| | | Thermal treatment | Yes | 60 sec | 0,0238 |
| | | MW | Yes | **30 sec** | **0,01** |
| TEXYLON (for fabrics) Argon | Solvent 5% 90924 Ethoxy propyl-acetate 40910 | IR | Yes | 30 sec | 0,0083 |
| | | Ambient drying | Yes | 1 h | N/A |
| | | Thermal treatment | Yes | 60 sec | 0,0238 |
| | | MW | No | N/A | N/A |
| Water based ink Argon | Solvent for water based inks 5% | IR | Yes | 30 sec | 0,0083 |
| | | Ambient drying | Yes | 1 h | N/A |
| | | Thermal treatment | Yes | 60 sec | 0,0238 |
| | | MW | Yes | **20 sec** | **0,0067** |
| LACPRINT A FREDDO 303080 Engler Italia s.r.l | ENGLER LACPRINT A FREDDO CATALYST 303099 | IR | Yes | 30 sec | 0,0083 |
| | | Ambient drying | Yes | 1 h | N/A |
| | | Thermal treatment | Yes | 60 sec | 0,0238 |
| | | MW | Yes | **15 sec** | **0,005** |

The results show that the MW-assisted drying method is able to dry all polar inks tested quicker using significantly lower energy. It offers definite advantages for drying all inks based on polar solvents, especially water-based ones, both in terms of effectiveness and speed of drying and lower production costs.

In addition, the higher speed of drying allows some definite improvements in overall productivity and capability of printing systems.

Furthermore, the higher speed of drying offered by the assisted microwave systems studied in this work shows that substantial environmental benefits are possible for most of the inks used.

## 3. Discussion

It is obvious that MWs are not the optimum drying mechanism for every ink type. In the table one we may observe that offset printing inks do not dry with the use of MWs, as these inks cannot absorb microwave energy.

On the other hand water based inks that are used in flexography and screen printing dry much more effectively than with ambient drying and even with the other -energy consumptive- methods.

Especially, water based inks for flexographic printing dry much more effectively than with the IR drying method. A 33% of time save and a 19% of energy consumption save was measured, increasing the productivity as well as the energy efficiency of the method.

Many of the screen printing inks seem to present a similar behavior. In the situations that MW drying for screen printing inks is applicable, time reduction of the drying process was estimated between 0% and 50% in comparison with the IR drying systems, which are the most effective systems used in the industry at present. Energy consumption seems to be reduced by up to 40% in some cases (Table 3 - Lacprint a Freddo screen printing ink).

Not only water based inks but also inks with several polar solvents dry effectively with the use of MW systems with significant benefits in productivity, cost and energy consumption.

The use of MW-assisted drying may thus allow the replacement of VOC-based solvents with water based inks, will offer a substantial environmental benefit as well.

## 4. Conclusions

This study clearly shows the potential of microwave systems to dry effectively the ink on the substrates examined, rapidly and efficiently. It also demonstrates the environmental benefits of the use of MW-assisted drying systems compared to conventional ones since it offers the possibility for use of water-based inks instead of solvent-based ones.

The use of MWs for drying may offer significant energy and cost efficiencies and quality of rapid offset printing will improve as well with the use of MW systems for paper drying between the printing units (wet on wet printing). The financial benefits that may occur as a result of a possible replacement of drying mechanisms in the productive process of graphic arts are clear but further work is needed to elucidate the details of an application.

## 5. Future R&D plans

To incorporate a MW drying system in Graphic Arts production we have already started a collaboration with a Greek SME with extensive expertise in industrial microwave drying systems. The first design for two prototypes MW-assisted dryers for a flexography and an offset printing press incorporates special field traps for safety, special field distributors (ensuring good field distribution) and measurement of surface humidity at the entrance and exit of the paper. We expect to have the pilot prototypes ready for testing in the next few months to carry out tests under real production conditions. Our aim is to determine all major industrial parameters such as printing quality, cost benefit, maximum possible printing speed improvements, energy consumption and environmental sustainability benefits.

## References

Cheeseman Dennis, (2002) Pressdoctor 2002 - A Web Offset Newspaper Guide, US Ink

Huang Y. F., Kuan W. H., Lo S. L. & Lin C. F., (2008) *Total recovery of resources and energy from rice straw using microwave-induced pyrolysis*, Bioresource Technology, 99, pp. 8252–8258

Jun Wang & Kuichuan Sheng, (2006), Far-infrared and microwave drying of peach, LWT - Food Science and Technology, Volume 39, Issue 3, pp. 247-255

Kipphan Helmut et al., (2001), Handbook of print media: technologies and production methods, ed. Helmut Kipphan, Springer Verlag, ISBN: 3-540-67326-1

Leonelli, C., Veronesi, P., Boccaccini, D. N., Rivasi, M. R., Barbieri, L., Andreola, F., Lancellotti, I., Rabitti, D., Pellacani, G. C., (2006), *Microwave thermal inertisation of asbestos containing waste and its recycling in traditional ceramics*, Journal of Hazardous Materials, B135, pp. 149-155

Martin, D. I., Margaritescu, I., Cirstea, E., Togoe, I., Ighigeanu, D., Nemtanu, M. R., Oproiu, C., Iacob, N., (2005), *Application of accelerated electron beam and microwave irradiation to biological waste treatment*, Vacuum, 77, pp. 501-506

Nomikos Spyridon, (1998), Flexography, academic material, TEI of Athens, (in Greek)

Ploumi Eugenia, (2009), Microwave application for the construction of a printing drying system, BSc. Thesis, TEI of Athens, (in Greek)

Stanganellis Dionysis, (1995), Offset Printing I & II, academic material, TEI of Athens (in Greek)

Sutton H. Willard, (1989), *Microwave Processing of Ceramic Materials*, Ceramic Bulletin, 68, pp. 376-385

Tao Wu, Linchun Mao, (2008), *Influences of hot air drying and microwave drying on nutritional andodorous properties of grass carp (Ctenopharyngodon idellus) fillets*, Food Chemistry, 110, pp. 647-653

Thompson Bob, (1995), Inks and printing coatings, PIRA International

Todd E. Ronald, (1997), Printing inks, Formulation principles, manufacture and quality control testing procedures, PIRA International, ISBN: 978-1858020271

Tsimi Diana, (2010), Rotogravure Printing, In Press, (in Greek)

Zheng-Wei Cui, Shi-Ying Xu, Da-Wen Sun, (2004), *Microwave-vacuum drying kinetics of carrot slices*, Journal of Food Engineering, Volume 65, Issue 2, pp. 157-164

# Improving reliability-based maintenance culture in the printing industry

*Csaba Horváth*[1]*,Erzsébet Novotny*[2]

[1] Óbuda University/Nyomdatechnika Kft.
  Doberdó út 6, H-1034 Budapest, Hungary

  E-mail: horvath.csaba@rkk.uni-obuda.hu

[2] PNYME/Állami Nyomda Nyrt.
  Fő utca 6, H-1027 Budapest, Hungary

  E-mail: novotny@any.hu

### Abstract

In several aspects, maintenance organization relies on the results of organization sciences, and therefore the results, correlations surfacing during the analysis and examination of organizational cultures may as well be applicable to this field of studies. Cultural elements can be clearly linked to the maintenance strategic model elaborated by the authors, thus demonstrating that the improvement of maintenance efficiency and changes in certain elements of the organizational culture can be assigned to each other. The authors have worked out correlations and methods, conducted studies to see how in contrast with the reactive (troubleshooting) maintenance approach the foresighted reliability culture can be made a part of the corporate culture at printing businesses, what steps, procedures are needed for a successful change.

**Keywords:** reliability; corporate culture; maintenance; printing industry

## 1. Scope of the research

With a focus on the development of maintenance organization, as part of a larger work we assessed the situation of maintenance in printing industry maintenance, at Hungarian printing enterprises in 2003 and 2004. A series of questionnaire-based surveys conducted with the involvement of professionals working in the examined field formed the basis of the assessment. With respect to the production value created, the survey could be performed at 26 of the 30 largest printing companies. At that time, these printing enterprises represented approximately 60% of the registered production volume of the sector. All the competent maintenance managers - altogether 67 people - responded to our questions. From the "private soldiers" of maintenance, we sought for and received answers from almost 20% of the representatives of the profession.

This questionnaire-based survey of the existing conditions tried to reveal the situation of maintenance in printing industry at that time, the professional preparedness and organization of these activities, technical facilities, expectations and the foreseeable tendencies of development (Horvath, Gaal, Kerekes, 2009).

Some of the questions in the survey also concerned problems relating to corporate culture, and the responses implied that in printing industry - including maintenance - traditions, the printer attitude and insistence on well-established ways of behaviour. It was apparent that major internal changes took place at the company, accompanied by a change in the culture. These factors have motivated us to examine whether the available means of organizational culture can contribute to the efficient adoption of the reliability-centered orientation in maintenance. Hereunder, our associated researches are presented.

## 2. Methodology of the research

When we were framing our integrated maintenance model, we considered all those means and abilities that were needed for the betterment of maintenance, expected to allow the implementation of efficient foresighted maintenance management in printing industry, and at the same time comprised the elements of the structuring of our maintenance model. Some of these elements belong to *hard means* or *hard skills* as they are called in Anglo-Saxon technical literature. They cover all those knowledge, professional contents, abilities that are needed for the performance of foresighted maintenance. They include tangible means such as professional and time planning, the performance of operating and stewardship tasks, condition monitoring, failure analysis, servicing know-how and so on.

*Key abilities* or in English terminology "soft skills" are not associated with the given profession, but rather successful work. On the other hand, there are so-called "intangible" characteristics, behavioural patterns and practices; long-term plans, short-term goals, personal management, communication and cooperation, problem solving and the assumption of responsibilities, learning skills and capabilities, team work, performance and evaluation skills.

Figure 1 shows how the pyramid of "hard" skills is built upon the foundation formed by the "soft" key abilities. Nevertheless, the deep foundation of both these types of skills is in fact the organizational culture. In the light of this attitude, the structuring of the corporate culture should unavoidably be associated with the development of a maintenance model.



*Figure 1: The pyramid of means and abilities stands on a foundation formed by organizational culture (Thomas, 2005)*

It has been examined how the reliability-centered culture can be incorporated into the work processes of the improvement of maintenance organization, how it is based on this maintenance model. The interpretation of the reliability-centered attitude is demonstrated via ways of behaviour matched up and described in Figures 2 and 3.

| Engineer Culture Change | |
|---|---|
| *Mechanic* | *Technician* |
| Lone ranger | Works in a team |
| Lubrication (if there is sufficient time) | Technically demanding |
| Inspection (if there is sufficient time) | Diagnostic and forecast |
| Troubleshooting panic | Works along time plans |
| Repeat breakdowns | Specialist of the given field |
| Permanent stress, but not a challenge | Challenging, but not stress |

*Figure 2: Repair-oriented and reliability-centered culture of engineers (Hair, 2002)*

Today, the execution of maintenance tasks calls for a technician of independent and synthesized thinking rather than a repair-oriented workfellow who tends to lean back and regard himself to be a hero after any successful troubleshooting.

| Management Culture Change | |
|---|---|
| *Repair servicing administrator* | *Engineering manager* |
| Get it fixed | Why did it break? |
| Work acceptability | What caused the work? |
| How much does it cost? | What caused the costs? |
| Inflexible in the face of budget constraints | To review the investment and planning |
| When will something break again? | Can do we prevent it? |
| Survived another week | How do we improve? |

*Figure 3: Repair-oriented and reliability-centered culture of maintenance management (Hair, 2002)*

Similarly, completely different mentality and requirements are valid for a manager who plans maintenance with respect to reliability in comparison with a leader always waiting for the following day to come. In the processes of maintenance organization, proper attention should be paid to supporting the forms of behaviour described in the right columns.

## 3. Structuring of a reliability-centered culture

Changes are always induced by economic factors, it is never the culture that itself "demands" change. In our case, the necessity to change the maintenance strategy is the main drive behind the change of the culture.

The control of the efficiency of the steps of change calls for the selection of such a cultural model where the concept of measurability can also be interpreted properly.

The cultural model suggested by Thomas (Thomas, 2005) assumes the existence of correlations among the eight concepts used in change management: the elements of change and the four fundamental elements of organizational culture as provided in Figure 4.

A scoring system can be worked out for the evaluation of the 8 elements of changes in the organizational culture model. The properties of the 32 correlations shown in *Figure 4* can be measured with tests. From the positive statements describing these correlations a test can be compiled. The responses can be evaluated via the grades of agreement pertaining to the elements of culture and focusing on the positive statements in view of the elements of changes, in a scale of 5 grades. The given responses can be summed up and evaluated towards the direction of the elements of changes. As a consequence, the tests to be compiled should minimally consist of 32 questions or the multiple of 32 questions.

| Eight Elements Of Change | Four Elements of Culture | | | |
|---|---|---|---|---|
| | Values | Role Models | Rites & Rituals | Cultural Infrastructure |
| Leadership | M | M | M | m |
| Work Process | M | M | M | m |
| Structure | M | m | M | m |
| Group Learning | M | M | m | m |
| Technology | M | M | M | m |
| Communication | M | M | M | M |
| Interrelationships | M | M | m | M |
| Reward | M | M | m | m |
| M - Major Interaction | | m - minor interaction | | |

*Figure 4: Correlations of the organizational culture and the elements of changes (Thomas, 2005)*

With respect to the foregoing, such a questionnaire of 32 questions has been worked out that is suitable for testing our status and progress in the structuring of a reliability-centered maintenance culture. The test is based on the 8 pillars of the change of culture, in view of the four elements of culture. The responses and thus the extent of satisfaction reflect positive trends. In this case, the evaluation can be interpreted in a scale of 20 points in relation to each element of change.

The questionnaires can be processed, and the changes can be evaluated with the use of ordinary web or column charts. The direction of changes indicates our further orientation that we should take in our work of culture building.

As an example, below the statements from the questionnaire concerning structural issues are provided.

31. It is clear for everyone that reliability and maintenance affect the entire operation of the company.

32. The necessary structural changes always influence maintenance management.

33. The structure of the company (hierarchical order) corresponds to the regular activities determined by the work processes of maintenance.

34. The company's management system minimizes the effects caused by whispering and corridor information exchange.

Figure 5 presents a situation assessment made in relation to a real maintenance workshop and shows the average changes of the reliability culture based the answers of 3 managers and 9 workers.
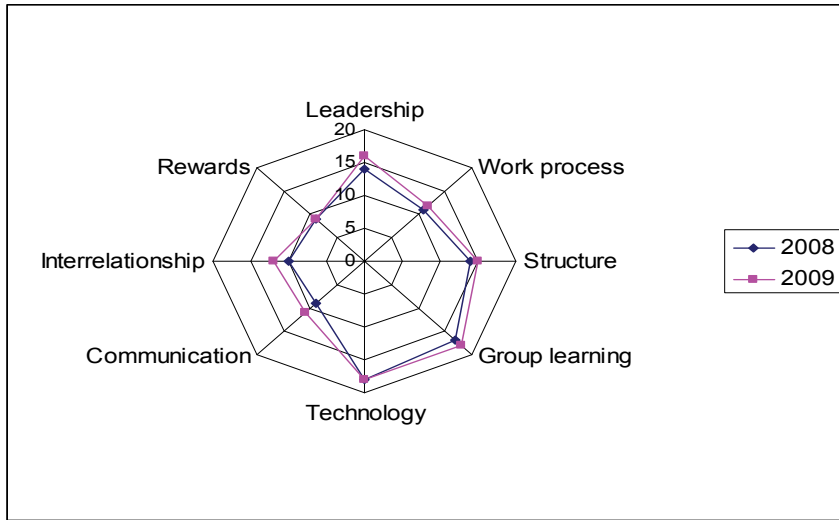
*Figure 5: Evaluation of the changes of organizational culture in a web chart*

## 4. Conclusion

An important and brand new element of the maintenance organization model is the maintenance reliability culture structuring module (Figure 6) that relies on the results of the questionnaire-based assessment (culture test), and thus provides for a framework of continuous development and the secure sustainment of the achievements made. It calls for a novel approach, and is incorporated into all the organizational processes represented by information and managerial chains, relations. We have tested this method in 10 printing companies. The used it with success to test and improve their reliability culture.
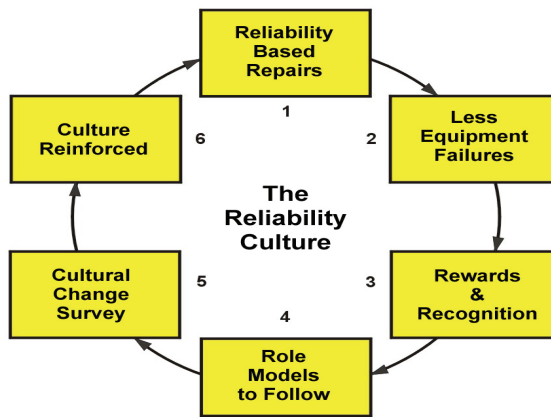


*Figure 6: Model for the improvement of the maintenance culture at the printing businesses*

## References

Hair, T. (2002): Improving Maintenance through operators, PIRA International Conference Proceedings, Best Practice Maintenance, Manchester

Horvath, Cs. - Gaal, Z. - Kerekes, K. (2009) : Extended model for modern printing machines

IARIGAI, Advances in Printing and media Technology, Vol. XXXV. p.129-136

Thomas S. T. (2005): Improving Maintenance Reliability Through Cultural Change, Industrial Press, NY, p. 356

**4**

*Innovative use of printing*

# Screen printing of thin, flexible primary and secondary batteries

*Michael Wendler*[1]*, Gunter Hübner*[1]*, Martin Krebs*[2]

[1] Hochschule der Medien (HdM), Institute for Applied Research (IAF)
 Nobelstraße 10, D-70569 Stuttgart, Germany
 E-mails: wendler@hdm-stuttgart.de; huebner@hdm-stuttgart.de

[2] VARTA Microbattery GmbH, R&D
 Daimlerstraße 1, D-73479 Ellwangen, Germany
 E-mail: martin.krebs@varta-microbattery.com

**Abstract**

Printed rechargeable (Nickel/Metal hydride) and non-rechargeable (Zinc/Manganese Dioxide) batteries are produced via screen printing onto a film substrate. First trials were carried out using standard electrode pastes (slurries) as they are used for conventional batteries. Due to the poor print quality characteristics of these pastes the reproducibility of the layers was not satisfying; especially the generated film thickness was very hard to determine. Therefore new, improved electrode pastes had to be developed that are specifically tailor-made for the screen printing process. Finally by using the new electrode pastes a battery cell was printed and successfully tested for the electrochemical performance (cycling) at the VARTA Microbattery GmbH.

**Keywords:** screen printing; printed batteries; thin flexible batteries; NiMH; rechargeable;
 non-rechargeable; electrode pastes

## 1. Introduction

NiMH-batteries (rechargeable) are well known since the 90's as commercial products [1], typically as cells of size AA or AAA. For more than 10 years it is reported of film type batteries. In this area, the Fraunhofer Institute for Electronic Nanosystems has been engaged and announced film and rechargeable batteries for the beginning of the new millennium e.g. for PDAs [2].

Since about 1995 an Israeli company with the same name offers commercially printed batteries so-called "Power Paper", see Figure 1a.

These thin, flexible film battery cells are patented and based on a zinc-manganese-electrolytic-gel chemistry. These batteries are not rechargeable and produce 1.5V voltage. They have a shelf life of about three years, similar to conventional batteries. In July 2009, the Fraunhofer Research Institution for Electronic Nanosystems announced in a press release a screen-printed battery. This printed battery is also based on the zinc-manganese system (Figure 1b).



*a)*                                                    *b)*

*Fig. 1: Thin flexible batteries by*
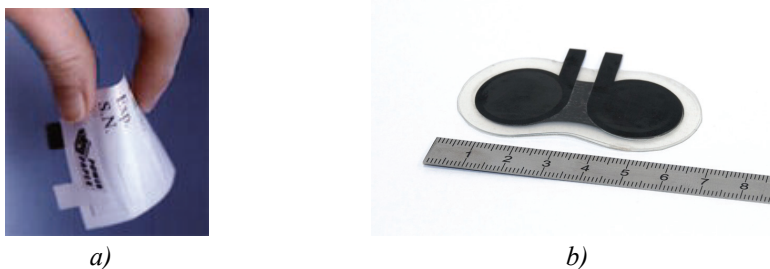*a) Power Paper (www.powerpaper.com) and b) Fraunhofer-Gesellschaft*
*(http://www.fraunhofer.de/presse/presseinformationen/2009/juli/batterien-drucker.jsp)*

All these products are novelties in thin, flexible energy sources, however, none of these products are based on the rechargeable NiMH technology and a commercially available rechargeable application is not yet in the market.

In principle, many electrochemical systems are considerable for printed batteries (Table 1); however, there are major differences in the required process technology. For example, Lithium-based systems are extremely hygroscopic and must be processed in an inert atmosphere making the production equipment rather complex and expensive.

From Table 1 it can be derived that Zinc/Manganese systems are the easiest to be printed but those who employ alkaline electrolyte are not much more complicated to print at room atmosphere as long as the electrolyte handling is mastered.

*Table 1: Possible chemical systems for printed batteries*

| Electrochemical systems | Voltage | Electrochemical reaction | Applicability for printed battery |
|---|---|---|---|
| **non rechargeable** | | | |
| Zinc/Manganese Dioxide | 1,5V | $Zn + 2\ MnO_2 + H_2O \rightarrow ZnO + 2\ MnO(OH)$ | Easy to print, open system |
| Zinc/Air | 1,4V | $2\ Zn + O_2 + 2\ H_2O \rightarrow 2\ Zn(OH)_2$ | Cathode complicated, alkaline |
| Zinc/Silver oxide | 1,5V | $Zn + Ag_2O \rightarrow 2\ Ag + ZnO$ | Alkaline |
| Lithium/ Manganese Dioxide | 3,0V | $Li + MnO_2 \rightarrow MnOOLi$ | Humidity/Water sensitive |
| **rechargeable** | | | |
| Nickel/Metal hydride | 1,2V | $Metal\text{-}H + 2\ NiOOH \rightarrow Metal + 2\ Ni(OH)_2$ | Alkaline |
| Lithium-Ion | 3,7V | $Li_{1-x}Mn_2O_4 + Li_xC_n \rightarrow LiMn_2O_4 + nC$ | Humidity/Water sensitive |

## 2 Methods

The principal structure (Figure 2) of a printed battery differs only marginally from that of a conventional battery.



Legend:
- Carrier foil
- Current collector
- Anode
- Cathode
- Separator

In case of NiMH Cell
- Current Collectors: Carbon Black / Silver
- Anode: printed MH-Paste
- Cathode: printed NiOOH-Paste
- Separator: Fleece soaked in causted potash solution (25%)
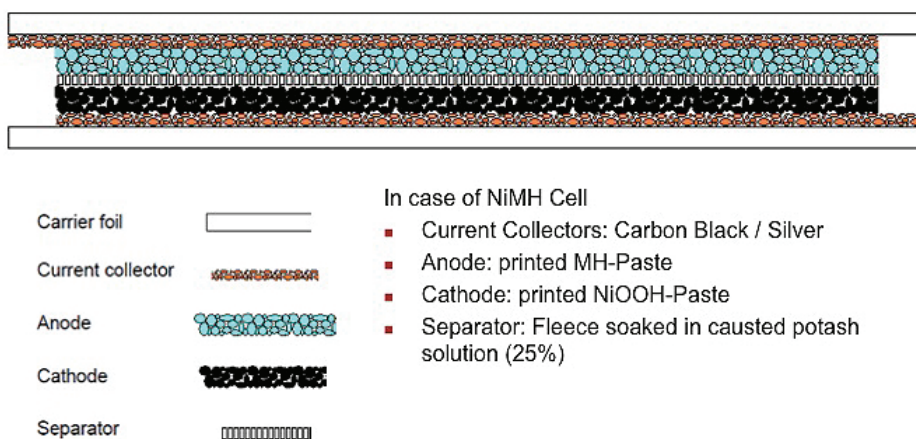
*Fig. 2: Basic printed battery cell concept*

For printed batteries two basic design concepts exist, the stack-type and the co-planar-type that both will be considered here. The differences of the design influence their performance as well as their complexity in manufacturing.

The cells in the stack-type design (see Figure 3) have lower internal resistance, and therefore allow lower charging times. They are able to deliver higher peak currents in a short period of time than the cells of the co-planar type design. Stack type cells have a higher capacity at the same dimensions, because they comprise of

about twice the amount of active electrode material on the same base area. These cells could therefore be used for "demanding" applications. A major disadvantage of the stack concept, however, is the need to bring a separator in between the two electrodes in order to protect the cell against an electrical short circuit.

This additional separator is quite a bit in contradiction to the demand for the low cost production principle of printed batteries. In conventional batteries the separator often is a piece of fleece material typically soaked with electrolyte. Considering an in-line production process the inlaying of the classical separator fleece would be a rather difficult step and maybe would have to be done off-line before the encapsulation.
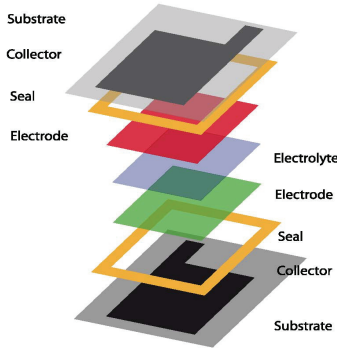


*Fig. 3: Battery design concept in stack-type*

The decisive advantage of the co-planar cell concept (see Figure 4) is that no separator is needed in the cell since the electrodes are located side by side on the same layer. Further reduction of the manufacturing costs in comparison to the stack-type is achieved because at the same lateral dimensions of the cell only about 50% of the collector material is needed.

However, the internal resistance of a co-planar cell is significantly higher, because the ion flux is primarily within the small gap region and rather slowly spreads over the whole electrode surface unlike the stacked cell, where the ion flux is distributed evenly over the entire electrode surface. The capacity is lower, since for the same size only about half of the electrode material is incorporated in the cell.
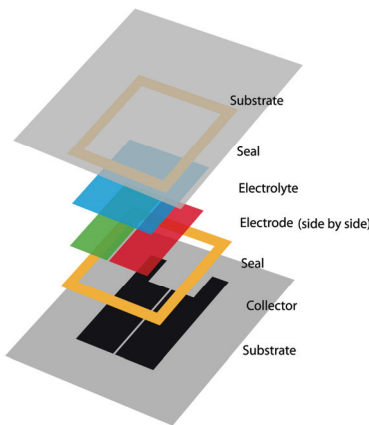


*Fig. 4: Battery concept in co-planar-type*

The core elements of the printed batteries are the electrode pastes, which are crucial for the electrochemical function of the cell. For example the detailed chemical processes of a NiMH battery during discharge, are described in the following formulae:

The metal hydride (anode) emits an electron (it gets oxidized):

$$MH + OH^- \rightarrow M° + H_2O + e^- \qquad\qquad -0,83V \qquad\qquad (1a)$$

The Nickeloxyhydroxide (cathode) receives the electron (it gets reduced):

$$NiO(OH) + H_2O + e^- \rightarrow Ni(OH)_2 + OH^- \qquad\qquad +0,52V \qquad\qquad (1b)$$

The overall reaction during discharge:

$$MH + NiO(OH) \rightarrow M° + Ni(OH)_2 \qquad\qquad 1,35 \text{ V (idle voltage) [4]} \qquad\qquad (1c)$$

In the charged state Nickeloxyhydroxide is the active material of the cathode and hydrogen is bound in a metal hydride, the active material of the anode. The metal alloy of the anode is responsible for that during the charging and discharging reaction. A reversible hydrogen absorption/desorption reaction takes place [3].

In the beginning of our research on printed NiMH batteries, standard electrode pastes (slurries) were provided by the VARTA Micro Battery GmbH. These pastes are composed of the following substances:

- Cathode-paste:
  - Nickeldihydroxide
  - Nickel-metal powder
  - Cobalt oxide
  - Cobalt metal powder
  - Binder
  - Water
  - Potassium hydroxide

- Anode-paste:
  - Mixed metal-nickel alloy
  - Binder
  - Water
  - Potassium hydroxide

The main components of these pastes are the Nickeldihydroxide particles (50-70% by weight) and the mixed metal-nickel alloy (50-80 wt%) respectively accompanied by water and binder. The pastes have a rather high particle volume concentration. The electrode pastes as provided by VARTA were used for filling up the metal housings of the conventional battery cells are not optimized for the screen printing process, at all.

Initial print trials of these electrode pastes without any modification did not provide satisfactory print results. As shown in Figure 5a) the anode paste tends to a pronounced unevenness and inhomogeneity. This phenomenon can be attributed to the unsuitable binder system. A similar problem occurs in the cathode paste (Figure 5b). However, here the influence of the inadequate binder system can be observed by an adhesive/cohesive failure in the printed electrode layer.



*a)*       *b)*
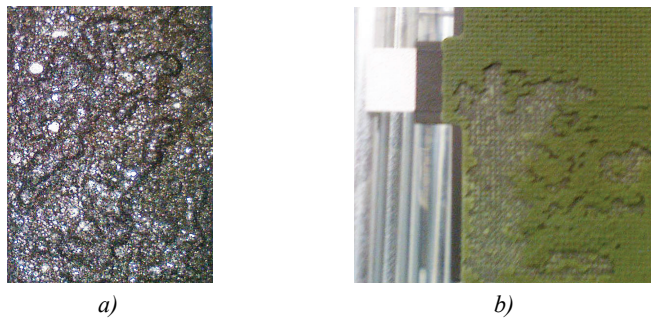
*Fig. 5: Electrode pastes - a) anode, b) cathode*

Relatively homogeneous layers can be realized by printing the electrodes several times on top of each other with intermediate drying, see figure 6.



*Fig. 6: Electrode layers printed several times with intermediate drying*
*cathode (left) and anode (right)*

To prove the feasibility of these pastes a battery cell was printed in accordance with the schematic layout shown in Figure 3. In Figure 7 the first prototype of a completely assembled cell is shown. That was done in 2006 as a feasibility study during a diploma thesis [5]. The separator was a fleece soaked in potassium hydroxide (25%). Figures 8 and 9 show the electrical performance measurements of this first prototype cell.

These measurements proved the concept that the secondary battery cell could be manufactured by screen printing technology. As the substrate PET had been used to see the inside of the cell. Today, during the research project the PET has been replaced by composite foils in order to improve the leak tightness and having a "nicer" look.



*Fig. 7: The first prototype of secondary cell (in PET) [5]*

Some sample results for testing the electrical performance of the first prototypes of the secondary batteries are shown in Figures 8a) and b).



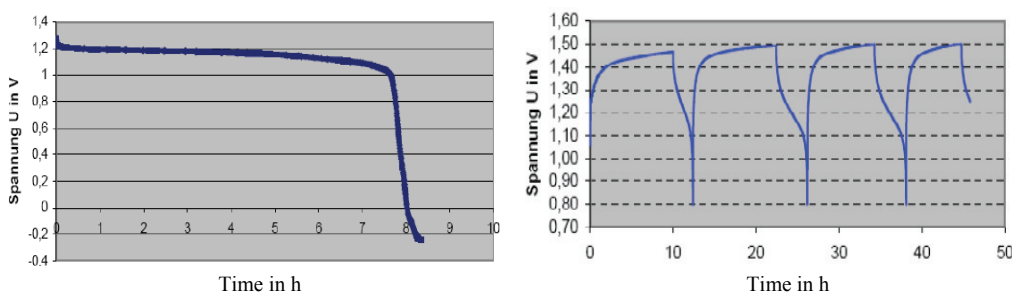*Fig. 8: a) discharging curve of the first prototype of a printed NiMH cell [5]*
*b) Charging and discharging curve (cycling) of a printed NiMH-cell. [5]*

The specific capacity of the positive electrode paste used in this prototype and in further investigations was reported by the provider VARTA with 253mAh/g, the negative electrode paste has a capacity of 276mAh/g. When a battery cell gets overloaded during the charging process then at the positive electrode hydrogen is generated, which must be bound by the negative electrode. Therefore, the negative electrode should have a higher capacity by about 10% over the positive electrode. Fortunately this would be achieved with a mass ratio of the two pastes of approximately 1:1. The dry density of the negative electrode paste is 6.74g/cm³ whereas the density of the positive electrode paste is 2.85g/cm³. Since the density of the negative electrode paste is higher by the factor of 2.27 and, based on the capacity consideration above, the mass of both electrode layers should approximately equal each other the thickness of the positive electrode layer should be 2.27 times greater than the thickness of the negative electrode layer [5].

Due to the poor print quality characteristics of these pastes the reproducibility of the layers was too low; especially the generated film thickness was very hard to determine (see Figure 9). Therefore electrode pastes had to be developed that are specifically tailored for the screen printing process.

While improving the printing properties it was tried simultaneously to achieve a capacity compensation of both electrodes by mixing the same mass of anode and cathode material with the appropriate amount of binder. This helps to ease the screen printing process.

One of the most important criteria in selecting an appropriate binding agent is the alkali resistance because in NiMH batteries potassium hydroxide is used as the electrolyte.

To find the appropriate binder a large set of experiments were carried out using the "one-factor-per-time" method. To a predefined volume of solvent a binder is added gradually to reach the optimum in viscosity of the varnish. After that not the slurry but dry pigments of Nickeldihydroxide (for the anode) and mixed metal-nickel alloy (for the cathode) were stirred into to the varnish resulting in the functional electrode paste. In the print experiments carried out with quite a lot of such varnish/pigment compositions during a bachelor thesis [6] several solvents were tried. It turned out that three combinations of materials showed promising results

and from them the solvent with the lowest volatility turned out to be the best. The criteria for the choice were the layer evenness and the printability. The significant increase in print quality can be observed by comparing the figures 9 and 10 (here the anode paste is shown).



*Fig. 9: poor print quality of
the first pastes*

*Fig. 10: improved pastes developed
for screen-printing*

Using the optimized electrode pastes a battery cell analogue to the prototype shown in fig. 7 was printed in stacked style (Figure 11) and tested for the electrochemical performance (cycled) at VARTA Microbattery GmbH. Instead of PET in this cell a barrier film substrate was used as substrate. Using these substrates with very low migration properties the lifetime of this cell can be increased significantly. The cell must be sealed on one hand against $CO_2$ that could migrate into the cell and influence the chemistry and on the other hand against drying which means that during the whole lifetime the electrolyte must be kept humid.



*Fig. 11: Battery concept in stacked-type*

In Table 2, the theoretical electro chemical capacities of the printed electrodes are shown. By multiplying the electrode weight by the specific capacity the theoretical capacity (last column in the table) of the cell can be estimated.

*Table 2: Theoretical capacity of the printed electrodes*

| Electrode | Layer thickness in µm | Electrode weight in g | Specific capacity Cspez | Theoretical capacity Cth |
|-----------|----------------------|----------------------|------------------------|--------------------------|
| cathode | 120 | 0,130 | 253 mAh/g | 33 mA/h |
| anode | 128 | 0,137 | 275 mAh/g | 38 mA/h |

The Figures 12 and 13 show the results of the battery cycling (using the cell from fig. 11 with the properties of table 2) over 70 cycles (charge / discharge) for in sum 2300 hours, in which the first 25 cycles were carried out at a charge current of 500µA. Since the cell has a much higher capacity than expected in the first moment, the charge current was increased from 500µA to 2mA starting with the 25th cycle. As shown in figure 12, the cell provides from the 27th cycle a constant capacity of about 31mAh, this is very close to the theoretical capacity of the electrode layers (table 2).

As the work on the electrode pastes turned out to deliver excellent results for the secondary battery, why not adapting it to primary cells just by changing the electrochemically active material? For this purpose, the cathode material for secondary battery NiO(OH) was replaced by Manganese Dioxide ($MnO_2$) and the anode material by Zinc (Zn). With these "primary pastes" non rechargeable batteries analogue to the cell design of figure 3 (stack type) were printed. For this chemical system the voltage of a single cell is about 1.5V. This primary battery cell does not need to be charged, i.e. these cells are immediately ready to use after activation with the electrolyte (zinc chloride). Because of the immediate activation this electrochemical system is ideal for testing new cell concepts, e.g. to test series circuits. The basic layout is shown in fig.14.
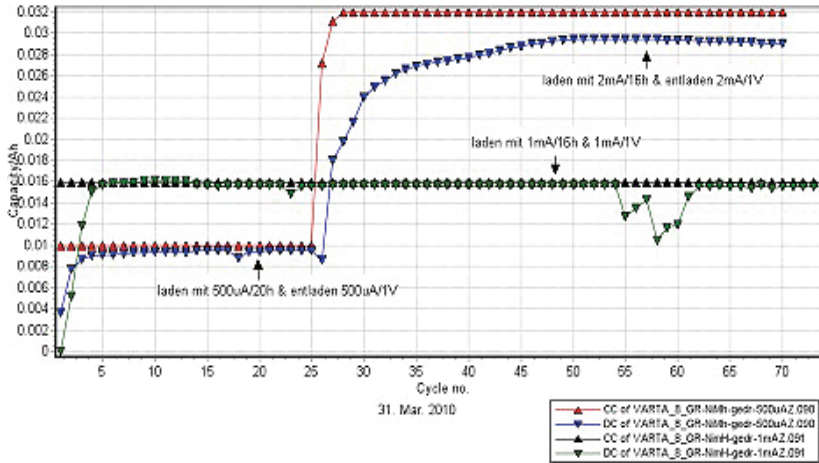
*Fig. 12: Battery capacity during the cyclization*



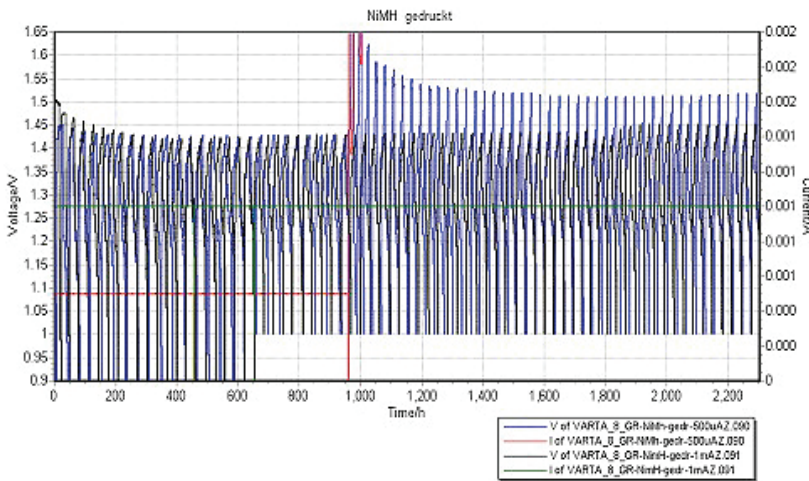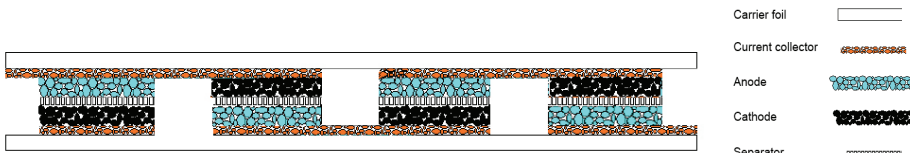*Fig. 13: Voltage during cyclization*



*Fig. 14: Series connection of printed battery cells*

To ease the printing process the collectors and electrodes are printed on a flat sheet of substrate and after adding the electrolyte/separator the cell is completed by flapping on half on top of the other half as indicated in Figure 15.
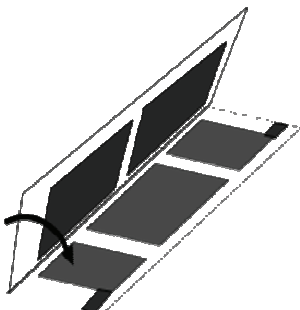


*Fig. 15: finishing of the series connection of printed battery cells*

For a functional test, a series circuit of five cells, corresponding to a cell voltage of 7.5V, was printed according to the technique shown in Figure 16. The final cell is depicted in Figure 16. To visualize the function of this cell with a practical example a screen printed electroluminescent lamp was driven with the printed battery. To drive such an electroluminescent lamp an inverter is needed which converts the current (DC) from a battery into alternating current (AC). The specifications of the inverter used are listed in Table 3.



Fig. 16: Five printed zinc-manganese dioxide cells in series connection

Table 3: EL-Inverter specifications

| Type | Input Voltage (V) | Input Current (mA) | Output Voltage (V) | Output Frequency (Hz) | Drive Area (cm$^2$) |
|------|-------------------|--------------------|--------------------|-----------------------|---------------------|
| WE5-50 | 5 VDC | 50 | Ca. 60 | 600 | 30-105 |

As can be seen from the table 3 the required 50mA current is demanding and therefore a challenge for the battery. To our great pleasure it was possible to operate the electroluminescent lamp with the printed battery (see Figure 17).
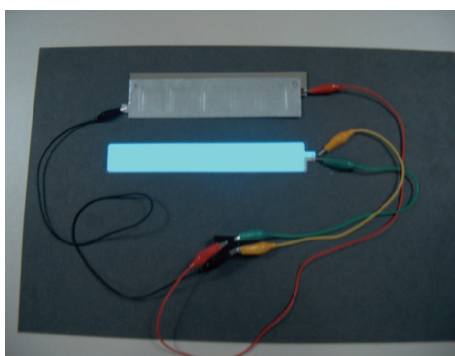


Fig. 17: Printed electroluminescent lamp powered with a printed battery

As mentioned above one of the great challenges of the manufacturing technique of printed batteries is the leak tightness. Especially the sealing of the collector lead-throughs is very problematic. As shown in Figure 18 this problem could be solved by printing a sealing layer around the collectors and electrodes. The sealing layer is a polymer that can be activated by heat application. The cell is finalized after filling in the electrolyte/separator by flapping one side on top of the other and then apply heat to the sealing. The principle of this process is shown in Figure 19.
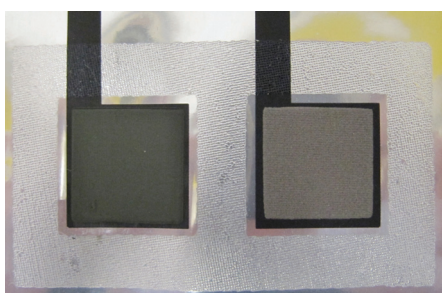


Fig. 18: Sealing printed around the collectors and electrodes
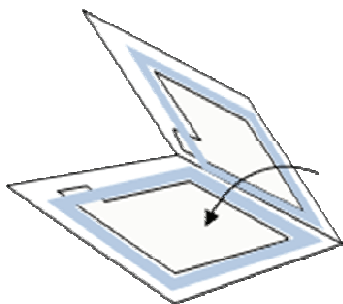
*Fig. 19: Finishing the cell*

One of the major problems in manufacturing thin flexible printed batteries is the handling of the electrolyte/separator. As mentioned above in conventional battery manufacturing the separator is a fleece material soaked in electrolyte and then placed onto the electrodes. For manufacturing the batteries using printing processes, solely, a printable electrolyte/separator layer (for stack type) or printable electrolyte (for co-planar) type is extremely desirable. In a large scale experiment setup a numerous combination of thickening agents and other additives was tested to bring the 25% caustic potash into printable form without influencing the electro chemical properties. After numerous trials we succeeded in finding a formula which works quite well. A patent is applied for that.

## 3. Discussion

The printing process for manufacturing thin and flexible battery cells offers great advantages in the easiness and flexibility of the design and layout. The batteries can for instance be combined with any smart object, display or sensor that needs power supply. It can be thought of printing such devices onto the same substrate. It could also be thought of manufacturing the batteries as self adhesive labels or stickers to connect them to the devices requiring the power supply. Interconnections with photovoltaic applications for storage purposes are very promising. With all these possible applications this technique offers great opportunities and future markets.

However, there are still some challenges. First of all the selling prices: to open up a mass market for printed batteries the prices should not exceed some few cents. In order to achieve that purpose fully integrated in-line manufacturing processes are needed. Our next step in the project therefore is to design such a manufacturing process. For this process some of the drying steps needed in-between the printing units require special considerations.

Other topics that need to be investigated in the next future are the possibility of intermediate storing the primary cells without electrolyte. Can they be finalized and activated by adding the electrolyte some weeks or months after printing? Other topics of the project are long-term tests and investigations about the shelf life time.

## 4. Conclusions

In a feasibility study during a diploma thesis it could be shown that printing thin, flexible NiMH-batteries is possible. Starting from that point VARTA Microbatteries GmbH, etifix GmbH and the Hochschule der Medien (HdM) initiated a research project that is funded by the FHProFunt programme of the German ministry for education and research.

During that research project the printing processes and the pastes have been improved to a great extent. New electrode pastes adapted to the screen printing process were developed. To test the functionality of the electrode pastes NiMH batteries were printed and electrical tested by the VARTA Microbatteries GmbH. The results of the electrical tests show that the cells perform well and can be cycled at least 100 times and more.

A printing paste could be developed that enables us to apply the electrolyte separator combination in the screen printing process, also. This allows the manufacturing of a 100% printed stack-type battery.

The printing technology offers a wide range of new possibilities for the production of energy storage in the form of printed thin and flexible batteries.

**References**

[1] Kiehne, Heinz Albert (5 Aufl. 2003): Batterien Grundlagen und Theorie, aktueller technischer Stand und Entwicklungstendenzen, Expert Verlag, Renningen, ISBN 3-8169-2275-9

[2] Dietmar Müller, Wiederaufladbare Folienbatterien für PDAs http://www.zdnet.de/news/hardware 0,39023109,2096794,00.htm

[3] David Linden. Handbook of batteries. McGraw-Hill handbooks. McGraw-Hill, New York, 2nd ed. edition, 1995.

[4] Horst Bannwarth. Basiswissen Physik, Chemie und Biochemie: Vom Atom bis zur Atmung für Biologen, Mediziner und Pharmazeuten. Springer-Verlag Berlin Heidelberg, Berlin, Heidelberg, 2007. In: Springer-Online http://dx.doi.org/10.1007/978-3-540-71239-8 Letzter Zugriff am 08.08.2009.

[5] Vindus, Boris "Feasibility Studie zum Drucken von NiMH-Akkumulatoren" Diplomarbeit im Studiengang Druck- und Medientechnologie der HdM Stuttgart 10/2006

[6] Rico, Hagedorn "Optimierung einer im Siebdruck hergestellten elektrochemischen Zelle" Bachelor Thesis im Studiengang Druck- und Medientechnologie der HdM Stuttgart 08/2009

# Fabrication of a printed alkaline battery using a new method for manganese dioxide cathode ink preparation

*Andrew Henry, Scott Williams*

School of Print Media
Rochester Institute of Technology
Rochester, New York, 14623, USA

E- mail: sawppr@rit.edu

**Abstract**

We have developed a new cathode ink formulation for the fabrication of a primary $MnO_2$- Zn alkaline battery power source on paper using flexography. Our long-term research objective is to establish a print-centric fabrication protocol that would be leveraged to explore new materials for power source production. In this paper, we report a novel approach that involves the in situ synthesis of the manganese oxide cathode.

Our approach would provide a production advantage over the current industry practice of dispersing an expensive electronics-grade manganese oxide pigment in a vehicle. We also have developed ink that incorporated nanoparticle zinc metal in a printable vehicle system. Our paper-based battery, printed with the new cathode ink system, delivered a favorable discharge capacity relative to an existing alkaline battery, but several challenges were realized. A discussion about our battery performance and future developmental pathways is provided.

**Keywords:** printed electronics; alkaline battery; flexography; manganese oxide; zinc metal; anode; cathode; electrolyte; primary battery

## 1. Introduction

One of the current limitations that constrain electronic device miniaturization is the size of the power source. Significant research and developmental effort is currently directed into making a portable battery both small and lightweight. A miniaturized battery, however, must still deliver the load currents required by the device and retain sufficient long-term charge capacity. That is, battery miniaturization will necessarily be limited by the mass of active electrochemical materials - cathode, anode and electrolyte. Developing a battery that conforms to the electronic packaging shell provides a useful path in overcoming weight and size limitations. The packaging shell could be a plastic case such as a cell phone, but also can be fabric or paper for such applications as active RFID. Battery development methodologies that allow for low cost web printing of fabric, plastics and paper electronic technologies are the focus of our current research.

Polaroid [Land, 1978] and Sharp [Oogita et al., 1988] Corporations lead early development of thin planar battery technologies that were coated onto plastic or paper supports. With recent advances in low cost and portable electronics produced using the printing method, new life has been breathed into thin-film battery research. Paper-based batteries have been developed by either printing on paper using a plurality of printing methods [Ghiurcan et al., 2003, Hilder et al., 2009, Huang et al., 2008, Kim et al., Nystrom et al., 2009, Park, et al., 2007, Southee et al., 2007, Tam et al., 2007, Zhao, et al., 2006], or incorporating electrochemical compositions, such as carbon nanotubes, into the cellulose fiber structure [Kiebel and Gruner, 2007, Landi, et al., 2009, Liu et al., 2009, Ollinger et al., 2006].

When the battery was produced using the printing method, printable inks were formulated using existing electrochemical materials such as zinc powder or manganese dioxide. Such electrochemical ink formulations were either highly viscous preparations that required screen or lithographic printing, or are advanced synthetic technologies that might be cost prohibitive when scaling up for large volume production.

Our approach focuses on the synthesis of battery component materials during the ink formulation or printing application stage thereby eliminating the need to develop complex pigment dispersing methodologies. In this paper, we report results for in situ manganese dioxide pigment synthesis from a water-soluble manganese permanganate starting material. Our simplifying ink formulation strategies may one day lend themselves to producing a high capacity thin film battery using conventional web printing techniques, such as flexography.

## 2. Methods

### 2.1 Cathode ink formulation

Manganese oxide ($MnO_2$, abbrev. MnO) was synthesized in situ by combining a two-part (A and B) solution preparation under vigorous stirring.

### 2.1.1 Part A Solution

Part A solution was prepared by dispersing five percent carbon (Cabot Vulcan XC72R) in water with one percent Zetasperse 2300 (Air Products) as a dispersing aid. Then, 0.028 moles of potassium permanganate (Fisher) were dissolved into the carbon dispersion.

### 2.1.2 Part B Solution

Part B Solution was prepared by dissolving 0.11 moles of potassium hydroxide (Sigma) into 20 milliliters of 10% carboxymethyl cellulose (CMC, 250,000 MW, Sigma) aqueous solution. Ten percent polypropylene glycol (PPG, Sigma) was added to this solution as both a humectant and viscosity modifier.

### 2.1.3 MnO synthesis

MnO was synthesized in situ by the slow addition of Part B to A under vigorous stirring for 30 minutes.

### 2.2 Anode ink paste formulation

Nano-particle zinc metal-carbon paste was prepared by mixing zinc and carbon powders in a 12:1 (w/w) ratio in five milliliters of polyethylene glycol (PEG, 400 MW, Aldrich).

### 2.3 Potassium hydroxide electrolyte

A six (6) molar potassium hydroxide electrolyte solution was prepared by mixing the salt into 40 ml of a five percent CMC solution that contains 10% PPG.

### 2.4 Battery fabrication

### 2.4.1 Terminals

Aluminum foil (Aldrich), copper foil (Aldrich), printed colloidal silver on a separate piece of paper (silver paper strips) and silver colloidal pastes and epoxies (Electron Microscopy Sciences), that was directly coated onto the battery paper support, were conductive materials tested for functional compatibility as the battery terminals. When a colloidal silver composition was used, these were applied to the paper and overprinted with either the cathode or anode ink.

### 2.4.1 Cathode ink

The cathode ink was printed on an IGT Reprotest Flexography Printability Tester (Model F1, Serial 432.B.033) located in the Printing Applications Laboratory at RIT. Dupont Cyrel photopolymer plates were imaged and processed through a DuPont Cyrel 3002i continuous flow plate processor provided by Adflex Corporation (Rochester, NY). An image of the file is illustrated in Figure 1. A #12 metering rod was selected when thicker ink films were required. We also modified a Little Joe lithographic proofing press to simulate a rotary screen printing process by mounting a nylon screen onto the plate section that inked our flexographic plate mounted on the blanket section of the proofing press. The paper substrate was fixed at the normal paper print section of the proofer.



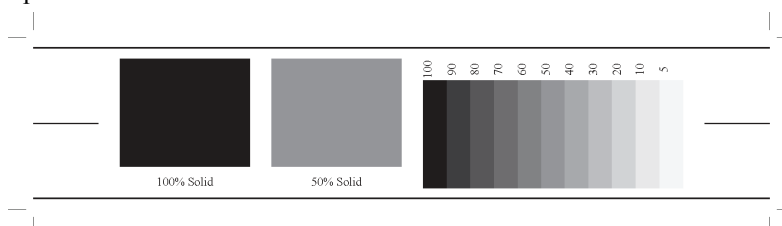*Figure 1: IGT Dupont Cyrel plate for ink print testing*

### 2.4.2 Electrolytic ink

Whatman #31 filter paper was used as an electrolytic separator for the battery. The filter paper was allowed to soak in the electrolyte until the battery was ready for final assembly. This filter paper separator was removed from the electrolyte solution, blot dried, and then applied over the anode and cathode printed patch.

### 2.4.3 Anode ink

The anode ink was printed using the same modified Little Joe in the "rotary screen" configuration.

### 2.4.4 Battery assembly

After the silver leads, anode and cathode patches are printed, the electrolyte-saturated filter paper was sandwiched between two pieces of printed patches. The battery was then sealed using 3M packaging tape to simulate lamination applied on a flexographic press.  Figure 2 illustrates the battery design that resembled a flat pouch design.
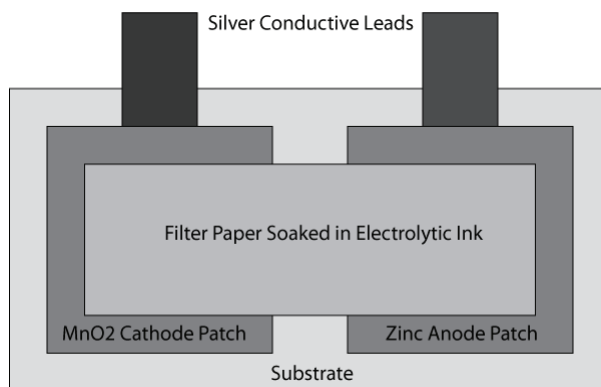


*Figure 2: Battery schematic*

## 2.5 Battery characterization

Open circuit voltage values were obtained using a standard electronics (VOM) multimeter.  Load and discharge capacity were measured with an Optim Engineering CBA III Computerized Battery Analyzer.  The discharge current was set to 0.25A. Theoretical battery capacity was calculated by multiplying the electrode mass with the electrochemical equivalence values for MnO (0.279 Ah/g) and zinc (0.821 Ah/g) electrodes. Discharge versus time profiles were measured using the Optim system.

## 3. Results

## 3.1 Cathode ink formulation

Our long-term research goal is to learn how we can modify electrochemical formulations to make them press-ready, while at the same time maintaining their functional role. In an alkaline battery, both electrodes are applied as thick pastes usually applied using coating or screen printing processes. The MnO cathode, for example, would typically be prepared by dispersing manganese dioxide pigment into a high viscosity paste comprising conductive carbon, an alkaline electrolyte such as potassium hydroxide, and aqueous binder such as carboxymethyl cellulose (CMC). When we attempted to prepare the same formulation with higher water content, and thus a lower viscosity, we found the MnO pigment dispersion to be unstable and prone to rapid flocculation.

Upon considering both the ink vehicle system and the paper support that the formula would be printed onto, we noticed one important common chemical property - most of the vehicle components (carbon and CMC in the presence of base) and paper could be reducing agents relative to potassium permanganate [Ladbury and Cullins, 1958]. We, therefore, decided to synthesize the MnO in situ with potassium or sodium permanganate as the starting material. Chemical tests indicated a high yield of MnO production although at the time of this manuscript submission the chemical characterization was still ongoing.

## 3.2 Cathode ink rheology and printing characteristics

As shown in Figure 3, we produced press-ready flexographic MnO cathode ink with the proper rheological properties.  The shear thinning rheology for our cathode ink settled to an optimum value of about 150 cP at 100 rpm (Brookfield, #1 Spindle). Good overall print quality, defined printed halftone dots, and excellent tape adhesion to uncoated paper was also found (Figure 3 Inset) over the 5 - 100% gradient range tested.  The dried electrode ink film weight ranged from about 0.5 grams when printed off a flexographic plate to over a gram when coated with a #12 metering rod.
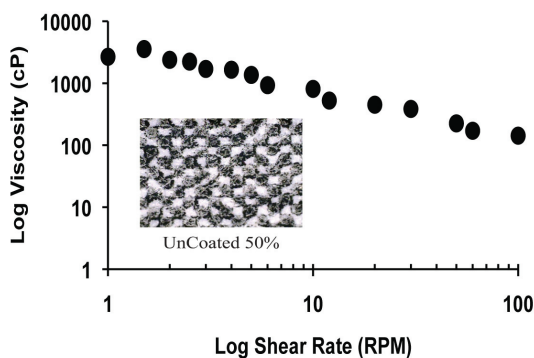
*Figure 3*
*Cathode ink rheology and printed image (50% Tint) from*
*an IGT Proofer. Viscosity was measured by varying the*
*spindle speed (RPM) using a Brookfield DV-I*
*Viscometer and #1 Spindle*

### 3.3 Anode ink formulation and printing

The selected zinc anode formulation was made using a typical formulation used in the electronics industry as described in Methods with only slight modifications. The zinc anode ink had a thick, paste ink, consistency that coated out well using a #12 metering rod. The anode ink also printed well onto paper when using our rotary screen proofer. Modifying the anode ink to be press-ready for flexography will be the subject of future research.

### 3.4 Electrolyte separator

The electrolyte separator was prepared by saturating the selected paper-based material in the alkaline electrolyte solution. Moisture was maintained by the incorporation of humectants and sealing the battery in packaging tape. Developing a printable separator will be the subject of future research.

### 3.5 Battery assembly and testing

Our assembled battery, regardless of terminals used, produced open circuit voltages (no load) of between 1.2-1.4 V. We did notice that the open voltage did oscillate with hand pressure applied to our flat pouch design with a separate foil or silver paper strip as opposed to directly coated silver terminals.  Such variation was expected given the importance of intimate contact between the active surfaces within a battery.  Any gap between the terminal, electrolyte separator and/or either electrode would result in the artificial introduction of an internal resistance created by poor electrical contact. Battery performance analysis, therefore, required that the pouch be placed under moderate pressure by sandwiching the battery between two pieces of wood block tightened with C-clamps.
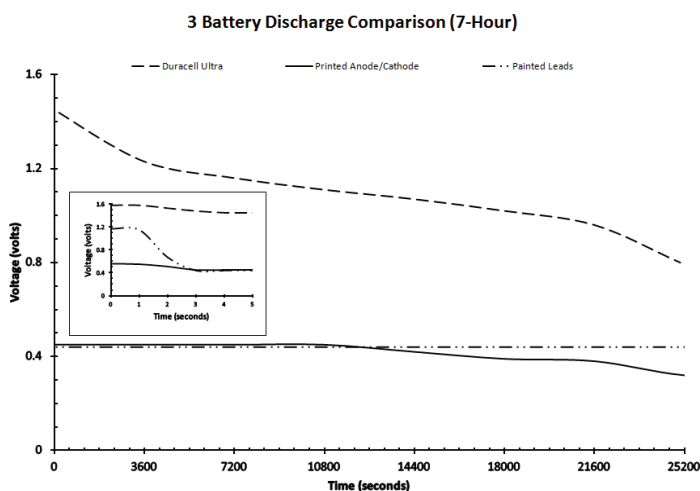


*Figure 4: Battery discharge comparison test under 250mA load. (Inset) Amplification of the first five (5)*
*seconds illustrating the IR drop region of the discharge profile*

Figure 4 illustrates the battery performance characteristics for our printed battery with both silver paper strip and coated ("painted") terminals, compared to a Duracell Ultra AA (1.5V) alkaline battery. Under a moderate discharge rate for an alkaline battery (250 mA or 0.25 A), the Duracell battery performed with a seven hour service life (discharge to 0.8 V) or a discharge rating of 1.75 Ah, a typical value for a AA battery.

With our printed battery, however, a significant IR drop (a voltage (E=I*R) drop that occurs do to do the onset of internal resistance within an electrochemical cell) was observed most likely from the rapid onset of polarization effects. The IR drop was greater when the separate silver paper strip terminal was used as opposed to a coated terminal that was in direct contact with the electrode film and allows little ability for the terminal to separate from the anode or cathode. As might be expected from the lower output voltage under load, the discharge capacity for the printed battery ranged from 4.71 Ah, for a battery with coated terminals, to over 10 Ah for a battery built using the silver paper strip terminals.

## 4. Discussion

We have demonstrated that a new design path towards the development of a printable alkaline battery is possible by modifying a typically high viscosity MnO paste composition, currently used in the industry, with a "cathode ink" formulation that has press-ready rheologies suitable for the higher speed printing techniques such as flexography. Our in situ synthesis protocol for MnO has been found to produce the cathode electrode in high yield as evidenced by chemical analysis and open voltage potentials approaching the theoretical maximum of 1.5V for the alkaline MnO-Zn battery system. The result, however, that our printed battery open voltage did not rise to the 1.5V level is the subject of ongoing research. The MnO purity and crystalline form are key factors in being able to obtain the open voltage or equilibrium result predicted by the Nernst equation for our system. Now that we are confident in our ability to synthesize MnO coincident with the ink formulation step, and thereby producing a more stabilized ink dispersion than if we tried to suspend a commercially produced MnO pigment, we can now turn our attention to the chemical factors that control MnO purity, yield and crystalline type. By moving beyond just the cathode material chemical study to the performance of the full alkaline battery system, however, the future challenges became apparent.

Our printed battery demonstrated well-established factors that increase internal resistance require special attention. As shown in Figure 4, a significant IR drop was observed with our printed batteries within seconds of applying a modest 250 mA load. We realize that our applied load was high for paper-based designs, but we chose to push the comparison relative to a standard alkaline cell. Polarization effects likely caused the IR drop. A Nernst calculation for the MnO-Zn system would predict a theoretical voltage of 1.5V. This voltage represents the equilibrium value, or a value under no load - the open circuit voltage. Once a battery is placed under a load, the electrochemical system is driven out of equilibrium by the applied current. If the system is not able to respond to this deviation from equilibrium, the battery becomes polarized due to the immediate electrical (as opposed to mechanical) creation of internal resistance (hence, the "IR drop"). The Duracell battery is designed to minimize polarization effects through intimate contact between the electrodes, the electrolyte separator, and the terminals through mechanical pressure in the winding and canning process. That is, if mechanical and chemical efficiencies are maximized, the overall effectiveness and capacity of the battery is maximized. Compared to our findings, however, such as variation in open voltage potential with applied pressure, polarization that might result from issues surrounding our non-optimized paper electrolyte separator, and the selection of the terminal design, all suggest that we have not optimized many key parameters in developing a useful printed battery- all issues directed to future research.

We suspect that our current design promote mechanical barriers that create internal resistance within the printed battery. Clearly, we do not have efficient contact between the electrode-terminal and electrode-separator interfaces. The corrosive nature of the alkaline chemistry is less of a concern since our printed battery capacity and efficiency issues occurred immediately when placed under a service load, a much shorter time than required for efficiency loss due to such mass transport effects as corrosion. We likewise suspect that dynamic, or load induced, increases in internal resistance are created by the arbitrary filter paper selection as a battery separator. Battery separator properties are oft overlooked, but are key to the battery performance quality. Filter paper is simply too thick and possess an inhomogeneous porous structure to be an efficient choice.

## 5. Conclusions

The developmental pathways to a functional and useful printed alkaline battery are clearly advanced through our findings. We can translate an electrochemically active composition that is unsuitable for high speed printing to a formulation that is both printable and press-ready, with apparently comparable discharge capacity. Given the caveats already discussed, our printed batteries consistently performed for many hours

longer than a typical AA alkaline battery per gram of electrode material. It may be possible that overall battery efficiency would be greatly enhanced by greater electrode surface area contact created by printing thinner films over a wider area. To equal a typical AA alkaline battery performance (MnO, 0.279 Ah/g), about 10 grams of MnO will need to be printed over a projected area of about 100 cm$^2$. The rush to develop such a large area battery, however, must be tempered by the prohibitive cost that terminal technology still present. Colloidal silver and conductive organic polymer costs per gram, for example, remain comparatively expensive. Although printing terminals are now a reality, lowering the terminal cost will be a major challenge.

Our research leads us into a design path suggesting that every active layer must be printed with direct contact between the active surfaces for the printed battery to be efficient. Internal resistances must be minimized. As with newer rechargeable secondary battery and fuel cell systems, a novel electrolyte separator innovation will be the technical gateway that must be crossed. Research into translating an anode formulation to a press-ready form, and the daunting task of developing a printable separator remain future research challenges.

# References

1.  Ghiurcan, G. A., Liu, C. C., Webber, A., and Feddrix, F. H. (2003). Development and characterization of a thick-film printed zinc-alkaline battery. Journal of the Electrochemical Society, 150(7), A922-A927.

2.  Hilder, M., Winther-Jensen, B., and Clark, N. B. (2009) Paper-based, printed zinc-air battery. Journal of Power Sources, 194(2), 1135-1141.

3.  Huang, J., Yang, J., Li, W., Cai, W., and Jiang, Z. (2008) Electrochemical properties of $LiCoO_2$ thin film electrode prepared by ink-jet printing technique. Thin Solid Films, 516(10), 3314-3319.

4.  Kiebele, A., and Gruner, G. (2007) Carbon nanotube based battery architecture. Applied Physics Letters, 91(14),144104 (1-3).

5.  Kim, H. S., Kang, J. S., Park, J. S., Hahn, H. T., Jung, H. C., and Joung, J. W. (2009) Inkjet printed electronics for multifunctional composite structure. Composites Science and Technology, 69(7-8),1256-1264.

6.  Land, E. (1978)  U. S. Patent No. 4,751,150. Washington, DC: U.S. Patent and Trademark Office.

7.  Landi, B. J., Dileo, R. A., Schauerman, C. M., Cress, C. D., Ganter, M. J., and Raffaelle, R. P. (2009) Multi-Walled Carbon Nanotube Paper Anodes for Lithium Ion Batteries. Journal of Nanoscience and Nanotechnology, 9(6), 3406-3410.

8.  Liu, S. Q., Shi, X. H., Huang, K. L. and Li, X. G. (2009) Characteristics of Carbon Paper as Electrode for Vanadium Redox Flow Battery. Journal of Inorganic Materials, 24(4), 798-802.

9.  Nystrom, G., Razaq, A., Stromme, M., Nyholm, L. and Mihranyan, A. (2009) Ultrafast All-Polymer Paper-Based Batteries. Nano Letters, 9(10), 3635-3639.

10. Ollinger, M., Kim, H., Sutto, T. and Pique, A. (2006) Laser printing of nanocomposite solid-state electrolyte membranes for Li micro-batteries. Applied Surface Science, 252(23),8212-8216.

11. Oogita, Y. and Nakao, K. (1988) U.S. Patent No. 4,751,150. Washington, DC: U.S. Patent and Trademark Office.

12. Park, M. S., Hyun, S. H. and Nam, S. C. (2006) Characterization of a $LiCoO_2$ thick film by screen-printing for a lithium ion micro-battery. Journal of Power Sources, 159(2), 1416-1421.

13. Park, M. S., Hyun, S. H. and Nam, S. C. (2007) Mechanical and electrical properties of a $LiCoO_2$ cathode prepared by screen-printing for a lithium-ion micro-battery. Electrochimica Acta, 52(28), 7895-7902.

14. Southee, D., Hay, G. I., Evans, P. S. A. and Harrison, D. J. (2007) Lithographically printed voltaic cells - a feasibility study. Circuit World, 33(1), 31-35.

15. Tam, W. G. and Wainright, J. S. (2007) A microfabricated nickel-hydrogen battery using thick film printing techniques. Journal of Power Sources, 165(1), 481-488.

16. Zhao, Y. M., Zhou, Q., Liu, L., Xu, J., Yan, M. M. and Jiang, Z. Y. (2006). A novel and facile route of ink-jet printing to thin film $SnO_2$ anode for rechargeable lithium ion batteries. Electrochimica Acta, 51(13), 2639-2645.

17. Ladbury, J. W. and Cullis, C. F. (1958) Kinetics and Mechanisms of Oxidation by Permanganate. Chem. Rev., 58(2), 403-438.

# Printing of catalyst layers used in fuel cells membrane electrode assemblies

*Anne-Gaëlle Mercier[1], Rémi Vincent[1], Christine Nayoze[1], Anne Blayo[2], Arthur Soucemariandin[3]*

[1] Atomic Energy and Alternative Energies Commission (CEA)/DRT/LITEN, Laboratory of Components for Fuel Cells and Electrolysers and of Modeling (LCPEM), 17 rue des Martyrs, F-38054 Grenoble, France
  E-mail: anne-gaelle.mercier@cea.fr

[2] Laboratory of Pulp and Paper Science and Graphic Arts (LGP2) (UMR 5518 CNRS-CTP-INPG), Grenoble Institute of Technology (INP Grenoble - PAGORA), 461 Rue de la papeterie, BP 65, F-38402 St Martin d'Hères, France
  E-mail: anne.blayo@pagora.grenoble-inp.fr

[3] Laboratory for Geophysical and Industrial Flow Research (LEGI) (UMR 5519 CNRS-UJF-INP Grenoble), Domaine universitaire, BP53, F-38041 Grenoble, France
  E-mail: arthur.soucemarianadin@ujf-grenoble.fr

**Abstract**

In this work, cathode catalyst layers of membrane electrode assemblies for proton exchange membrane fuel cells (PEMFC) were made by using inkjet printing. First, formulation of catalyst inks comprising carbon-supported platinum and Nafion® polymer solution was developed by testing different dispersion techniques and adapting the solvents to the process and substrates. Inkjet printed catalyst layers were then compared with electrodes realized with conventional deposition methods: blade coating, screen printing and spray coating.

Best inks characteristics meet inkjet requirements concerning dispersion, stability and ejectability. Morphology observations show that all catalyst layers have similar thicknesses. The inkjet printed MEAs single cell performances are equivalent to those obtained with the conventional processes, achieving power densities of 650mW/cm² for inkjet printing in automotive conditions. Thus, this work stands for an important step in the use of inkjet printing for MEAs manufacturing. The versatility of this process offers new opportunities to optimize the structure of the electrodes and platinum utilization in order to increase MEAs performances and reduce manufacturing costs.

**Keywords:** inkjet printing; PEM fuel cells; membrane electrode assembly (MEA);
            catalyst ink formulation; single cell performances

## 1. Introduction

Fuel cell manufacturing remains a challenge both for researchers and industrialists and a breakthrough is needed to meet the requirements of new sources of energy. Proton exchange membrane fuel cells (PEMFC) are considered as one of the promising environmentally friendly technologies to produce electricity by direct electrochemical conversion of hydrogen and oxygen into water. However, several barriers prevent their commercialization: the issues of durability, performance and the reduction of manufacturing cost. The last point gains attention and implies simplifying the MEA fabrication process and reducing materials costs, especially of membranes and noble metals such as platinum used to catalyze the oxidation and reduction reaction (Stone *et al.*, 2002).

Platinum utilization of commercially prototype fuel cells remains low. It indicates that efforts can still be done to reduce catalyst loading levels, which have already been lowered from 4 to below $0.2 mgPt.cm^{-2}$ without loss of performance with traditional method such as blade coating, screen printing or spray painting (Kocha, 2003). Catalyst deposition at ultra low loadings has also been investigated with techniques such as sputtering or electrodeposition, but they present several drawbacks, for instance, the uniformity of catalyst layer, MEA life time or the impossibility to deposit the electrolyte simultaneously for sputtering (Wee *et al.*, 2007).

The use of inkjet printing to deposit catalyst layer onto gas diffusion layer or perfluorosulfonic polymer membrane (Nafion® type) can overcome some of these limitations. In the last few years, it has been used for industrial applications involving deposition of ceramics, organic light emitting diodes, assemblies of periodic structures, structural polymers (Calvert, 2001). In the field of PEMFC, this free-form fabrication method

enables to explore both reduction of Pt loading and the design of structures improving catalyst utilization thanks to its versatility, adaptability and reproducibility (Taylor *et al.*, 2007; Towne *et al.*, 2007). Nevertheless, ink jet printing remains a complex process because ink composition must meet strict requirements to avoid clogging of the printer nozzles. Thus, the objective of this study is to formulate electrocatalyst inks that match the requirements of conventional inkjet printing inks. Our purpose is to show that MEA printed with a piezoelectric inkjet printer may achieve comparable performances to MEA produced by standard fabrication techniques like blade coating or screen-printing.

## 2. Methods

### 2.1 Preparation of catalyst inks

Catalyst inks compatible for a piezoelectric inkjet printer have been developed. They are prepared from carbon-supported catalyst (46% w/w platinum on Vulcan XC-72R; Tanaka) and Nafion[®] solution (20wt% in alcohol and water), dispersed in a suitable mixture of solvents. A crucial problem in inkjet printing is nozzle clogging which may occur since Pt/C particles tend to agglomerate, leading to particle sizes up to 10 μm, whereas they should ideally be less than 1 μm. In order to achieve a suitable dispersion, two ways of improvement have been explored: the use of a Triton X-100 or carboxyl-methyl cellulose (CMC) to limit sedimentation, and techniques for dispersing Pt/C powder, such as sonication or magnetic agitation. For each ink composition, agglomerate size distribution was measured with a light scattering instrument (Malvern Mastersizer). Measures were carried out at natural ink pH, which is acidic due to Nafion[®] polymer dispersion made from chemically stabilized perfluorosulfonic acid/PTFE copolymer in the acid ($H^+$) form.

Clogging can also be caused by ink drying in and around the nozzle. That's why humectants, that is to say low volatility water-miscible solvents, such as glycols, are traditionally added to prevent drying. Different solid contents, natures and proportions of solvents were investigated according to these issues.

Regarding the solvents, three quantities of ethylene glycol were tested: 0%, 15% and 32% by weight. Water and isopropanol were also added to the slurry to adjust the viscosity, the surface tension, the particle size, the wettability and the drying rate of the inks as described by (Towne *et al.*, 2007). Viscosity is measured with a cone/plate rheometer (Anton Paar, Modular Compact Rheometer MCR 300) and contact angle visualizations were carried out using a drop shape analysis system (KRÜSS DSA-10MK2).

### 2.2 Inkjet printing of catalyst inks

The formulated inks were printed with a laboratory piezoelectric inkjet printer developed by Siliflow[®] and consists of a single nozzle of 150 μm diameter. Due to its single nozzle, the printing time is rather long, but this equipment presents the benefits of being robust and more reliable than conventional inkjet printers. Thus, thanks to its ability to purge the ink if the nozzle is clogged and to change the ink very easily, it enables to develop catalyst inks that could not be used at the beginning in conventional inkjet printer due to poor dispersion and quick sedimentation.

The printing parameters were optimized to achieve the better deposit: wave forms, amplitude and duration, applied to the piezoelectric element, were adapted to each ink. Inks were printed on two hydrophobic substrates: a Nafion[®] polymer membrane (Nafion[®] NRE 212) and a gas diffusion layer (SGL 24BC), which is a paper-type product based on carbonized fibers coated with a microporous layer. A distance of 500μm between droplet impact centers was chosen to completely cover substrates with several passes, both on membrane and gas diffusion layer. This drop spacing enables to have a more uniform layer, without ink coalescence. Separated dots instead of continuous lines were printed to limit also polymer membrane swelling, which was also decreased thanks to the action of a vacuum and thermal plate. It is indeed important to limit membrane deformation so that no mechanical strain may weaken the membrane and damage it during fuel cell operating. Substrates were heated at 60°C during printing to improve ink drying.

Uniform catalyst layers of 25 cm$^2$ were printed with a succession of several passages to achieve the desired loading of 0.4 mg Pt.cm$^{-2}$, corresponding to a cathode catalyst layer.

### 2.3 Preparation and characterization of membrane electrode assemblies

For comparison to inkjet printed cathode catalyst layers (0.4mg Pt.cm$^{-2}$), three other processes were used to fabricate cathodes: blade coating, screen-printing and spray coating. All cathode catalyst layers had a Pt loading of approximately 0.4 mg.cm$^{-2}$ and the anodes were always blade coated catalyst layers (0.2 mg Pt.cm$^{-2}$). The

inks used to produce cathode catalyst layers were adapted to processes by adjusting solid content, with the same Nafion[®]/Pt ratio. Thus, the main difference between inks was the quantity of ethylene glycol added to inkjet inks. MEAs were then made by hot pressing the gas diffusion layers, the catalyst layers and the membrane.

Optical microscopy observations were made to control uniformity and print quality of catalyst layers. SEM observations were achieved on MEAs cross-sections embedded in epoxy resin in order to determine more precisely their thickness and to verify the uniformity and adhesion to Nafion[®] membrane.

Fuel cell performance measurements were performed using a single cell test system. After conditioning for several hours, measurements were done with a fuel cell temperature of 80 °C, and the reactant gas ($H_2$ for anode and air for cathode) were injected at 0.15MPa; the relative humidity is 50% on each side. Cyclic voltammetry measurements were also conducted to determine the electrochemical active surface area (ECA), which was obtained from the area of hydrogen desorption peak using the formula (1) given below:

$$\text{ECA (cm}^2\text{/mg Pt)} = \frac{H_2 \text{ desorption peak area}}{\text{Sweep rate} \times 210 \times \text{Electrode surface}} \qquad (1)$$

(by assuming a value of 210 µC/cm² for the oxidation of atomic hydrogen on a smooth Pt surface).

Impedance spectroscopy measurements were also performed to measure the resistance of fabricated MEAs.

## 3. Results and discussion

### 3.1 Catalyst ink compatibility with inkjet printing

The particles size measurements showed that the suspension stability is influenced by mixing conditions and ink composition. With ultrasonic bath, particle sizes of less than 1 µm were achieved for the best inks, which was a sufficient colloidal stability to pass through the nozzle of 150 µm diameter for the period needed in this field of development application. The resulting suspension is found to be stable for a few days.

Otherwise, the solid content was adjusted at 3% by weight. Lower solid contents (for example 1%) led to too low printing speeds, whereas higher solid loadings increased ejection instability. The increase of ethylene glycol content enabled to improve ejection stability and to multiply by 6 the potential printing time. Isopropyl alcohol was also added to improve ink wettability on the two printed hydrophobic substrates: Nafion[®] polymer membrane (Nafion[®] NRE 212) and gas diffusion layer (SGL 24BC). The minimum isopropyl alcohol quantity was determined by contact angle visualization as illustrated by Figure 1.
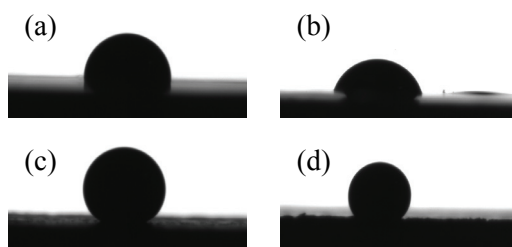


*Figure 1: Effect of isopropyl alcohol on the ink wettability on Nafion[®] membrane without (a) and with isopropyl alcohol (b) and on gas diffusion layer without (c) and with (d) isopropyl alcohol*

The formulated inks showed low viscosities, less than 10 mPa.s, more precisely 5 mPa.s for inks based on 32% ethylene glycol solvent, at 20°C, a shear rate of 2500 s^{-1} and of quasi-Newtonian behavior. Surface tension was also in accordance with ink jet printing requirements. Thus, the inks were compatible with the piezoelectric inkjet printer, causing no problem of dripping, drying or clogging and sufficient wetting of substrates.

### 3.2 Morphology characterization of printed catalyst layers

The optical microscopy observations showed that the print quality was achieved both on Nafion[®] polymer membrane and on gas diffusion layer with the same ink. Defaults such as coffee ring or inhomogeneity at the

scale of a droplet impact were observed, but the adjustment of solvent ratio and the increase of solid content seems to limit this phenomenon.
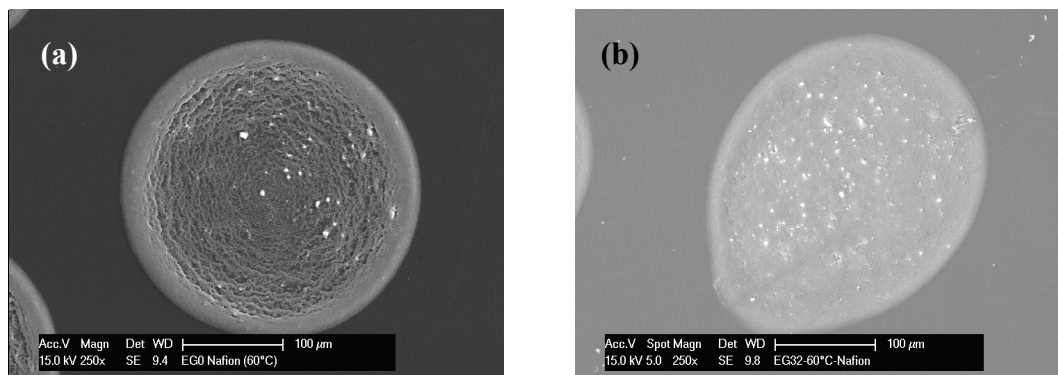


*Figure 2: SEM images of inkjet droplet impact with 0% (a) and 15% (b) of ethylene glycol on Nafion® membrane heated at 60° C*

Especially, Figure 2 outlines that the addition of ethylene glycol limits the coffee ring formation on Nafion® membrane heated at 60°C. This phenomenon may be explained by the apparition of a Marangoni flow. Since ethylene glycol has a high boiling point (198°C), its concentration may increase at the edge of the droplet where the lower boiling point solvents will evaporate faster. The resulting surface tension gradient can cause a Marangoni-type flow that will transport particles from low surface tension regions to high surface tension regions, that is to say, from the edge of the droplet to the center, conter-balancing therefore the outward convective flow induced by the evaporation at the droplet contact line (Kim, *et al.,* 2006). The decrease of coffee ring thanks to the addition of ethylene glycol was even more pronounced on gas diffusion layer, which could be explained by the less important spreading of catalyst ink on this substrate, as illustrated in Figure 1. This difference of spreading led to droplet impact diameter of around 170 µm on gas diffusion layer and around 280 µm on Nafion® membrane. The smaller diameter on gas diffusion layer may make easier the circulation of particles, thus enable a more uniform repartition.

Otherwise, SEM observations of MEAs cross-sections (cf Figure 3) show that the quality of catalyst layers achieved with inkjet printing, which is a discontinuous deposition process, is comparable to those obtained with a continuous process like blade coating.
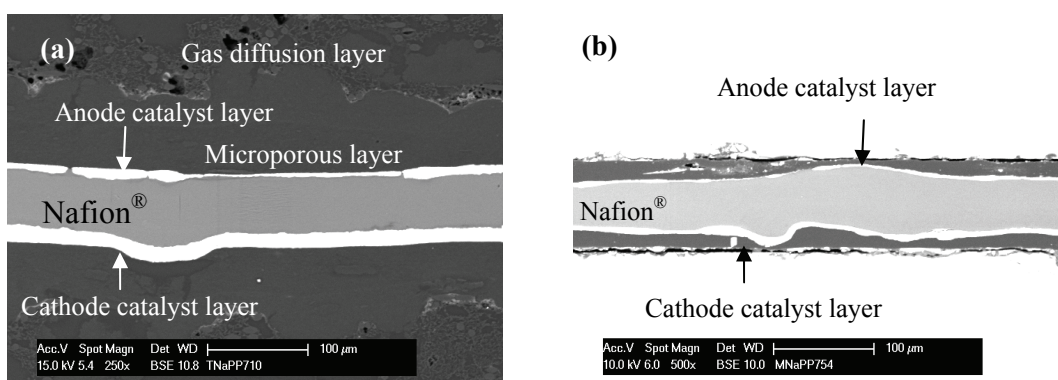


*Figure 3: SEM cross-section of MEA fabricated from blade-coated catalyst layer (a) and inkjet printed catalyst layer (b)*

The observation of MEAs with the same Pt loading showed that the thicknesses of catalyst layers were comparable for the four processes, approximately 12 µm for cathode catalyst layers and 5 µm for anode catalyst layers. These SEM images show that inkjet catalyst layers are continuous, present a good adhesion to Nafion® membrane, but may be less uniform.

The impact of inkjet printing parameters (for example drop spacing) and of coffee ring on single cell performances were not yet evaluated. This impact must be limited by the number of passes necessary to obtain a cathode catalyst layer with a Pt loading of 0.4mg.cm⁻², but it can have an influence for instance on the anode catalyst layer quality since the number of passes would be lower.

### 3.3 Single cell performances

The single cell performances, active surface areas and resistances were measured on fabricated MEAs. These measurements give information about two major concerns linked to the use of a new process like ink jet printing: first, a possible modification of the structure of catalyst layer implied by ink jet printing and secondly an impact on fuel cell performances due to the presence of a high boiling point solvent (Chisaka *et al.,* 2009). Due to that property, a part of ethylene glycol may remain in the catalyst layer, which could lead to a decrease of cell performances.

Figure 4 shows the electrochemical active surface areas of cathode catalyst layers produced with the different processes. This area stands for the platinum in contact with the ionomer and carbon, which corresponds to active sites where electrochemical reactions occur. It can be observed that the catalyst layers present an active surface area rather close for the different processes and which is more influenced by the type of MEA (CCB or CCM) than the process used to apply the catalyst layer. The electrochemical areas are indeed lower for CCM catalyst layers than for CCB catalyst layers, with an average difference of around 140cm²/mg. This might be explained by the different affinity between the ink and the two substrates, and especially the way the structure is formed during ink drying.
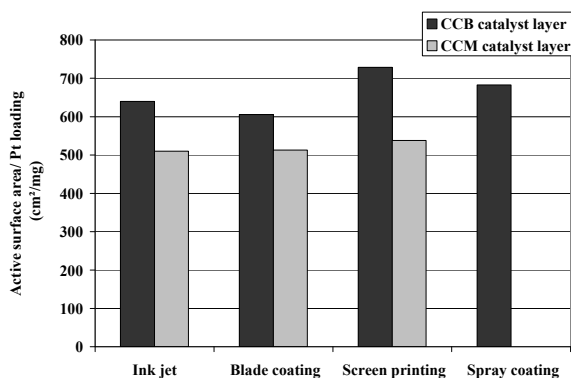


*Figure 4: Electrochemical active surface areas for the different cathode catalyst layers. Scan rate = 50mV/s,*
*Ca./An. = $N_2/H_2$, T = 80°C, RH = 100% and P = 0.15 Mpa*

Anyway, an important point is that the quantity of platinum that may be used for electrochemical reactions for inkjet printed catalyst layers is as high as for the other processes .This observation implies that the quantity of catalyst in the electrode structure in contact with the ionomer is sufficient. Otherwise, platinum is sensitive to physisorption pollution, ethylene glycol could also limit adsorption of Nafion® on platinum, leading to a decrease of platinum usefulness to the reaction catalysis. According to these results, even if this pollution may exist, ethylene glycol doesn't cause an important catalyst poisoning.

However, the electrochemical area is measured at low current densities and it doesn't take into account gas accessibility to platinum active sites. That's why fuel cell performances are also evaluated by polarization and power curves shown in Figure 5 and Figure 6.
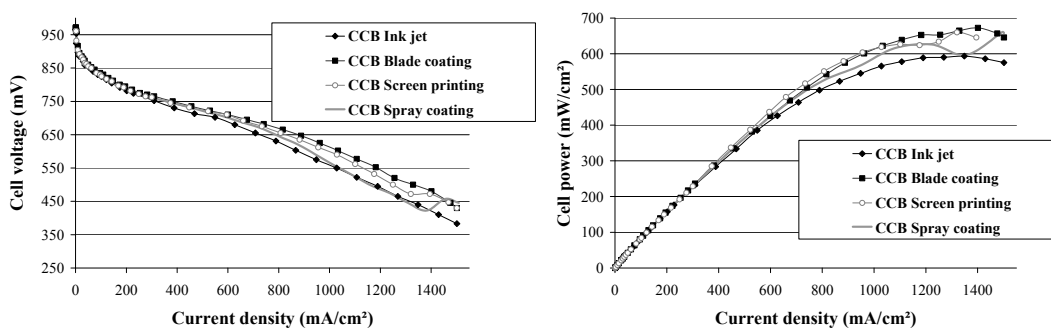


*Figure 5: Polarization and cell power curves comparing cathode catalyst layers printed with the different processing*
*techniques on gas diffusion layer (CCB). Ca./An. = Air/$H_2$, T = 80°C, RH = 50% and P = 0.15 Mpa*
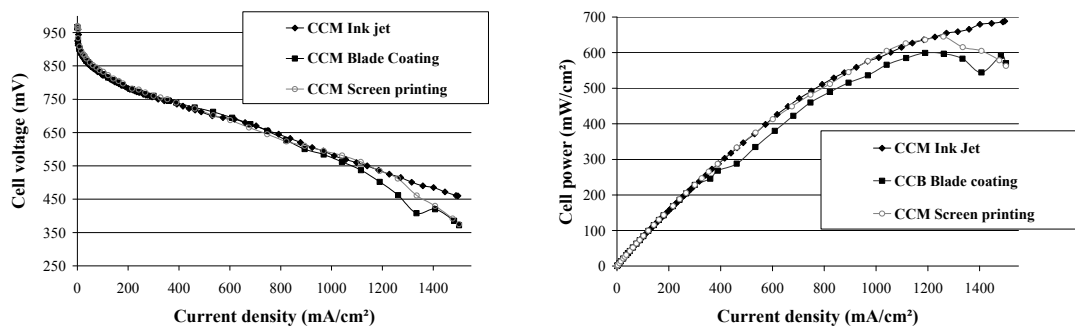*(Pt loading: approximately 0.4mg.$cm^{-2}$)*

*Figure 6: Polarization and cell power curves comparing cathode catalyst layers printed with the different processing techniques on Nafion® membrane (CCM). Ca./An. = Air/H2, T = 80°C, RH = 50% and P = 0.15Mpa (Pt loading: approximately 0.4mg.cm⁻²)*

The polarization and power curves show that at equivalent Pt loading (around 0.4 mgPtcm$^{-2}$), the cell performances of ink jet printed catalyst layers are really close to performances achieved with screen-printing, blade coating or spray coating. Impedance spectroscopy showed that the resistances associated with polymer electrolyte of all the electrodes were similar for the four processes and close to 0.15 Ohm.cm$^2$. Furthermore, the CCB inkjet printed MEA had a peak power density of 633 mW.cm$^{-2}$, which is only 6 % less than blade coating MEA and 4 % less than the screen-printed MEA. These results confirm that ethylene glycol doesn't seem to poison catalyst particles, even though it may remain a part of this solvent in the catalyst layer due to its high boiling point. Moreover, ethylene glycol does not affect to a great extent fuel cell performances by decreasing catalyst layer porosity by blocking pore layers and thus gas diffusion/accessibility to catalytic sites. The difference of performance may be all the same linked to the influence of ethylene glycol or iso-propanol on the catalyst layer structure formation (Chisaka *et al.,* 2009; Shin *et al.,* 2002; Towne *et al.,* 2007). That's why an experiment has also been made in order to see if inkjet printed MEAs cell perfor-mances could be improved by a heating treatment consisting in drying the catalyst layer at 120°C for 2h to remove a more important quantity of ethylene glycol. The performances are depicted in Figure 7.
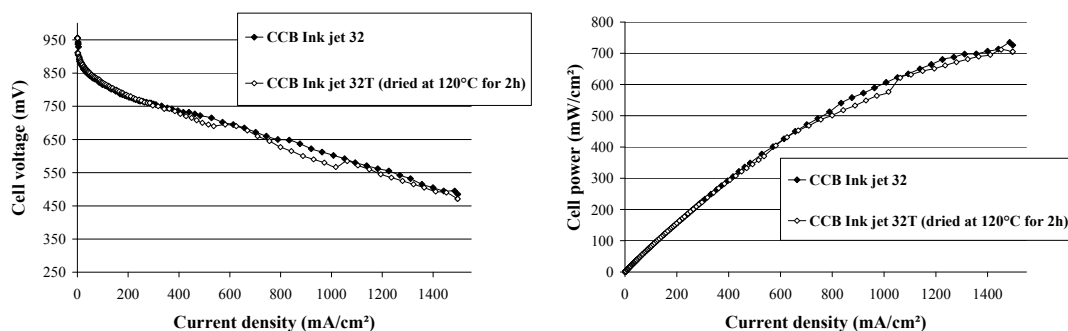


*Figure 7: Polarization and power curves comparing inkjet printed cathode catalyst layers with and without a drying step at 120°C during 2h. Ca./An. = Air/H₂, T = 80°C, RH = 50% and P = 0.15Mpa*

These results indicate that the treatment at 120° C has no impact on fuel cell performances. A possibility may be that ethylene glycol may be eliminated by water flow produced by the cell and evacuated during cell functioning, which could liberate pores that could have been filled by ethylene glycol. It validates that typical inkjet inks containing a humectant can be used to produce catalyst layers and to have similar performances to conventional inks without humectants.

## 4. Conclusion

This study enabled to formulate catalytic inks that meet the strict requirements of piezoelectric inkjet printing. The inks prepared showed a suitable dispersion, viscosity and surface tension. According to the printed catalyst layers, the inkjet method doesn't seem to modify catalyst layer structure, or the possible change may be balanced by the introduction of ethylene glycol and isopropanol. The single cells performan-ces are indeed comparable to MEAs fabricated by screen printing, blade coating or spray coating, regarding

fuel cell performances, electrochemical active areas or resistances. To summarize, this study has demonstrated the possibility of using inkjet printing to produce PEMFC MEA. From a production point of view, the single nozzle is not enough competitive for the moment, but this work of validation of solid areas catalyst layers stands as an important first step with two outlooks enabled by inkjet possibilities. The benefits offered by this technique can be indeed exploited in two ways: on one hand, an increase of productivity by the integration of a multi-nozzle equipment to print solid areas and thus achieve printing speeds more comparative to competitive methods like screen printing and blade coating, and on the other hand, the utilization of inkjet printing versatility to increase MEAs performances by an optimization of the structure of the electrodes and the Pt utilization.

## References

Calvert, P., (2001), *Inkjet Printing for Materials and Devices, Chem. Mater., 13, 3299-3305*

Chisaka, M. and Hirofumi, D., (2009), *Effect of Organic Solvents on Catalyst Layer Structure in Polymer Electrolyte Membrane Fuel Cells, Journal of The Electrochemical Society, 156 (1), B22-B26*

Kim, D., Jeong, S., Park, B. K., Moon, J., (2006), *Direct writing of silver conductive patterns: Improvement of film morphology and conductance by controlling solvent compositions, Applied physics letters 89, 264101*

Kocha, S. S., (2003), *Principles of MEA preparation. In: Handbook of Fuel Cells - Fundamentals, Technology and Applications, Edited by Wolf Vielstich, Hubert A. Gasteiger, Arnold Lamm, Volume 3: Fuel Cell Technology and Applications*

Shin, S.-J., Lee, J.-K., Ha, H.-Y., Hong, S.-A., Chun, H.-S., Oh, I.-H., (2002), *Effect of the catalytic ink preparation method on the performance of polymer electrolyte membrane fuel cells, Journal of Power Sources 106, 146-152*

Stone, C., Morrison, A.E., (2002), *From curiosity to "power to change the world®", Solid State Ionics 152-15, 1-13*

Taylor, A. D., Kim, E.Y., Humes, V.P., Kizuka, J., Thompson, L.T., (2007), *Inkjet printing of carbon supported platinum 3-D catalyst layers for use in fuel cells, Journal of Power Sources 171, 101-106*

Towne, S., Viswanathan, V., Holbery, J., Rieke, P., (2007) *Fabrication of polymer electrolyte membrane fuel cell MEAs utilizing inkjet print technology, Journal of Power Sources 171, 575-584*

Wee, J.-H., Lee K.-Y., Kim S. H., (2007), *Fabrication methods for low-Pt-loading electrocatalysts in proton exchange membrane fuel cell systems, Journal of Power Sources 165, 667-677*

# Manufacturing of modular electronic devices employing the concept of functionality separations: towards an adapted workflow for functional printing

*Reinhard R. Baumann*[1, 2]*, Andreas Willert*[2]*, Thomas Blaudeck*[1]

[1] Chemnitz University of Technology
  Institute for Print and Media Technology, Digital Printing and Imaging Technology
  Reichenhainer Str. 70, D-09126 Chemnitz, Germany
  E-mails: reinhard.baumann@mb.tu-chemnitz.de, thomas.blaudeck@mb.tu-chemnitz.de

[2] Fraunhofer Research Institution for Electronic Nano Systems ENAS
  Department Printed Functionalities
  Technologie-Campus 3, D-09126 Chemnitz, Germany
  E-mails: andreas.willert@enas.fraunhofer.de, reinhard.baumann@enas.fraunhofer.de

### Abstract

During the last decade, several approaches have been published, which employ printing technologies for the solution based manufacture of electronic components and devices. The printed layers are made from new functional inks which targeted functionalities are not the regular process colours CMYK but functionalities beyond colour, e.g. electrical conductivity or semi conductivity. In this paper, we introduce the concept of *functionality separations* as a new basic methodology to organise the workflow of functional printing, where the well introduced *colour separations* are considered as the basic subset. In that context, *functional printing* shall represent the full set of technological approaches to extend and exploit the potential of state-of-the-art printing technologies for the fabrication of printed items or devices with advanced - "not only graphical" - functionalities. The paper will exemplify this approach by three particular cases: (i) printed electrical conductive patterns, (ii) printed RFID applications and (iii) printed modular batteries.

**Key words:** printed functionalities; functionality separations; workflow; fabrication of printed electronic devices

## 1. Introduction

After half a millennium of technological development printing has achieved the quality level to meet the requirements of its mission: to convince the human eye to recognize a well defined ensemble of discrete coloured screen dots as a perfect halftone image. And this quality level applies to printing on endless paper web or paper sheets and on a broad variety of substrates additionally. Nowadays developments of industrial printing are more or less solely addressing improvements of the production efficiency.

During the last decade, several approaches have been published, which employ printing technologies for the solution based layer-by-layer manufacture of electronic components and devices. The printed layers are made from new functional inks which targeted functionalities are not the regular process colours CMYK but functionalities beyond colour, e.g. electrical conductivity or semi conductivity. These applications, contradictory to lithography, utilize the advantages of printing as an additive material deposition technology: the functional materials are only deposited in areas of the substrate, where their functionality is essential for the final electronic devices. In this paper, we introduce the concept of *functionality separations* as a new basic methodology to organise the workflow of functional printing, where the well introduced *colour separations* are considered as the basic subset. Following this route it becomes obvious that the printers have already the fundamental toolbox to start printing beyond colour. In that context, *functional printing* shall represent the full set of technological approaches to extend and exploit the potential of state-of-the-art printing technologies for the fabrication of printed items or devices with advanced - i.e. "not only graphical" - functionalities. The paper will exemplify this approach by three particular cases: (i) printed electrical conductive patterns, (ii) printed RFID applications and (iii) printed modular batteries.

## 2. Printed functionalities beyond colour

With respect to literature, the concept of colour separations is considered one of the few in printing and media technology that is accepted as a basic methodology and multidisciplinary concept independent of the

details of the particular printing technique [Mandel 2010]. It is closely related to the development of quantitative models and explanations of autotype colour mixing in multi-colour printing, with its roots traced back to the efforts of Neugebauer, Demichel, Kubelka and others in the first half of the 19th century [Amidror 2000]. Recent publications show that there is a clear trend in graphical printing towards an integration of additional process colours (beyond cyan, magenta and yellow) into traditional [Koirala 2008, Chen 2008] or advanced [Esler 2009, Wang 2009] colour management concepts for a faithful colour reproduction. However, as soon as this reproduction becomes different to the traditional concept of autotype colour mixing, a conceptual separation into layers is still useful for the sake of an efficient process workflow. For example, true-colourcolour holographic stereometry is based on multiple layers of photopolymers [Hubel 1992]. In this concept, there is colour distinct from the traditional autotype colour mixing, but the design of the printing workflow relates to the individual photopolymer layers to give holographic effects, showing that the concept of colourcolour separation has turned into the concept of a functionality separation.

Analysing the future requirements of printed products, for example of being elements of automated supply chains or highly secure medication systems, it is evident that the products made on an industrial print production line have to have more functionalities than just merely colour.

As outlined above in this chapter, printers are currently printing inks which are creating the functionality "process colour" on the substrate. For the deposition of each process colour a *colour separation* has to be prepared to make the right plate for the underlying printing process (in case of inkjet printing these separation data are directly used to fire a nozzle at the right position of the substrate). In analogy the printer has also to prepare a separation for the deposition of inks which do not generate the functionality colour but other functionalities, e.g. conductivity. To keep the termini for functional printing in accordance with graphical printing we propose to define all separations made for any functionalities "functionality separations" and recognize that the good old colour separations are a subset of the introduced, more general term. In parallel helps this definition easily to understand that the printers have already the general toolbox to make ALL functional separations. Further development approaches have to be executed to choose the right materials for making the appropriate forms and to find and define all the meta data which are necessary for the printing process.

| Functionality | Application |
|---|---|
| Color Cyan<br>Color Magenta<br>Color Yellow<br>Color Black | Process Colors |
| Gloss & Protection | Coating |
| Electrical Conductivity<br>Adapted Dielectric Properties<br>Electrical Semi-Conductivity<br>Electro-Luminescence / Light Emission<br>Electric Power | Circuitry |
| Sensing Environment | Sensors |
| Surface Modification<br>Surface Protection<br>Catalysis<br>Porosity | Process Support |
| Intelligence via Si-Chip and / or Supplemental Electronics<br>Geometric Shape / Laser Cutting | Hybrid Tech |

*Figure 1: Traditional and future functionalities manufactured by printing*

Figure 1 summarizes different groups of functionalities of future printed products. The functionality *process colour* is generated by transferring a coloured ink to the substrate dot wise. In any case the ink has to be optimized for a designated printing technology. The setting of the rheological properties of these inks, determined by the chosen printing process, allows almost all possible low prized solutions to be used, as long as the targeted colour fits the standards.

Contemplating other functionalities included in Fig. 1 it becomes obvious that the number of applicable materials to adjust the rheological properties of an ink is seriously limited. For instance, UV curable inks

used to generate the functionality *gloss* can only be composed from materials that neither inhibit the photochemistry nor the polymerization itself. Considering the optimization of those inks which will generate the functionalities of electrical circuitries in multilayer arrangements, the material scientists are facing a rather narrow window of opportunities to combine the targeted functionality of the printed element and the required rheological properties of an appropriate ink.

Nevertheless, printing technologies including the digital, non-impact ones will enable a new field for print applications and subsequently a new market: printed low-end electronics. They are expected to enable a variety of new products that will not meet the top-notch specs of silicon electronics but will be manufactured on flexible substrates, at low production costs, under ambient conditions and in (very) large quantities, typical for printing lines. And these manufacturing details are illustrating the potential of low-end electronics becoming a value-adding part of printed products.

## 3. Method

As for any production technique, the workflow for functional printing is a crucial part in further developments. The workflow definitions ensure that the different materials (inks and substrates) are processed with the right set of parameters and combined in the right manner to achieve the required quality at the end of the production process. For graphical printed products the workflow is well established and widely known comprising the production stages *prepress*, *press*, and *postpress*.

On the *prepress* stage is usually organized how the layout and applying meta data have to be handled to make the printing form. Figure 2 contains the further derivation of a workflow concept for a *functional prepress* stage. It visualises the preparation for handling and usage of functional inks before the printing and manufacturing process from the state-of-the-art workflow of the production of a common coloured print result (Fig. 2 A). In this context, the raster-image processing (RIP) separation algorithms are sufficient to handle this task.

To improve the production efficiency and to decrease the time of production of a job, the JDF (job definition format) workflow concept has been developed for a long period of time (Fig. 2 B). Using this concept, relevant process data can be handled such as the run length, the substrate, the inks but also predefinitions of machinery equipment such as ink zones or intended formats for the initialisation of cutters.

Within the JDF concept, also the application of spot colours can be handled (Fig. 2 C). Taking the spot colour into account, the separation of the printout in only four colours is not longer sufficient. At this step of the development, an additional separation is needed to control the printing of the spot colour. Therefore, the term *functionality separation* enters the stage: instead of splitting the colour information into four layer channels (cyan, magenta, yellow and black) only, one additional layer is needed, namely for the functionality *spot colour* or even *spot colours*. A similar situation becomes true when dealing with spot varnishing. In this case the information of the locations of the varnish has to be handled as the functional layer *varnish*. This concept is similar to that presented in the preceding clause (Fig. 2 C).

Thinking of functionalities other than colour or varnish, functional layers for devices or circuitries come into mind. Finally, these functional layers require dedicated printing units to apply functional ink at defined locations on the printing product. To jump from the lab into a manufacturing workflow a new concept is needed to join new demands with already established technologies.

In Figure 2 D, a concept is shown to integrate the handling of new functional inks into the already existing print prepress workflow: Layer requirements concerning areas for application of functional material for devices can be encoded e.g. using encapsulated post script (EPS). The JDF concept enables to encode in addition to the EPS information about layer thicknesses, printing and curing conditions, etc. Therefore all information necessary to manufacture e.g. a printed battery consisting of the different layers and their requirements can be encoded for the manufacturing process by using EPS and JDF information. All this information shall be collected in an adequate container-like PDF.

Having all information concentrated in only one PDF container enables the RIP to separate all needed information for every printing and processing unit required for manufacturing the intended print product. The RIP separates the colour information as described above. Additionally, the functional layers are being

separated by the RIP to use the required machinery information to manufacture the desired functionality. The manufacturing data are complemented by the JDF data.
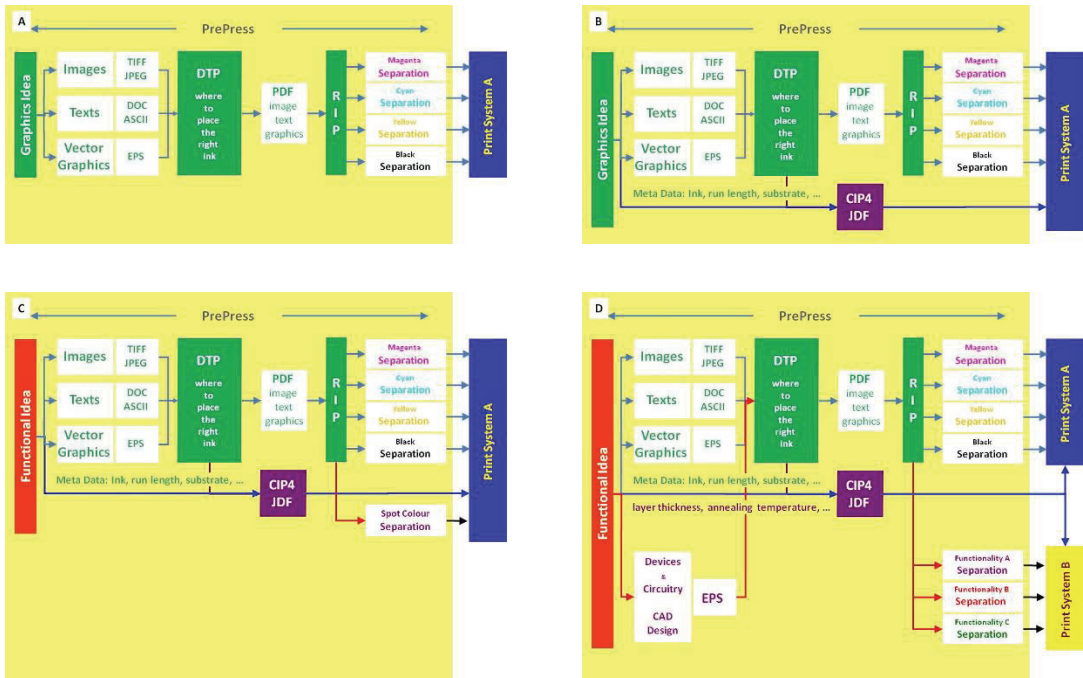


*Figure 2: Workflow systems used for graphical print production (A, top left), using meta data (B, top right) and spot colours (C, bottom left) and final extension to use of functional inks (D, bottom right)*

Having introduced particular prepress aspects for functional printing, it is important to identify the relevant differences of functional printing and graphical printing with respect to layer formation and functionality forming during the production process. Figure 3 contains a simplified flowchart showing the production stages of *functional printing* versus the classical micro structuring technique of *graphical printing*.
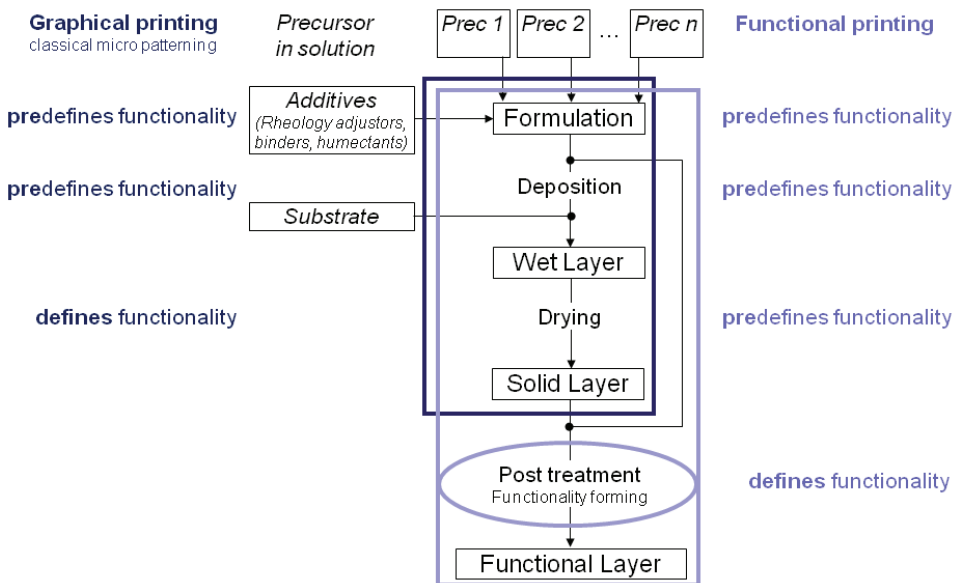


*Figure 3: Simplified flowchart of the production stages in functional printing with respect to graphical printing as a classical micropatterning technique (Figure adapted from Čermák, 2009)*

It turns out that, in the case of graphical printing, drying (by hot air, IR or UV) of the deposited layer generates already the desired functionality *process or spot colour*. On the contrary, most of the functional layers require in addition to drying particular post-treatment steps, which are basically as important as the

choice of the particular deposition or printing process itself. The challenge for functional layers manufacturing becomes the integration of the new functionality forming processes into the traditional value chain in addition to drying. As discussed in more detail later, such additional processes are necessary to transform the printed, pre-functional layer (i.e. metal particles containing ink) by curing, annealing or sintering to form the desired functionality (i.e. conductivity).
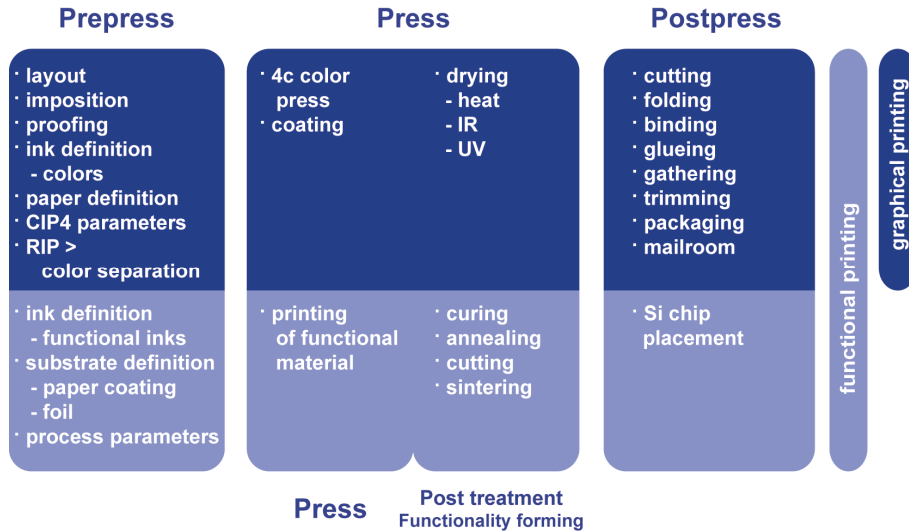


*Figure 4: Comparison of the workflow of graphical arts print production (upper part, blue) and additional processes needed for functional inks (lower part, green) (Figure adapted from Willert, 2009b)*

In the light of the particular importance of this transforming step, we suggest to differentiate between the printing processes themselves and a variety of required post-treatment processes in the production stage. Figure 4 shows a listing of selected individual manufacturing steps for graphical arts printing (upper part) and functional printing (lower part). It is obvious that the production stages prepress, press and postpress for coloured products and functional layers show - truly expected - similarities. However, the set of integrated manufacturing techniques in functional printing may highly differ from graphical printing.

## 3. Results and discussion

In this chapter, the concept of functional layer separation is applied for the manufacturing of three different kind of printed items: (i) printed electrical conductive patterns, (ii) printed RFID applications and (iii) printed modular batteries.

### 3.1 Printed electrical conductive patterns

Electrical conductive patterns can be considered as a passive component of printed electronics with rather low complexity. The manufacturing workflow can be based on printing of silver-particle-filled (Perelaer, 2006) or metal-organic decomposition silver precursor inks (Jahn, 2010a; Jahn, 2010b) with subsequent post-treatment (plasma, UV or laser light, microwaves etc.) (Reinhold, 2009) to form conductive layers. This example of printed electrical conductive layers may help to anticipate the major difference of functional and graphical printing: the printed and dried Silver layers are not at all functional regarding their targeted functionality which is formed only after an additional, successful post-treatment. That means, the particular process conditions as well as layer parameters measured in-line (such as spatially resolved conductivity) are important meta data to be held and distributed in the workflow system.

### 3.2 Printed RFID applications

The integration of RFID communication into packaging products is an example of the next complexity level for functional printing which could be successfully demonstrated at DRUPA in 2008 as a result of a German research consortium (Locostix, 2008). (cf. Figure 5). The challenge for this group of applications so far is the fact that the performance of a RFID antenna is strongly affected by its particular dielectric environment described by the elementary Maxwell's equations. Consequently, each RFID tagged object needs a dedicated antenna design depending on its geometry, its resulting electrical permittivity and the general permittivity of

its neighbourhood to perform at an optimal communication quality. Therefore the number of copies of the antenna is identical with the number of the printed product itself, suggesting to print the antenna "in-line with the pictures". A proof of this concept has been published recently (Zichner, 2009). Figure 5 shows printed objects with integrated antennas made by functional printing. Consequently, in addition to the separations for the *process colours* a functionality separation to print the functionality *conductivity* for these antennas was necessary. The subsequent interconnection of antenna and RFID chip (which is made from Si) based on interposer technology and its integration into the workflow for the manufacture of the final product is a challenge to get over is still left for the future. Figure 6 shows the appropriate manufacturing steps which needs to be integrated into the overall workflow (see Fig. 2).



Figure 5: Packages with RFID functionality based on printed RFID antennae



Figure 6: Workflow concept to manufacture a package with included RFID functionality: antenna design, simulation, conductive ink printing, interposer mounting of Si microelectronics, tag characterization (from left to right). For this procedure, an adaptation in the software workflow concept is required.

In case of antennas, there is only one additional layer necessary for the printing process. Nevertheless, there are additional steps required due to the fact of connecting the silicon chip as a microelectronic device with the printed structures. As indicated in Figure 4, placement and mounting of the silicon chip can be considered as a postpress step. From a conceptual point of view, these manufacturing steps have to be described in a way compatible to the established printing workflow process, possibly with an extension of the exisiting PDF/JDF workflow concepts.

### 3.3 Printed modular batteries

The printing of  thin-film batteries is addressing several draw-backs  which state-of-the-art batteries have :static, regulated geometrical form and static contend of energy, which in some cases exceeds by far the consumption the driven circuit during its live cycle. Recently, Willert et al. could present a modular concept for printed serial connections of battery cells based on the zinc-manganese dioxide system elucidating that manufacturing based on the printing workflow is an alternative to contemporary manufacturing techniques (Willert, 2009a) (cf. Figure 7). From the viewpoint of the classical printing workflow, it turns out that the concept of functional printing rather focuses on the particular patterned functional layer as the elementary information than the individual component. In some sense, the patterned functional layer is thus comparable to the halftone elements in the reproduction of colour enabling new modular design concepts of complete electronic systems comprising both power sources, wiring and consumers (Liu, 2009).

Hence, in case of the printed thin-film batteries, the prepress workflow has to cope with the demands of the particular application. As the design determines the layout of each individual required functional layer for the printed battery, the transition from *color separation* to *functionality separation* within the RIP is intriguing.

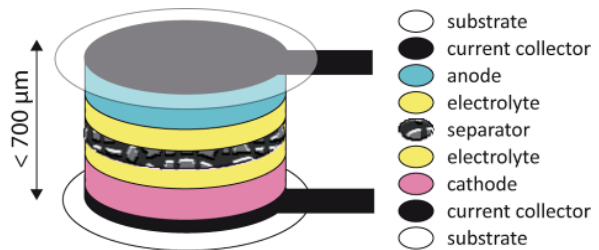*Figure 7: Flexible printed thin-film-battery consisting of two cells*



*Figure 8: Layout of a printed thin-film battery*

In Figure 7 the required layers for a battery setup are shown. Depending on the design concept at least four functional layers needs to be printed. In case of a battery, in the framework of the concept of functionality separations, the definition of the battery layers in term of thickness, printing technology, patterning, drying conditions, etc. can be carried out in the *functional prepress* aside with the definition of e.g. a package where the battery should fit into. All information can be gathered in a PDF/JDF container for manufacturing the package and the battery.

## 4. Conclusions

For the emerging field of functional printing, a concept of *functionality separations* has been derived in analogy to the concept of colour separations in graphical arts printing. The transition from graphical to functional printing requires extensions of the existing printing workflow schemes by post-treatment steps (e.g. curing, annealing, sintering) that are necessarry for the new printed functionalities (e.g. conductivity) and post-press steps (e.g. placement of a Si chip). In the three described examples , conductive patterns, RFID applications and thin-film batteries, the manufacturing of products based on printing technologies requires appropriate modifications of the regular workflow of graphic arts industry. We suggest to introduce new elements into already existing data containers represented as layer information (EPS) or process information (JDF). These information will be separated subsequently in the raster image processor (RIP) for the applying process steps. This extension of the workflow definitions opens additionally opportunities of the integration of further postpress steps, e.g. the electrical connection of supplementary microelectronics with printed layers.

### References

Amidror, 2000   I. Amidror, R. Hersch: *"Neugebauer and Demichel: Dependence and Independence in n-Screen Superpositions for Colour Printing" Colour Research and Applications 25 (4), 267-277 (2000).*

Čermák, 2009   D. Čermák, J. Hammerschmidt, C. Rahnfeld, S. F. Jahn, T. Blaudeck, D. A. M. Egbe, A. Willert, R. R. Baumann, *Digital Fabrication of Functional Nanostructured Layers by Inkjet Printing, Proceedings of Large-Area, Organic and Polymer Electronics Convention 2009 (LOPE-C 09), Frankfurt/M., June 2009, paper no. 1.5.*

Chen, 2008        Y. Chen, R. S. Berns, L. A. Taplin, F. H. Imai: *„Multi-ink colour separation algorithm improving image quality", Journal of Imaging Science and Technology 52 (2), 20604-20609 (2008).*

Jahn, 2010a       S. F. Jahn, A. Jakob, T. Blaudeck, P. Schmidt, H. Lang, R. R. Baumann, *Inkjet printing of conductive patterns with an aqueous solution of [AgO2C(CH2OCH2)3H] without any additional stabilizing ligands, Thin Solid Films 2010 518, 3218-3222 (2010).*

Jahn, 2010b       S. F. Jahn, T. Blaudeck, R. R. Baumann, A. Jakob, P. Ecorchard, T. Rüffer, H. Lang, P. Schmidt, *Inkjet Printing of conductive silver patterns by using the first aqueous particle-free MOD ink without additional stabilizing ligands, Chemistry of Materials 22, 3067-3071 (2010).*

Kiorala, 2008     P. Koirala, M. Hauta-Kasari, B. Martinkauppi, J. Hiltunen: *„Colour Mixing and Colour Separation of Pigments with Concentration Prediction",Colour Research and Applications 33 (6), 461-469 (2008).*

Liu, 2009         J. Liu, I. Engquist, M. Berggren, P. Norberg, M. Lögdlund, S. Nordlinder, A. Sawatdee, D. Nilsson, H. Gold, B. Stadlober, A. Haase, E. Kaker, M. König, G. Klink, K. Bock, T. Blaudeck, U. Geyer, R. R. Baumann, *Integration of Two Classes of Organic Electronic Devices into One System, Proceedings of Large-Area, Organic and Polymer Electronics Convention 2009 (LOPE-C 09), Frankfurt/M., June 2009, paper no. 3.8.*

Locostix, 2008    M. Beigl (ed.): *Low-cost smart labels for logistic processes in consumer retail (Locostix), final report, URL http://www.ft.uni-karlsruhe.de/FORDAT/PROJEKTE/ka9819.htm*

Mandel, 2010      R. Mandel: *"Colour separations revisited", Screen Printing 100 (1), 12-13 (2010).*

Perelaer, 2006    J. Perelaer, B. J. de Gans, U. S. Schubert*, "Inkjet printing and microwave sintering of conductive silver tracks", Advanced Materials 18 (16), 2101-2104 (2006).*

Reinhold, 2009    I. Reinhold, C. E. Hendricks, R. Eckhardt, J. M. Kranenburg, J. Perelaer, R. R. Baumann, U. S. Schubert: *Argon plasma sintering of inkjet-printed silver tracks on polymer substrates; Journal of Materials Chemistry 19 (21), 3384-3388 (2009).*

Willert, 2009a    A. Willert, A. Kreutzer, U. Geyer, R. R. Baumann, *Lab-manufacturing of batteries for smart systems based on printing technologies, Smart Systems Integration 2009 - 3rd European Conference & Exhibition on Integration Issues of Miniaturized System s, March 10-11, 2009, Brussels, Heidelberg: AKA Verlag, 2009, pp. 556-559.*

Willert, 2009b    A. Willert, T. Blaudeck, R. R. Baumann, *Printing Technologies for Functional Layer and Device Manufacturing, 9th Seminar in Graphic Arts, Pardubice/Czech Republic, September 2009, Proceedings, pp. 75-80*

Zichner, 2009     R. Zichner, R. R. Baumann, *Customised Printed RFID Antennas for Various Environments, Proceedings of Large-Area, Organic and Polymer Electronics Convention 2009 (LOPE-C 09), Frankfurt/M., June 2009, paper no. 3.11.*

# Printed electrodes on tailored paper enable extended functionalization of paper

*Jouko Peltonen[1], Anni Määttänen[1], Roger Bollström[1], Martti Toivakka[1], Milena Stępień[1], Jarkko Saarinen[1], Petri Ihalainen[1], Ulriika Mattinen[2], Johan Bobacka[2]*

[1] Centre of Excellence for Functional Materials, Laboratory of Paper Coating and Converting, Åbo Akademi University

 E-mail: Jouko.Peltonen@abo.fi

[2] Process Chemistry Centre, Laboratory of Analytical Chemistry, Åbo Akademi University
 Piispankatu 8, FIN-20500 Turku, Finland

**Abstract**

Silver electrodes were flexographically printed on a paper substrate with controlled smoothness, surface energy and barrier properties. The printed electrodes were utilized for further functionalization of the paper substrate. In the first case study, a droplet of water was placed between the printed electrodes and voltage-induced increase of wetting (decrease of contact angle) in the direction parallel to the electrodes was demonstrated. In the second case study, a polyaniline (PANI) layer inkjet-printed on the silver/paper substrate acted as a working electrode on which a layer of poly(3,4.ethylenedioxythiophene doped with chloride (PEDOT-Cl) was galvanostatically grown in an electrochemical cell.

**Keywords:** printed electrodes; functionalization of paper; contact angle

## 1. Introduction

Currently most of the applications of printed functionality are established on plastic films. However, the recyclability of such devices is poor. A more sustainable alternative is to use paper as the printing substrate. For example, thin, lightweight, and foldable thermochromic display has been realized on a regular copy paper (Siegel, 2009). Paper provides an excellent writing and printing substance, but being a porous, permeable, uneven, and rough network of wood fibres, a specific coating structure is needed to control the roughness and barrier properties of paper.

In this work we demonstrate that a paper substrate with controlled smoothness and barrier properties is suitable for various electrical applications. It has previously been shown that a transistor can be realized on such a paper substrate by all-printing process (Bollström, 2009). Here we show that, thanks to the superior barrier properties of the paper substrate, electrodes printed on it can be applied in liquid environment for e.g. electrowetting (Lippmann, 1875) and electrodeposition (Gerard, 2002) experiments.

## 2. Materials and methods

### 2.1 The paper substrate

The used paper substrate consists of the following coating layers: precoating, smoothing layer, barrier coating and a top coating (Bollström, 2009). Each of the layers has its specific function that allows a printed device to operate successfully. The precoated basepaper ($90 \text{ g/m}^2$) was first blade-coated with a $7 \text{ g/m}^2$ kaolin layer to decrease the roughness. On this smoothing layer a barrier layer was coated, consisting of acrylic or styrene acrylic copolymer latex either as 100% latex or blended with mineral pigments (coat weight $0.5\text{-}20 \text{ g/m}^2$). The surface was made polar by blending mineral pigments (PCC) with the barrier latex, which makes it possible to coat an aqueous top coat on the barrier layer. The top layer is thin and smooth (coat weight $0.7\text{-}5$ $\text{g/m}^2$, layer thickness 0.5-10 μm and RMS surface roughness 55-75 nm) consisting of mineral pigments blended with 7-12 pph of styrene-butadiene latex as binder. PCC and Kaolin were used in this layer in order to provide different absorption properties. The sorption properties can be adjusted through controlled thickness and porosity enabling optimized printability of given functional materials. The materials in the coating structure were chosen in order to retain the recyclability and sustainability of the substrate.

## 2.2 UVC-treatment of the coated samples

An ozone-free low-pressure vapor mercury lamp (Heraeus NNI 120/44U, Germany) was used as the UVC radiation source. The lamp emits UV radiation mainly at 254 nm. The distance between the UV source and the sample was set to 2.5 cm. At this distance, the lamp provided a radiation intensity of 50 mW/cm$^2$. All the treatments were done in ambient conditions. The UVC treatment time was 60 s.

## 2.3 Printing experiments

Flexography printing was carried out using an IGT GST2 laboratory scale printability tester equipped with a commercial OHKAFLEXr (Shore A 64º - 66 º) photopolymer plate. The anilox cylinder had 40 lines/cm and a volume of 20 ml/m$^2$. The printing speed was set to 0.5 m/s. All printings were performed at 23.0 ± 0.2 º C temperature and 50 ± 2 % relative humidity. The conductive ink used in the experiments was a commercial silver ink designed for pad printing (supplied by Creative Materials) and diluted in methyl ethyl ketone (1:5, 17 vol%). The printed Ag electrodes were cured using an infrared (IR) drier (IRT systems, Hedson Technologies AB, Sweden).

Conductive polyaniline (PANI, emeraldine salt, 6.3 wt % dispersion in toluene) was obtained from Panipol Ltd. (Finland). The printing ink was a mixture of PANI (in toluene) and o-dichlorobenzene (o-DCB) with a weight ratio of 1:2. The ink was filtered with 0.2 μm polypropylene (PP) filter prior to printing with a laboratory scale piezoelectric inkjet printer Dimatix DMP-2800 (Fujifilm Dimatix Inc., Santa Clara, USA).

## 2.4 Electropolymerization

The EDOT monomer was purchased from Sigma-Aldrich and KCl (≥99%) from Fluka. Electrochemical polymerization was done with Autolab General Purpose Electrochemical System (PGSTAT 20, Eco Chemie, The Netherlands) in a three electrode system and a one-compartment electrochemical cell, using platinum wire as counter electrode, Ag/AgCl quasi-reference electrode as reference and the paper/Ag/polyaniline (0.44 cm$^2$) as a working electrode.

## 2.5 Contact angle study of electrowetting

The contact angle measurements were performed with a commercial contact angle goniometer KSV CAM 200 (KSV Instruments Ltd., Finland) with an automatic dispenser and motorized sample stage. The images were captured by a digital CCD camera with telecentric zoom optics with a 55 mm lens, and analyzed using the KSV CAM software. The static contact angles of water (Millipore) on Ag film surfaces with 1–4 print layers were measured in air in ambient conditions (RT 23 ± 1 ∘C, RH 30 ± 5%). The size of the droplets in these measurements was approximately 1 μl. Cationic polyDADMAC (CibarAlcofixr169, Ciba Specialty Chemicals) with high ionic conductivity was dissolved in deionized water in different amounts (1, 10, and 20 wt%). All measurements were done in ambient conditions. Contact angles were measured as a function of time and applied voltage. The power source was Kikusui PMC250-0.25A (Kikusui Electronics Corporation, Japan). Measurement time was set to 90 s with a frame rate of 1/s. EW was triggered by applying external potential (voltage of 20 V and a current of 5 mA) at 30s.

## 3. Results

The structure, barrier properties and printability of the paper substrate comprising a precoating, barrier and topcoat layer has been reported previously (Bollström, 2009). The barrier properties appeared to be superior as compared with commercial fine paper and copy paper, and the printability properties clearly better than that of PET. Furthermore, the surface energy of the substrate can be tuned by varying the composition of the topcoating, or by treating it with UVC irradiation, as shown in Figure 1.

The smallest surface energy was observed for the thick PCC top coating. The increasing thickness of the Kaolin top coating also increased the surface energy. Additional increase of surface energy could be generated by UVC-treatment, making the surface more hydrophilic. The benefit of being able to tune the surface energy is obvious, it provides a way of adjusting the print resolution, i.e. the spreading of a functional ink.

Further applications of this substrate in electrowetting and electropolymerization experiments are described in the following.
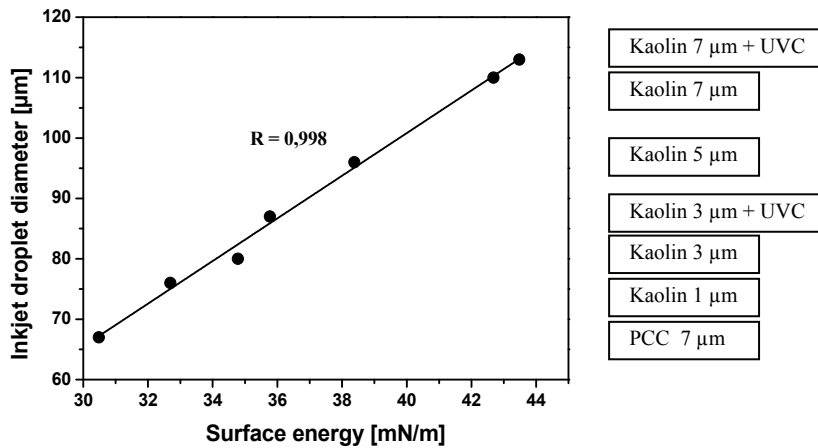
*Figure 1: Spreading and print resolution of a semiconductor ink (Poly(3-hexylthiophene)) as a function of the surface energy of the paper substrate. The composition and thickness of the top coating and possible UVC-treatment for the respective data points is indicated on the right*

### 3.1 Electrowetting

We studied how an external electric field can be used to control wetting of liquids on a substrate. To the best of our knowledge, this is the first time when electric field assisted wetting is demonstrated on a paper substrate. Contact angle (CA) of water (Figure 2) and polyDADMAC solutions as a function of time were analysed. A drop of liquid was injected onto the substrate bridging over the Ag electrodes being printed on it. After a stabilizing period, the electric field triggering was done at 30 s (Figure 2). A voltage-induced abrupt decrease of the contact angle is obvious. Similar kind of effect was found for polyDADMAC, for which the change of contact angle was dependent on, and became slower with increasing concentration of polyDADMAC.

In electrowetting, one is generically dealing with droplets of partially wetting liquids on planar solid substrates. In most applications of interest, the droplets are aqueous salt solutions (Lippmann, 1875; Mugele, 2005). In another approach, an electric field may also be used to modify the surface energy of the surface on which a drop of liquid is brought. Chibowski et al. have shown that surface energy of minerals, e.g. $CaCO_3$ and $Al_2O_3$ can be influenced by an external electric field (Chibowski, 1994; Lubomska, 2001). This situation is quite analogous to the system of this study, where a droplet of pure water is placed on pigment-coated paper between two electrodes. As demonstrated in the schematic drawing of Figure 2, the voltage-induced increase of wetting (decrease of contact angle) indeed takes place in the direction parallel to the electrodes, strongly indicating, that the surface energy of the substrate was modified.
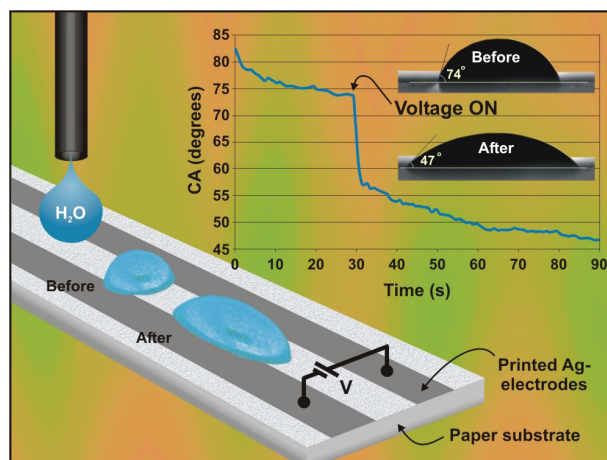


*Figure 2: Contact angle (CA) of water as a function of time. The electric field triggering is done at 30 s, which is clearly seen as a step like function in the contact angle*

### 3.2 Electropolymerization

The setup for the electropolymerization experiments is illustrated in Figure 3. The silver electrodes were flexographically printed on paper, on top of which PANI was inkjetted. In the one-compartment electrochemical cell PANI acted as the working electrode, whereas a platinum wire was used as counter electrode and Ag/AgCl quasi-reference electrode as reference.
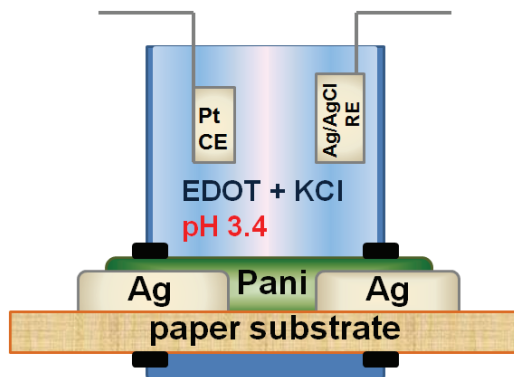


*Figure 3: A schematic illustration of the setup for electropolymerization experiments*

Electrochemical polymerization of (PEDOT-Cl) onto silver/polyaniline (Ag/PANI) electrodes printed on paper was demonstrated. During galvanostatic deposition, the potential of the electrode was measured at constant current density of 0.08 mA/cm$^2$ (Figure 4). The potential-time transient curve for printed Ag/PANI electrode shows three different regions. An initial region, where potential changes sharply with time, corresponds to the charging of the double layer (including oxidation of PANI) and the formation of PEDOT-Cl nuclei (Greef, 1985). The growth of the polymer layer continues in the region where the potential remains approximately constant at about 0.98 V.  This initial time-potential transient is similar to that observed for electropolymerization of PEDOT-Cl on platinum (Bobacka, 2000). This is followed by a region where the potential slowly increases with time up till the end of the experiment. In comparison, the deposition of PEDOT-Cl on TO-glass electrode occurs at about 0.87 V with same current density. The curve lacks the initial region, indicating much faster double layer charging and PEDOT-Cl nucleation kinetics on TO-glass compared to printed Ag/Pani electrode. This can be most probably attributed to a higher conductivity of TO-glass substrate and the absence of elctrochemical oxidation of the substrate itself that may take place in the case of printed Ag/Pani electrodes. In addition, after the short initial stage the potential remains constant throughout the whole deposition process on TO-glass.

The size of the printed PANI area was $1 \times 1$ cm$^2$ (Figure 5A) and the resistance over PANI film was about 50Ω. The deposited PEDOT-Cl appeared as a black circular area on a green Ag/PANI electrode (Figure 5B).
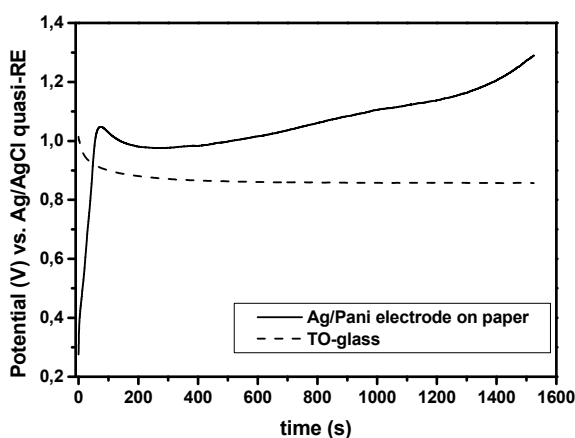


*Figure 4: Potential transient for electrodeposition of PEDOT-Cl on Ag/PANI and TO-glass electrodes at current density of 0.08 mAcm$^{-2}$ in 0.1 M KCl + 0.01 M EDOT*
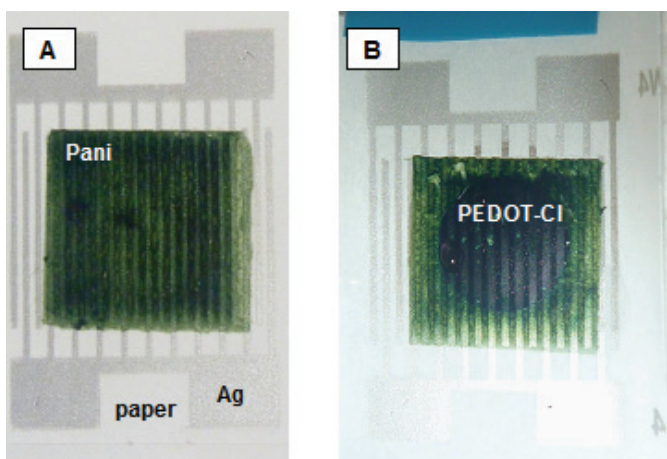
*Figure 5: Digital images of printed Ag/PANI electrodes (A) before and (B) after the electrodeposition of PEDOT-Cl. The Ag pattern was formed with flexographic printing and PANI polymer film with inkjet printing*

## 4. Conclusions

The presented results show that a paper substrate with controlled smoothness, barrier properties and surface energy is suitable as a printing substrate for functional inks like metals and conducting polymers. The print characterisics may be tuned by the choice of the top coating parameters like type of pigment, layer thickness and pretreatment. As a results, printed electrodes together with superior barrier properties of the paper substrate enabled the demonstration of various applications in liquid environment. In summary, the paper substrate provides a cheap, flexible and sustainable platform for developing various functional devices for e.g. printed electronics and smart packages.

## Acknowledgements

## References

Bobacka J., Lewenstam A., Ivaska A., (2000), *Electrochemical impedance spectroscopy of oxidized poly(3,4-ethylenedioxythiophene) film electrodes in aqueous solutions, J. Electroanal. Chem., 489, 17-27*

Bollström R., Määttänen A., Tobjörk D., Ihalainen P., Kaihovirta N., Österbacka R., Peltonen J., Toivakka M., (2009), *A multilayer coated fiber-based substrate suitable for printed functionality, Organic Electronics, 10, 1020-1023.*

Chibowski E., Holysz L., Wojcik W., (1994), *Changes in zeta potential and surface free energy of calcium carbonate due to exposure to radiofrequency electric field, Colloids and Surfaces A, 92, 79-85*

Gerard M., Chaubey A., Malhotra B. D., (2002), *Application of conducting polymers to biosensors. Biosens. Bioelectron., 17, 345-359.*

Greef R., Peat R., Peter L. M., Pletcher D., Robinson J., (1985), *Instrumental Methods in Electrochemistry, Ellis Horwood: Chichester, UK.*

Lippmann G., (1875), *Relations entre les phénomènes électrique et capillaries, Ann. Chim. Phys., 5, 494-549.*

Lubomska M., Chibowski E., (2001), *Effect of radio frequency electric fields on the surface free energy and zeta potential of $Al_2O_3$, Langmuir, 17, 4181-4188*

Mugele F., Baret J.-C., (2005), *Electrowetting: from basics to applications, J. Phys.; Condens. Matter, 17, R705-R774*

Siegel A. C., Phillips S. T., Wiley B. J., Whitesides G. M., (2009), *Thin, lightweight, foldable thermochromic displays on paper, Lab Chip, 9, 2775-2781.*

# The impact of paper coatings on printed electronics

*D. C. Bould, T. C. Claypole and D. T. Gethin*

Welsh Centre for Printing and Coating, Swansea University
Singleton Park, Swansea SA2 8PP, United Kingdom
E-mail: d.c.bould@swansea.ac.uk

**Abstract**

The ability to use paper as a substrate for printed electronics is limited by the tendency of the ink to penetrate into the internal structure of the paper, resulting in breaks in the conductive tracks. It is possible to alleviate this by selection of a suitable coating to be applied to the paper substrate, to prevent excessive penetration of ink away from the paper surface. An investigation has been performed whose objective was to assess the conductivity of silver and conductive carbon inks on a range of coated paper samples, to determine the effect that the type of coating and the coating weight has on the conductivity of printed tracks. Conductive silver and carbon inks were printed onto different paper coatings and their resistivity determined.

It was concluded from the investigation that the roughness of the paper surface has an effect on the conductivity of the samples. Improved line structure was observed where the liquid phase of the ink was able to penetrate more easily away from the paper surface, than where immobilisation into the substrate was restricted.

**Keywords**: flexography; electronics; barrier coatings

## 1. Introduction

The ability to use paper as a substrate for printed electronics is limited by the tendency of the ink to penetrate into the internal structure of the paper, resulting in breaks in the conductive tracks. It is possible to alleviate this by selection of a suitable coating to be applied to the paper substrate, to prevent excessive penetration of ink away from the paper surface.

The selection of the paper coating can potentially have a large impact on the range of applications for printed electronics on paper. These range from interactive or addressable posters, to printed sensors. Although a limited amount of research has been performed into the printing of conductive inks on paper, the majority of previous research focuses on the deposition of functional materials on planarised polymer films, where it is possible to create high value added devices. However, Claypole et al (2004) showed that it is possible to deposit conductive tracks onto a porous substrate, whilst still maintaining functionality. However, this study was performed using offset lithography, where, due to the low film weights, it was not possible to draw explanations to some of the trends observed.

The objective of this investigation was to assess the conductivity of silver and conductive carbon inks on a range of coated paper samples, to determine the effect that the type of coating and the coating weight has on the conductivity of printed tracks. The flexographic printing process was adopted as the process of choice, to deposit higher film thicknesses than those obtained by Claypole et al (2004).

## 2. Methodology

### 2.1 Sample preparation

To improve the understanding of how paper coatings can affect the conductivity of printed track on a porous substrate, different coating types, which varied according to coating pigments, were applied to a common paper stock. The samples used for the experimental investigation were prepared by Imerys Pigments for Paper Ltd. The coatings were applied to the paper surface by blade coating. Although a wide range of different samples were prepared, analysis is restricted to three different coating types, for the purposes of this investigation. For each case, the coating weight was maintained at 7 gsm, although in the case of Coating A, an additional top coat of latex was applied to the coated paper surface. The paper samples were characterised according to surface roughness, using a Parker Print Surf 1000. The roughness for each of the samples analysed is shown in Table 1.

*Table 1: Roughness of coated paper samples*

|  | Surface Roughness ($\mu$m) |
| --- | --- |
| Coating A | 0.53 |
| Coating B | 1.73 |
| Coating C | 4.63 |

In addition to the printing of the paper samples, a filmic substrate, whose surface has previously been shown to be receptive to solvent based conductive inks, were also assessed, for the silver ink only. The roughness of the filmic substrate was measured as 0.20$\mu$m.

## 2.2 Printing trials

The experimental investigation was performed using an RK Flexiproof 100 Printability Tester. The paper and filmic samples were printed using flexographic conductive silver and carbon inks, supplied by Gwent Electronic Materials Ltd, although the filmic substrate was printed for the silver ink only, as stated above. An Asahi AWP plate was supplied by Asahi Photoproducts. As the anilox on the RK Flexiproof comprised two discrete bands, the image was designed accordingly, allowing the performance of the coated paper samples to be assessed for two different anilox volumes. The anilox volumes selected were 13cm$^3$m$^{-2}$ and 18cm$^3$m$^{-2}$. The image used is shown in Figure 1. For the purposes of the investigation, only the horizontal and vertical lines were analysed.
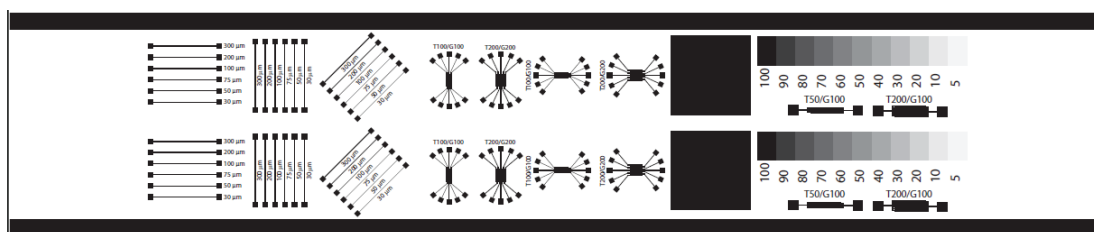


*Figure 1: Image for trial*

The printing speed was maintained at 25m/min for all samples. The pressure between both the anilox-plate and plate-substrate was also held constant for the duration of the experiment. To improve the conductivity of the samples, each sample was printed twice, with the second pass immediately following the first, without removing the sample from the printability tester. No registration issues were observed between the first and second pass. After each sample had been printed, it was dried in an oven, at 60°C for 10mins. This was shown not to have a long term effect on the paper samples, as although moisture was removed from the substrate during drying, the samples were allowed to reabsorb moisture before analysis, returning them to their original condition.

## 2.3 Analysis

Following the printing of samples, the resistances (in ohms) of the lines were quantified using a Keithley 2 point probe measuring system. It should be noted that due to the porous nature of the paper substrates, some of the charge carrying conductive particles may have penetrated into the paper structure, which could have an influence on the conductivity measurements. However, it was considered that the overall impact of this phenomenon would be low as once the particles have penetrated away from the paper surface, their ability to transmit charge along the printed track will be limited.

White light interferomentry was used to assess the topographical profile of the printed lines. The data obtained from the white light interferometry measurements was used to determine the height of each line, as well as to assess the overall printed line quality. Using the data generated from the resistance measurements, using the 2 point probe system, in conjunction with the white light interferometry analysis, the resistances were converted to give data in terms of Ohms/square. This was to normalise the effect of printed line width and ink film thickness due to the different line widths and anilox volumes.

Due to difficulties differentiating between substrate and ink, for some measurement, using white light interferometry, Focused Ion Beam measurements were also used to provide an assessment of the topographical structure of the line.

## 3. Results

The normalised data for the 300μm silver printed lines is presented in Figure 2, and the data for the 100μm silver printed lines is presented in Figure 3. For both sets of data, the three paper coating types are compared to the filmic substrate. For both line thicknesses, Coating A provides the lowest resistance, followed by Coating B and then Coating C. However, in all cases, the resistances are lower than those obtained when printing onto the filmic substrate, with the exception of the 100μm vertical lines for the 13cm$^3$m$^{-2}$ anilox, where no conductivity was obtained on the paper samples, and also the 100μm horizontal lines for the 18cm$^3$m$^{-2}$ anilox, where the normalised resistance of the filmic substrate was lower than for Coating C. The lack of data for the 100μm vertical lines for the 13cm$^3$m$^{-2}$ anilox on the paper samples was attributed to a small break in the line on the plate. For the filmic substrate sample, as no ink penetrated into the substrate, the squeezed ink film was able to overcome this gap, providing continuity. However for the paper samples, as the ink was absorbed by the substrate, there was less ink squeeze on the surface of the substrate, and the break in the line remained un-bridged.
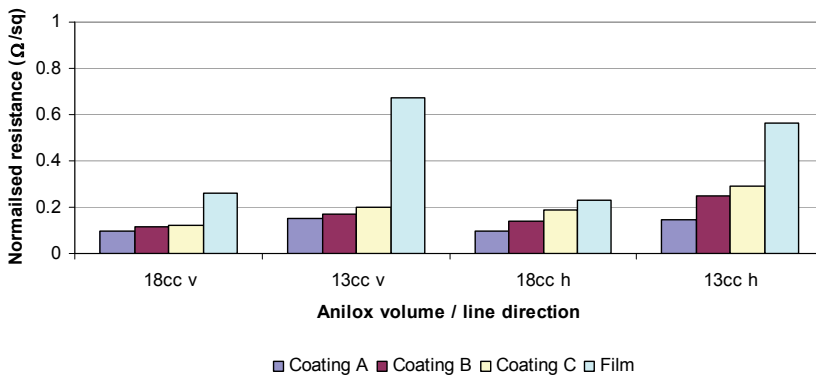


*Figure 2: Normalised resistances for horizontal and vertical 300μm lines - Silver ink*
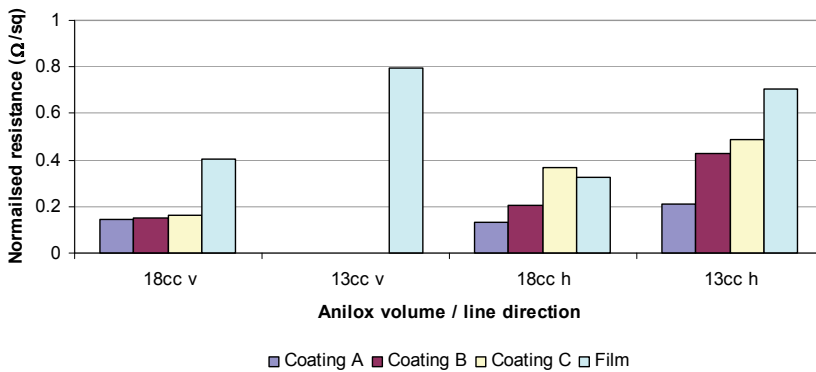


*Figure 3: Normalised resistances for horizontal and vertical 100μm lines - Silver ink*
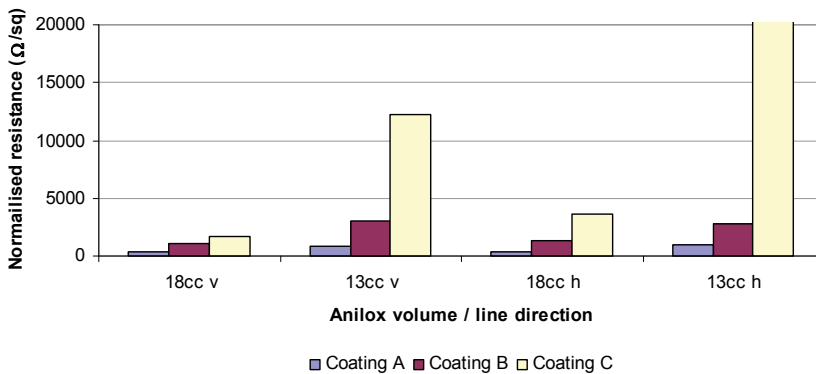


*Figure 4: Normalised resistances for horizontal and vertical 300μm lines - Carbon ink*

The normalised data for the 300µm carbon lines is presented in Figure 4. Similar trends were observed for the 100µm lines. The resistances of the carbon tracks are three to six orders of magnitude greater than those observed for the silver lines. Figure 4 also shows much greater differences in resistance between the coating types, particularly for Coating C, whose resistances were generally much greater than Coatings A and B. the normailsed resistance of the horizontal line for Coating C at 13cm$^3$m$^{-2}$ was observed at being 58kΩ/sq. With the exception of the results for Coating C, there was little difference in the resistances between the vertical and horizontal lines, for the carbon inks.

White light interferometry images of the 300µm lines for Coatings A and B are presented in Figure 5. Due to the high roughness of the substrate surface for Coating C, it was not possible to detect the printed profile of the lines for that particular paper coating. The images show that whilst the printed line is more clearly defined for the smoother paper surface (Coating A), the ink has been squeezed to the edges of the line structure. For the line printed on Coating B, although the line is less clearly defined, compared to the roughness of the paper surface, the line appears to have much greater homogeneity. As Coating A has the additional top coat of Latex, there is less penetration of the liquid phase of the ink for Coating A, forcing the ink to be squeezed laterally, in the printing nip. As the amount to which an ink can be immobilised in the paper increases, the liquid phase of the ink is able to penetrate into the paper structure through the printing nip, resulting in reduced ink film squeeze, and greater homogeneity of printed line structure.
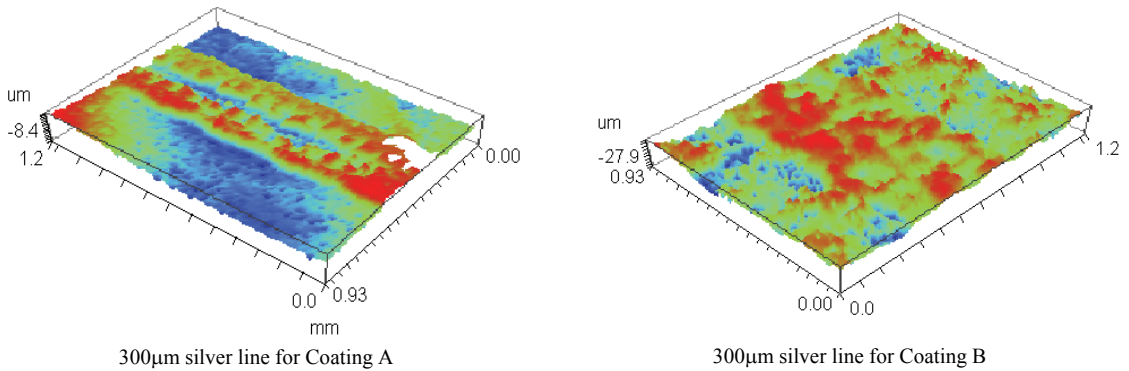


300µm silver line for Coating A          300µm silver line for Coating B

*Figure 5: White light interferometry images of 300µm silver lines for Coatings A and B*

In order to investigate further the effect of ink penetration into the substrate and its effect on the topographical profile of the printed line, Focused Ion Beam (FIB) images were obtained for two lines; a 300µm line for Coating B, where good uniformity of the line was observed using white light interferometry, and a 300µm line printed on the filmic substrate, where no penetration into the substrate structure is possible. The results, shown in Figure 6, confirm that where the liquid phase of the ink is able to penetrate into the paper, improved line profiles are obtained. For the case of the filmic substrate, the ink is squeezed such that the 300µm line has split into two discrete lines.
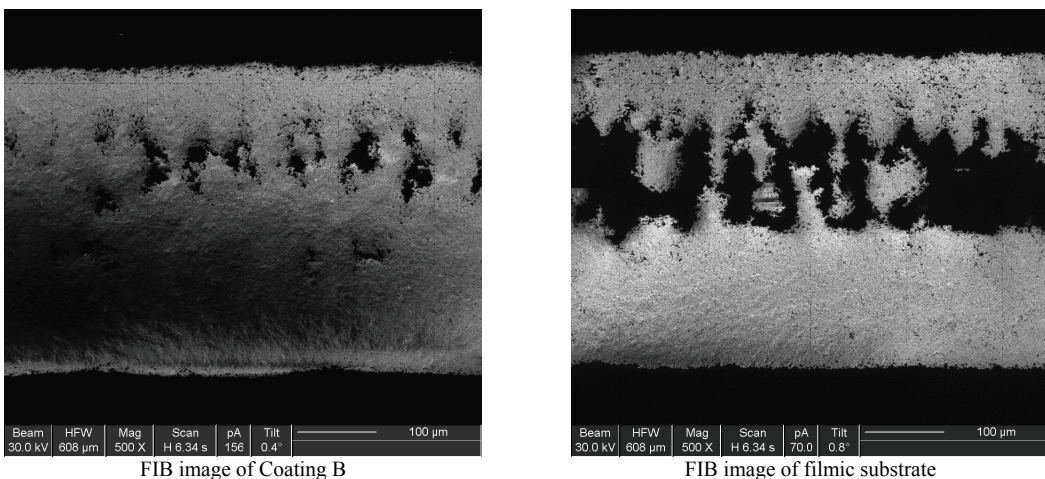


FIB image of Coating B          FIB image of filmic substrate

*Figure 6: Comparison of Focused Ion Beam images for line profiles of Coating B and filmic substrate*

## 4. Discussion

This investigation has highlighted the potential for the use of paper, as a substrate for plastic electronics. During the course of the investigation it has been noted that the paper samples coated with Coating A provide the best conductivity, giving superior results to those obtained using a filmic substrate. However, it was also observed that the best line structure was obtained for Coating B, where the liquid phase of the ink was able to penetrate into the paper structure, rather than being squeezed laterally in the printing nip. From these results, it is possible to further optimise the paper surface structure to give the conductivities of Coating A, whilst producing the line structure of Coating B.

For the silver inks, the resistances for the horizontal lines were slightly greater than the lines running in the direction of print. However, little difference was observed between the two print directions for the carbon inks. A previous investigation into the printing of functional lines by flexography (Bould et al., 2009), showed that horizontally printed lines showed lower resistances than vertical lines. Further investigation is required to fully understand the effect of line direction on the functionality of a printed line.

The results obtained in the investigation demonstrate that whilst paper will not be a suitable substrate for printed electronics where low surface roughnesses are required, it is a suitable substrate, and may even be a superior substrate for low mobility devices, due to the improved conductivity over the filmic substrate. A further benefit is the reduced environmental impact of using paper over plastic film. However, a key challenge that needs to be investigated further is the improved barrier performance of the paper coatings, so that functionality is not compromised by moisture or the presence of oxygen over the lifetime of the device.

## 5. Conclusions

As a result of the investigation, it has been concluded that:
- Good conductivities can be obtained on coated paper samples;
- Smooth paper surfaces offer improved resistance over rougher paper samples;
- The printed line structure is best where the liquid phase of the ink is able to penetrate into the substrate structure in the printing nip, rather than being subjected to lateral squeeze;
- Silver inks give conductivities three to six orders of magnitude better than those obtained for conductive carbon inks, for the same printing conditions.

### Acknowledgements

### References

Bould D. C., Claypole T. C. and Gethin D. T. "An Investigation into the performance of biodegradable plastic electronics by flexography", Advances in Printing and Media Technology, Vol. 36, pp415-420, 2009

Claypole T. C., Jewell E. H. and Ray W. J "Printing of conducting inks on paper", Proceedings of the 56th Annual TAGA Technical Conference, pp541-550, 2004

# Production of colored nanocrystalline cellulose (NCC) films

*Christine Canet*[1]*, Alice Vermeulin*[1]*, Fyrial Ghozayel*[1]*, Jean-David LeBreux*[1]*,*
*Yasser Kadiri*[2]*, Gilles Picard*[2]*, Dominique Simon*[2]

[1] QIGC - The Quebec Institute of Graphic Communications
999 Emile Journault Avenue East, Montréal (Québec), Canada H2M 2E2

E-mails: ccanet@icgq.qc.ca, avermeulin@icgq.qc.ca, fghozayel@icgq.qc.ca, jdlebreux@icgq.qc.ca,

[2] Ahuntsic College
9155 Saint-Hubert, Montréal (Québec), Canada H2M 1Y8

E-mails: yasser.kadiri@collegeahuntsic.qc.ca, gilles.picard@collegeahuntsic.qc.ca
dominique.simon@collegeahuntsic.qc.ca

### Abstract

The Quebec Institute of Graphic Communications (QIGC) has been conducting a three-years R&D project aiming at developing a liquid printing material made of nanocrystalline cellulose and its print applications. Among the vast area of promising applications NCC might offer, QIGC has decided to focus on developing a liquid printing material made of NCC in order to introduce security elements like latent patterns and/or specific colors in a print. Color produced by thin NCC films is not due to the presence of pigmented element, but results from light interferences on NCC self-organized as a Bragg network. Counterfeiting of such an "ink" will thus be seriously compromised. This project comprises several steps, among which: 1/ The identification and understanding of parameters controlling the color of a thin NCC solid film; 2/ The characterization and mapping of the whole range of reproducible colors; 3/ The formulation of a printing material made of NCC and 4/ The development and establishment of a procedure to obtain predictable and consistent target colors. The present paper aims to present used methodology. It also highlights achieved results-to-date and describes future steps and main issues to overcome to complete successfully this project.

**Keywords:** nanocrystal; color; new generation ink; nancrystalline cellulose films

## 1. Introduction and background

Two years ago, the Quebec Institute of Graphic Communications (QIGC) was awarded a grant of half a million Canadian dollars by the Quebec government (the MDEIE department: Ministère du Développement Économique, de l'Innovation et de l'Exportation) to conduct a three-years R&D project aiming at developing a liquid printing material made of nanocrystalline cellulose and its print applications. Initiated by the QIGC, this highly promising nanotechnology development project is carried out in partnership with FPInnovations.

Although cellulose whiskers (nanocrystalline cellulose, NCC hereafter) have existed for a few decades, FPInnovations only recently developed and patented (in 2006) the process enabling a large-scale production of these nanocrystals. Thanks to this brand new material availability, its potential industrial applications now become of interest. Among the interesting NCC properties, one holds our attention: NCC in suspension tends naturally to self-assemble in a liquid crystalline texture, producing solid films showing various iridescence colors once dried.

*NCC or nanocrystalline cellulose is a colloidal particle of about 150 nanometers length and 10 nanometers width. It deals with the smallest solid cellulose entity isolated successfully today.*

The behaviors of NCCs are still not well understood. Moreover, in most of the currently existing application developments, NCC is mostly being used as an additive aiming at improving mechanical properties. Only very few people are currently working on NCC's color properties.

## 2. Objective

Among the vast area of promising applications NCC might offer, QIGC has decided to focus on developing a liquid printing material made of NCC in order to introduce security elements like latent patterns and/or specific colors in a print. Color produced by thin NCC films is not due to the presence of pigmented ele-

ments, but results from light interference on self organized NCCs acting as a Bragg network. Counterfeiting of such an "ink" will thus be seriously compromised.

Several steps are required to complete the project:

◊ Identification and understanding of parameters controlling the color of a thin NCC solid film;

◊ Characterization and mapping of the whole range of reproducible colors;

◊ Formulation of a printing material made of NCC;

◊ Development and establishment of a procedure to produce predictable and consistent target colors.

## 3. Research methods

Based on our previous literature review, NCC will very likely be used in suspension. Compatible materials and key parameters such as concentration and rheological properties need to be identified to create the final printable NCC formulation.

Three research steps were required prior to the realization of this project.

A. Characterization of liquid NCC suspensions:

A specific methodology was developed to determine the mechanical and dynamic behavior of cellulose nanocrystals in an aqueous suspension.

B. Characterization of thin NCC films:

The purpose was first to lay down a thin layer of NCC. A methodology was then developed to measure the spectral response of NCC thin films as a function of the wavelength. Films were measured in both transmission and reflection modes.

C. Identification and understanding of NCC suspension deterioration over time:

As some bacteria formation was identified in the suspension, a methodology was developed to prevent contamination by some microorganisms. It is now possible to use a NCC suspension whatever its age so long as it is decontaminated using this methodology.

To guarantee the project success, QIGC has gathered a team made of experts and specialized scientists in cellulose whiskers, in assembling and auto-assembling of nanomaterials, in mathematic modeling and in simulation of nanostructured materials as well as in printing technologies, in colorimetry and in polymer chemistry. FPInnovations works in collaboration with the group at QIGC by sharing their NCC knowledge and expertise to support these studies.

Our chosen methodology consists of building a mathematical modelling to simulate light interference in dried NCC films. Experimental data have been used to fit the model and be able to predict colors. Realization and characterization of thin NCC films allow for instance validation of the different parameters responsible for color such as NCC concentration, additives etc. These parameters will help to define specifications required to build a color map of reproducible colors. Finally, formulation and properties of NCC printing material will remain to be adjusted and fine-tuned.

## 4. Summary of experimental results

Main advances will be first released at the IARIGAI conference 2010. The most significant and relevant experimental results related to either the identification and understanding of some parameters controlling the color of solid NCC films will be presented.

When the NCC concentration exceeds 4.5% (w/w), a NCC suspension has a cholesteric structure, which forms a helical pattern. The helix pitch can be determined by using a laser diffraction technique. The drying of NCC suspensions permits the formation of chiral nematic iridescent NCC films. After having tested various initial NCC states to evaluate their effects on the resulting colors, it was found that a color shift from blue to red in iridescent dried NCC films can be achieved via a patent pending pre-treatment - developed by FPInnovations - applied to the NCC suspension prior to film casting. Also an addition of NaCl salt moves the color back towards the blue end of the spectrum.
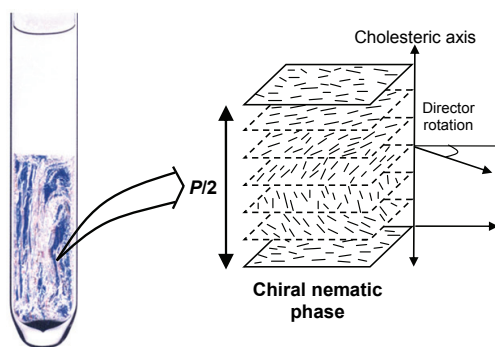
*Fig. 1: Illustration of NCC cholesteric structure*
*Source: Xue Min Dong and Derek G. Gray, Langmuir, 13, 2404-2409 (1997)*

According to the Bragg law, the achieved colors correlate with the helix pitch of the NCC film and thus with the pre-treatment and salt addition.

The pre-treatment methodology was further developed and different parameters were fine-tuned. Parameters influencing the film color were also identified, such as: the NCC concentration, quantity of salt added and parameters of the pre-treatment.

For the moment, the obtained films are iridescent. In other words, the color and intensity of the dried NCC films depend on the viewing angle. Moreover, the time scale for NCC auto-organization is on the order of minutes. But this result is already promising for a potential application.

However, to fit in an industrial context, some characteristics need to be improved, including the color intensity and the opacity of the dried film as well as the time required to show colors.

Once the parameters ensuring consistency of color reproduction are identified, three remaining steps have to be completed:

◊ A printing material has to be formulated. It has to be compatible with the selected printing process in terms of rheological, transfer and drying properties, press stability, resistance properties once dried, etc.

◊ Achieved colors with the formulated NCC dispersion laid down with the selected printing process have to be characterized and mapped. Also the combination of one or several different printing materials composed of different NCC states will be investigated.

◊ A procedure to reproduce consistent target colors has to be established and developed.

## 5. Conclusions

Emphasis is right now put on the critical point, which consists of establishing a normalization method of NCC suspensions taking into account parameters such as pH, nanocrystal size and shape, viscosity, density, etc. This will guarantee the reproducibility of targeted colorimetric effects from batch to batch. Measuring methods are also being developed and need to be validated.

Then challenges identified as further priority axes in this project consist in accelerating the NCC auto-organization process and improving the film colorimetric properties (i.e. increase areas where color is uniform). Actually, even if NCC auto-organization is feasible on-demand, it takes a long time and colorimetric discontinuity (i.e. a kind of iridescence) is noticed.

Potential applications of this project are wide for the graphic industry. Hereafter a non-exhaustive list introduces some of them:

◊ Security elements printed with this new "ink" would be almost impossible to counterfeit in color, as the material does not contain any physical color,

◊ This new printing material could replace some specific inks or varnishes,

◊ Thanks to such a project, this new "ink" could be ultimately substituted for quadrichromic inks (cyan, magenta, yellow and black) traditionally used in the printing industry.

Printing presses would be extremely simplified: laying down by successive printing of layers of this new NCC fluid, *a priori* totally recyclable (printing of cellulose on cellulose). Besides, if all of these project phases pass, the whole graphic chain will be changed as traditional proofing and color management systems would have to be completely rethought.

## Acknowledgments

## References

[1] Y. Habibi, L. A. Lucia and O. J. Rojas, Cellulose Nanocrystals: Chemistry, Self-Assembly, and Applications, Chem. Rev., 2010.

[2] D. Simon, Y. Kadiri and G. Picard, Nano cellulose crystallites: optical, photonic and electro-magnetic properties, NSTI, 2008.

[3] Y. Kadiri, D. Simon, G. Picard, F. Ghozayel and J.-D. Lebreux, Nano Crystalline Cellulose - Structural and Optical Properties by Molecular Dynamic Simulations NSTI, 2010.

# Printing and coating of T4 phage based bioactive paper

*Tarik Jabrane*[1]*, Meije Laloi*[1,2]*, Martin Dubé*[1]*, and Patrice J. Mangin*[1]

[1] Centre Intégré en Pâtes et Papiers (CIPP)
 Université du Québec à Trois-Rivières
 3351 boul. Des Forges, C.P. 500 Trois-Rivières, Québec, Canada G9A 5H7

 E-mails:Tarik.Jabrane@cipp.ca, Martin.Dube@cipp.ca, Patrice.Mangin@cipp.ca

[2] PAGORA, 461 Rue de la papeterie, BP 65
 F-38402 Saint-Martin d'Hères, France

 E-mail: meijelaloi@gmail.com

### Abstract

Several bio-agents such as enzymes, viruses or antibodies, can be deposited on paper in order to increase its functionalities. In this work, we demonstrate that a bioactive paper that can destroy *E. Coli* bacteria can be effectively produced by printing or coating a solution containing T4 phage. We show that the T4 phage resists to the shear stress and infrared drying encountered in printing and coating operation but that a bioactive paper containing only T4 phage on its surface rapidly becomes inefficient though drying.

This problem is solved using inks and coating colour containing gelatine. We show that the gel formed at the surface after coating protects the phage from moisture loss for time periods extending to several days.

**Keywords:** bioactive packaging; printed functionality; pathogen disabling

## 1. Introduction

Complex bio-molecules such as enzymes and proteins can now be directly printed on a support (either rigid or flexible) for applications as diverse as protein analysis (Roda, 2000), DNA sampling (Okamoto, 2000), neural science (Sanjana, 2004) or even tissue engineering (Boland, 2006). The development of reliable printing techniques based on ink-jet technologies (Di Risio, 2007, Bruzewicz, 2008), microcontact printing (Renault, 2003) or soft lithography (pad printing (Thibault, 2007)) whether used alone or in combination with sol-gel technology (Hossain, 2009) has opened extremely rich possibilities for research. It is already clear that deposition of bio-molecules on paper can provide an effective and low-cost platform for several types of diagnosis (Pelton, 2009).

Bacteriophages, commonly called phages, are particularly interesting in light of bio-active paper production. These viruses, non-harmful to humans, can infect and destroy several types of bacteria, are abundant and cheap to produce and, if combined to food, do not alter its properties. In this work, we use the T4 phage, acting specifically on the *E. Coli O157:H7* bacteria stain (Oda, 2004). Since this strain can easily contaminate ground beef, raw milk and chicken as well as water (McMeekin, 2003), a bioactive paper containing T4 phage could be used as packaging.

There are several techniques to immobilize phages on a substrate (Zourob, 2010). Physical adsorption is the simplest, but results in very weak adhesion and efficiency (Su, 2007). Phage grafting on cellulose is possible (Gervais, 2007; Ong, 1989), but is not necessarily an economical way to produce bioactive paper. We have previously shown that T4 phages could be printed on paper using conventional printing equipments (Jabrane, 2008), with improved efficiency coming from a cationic pre-layer (Jabrane, 2009). In this work, we use image analysis to quantify bioactive paper production using printing and coating. We show that the bacteriophages are extremely resistant to the shear stresses and infrared-drying encountered during these processes but that open-air storage will harm their efficiency. To remediate to this problem, we use type-A gelatine as a moisture-retaining network that can increase paper bioactivity for several days.

This work is carried within the Sentinel Network (www.bioactivepaper.ca), a broad collaboration of Canadian universities, research centres and industrial partners which aims to develop the biological potentialities associated with paper, whether as filter papers, bio-sensors or virus deactivators.

## 2. Materials and Methods

### 2.1 T4 Bacteriophage

The T4 phage can be represented as an oblong molecule of about 200 nm in height for 60 nm in diameter. It is composed of a negatively charged "head" and a "tail" that binds to the bacteria (Fig. 1). T4 phage is specific to *E.Coli* bacteria. The infection mechanism by T4 virus takes approximately 30 minutes at 37°C. It begins with the adsorption of the phage with the long fibres. A contractile tail shortens to allow a syringe-like tube to enter the cell membrane, emptying the DNA content of the head into the bacterium. Once the genetic material is introduced, the phage replicates its genome and uses the bacterium's metabolic machinery to synthesize phage enzymes and phage structural components. The phage parts assemble around the genomes, and hundreds of new viruses are generated inside each bacterium until it bursts open (being effectively killed). The newly released bacteriophages are then free and ready to infect other bacteria. T4 bacteriophage lysate stock of $10^9$ phage/ml (plaque forming unit) was obtained by enrichment and concentration of an initial stock obtained from the microbiology laboratory of the Université du Québec à Trois-Rivières (UQTR, Trois-Rivières, Québec).
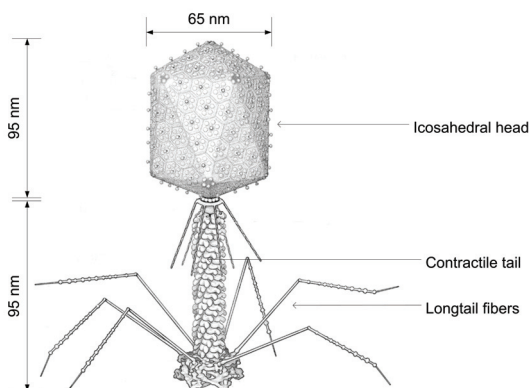


*Fig. 1: Schematic representation of T4 bacteriophage, composed of an anionic head and a tail terminated by long tail fibres. To infect and destroy bacteria, the phage tail fibres must be in contact with bacteria*

### 2.2 Printing system and bioactive ink formulation

The water-based bioink was composed of 0.9% in weight of sodium chloride (to assure osmotic pressure equilibrium) in which were diluted $10^7$ phages/ml and 1% in weight of Carboxy Methyl Cellulose (CMC) as viscosity modifier. The viscosity of the bio-ink was 50 mPa.s as measured from a Brookfield viscometer.

The bioink was printed onto 50x300 mm paper strips using an IGT Global Standard Tester 2 with gravure printing disc (Fig. 2) at velocities ranging from 0.2 to 2m/s and printing force from 100 to 600N. Printing was done in conditioned atmosphere, 50% relative humidity and 23°C according to TAPPI standard method T 402 sp-03. A softwood mechanical pulp base paper (basis weight 44g/m²) was used.
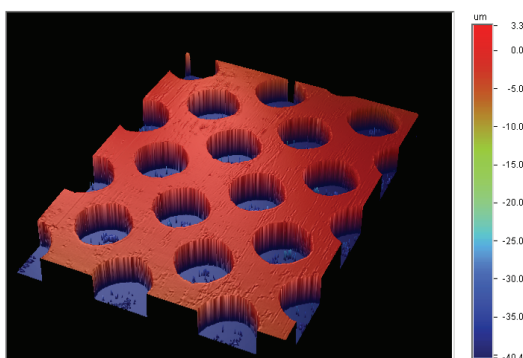


*Fig. 2: Gravure printing disc surface characterization. Coverage is 42% with dot radius of 95 microns and depth of 30 microns*

Ink transfer characteristics of the ink/gravure disk system were evaluated by adding a dye to the bio-ink and recording the colour change using a spectrometer (Technidyne Color Touch). The CIE L*a*b* color system (Kipphan, 2001) was used and color changes were quantified with the ΔE value. The results, illustrated on Fig. 3 show essentially that an increasing printing speed from 0.2 m/s to 2m/s do not significantly affect the ink transfer rate, while on the other hand, an increase of the printing force (an indication of printing pressure) from 100N to 600N tends to increase the ink transfer rate to the paper (De Grâce, 1984) .
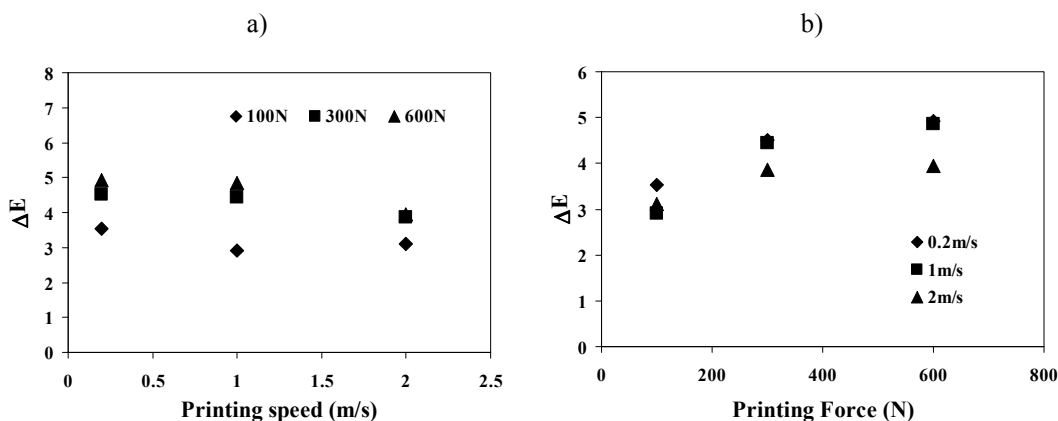
a)                                                                                    b)



Fig. 3: Ink transfer characteristics. At constant force, transfer is relatively constant while it increases with printing force at constant velocity

## 2.3 Coating system and bioactive coating colour formulation

Coating was performed with a Cylindrical Laboratory Coater (CLC-7000, Simutech). This instrument is designed to reproduce the complete coating process on a laboratory scale. It can coat a wide range of base papers at speeds (up to 800 m/min) comparable to pilot machines and offers great flexibility in the choice of coating color (pigments, binders and other additives) and coating method (blade or rod coating). Blade coating experiments were done with a steel blade of 0.018 in thickness. Coat weight deposition can be controlled through *i)* coating colour viscosity *ii)* coating speed and *iii)* blade pressure, this last parameter being effectively adjusted by controlling the gap between the blade and the paper surface. Increases in viscosity, coating speed and blade pressure all result in an increase in the shear stress sustained by the biomolecules. In general, increasing the coating speed and coating color viscosity will increase the coat weight applied while increasing the blade pressure will reduce coat weight.

Pork type-A gelatine was obtained from Fisher Scientific. Various solutions containing up to 10% gelatine in weight were prepared. The gelling point of a 1% gelatine solution was 20 °C while the gelling point was of 30 °C for a 10% in weight gelatine solution. Above the gelling temperature, the viscosity of the solution ranges from 5 mPa.s to 40 mPa.s as shown in Fig. 4.
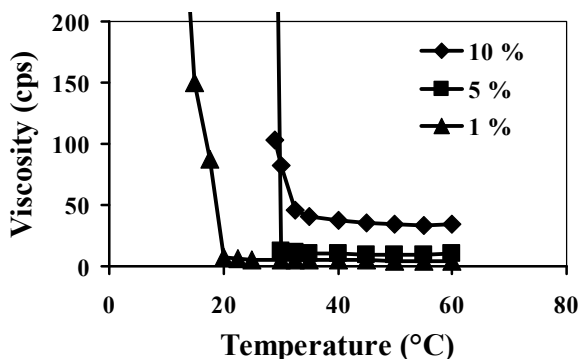


Fig 4: Gelling point and viscosity of bioactive coating color formulation

Two different coating colours were prepared. A first coating colour with a viscosity of 100 mPa.s was prepared with $10^7$ phages/ml, 5% in weight gelatine and 3% in weight CMC. The second coating colour was prepared similarly but with 5% in weight CMC, yielding a viscosity of 250 mPa.s.

## 2.4 Assessment of biological efficiency

Quantitative measurement of the bioactivity of the papers is obtained from a culture method. An *E. Coli* bacterial broth culture is first prepared according to standard techniques (Kropinski, 2008). The printed/coated bioactive papers are then cut into 6 mm diameter discs, and carefully placed on top of the bacterial lawn. The bioactive paper/bacteria is then left to incubate for 12 hours at 37°C. Regions with bacterial activity are optically turbid and can thus be differentiated from transparent regions in which phages have impeded bacterial growth. The area of the transparent zones can be measured through image analysis using Adobe Photoshop CS3 and is taken as the metric of bioactivity. In this work, the lysis area is denoted A and has units of [mm$^2$]. This method cannot be used to obtain the quantity of phages effectively deposited on the paper but allows comparative studies of different deposition methods (printing, coating) and parameters, different base papers and different bio-ink or coating colour formulations.
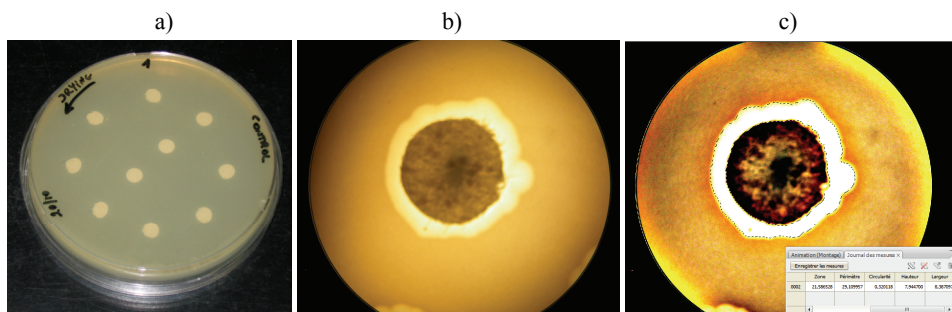


a)                                   b)                                   c)

*Fig 5: Illustration of the method to measure bioactivity through photographs of printed paper samples in contact with E.Coli bacteria. Inset a) shows the bioactive paper disc on top of E.Coli lawn plate before incubation. Inset b) corresponds to the qualitative assessment of phage bioactivity after incubation with optical microscopy.Inset c) is the result of image treatment, lysis zone selection and measurement of the transparent zone area (mm²)*

It is clear that the amount of phage deposited on paper will influence paper bioactivity. In order to estimate this effect, it is convenient to use the specific surface area:

$$A_s = \frac{A}{\beta},$$                                                                                                        *(1)*

where β is the dry basis weight of the bioink/coating colour. Since the basis weight is customarily measured in [g/m$^2$] the specific area as unit [g$^{-1}$].

## 3. Results and Discussion

### 3.1 Phage printing

Previous work has shown that phages could be printed on paper using printing equipment. However, it is also known that the shear stress arising in the printing nip can be harmful to the biomolecules. Detrimental effects on bioactivity were demonstrated for enzyme-based bioactive paper but no information is available for phage-based paper.
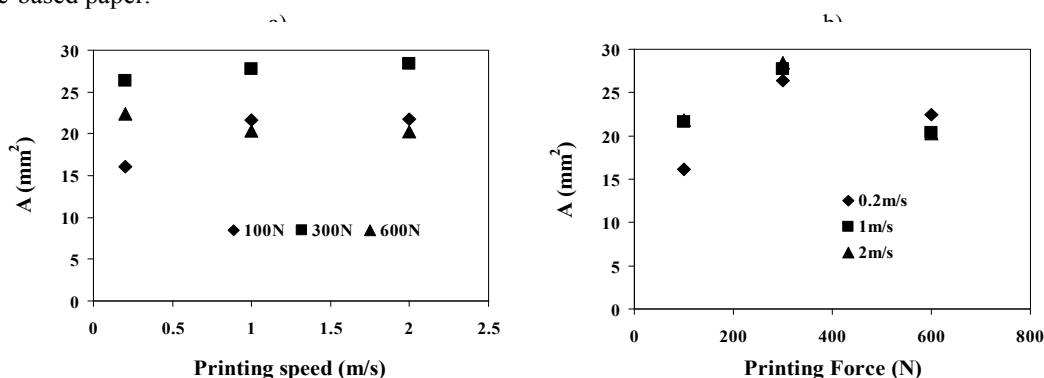


*Fig 5: Influence of printing speed and force on bioactivity.Bioactivity increases slightly with printing force but, at constant velocity, reaches an optimium for a printing force of 300 N.*

Paper bioactivity was measured immediately after printing (without a drying phase) in order to exclude moisture effects from the factors influencing phage activity on paper. Figure 5 shows that phage activity remained constant and was not affected by an increased in the shear rate associated with an increased printing speed. On the other hand, Figure 5b) shows that a high printing forces (between 300N and 600N) have a detrimental effect on paper bioactivity even though there is an increased transfer of bioink.

## 3.2 Influence of humidity and gelatine protection

It is already known that drying is detrimental to paper bioactivity (Jabrane, 2009). This is quantitatively demonstrated in Fig. 6a), which represents the moisture content (in mass) and bioactivity of a paper uniformly impregnated with bioinks containing different concentrations on phages and left to dry time at 50% relative humidity and 23°C. Both paper bioactivity and moisture content were measured at regular intervals over 30 mins. After this time, paper bioactivity is essentially zero. As shown on Fig. 6a), this decrease is clearly associated with the decrease in paper moisture content, independently of the quantity of phages originally present on the paper.
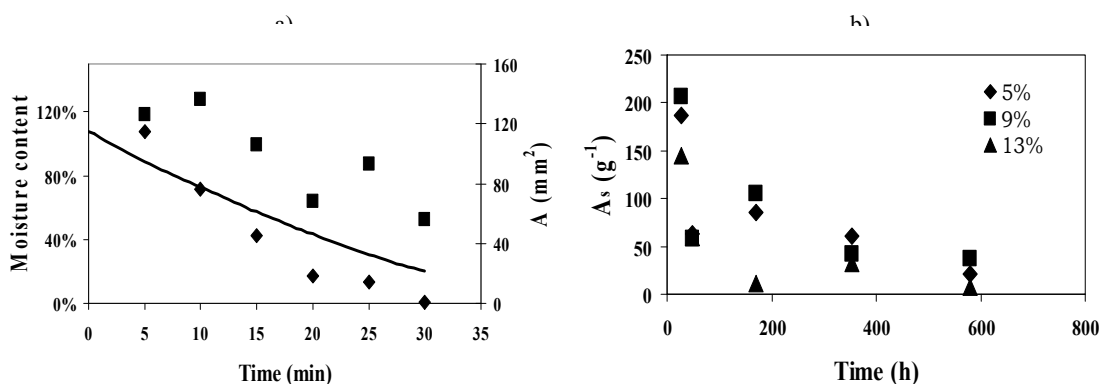


*Fig 6: Influence of humidity on bioactivity Inset a) Influence on drying time on paper bioactivity for phage solutions impregnated on paper. The solid line linked to the left vertical axis represents the moisture loss behaviour of the three paper samples. The right vertical axis represents the phage activity expressed in lysis area (mm²) for both $10^5$ phage/ml (diamonds) and $10^9$ phage/ml (squares) impregnated papers. Inset b) Influence of storage time on paper activity for phage/gelatine solutions drop-deposited on paper*

The impact of drying can be drastically attenuated by including gelatine in the bioink. The experiment was done with drop-deposition of a controlled amount of gelatine-coating colour of 5%, 9% and 13% in mass on pre-cutted 6mm diameter paper discs. Figure 6 b) represents the specific lysis area as a function of storage time at 50% relative humidity and 23°C for different proportion of gelatine and shows that the decay time of bioactivity can be increased up to a thousand fold, with little dependence on the gelatine concentration.

## 4.3 Coating

Coating experiments were designed to test the feasibility to industrially produce bioactive papers with this process. Emphasis was placed on phage resistance to shear stress and on temporal conservation of bioactivity, using gelatine. After coating, all samples were dried for 30 sec. with high intensity infra-red lamps.

Figure 7 relates the bioactivity of papers immediately after coating to the gap between paper and blade (which controls blade pressure). A general increase of bioactivity with increasing gap opening (reduced blade pressure) is first shown in Fig. 7a). This increase in bioactivity can arise either from an increase in coat weight (simply depositing more phages on the paper) or from an increase in phage survival to coating (coming from the reduced blade pressure). Coat weight can be factored out using the specific lysis area (cf., Eq. (1), as shown in Fig. 7b). The data collapse to a single curve implies that viscosity has no effect on bioactivity other than fixing the coat weight, ie., increased shear stresses resulting from higher viscosity are not harmful to phage efficiency. The shape of the curve, showing a higher specific lysis area at low coat weight, indicates that not all phages deposited on paper participate in bacteria destruction. At a fixed bacteria concentration, increasing the phage quantity has little effect since they can only move through diffusion (Krone 2008). In addition, phage diffusion rates may be influenced by CMC and gelatine.

Paper bioactivity as a function of coating speed is shown in Fig. 8. Blade opening was set to 0 and paper bioactivity was measured immediately after coating. The lysis area, shown in Fig. 8a) displays a slight

decrease with coating speed. It is however clear that high speed coating (up to 600m/min) did not appreciably harm the phage activity. The specific area, shown in Fig. 8b), again demonstrates that coating colour viscosity has little effect on paper bioactivity.
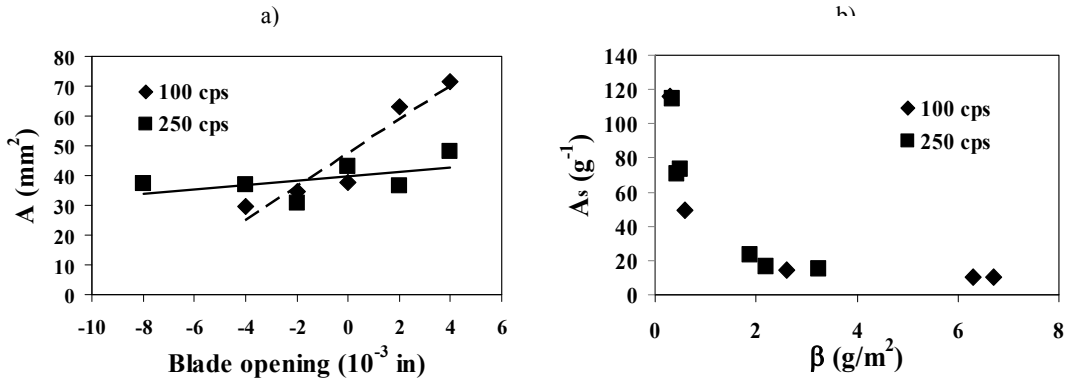


*Fig 7: Influence of blade pressure on bioactivity. Paper bioactivity increases slightly with decreasing blade pressure, as shown in inset a). Inset b) shows that viscosity has little influence on bioactivity other than through increased coat weight*
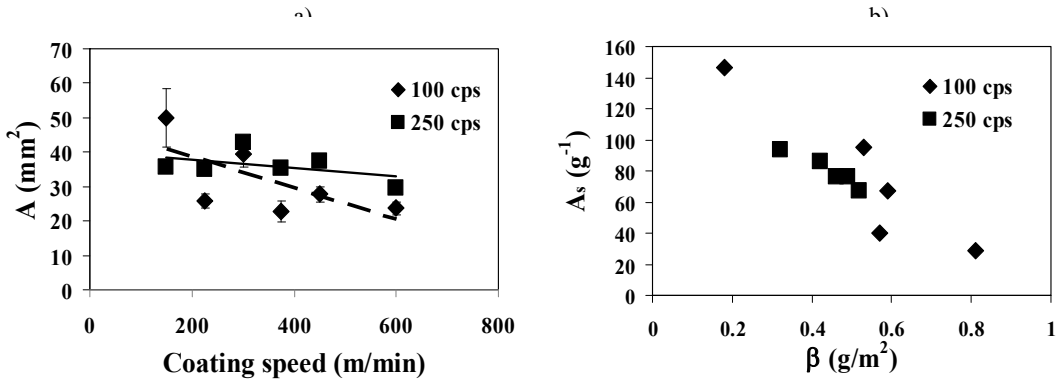


*Fig 8: Influence of coating velocity on bioactivity. For both viscosities, coating speed has virtually no influence on the lysis area. On the right, inset b) shows that viscosity influences bioactivity mostly through the coat weight of the deposited layer*

Finally, the influence of storage time on the bioactivity of paper coated at 600 m/min for two blade openings is shown in Figure 9. Storage was at room temperature in the dark, without humidity control. The results clearly show that a bioactive paper coated with phage and gelatine can retain its activity for a period of several days. Moreover, increasing the coat weight (using a blade opening of 0.004 in instead of 0.002 in) increases the longevity of the papers.



*Fig 9: Decay of bioactivity as a function of time for bioactive paper produced by coating at 600 m/min for two different blade pressures*

## 5. Conclusion

In conclusion, we have shown that the T4 bacteriophage is extremely resistant to the conditions (shear stress and IR drying) encountered in industrial printing and 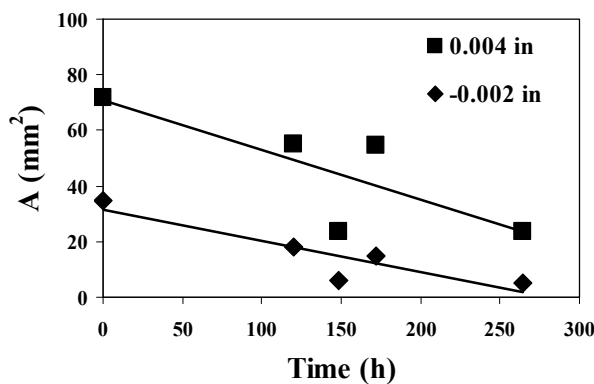coating processes. In addition, the detrimental effects of storage can be alleviated by using gelatin as a moisture retention agent. This complicates the printing/coating operations since the gelling transition temperature of gelatin is relatively high. However, other gels or combinations of gel/viscosity modifiers can be used and this possibility will be explored in the future.

In addition, the phage are resistant to IR drying printing process conditions of 0.2-2m/s printing speed and 100-600N printing force, the T4 bacteriophage resist greatly to the shear stress and constraints between the printing disc and the doctor blade, and into the printing nip.

## References

1. Boland, T., Xu, B., Damon X. (2006) *"Application of inkjet printing to tissue engineering"*, *Biotechnol J* **1** (9), 910-917.

2. Bruzewicz, D. A., Reches, M., and Whitesides G. M. (2008) *"Low-Cost Printing of Poly(dimethylsiloxane) Barriers To Define Microchannels in Paper"*. *Analytical Chemistry*, 80(9): p. 3387-3392.

3. De Grâce J. H., Mangin, P. J. (1984) *"A mechanistic approach to ink transfer. Part I: Effect of substrate properties and press conditions"*, Advances in Printing Science and Technology, W.H. Banks Ed., Pentech Press (London) **17**, 312.

4. Di Risio, S., Yan, N. (2007) *"Piezoelectric ink-jet printing of horseradish peroxidase: Effect of ink viscosity modifiers on activity"*. *Macromolecular Rapid Communications*, 28, 1934-1940.

5. Gervais, L., Gel, M., Allain, B., Tolba, M., Brovko, L., Zourob, M., Mandeville, R., Griffiths, M., Evoy, S. (2007) *"Immobilization of biotinylated bacteriophages on biosensor surfaces"*. *Sensors and Actuators B* **125** (2), 615-621.

6. Hossain, S. M. Z., Luckham, R. E., Smith, A. M., Lebert, J. M., Davies, L. M., Pelton, R. H., Filipe, C. D. M., and Brennan, J.D. (2009) Development of a Bioactive Paper Sensor for Detection of Neurotoxins Using Piezoelectric Inkjet Printing of Sol-Gel-Derived Bioinks. *Anal. Chem.,* **81** (13) 5474-5483.

7. Jabrane, T., Jeaidi, J., Dubé, M. and Mangin, P. J. (2008) *"Gravure Printing of Enzymes and Phages"*, Advances in Printing and Media Technology Vol.35: 279-288.

8. Jabrane, T., M. Dubé and P.J. Mangin, (2009) *"Bacteriophage Immobilization on Paper Surface: Effect of Cationic Pre-Coat Layer"*, Proceedings of Pulp and Paper Technical Association of Canada, Vol. 95:311-315.

9. Kipphan, H. (2001) *"Handbook of Print Media"* (Springer).

10. Krone, S. M. and Abedon, S. T. (2008*) "Modeling Plaque Growth"*. *Bacteriophage Ecology*, Cambridge University Press, pp 415-438.

11. Kropinski, A. M., Mazzocco, A., Waddell, T. E., Lingohr, E. and Johnson, R. P. (2008*) "Enumeration of Bacteriophage by double Agar Overlay Plaque Assay"*. *Bacteriophages, Methods and Protocols*, 69-76.

12. McMeekin, T. A (2003) "Detecting Pathogens in Food". (Woodhead Publishing).

13. Oda, M., Masamoto, M., Unno, H., Tanji, Y. (2004) *"Rapid Detection of Escherichia Coli O157:H7 by Using Green Fluorescent Protein-Labeled PP01 Bacteriophage"*. *Appl. Environ. Microbiol*. **70**, 527-534.

14. Okamoto, T., Suzuki T., Yamamoto N. (2000) *"Microarray fabrication with covalent attachment of DNA using bubble jet technology"*. *Nat. Biotechnol*. **18**, 438-441.

15. Ong, E., Gilkes, N. R., Antony, R., Warren, J., Miller, R. C., Kilburn, D. G. (1989) *"Enzyme immobilization using the Cellulose-Binding Domain of a Cellulomonas Fimi Exoglucanase"*. *Bio/Technology* **7**, 604-607.

16. Pelton, R. (2009*) "Bioactive Paper - a Low Cost Platform for Diagnostic"*. *Trends Anal. Chem*. **28** (8), 925-942.

17. Renault,J. P., Bernard, A., Bietsch, A., Michel, B., Bosshard, H. R., *et al.* (2003) *"Fabricating arrays of single protein molecules on glass using microcontact printing"*, *J Phys Chem B* **107** (3), 703-717.

18. Roda, A., Guardigli, M., Russo, C., Pasini, P., Baraldini, M. (2000) *"Protein microdeposition using a conventional ink-jet printer". Biotechniques* **28**, 492-496.

19. Sanjana N. E., S. B. Fuller S. B. (2004*) "A fast flexible ink-jet printing method for patterning dissociated neurons in culture"*, *J Neurosci. Methods* **136** (2), 151-163.

20. Su, S., Razvan, N., Flilipe, D. M., Li, Y., Pelton, R. H. (2007) *"Adsorption and Covalent Coupling of ATP-Binding DNA Aptamers onto Cellulose". Langmuir* **23** (3) 1300 - 1302.

21. Thibault, C. (2007) *«Impression de biomolécules par lithographie douce: application pour les biopuces, de l'échelle micrométrique à nanométrique»*. Thesis, Université de Toulouse.

22. Zourob, M. and Ripp S. (2010). *"Bacteriophage-Based Biosensors in Recognition Receptors in Biosensors"*, Springer. 415-448.

# Paper-supported assay for the quantification of alkaline phosphatase activity

*Scott Williams, Lindsay Cade and Daniel Clark*

School of Print Media and Printing Materials and Applications Laboratory
Rochester Institute of Technology, Rochester, NY 14623, USA

E-mail: sawppr@rit.edu

**Abstract**

A current medical diagnostic assay for alkaline phosphatase (ALKPHOS, ALP) was adapted to a paper support in order to determine whether a clinically relevant (30 to 202 IU/L) enzyme activity level could be both detected and differentiated. Bioactive paper developments have received significant attention in recent months due to exciting new developments in paper-supported assay platforms and methodologies. We conducted our experiments in order to determine whether a clinically established and certified clinical assay could be directly translated to a paper-supported platform, and return results that are accurate and sensitive enough to be visually quantitative. We also wanted to explore how paper properties, such as permeability might affect the efficacy of such an assay and how differing paper properties might facilitate the use of clinical diagnostics to a *point-of-care* location. Reaction time course and time-limited ALPase concentration assays were done and it was found that the reaction time course extended over a much longer time than anticipated, and optimizing the reaction time was critical in the development of a useful protocol. We also demonstrated that low alkaline phosphatase activity levels are detectable and may be differentiated using optical instrumentation, but cannot easily be visually resolved. Both physical and structural paper properties were found to influence the rate of enzyme reactions.

**Keywords:** paper-supported assay; bioactive paper; enzyme kinetics

## 1. Introduction

Paper is an inexpensive, lightweight and portable substrate that has found many uses in clinical applications. Paper-supported lab-on-a-chip technology has been recently demonstrated for the screening of clinically relevant analytes in urine [Bruzewicz et al., 2009, Martinez et al., 2008, Dungchai et al., 2009, Abe et al., 2008] and as a new way to conducting well-plate assays [Carrilho et al., 2009]. Paper, however, is not new to clinical chemistry. Lateral flow assays [Wong, 2009, Posthuma et al., 2009, Fenton et al., 2009, Hossain et al., 2009, Su et al., 2008, Thornton, 2008] and dipstick technologies [Senturk et al, 2009, St. John et al., 2006, Dyerberg et al., 1978] have been used for some time. Bioactive paper is a new and exciting area of research that includes not only these clinical developments, but also a broader range of technologies, including anti-microbial paper, biosensors and pathogen detection [Pelton, 2009].

Analyte detection with bioactive papers usually involves measuring or observing a colorimetric or fluorescent signal. A successful biosensor methodology will be able to detect an analyte with a signal that is sensitive or intense enough to dependably achieve a confident result. In many cases, only a qualitative YES-NO result is required. When a paper-supported assay relies on a quantitative answer, however, reliability becomes an issue [Ellerbee et al., 2009, Martinez et al., 2008]. The heterogeneous composition and physical properties of paper can play a role [Pelton, 2009, Martinez et al., 2008], and may require the incorporation of internal standards that may further complicate the design or raise the cost.

We conducted a study to compare the kinetics of a clinically relevant enzyme reaction, blood serum alkaline phosphatase (ALK PHOS or ALP), on paper and in a buffered solution. There have been other interesting studies of enzymes being printed onto paper [DiRisio et al., 2008,2009] and investigations looking into the thermal stability of enzymes on paper [Khan et al., 2010]. We are not aware, however, of any studies that have investigated the impact the physical properties of paper, such as porosity or formation, on the kinetics of a paper-supported enzyme activity assay using a clinically relevant enzyme concentration range (30-120 IU/L, ALP for normal adults [Bowers and McComb, 1975]).

In addition, with many of the bioactive papers research, the biologically active component is chemically tethered to the paper [Pelton, 2009]. In our case, however, the analyte would be in the blood serum. Therefore, the assay chemistry must necessarily be the component adsorbed or tethered to the paper fiber. Since the enzyme substrate would be physically adsorbed to the paper fiber, the physical properties of the

paper, such as porosity and formation, may play a role in regulating the enzyme reaction. Three filter paper types were selected, with varying porosity and formation properties, to investigate the role of paper property on the kinetics of an enzyme reaction.

## 2. Materials and methods

### 2.1 Filter Paper Selection and Physical Property Measurement

Whatman #1, Whatman #31 and VWR 410 filter paper grades were selected based on their different application and porosity properties. Paper property tests were conducted in the Printing Applications Laboratory at RIT using established TAPPI methods. Paper porosity was measured using a Gurley TAPPI T460 protocol. Paper grammage was measured using the TAPPI T410 standard. Paper formation was measured using a method developed at RIT (RIT PAL, unpublished results).

### 2.2 Assay Solution Preparation

Bovine intestinal alkaline phosphatase (ALPase, EC 3.1.3.1) was assayed using the Rochester General Hospital clinical protocol. A 0.5M AMP (2-amino-2-methylpropanol, Aldrich) buffer, pH 10.35, with 2.3mM magnesium chloride (USB), and 80 micromolar zinc chloride (Aldrich) was prepared using glass distilled water. A 20mM p-nitrophenol phosphate (pNPP, disodium salt, Fluka) substrate solution was prepared using the AMP buffer. Bovine intestinal alkaline phosphatase (Sigma) was dissolved into the AMP buffer at a stock concentration of 8.61 mg/ml. Activity levels were experimentally determined by measuring the absorbance change at 410nm per minute over the initial linear portion of the absorbance versus time profile on a PerkinElmer Lambda 25 spectrophotometer in Kinetics mode. The substrate concentration was one millimolar p-nitrophenyl phosphate in AMP buffer at $25^{o}$C.

### 2.3 Paper saturation and paper-supported activity assay

Six millimeter paper disks were punched out of the selected filter paper sheets using a standard single hole paper punch. The paper disks were then saturated with selected substrate concentrations by immersion, blotted and dried for five (5) minutes at $60^{o}$C. Substrate-saturated disks were stored at $4^{o}$C. ALPase assay solution was prepared by diluting the ALPase stock solution with AMP buffer so that the enzyme activities would fall into a range from 30 to 1000 IU/L. An activity unit (IU) is defined as the conversion of micromoles of substrate to product per minute.

A substrate and enzyme concentration assay series was prepared, for each filter paper studied, by fixing each selected substrate paper disk onto the adhesive side of optically clear Scotch brand tape. The disks were fixed onto optically clear adhesive tape so that the reaction would be confined to the paper disk. Five to ten (10) microliters of each enzyme concentration were then dispensed onto each disk. The enzyme reaction was then allowed to proceed at room temperature ($25^{o}$C). After the reaction was allowed to proceed for a fixed time that ranged from a few minutes to several hours (in order to learn about the reaction time course), the disks were then covered with clear optical tape and directly measured. Optical reflectivity at 410 nm and colorimetric data, using an XRite Digital Swatchbook, were recorded. Optical reflectivities were then converted to absorptivities using standard equations. The enzyme activity time profile was measured in a similar fashion by measuring the absorbance with time using the XRite Swatchbook. Xrite Swatchbook linearity over the absorbance values measured in this study was confirmed by measuring a lithographically printed yellow vignette from 0 to 100% tint coverage (0 to 1.0 OD at 410 nm).

## 3. Results

### 3.1 Filter paper physical properties

Table 1 lists the physical properties of each filter paper grade. As expected, the higher grammage filter papers exhibit lower dry Gurley porosity. The fiber distribution with VWR 410 paper also was found to be more randomly distributed compared with the Whatman papers. This may translate into more variability in fluid flow properties thus affect the rate of a color forming reaction.

What we found to be even more interesting was the magnitude of the change in air permeability once the filter paper became wet. We would, of course, expect a decrease in air permeability with the exposure of paper fiber to water, but the variable nature of the change was unexpected. As shown in Table 1, air per-

meability varied greatly once the filter paper became wet. Whatman #1 filter papers decreased in the passage of airflow by about 25%. Whatman #31 paper exhibited a 275% decrease in air permeability while VWR 410 paper became impermeable.

*Table 1: Physical properties of three filter paper grades*

| Filter Paper Grade | Grammage[a] | Formation[b] | Gurley Porosity[c] seconds | |
|---|---|---|---|---|
| | | | Dry | Wet |
| Whatman #31 | 92 (2.85) | 15.5 | 1.14 (0.21) | 4.27 (0.18) |
| Whatman #1 | 97 (1.31) | 14.9 | 2.90 (0.21) | 3.61 (0.58) |
| VWR 410 | 114 (1.18) | 18.6 | 20.62 (0.75) | Impermeable[d] |

## 3.2 Time-independent ALPase concentration assay

As shown in Figure 1 (inset), when the ALPase concentration series was assayed with 1.0mM pNPP using a standard solution-based procedure, the enzyme activity increased linearly with concentration. When the same ALPase concentration series was assayed on the paper disks saturated in a 1.0mM pNPP substrate solution, enzyme activity was non-linear, nearly independent of enzyme concentration, and this kinetic result was independent of paper grade. With all three filter paper grades, apparent enzyme saturation of the assay occurs at very low concentration corresponding to about 50 IU/L, a normal ALPase level in human serum. The time course for the reaction illustrated in Figure 1 was three (3) hours – clearly long enough for a departure from pseudo-first order reaction kinetics.
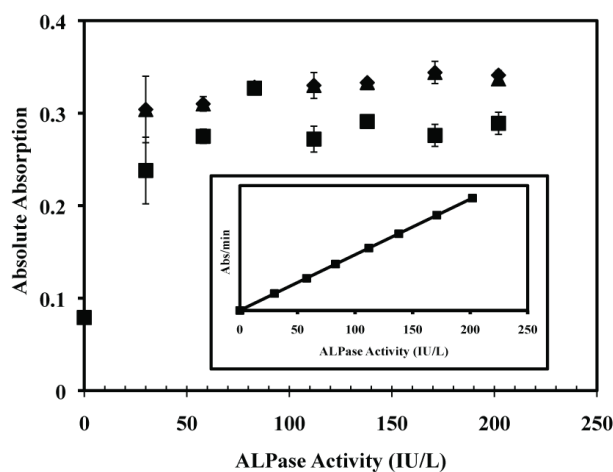


*Figure 1. ALPase concentration dependence assay on Whatman #1 (■), Whatman #31 (◆), and VWR 410 (closed triangle) Filter Paper. pNPP substrate concentration was 1.0mM. Absorbance values were retained on the ordinate to illustrate the signal level corresponding to product (pNPP hydrolysis) formation measured after a three (3) hour time period. (Inset) ALPase activity assay using a standard initial rate kinetic method in solution*

## 3.3 Reaction time course for the paper-supported reaction

Figure 1 illustrates that, in order for a paper-supported assay to be sensitive to changes in one of the reactants (ie., enzyme concentration), the measurement conditions must obey the pseudo-first order reaction kinetics under saturating substrate concentration. So, how long does this condition apply, and does the reaction proceed over a much longer time than we would anticipate given such conditions as paper wicking and solvent evaporation? Figure 2 illustrates the time course for a reaction conducted on Whatman #31 filter paper and a physiological normal activity level of ALPase. As shown, the linear portion of the pseudo-first order enzyme reaction process occurs only over the first 120 seconds. Non-linearity, corresponding to first order kinetic departure, occurs thereafter. Interestingly, however, the reaction proceeds over a much longer time scale that one might anticipate given normal paper properties and ink jet ink drying, for example. In some cases, the reaction proceeded over an open-air time of one hour (data not shown). Clearly, allowing the

reaction to proceed for three (3) hours and assuming that the reaction would simply slow down and stop over a few minutes due to drying proved to be incorrect. Conditions used to produce an assay as illustrated will simply not work in practice. The color formation reaction will require a "stop time" of a few minutes depending on the selected assay conditions.
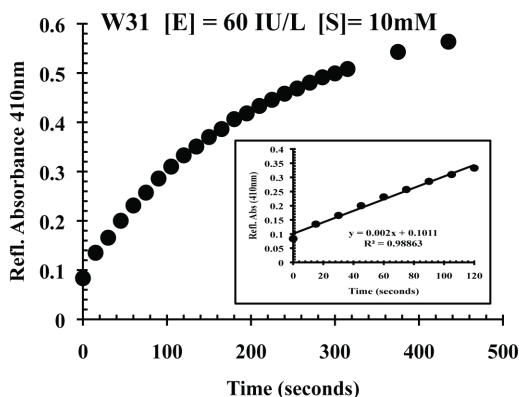


*Figure 2: ALPase reaction rime course*

### 3.4 Time-limited ALPase concentration assay

Knowing that we need to time limit the reaction time to two (2) minutes or less, an ALPase paper-supported assay was performed over varying substrate and enzyme concentration (Figure 3A,B). When the color-forming product reaction was measured after two (2) minutes, linear pseudo-first order kinetics were obeyed and the rate of the reaction varied proportionally (slope of the line) with ALPase concentration over a clinically relevant range (Figure 3A). Under the time-limited condition, differences in the rate of product formation were also filter paper type specific (Figure 3B). Over the same reaction time, the more permeable Whatman 31 filter paper yielded more color density per substrate concentration level compared to VWR 410. As shown in Table 1, the permeability of the VWR 410 paper significantly decreased with moisture contact, and presumably, making less substrate available for the enzyme reaction. Non-linear kinetic behavior did appear to set in when the enzyme activity rose to levels that might be expected for abnormal physiological conditions (greater than 120 IU/L; see Figure 3A).
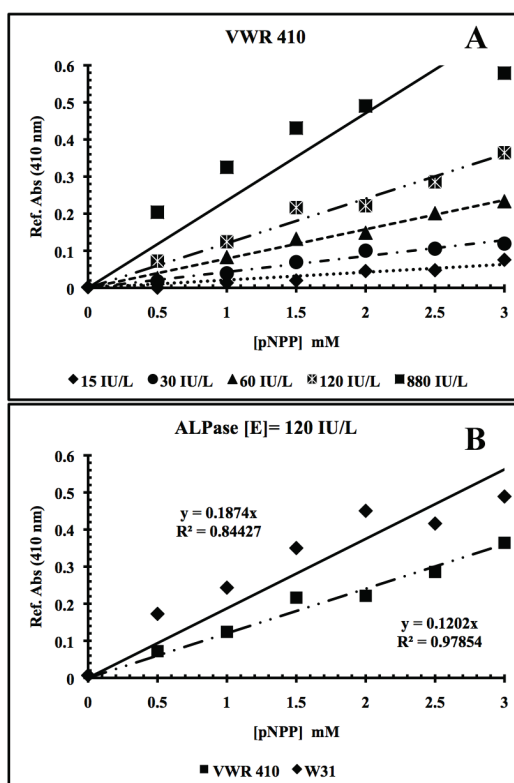


*Figure 3*
*(A) Time-limited ALPase concentration assay*
*as a function of substrate concentration.*
*(B) Comparison of the same assay conditions*
*between Whatman #31 and VWR 410 papers*

This might suggest that a normal disease state determination, a yes/no type of assay, may be possible, but visually quantifying abnormal enzyme activity levels may not be possible given the apparent insensitive nature of our assay design conditions.

## 4. Discussion

Recent developments have pointed to paper as a new platform for performing more advanced clinical diagnostic investigations rather than common lateral flow or dipstick tests. Many paper-supported tests, for example, are well characterized to provided sensitive yes/no answers through color change. The challenge becomes whether paper-supported tests can deliver quantitative answers to more complex clinical processes such as an enzyme assay or immunochemistry analysis. One goal would be to print a medical diagnostic device that can then be transported and used more safely in the field, whether in urban or rural settings. We conducted a study to determine whether a clinically relevant enzyme, ALPase, could be assayed on a paper medium using typical blood serum concentrations. The assay conditions are those currently used at the Rochester General Hospital (Rochester, New York (USA) only translated from solution to a paper-supported protocol as described. The visible color forming reaction is monitored by a change from a colorless reactant (p-nitrophenyl phosphate) to a yellow product (p-nitrophenol) monitored at 410 nm. Our results indicate that the kinetics of this enzyme-catalyzed reaction can be easily detected on paper at activity levels as low as 30 IU/L, but the assay conditions lack the sensitivity to be a useful visual method in the field.

When the clinical ALPase assay conditions were translated from solution to a paper-supported medium, we anticipated that the enzyme would be immobilized and deactivated during the burst or linear portion of the reaction kinetic curve due to evaporation or solvent wicking through the paper fiber network. If pseudo-first order reaction kinetics applied, then the rate of color change would vary linearly with enzyme concentration. If the enzyme remained active over a sustained period of time, than we would expect lower order kinetic terms would enter breaking the linear enzyme concentration dependence. Figure 1 illustrates that paper was capable of sustaining an enzyme reaction. Our results show, in Figure 2, that the reaction can proceed over much longer than expected times; not a few minutes, but tens of minutes. Clearly, the ALPase reaction may be sustained on paper long after product formation over the initial linear portion of the kinetic profile.

When we measured the time profile for the ALPase reaction performed under our conditions, we found that pseudo-first order conditions may be obeyed as long as the observation time was kept shorter than two minutes (see Figure 2). As shown in Figure 3A, a linear dependence with enzyme and substrate concentration may be maintained if the enzyme activity was less than a few 100 IU/L, the substrate concentration was less than about three millimolar p-nitrophenyl phosphate, and the reaction was allowed to proceed for only a few minutes. Clinically high ALPase concentrations of about 800 or more IU/L did not linearly depend on a substrate concentration used in our experiments. We also suspected that variations in paper formation and permeability would affect the rate of the color forming reaction. As shown in Figure 3B, the rate of product formation was different among the filter papers tested. Depending on the conditions, the difference in product formed could be as high as 100% or a factor of two. So, the visual color density formed would depend on paper properties. This result has been demonstrated with other enzyme systems [DiRisio, 2009].

In order for our paper-supported reaction to be visually useful as a way of quantifying enzyme activity levels, the assay must be sensitive enough to amplify differences in enzyme concentration. When we ran the paper-supported (Whatman #31) assay using the two millimolar substrate and two minute reaction time conditions, the color difference (ΔE) measured (calculated based on a 120 IU/L ALPase activity level) was not greater than eight (data not shown). In the yellow portion of the visible spectrum, this was a very difficult change to visually detect. A color change was perceptible, but not at visual difference that would suggest an eight fold change in enzyme activity level (120 IU/L vs. 880 IU/L). The apparent non-linear departure of enzyme activity at the levels of ALPase that would be considered abnormally high (greater than 120 IU/L) lessens the sensitivity of the paper-supported assay over a solution-based method.

## 5. Conclusions

We have demonstrated that a clinically relevant ALPase assay may be translated from the current solution-based method to a paper-supported method. We report the assay conditions that provide the ability to quantify enzyme activity level over the range typically found in human serum. Such a paper-supported assay

would allow for ALPase, a key marker for liver and cellular function, to be administered in conditions where full laboratory support was not possible. Our results, however, also demonstrate that some instrumentation would still be required for this quantification. The yellow product color differences obtained, under our optimized conditions, were not perceptible enough to visually ascertain the magnitude between physiologically relevant enzyme activity levels. We might be able to suggest that our paper-supported protocol would allow for the detection of a normal versus abnormal (yes versus no) result, but the visual sensitivity to detect and report the level of abnormal activity was lacking.

A plethora of ALPase assay protocols have been reported in the literature and used as a marker for a variety of scientific investigations, some even paper-supported, such as ELISA analysis. The purpose of this study was not to find the best assay, but to see if an already clinically accepted and approved assay could be simply translated from an approved solution-based protocol and used in a new way. Our results would seem to suggest that for ALPase, the search for a more sensitive test with a more favorable visual color change, may be more fruitful if the intent is to develop a instrument-independent field test. The change to a paper-supported assay, however, may have more value than just point-of-care applications. The clinically accepted ALPase protocol may be developed to a paper-supported medium in order to increase throughput, reduced cost or chemical waste. Since the clinically approved assay is already accepted, a shorter path to development for laboratory-based applications may be plausible.

## Non-standard abbreviations

ALPase, alkaline phosphatase; ALP or ALK PHOS, alkaline phosphatase assay; pNPP, p-nitrophenyl phosphate; AMP, 2-amino-2-methyl-1-propanol; MM, Michaelis-Menton kinetics; DBS, dried blood spot.

## References

1. Abe K, Suzuki K, Citterio D. Inkjet-printed microfluidic multianalyte chemical sensing paper. Anal. Chem. 2008; 80(19): 6928-6934.

2. Bowers GN, McComb RB. Measurement of the total alkaline phosphatase activity in human serum. Clin. Chem. 1975; 21(13):1988-1995.

3. Bruzewicz DA, Reches M, Whitesides GM. Low-cost printing of poly(dimethylsiloxane) barriers to define microchannels in paper. Anal. Chem. 2009; *80* (9):3387-3392.

4. Carrilho E, Phillips ST, Vella SJ, Martinez AW, Whitesides G. Paper microzone plates. *Anal. Chem.* 2009; *81* (15):5990–5998.

5. DiRisio S, Yan N. Adsorption and inactivation behavior of horseradish peroxidase on cellulosic fiber surfaces. Journal of Colloid and Interface Science 2009; 338:410-419.

6. DiRisio S, Yan N. Piezoelectric ink jet printing of horseradish peroxidase on fibrous supports. J. Pulp Pap. Sci. 2008; 34(4):203-211.

7. Dungchai W, Challapakul O, Henry CS. Electrochemical detection for paper-based microfluidics. *Anal. Chem.* 2009; *81*:5821-5826.

8. Dyerberg J, Pedersen L, Aagaard O. Evaluation of a dipstick test for glucose in urine. Clin. Chem. 1978; 22(2):205-210.

9. Ellerbee AK, Phillips ST, Siegel AC, Mirica KA, Martinez AW, Striehl P, Jain N, et al. Quantifying colorimetric assays in paper-based microfluidic devices by measuring the transmission of light through paper. Anal. Chem. 2009; 81(20): 8447-8452.

10. Fenton EM, Mascarenas MR, Lopez GP, Sibbett SS. Multiplex lateral-flow test strips fabricated by two-dimensional shaping. ACS Appl. Mater. Interfaces 2009; 1:124-129.

11. Hossain SMZ, Luckham RE, McFadden MJ, Brennan JD. Reagentless bidirectional lateral flow bioactive paper sensors for detection of pesticides in beverage and food samples. Anal. Chem. 2009; 81:9055-9064.

12. Khan MS, Li X, Shen W, Garnier G. Thermal stability of bioactive enzymatic papers. Colloids and Surfaces B: Biointerfaces. 2010; 75(1):239-246.

13. Martinez AW, Phillips ST, Whitesides GM. Three-dimensional microfluidic devices fabricated in layered paper and tape. Proc Natl Acad Sci U S A. 2008;105(50):19606-11.

14. Martinez AW, Phillips ST, Carrilho E, Thomas SW, Sindi H, Whitesides GM. Simple telemedicine for developing regions: camera phones and paper-based microfluidic devices for real-time, off-site diagnosis. Anal. Chem. 2008; 80(10):3699-3707.

15. Pelton R. Bioactive paper provides a low-cost platform for diagnostics. TrAC 2009; 28(8):925-942.

16. Posthuma GA, Korf J, van Amerongen A. Lateral flow (immuno) assay: its strengths, weaknesses, opportunities and threats. A literature survey. Anal Bioanal Chem 2009; 393:569-582.

17. Senturk BA, Akgol E, Ince DA, Ustuner I.  Evaluation of dipstick urinalysis for urinary tract infection. Clin. Biochem. 2009; 42(4-5):339-340.

18. St. John A, Boyd JC, Lowes AJ, Price CP. The use of urinary dipstick tests to exclude urinary tract infection - A systematic review of the literature. Am. J. Clin. Path. 2006; 126(3):428-436.

19. Su S, Ali MM, Filipe CD, Li Y, Pelton R.  Microgel-based inks for paper-supported biosensing applications. Biomacromolecules 2008; 9(3):935-941.

20. Thornton CR. Development of an Immunochromatographic lateral-flow device for rapid serodiagnosis of invasive apergillosis. Clinical and Vaccine Immunology 2008; 15(7):1095-1105.

21. Wong R, Tse H. Lateral flow immunoassay. New York: Humana Press; 2009.

# Factorial experiment to identify significant factors affecting electrical conductivity of blood glucose test strips

*Yung-Cheng Hsieh, Suu-Yi Cheng*

Department of Graphic Communication Arts, National Taiwan University of Arts
59, Section 1, Ta-Kuang Rd., Pan-Chiao City, Taipei County, Taiwan R.O.C.
E-mails: ych@ntua.edu.tw, cindy9518183@gmail.com

**Abstract**

As the global diabetic population expands, with the global diabetic population exceeding 250,000,000 diabetics, given such a massive worldwide diabetics market, the need for diabetic blood monitoring equipment is naturally growing rapidly. The most frequently replaced part of blood glucose monitoring equipment is the blood glucose monitoring strips. These test strips are often produced using screen printing. Currently in Taiwan there is no uniform standard for the screen printing manufacturing process. Most of the academic literature in the blood glucose test strip field focuses on aspects of the biochemical reactions involved, but little study has been conducted on the screen printing processes. Thus this study intended to fill the gap by study conductivity of screen printed blood glucose test strips to explore and develop a resistance model for predicting electrical conductivity, for reference by the industry. A $2^3$ factorial experiment was conducted to explore the major factors which impact resistance in blood glucose test strips. Three possible influential factors, conductive silver ink film thickness, conductive carbon ink film thickness, and the mesh count number for the silver ink screen mesh were investigated. This $2^3$ factorial experiment yielded 8 different printing combinations. The study found that when using the silver ink screen with a mesh count of 250 meshes, conductive ink silver thickness ($X_1$) of 14μm, and conductive ink carbon thickness ($X_2$) of 12μm, one can obtain the most optimum combination for achieving the minimum resistance value for the test strips, with an average resistance value of 7.046.

**Keywords:** screen printing; blood glucose test strips; resistivity; factorial experiment

## 1. Introduction

### 1.1 Background to the study and research motivation

Preventive medicine and personalized medicine represent the latest trends for the biotech industry's emerging research. According to the International Diabetes Federation (IDF) there are more than 250 million people worldwide who suffer from diabetes, with more than 3.8 million people worldwide each year who die from diabetes and diabetic heart disease or high blood pressure complications. Regular blood glucose monitoring in diabetic patients is very important, but trips to the hospital for blood glucose testing requires many complex processes, consuming much manpower and time resources, and results provided by detection through their large laboratory instruments are not immediately available, so personal home blood glucose detector provides a simple, rapid and accurate testing method so that patients during the course of their regular life activities can monitor their disease status through blood glucose detection. The Blood glucose tester is a form of biosensor. Bio-sensors are used in the identification of biological molecules, such as: enzymes, and antibodies, to capture the materials under examination, and then convert their presence into electronic signals through the sensor processes as illustrated step by step in Figure 1.
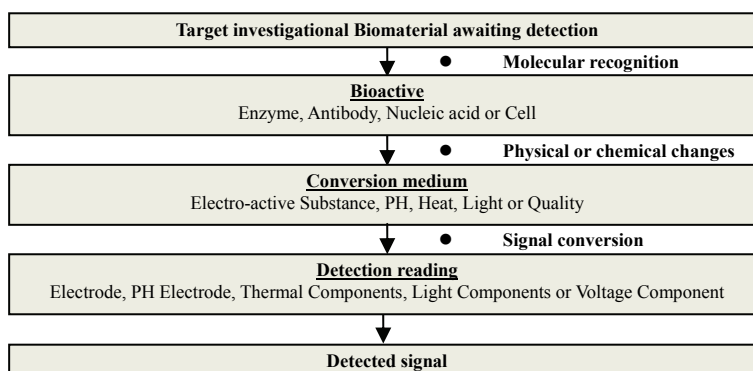


*Figure 1: Flowchart of biosensor operational principles*

This study focuses on home blood glucose monitoring in relation to the screen printing process variables for the blood glucose test strip pieces which are most often purchased with high consumption rates, and a flowchart of this study's investigational processes for these blood glucose test strips is shown in Figure 2.
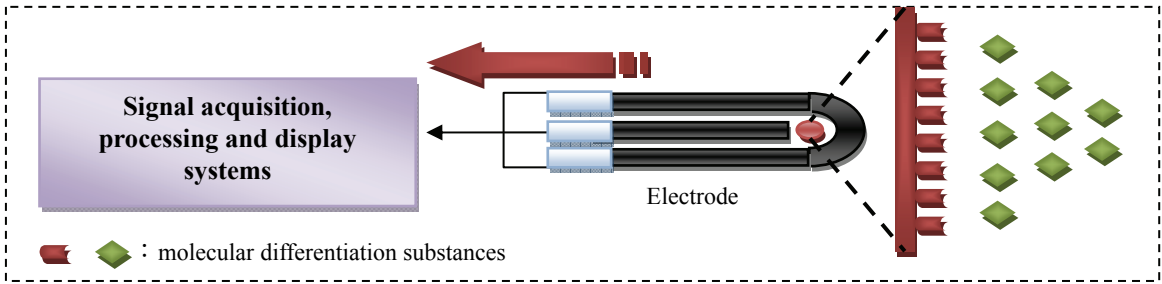


*Figure 2: Flowchart of blood glucose test strips operational principles*

## 1.2 Research objectives

This study aims to identify the ideal combination of factors assuring maximal stability for blood glucose test strips by exploring the blood glucose test strip screen printing processes which yield stable results in the printing processes.This study conducted experiments on blood glucose test via screen printing processes, to explore the relationships between conductive ink film thickness and screen mesh counts, measuring conductivity through the resistance of target blood glucose test strips, then using SPSS17.0 and Minitab14 .0 statistical software to calculate and analyze the experimental data, applying the process-capability ratio (PCR) to examine process stability, and identify a set of appropriate factors for a screen printing glucose test strip predictive model. The purposes of this study are as follows:

1. Explore the significant factors influencing blood glucose test strip resistance values, including the relative size of the impacts and the means by which they exert their influence.
2. Explore how to obtain factorial combinations to achieve the smallest blood glucose test strip resistance, and identify the optimal combination for conductivity with minimal resistance.
3. Establish a regression model of factors for prediction of screen printed blood glucose test strip resistance.

## 1.3 Research framework

This study employs the screen printing process, using 75μm PET printing substrate to examine the three major factors affecting test strip resistance, silver ink screen mesh counts, conductive silver (Ag) ink film thickness, and conductive carbon (Carbon) ink film thickness, applying multi-factor impact testing to identify significant factors in the blood glucose test strips and their respective effects and magnitude, to ascertain the optimal combination of conductivity and minimal resistance for process stability and yielding a prediction model, pursuant to the study flowchart as illustrated below (Figure 3).
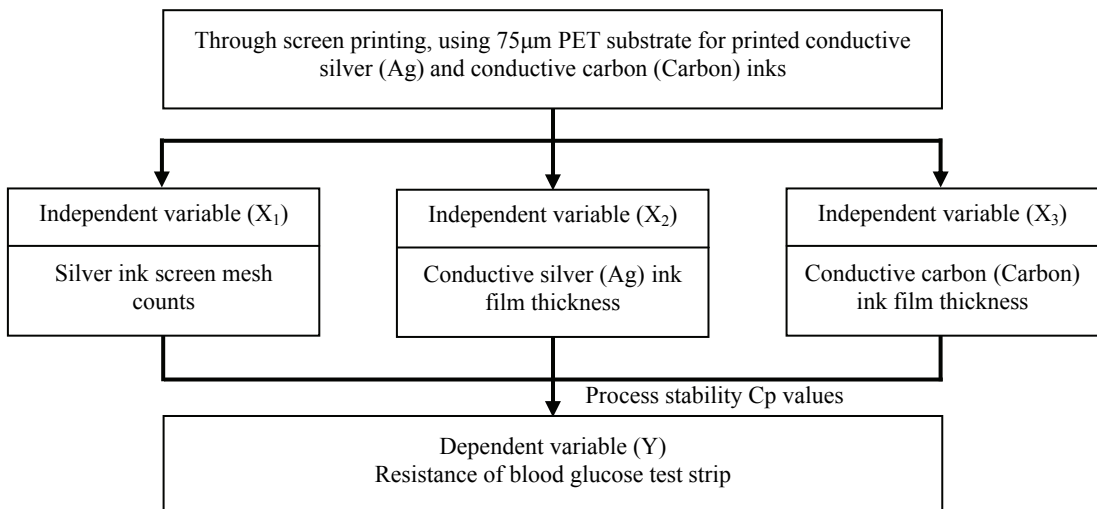


*Figure 3: Research framework*

## 1.4 Research hypotheses

Under the same standardized processes, there exist significant effects on blood glucose test strip resistance from silver ink screen mesh counts, and from different thicknesses of the conductive silver (Ag) ink and conductive carbon (Carbon) ink. Namely:

$$Y = \alpha + \beta_1 X_1 + \beta_2 X_2 + \beta_3 X_3 + \beta_4 X_1 X_2 + \beta_5 X_1 X_3 + \beta_6 X_2 X_3 + \beta_7 X_1 X_2 X_3 + E \tag{1}$$

$$Ha : \beta i \neq 0 \ \ i = 1, 2, 3, 4, ....7 \ (\beta i \neq 0) \tag{2}$$

$$Ho : \beta i = 0 \ \ i = 1, 2, 3, 4, ....7 \tag{3}$$

($\alpha$, $\beta$ as coefficients, Y is resistance, $X_1$ for silver ink screen mesh counts, $X_2$ for conductive silver (Ag) ink variable film thickness, $X_3$ for conductive carbon (Carbon) ink variable film thickness, and E is a random error term.)

## 2. Methods

### 2.1 Research flowchart

This study is a true experiment in nature, using $2^3$ factorial experimental design, which aims to investigate the influential factors affecting screen printing blood glucose test strips, to ascertain the optimal process combination of the three factors of silver ink screen mesh count number, conductive silver (Ag) ink film thickness and conductive carbon (Carbon) ink film thickness. The research process flowchart is illustrated in Figure 4.
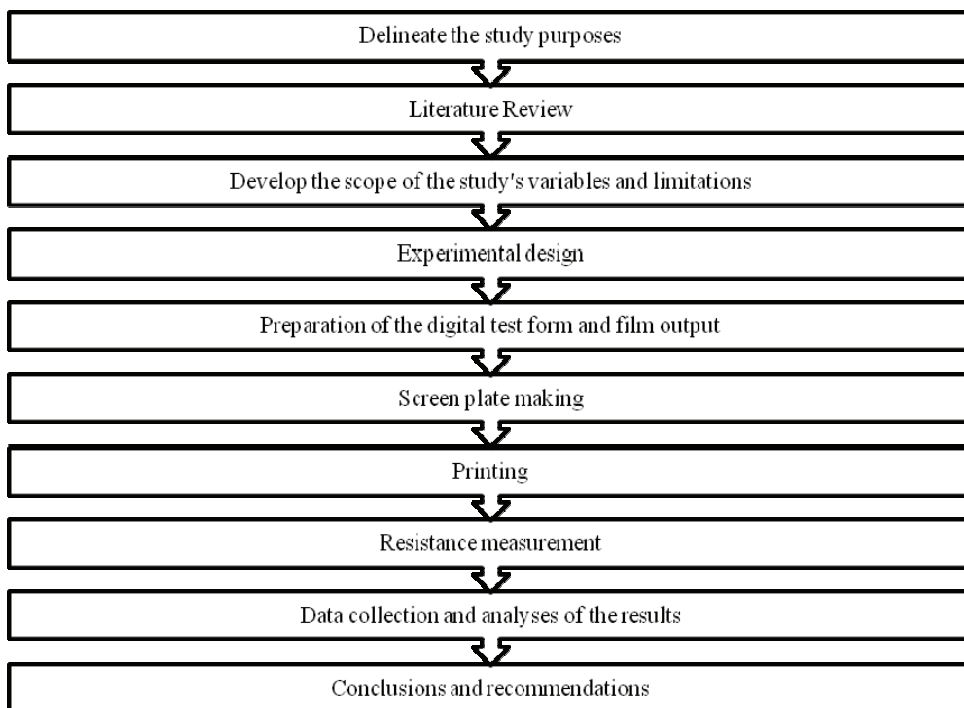


```
┌─────────────────────────────────────────┐
│         Delineate the study purposes      │
└─────────────────────────────────────────┘
                    ⇓
┌─────────────────────────────────────────┐
│              Literature Review            │
└─────────────────────────────────────────┘
                    ⇓
┌─────────────────────────────────────────┐
│  Develop the scope of the study's variables and limitations │
└─────────────────────────────────────────┘
                    ⇓
┌─────────────────────────────────────────┐
│              Experimental design          │
└─────────────────────────────────────────┘
                    ⇓
┌─────────────────────────────────────────┐
│  Preparation of the digital test form and film output │
└─────────────────────────────────────────┘
                    ⇓
┌─────────────────────────────────────────┐
│             Screen plate making           │
└─────────────────────────────────────────┘
                    ⇓
┌─────────────────────────────────────────┐
│                 Printing                  │
└─────────────────────────────────────────┘
                    ⇓
┌─────────────────────────────────────────┐
│            Resistance measurement         │
└─────────────────────────────────────────┘
                    ⇓
┌─────────────────────────────────────────┐
│   Data collection and analyses of the results │
└─────────────────────────────────────────┘
                    ⇓
┌─────────────────────────────────────────┐
│       Conclusions and recommendations     │
└─────────────────────────────────────────┘
```

*Figure 4: Research flowchart*

### 2.2 Experimental design

Experimental design relies on a $2^3$ factorial design (a total of three factors, with each factor having two levels). Three factors are: (1) Silver ink screen mesh counts ($X_1$), (2) conductive silver (Ag) ink film thickness ($X_2$), (3) conductive carbon (Carbon) ink film thickness ($X_3$). For details of the $2^3$ factorial designs, see Table 1. Each factor was divided into high and low levels(+, -). The experimental design provided for a total of eight different combinations, with each of the eight combinations conducted in random order as determined by the experiment processes, and each combination had a printing run of 150 samples, numbered sequentially from 1 to 150, from which we then used Systematically Random Sampling to select 50 investigational samples. Therefore, our results come from 400 measured samples.

*Table 1: The eight different combinations of the $2^3$ factorial experimental design*

| Combination number | factors | | | Run order | Total samples | Randomly selected investigational samples | Total investigational samples |
|---|---|---|---|---|---|---|---|
| | $X_1$ | $X_2$ | $X_3$ | | | | |
| 1 | - | - | - | 6 | 150 prints | 50 prints | |
| 2 | + | - | - | 3 | 150 prints | 50 prints | |
| 3 | - | + | - | 1 | 150 prints | 50 prints | |
| 4 | + | + | - | 7 | 150 prints | 50 prints | |
| 5 | - | - | + | 2 | 150 prints | 50 prints | 400 prints |
| 8 | + | - | + | 8 | 150 prints | 50 prints | |
| 7 | - | + | + | 5 | 150 prints | 50 prints | |
| 8 | + | + | + | 4 | 150 prints | 50 prints | |

| Factor | Factor levels (+, -) | |
|---|---|---|
| | - | + |
| $X_1$: variable silver ink screen mesh net mesh | 250 lines/inch | 300 lines/inch |
| $X_2$: conductive silver (Ag) ink variable film thickness | 8μm | 12μm |
| $X_3$: conductive carbon (Carbon) ink variable film thickness | 12μm | 14μm |

## 2.3 Experimental procedure

The experimental procedure consists of three phases: first, digital test forms are prepared for film output and plate making; second, the blood glucose test strips are screen printed, and the third stage with analyses and measurement of resistance. (As illustrated in Figure 5)
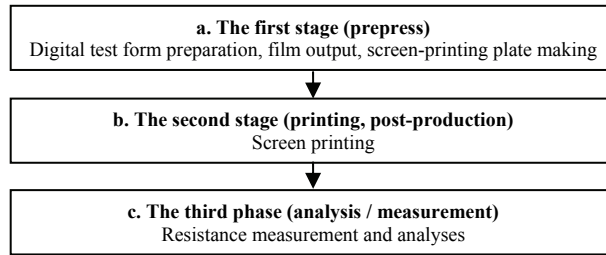


**a. The first stage (prepress)**
Digital test form preparation, film output, screen-printing plate making

↓

**b. The second stage (printing, post-production)**
Screen printing

↓

**c. The third phase (analysis / measurement)**
Resistance measurement and analyses

*Figure 5: Experimental steps*

a.  **First phase (pre-press)**
    The first step for the prepress stage involves preparation of the digital test forms, of which there are two designed respectively for 1) the Conductive silver ink digital test form; and 2) the conductive carbon ink digital test form (see Figure 6). To design good digital test form for the conductive silver ink and conductive carbon ink, we must consider the screen printing process and provide for the variable parameter settings for the output film, and then engage in the screen preparation and plate-making processes.
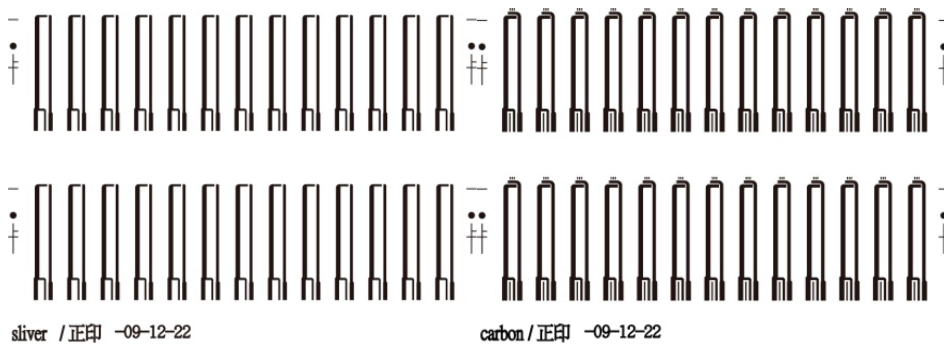


sliver / 正印 −09-12-22                     carbon / 正印 −09-12-22

*Figure 6: Digital test form designs for the conductive carbon and conductive silver inks*

b.  **The second phase (printing, post-production)**
    The second stage is screen printing of the blood glucose test strips, with the blood glucose test strips structure illustrated in Figure 7. Table 2 shows the parameter setting of control variables for the printing process according to our experimental steps.
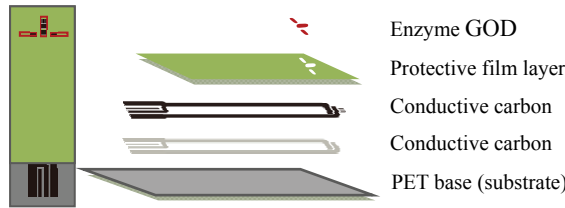
*Figure 7: Structure of the blood glucose test strips*

*Table 2：Screen printing process steps*

| Printing process step | Material | Notes |
|---|---|---|
| | PET substrate | Thickness of 0.75µm |
| 1  Print run I | Conductive silver (Ag) ink | Drying at 120$^{o}$ C for 15 minutes |
| 2  Print run II | Conductive carbon ink | Drying at 120$^{o}$ C for 5 minutes |
| 3  Print run III | Conductive carbon ink | Drying at 120$^{o}$ C for 5 minutes |

*c.* ***Third phase (measurement/analysis)***

400 printed samples were systematically random selected and measured, using the DH-303 indicators to measure the blood glucose test strip resistance. Resistance measurement was made in a zone 0.5cm from the working electrode ends of blood glucose test strips, as shown in Figure 8. The data collected was analyzed using the SPSS17.0 and Minitab14.0 statistical software packages.



Resistance measurement zone 0.5cm
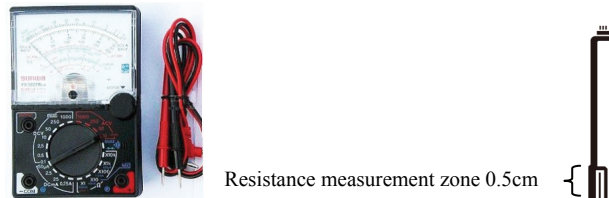
*Figure 8: Range and measurement scope of the DH-303 resistance meter employed in this study*

## 2.4 Analysis of the reliability and validity of the detection device used in the experiment

In this study, Factor Analysis was employed to test the construct validity of the experimental instrument through Principal Component analysis, with Eigen values set to 1. R-Square value explains the percentage of the total variance in the blood glucose test resistance contributed by the instrument. R-Square in this study was 99.11% (see Table 3), meaning all the measured values taken by the experimental instrument can collectively explain 99.11% of the total resistance variance. The results indicated that the construct validity is quite high for the DH-303 measurement instruments.

*Table 3: R-Square values*

| S | R-Sq | R-Sq (adj) |
|---|---|---|
| 0.0247 | 99.11% | 99.10% |

## 2.5 Process stability

This study used process-capability ratio (PCR) to assess the stability of the processes. Processing capability ratio PCR (Cp value) uses upper specification limit (USL) and lower specification limit (LSL) to measure process capability, and measures process variation (σ, because σ is usually unknown, it is generally estimated with the sample standard deviation S). Cp value is an indication of the process stability. High Cp value means low quality variation, moreover, better process capability. The formula is calculated as follows:

$$PCR = \frac{USL - LSL}{6\sigma}$$

(4)

Using the Minitab14.0 I-MR statistical software I-MR control chart, excluding those samples falling outside the specification limits, the combination of the samples within specification limits were controlled by the I-MR control chart, with each combination of Mean $_{revised}$ and corrected specifications and under the specifications of 3σ $_{revised,}$ to further obtain the combination of the 8 treatments under the standard 3σ $_{revised}$ spe-

cifications and the average (of 0.112. Finally we obtained the LSL $_{final}$ and USL $_{final}$ values, and calculated process capability Cp values using statistical software, as shown in Table 4.

$$3\hat{S}_{revised}=(3\sigma_1+3\sigma_2+3\sigma_3+3\sigma_4+3\sigma_5+3\sigma_6+3\sigma_7+3\sigma_8)/8 \qquad (5)$$

LSL$_{final}$   Mean$_{revised}$   3 $_{revised}$

USL$_{final}$   Mean$_{revised}$   3 $_{revised}$

In this study, among the 8 treatment combinations, the best one for process capability yielded a Cp value of 1.17, namely the (+,-,-) combination; with silver ink screen mesh counts of 300 mesh, conductive silver (Ag) ink film thickness of 8μm, and conductive carbon (Carbon) ink film thickness of 12μm.

*Table 4: Process capability Cp values*

| Experimental combination | Factors | | | Mean revised | 3σ revised | 3$\hat{S}$ revised for the 8 groups | USL$_{final}$ | LSL$_{final}$ | Cp value | Cp sequence of the Cp values (magnitude) |
|---|---|---|---|---|---|---|---|---|---|---|
| | X$_1$ | X$_2$ | X$_3$ | | | | | | | |
| 1 | - | - | - | 7.524 | 0.087 | | 7.636 | 7.412 | 0.83 | 2 |
| 2 | + | - | - | 8.746 | 0.065 | | 8.858 | 8.634 | 1.17 | 1 |
| 3 | - | + | - | 7.046 | 0.109 | | 7.158 | 7.034 | 0.44 | 6 |
| 4 | + | + | - | 8.052 | 0.118 | 0.112 | 8.164 | 7.940 | 0.51 | 5 |
| 5 | - | - | + | 7.800 | 0.130 | | 7.912 | 7.688 | 0.75 | 4 |
| 8 | + | - | + | 8.958 | 0.114 | | 9.070 | 8.846 | 0.79 | 3 |
| 7 | - | + | + | 7.306 | 0.109 | | 7.418 | 7.194 | 0.79 | 3 |
| 8 | + | + | + | 8.536 | 0.160 | | 8.648 | 8.424 | 0.51 | 5 |
| Factor | | | | | | | Factor levels (+, -) | | | |
| | | | | | | | - | | + | |
| X$_1$: variable silver ink screen mesh counts | | | | | | | 250lines/inch | | 300lines/inch | |
| X$_2$: conductive silver (Ag) ink variable film thickness | | | | | | | 8μm | | 12μm | |
| X$_3$: conductive carbon (Carbon) ink variable film thickness | | | | | | | 12μm | | 14μm | |

## 3. Results

### 3.1 Descriptive statistics

Average measurement was taken for the 8 treatment combinations, on each of 50 samples, for averages from a total of 400 measured values. As can be seen from Table 5 the average value of the 400 samples was 7.9960: with a maximum of 9.1; and a minimum of 6.1; and a standard deviation of 0.6578; Skewness was 0.07628, with the 0.07628 lying between positive and negative 1; this means the data distribution was approximately normal. In addition, the peak state coefficient of -1.38123, being less than 3 evincing a flat broad peak, indicating that this data is effectively responsive for the overall sample.

*Table 5: Typical descriptive statistics*

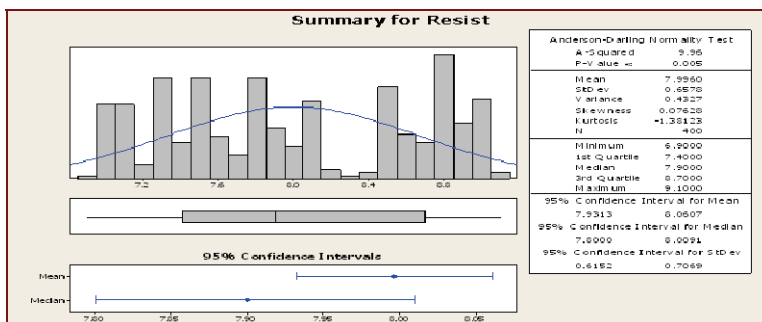| Dependent variable | N | Minimum | Maximum | Mean | Kurtosis | Skewness | Std. Deviation |
|---|---|---|---|---|---|---|---|
| Resistance value | 8 | 6.9 | 9.1 | 7.9960 | -1.38123 | 0.07628 | 0.6578 |



*Figure 9: Illustrative chart for descriptive statistics of the blood glucose test strip resistivity*

Figure 9 provides a simple chart of the central tendency estimates for the resistance value measurements for the blood glucose test strips according to descriptive statistics. From the figure we can see that there is a normal distribution to be found among the 400 samples' resistance values, using a box-shaped graph to assess the median and mean, we estimate the median to be 7.996 or slightly larger than the mean of 7.9, with most of the resistance value measurements concentrated in the latter part.

## 3.2 Hypothesis testing

Using the Minitab statistical software Fit Faction Model to perform hypothesis testing, with a significant level at an α value of 0.05, we can see from Table 6, that $P = 0.000 < α$ (significance level) $= 0.05$, so we reject Ho, and accept Ha, that is at least one factor has a significant impact on the test strip resistance.

*Table 6: Significance levels for effects on blood glucose test strip resistivity*

| Source | DF | SS | MS | F | P |
|--------|-----|---------|---------|---------|-------|
| Main Effects | 7 | 171.124 | 24.4463 | 6265.00 | 0.000 |
| Pure Error | 392 | 1.530 | 0.0039 | | |
| Total | 399 | 172.654 | | | |

## 4. Discussion

### 4.1 Main effects on resistivity in the blood glucose test strips

Figure 10 provides a Pareto chart for the blood glucose test strips' resistance, where the factors' do not reach the dotted line this means the factor had no significant effect on the dependent variables. From the chart we can see that each factor had significant effects on the conductivity of the blood glucose test strips.
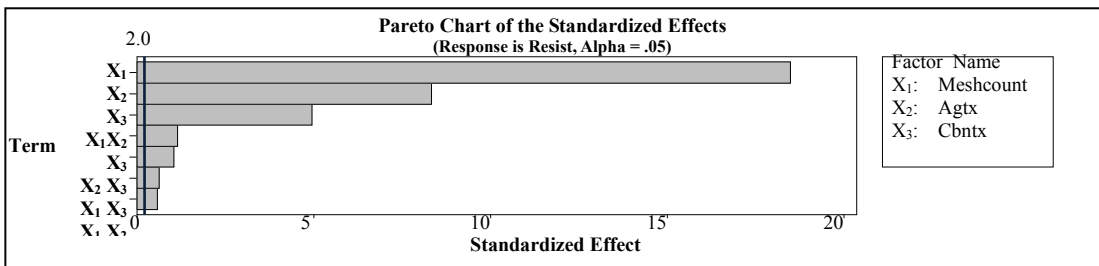


*Figure 10: Pareto chart of the blood glucose test strips resistance*

Figure 11 illustrates a plot of the main effects on the resistance of the blood glucose test strips, with the greater the slope rate representing a stronger significant effect on the blood glucose test strip resistance. The chart shows that the Silver ink screen mesh counts ($X_1$) had the maximum slope rate, yielding the greatest impact on the blood glucose test strips resistance value (Y).
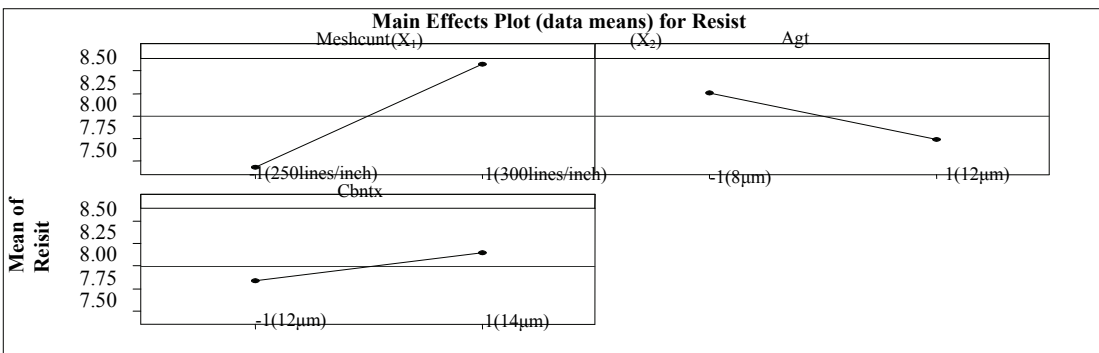


*Figure 11: Main effects plot of blood glucose test strip resistance values*

Table 7 provides a multi-factor analysis of resistance for the blood glucose test strips from the Effect value to determine the size of the absolute value of the factor on resistance. The silver ink screen mesh counts ($X_1$)

had the greatest resistance impact (Effect value = 1.154), and the impact was positive. The table shows that each of the eight independents variables has significant effects on the resistance of blood glucose test strips.

*Table 7: Factorial analysis of the blood glucose test strips' resistance*

| Term | Effect | Coef | SE Coef | T-value | P |
|---|---|---|---|---|---|
| Constant | | 7.9960 | 0.003123 | 2560.10 | 0.000 |
| $X_1$ (Meshcount) | 1.1540 | 0.5770 | 0.003123 | 184.74 | 0.000 |
| $X_2$ (Agft) | -0.5220 | -0.2610 | 0.003123 | -83.57 | 0.000 |
| $X_3$ (Cbnft) | 0.3080 | 0.1540 | 0.003123 | 49.31 | 0.000 |
| $X_1 X_2$ (Meshcount*Agft) | -0.0360 | -0.0180 | 0.003123 | -5.76 | 0.000 |
| $X_1 X_3$ (Meshcount*Cbnft) | 0.0400 | 0.0200 | 0.003123 | 6.40 | 0.000 |
| $X_2 X_3$ (Agft*Cbnft) | 0.0640 | 0.320 | 0.003123 | 10.25 | 0.000 |
| $X_1 X_2 X_3$(Meshcount*Agft*Cbnft) | 0.0720 | 0.0360 | 0.003123 | 11.53 | 0.000 |

## 4.2 The most optimal combination for maximal conductivity (minimal resistance)

Figure 12 provides a cube plot for the blood glucose test strips resistance. The cube plot presents the average values of test strip resistance for the eight different combinations. The average values are labeled at each corner of the Cube. As shown in Figure 12, when the combination of (-1, 1, -1) is used, that is the silver ink Screen mesh counts ($X_1$) value of 250; conductive silver (Ag) ink film thickness ($X_2$) of 12μm; and conductive carbon (Carbon) ink film thickness ($X_3$) of 12μm, then the blood glucose test strip resistance (Y) is at the minimum value of 7.046.
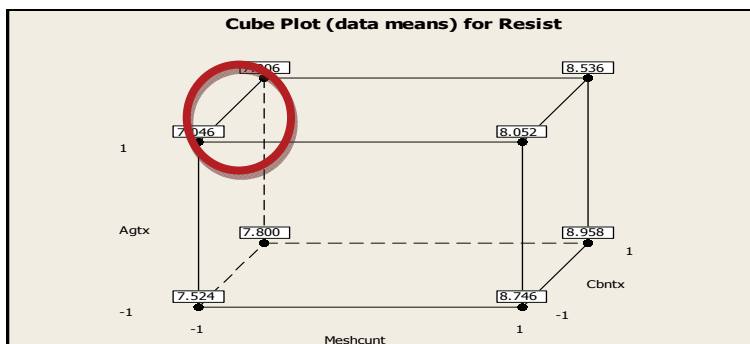


*Figure 12: Cube plot of the blood glucose test strip resistance*

## 4.3 Forecasting model

Using Stepwise Regression analyses, this study obtains regression analysis of the blood glucose test strip resistance values. From the Coef (Coefficient) value in Table 7 we can derive a prediction model for the blood glucose test strips resistance values, as:

$$Y = 7.996 + 0.557X_1 - 0.261X_2 + 0.154X_3 - 0.018X_1X_2 + 0.02X_1X_3 + 0.32X_2X_3 + 0.036X_1X_2X_3 \qquad (6)$$

Therefore when the combination yielding the minimum resistance value is deployed (-1, 1, -1), namely with the silver ink screen mesh counts ($X_1$) of 250; conductive silver (Ag) ink film thickness($X_2$) of 12μm; conductive carbon (Carbon) ink film thickness($X_3$) of 12μm, the prediction model estimates a blood sugar test strip resistance value (Y) of 6.788.


## 5. Conclusions

The overall results of Factorial and Regression analyses of the study, as shown in Table 8, indicate that all the eight factors, main effects and interaction effects, had significant influence on blood sugar test strip resistance (conductivity). The most optimal combination of the three factors to achieve the minimal resistance (or the maximum conductivity) is when screen mesh counts ($X_1$) of 250, conductive silver (Ag) ink film thickness($X_2$) of 12μm, and conductive carbon (Carbon) ink film thickness($X_3$) of 12μm. In addition, the optimal prediction model of all the factors, with a high R-square value of 99.11%, is "Y = 7.996 + 0.557X1 - 0.261X2 + 0.154X3 - 0.018X1X2 + 0.02X1X3 + 0.32X2X3 + 0.036X1X2X3", with a minimal estimated resistance value at 6.788.

*Table 8: Overall results and findings of the study*

| | |
|---|---|
| Optimal (maximal) process combination | (+, -, -); screen mesh counts number(X1)= 300; conductive silver (Ag) ink film thickness(X2)=8μm; conductive carbon (Carbon) ink film thickness(X3)=12μm , yields the best Cp value of 1.17. |
| $R^2$ | $R^2$ (R Square) = 99.11% |
| Significant effects | X1 (Meshcount) X2(Agft) X3(Cbnft) X2X3(Agft*Cbnft) X1X3(Meshcount*Cbnft) X1X2(Meshcount*Agft) X1X2X3(Meshcount*Agft*Cbnft) |
| Optimal combination for obtaining minimal resistance | (-, +, -); screen mesh counts number(X1)= 250; conductive silver (Ag) ink film thickness(X2)=12μm; conductive carbon (Carbon) ink film thickness(X3)=12μm |
| Prediction model | Y = 7.996 + 0.557X1 - 0.261X2 + 0.154X3 - 0.018X1X2 + 0.02X1X3 + 0.32X2X3 + 0.036X1X2X3 |
| R2 (R Square) | 99.11% |
| Estimated minimal resistance value of blood sugar test strip | 6.788 |

## Acknowledgements

## References

Olga, S. (2010). *The influence of external factors on the operational stability of the biosensor response. Talanta. 11, 1245-1249.*

Liao, C. N. (2008). Research and Implement on the Intelligent Glucose Meter. (Master thesis, University of Bioengineer Tatung, 2008).

Nan, C. (2008). Fabrication and Analytical Application of Glucose Biosensors. (Master thesis, University of Shanxi, 2008).

Taufik, P. (2007). Fabrication of a Disposable Glucose Biosensor on Screen-printed Carbon Electrodes. (Master thesis, University of National Taiwan, 2007).

Liou, Y. C. (2007). *The Research of Glucose Biosensors on Screen-printed. Printing Industry. 4, 17.*

# Hybrid media on packages

*Ulf Lindqvist* [1]*, Maija Federley*[1]*, Liisa Hakola*[1]*, Mikko Laukkanen*[2]*,*
*Aino Mensonen*[1]*, Anna Viljakainen*[1]

[1] VTT Technical Research Centre of Finland
  P. O. Box 1000, FI-02044 VTT, Finland
  E-mail: firstname.surname@vtt.fi

[2] Aalto University, School of Economics
  P. O. Box 1210, FI-00101 Helsinki, Finland
  E-mail: firstname.surname@hse.fi

### Abstract

The packages are expected to carry ever more information in a limited space. One solution is hybrid media, i.e. printing intelligent elements on the packages. The aim of this study was to find the best way to produce additional business to the value chain of packages via already existing technologies for hybrid media.

The approach included a technology survey about 2D applications, interviews with industrial experts from the package value chain, two industrial case pilots with user studies and a study tour to forerunner companies in Japan.

Hybrid media can give benefits in form of cost savings, new business opportunities, additional value to already existing business and increased customer loyalty to all players in the value chain. Available hybrid media technologies are 2D bar codes, digital watermarks, image recognition, fibre matrix, RFID tags and magnetic codes.

Pilot tests and user studies showed that additional hybrid media service should include detailed product data, recipes, nutrient need, user instructions and matching of user demand. Obstacles for use are costs, time consuming and complexity.

In Japan mobile barcodes are part of everyday life, well known to consumers and used on flat rate basis. The introduction was from the beginning based on consumers' needs, not on early profit. Today it operates on a win-win principle with benefits for all the players in the value chain and several traditional printers have created completely new service concepts for their customers.

**Keywords:** hybrid media; packaging; printed functionality; business models; user studies

## 1. Introduction

The role of the packages as a communication media is increasing and they are expected to carry more information and to give additional value instead of just being a cover for the product. On the other hand, the surface area of the package available for additional information - useful or entertaining - is decreasing as more space is needed for compulsory information set by legislation and authorities, and by e.g. versions in different languages.

Hybrid media, i.e. the integration of printed and electronic media, is one way to increase the amount of information applicable to a package. In its simplest form hybrid media includes printing of a 2D code on a package, reading the code with a mobile phone equipped with a camera, and access via the interpreted information to an Internet address to receive additional information. However, hybrid media may also have a wider meaning like interpreting an intelligent printed element, like a code, an image, a fibre structure, active particles etc., by a reader giving access to an electronic service or additional information.

The aim was to clarify the opportunities in hybrid media for the packaging industry and to find the best ways to produce additional business values. The project concentrated on existing exploitable technologies and analysed them from the aspect of applications, services, business potential and consumers' attitudes.

The project resulted in a generic analysis of applications, where hybrid media offers additional values for the players in the value chain.

## 2. Research methods

The work started with a technology survey with the objective to analyze available hybrid media technologies and their differences. The technologies under study were mainly limited to optically readable. Camera phones were considered as a primary reading device. Also code contents were analyzed.

More than 40 industrial experts from 20 companies in the package value chain were interviewed. The companies represented manufacturers of raw materials, package manufacturers, printers, brand owners, technology providers and vendors, retailers, logistic companies, advertising agencies and consumers. The themes of the interviews were the position of the company in the package value chain now and in the future, new opportunities for the company and the company's need to communicate with the consumers.

The purpose of the case studies was to simulate an actual hybrid media service implementation process without delivering the packages to consumers through retail stores or similar delivery channels. The packages were used for individual consumer interviews in controlled environment. The case study concepts were defined based on rough ideas collected from companies during interviews.

Consumer studies with the pilot services were performed with four consumer groups. Each group consisted of ten persons and represented different ages and educational levels. The groups were balanced in respect to gender. The aim was to find out which services were of interest to the consumer, what ties the consumer to the brand, opinion about hybrid media, suitability of hybrid media in the cases, functionality and obstacles for use.

The international state of the art of hybrid media in packages was evaluated with special emphasis on additional services, information, amusement and games. Finally, industrial pilots including services based on 2D codes were developed and new business models for these services were outlined.

## 3. Results

Based on company interviews the general package value chain was defined (Figure 1) together with the information flow between different parties.

The package already acts as an information carrier, the legally required information is huge and "excess" codes waste surface area from a package that should be as attractive as possible. The brand owners accept a rise in price to reach visibility.

Hybrid media is used to reach cost savings, new business and additional value to existing business. In the customer interface it may create loyalty, information and additional sale. Motivating the customer to use it is essential. The brand owner can get valuable information about the using context.

Applications in logistics give the fastest pay-back. The future role of logistics may include managing the entire business chain and minimizing storing at the retailer. In valuable products RFID tags will be used.

Available hybrid media technologies include 2D bar codes, digital watermarks, image recognition using fibre matrix, RFID tags and magnetic codes. These all can be used for hybrid media services in packages although dependent on service type. RFID tags and magnetic codes are especially suitable for logistics and security applications. For consumer applications, 2D bar codes and digital watermarks are ideal as they are inexpensive to produce and the codes can be interpreted with a camera phone.

Consumers can read the data content of a code symbol by camera phone equipped with suitable software. The data content is typically a link to a web service giving additional information about the product or access to some kind of contest etc. A 2D-code requires space on a package but on the other hand methods for customizing the code symbol have been developed so that it would better match the appearance of the package.

In Japan hybrid media has been utilized since 2003. In Finland the first hybrid media service was used in summer 2004. During 2008 several services have been introduced in several countries in Europe, Asia and Americas. The services have mostly been attached to publications, advertisements and business cards, but

also in the packaging industry some services have been tested. The technology has been globally established during the recent years and consumers are becoming familiar with it.
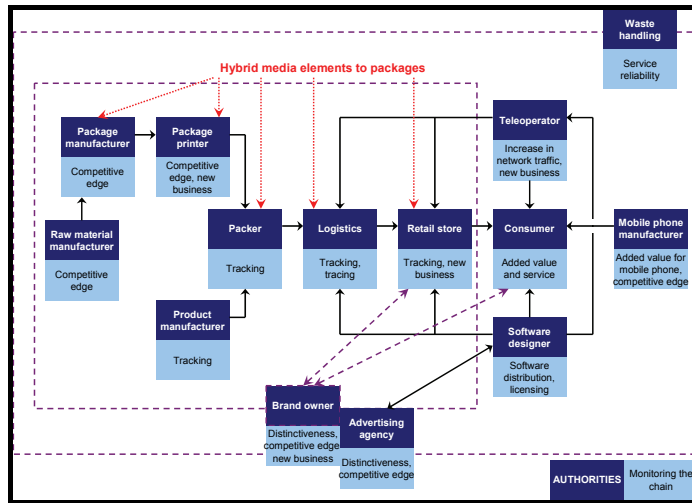


*Figure 1: Package value chain with potential parties who could add the hybrid media elements and benefits that hybrid media could bring*

Consumers can read the data content of a code symbol by camera phone equipped with suitable software. The data content is typically a link to a web service giving additional information about the product or access to some kind of contest etc. A 2D-code requires space on a package but on the other hand methods for customizing the code symbol have been developed so that it would better match the appearance of the package.

In Japan hybrid media has been utilized since 2003. In Finland the first hybrid media service was used in summer 2004. During 2008 several services have been introduced in several countries in Europe, Asia and Americas. The services have mostly been attached to publications, advertisements and business cards, but also in the packaging industry some services have been tested. The technology has been globally established during the recent years and consumers are becoming familiar with it.

The lack of standardization, especially with the code content, limits the use of hybrid media technologies. Hybrid media is still a technology under development and currently it has a risk of conflicting standards that can complicate its use. In order that hybrid media would become a success story, different parties should be able to count on that the basic technology will remain unchanged.

The objective of the technology pilots in the project was to 1) produce demonstration packages and services for consumer studies and to 2) precisely report how an example hybrid media service is implemented. The technology pilots were designed to give information on how willing consumers are to use hybrid media services as well as what are consumer opinions on usefulness, functionality and ease-of-use of these services.



*Figure 2: Coffee and cereal packages with hybrid media codes used in the pilot tests*

The results clearly showed that grown-ups tend to be in a hurry when shopping and that any service that eases their shopping would be useful. Such a service should work only on-request. For some users the data transfer fee is an obstacle for using this kind of services, but for many users it is important only to know the magnitude of costs.

Based on the user studies the service could include:

- Recipes and shopping list based on user's choices. For one day or for whole week depending on user's choices.
- Service that tells the user how much of daily need of each nutrient he has had after each meal/snack. Service could recommend healthier choices if requested.
- Ideas of new ways to use the product.
- Very detailed information of the food stuff like the origin of each component.
- Information on how well a new product meets the demands set by the user. The criteria could be defined in a user profile of the service. The most common restrictions in diet are due to allergies but some users also want to avoid certain ingredients (e.g. aspartame, fat or specific e-numbers) for other reasons.

The biggest obstacles for using code were:

- The costs; the users are not willing to pay for additional information of the product. The data transfer fee was not an obstacle for highly educated users or for users over 40 years old, if the service was found useful.
- The mobile phone or the application; the users found their own mobile incapable of using the services and they were lazy to download applications, while their experience of downloading was sometimes troublesome.
- It is time consuming; users are not willing to spend time on codes. Especially this concerns the time spent shopping groceries.

Things that would promote the usage of the codes:

- Young people find it frustrating to write text messages, codes are simpler to use.
- Users tend to have the mobile available somewhere near.
- Middle-aged users have problems in seeing small text.

An analysis of business models associated with using hybrid media on packages was carried out. The aim was to discover the different solutions for taking advantage of hybrid media and the requirements that the implementation of these solutions place on the way the firms do business. For the purposes of this study, business models were understood to mean the logic behind how a firms aims to generate revenue by creating value for its customers and the way in which the firm organizes its resources in order to do so.
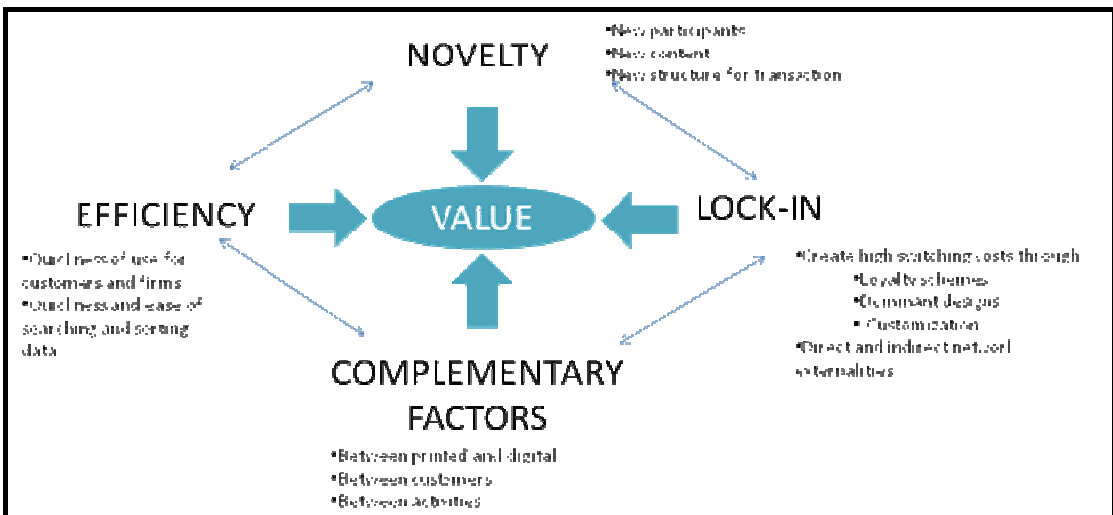


Figure 3: A value driven model for hybrid media solutions

A two-tiered approach was undertaken that included interviews in Finland with managers of firms about the benefits they envision hybrid media could provide and how they would organize their business to take advantage of these benefits, as well as interviews with firms' management in Japan, where hybrid media solutions had been successfully integrated into products and firms were able to benefit from using hybrid media.

The interviews in Finland revealed that some of the representatives of the Finnish firms were extremely cautious about integrating new technology into their existing offerings. Their concerns seemed to be mostly with the added costs and high risk associated with undertaking a new type of solution. While many interviewees in Finland seemed convinced that hybrid media solutions could offer added value to their customers and therefore be worthwhile for the firm, they were afraid the changes required in their existing business models to incorporate the new solution would be substantive and possibly detrimental. Many firm representatives said they would be more likely to be willing to take the risk once other firms had shown that hybrid media can be used successfully.

Meanwhile, the Japanese interviewees seemed convinced that the business model of the firm should always be aimed at providing maximum value for their customers, and that in order to do this, they must be able to incorporate new ways to deliver value into their existing business model. They appeared to view the integration of hybrid media into existing products as merely an added component to their offering and not something that requires a total overhaul of their business model. Their views also seemed to be in stark contrast to those of their Finnish counterparts regarding the time a firm should wait for positive returns before terminating a new venture. While some of the Finnish interviewees were keen on seeing a clearly defined ROI analysis that could be conducted after a given period time, the Japanese appeared to be more willing to provide new services even without a clear and identifiable revenue stream. It was enough for them that they judged the new services to be of value to their customers.

## 4. Conclusions

Hybrid media has proven to be an efficient way to increase the amount of information on packages. Intelligent printed elements, readable e.g. by mobile phones, can be used for giving additional information in different languages about the product, raw materials, manufacturing process, advises to use, recipes, restrictions and regulations. It also enables feedback from customers and additional service like entertainment, special offers and advertising. The same elements can also be used to send information between the different partners in the value chain.

In Japan hybrid media has been used generally in packages since 2003. The lack of standards has been the main obstacle for international utilisation of the hybrid media technology. Technology pilots were carried out for consumer studies and to find the best way to implement hybrid media service. It was found that consumers are most interested in the product itself and want to find more information about it via the intelligent elements. However they need the software ready installed in their mobile phones, and they are also concerned about data transfer fees.

The additional hybrid media services need new business models to become profitable. Examples of successful campaigns and service business can be found in Japan, where the brand owners often see the additional services as a marketing tool.

## Acknowledgements

## References

**Lindqvist, U., Federley, M., Hakola, L., Mensonen, A., Moilanen, P., Viljakainen, A., (2010)**, Hybrid Media in Packaging. VTT Working Papers, Espoo, 2010. To be published.

**Lindqvist, U., Moilanen, P., (2008)**, Business from hybrid media and printed functionality. ed.: Enlund, N., Lovrecek, M., Advances in Printing and Media Technology, Vol. XXXV. Darmstadt, 2008, p. 101-106.

**Lindqvist, U., Hakola, L., Linna, H., Moilanen, P., Siivonen, T., (2007)**, New business models for printed functionality. ed.: Enlund, N., Lovrecek, M., Advances in Printing and Media Technology, Vol. XXXIV. Darmstadt, 2007, p. 395-400.

**Hakola, L., Lindqvist, U., Linna, H., Siivonen, T., Södergård, C., (2007)**, Roadmap on printed functionality and hybrid media. ed.: Enlund, N., Lovrecek, M., Advances in Printing and Media Technology, Vol. XXXIII. Zagreb 2007, p. 103-109.

**Hakola, L., Linna, H., (2006)**, Detection of printed codes with a camera phone. ed.: Enlund, N., Lovrecek, M., Advances in Printing and Media Technology, Vol. XXXII. Zagreb 2006, p. 11-16.

# Printing of identification characters on vanishing micro-pattern of plasticized polymers as the means of polygraphic protection

*Akakiy Dzhvarsheishvili, Alexandr P. Kondratov and Evgeny B. Bablyuk*

Moscow State University of Printing Arts
2a, Prianishnikova Street
RU-127550 Moscow, Russia

E-mails: koks85@bk.ru, apk@newmail.ru, evgeny.bablyuk@mgup.ru

**Abstract**

A rapid development of the most diverse consumer goods' counterfeit and adulterations industry is determining the increase of counterfeit package's production volumes. Exactly the package contains the inside's anticounterfeit features and is most often forged by simple photocopying by applying the small-offset printing methods. The easiest way to do it is when the packing material to be sealed is presented by a large capacity polymer, and a barcode is used as the goods' means of identification. The technological tools of small-offset printing allow a quick receiving of goods label's copy with a bar-code of a considerably high quality, and the film filler polymer materials to be sealed, as a general rule, are widely presented in the market. Within the framework of polygraphic industry the struggle against counterfeiting of consumer goods is focused on the search of original optical, chemical, thermo-chromic and other physical effects that allow producing the identification seal that virtually can not be reproduced by counterfeiters.

The development objective is to create a technology when a printed image, containing the informative component, protected against forgery, for instance, a bar-code, is applied on a polymer base surface (stamp, label), enabling its duplication in numbers of copies with no high technological costs and impossibility of adulteration. The principal research interest is the polymer-solvent system, carried out by studying the kinetics and thermodynamics of the interaction of polymers with low-molecular fluids.

In this paper we propose a unique method of protecting information, which is based on the process of swelling of the polymer material. To find the optimal polymer-solvent system we investigated kinetics of swelling different polymers in low-molecular liquids. Constants of speed, Flory-Huggins parameters, diffusion coefficient D for each solvent was determined. The changes of the basic thermodynamic functions $\Delta G$, $\Delta S$, $\Delta H$ of swelling, differential molar isosteric heats of sorption are calculated. The data obtained allow to choose a suitable polymer material for the problem posed

**Keywords:** counterfeiting; Flory-Huggins parameter; plasticized polymers; swelling

## 1. Introduction

The problem of counterfeit goods in the consumer market is not new. Scope of the various imitations worldwide is very wide and extends from the production of low-quality food products to the manufacture of cheap non-standard components in the electronics industry. Thus, according to the International Anti-Counterfeiting Coalition (international organization coordinating the effort to eliminate counterfeiting ), an annual global volume of the "parallel" trade (i.e. trade in counterfeit goods) is a figure close to 500 billion dollars a year. Combating counterfeiting of consumer goods in the printing industry is focused on finding the original optical, chemical, thermo chromic and other physical effects that make the identification seal virtually non-reproducible. Therefore, the creation of new technologies that allows protecting, printing products from counterfeiting is one of the most promising goals to date.

In the late 50-ies of the XX century, academician Kargin V. A. and co-workers put forward a number of fundamentally new hypotheses concerning the structural heterogeneity of amorphous and crystalline polymers (Kargin, V. A., Slonimsky, G. L., 1967). These views were so new and revolutionary, that for their experimental validation new methods and approaches were needed. As a basis for such an approach acad. Kargin V. A. used the principle of visualization of amorphous (structureless) polymer systems and phenomena occurring in them.

A structured approach to the study of various phenomena in polymers is a valuable scientific heritage of acad. Kargin V. A., and certainly merits further development. The phenomenon of structural heterogeneity of

polymer material opens up new possibilities in the development of new technology for printing products to protect against counterfeiting. Our development is based on the unique effect of the appearance and disappearance of micro-topography cross-linked rubber and polymer composites accompanying the sorption of "good" solvents. This effect is proposed to be used for marking and protecting against forgery of valuable products or products with limited shelf life. This should make printing images carrying information about the object on the polymer at the time of appearance of micro-relief on its surface. After printing an informative sign, for example, a linear or two-dimensional bar code on the uneven surface of the swollen polymer material and the desorption of solvent from the polymer material, the specific micro relief of the surface disappears (or is smoothed), and an information sign "splits" into pieces, therefore separated by spaces and as a consequence of this, is not perceived by a scanner (see fig. 1). Printing of the information sign is done at the moment of maximum distortion of the wavy surface which is plasticized by the liquid polymer. The plasticized surface layer of liquid polymer at the optimal time for printing is created by closed/dense ridges formed by waves, when grooves are at their maximum depth.



*Fig. 1: "Collapse" into pieces of bar-code applied to a contoured surface of the swollen rubber*

The solution to this problem will create a so-called temp sensor, which can be used for products with limited shelf life. At the same time, "life" image bar code must match the time and date of the product depending on the properties of the polymer and the volatility of the solvent.

Protection of the products or packaging from forging is provided by the inverse problem solution, hence once the barcode disintegrated into fragments, the polymeric material is exposed to interact with specifically selected solvent, and due to swelling and the formation of relief structures in polymer materials, sizes of cracks are reduced, resulting in the bar code becoming unreadable for the scanner.

## 2. Mathematical model of a swelling process

The swelling of a material in a liquid is a superposition of two simultaneous processes. These are, on the one hand, diffusion of the liquid and, on the other hand, deformation of the polymer matrix induced by absorption of the liquid. These processes are interrelated because a nonuniform distribution of the liquid arising in the course of diffusion induces heterogeneous strain and stress fields, which can affect the diffusion kinetics of the material swelling. This effect increases with increasing deformation of a material, being most pronounced in strongly swollen materials. The mathematical model constructed in (Denisyuk E. Y. and Tereshatov V. V., 2000; Dzhvarsheishvili A. I., 2008) describes the nonequilibrium process of swelling that takes place with finite strains for a plane elastomer sample or a polymer gel. Let us use this model to analyze the kinetics of swelling of polymers in solvents of various thermodynamic qualities. At first, let us introduce some definitions:

$u(x; \tau)$ - is a solvent concentration;

$\varphi(x; \tau)$ - is a local volume fraction of polymer;

$\varphi_E(x)$ - a volume fraction of polymer in an equilibrium swelling state;

$J(x; \tau)$ - describes the current local bulk deformation of swelling material;

$v = v(\tau)$ - is a longitudinal relative elongation of a specimen;

$\chi$ - is the Flory-Huggins parameter;

$Z = V_2 / V_1$ - is a dimensionless parameter;

$V_1$ - is a molar volume of solvent;

$V_2$ - is a molar volume of polymer network subchains;

$D$ - is the solvent diffusion coefficient in the material.

This mathematical model is considered for the polymer $2h$ thick with an infinite length to both sides. The model includes the following system of equations and initially boundary-value conditions:

$$u'_\tau = u''_{xx}, \quad u = u(x,\tau), \quad 0 \le x \le 1, \tag{1}$$

$$u(x,0) = 0, \quad u'_x(1,\tau) = 0. \tag{2}$$

$$v(\tau) = (\int_0^1 J(x,\tau)dx)^{\frac{1}{6}}, \tag{3}$$

$$\ln(1-\varphi) + \varphi + \chi\varphi^2 + Z^{-1}\varphi_E^{\frac{4}{3}}\varphi^{-1}v^{-4} = 0. \tag{4}$$

At $x = 0$

$$\varphi = \frac{\varphi_E}{J} \tag{5}$$

$$J = (1-\varphi_E)u + \varphi_E \tag{6}$$

The problem (1)-(6) is represented in a dimensionless form and describes free swelling of a flat specimen in the proximity of the infinitely long layer. The units of measurement of a distance and time are a semi-thickness of a specimen in a reported state, $h$, and the value of $h^2/D$. Equations (1) and (2) describe the diffusion process, equations (3), (5), (6) - the deformation process of a polymer network.

The longitudinal deformation of a specimen leads to the higher thermodynamic polymer-solvent compatibility and causes the solvent concentration growth in the surface layer of a specimen. This circumstance takes into account boundary condition (4). It follows from the condition of a thermodynamic equilibrium on the specimen-solvent interface that is expressed in the equality of chemical potentials of a liquid phase and a solvent absorbed by the material.

The boundary-value problem (1)-(6) are written down for a reference state that is assumed here to be the equilibrium swelling state of the material.

Taking into consideration boundary-value problem (1)-(6) we can derive the asymptotic equation of a kinetic curve at the terminal swelling stage

$$\alpha_1^2 \cdot h^{-2} \cdot D \cdot t - \ln C = -\ln(1 - g(t)) \tag{7}$$

where $g(t) = m(t)/m_E$ is a kinetic swelling curve; $m(t)$ is the current value of fluid mass absorbed by a specimen; $m_E$ is the maximum value of fluid mass absorbed by a specimen; $C$ is a constant, $h$ -1/2 of the specimen thickness in the equilibrium swelling state; $\alpha_1$ is the first positive root in the following equation

$$\alpha = \gamma \cdot tg\alpha, \tag{8}$$

where

$$\gamma = \frac{4(1-\varphi_E)}{3 \cdot [Z \cdot \varphi_E^{\frac{5}{3}}(1 - 2\chi + 2\chi\varphi_E) + 1]}. \tag{9}$$

Equation (7) is the basic for estimation of the diffusion coefficient.

## 3. Methods

For exposure of macroscopic structure of investigated samples we used the method proposed in (Kondratov A. P. Patrikeev G. A., 1988). Dispersed dye, the powder with hue contrast to the hue of elastomer (for example, for white rubber we used the magenta pigment), carried to the elastomer surface by the roller moistened with the solvent at the beginning moment of symmetric swelling. The adhesion marks were carried in definite time intervals, namely in 5, 7, 10, 20, 30, 40, 50, 60, 120, 180, 1440 minutes of swelling. It is important to note, that in case of flocculation the contrast substance doesn't penetrate to the small cavities between closed surfaces, to the cavities of lengthwise grooves and others. It is proposed to differ the three types of large-scale relieves of swelled rubbers surfaces: A, B and C. The relative (without scaling) schemes of relieves cross-sections shown at fig. 2.

As a result of contrasting of swelling relief with the structure marks method, the closing surfaces stay uncolored, that gives the possibility to estimate approximately, using measuring microscope, their typical transverse sizes, corresponded to the depth of resulting cavities
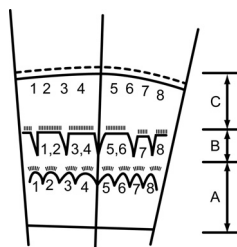


*Fig. 2*
*Diagrams of distinctive pattern's cross sections of cross-linked elastomeric material's surface layers in the initial stage in undistorted state*

As a result of contrasting of swelling relief with the structure marks method, the closing surfaces stay uncolored, that gives the possibility to estimate approximately, using measuring microscope, their typical transverse sizes, corresponded to the depth of resulting cavities. The A type relief should be formed under a short-term contacting sample surface with solvent thus characterizing by some chaotic bulges and cavities having its shapes and dimensions which depend significantly upon a type of sewn elastomer, sample thickness, technological compound factors, swelling degree or etc. Under sorption of the solvent by sample during several minutes these cavities' lateral surfaces join together, i.e. the B type relief occurs. The A relief transfers into the B relief along with a smallest particles "disintegration" or, in other words, the A relief becomes larger one. Such process is shown in the diagram as an elimination of cavities between relief elements (1-2, 3-4, 5-6). The cavities between elements 7 and 8 as well as 2 and 3 are enlarged by size and under swelling pressure are closed and compressed crosswise. Under long-term contacting with solvent the sewn elastomers' surface is aligned completely. This condition of the sample's bulged and superficial layer is shown as C in fig. 2. The contrasting process enables to "fix" a relief at the moment of its maximal occurrence and to determine any dimensions of its major elements. The longitudinal grooves in its transverse direction appear as some alternate regular bulges and cavities which are sketched in figure 2. The cross section dimensions of the longitudinal grooves can be measured only by respective adhesional mark points upon solvent desorption. The elastomers' surface morphology has been surveyed by way of analyzing relevant photomicrographs made by using the Polam P-312 polarization microscope.

To study the kinetics of swelling, disk-shaped samples were prepared. The kinetics of swelling were monitored by the gravimetric technique: the sample was placed into the solvent and periodically weighed with an analytical balance. The experiment was complete after the sample attained the equilibrium degree of swelling. The swelling experiments were conducted at 25°C. The Flory-Huggins parameter $\chi$ was found from

$$\ln(1-\varphi_E) + \varphi_E + \chi\varphi_E{}^2 + Z^{-1}\varphi_E{}^{1/3} = 0 \qquad (10)$$

Characteristics of the polymer network was determined by the method of Cluff-Gleding (Cluff E., Glading E., Pariser R., 1960). Applying the experimental data the kinetic swelling curves were plotted. Then the diffusion coefficient $D$, for each solvent was calculated by relationship (7), by the terminal parts of kinetic swelling curves having represented them in coordinates ($t$ ; $-\ln(1-g(t))$, in which at $g(t) \geq 0.5$ they take the the form of a straight line with slope $\alpha_1^2 \cdot D \cdot h^{-2}$. The value of $\alpha_1$ was found from equation (8) after preliminary calculation of $\gamma$ by formula (9).

## 4. Results and discussion

Print on swollen polymer materials was carried out using automatic screen printing machine - Synchroprint 4000 AC (MHM, Austria). Two types of inks were used: UV and alcohol based. For the printed material we have used natural rubber that had thickness of 4 mm. Usual bar code was used as an element of protection, which is printed at different angles in relation to the created grooves in the polymer material.

There was a preliminary experiment on the selection of colors. Figure 3 clearly shows that the effect of cracking of the ink layer after solvent desorption is observed for both alcohol and for UV inks. After analyzing the micrographs, we concluded that the cracks in ink are clearly recognized as a class of UV curing inks. It should be noted that the adhesion of inks in the formation of cracks in the ink, remains good.
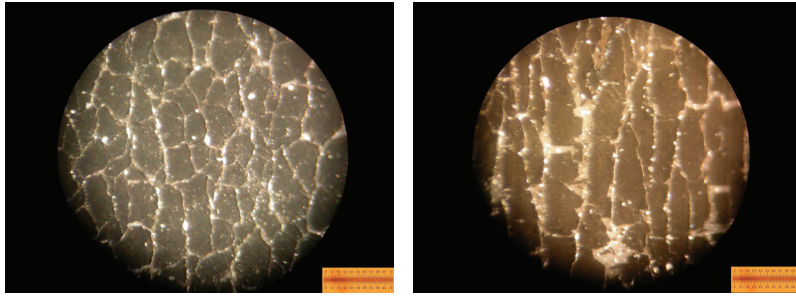
*Fig. 3: The formation of cracks in the layer of alcohol and UV inks after desorption solvent
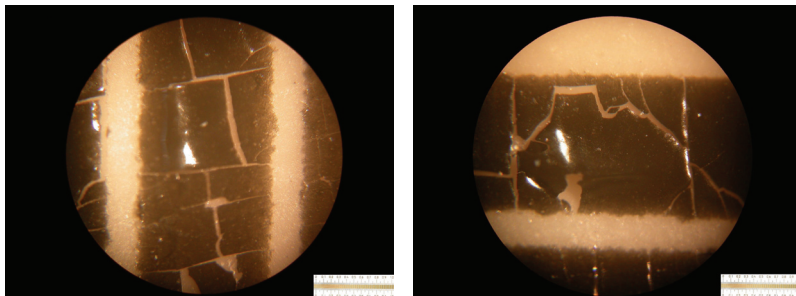(Scale with a scale division 5 microns)*



*Fig. 4: The formation of cracks in the form of bar code under UV - printing on polymer materials
is subjected to a 10 minute swelling after the desorption solvent. Print bar code carried in the
direction of education grooves
(Scale with scale division of 5 microns)*

Analyzing the resulting micrographs we concluded that the effect of crack formation (fig. 4) is more pronounced in the case of printing a barcode in the direction of education striped structure. From the experimental data there was made a general conclusion that the effect of the crack formation in the consequence of disappearance of the striped structure is the case. The opposite effect, i.e. sorption-desorption cycle, showed that the cracks in the paint are on the decline due to, once again, developed furrowed structure, with the adhesion of ink to the polymer that does not deteriorate. When reducing the cracks into the ink, bar code once again becomes readable for the scanner.

Further model experiments were conducted to identify the optimum time of swelling for the polymer material in various solvents, in order to determine the maximum width of grooves formed at the sorption of solvent.

Based on a mathematical model of the swelling of polymers, proposed above, the kinetic and thermodynamic parameters of interaction in the polymer-solvent have been calculated. From the results we can conclude that most thermodynamic affinity (Flory-Huggins parameter takes the lowest value) to the natural rubber has chloroform followed by (in order of decreasing affinity), carbon tetrachloride, toluene, dean, hexane, ethyl acetate and isopropanol. When increasing the thickness of the rubber, Flory-Huggins parameter when interacting with all solvents was decreased, although according to the theory of Flory-Huggins this parameter must be a constant no matter of the thickness of the polymer material.

This provision is an experimental refutation of the monograph Tager A. A (Tager A. A., 2007). In some systems (natural rubber, isopropanol, natural rubber - ethyl acetate), there was a rapid absorption of the solvent in the first moments of time, and then a gradual swelling. This phenomenon can be explained by two reasons:

a) Presence in polymer of micro-voids, which are being quickly filled with solvent within the initial moment of time;

b) Quick penetration of molecules of solvent along solvate shells of macromolecules with their subsequent slow-flowing diffusion into phase of polymer.

Below provides a summary table of calculations of parameters the kinetic curves of swelling (table 1-2).

*Table 1: Parameters of the kinetic curves of swelling of natural rubber of various thicknesses in solvents of different thermodynamic quality*

| Solvent | The thickness of the polymer. h (cm) | The Flory-Huggins parameter ($\chi$) | The diffusion coefficient, $Dx10^8$ $cm^2/sec$ | Equilibrium degree of swelling, % |
|---|---|---|---|---|
| Chloroform | 0,4 | - 0,858 | 3,531 | 713 |
| | 0,5 | - 0,428 | 6,875 | 550 |
| | 0,6 | - 0,329 | 23,526 | 534 |
| Carbon tetrachloride | 0,4 | - 0,789 | 9,147 | 744 |
| | 0,5 | - 0,195 | 18,095 | 580 |
| | 0,6 | - 0,179 | 23,593 | 562 |
| Toluene | 0,4 | - 0,363 | 2,289 | 316 |
| | 0,5 | - 0,035 | 3,433 | 255 |
| | 0,6 | - 0,188 | 17,96 | 241 |
| Dean | 0,4 | - 0,104 | 1,835 | 159 |
| | 0,5 | 0 | 5,032 | 126 |
| | 0,6 | 0,195 | 17,041 | 109 |
| Hexane | 0,4 | 0,231 | 0,778 | 133 |
| | 0,5 | 0,401 | 8,823 | 111 |
| | 0,6 | 0,415 | 8,850 | 109 |
| Ethyl acetate | 0,4 | 0,865 | 1,221 | 46 |
| | 0,5 | 0,871 | 1,342 | 45 |
| | 0,6 | 0,876 | 2,125 | 43 |
| Isopropanol | 0,4 | 3,171 | 1,371 | 1 |
| | 0,5 | 3,183 | 5,431 | 1 |
| | 0,6 | 3,189 | 6,543 | 1 |

*Table 2: Parameters of the kinetic curves of swelling of natural rubber of various thicknesses in solvents of different thermodynamic quality*

| Solvent | The thickness of the polymer. h (mm) | $\phi_E$ | $\alpha$ | Maximum width of grooves (mm) |
|---|---|---|---|---|
| Chloroform | 4 | 0,132 | 1,2479 | 1 |
| | 5 | 0,163 | 1,254 | 0,8 |
| | 6 | 0,191 | 1,2663 | 0,6 |
| Carbon tetrachloride | 4 | 0,148 | 1,5361 | 0,9 |
| | 5 | 0,202 | 1,2663 | 0,75 |
| | 6 | 0,204 | 1,2725 | 0,55 |
| Toluene | 4 | 0,186 | 1,2663 | 0,2 |
| | 5 | 0,235 | 1,2786 | 0,15 |
| | 6 | 0,236 | 1,2786 | 0,1 |
| Dean | 4 | 0,286 | 1,2908 | 0 |
| | 5 | 0,316 | 1,5484 | 0 |
| | 6 | 0,356 | 1,3276 | 0 |
| Hexane | 4 | 0,339 | 1,3337 | 0 |
| | 5 | 0,458 | 1,4073 | 0 |
| | 6 | 0,462 | 1,3276 | 0 |
| Ethyl acetate | 4 | 0,667 | 1,5361 | 0 |
| | 5 | 0,679 | 1,53 | 0 |
| | 6 | 0,684 | 1,5178 | 0 |
| Isopropanol | 4 | 0,952 | 1,5669 | 0 |
| | 5 | 0,957 | 1,5669 | 0 |
| | 6 | 0,967 | 1,5669 | 0 |

When processing the results there was a clear pattern distinguished - at the deterioration of the thermodynamic quality of solvent the maximum width of grooves decreases for each type of polymer. This trend can be seen in figure 5. The formation of grooves in the swelling of polymeric materials was observed for three kinds of solvents - chloroform, carbon tetrachloride and toluene. And the grooves for all the polymers reached its maximum width of the swelling of natural rubber in chloroform, followed by carbon tetrachloride and toluene. Kinetics of the width of the grooves in the swelling of the polymer material in these solvents is shown in figure 6.
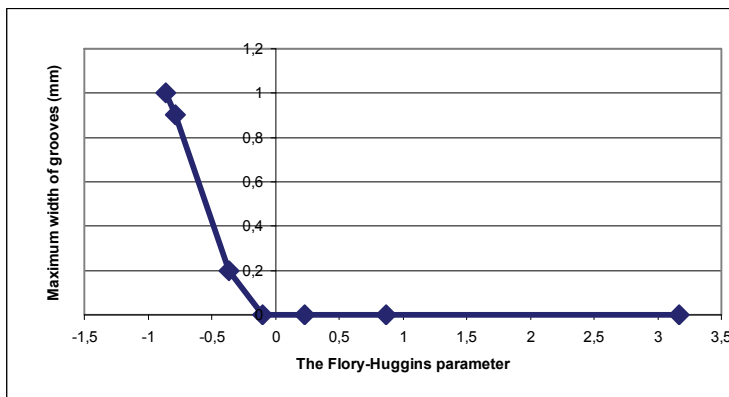
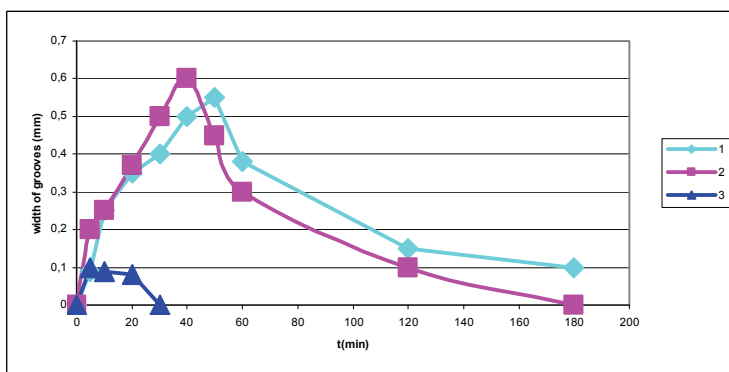*Fig. 5: The dependence of the parameter Flory-Huggins of the maximum width of grooves*



*Fig. 6: The dependence of the change in the width of grooves on the time of swelling of rubber 6 mm thick, in solvents of different thermodynamic quality. 1-carbon tetrachloride, 2 - chloroform, 3 - toluene.*

For natural rubber, thickness 4 mm, maximum width of the groove is achieved by swelling of the polymer in chloroform, and is equal to 1 mm, and 0,9 mm. in carbon tetrachloride, at the time of swelling for 30 minutes, in either case. It is expected that if the conditions of the technological process are met, (30 minutes, the swelling of natural rubber (4 mm) in chloroform and four chloride, carbon tetrachloride), the cracks in the paint layer, would reach their maximum value. It should be noted that increasing the thickness of polymer material - the width of the grooves when the swelling decreases, such as: swelling of 5 mm natural rubber in chloroform, the maximum width of the grooves reaches 0.75 mm and 6 mm - 0,55 mm. More clearly the effect is demonstrated in figure 7.
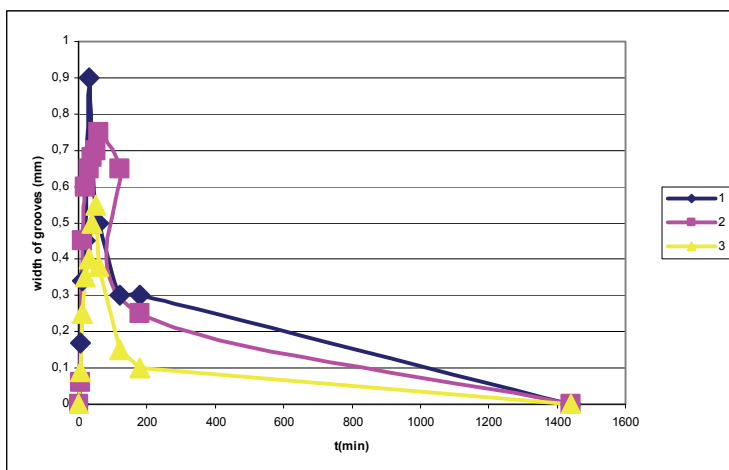


*Fig. 7: The dependence of the width of the grooves on the time of swelling of rubber in carbon tetrachloride. The thickness of the sample: 1 - 4 mm, 2 - 5 mm., 3 - 6 mm*

A similar pattern is observed for other solvents, i.e. thickness of the polymer material is inversely proportional to the width of the grooves. This is due to a decrease in the degree of swelling of polymer material with an increase in its thickness.

It should be noted that the interaction with all three solvents for all studied polymer Flory-Huggins parameter is less than 0. It can be assumed that the formation of the striped structure can be observed only in highly corrosive solvents, where the crosslinked polymer swells to become 5-10 times thicker.

The formation of grooves on the sample's surface can be explained in several ways:

1) Education grooves associated with the supramolecular structure of polymer material. Namely, the relative positions in space, the internal structure and nature of the interaction between the individual elements constituting the macroscopic polymer body. Some polymers may be obtained completely amorphous or completely crystalline, but the majority of known polymers after crystallization always keeps the area with malouporyadochennoy amorphous structure, therefore, these polymers are partially crystalline (semi-crystalline). One can assume that this is a semi-crystalline polymer, i.e. consists of both amorphous and crystalline parts. The crystalline part of the polymer swells significantly worse than the amorphous part. This is due to the large intermolecular interactions. Due to this it displays a specific surface topography.

2) We can assume that the heterogeneous topography of the polymer material swelling, seen in connection with the inhomogeneous crosslinking degree of the polymer. Because of the heterogeneous crosslinking, studied natural rubber, the material swells nonuniform (increasing the number of cross-links leads to a decrease in the ability of the polymer to absorb low-molecular liquid).

For all the investigated polymers there was observed a general pattern, where the width of the grooves with increasing time of swelling is increasing until a certain point, then it begins to decrease, due to the effect of closing the neighboring grooves. Visually, this phenomenon demonstrated in figure 8.
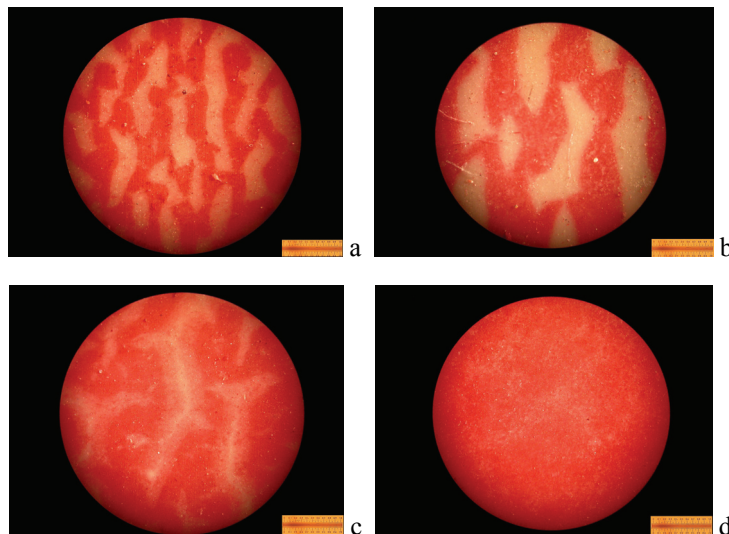


*Fig. 8. The planar form of grooves formed on the surface of natural rubber (5 mm thick) swelling in carbon tetrachloride. Time of swelling: a) 10 min., b) 60 min., c) 180 min. d) 1440 min.*

As shown above, the swelling of the polymer material "exhibit", in liquids, the width of grooves increases to a certain point of time, but then goes its further reduction. Such trends were noticed in the papers (Kondratov A.P. Patrikeev G.A., 1988), but in these works, the studies of the formation of grooves were introduced during the short time of swelling of polymeric materials (0,5 - 10 min). We have shown that the effect of the formation of grooves for natural rubber can be observed at the time of swelling of 1440 minutes (i.e. grooves at t = 1440 minutes do not join). This result fundamentally changes the idea of clamping grooves in the swelling of the polymer material. In (Kondratov A.P. Patrikeev G.A., 1988), the process of the relief formation (see fig. 2) is reasoned by the fact that prolonged contact with the solvent, the surface of sewed elastomers is completely flattened, so as not swollen core sample from the surface, completely loses touch with mouths of the depressions, which leads to the elimination of local internal stresses and the "dis-

integration" of the relief formed. It is based on this fact in (Kondratov A. P. Patrikeev G. A., 1988) where asymmetric swelling of polymeric materials with low sorption time were studied. However in this current paper, we showed that the development effect of the furrowed structure is more pronounced in symmetric swelling, with the full closure grooves can occur at the time of swelling of more than 1440 minutes. This result is new for the physical chemistry of polymers and deserves further study.

In the analysis of micrographs of grooves we came to the conclusion that the "picture" of the striped structure retains its shape after repeated swelling. Consequently, a model experiment can be assumed that the crack into the paint for a continuous cycle of sorption-desorption will be generated in the same field.

In the chaotic striped structure observed in all the micrographs, there is a defined system of the grooves arrangement. It can be assumed that the different nature of polymeric materials have their own unique cycles in the "sorption-desorption" liquid (unique) structure, which revealed swelling of the polymer material and can serve as a means of identifying a given sample of polymer material - like a fingerprint could be used for human identification (if there is information about it in the database). The above-described technology can protect information from a fake. Clearly, this development requires further study.

## 5. Conclusions

1. For the first time such reliable relationship had been found as for occurrence of specific micro-relief of the elastomer's surface and solvent's thermodynamic quality while the elastomer is swelling. The solvent's thermodynamic quality is defined by the Flory-Higgins parameter which at five-tenfold elastomer swelling becomes negative being increased monotonously within such liquid products as chloroform, carbon chloride, toluene, hexane.

2. It was suggested to print any information and protection symbols onto some plasticized polymers at the moment of the micro-relief's maximal occurrence featuring with the grooves' depth of 0,4-0,5 mm. The image of the sewn elastomer on the surface with micro-relief disintegrates into some "unreadable" fragments under drying procedure and restores under repeated swelling process which can be utilized for technology of identifying any print products and any other items protected by its polymer coating.

3. The adhesion degree of the paint layer under applying any information and protection symbols on the sewn elastomer's surface upon swelling (screen print process) is quite high. For printing purposes such materials as solvent paints having its spirits and ethers and UV drying acryl compositions are used. The bar code imprints on the natural rubber's resin may endure several cycles of the solvent "sorption-desorption" process when a multiplied and restored picture and surface micro-relief are such unique appanage of each polymer sample as any human being's fingerprint and can serve an identification method.

## References

1. Cluff E., Glading E., Pariser R. (1960). A new method for measuring the degree of crosslinking in elastomers, J. Appl. Polym. Sci., V. 45, No. 8, p. 341-345.

2. Denisyuk E. Y. and Tereshatov V. V. (2000). A nonlinear theory of the process of elastomer swelling in low-molecular-mass liquids, Polymer Science, Ser. A,, V.42, No. 1, pp 56-67.

3. Dzhvarsheishvili A. I. (2008). The effect of the thermodynamic quality of solvent on the kinetics of screen printing squeegees swelling. Proceedings of the 1st International student conference P.D.P convention. p.48-55.

4. Kargin, V. A., Slonimsky, G. L. (1967). Short Course of the Physical Chemistry of Polymers. Khimiya. p.232 (in Russian)

5. Kondratov A. P. Patrikeev G. A. (1988). The method of evaluating the structural heterogeneity of elastomers, copyright certificate USSR 1406480.

6. Tager A. A., (2007). Physical chemistry of polymers. Nauchni Mir., P. 576 (in Russian).

# Examination of the factors influencing the adhesion power between the layers of laminated plastic cards

*Erzsébet Novotny*[1]*, Ildikó Endrédy*[2]*, Csaba Horváth*[3]

[1] PNYME/Állami Nyomda Nyrt.
   Fő utca 6, H-1027 Budapest, Hungary
   E-mail: novotny@any.hu

[2] Óbuda University
   Doberdó út 6, H-1034 Budapest, Hungary
   E-mail: endredy.ildiko@rkk.uni-obuda.hu

[3] Óbuda University/Nyomdatechnika Kft.
   Doberdó út 6, H-1034 Budapest, Hungary
   E-mail: horvath.csaba@rkk.uni-obuda.hu

**Abstract**

Plastic cards are applied in many fields of our lives. They can be documents and bank cards, as well as club cards and loyalty cards. Their body is made of several plastic foil layers with lamination.

Our research focuses on the adhesion problems between plastic foil layers which can be influenced by several factors during the manufacturing process, including the type of ink, the quality of the foil and total ink coverage. The most important of them is the effect of the printed surface's total ink coverage. The purpose of our investigation is to determine the maximum total ink coverage that provides a just appropriate layer adhesion after lamination.

We printed plastic card samples with different TIC values, using CMYK process inks. We established that from the point of applicability maximum total ink coverage can be 280-300% and individually the four basic colours show very good layer adhesion results. The presence of black and cyan colours in high percentages adversely influences the adhesion force between the layers. The maximum total ink coverage can be increased if their proportions are reduced, this would, however, result in a lighter shade of colours not suitable for all card designs.

**Keywords:** plastic card manufacturing; total ink coverage; adhesion between layers

## 1. Introduction

By fulfilling more and more functions plastic cards are applied in many fields of our lives. Nowadays plastic cards can be documents, bank cards, phone cards, different ID cards, PKI cards and loyalty cards, as well as club cards. Card bodies are made of several plastic foil layers with lamination by reason of their application method and durability requirements. One of these requirements is the value of adhesion power arising between layers.

Our research focuses on the adhesion problems between foil layers due to which the cover foil may separate from the core foil after lamination during the manufacturing of the cards or during their use, respectively. This represents a serious problem for manufacturers, card issuers and users equally.

Several factors can influence the adhesion power between layers during manufacturing, including the type of ink, the quality of the foil, the evenness of drying and the total ink coverage. The most important of the factors we investigated is the effect of the printed surface's total ink coverage.

The thickness of the ink layer between the core foil and the cover foil varies depending on the graphic appearance of the card. The adhesion problem between the layers can be observed primarily at cards where the area filling ratio is high. The purpose of our investigation is to determine the maximum total ink coverage that provides a just appropriate layer adhesion after lamination. Furthermore, we investigated if there is any difference between the adhesion values of layers formed by the individual basic colours. Our goal was to filter out before manufacturing those card graphics that can be produced by us in proper quality only after

modifying the colour composition, when using the given card base material and standard lamination parameters (temperature and pressure) before manufacturing. The customer may insist on the original design but in this case the technology or the base material should be changed in order to achieve the appropriate adhesion of layers.

These tests were performed for the combination of several plastic foils, ink types and laminating machine settings; out of these the data pertaining to PVC card bodies are included in the paper.

## 2. Plastic card manufacturing

A plastic card basically consists of two core foils and two cover foils. The cover foil for the back is equipped with a magnetic strip if required. Card manufacturing consists of the following steps:

- printing,
- laminating and punching,
- applying hologram and chip insertion.

Laminating is placing a protective plastic foil on both sides of the print that protects it from incidental contamination and makes the card body more durable. This takes approx. 17-25 minutes by a pressure of 100-150 N/cm$^2$ on 125-150 $^o$C for PVC and on 170-200 $^o$C for PC. During lamination a periodic pressing takes place with heat transfer and as an effect the foils soften and their structure becomes homogeneous. After laminating, punching is the next step where cards are cut to the given size.

## 3. Test card manufacturing

Because the adhesion power between layers is mostly influenced by the total ink coverage (TIC) we printed plastic card samples with different TIC values, using CMYK ink. Furthermore we examined if there was any difference between the adhesion values of the four basic colours. There should be at least 0.35 N/mm binding force by layer between the base material components forming the structure of cards. The machines and materials at our research were the followings:

- Printing press: Heidelberg SM 52 UV
- Basic material: PVC core foil (300 x 500 mm, thickness: 310 μm).
- Ink: Sicpa 770 UV Process
- Cover foil: PVC (composition was the same as that of the core foils but thinner and translucent)
- Laminating machine: Bürkle type two tower laminating machine.

Before lamination a strip made of a 5 μm thin metal foil was placed between the core foil and the cover foil. Where such foil existed the cover foil did not merge with the core foil after lamination. The cover foil was then separated from the core foil by cutting the laminated sheet at this non-merged portion thus obtaining the surface that should be put into the clamps of the tensile testing machine.
We measured the adhesion values by Zwick Roell tensile testing machine type BDO-TB 0.5 TS.

## 4. Evaluation of the results

### 4.1. Basic colours
In the first printing phase the four basic colours were examined separately with different filling ratios. In the different printing phases FM-screening were applied always with the same rotation. 32 pcs of 20 x 120 mm specimens suitable for testing the adhesion force between layers were placed on a sheet; 8 pcs with 25%, 8 pcs with 50%, 8 pcs with 75% and 8 pcs with 100% filling values, under standard circumstances and normal load. At the very first measurement an unprinted sheet was laminated and then the layer adhesion test was performed on it. From here on samples prepared with each filling ratio were measured three times and then the average value of these measurements was taken into account. The average layer adhesion value of the unprinted sample was 13.46 N/cm. The cover foils of specimens with 25, 50 and 75% filling ratio broke during the measurements i.e. the adhesion force between the layers was higher than the force required to break the cover foil. The measurement results show that the basic colours comply with the layer adhesion requirements. This means that they have complied with the stipulated requirement. (Table 1)

*Table 1 Measurement results of the first printing phase*

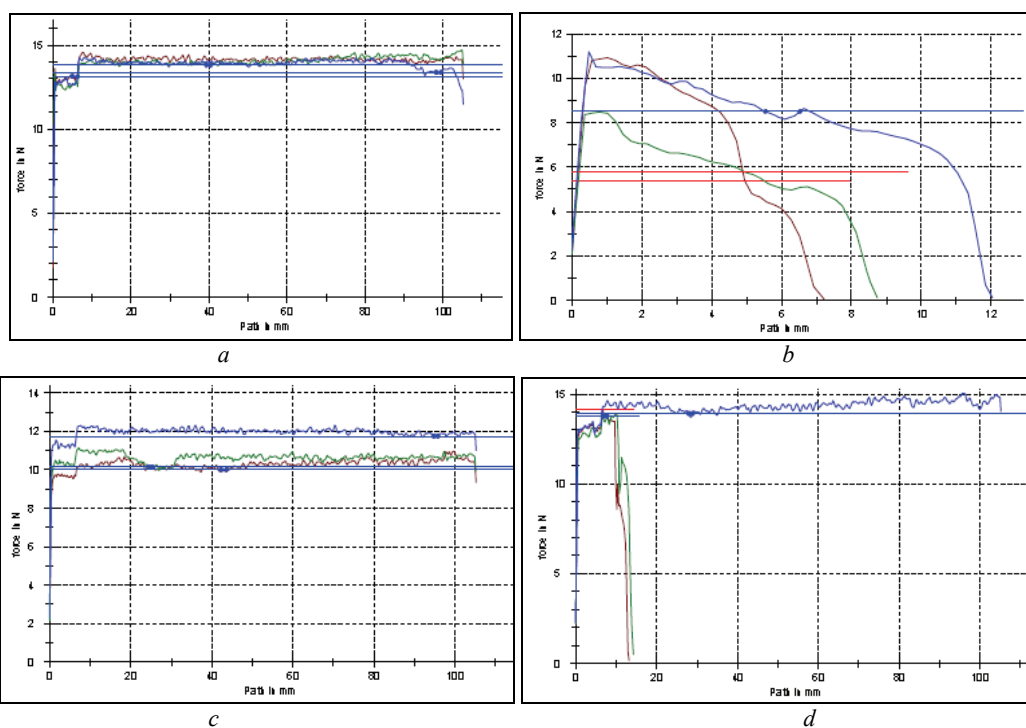| TIC % | Layer adhesion (N/cm) |
|---|---|
| unprinted 0 | 13.46 |
| C 75 | foil break |
| M 75 | 10.62 |
| Y 75 | foil break |
| K 75 | 13.65 |
| C 100 | 13.71 |
| M 100 | 11.7 |
| Y 100 | 13.94 |
| K 100 | 11.54 |



*Figure 1: Adhesive strength between layers - a: unprinted, b: C75%, c: M75%, d: Y100%*

## 4.2. Overprints 1

In the second printing phase the critical total ink coverage was determined. The overprints were printed with equal filling ratios of basic colours. It turned out that there was a big deviation between specimens with 280 and 300% during the measurements. The average value of the adhesion force between layers was reduced from 14 N/cm to 4.5 N/cm (*Table 2*).

*Table 2: Measurement results of the second printing phase*

| TIC % | Layer adhesion (N/cm) |
|---|---|
| 100 (4x25%) | 13.7 |
| 200 (4x50%) | 13.27 |
| 240 (4x60%) | foil break |
| 260 (4x65%) | 14.51 |
| 280 (4x70%) | 14.9 |
| 300 (4x75%) | 4.16 |
| 320 (4x80%) | 4.46 |
| 340 (4x85%) | 4.15 |
| 360 (4x90%) | 4.34 |
| 380 (4x95%) | 3.1 |
| 400 (4x100%) | 2.38 |

*a*

*b*





*c*

*d*
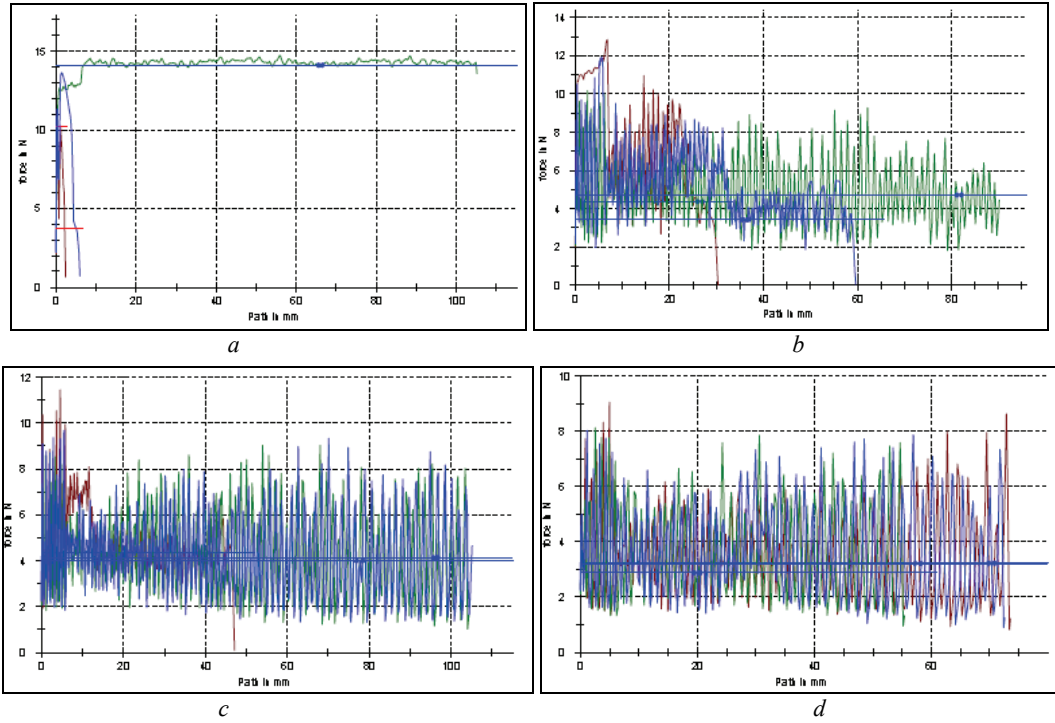
*Figure 2: Adhesive strength between layers - overprints*
*a:TIC280(4x70% ), b:TIC300(4x75%), c: TIC340(4x85%), d: TIC380(4x95%)*

## 4.3. Overprints 2

In the third printing phase the filling ratios of the basic colours were present in different quantities within one specimen. It can be observed in these measurements that if black or cyan colours are present in bigger quantities then the value of the adhesion force between layers reduces by a greater extent as if the sample contained magenta or yellow colours in the same proportion. From the measurement results it turned out - contrary to the second printing phase in which we examined the basic inks - that while magenta does not reduce the bonding force of lamination, cyan does. (Table 3)

|  | TIC % | Layer adhesion (N/cm) |
|---|---|---|
|  | 250 = C100% M80% Y70% K0% | 13.6 |
|  | 260 = C100% M100% Y30% K30% | 9.09 |
|  | 260 = C30% M100% Y100% K30% | 12.84 |
|  | 300 = C100% M100% Y50% K50% | 4.9 |
|  | 300 = C50% M100% Y100% K50% | 11.3 |
|  | 325 = C75% M75% Y75% K100% | 4.42 |
|  | 335 = C80% M85% Y75% K95% | 3.5 |
| *Table 3* | 340 = C70% M100% Y100% K70% | 6.2 |
| *Measurement results of* | 350 = C100% M75% Y75% K100% | 3 |
| *the third printing phase* | 355 = C85% M85% Y85% K100% | 4.19 |
|  | 370 = C100% M85% Y85% K100% | 2.73 |





*a*

*b*
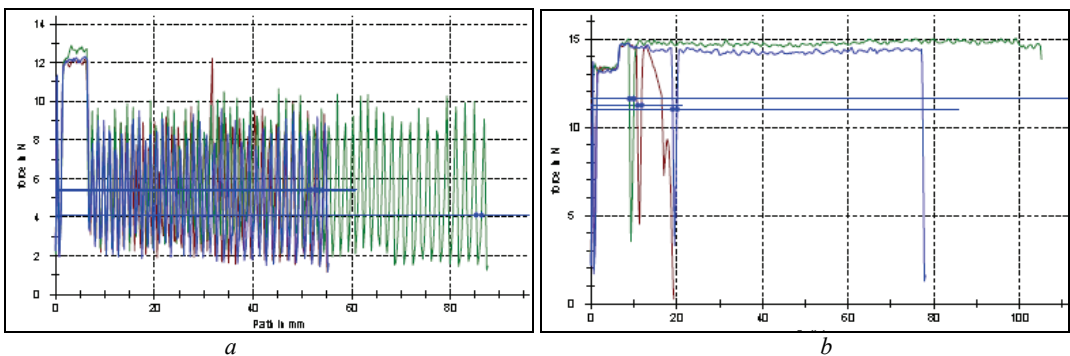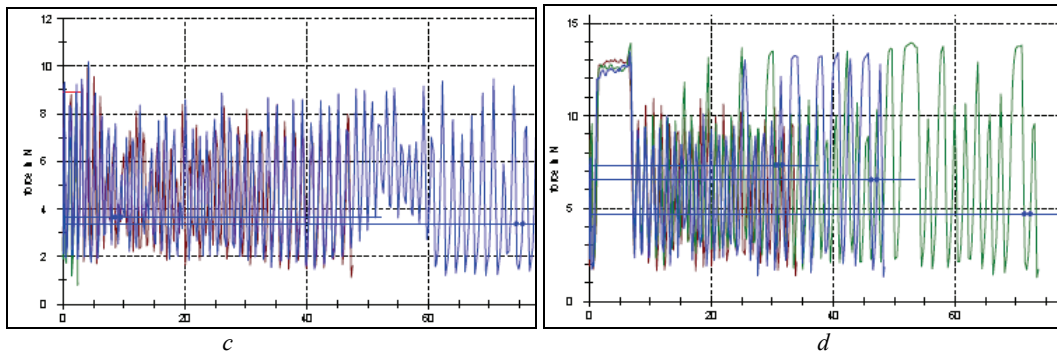
*Figure 3: Adhesive strength between layers - overprints*
*a: TIC 300% (C100%M100%Y50%K50%), b: TIC 300% (C50%M100%Y100%K50%),*
*c: TIC 335% (C80%M85%Y75%K95%), d: TIC 340% (C70%M100%Y100%K70%)*

## 5. Conclusion

Based on our results we can be establish the following statements:

- individually the four basic colours show very good layer adhesion results (12-14 N/cm); the adhesion of the cover foil was smaller than the adhesion force between layers and thus the cover foil broke;
- a minimal deviation can be observed between the basic colours and no significant conclusion could have been drawn from this issue after the first printing phase;
- from the point of applicability the maximum total ink coverage can be 280-300%, or even 360% based on the requirements of the standard;
- the presence of black and cyan colours in high percentages adversely influences the adhesion force between the layers;
- the maximum total ink coverage can be increased if the proportion of cyan and black colours are reduced; this would, however, result in a lighter shade of colours not suitable for all card designs (in this case an other basic material have to be chosen).

These useful pieces of information gained for plastic card design and manufacturing by our examination and measurements can improve the quality and durability of our products nowadays and in the future as well.

## References

1. Jakab, Á., Thurzó, Gy. Zinz, B. *A PVC előállítása, feldolgozása és alkalmazása Műszaki Könyvkiadó Budapest*

2. Szilágyi, T. *UV-ofszet - a jövő útja 2005 Print Consult Budapest*

3. www.bankkártya.hu

4. www.ISO/IEC7810szabvany.hu

5. www.ISO/IEC10373-1szabvany.hu

# Ensure product longevity and quality at printing on balloons and other stress-deformed materials

*Anna V. Erofeeva, Alexander P. Kondratov and Evgeny B. Bablyuk*

Moscow State University of Printing Arts
2a, Prianishnikova Street
RU-127550 Moscow, Russia

E-mails: anna.erofeeva@gmail.com; apk@newmail.ru; evgeny.bablyuk@mgup.ru

**Abstract**

One of the main problems of screen-printing on the deformed surfaces of elastic materials, in particular on elastic balloons, is a limited range of inks that can be used for working on elastic materials. It is explained by their low durability in stressed-deformed state and low resistance to solvents and other ink organic components, in which the balloon material (latex film, rubber, synthetic elastomer) intensively swells, or which can cause cracking of its surface.

To increase technological capabilities and competitiveness of specialized printing companies dealing with printing on balloons and other products made of deformable elastomers, the following are essential: carefully selected formulas of the used materials, improved ways of screen-printing and research of the three-dimensional rubber deformation features. These problems can be solved by physical simulation of a three-dimensional rubber deformation processes in contact with aggressive liquids.

**Key words**: screen printing; solvent; balloon; longevity; deformation limit; latex rubber

## 1. Introduction

One of the main problems of screen-printing on the deformed surfaces of elastic materials, in particular on elastic balloons, is a limited range of inks that can be used for working on elastic materials. It is explained by their low durability in stressed-deformed state and low resistance to solvents and other ink organic components, in which the balloon material (latex film, rubber, synthetic elastomer) intensively swells, or which can cause cracking of its surface. To increase technological capabilities and competitiveness of specialized printing companies dealing with printing on balloons and other products made of deformable elastomers, the following are essential: carefully selected formulas of the used materials, improved ways of screen-printing and research of the three-dimensional rubber deformation features. These problems can be solved by physical simulation of a three-dimensional rubber deformation processes in contact with aggressive liquids.

## 2. Methods

In practice, many well-known printing companies producing promotion materials use the following way of screen printing on balloons: fanning the workpiece balloons by compressed air to the size of components 30-80% of maximum deformation limit (strength), ink application to the surface of the balloon through the mesh stencil on a special equipment (machines for screen printing on the balloons), short-term preliminary image drying at the temperature of working area or airflow cooling within 3 ÷ 5 sec., the compressed gas removal, balloon size reduction to the baseline, final ink drying within 1 ÷ 3 hours and final packaging.

The current printing technology does not take into account such features of films and sheets of latex rubber as rapid changeability within time and dependence on the size and type of mechanical deformation parameters: modulus of elasticity, strength, durability. A drawback of production equipment is the lack of means for fixing the optimal size of the ball at the moment of printing the picture on the machines used in printing, which should be provided for screen-printing technology for elastomers and depend on the size, thickness and physical and mechanical properties of the latex intermediate (the balloon).

As a consequence of imperfections in equipment and technology we have decrease in accuracy of image reproduction in size, and increase of the amount of throwaways at the expense of destruction of the billets under the action of mechanical stress and aggressive ink components.

The practical objectives of the present development is the final printed production yield increase by reducing the number of damaged billets, enhancing the technological capabilities of screen printing, reducing the cost of inks used for printing images on a elastic material by increasing the number of permissible ingredients and increase the safe concentration of stencil inks. Achieving this goal can be accomplished through the use of basic knowledge about the structure of rubber in general, and structural mechanics of latex films, in particular, who are known experts in the field of mechanics of polymers as the effect Patrikeeva - Mallins [2]. The essence of the effect Patrikeeva - Mallins is a physical modification (irreversible restructuring) of the structure of rubber in the entire volume of material as a result of deformation and is traditionally illustrated by the diagram of cyclic stretching of the sample elastomer in the mode of constant strain rate [Patrikeev G. A., Baidakov D. I., 1972]. Restructuring of rubber in a single (first) stretching leads to "softening" and significantly reducing the stresses of the material, as with the partial reduction of up to a certain degree of swelling, and in repeated tension to the same degree of swelling. The graph of irreversible effects "softening" of elastomer looks like a hysteresis loop under cyclic tension and reducing the sample rubber (Fig. 1). The width of the loop depends on the material properties and conditions of the deformation (temperature, speed and type of stress state). During printing balloons get biaxial deformation of significant quantities at a rate determined by the flow and pressure of the compressed gas. At the moment of printing inside balloons the stresses are close to the ultimate strength, which leads to their rapid destruction in contact with the screen-printed form and ink application.
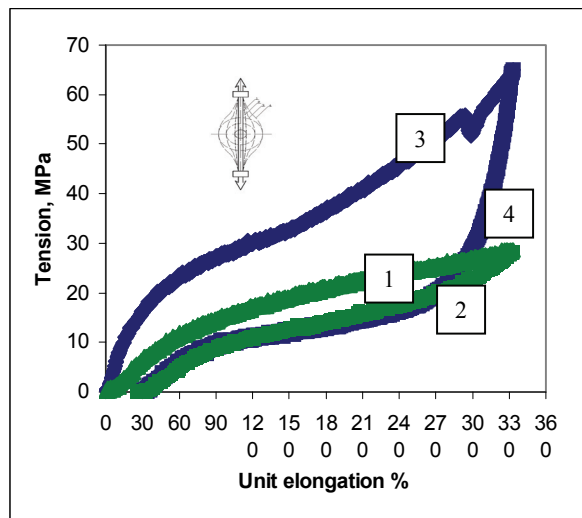


Fig. 1: Diagramm of stretching of balloons. Hysteresis loop.
1, 2 - uniaxial deformation of natural latex balloon;
3, 4 - deformation of the balloon of natural latex with a fixed transverse size (biaxial);
1, 3 - stretching balloon up to 330% ; 3, 4 - reduction to the original size

The difference between the stresses in the shell of the balloon under uniaxial extraction and swelling (biaxial strain) are quite essential, as reflected on the tension diagram. It can be seen (Fig. 1) that the hysteresis loop in the biaxial strain is much broader than under uniaxial drawing and the difference between the tension corresponding to a particular strain in tension and reducing the higher, the more elongation and the transverse size of the balloon.

## 3. Results

To study the effect of effect Patrikeeva - Mallins in the biaxial strain methodology of preparation of latex balloons to mechanical testing has been developed. The essence of the method consists in introducing into the cavity of the balloon a dosed amount of components required for the synthesis of light sphere of rigid polyurethane foam (aromatic polyol, water and toluene diisocyanate) inside the baloon.

After the synthesis of polyurethane foam inside the balloon, forming and curing the scope of polymer foam, which dimensions are determined by the number of components introduced, the samples look as shown in Figure 1, "a". Their transverse size in the center (the sphere diameter) is fixed initially before the mechanical testing. In the longitudinal stretching of the samples "with spherical inserts" on a tensile testing machine the

latex film undergoes stretching close to the three-dimensional deformation, realizing at the rupture of the baloon, and the chart shows the value of the tensile stress corresponding to its longitudinal component. On the stretching chart of the sample with fixed transverse size (Fig. 1 B) we can see that with the same degree of the balloon blowing (the strain in the same direction), for example, 270% (curve 3,4 biaxial stretching) corresponds to stress 51 MPa in tension and 20 MPa at a reduction. Thus, the balloon at the stage of blowing has a tension more than 2.5 times bigger than at the stage of reduction and, therefore, the probability of its failure (loss of the work piece, expensive paints and productivity) is significantly higher.

## 4. Discussion

The time up to the elastomer product destruction (longevity) depends on the magnitude of mechanical stress. This relation applied to cross-linked elastomers described by a power function as a result of compiling a set of experimental data on the destruction of elastomers under uniaxial strain [Bartenev G.M., Zuev U.S., 1964]:

$$\tau = C_1 \cdot \frac{1}{\sigma^b} \qquad\qquad (1)$$

where:  $\tau$ - time till sample destruction, sec.;
$\sigma$ - tension, Pa;
$b$ - constant (2,7-3,4);
$C$ - constant, sec $(Pa)^b$.

Assuming the power law, reflecting the relation of durability of elastomers and tension we can legitimately suppose, that, if the tension at which the balloon is inflated to the desired print size can be reduced by a factor of 2 due to the application of the proposed method, its longevity raises by 8 times. If the tension drops a multiple of 3-m, the durability of the balloon increases 27 times, etc.

The three-dimensional deformation occurring at the blow of elastomer hollow products can be studied by simultaneous measuring the gas pressure inside the shell and its dimensions. The result of these measurements is the "quaint" (in the form of "8") graph of the relation of the gas pressure inside the shell to the length or magnitude of the deformation of the equator of the sphere (Fig. 2).
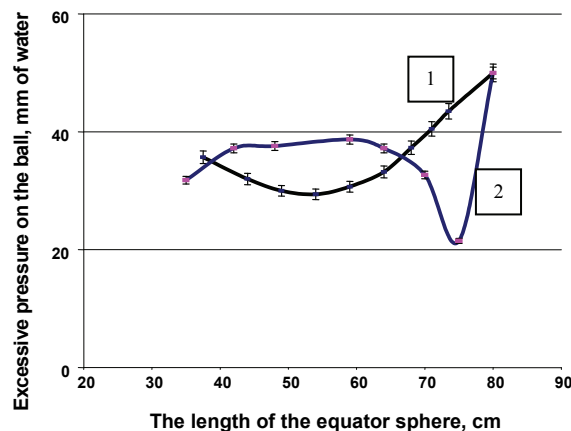


*Fig. 2: Relation of internal gas pressure with the length of the equator of the balloon filling and emptying.*
*1 - tension (blowing) balloon; 2 - reduction in air outlet*

In this case, by simultaneous shell stretching and increase of the curvature radius of the spherical surface the uniform dependence of stress on deformation, characteristic of the effect Patrikeeva - Malinza deformation on one and the same plane, is distorted [2; Patrikeev G. A., Baidakov D. I., 1972]. The effect increases sharply at the first moment of reducing the size of the sphere and decreases with significant reversible elastic deformation of the shell. Based on the facts established in this work and the known degree of durability depending on the tension we should expect the corresponding multiple increase of durability. The behavior of strained elastomers in contact with a liquid causing swelling (solvent) or cracking of the polymer surface (SAW) is less predictable.

As it was illustrated in 60-ies of the 20th century by Russian researchers Dogadkin, Fedyukin and Gul in the experiments over mechanical properties of rubber through various elastomers, the relation between the strength of rubber and the degree of swelling of rubber has a complex character [Dogadkin B. A., Fedukin D. L., Gul V. E, 1957]. The effect of the liquid on the durability of the stress-deformed elastomers is the most evidently seen in testing their durability and can be clearly observed in the graphs of dependence of durability of rubbers on the tension built in logarithmic coordinates (Fig. 3).
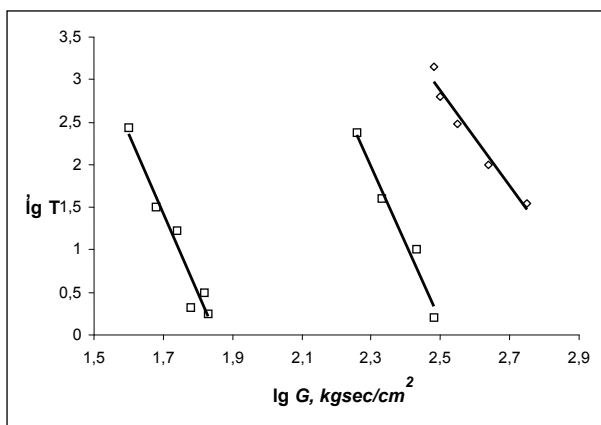


*Fig. 3*
*Influence of conditions of solvent (plastic -*
*plasticizer - dibutyl phthalate) on the durability of*
*rubber Nairit. Dependence of time to fracture (τ) of*
*rubber from the tension in logarithmic coordinates.*
*1 - an endurance test with constant load in air,*
*2 - test at constant load in air samples swollen*
*in the solvent, 3 - tested in contact with the*
*solvent after the pre-tension in the air*

In the circumstances before the favorable effect of the solvent as a plasticizer appears, it has such effect on rubber being already under great stress, the destruction of rubber in solvent media is much more intensive than the destruction of the rubber in the air and even rubber, solvent-like volume plasticizer in the amount exceeding 15% (mass) [Bartenev G. M., Zuev U. S., 1964; Dogadkin B. A., Fedukin D. L., Gul V. E., 1957]. In case of a short-term contact with the liquid, the effect of weakening the intermolecular interaction in a thin surface layer of the polymer evidently appears and the reduction of the polymer surface tension to the values close to zero occurs. The reduction of longevity becomes much stronger the more reduces the surface tension and intermolecular interaction. In the case of Nairit destruction under the action of the liquid goes with separate big cracks on the surface [S. Oswitsch, Reinforced Plast, 1963; Zuev U. S., 1972]. A similar picture is observed at the destruction of other polymeric materials [Kondratov A. P., Klendo E. M., Manin V. N., 1983; Kondratov A. P., Gromov A. N., Manin V. N., 1985] and latex spheres in contact with solvent inks.

The influence of "aggressive" components of paints, causing swelling of the elastomer, the destruction of the balloons in the printing process is illustrated by the diagrams of stretching balloons with short-term unilateral contact with organic solvents (Fig. 4).
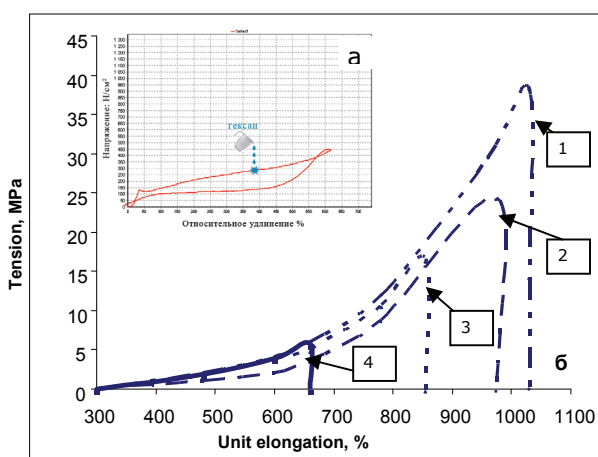


*Fig. 4*
*Diagram fragment of uniaxial stretching of balloon to*
*a fixed deformation with following*
*carbon tetrachloride wetting (contact)of cover part.*
*1 - stretching «in the air» to break (1040 %),*
*2 - stretching up to unit strain of 970 %, followed by*
*touching the tampon wetted with carbon tetrachloride;*
*3 - stretching up to unit strain of 840 %, followed by*
*touching the tampon wetted with carbon tetrachloride;*
*4 - stretching up to unit strain of 660 %, followed by*
*touching the tampon wetted with carbon tetrachloride*

As samples of "aggressive" ink components some volatile organic solvents were used in the development of this method: white spirit, benzene, carbon tetrachloride and chloroform. Samples of materials for balloons in the form of rings cut from the bottom of the cylindrical blanks were stretched at a constant speed in a tensile machine of the type RM-50 up to the strain component constituting 0.95, 0.8 and 0.65 of the maximum deformation of the material, which is 970, 840 and 660% of the relative deformation of the linear tension.

When the most aggressive of the tested solvents - carbon tetrachloride - was applied on the part of the sample deformed at 0.95 of the deformation limit (curve 2, Figure 3) with a cotton swab, the break of the latter occurs almost instantly, the balloon breaks within 2-4 sec.

When a cotton tampon with a carbon tetrachloride was applied to the sample deformed to 0.8 of the maximum material deformation (curve 3, fig. 4), the destruction occurred in 20 seconds. This result is better, but not enough for application and drying the ink based on the aggressive solvent. When a cotton tampon with a carbon tetrachloride was applied to the sample, which was under 0.65 of the maximum deformation (curve 4, Figure 4), the destruction occurred in 120 seconds. It's good for application and ink drying. The tension in this sample that did not break in contact with aggressive liquid double as less as in the previous example and can be reached by means of preliminary single or multiple blowing of an intermediates.

## 5. Conclusions

Physical and mechanical properties of materials were tested by the example of balloons, made from natural latex. Ring-shaped 10 mm wide samples were cut. Tensile strength and characteristics of deformability of material were measured: module of elasticity of 100 (E100), module of elasticity of 300 (E300), tension corresponding to extracts from 0.75 deformation limit under tension and reduction. The measurements of physical and mechanical parameters and the estimated coefficients reflected the state of the material at the moment of paint application are given in Table 1. It is evident that application of the proposed method can improve the reliability of the process of screen printing products at inflated elastomer items and increase their longevity in the stress state in 5 ÷ 20 times [Bablyuk E. B., Kondratov A. P., Erofeeva A. V., 2009].

*Table 1: The estimate and experimental deformative and  strength characteristics of latex rubber*

| Parameters and deformation type | Sample width (diameter) | Elasticity module $E_{100}$ | Elasticity module $E_{300}$ | Tension during printing |
|---|---|---|---|---|
| | мм | MPa | MPa | MPa |
| Film stretching | 20 | 15.4 | 27.0 | 21.0 |
| Film shrinking | 20 | 5.0 | 12.0 | 14.0 |
| Extinction coefficient, time | 20 | 3.0 | 2.3 | 1.5 |
| Longevity increasing, time | 20 | 27.0 | 18.3 | 2.4 |
| Ballooning * | 40 | 28.1 | 52.5 | - |
| Balloon reducing ** | 40 | 10.0 | 29.9 | - |
| Extinction coefficient, time | 40 | 2.8 | 1.8 | - |

\* Tension during balloon deformation is 75%  from limit deformation
\*\* Inflated balloon with fixed diameter tensile test (inset of hard polyurethane foam)

**References**

1. Laboratory test, Sharm-Art, Publishing house Sharm-Art, 2008, №2.

2. Polymer encyclopaedia, M., UE, 1972, T.1, p. 821.

3. Patrikeev G. A., Baidakov D. I., DAN USSR, 1972, t.207, №2, p. 381.

4. Bartenev G. M., Zuev U. S., Strength and destruction of  high-elasticity materials, M., Chemistry, 1964, p. 387.

5. Dogadkin B. A., Fedukin D. L., Gul V. E., Colloidal magazine, 1957, t.19, №1, p. 287.

6. S. Oswitsch, Reinforced Plast, 1963, v.8, №4, p. 116.

7. Zuev U. S., Polymer destruction under aggressive environment, M., Chemistry, 1972, t 45, p. 323.

8. Kondratov A. P., Klendo E. M., Manin V. N., High-molecular substances, 1983, ser.B, t.25, № 3, p. 202.

9. Kondratov A. P., Gromov A. N., Manin V. N., Plastic mass, 1985, №7, p. 40.

10. Bablyuk  E. B., Kondratov A. P., Erofeeva A. V., Screen printing method on balloon, Pat. RF, application № 2009136307 dd 30.10.2009

# Index of authors